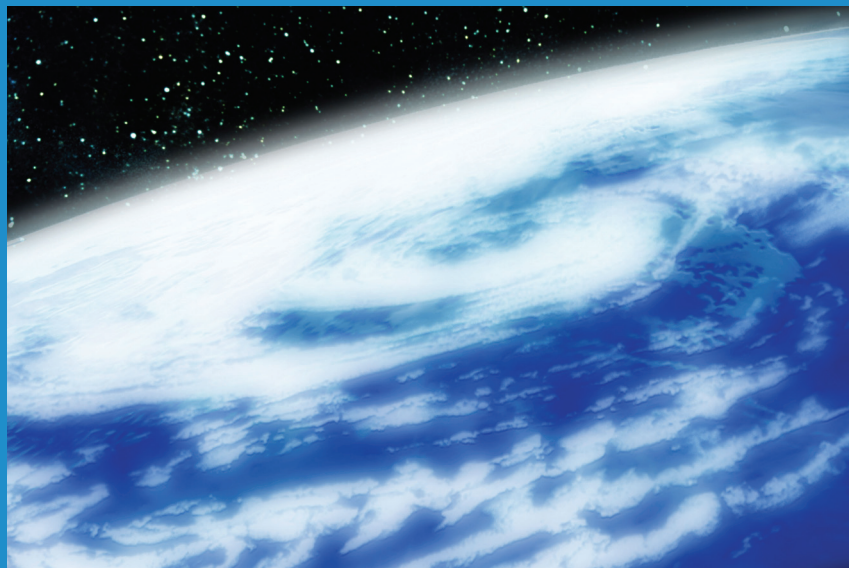


International Hydrological Programme



Satellite Remote Sensing of Atmospheric Constituents

-The Eighteenth IHP Training Course in 2008-



Edited by Hirohiko Masunaga

Hydrospheric Atmospheric Research Center, Nagoya University



United Nations Educational Scientific and Cultural Organization



The Eighteenth IHP Training Course
(International Hydrological Program)

Satellite Remote Sensing of Atmospheric Constituents

3-15 November 2008

Nagoya, Japan

Working Group for IHP Training Course,

Sub-committee for IHP

Japanese National Commission for UNESCO

Outline

As a part of the Japanese contribution to the International Hydrological Program (IHP), a short course on satellite remote sensing of atmospheric constituents will be conducted for participants from the Asia-Pacific regions. The course will be held for the period from 3 to 15 November 2008 at Hydrospheric Atmospheric Research Center (HyARC) and Information Technology Center, Nagoya University, Nagoya, Japan. The course includes a series of lectures in English, practical sessions, and technical tours.

Objectives

Satellite remote sensing is a unique tool to homogeneously observe our whole planet. A variety of meteorological satellites are currently in operation to monitor clouds, precipitation, aerosols, and different gaseous components of the atmosphere. The applicability of satellite data ranges over a broad area from operational use to climate studies. The 18th IHP training course will provide an opportunity for participants to learn the fundamentals of satellite remote sensing and its application to atmospheric sciences. The training course offers introductory lectures on the basics of meteorological satellite observations and the physical principles of retrieval algorithms. Also offered is a practical training course for the participants to establish basic skill to analyze satellite data.

Course Contents (convener: H. Masunaga)

Lecturers

Aonashi, Kazumasa (Meteorological Research Institute, Japan Meteorological Agency)

Higuchi, Atsushi (Center for Environmental Remote Sensing, Chiba University)

Iguchi, Toshio (Applied Electromagnetic Research Center, National Institute of Information and Communications Technology)

Kachi, Misako (Earth Observation Research Center, Japan Aerospace Exploration Agency)

Kawamoto, Kazuaki (Faculty of Environmental Studies, Nagasaki University)

Kubota, Takuji (Earth Observation Research Center, Japan Aerospace Exploration Agency)

Masunaga, Hirohiko (Hydrospheric Atmospheric Research Center, Nagoya University)

Nakamura, Kenji (Hydrospheric Atmospheric Research Center, Nagoya University)

Okamoto, Hajime (Center for Atmospheric and Oceanic Studies, Tohoku University)

Okamoto, Kozo (Forecast Department, Japan Meteorological Agency)

Sano, Itaru (School of Science and Engineering, Kinki University)

Ushio, Tomoo (Graduate School of Engineering, Osaka University)

Yamamoto, Munehisa K. (Center for Environmental Remote Sensing, Chiba University)

Yokota, Tatsuya (Center for Global Environmental Research, National Institute of Environmental Studies)

Lectures

- L0 Introduction H. Masunaga
- Guidance and outline of the IHP short course
- L1 Overview of Meteorological Satellites in Orbit H. Masunaga
- A brief summary of satellites and sensors being used for meteorological research and weather forecasting.
- L2 Satellite Remote Sensing of Clouds by Passive Sensors K. Kawamoto
- Methodologies to retrieve cloud physical properties from space
 - Applications to climate studies
- L3 Satellite Remote Sensing of Clouds by Active Sensors H. Okamoto
- Cloud profiling by ground-based and spaceborne W-band radars
 - Current and future satellite missions carrying cloud profiling radars
- L4 Satellite Remote Sensing of Aerosols I. Sano
- Methodologies to retrieve aerosol optical properties from space
 - Applications to climate and environmental studies
- L5 Satellite Remote Sensing by Temperature and Humidity Sounders K. Okamoto
- Methodologies of atmospheric sounding from space
 - Application to data assimilation
- L6 Geostationary Meteorological Satellites A. Higuchi
- Introduction to existing geostationary satellites for meteorological applications
 - Cloud and water-vapor monitoring by GMS/MTSAT: physical principles and applications
- L7 Tropical Rainfall Measuring Mission (TRMM) K. Nakamura
- Mission outline and precipitation data products available
 - Applications to climate studies and extreme weather monitoring
- L8 Space borne Precipitation Radars T. Iguchi
- Rainfall profiling by space borne K-band radars
 - Current and future satellite missions carrying precipitation radars
- L9 Precipitation Retrieval by Microwave Radiometers K. Aonashi
- Methodologies to retrieve precipitation from space
 - Applications to data assimilation
- L10 Global Satellite Mapping of Precipitation (GSMaP) T. Ushio
- Introduction to the GSMaP project

- Retrieval algorithms and data products

L11 Greenhouse Gas Observing Satellite (GOSAT)

T. Yokota

- Introductions to the GOSAT project
- Retrieval methodology and expected outcome.

Practices

P1 Geostationary Meteorological Satellite (GMS) Data Analysis

M. K. Yamamoto

- On-site computer exercise to analyze GMS data

P2 Real-time Global Precipitation Data Analysis

T. Kubota

- On-site computer exercise to analyze Global Satellite Mapping of Precipitation (GSMaP) data

Technical Tours

Japan Aerospace Exploration Agency in Tsukuba

- Guided tour
- Seminar for satellite data/images access through JAXA EORC WWW site

M. Kachi

Schedule (3-15 November 2008)

3 (Monday)	Arrival at Nagoya	Nagoya
4 (Tuesday)	10:00-12:00: Guidance (Lecture 0) and Lecture 1 by H. Masunaga 14:00-16:00: Lecture 2 by K. Kawamoto Reception at Nagoya University in the evening	Nagoya
5 (Wednesday)	10:00-12:00: Lecture 3 by H. Okamoto 14:00-16:00: Lecture 4 by I. Sano	Nagoya
6 (Thursday)	10:00-12:00 Lecture 5 by K. Okamoto 14:00-16:00 Lecture 6 by A. Higuchi	Nagoya
7 (Friday)	10:00-12:00: Practice 1 supervised by M. K. Yamamoto 14:00-16:00: Practice 1 (contd.)	Nagoya
8 (Saturday)	Japanese culture introduction and free time	Nagoya
9 (Sunday)	Technical Tour: Japan Aerospace Exploration Agency (JAXA) (Move to Tsukuba): Guided tour	Tsukuba
10 (Monday)	Technical Tour (contd.): JAXA EORC seminar by M. Kachi Move back to Nagoya	Tsukuba
11 (Tuesday)	10:00-12:00: Lecture 7 by K. Nakamura 14:00-16:00: Lecture 8 by T. Iguchi	Nagoya
12 (Wednesday)	10:00-12:00: Lecture 9 by K. Aonashi 14:00-16:00: Lecture 10 by T. Ushio	Nagoya
13 (Thursday)	10:00-12:00: Practice 2 supervised by T. Kubota 14:00-16:00: Practice 2 (contd.)	Nagoya
14 (Friday)	10:00-12:00: Lecture 11 by T. Yokota 14:00-: Closing Ceremony	Nagoya
15 (Saturday)	Departure from Nagoya	

- All lectures are held at the lecture room (3F) of the Hydrospheric Atmospheric Research Center, Nagoya University.
- Practices are held at the Information Technology Center, Nagoya University.

Lecture 1

Introduction and Overview of Meteorological Satellites in Orbit

Hirohiko Masunaga

Hydrospheric Atmospheric Research Center, Nagoya University

This opening lecture overviews the Earth observing satellites currently being operated for meteorological applications. Meteorological satellites may be classified into distinct categories by orbital configuration. Geostationary satellites, phase-locked with the Earth rotation, provide temporally continuous observation on a broad area facing the satellite. The low-Earth orbiting (LEO) satellites, in contrast, typically fly at altitudes of a few hundred to a thousand kilometers. LEO satellites carry a number of different sensors, including microwave radiometers and radars, that are not onboard the geostationary satellites. Governmental agencies operating these satellites may be divided into “operational agencies” and “space agencies”. The former is expected to provide continuous, stable services, while the latter develops satellites carrying technologically advanced sensors. Geostationary satellites, instrumental for daily weather monitoring, are typically operated by the operational agencies. Space-borne radars, in contrast, are relatively experimental for use by the weather bureaus and operated by the space organizations such as the Japan Aerospace Exploration Agencies (JAXA) and U.S. National Aeronautics and Space Administration (NASA).

Lectures in the training course are focused on a variety of satellite capabilities available to date. Physical principles to measure cloud properties from satellite remote sensing, with both traditional and newest technologies, are introduced (L2 and L3). Aerosol measurements are also important for monitoring and assessing air pollution and the aerosol impact on climate (L4). Sounding air temperature and humidity is crucial for numerical weather prediction (L5). Geostationary satellites are particularly useful for cloud and water vapor observations (L6). The second week of the training course starts with an introduction to the Tropical Rainfall Measuring Mission (TRMM) (L7), which is a recent technological progress in measuring global precipitation with the Precipitation Radar aboard (L8). Global precipitation estimates are now conveniently organized into user-friendly datasets by dedicated efforts across the world (L9). Finally, global monitoring of greenhouse gases by a newest satellite, to be launched just in a few months, is reviewed (L10).

Lecture 2

Satellite Remote Sensing of Clouds by Passive Sensors

Kazuaki Kawamoto

Faculty of Environmental Studies, Nagasaki University

This lecture describes a satellite remote sensing investigation with passive sensors, aiming following two points: 1) a methodology to retrieve cloud properties and 2) an extension to climate studies. To begin with, the basic conception of remote sensing is given by some examples such as the dragon and its tracks, and forward and backward problems. A target cloud type in this lecture is low-level water cloud, since radiative properties of non-spherical ice particles are still difficult to apply. After introducing aerosols and cloud properties such as optical depth and representative particle size, principles are explained in detail to retrieve the optical depth, effective particle radius and top temperature of clouds using visible ($0.6\mu\text{m}$), near-infrared ($3.7\mu\text{m}$), and thermal-infrared ($11\mu\text{m}$) spectral channels. A brief history of cloud remote sensing is also presented. Then geographical distributions of cloud properties on global and regional scales are shown, applying above principles to data from passive satellite sensors. Land-ocean contrasts and vertical profiles of cloud properties are consistent with cloud condensation nuclei (CCN) number density, as the Twomey effect suggests. Cloud properties thus obtained are compared with the aerosol abundance in East Asia. When aerosols increase, the optical depth and particle number density of clouds also increase, but the cloud effective particle radius decrease. These behaviors are understood by the Twomey effect. Finally relationships of cloud properties with the precipitation amount are examined. Analyses reveal that precipitation could be one of major controllers of cloud and aerosol properties. For future strategy, passive remote sensing should take synergetic uses with active remote sensing and numerical models.

Lecture 3

Satellite remote sensing of clouds by active sensors

Hajime Okamoto

Center for Atmospheric and Oceanic Studies, Graduate School of Science,
Tohoku University

In this lecture, I introduce the satellite and ground-based remote sensing of clouds (and aerosols). The lecture consists of 8 chapters. (1) what is active remote sensing, (2) About scattering and absorption by particles, (3) Lidar and radar equations, (4) why clouds are important, (5) Observations of clouds from radar and lidar, (6) Evaluation of the Clouds from the Atmosphere General Circulation Model, (7) Results from CloudSat and CALIPSO data, (8) Future satellite mission with radar. In chapter (1), I discuss about the differences between the widely used passive sensors and active sensors. Some measurements of high cirrus clouds from ground based radar and lidar are shown. Some materials are taken from the new satellite mission CloudSat and CALIPSO. In the next chapter, the basic concept about the extinction, scattering and absorption of particles are introduced by using electric and magnetic fields inside and outside the particles. Relation between pointing vectors and scattering cross sections are derived. Definition of backscattering coefficient is also treated here since this is the most relevant parameter in the active remote sensing. And the relationship between these scattering properties and microphysical properties such as size distribution, phase, refractive index, particle shapes are discussed. As a non-spherical particle scattering theory, some details about the discrete dipole approximation (DDA) are explained. Then lidar and radar equations are discussed. We might see the observables are finally related to the microphysics of particles through these equations. These two equations are very similar except for the dependence of single scattering properties on cloud microphysics. Basic features of lidar and radar are summarized. The differences in the features of the radar and lidar, may be easily understood from the knowledge already shown in the previous chapter and these differences also lead to the understanding of the basics of the particle sizing from the combination of these two different sensors. I also provide some basic knowledge about the discussions related to issues in the numerical modeling such as atmospheric general circulation models and concepts of cloud feed back processes. Then ship-based radar and lidar observations and results of analyses are discussed. Evaluation of the representation of clouds is examined. There are some efforts to develop radar and lidar simulators, i.e, signals are estimated from the model output and sensitivity of instruments and observational conditions are included. Results from CloudSat and CALIPSO are presented. And finally, outline of new mission EarthCARE, and scientific targets are introduced.

Lecture 4
Aerosol Remote Sensing

Itaru Sano
Faculty of Science and Technology, Kinki University

Incident solar radiation interacts with aerosol particles in the atmosphere. Such a phenomenon by aerosols as scattering and/or absorption of radiation directly affects Earth's radiation budget. The atmospheric aerosols also play an indirect effect in the radiation budget as the cloud condensation nuclei, because the cloud influences upon the radiation field and precipitation. Accordingly in order to evaluate the Earth's radiation system, the precise aerosol information and its role is desired in the globe scale.

This lecture focuses on the aerosol remote sensing from space. The idea of aerosol remote sensing is based on the fact that satellite has received the scattered light by the atmospheric particles. In other word, the satellite data could involve the scattering characteristics of aerosols. Certainly the surface properties should be considered for aerosol retrieval from satellite data. First, single scattering pattern is calculated as: Lorenz-Mie and Rayleigh theory for aerosols and molecular gases, respectively. Then multiple scattering problem is solved by using the adding-doubling method. It is enhanced that our calculation is made for semi-Stokes parameters $\{I, Q, U\}$, because polarization information is available for our aerosol retrieval. Finally, the numerical results are stored in the look-up tables. Then aerosol properties are retrieved in accordance with the optimized comparison of satellite data with the corresponding values in the look-up tables. In this lecture, the obtained global distribution of aerosol properties and their seasonal change are shown.

The NASA/AERONET ground based aerosol measurements are used for validation for the results of satellite aerosol retrieval. The federated sun photometer network (aerosol robotic network; AERONET) provides the aerosol properties all over the world, which include optical thickness at many wavelengths, refractive index of real and imaginary part at several wavelengths, volume size distribution and other valuable properties. Three AERONET stations have been operated inside Japan by myself collaborated with NASA/GSFC since 2000. All data are distributed to the researchers from the AERONET web (<http://aeronet.gsfc.nasa.gov>).

New generation aerosol sensors called JAXA/GCOM/SGLI are under developed. The reflectance data in the near UV wavelength and polarization information in the red and NIR wavelengths to be observed by SGLI sensor look promising for extracting aerosol information from space. These features are very unique in comparison with other sensor as VIIRS/NPOESS mission etc.

Lecture 5

Satellite Remote Sensing by Temperature and Humidity Sounders

Kozo Okamoto

Numerical Prediction Division, Forecast Department,
Japan Meteorological Agency (JMA)

This lecture shows features, principles and applications of passive atmospheric sounders. Sounders extract vertical distributions of temperature and atmospheric constituents such as humidity using a number of wavelength with different radiative characteristics. They have been long and widely used by operational and research communities. In particular, nadir-looking sounders in the infrared and microwave spectral regions are essential for data assimilation in numerical weather prediction (NWP) because of the ample information and wide coverage.

In the lecture, after the introduction of typical instruments and data examples, what defines a shape (peak height and sharpness) of “weighting function” and how to retrieve atmospheric parameters from radiances sounders measure are discussed. While various retrieval products are used in an environmental monitor, process study and, validation of models and other observations, recent NWP systems directly assimilate radiances. The direct assimilation more effectively and properly extracts observation information although it requires careful data pre-processing, including quality check and bias correction, and accurate radiative transfer models. The performance and pre-processings of the JMA’s operational system are given in the lecture.

Lecture 6

Geostationary Meteorological Satellites

Atsushi Higuchi

Center for Environmental Remote Sensing, Chiba University

This lecture focused on the Geostationary Meteorological Satellites (hereafter GMSs) operated by operational agencies. As well-known, the Earth images captured by GMSs widely apply for daily weather monitoring mainly via TV news or on website. GMSs are operated as phase-locked with the Earth rotation, thus biggest advantage of GMSs is high temporal observation with wide area coverage. Basic observation wavelengths derived from GMSs are consist of: One or two bands in thermal-infrared (IR), corresponding to atmosphere's window wavelength (10-13 micron), water vapor band of 7 micron, some of GMSs have middle-IR band for the water droplet in clouds (3 micron), and visible band. Currently, at least the six GMSs cover the whole of globe under the framework of World Meteorological Organization (WMO). Spacecrafts of GMSs are briefly divided into two types by the scanning and orbit-control methodology. One is spin type (e.g., Meteosat, Meteosat Second Generation (MSG) both operated by EUMETSAT, GMS-5 operated by JMA, FY2 Series by CMA). Spin type GMSs are rotate themselves for the observation and stabilization of them. The other is three-axes control type, such as new generation GOES operated by NOAA and MTSAT-1R (HIMAWARI-6) by JMA. In lecture time, I showed several animations (consist of hourly images in each observation band) derived from MTSAT-1R, for easy to understand how to visualize the feature of clouds by GMSs.

To describe and/or diagnose the feature of clouds from GMSs, several analyzing techniques are shown in this lecture. As example, simple method for the detection of convective activity is utilization of thermal-IR image. For the detection of low-level clouds, visible image is useful during daytime. In addition, Hovmoller diagram, time-longitude section of thermal-IR slice cutting of target latitude belt, is widely applied for the description of convective activity moving with time. Moreover, the combination technique of two or more band images are also widely applied for the field of meteorology. For example, the split window technique of which estimates two thermal-IR bands images difference, is used for the separation of cirrus and deep convective clouds. Such multi-bands or channels applications are adapted in International Satellite Cloud Climatology Project (ISCCP) product. At the end of this lecture, the activity in Center for Environmental Remote Sensing (CEReS), collecting and publishing the major GMSs dataset under the framework of four university's centers virtual laboratory formation (used this dataset in Practice 1) and inter-calibration of GMSs (Global Space-based Inter-Calibration System: GSICS) were introduced.

Lecture 7

Tropical Rainfall Measuring Mission (TRMM)

Kenji Nakamura

Hydrospheric Atmospheric Research Center, Nagoya University

The Tropical Rainfall Measuring Mission (TRMM) is a joint satellite venture between Japan and the U. S. The satellite was launched in November 1997, and is still working in orbit. The TRMM satellite is equipped with a rain radar (PR), a microwave radiometer (TMI), a visible/infrared radiometer (VIS), and a lightning sensor (LIS). As the instruments say, TRMM is dedicated for accurate rain measurement. Particularly, PR is a powerful instrument for observation of precipitation. PR has been developed in Japan, and the first spaceborne rain radar. PR and TMI both apply microwaves, and directly observe rain. The combination of PR and TMI has contributed much to the understanding of the precipitation features over tropical and subtropical regions.

Precipitation is one of the major players in the water cycle over the globe. Water evaporates from ocean or land surface, is transported by wind, and falls as the precipitation. In the global change, one of the key issues is the change of the water cycle, particularly, rain. For this issue, the achievements of TRMM is invaluable and include: much improved global rain distribution, latent heating profiles, and improvement of the rain retrieval algorithms from space. For example, currently, a few hourly near global rain distribution is generated using multi-satellite data with TRMM as a core data source.

Based on the science and engineering heritage of TRMM, a next generation satellite project has been launched as the Global Rainfall Measurement (GPM). GPM aims to provide at least three-hourly global rain distribution in near real time. GPM is a multi-satellite system with a core satellite as a TRMM follow-on and with constellation satellites with microwave radiometers. One of the main and unique sensors is the dual-wavelength radar (DPR) onboard the core satellite. DPR is expected to provide more accurate rain rate estimation and also make the solid precipitation retrieval possible.

Lecture 8

Space borne Precipitation Radars

Toshio Iguchi

National Institute of Information and Communications Technology

The lecture starts with an overview of the general principle of radar measurements of precipitation. It then explains the special conditions in precipitation measurements from space, and how these conditions result in peculiarities of satellite-borne radar. The major hardware constraints given to a space-borne radar are the size, mass, and power consumption together with the reliability. The observation conditions and geometry that are very different from a ground-based radar also constrain the design of a space-borne radar. Some of the important factors in this regard are the distance from the radar to the target, observation angles, existence of Earth's surface behind rain, and the motion of the platform. These factors affect the sensitivity, resolution, observable regions that are free from surface clutter and possibility of Doppler measurements. One good example is the use of relatively short wavelength of electromagnetic waves for the radar in order to realize a good horizontal resolution with a limited size of the antenna. Since high frequency radio waves suffer from attenuation by precipitation itself and other elements in the atmosphere such as water vapor, clouds, and oxygen molecules, a data processing for attenuation correction becomes an essential part of the rain retrieval algorithm. High frequency radio waves also create non-Rayleigh scattering and makes it difficult to estimate rain rates quantitatively. In the lecture, how these issues are handled in the current algorithm developed for the Precipitation Radar onboard the TRMM satellite. It will mention the importance of the drop size distribution information and the surface reference technique for attenuation correction. The lecture ends with an introduction of other current and future space missions that carry satellite-borne radars for precipitation and cloud observation. They include the Global Precipitation Measurement (GPM), CloudSat, EarthCARE, and ACE.

Lecture 9

Precipitation Retrieval by Microwave Radiometers

Kazumasa Aonashi

Meteorological Research Institute, Tsukuba, Japan

Heavy precipitation around meteorological disturbances often causes floods or other natural disasters. Hence, precipitation monitoring is very important task for disaster prevention agencies. Though, accurate precipitation observation data are sparse, especially over oceans.

As tools for global precipitation monitoring, satellite microwave radiometers have drawn attention recently. This is mainly because satellite microwave radiometer data give direct signals from hydrometers over wide ranges. This presentation describes the basic principles of the passive microwave precipitation retrieval, and the Global Satellite Mapping of Precipitation project (GSMaP) passive microwave precipitation retrieval algorithm using TRMM Microwave Imager (TMI) brightness temperatures (TBs). The GSMaP algorithm employs Polarization Corrected Temperature (PCT) at 37 and 85 GHz (PCT37, PCT85) over land and coast, TBs with vertical polarization at 10, 19, and 37 GHz (TB10v, TB19V, and TB37v) in addition to PCT37 and PCT85 over ocean.

In order to validate our algorithm, we compared its retrievals from TMI with the Precipitation Radar (PR) precipitation rates for some Baiu cases and global precipitation distribution in 1998. The results show:

- 1) The over-land and over-coast retrievals agreed better with PR than the retrievals only using PCT85, while the correlation degraded for precipitation heavier than 10 mm hr^{-1} . The over-land and over-coast retrievals underestimated PR precipitation rates for precipitation heavier than 10 mm hr^{-1} . These errors were caused by the problems in the forward calculation of scattering signals at the high frequencies. In order to alleviate this, we need to improve the precipitation-related variable models and RTM program for frozen precipitation.
- 2) The over-ocean retrievals agreed well with PR, in spite of slight overestimation of precipitation weaker than 10 mm hr^{-1} . This can be due to the neglect of the slant-path effect.
- 3) Our algorithm overlooked some weak precipitation areas over sub-tropical oceans. This arose from the forward calculation of emission signals. In order to improve the over-ocean precipitation detection method, we need to give more realistic humidity and CLWC for shallow precipitation regions.

This presentation also reports our current work on the assimilation of satellite microwave TBs into a cloud-resolving model.

Lecture 10

Global Satellite Mapping of Precipitation (GSMaP)

Tomoo Ushio

Department of information and communication engineering, Osaka University

This lecture overviews the Global Satellite Mapping of Precipitation (GSMaP) project with a particular emphasis on a system which has been recently developed and implemented that integrates passive microwave radiometer data with infrared radiometer data. In order to have high temporal (1 hour) and spatial (0.1 degree) resolution global precipitation estimates, the product (GSMaP_MVK) is produced based on a Kalman filter model that refines the precipitation rate propagated based on the atmospheric moving vector derived from two successive IR images. The method was introduced, evaluated and compared with other high-resolution precipitation products and the ground-based data collected by the Automated Meteorological Data Acquisition System (AMeDAS) near Japan. It was clearly shown that the approach described in this lecture performed better than without the Kalman filter, and the time series of the hourly global precipitation pattern demonstrated the potential capabilities for weather monitoring and typhoon tracking. The GSMaP_MVK product achieved a score comparable to the CMORPH and the 3B42RT products.

The 18th IHP Training Course

“Satellite Remote Sensing of Atmospheric Constituents”

Hirohiko Masunaga

Hydrospheric Atmospheric Research Center, Nagoya University

Program Aims

- ▶ IHP Nagoya Training Course
 - ▶ A part of the Japanese contribution to the UNESCO International Hydrological Program (IHP)
 - ▶ Held every year at the Hydrospheric Atmospheric Research Center (HyARC), Nagoya University.
 - ▶ The 2008 (18th) training course “**Satellite Remote Sensing of Atmospheric Constituents**” is aimed to offer an opportunity for participants to:
 - ▶ Learn the fundamentals of satellite remote sensing.
 - ▶ Earn the basic skill to analyze satellite data.
 - ▶ Lecturers, invited from across Japan, are all leading researchers in the relevant fields.



Logistics -1

▶ Overall schedule

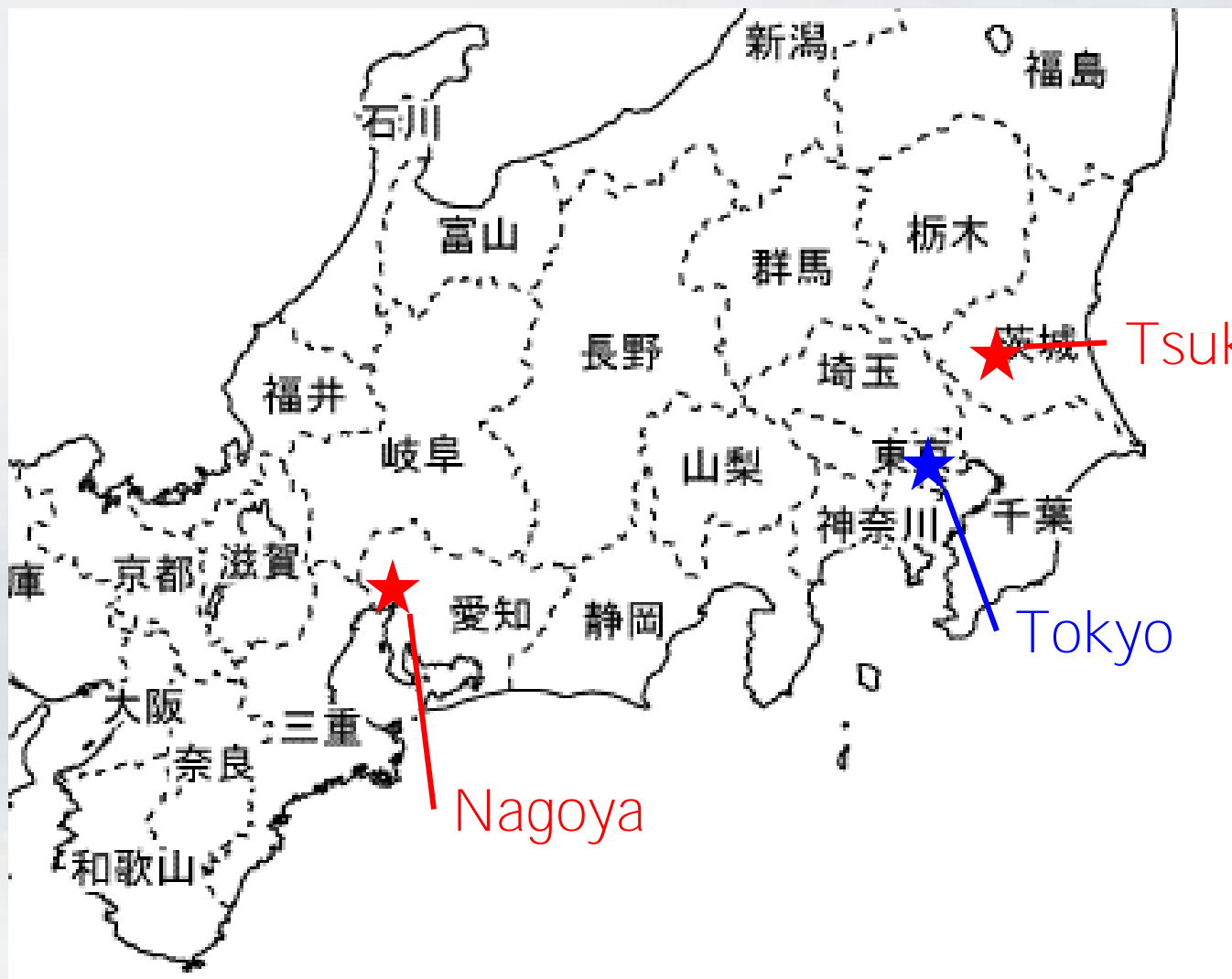
- ▶ Nov 3 (Mon): Arrival in Japan
- ▶ Nov 4 (Tue) – 6 (Thu): Lectures #1-6
- ▶ Nov 7 (Fri): Practice #1
- ▶ Nov 8 (Sat): (All day break)
- ▶ Nov 9 (Sun) – 10(Mon): Technical tour to Tsukuba
- ▶ Nov 11 (Tue) – 12 (Wed): Lectures #7-10
- ▶ Nov 13 (Thu): Practice #2
- ▶ Nov 14 (Fri): Lecture #11 and closing ceremony
- ▶ Nov 15 (Sat): Departure from Japan
- ▶ Each class is 2-hour long: morning class is 10:00-12:00 and afternoon class is 14:00-16:00.

Logistics -2

- ▶ Venue
 - ▶ All lectures are given at HyARC lecture room (301).
 - ▶ All practices are held at Information Technology Center (ITC).



- ▶ The trainees will make a two-day visit to the Japan Aerospace Exploration Agency (JAXA) in Tsukuba.



Logistics -3

- ▶ To be announced.



Overview of Meteorological Satellites in Orbit

HIROHIKO MASUNAGA

Hydropheric Atmospheric Research Center, Nagoya University



Atmospheric Constituents

▶ Gases

- ▶ Water vapor: a key of global water cycle
- ▶ Greenhouse gases (CO₂ etc.)



▶ Cloud

- ▶ **Cools the Earth's surface by reflecting solar radiation.**
- ▶ **Warms the Earth's surface by trapping** longwave radiation.

▶ Precipitation

- ▶ Provides water resource to all of us living on the Earth.
- ▶ Could causes devastating disaster.

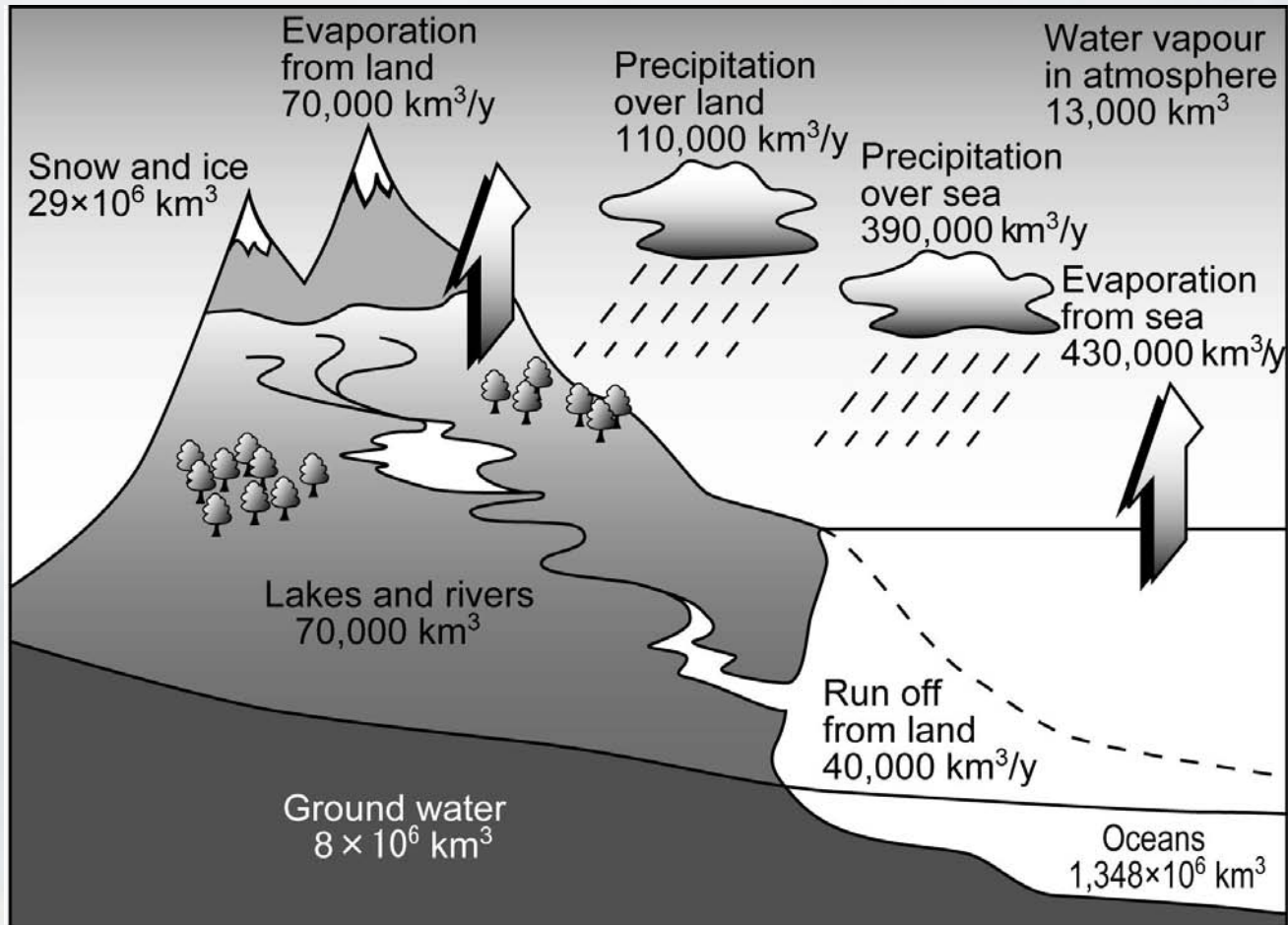


▶ Aerosol

- ▶ Soil dust, biomass carbon, anthropogenic pollutant, etc.
- ▶ A source of air pollution
- ▶ Could modify surface radiation flux in various ways.



Global water cycle



The amount of water

(Reference : ENCYCLOPEDIA of HYDROLOGY AND WATER RESOURCES, 1998)

Why do we need satellites? -1

- ▶ Think globally, act globally!
 - ▶ Satellites observe the Earth thoroughly and homogeneously.
 - ▶ The only tool to look into the vast majority of our planet that is beyond the reach of ground-based observations.



- ▶ Disaster prevention
 - ▶ Watching for severe storms potentially causing flash flood.
 - ▶ Tropical cyclone tracking.

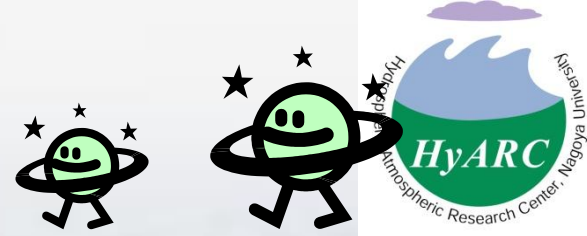


Why do we need satellites? -2

- ▶ Weather forecast
 - ▶ Data assimilation: satellite data help numerical models with better weather prediction.
- ▶ Climate monitoring
 - ▶ Impacts of cloud and aerosols on **the Earth's radiation budget**
 - ▶ Long-term change to global water cycle

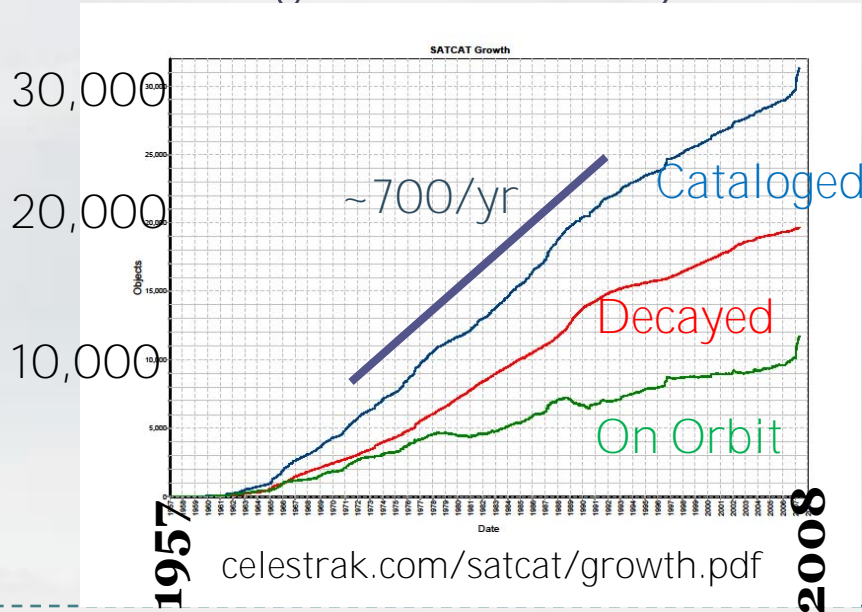


Satellites at dawn



▶ Our planet is now surrounded by...

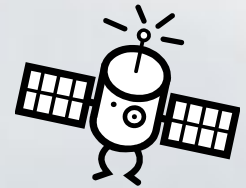
- ▶ 5,924 satellites (including those decayed) in orbit, as of May 14, 2007.
- ▶ 25,468 debris (source: celestrak.com/satcat/boxscore.asp)
- ▶ Growing in number by ~700/year



© Harald Edens
www.weather-photography.com

Meteorological satellites -Introduction

- ▶ Satellite categories – separated by orbital altitude
 - ▶ Geostationary satellites
 - ▶ Orbiting at ~36,000 km in altitude above the equator.
 - ▶ Constantly observe an area on the Earth facing the satellite.
 - ▶ Low-Earth orbiting (LEO) satellites
 - ▶ Altitude ranges from a few hundred to a thousand km.
 - ▶ Mostly sun-synchronous satellites (polar orbiting)
 - Observe a given area on the same local time almost every day.
 - ▶ Some are sun-asynchronous.
 - TRMM etc.



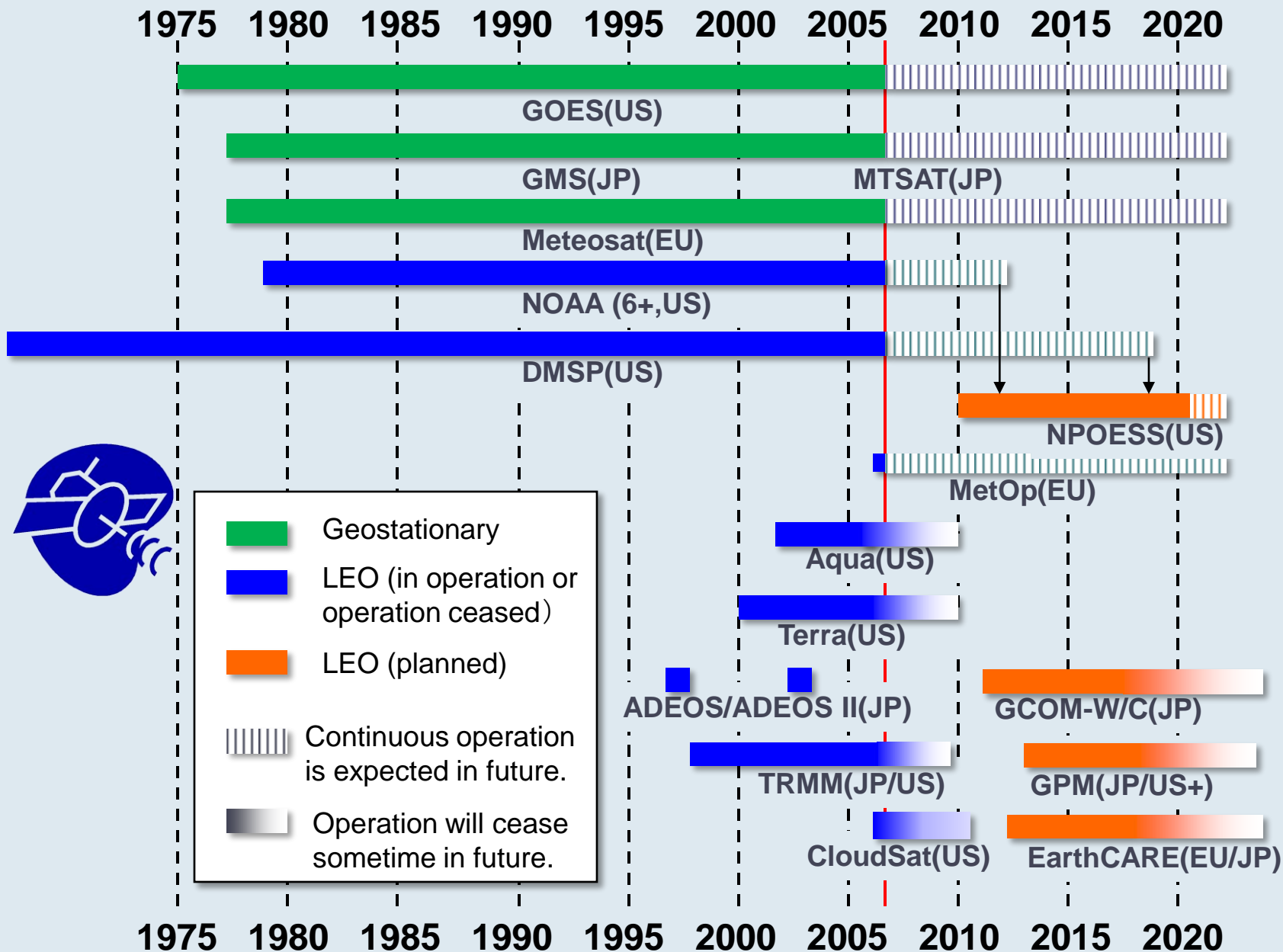
Satellite programs -1



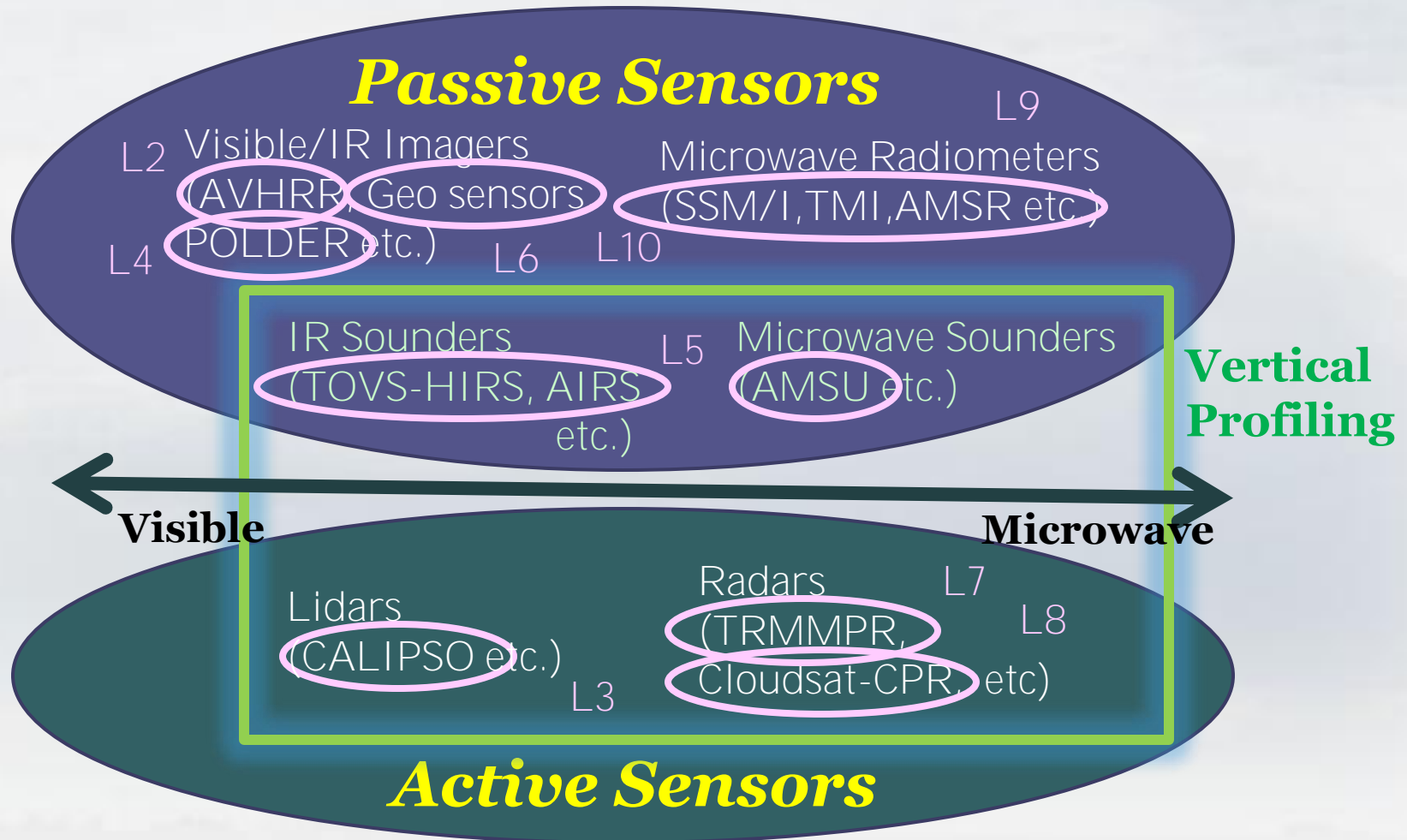
- ▶ Satellites maintained by operational agencies
 - ▶ Expected to provide continuous, stable services.
 - ▶ Geostationary satellites
 - ▶ **GMS** (Geostationary Meteorological Satellite) or currently **MTSAT** (Multi-functional Transport Satellite)
 - Japan Meteorological Agency (JMA)
 - ▶ **GOES** (Geostationary Operational Environmental Satellite)
 - US National Oceanic and Atmospheric Administration (NOAA)
 - ▶ **Meteosat**
 - European Organisation for the Exploitation of Meteorological Satellites (EUMETSAT)
 - ▶ **Fengyun**
 - China
 - ▶ Low-Earth Orbiting (LEO) satellites
 - ▶ **NPOESS** (Natl Polar-orbiting Operational Environmental Satellite System)
 - The U.S. tri-agency program to integrate existing independent programs.
 - ▶ **MetOp**
 - EUMETSAT

Satellite programs -2

- ▶ Satellites developed and operated by space agencies
 - ▶ Allowed to carry technologically advanced sensors.
 - ▶ Currently in orbit
 - ▶ **TRMM** (Tropical Rainfall Measuring Mission)
 - National Aeronautics and Space Administration (NASA)/Japan Aerospace Exploration Agency (JAXA)
 - ▶ **Terra, Aqua, and CloudSat**
 - NASA
 - ▶ Being planned
 - ▶ **GCOM** (Global Climate Observing Mission)
 - JAXA
 - ▶ **EarthCARE** (Earth Cloud, Aerosol, and Radiation Explorer)
 - JAXA/European Space Agency (ESA)
 - ▶ **GPM**
 - **NASA/JAXA/...**

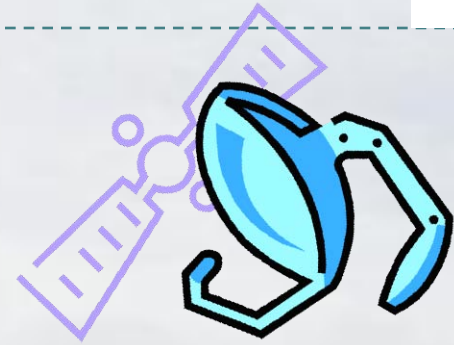


Satellite Remote Sensors



Passive versus Active sensors

- ▶ Passive remote sensors
 - ▶ Measure natural-origin radiation
 - ▶ Imager, radiometers, and sounders
 - ▶ Observe two-dimensional plan view.
 - ▶ Except for sounders, which measure vertical profiles as well.
 - ▶ Relatively inexpensive
- ▶ Active remote sensors
 - ▶ Send electromagnetic pulses and detect the strength and temporal delay of back-scattered signal.
 - ▶ Radars and lidars
 - ▶ c.f., scatterometers
 - ▶ Observe three dimensional structure
 - ▶ Tend to be expensive

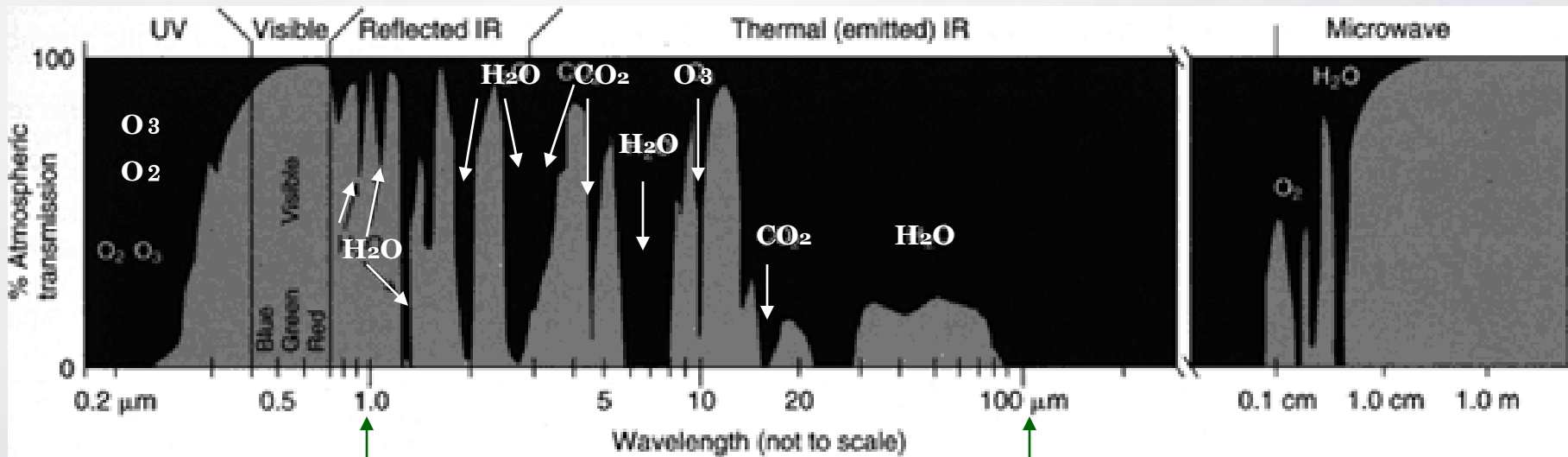


Different bands for different targets

- ▶ Visible light
 - ▶ Atmospheric particle scattering
 - ▶ Cloud and aerosol optical properties
- ▶ Infrared radiation
 - ▶ Cloud top temperature
 - ▶ Molecular absorption
 - ▶ Temperature and humidity sounding
 - ▶ Carbon dioxide retrieval (GOSAT)
- ▶ Microwave
 - ▶ Sensitive to liquid water when particles are large
 - ▶ Precipitation retrieval
 - ▶ Oxygen and water vapor absorption
 - ▶ Temperature and humidity sounding



Atmospheric Transmittance



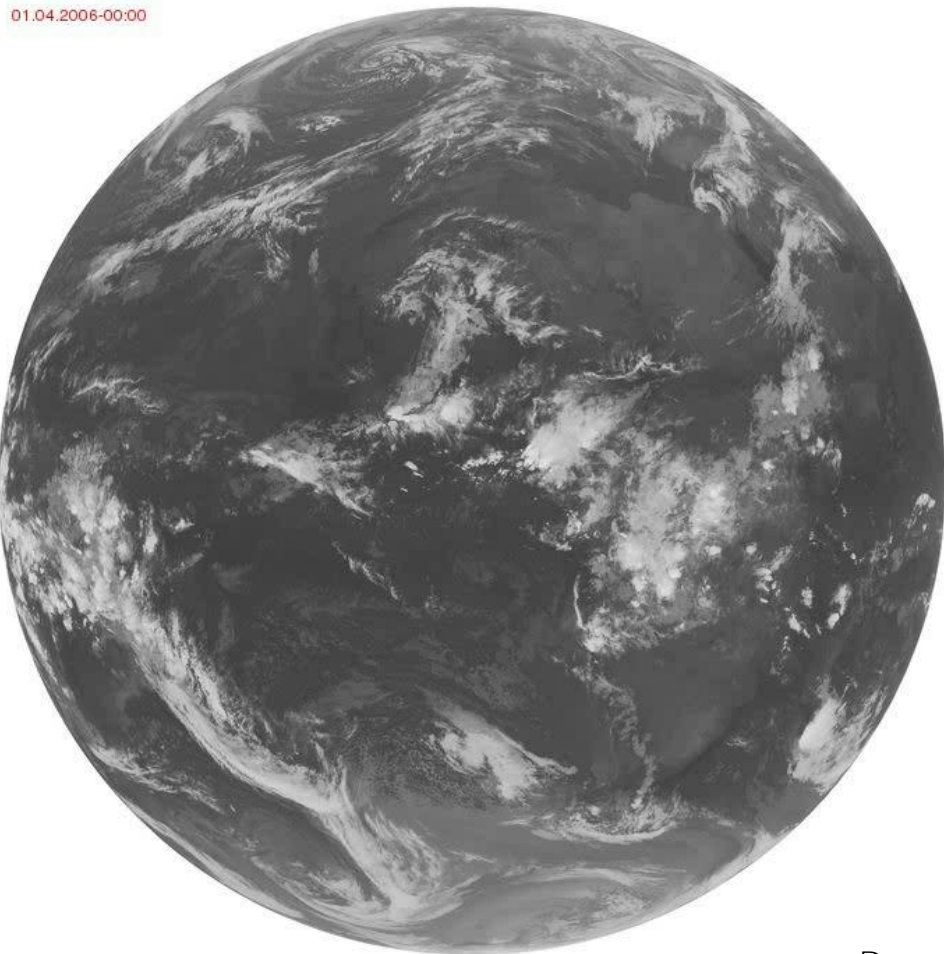
$1/1000\text{mm}$

Wavelength

$1/10\text{mm}$

<http://earthobservatory.nasa.gov>

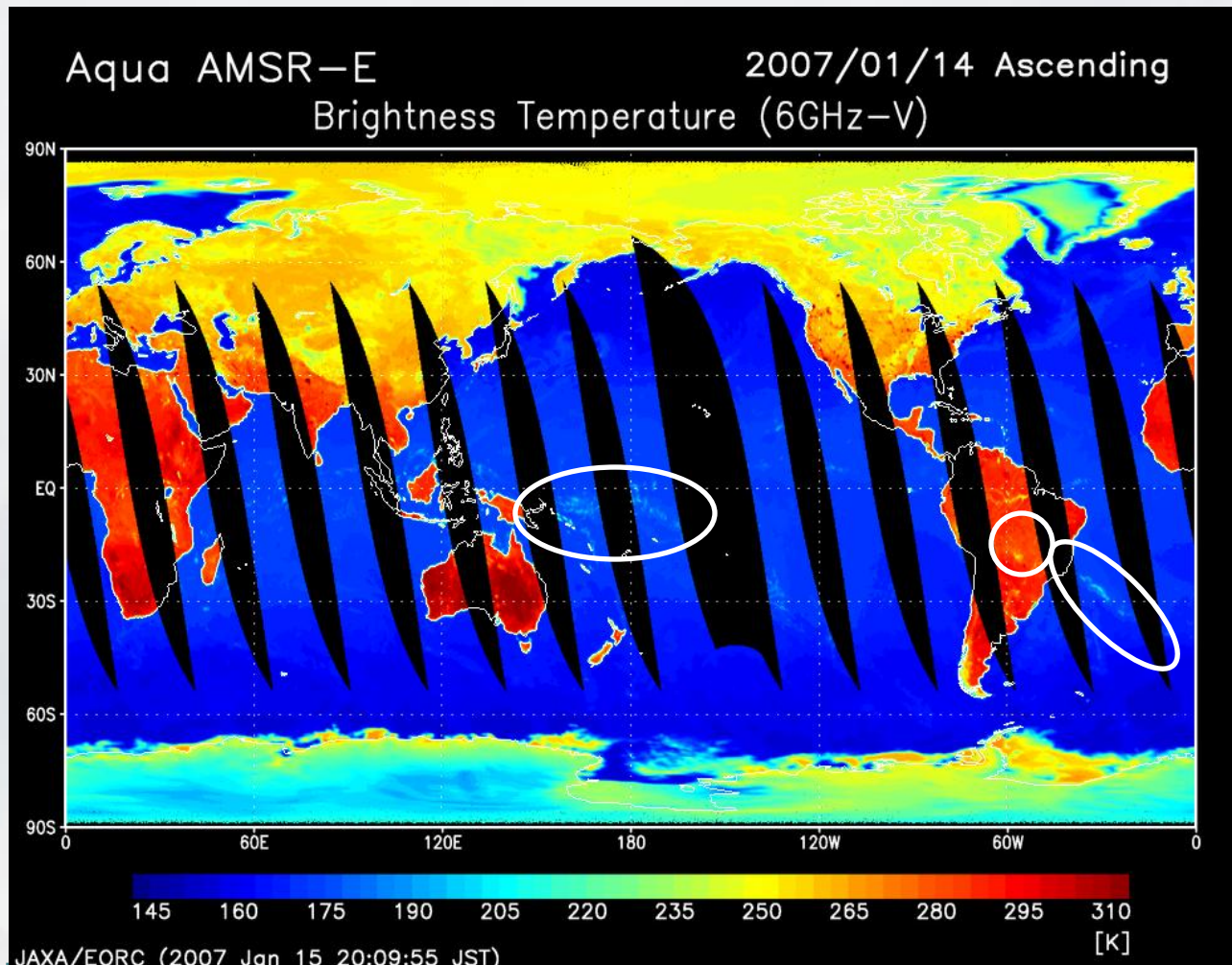
Meteosat infrared imagery



By courtesy of Prof. Raschke

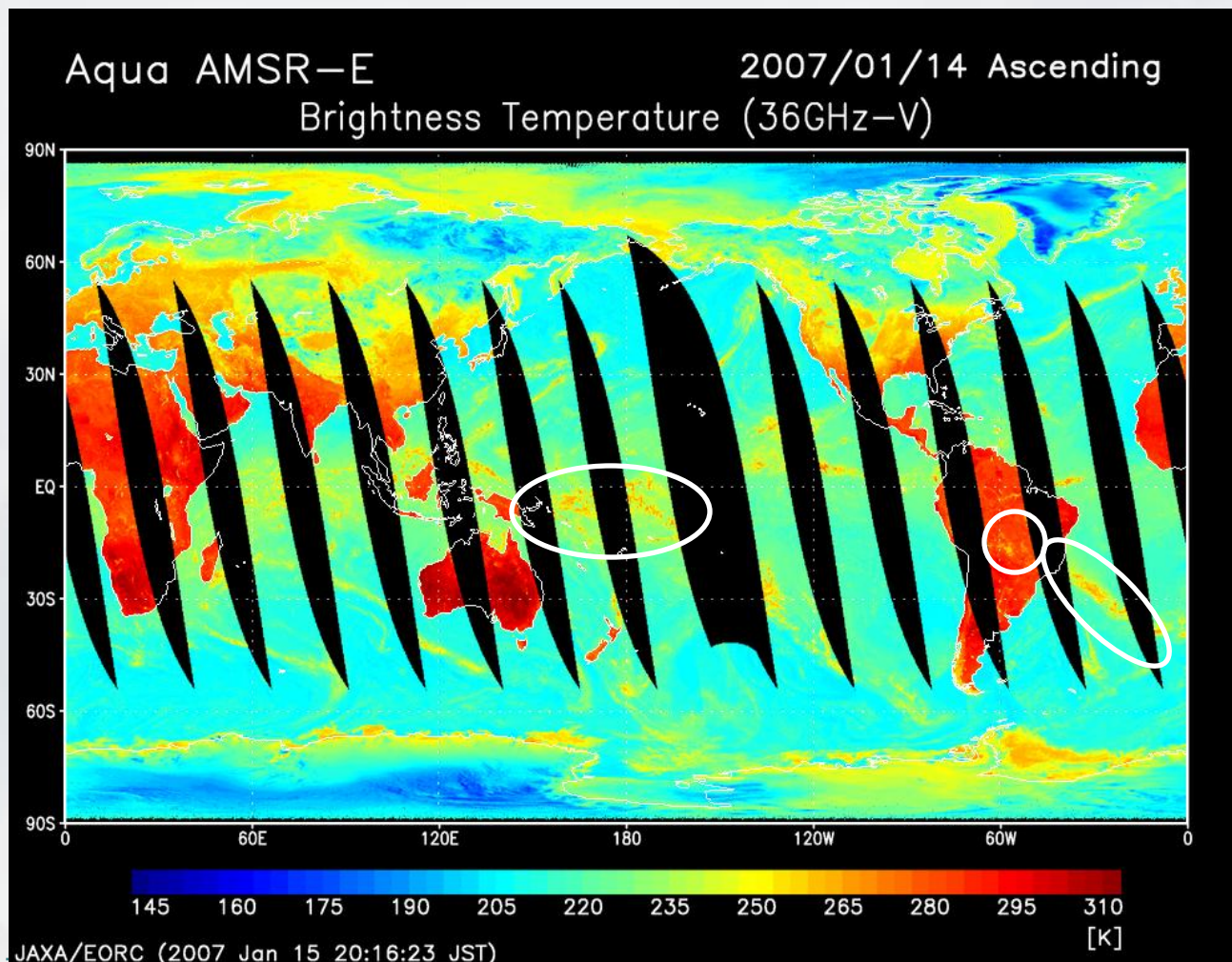
Microwave imagery: 6GHz

http://sharaku.eorc.jaxa.jp/AMSR/index_j.htm



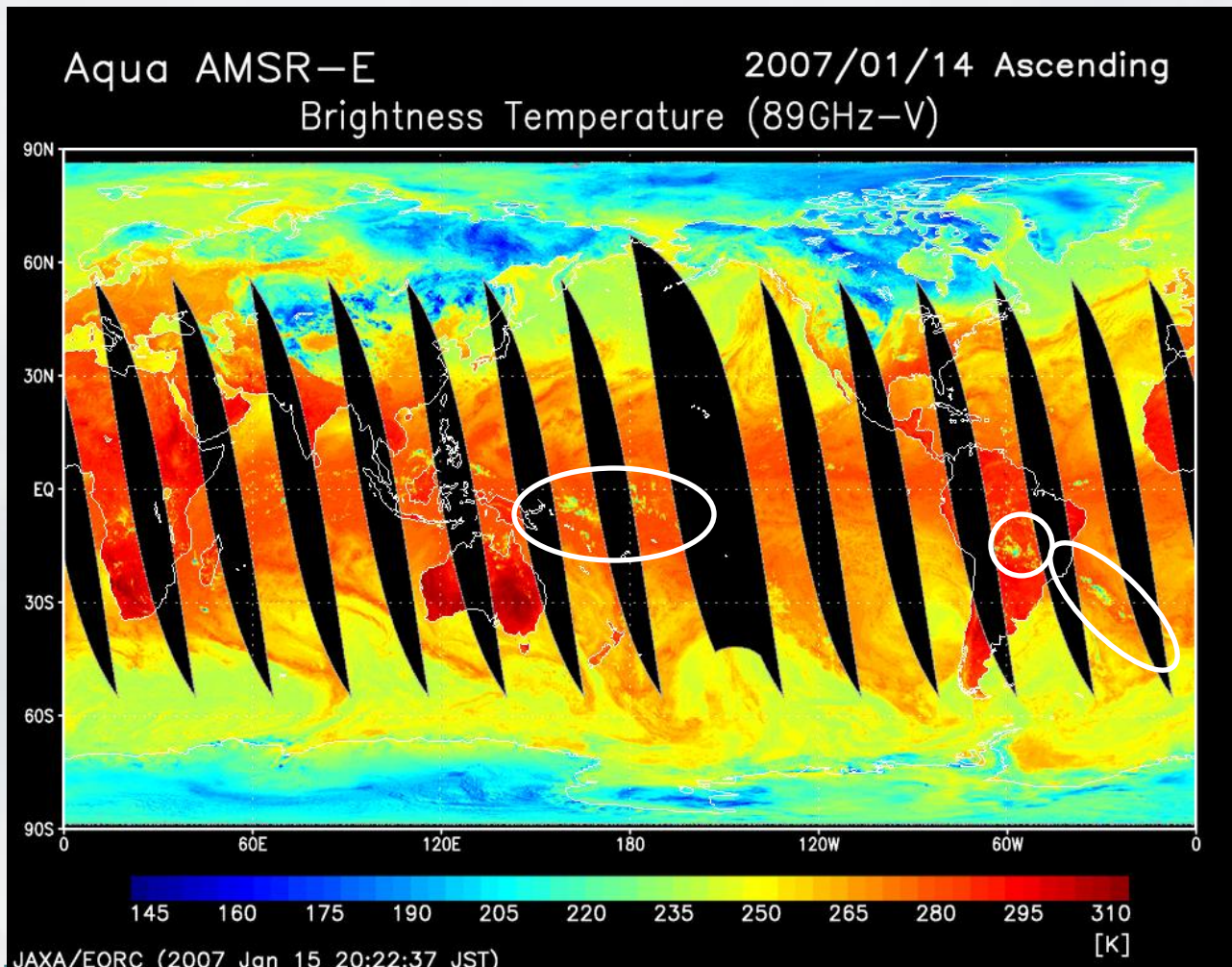
Microwave imagery: 36GHz

http://sharaku.eorc.jaxa.jp/AMSR/index_j.htm



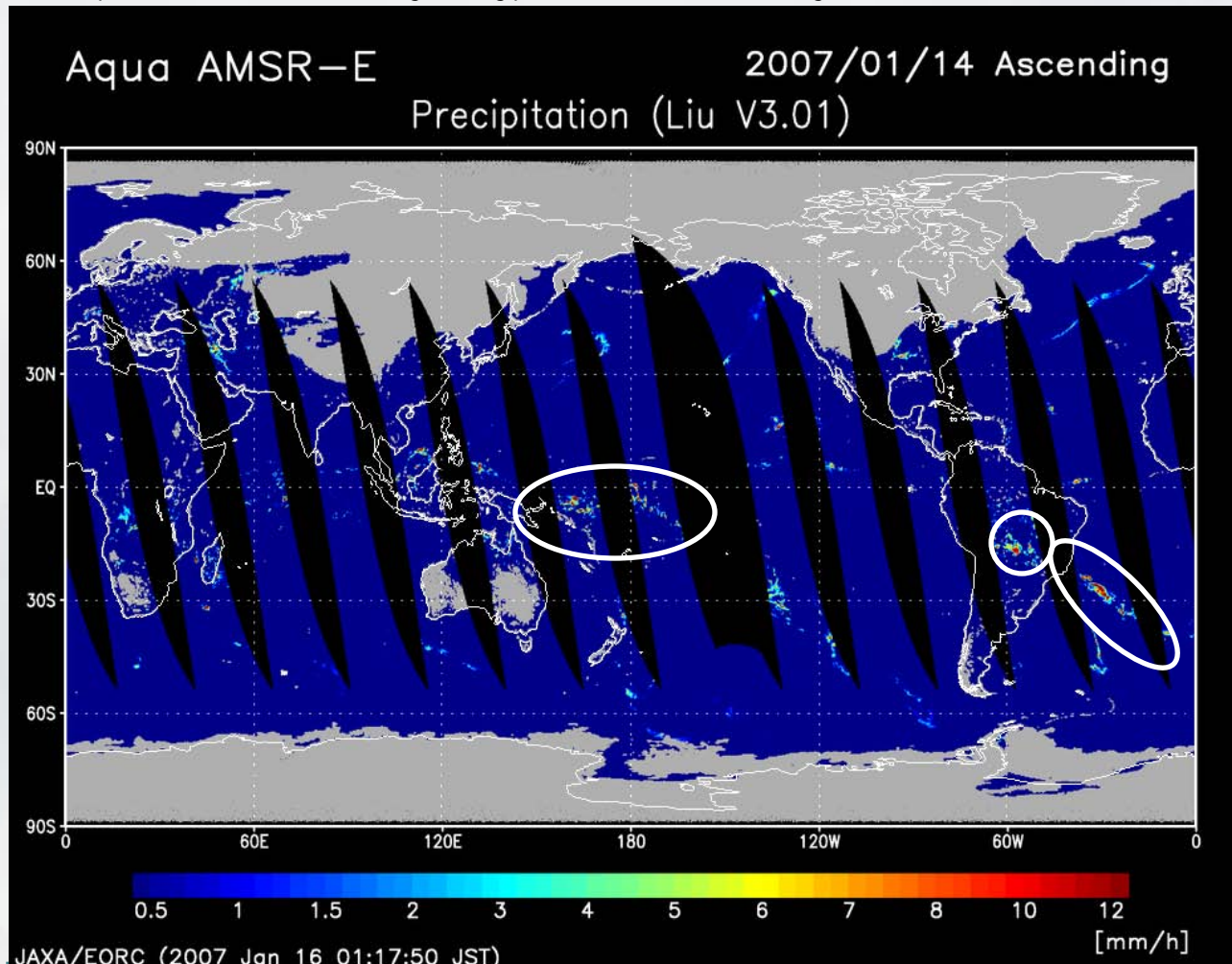
Microwave imagery: 89GHz

http://sharaku.eorc.jaxa.jp/AMSR/index_j.htm



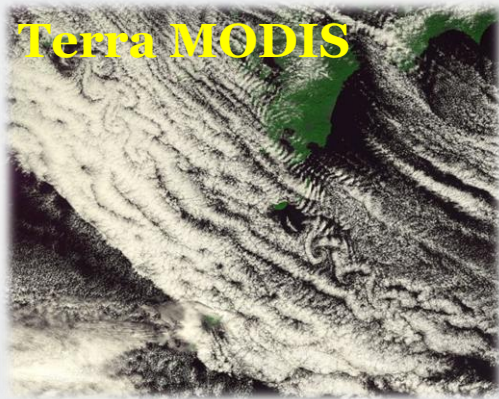
Microwave imagery: Retrieved rainfall

http://sharaku.eorc.jaxa.jp/AMSR/index_j.htm



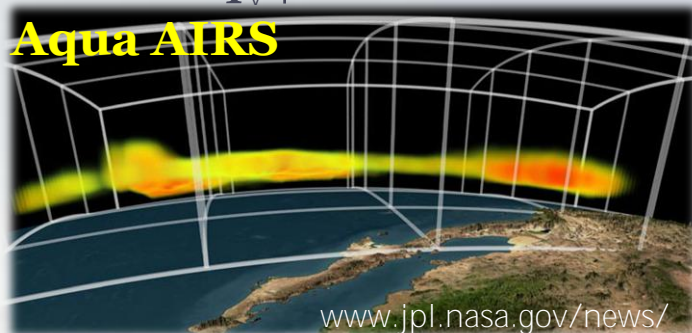
A variety of satellite sensors

- ▶ Visible/IR imager
 - ▶ Cloud and aerosol properties



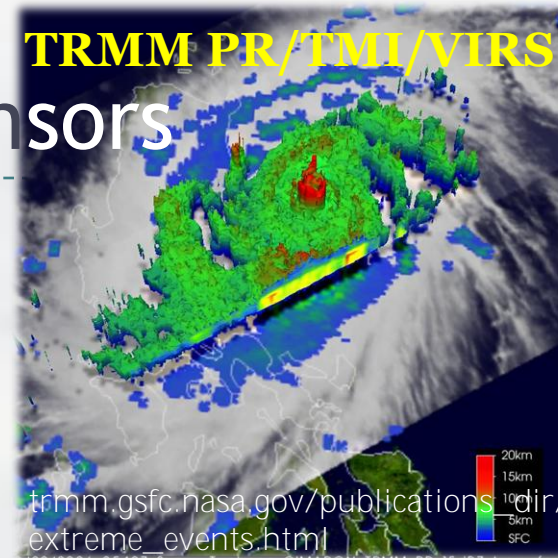
www.eorc.jaxa.jp/imgdata/topics/divide/atmosphere.html

- ▶ IR & microwave sounders
 - ▶ T and q_v profiles



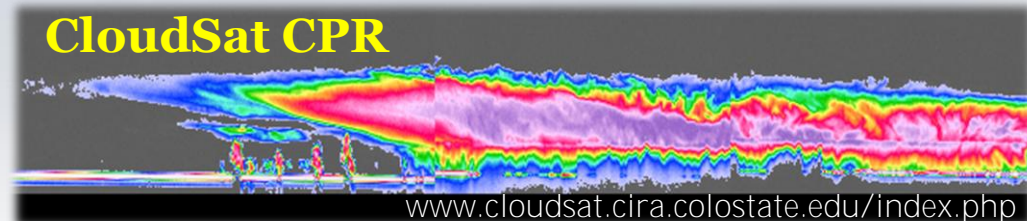
www.jpl.nasa.gov/news/

TRMM PR/TMI/VIRS

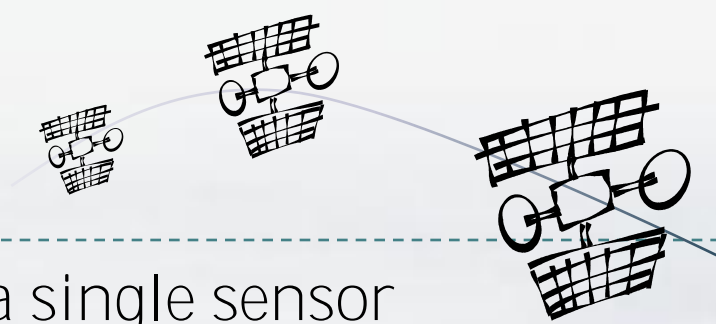


- ▶ Microwave radiometer
 - ▶ Cloud water & rain rate
 - ▶ SST and near-surface wind
 - ▶ Precipitable water
- ▶ Radar
 - ▶ Precipitation & cloud profiles

CloudSat CPR



Expand more!



- ▶ More channels on a single sensor
 - ▶ MODIS (Terra & Aqua): visible/IR imager with 36 channels
 - ▶ AIRS (Aqua): IR sounder with 2,378 (!) channels
- ▶ More sensors on a single satellite
 - ▶ 5 sensors on TRMM, 5 on Terra, 6 on Aqua, and 12 on MetOp.
 - ▶ NPOESS will have 4-9 sensors per satellite.
- ▶ More satellites collaborating together
 - ▶ A-Train: 6 satellites incl. CloudSat and Aqua fly in formation.
 - ▶ GPM: consists of a core satellite and ~8 constellation satellites.
- ▶ More “active”
 - ▶ Radars onboard: TRMM, CloudSat, EarthCARE, and GPM.
 - ▶ Lidars onboard: CALIPSO and EarthCARE
- ▶ More international
 - ▶ TRMM (US/JP), EarthCARE (JP/EU), and GPM (US/JP+)

Lecture plan summary -1

- ▶ L0: Introduction
 - ▶ Lecturer: Hirohiko Masunaga (Nagoya University)
 - ▶ Guidance and outline of the IHP training course
- ▶ L1: Overview of Meteorological Satellites in Orbit
 - ▶ Lecturer: Hirohiko Masunaga (Nagoya University)
 - ▶ A brief summary of satellites and sensors being used for meteorological research and weather forecasting.
- ▶ L2: Satellite Remote Sensing of Clouds by Passive Sensors
 - ▶ Lecturer: Kazuaki Kawamoto (Nagasaki University)
 - ▶ Methodologies to retrieve cloud physical properties from space
 - ▶ Applications to climate studies
- ▶ L3: Satellite Remote Sensing of Clouds by Active Sensors
 - ▶ Lecturer: Hajime Okamoto (Tohoku University)
 - ▶ Cloud profiling by ground-based and spaceborne W-band radars
 - ▶ Current and future satellite missions carrying cloud profiling radars

Lecture plan summary -2

- ▶ **L4: Satellite Remote Sensing of Aerosols**
 - ▶ Lecturer: Itaru Sano (Kinki University)
 - ▶ Methodologies to retrieve aerosol optical properties from space
 - ▶ Applications to climate and environmental studies
- ▶ **L5: Satellite Remote Sensing by Temperature and Humidity Sounders**
 - ▶ Lecturer: Kozo Okamoto (Japan Meteorological Agency)
 - ▶ Methodologies of atmospheric sounding from space
 - ▶ Application to data assimilation
- ▶ **L6: Geostationary Meteorological Satellites**
 - ▶ Lecturer: Atsushi Higuchi (Chiba University)
 - ▶ Introduction to existing geostationary satellites for meteorological applications
 - ▶ Cloud monitoring by GMS/MTSAT : physical principles and applications
- ▶ **L7: Tropical Rainfall Measuring Mission (TRMM)**
 - ▶ Lecturer: Kenji Nakamura (Nagoya University)
 - ▶ Mission outline and precipitation data products available
 - ▶ Applications to climate studies and extreme weather monitoring

Lecture plan summary -3

- ▶ L8: Space borne Precipitation Radars
 - ▶ Lecturer: Toshio Iguchi (Natl Institute of Info and Comm Tech)
 - ▶ Rainfall profiling by space borne K-band radars
 - ▶ Current and future satellite missions carrying precipitation radars
- ▶ L9: Precipitation Retrieval by Microwave Radiometers
 - ▶ Lecturer: Kazumasa Aonashi (Meteorological Research Institute)
 - ▶ Methodologies to retrieve precipitation from space
 - ▶ Applications to data assimilation
- ▶ L10: Global Satellite Mapping of Precipitation (GSMaP)
 - ▶ Lecturer: Tmoo Ushio (Osaka University)
 - ▶ Introduction to the GSMaP project
 - ▶ Retrieval algorithms and data products
- ▶ L11: Greenhouse Gas Observing Satellite (GOSAT)
 - ▶ Lecturer: Gen Inoue (Research Institute for Humanity and Nature)
 - ▶ Introductions to the GOSAT project
 - ▶ Retrieval methodology and expected outcome.



Practice and tech tour summary

- ▶ P1: Geostationary Meteorological Satellite (GMS) Data Analysis
 - ▶ Lecturer: Munehisa K. Yamamoto (Chiba University)
 - ▶ On-site computer exercise to analyze GMS data
- ▶ P2: Real-time Global Precipitation Data Analysis
 - ▶ Lecturer: Takuji Kubota (JAXA)
 - ▶ On-site computer exercise to analyze TRMM and Global Satellite Mapping of Precipitation (GSMaP) data
- ▶ Technical Tour to the Japan Aerospace Exploration Agency (JAXA) in Tsukuba
 - ▶ Guided tour
 - ▶ Briefing for satellite data/images access through JAXA EORC WWW site lectured by Misako Kachi (JAXA)

L2. Satellite Remote Sensing of Clouds by Passive Sensors

- Methodologies to retrieve cloud physical properties from space
- Applications to climate studies

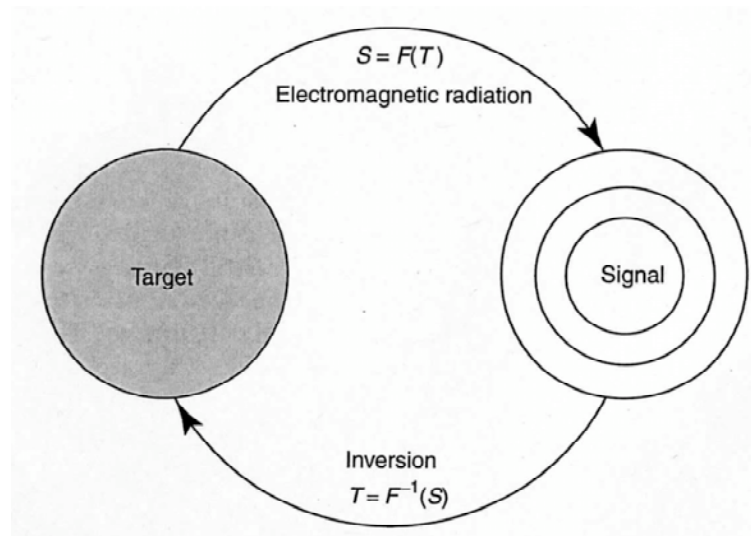
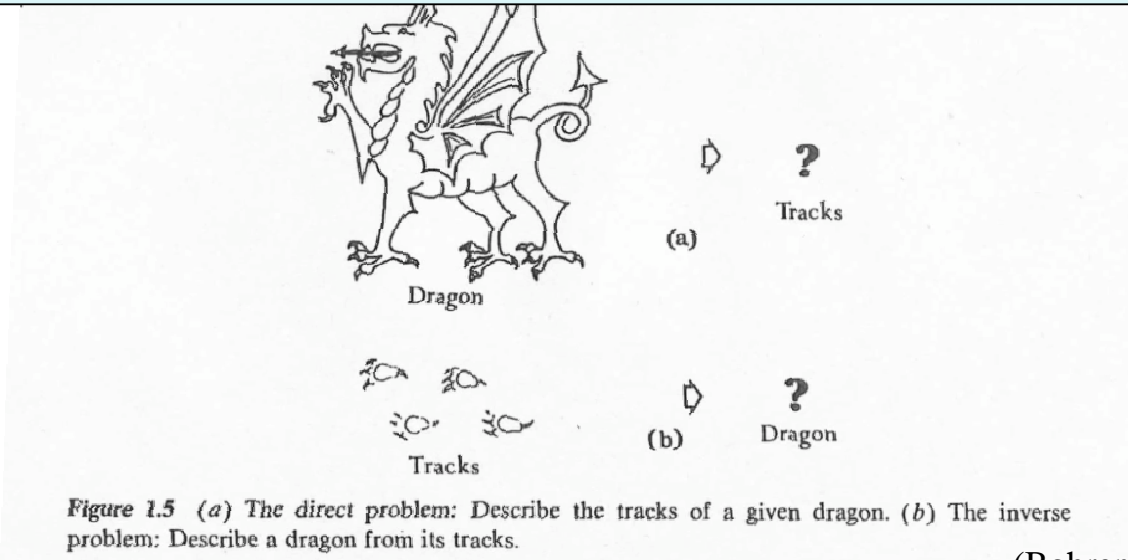
Kazuaki Kawamoto
Faculty of Environmental Studies
Nagasaki University

What is Remote Sensing?

To measure the characteristics (quality, quantity, etc.) of targets from remote place without touching

Electromagnetic wave is mostly used.

Inverse and forward problems ~Dragon and tracks~



(Liou 2002)

Importance of clouds in the climate system

Radiation budget
(reflection of solar radiation and
absorption/re-emission of earth's radiation)

Low clouds: cooling effect
High clouds: warming effect

Interactions with aerosols
Contribution to the water cycle through precipitation

Importance of cloud microphysics

Optical depth (τ_c) Effective Particle Radius (r_e)

- influence on cloud radiative properties (reflectivity, transmissivity and emissivity)
- development of clouds and precipitation
- interaction with aerosols (aerosol indirect effect)

Cf. Aerosol direct effect

=> scattering and absorption of solar radiation by aerosols

Cloud Physical Properties

Cloud amount (cloud fraction)

Cloud top height (cloud top pressure)

Cloud optical depth (thickness)

Cloud geometrical thickness

Cloud thermodynamic phase (water or ice)

liquid water content, ice water content

liquid water path, ice water path

Cloud droplet size (mode particle radius, effective particle radius)

Cloud reflectivity

Cloud transmissivity

Cloud emissivity

Basic principles to retrieve cloud properties

Passive method uses reflected solar radiation by clouds

Visible radiation(0.64micron) => little (negligible) water absorption
=> cloud optical depth

Near-Infrared (2.16 or 3.7 micron) => moderate water absorption
=> cloud effective particle

Infrared (11micron) => emission from the cloud top
=> cloud top temperature

Cloud Microphysics

cloud optical thickness

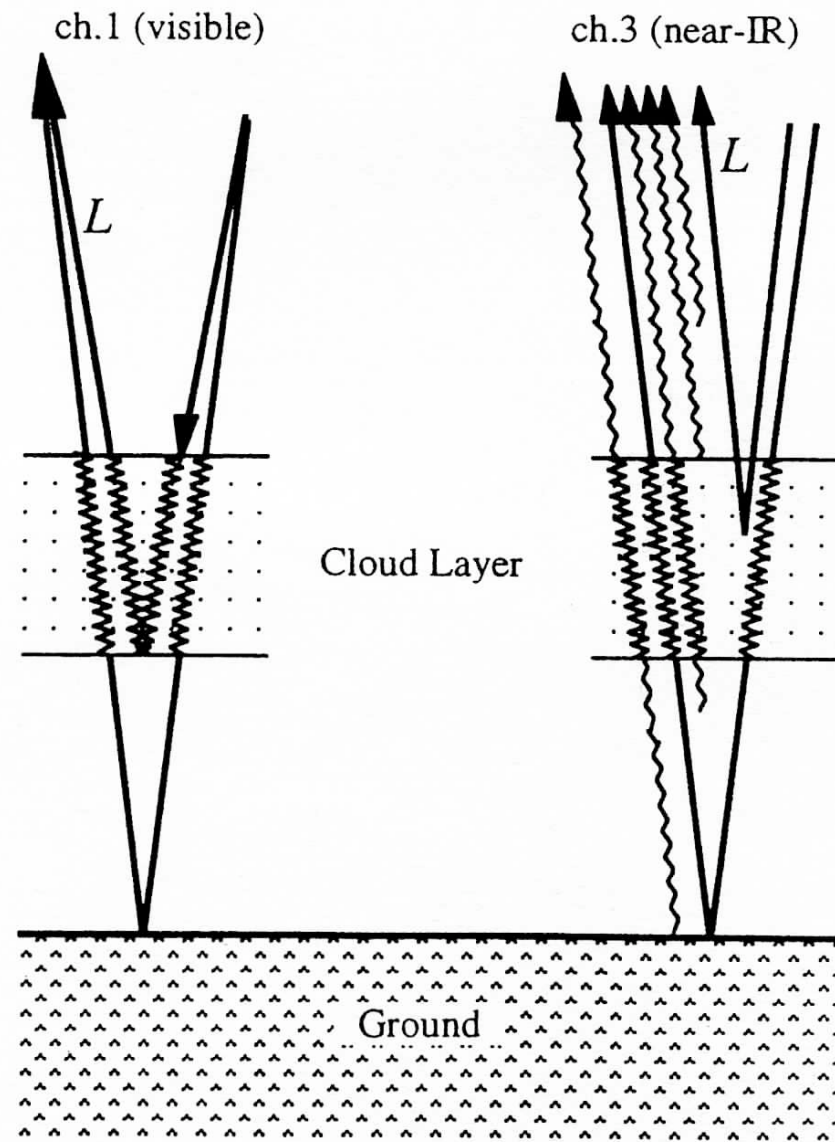
$$\tau_\lambda = \int_L \int_0^\infty \pi r^2 Q_{ext}(\lambda, r) n(r) dr dL$$

the effective radius of cloud droplets

$$r_e \equiv \frac{\int \pi r^3 n(r) dr}{\int \pi r^2 n(r) dr}$$

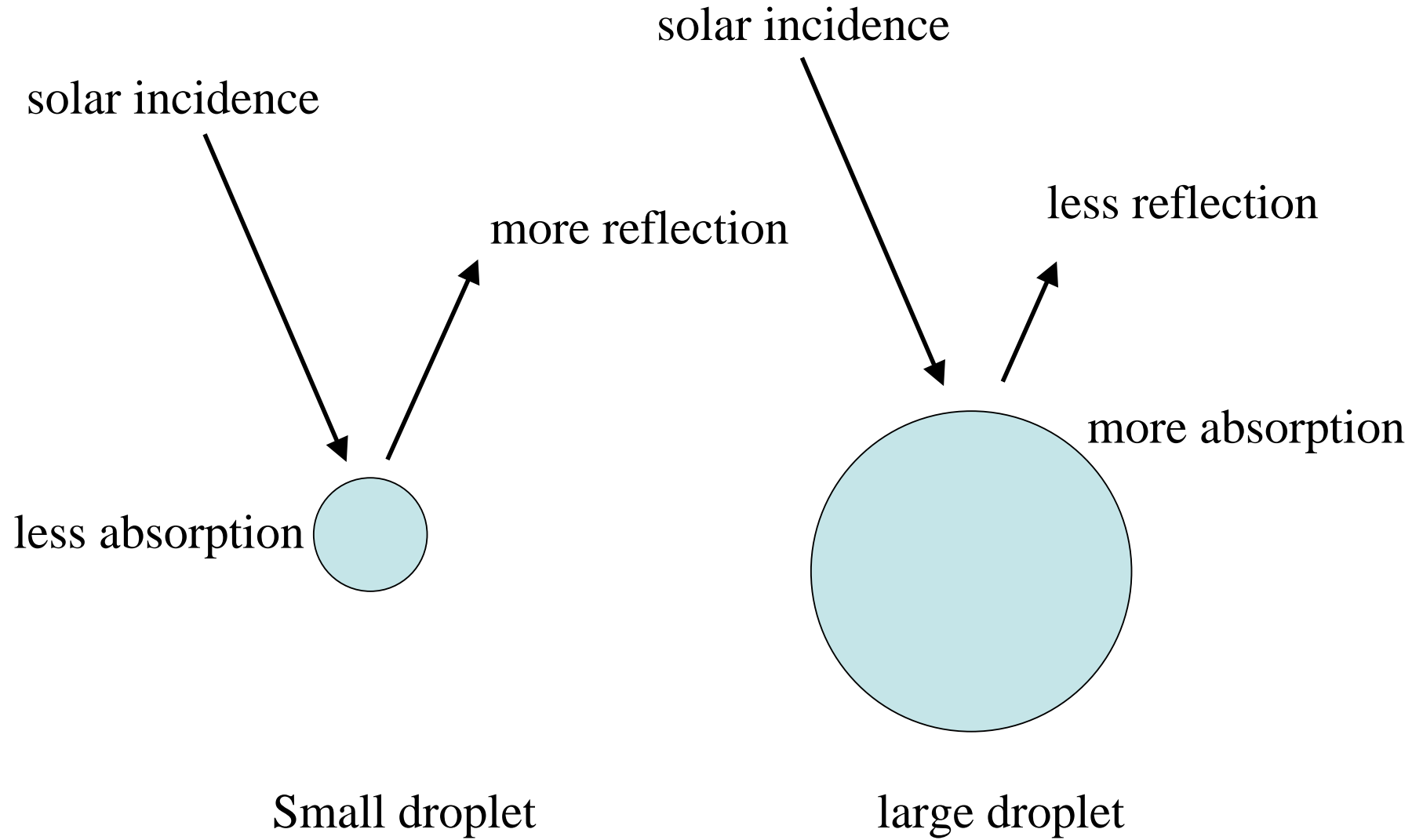
Cloud droplet size distribution : log-normal assumed

$$n(r) = \frac{N}{\sqrt{2\pi}\sigma} \exp\left[-\frac{(\ln r - \ln r_0)^2}{2\sigma^2}\right]$$



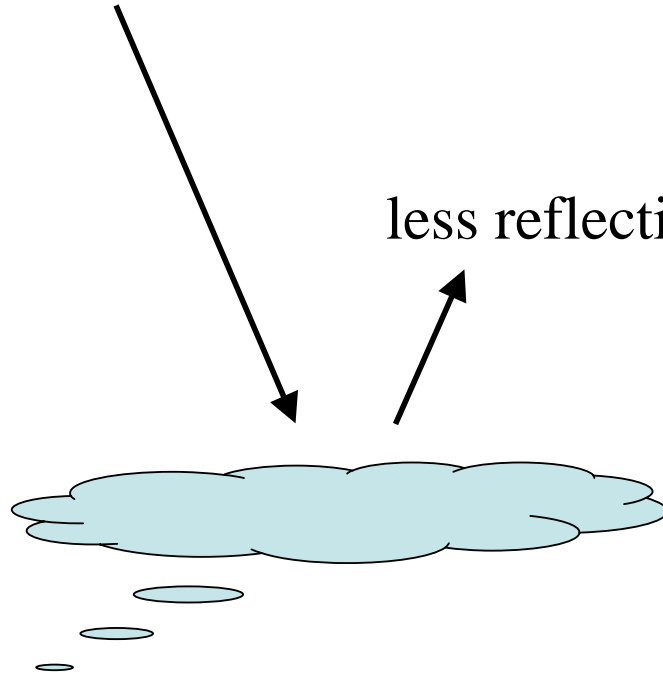
Schematic of passive remote sensing of clouds

For near-infrared radiation (particle size-sensitive)



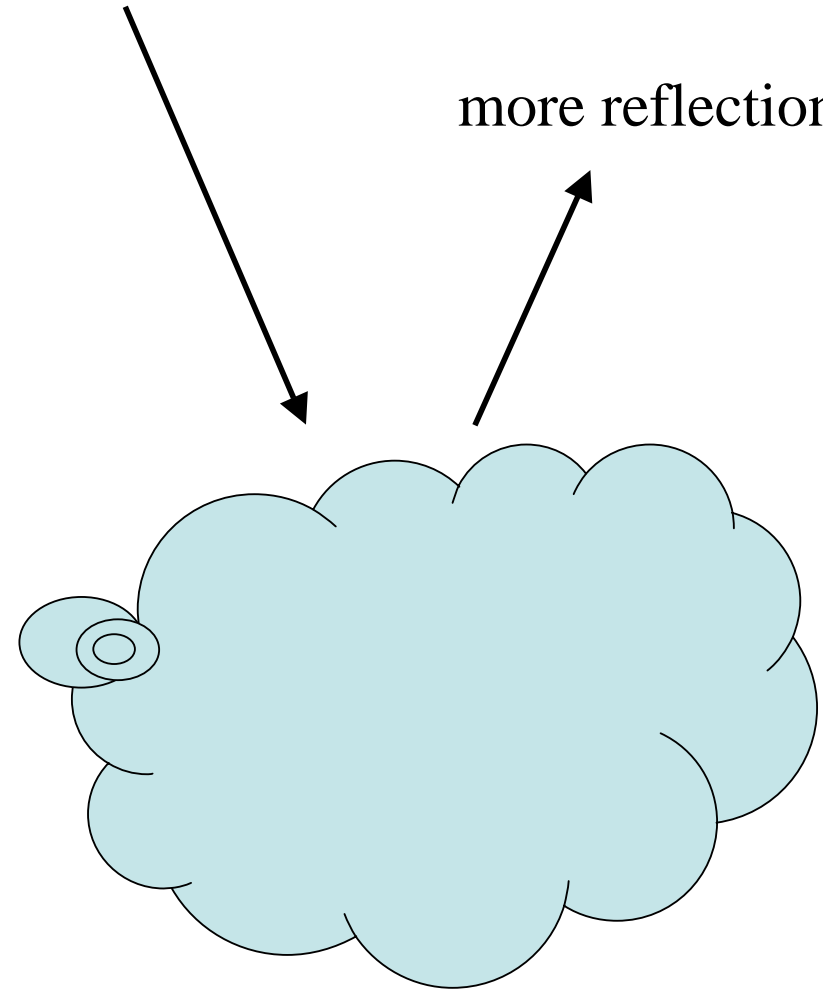
For visible radiation (optical depth-sensitive)

solar incidence



optically thin cloud

solar incidence

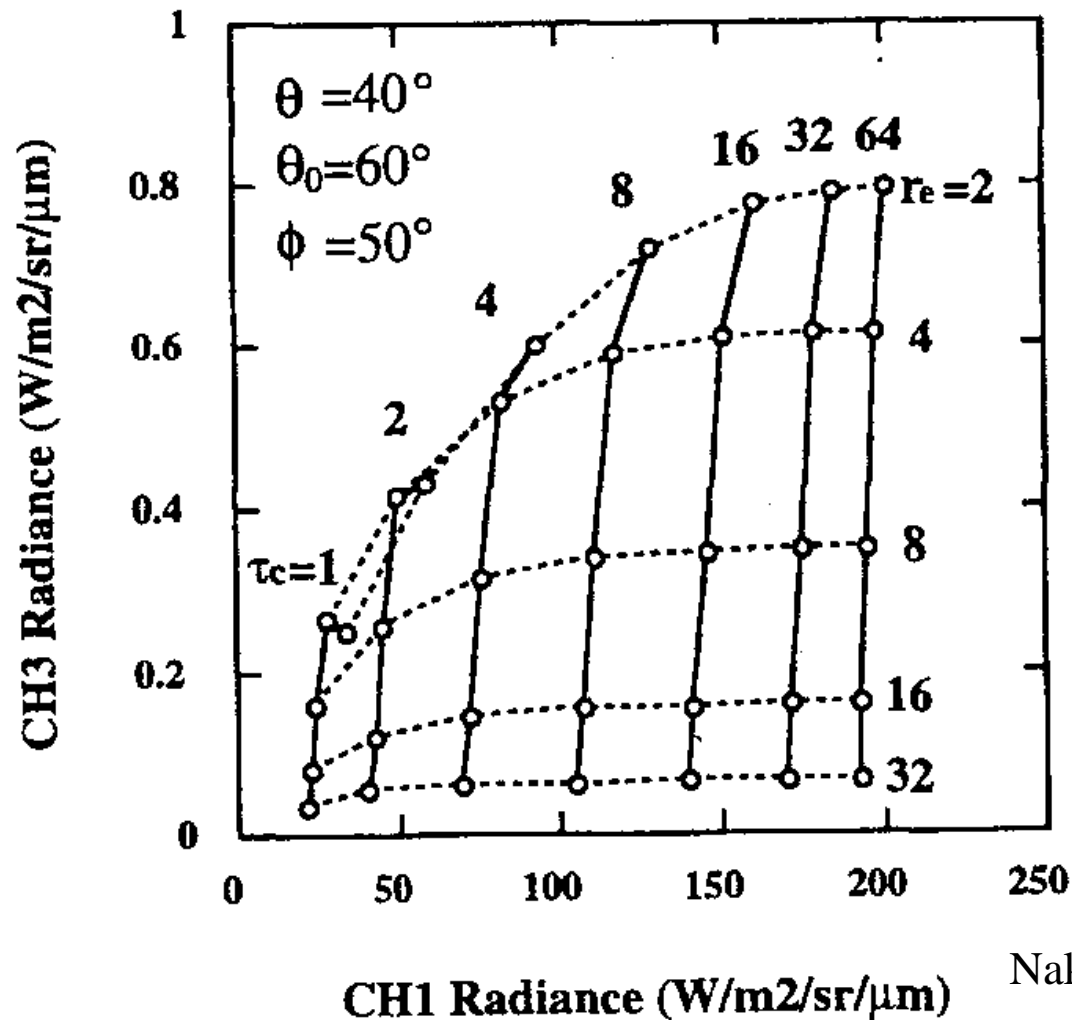


optically thick cloud

Simultaneous determination of τ_c and r_e

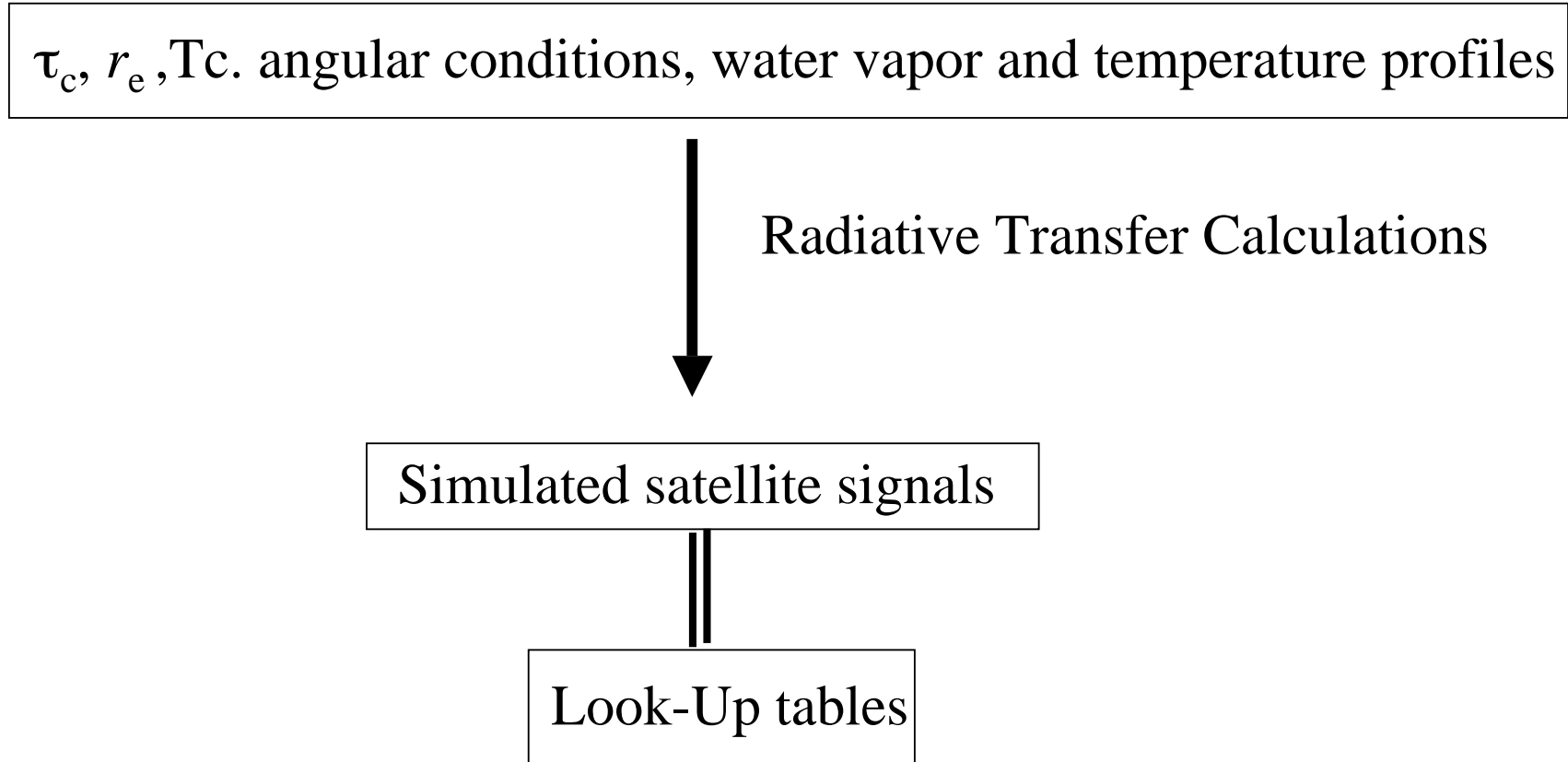
Reflected solar radiation by clouds

CH1. 0.64micron (no abs.), CH3. Near-Infra 3.73micron (moderate abs.)

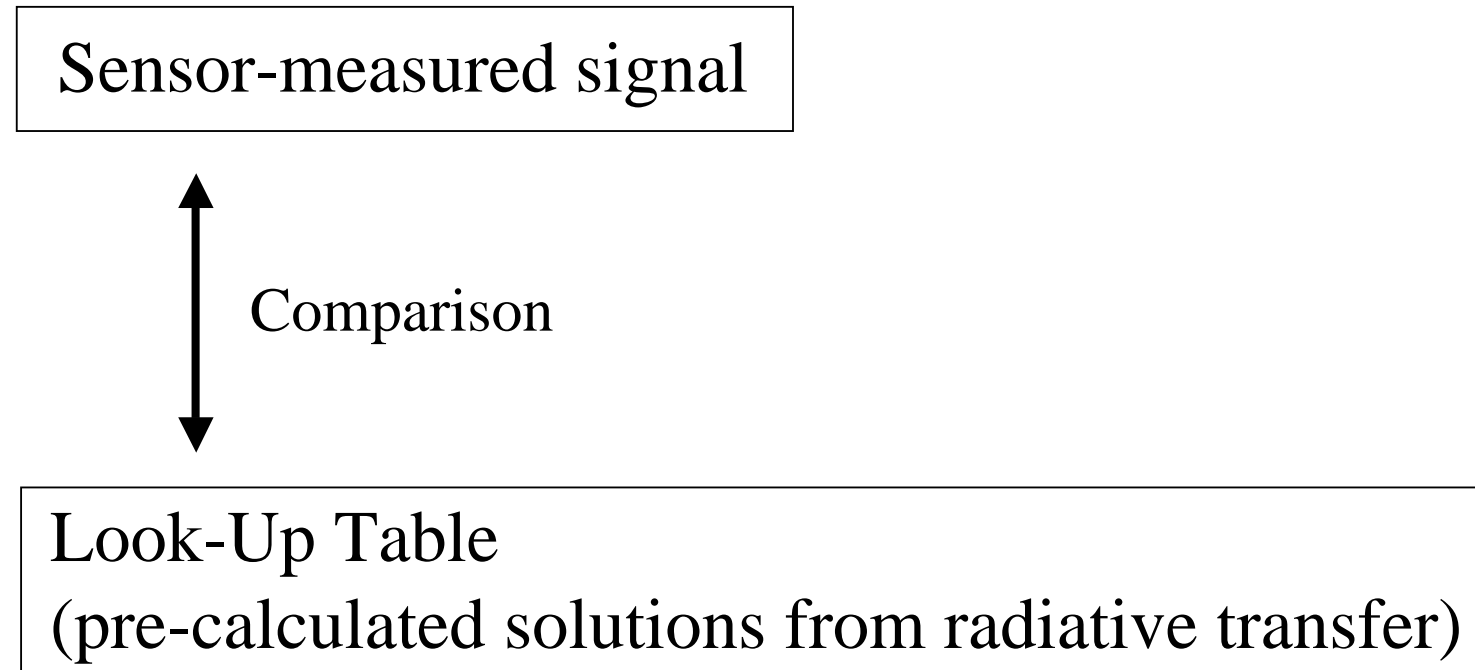


Nakajima and Nakajima 1995

Forward calculation



Then,



Iterations will be done until the best solution is determined.

History of remote sensing of cloud microphysics

Pioneering measurements at NIR (planetary sciences)

Blau et al. (1966)

Hovis and Tobin (1967)

Aircraft measurements (NIR: 1.6, 2.2 μ m)

Twomey and Cocks (1982)

Nakajima and King (1990)

Rawlins and Foot (1990)

Nakajima et al. (1991)

Satellite observations (NIR:3.7 μ m) on a regional scale

Platnick and Twomey (1994)

Nakajima and Nakajima (1995)

Platnick and Valero (1995)

Minnis et al. (1998)

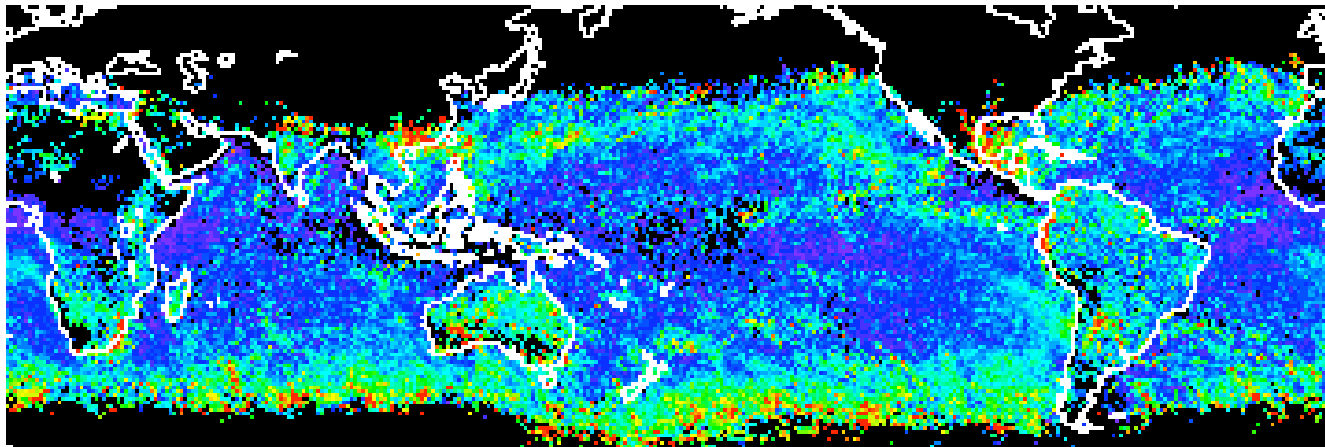
Satellite observations (NIR:3.7 μ m) on a global scale

Han et al. (1994) using ISCCP data

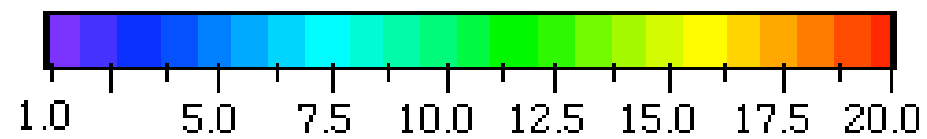
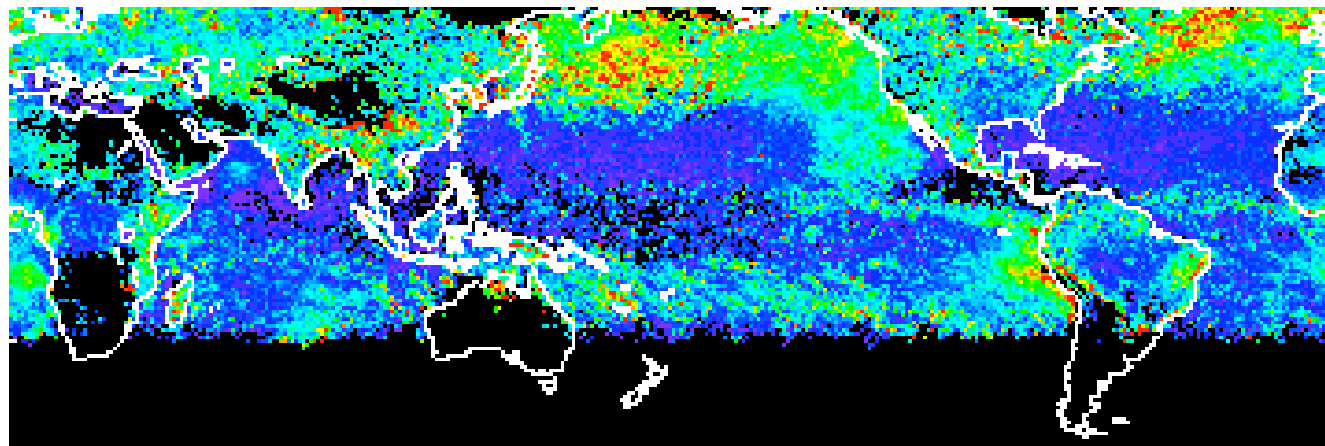
Kawamoto et al. (2001)

Cloud Optical Thickness

January

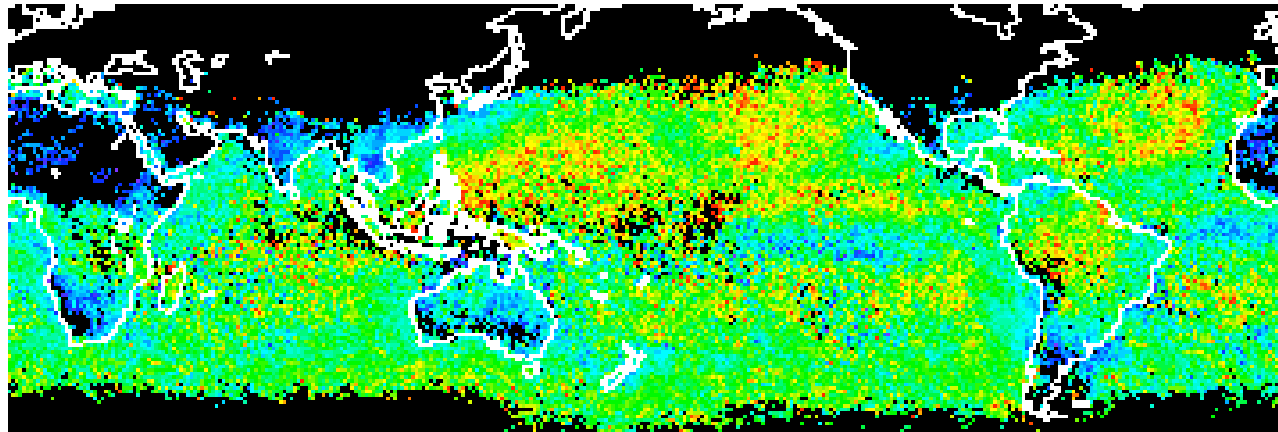


July

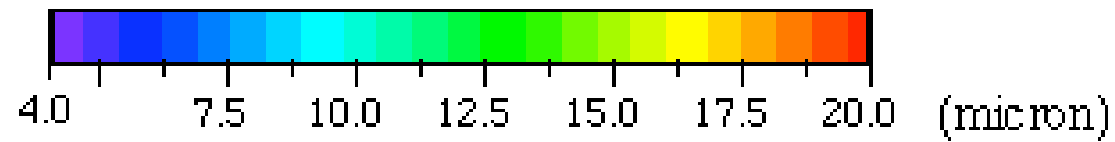
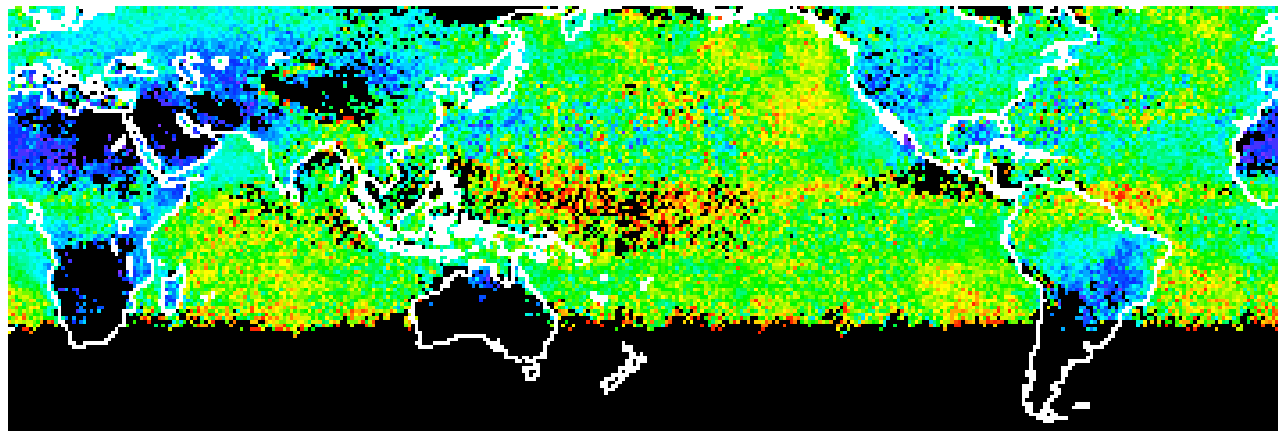


Effective Particle Radius

January

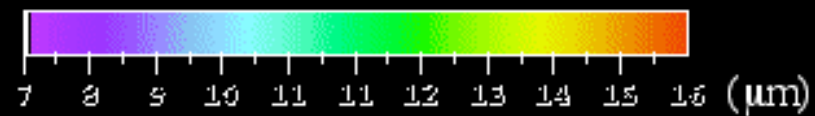
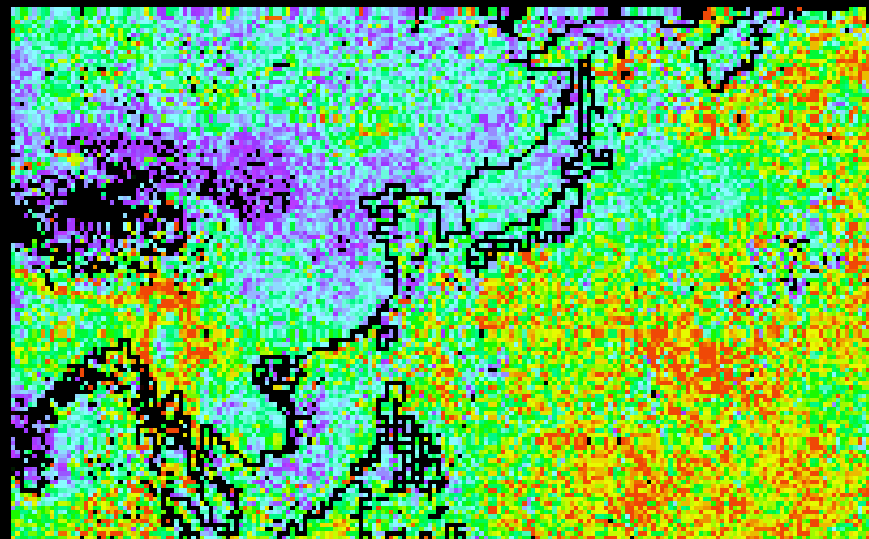


July



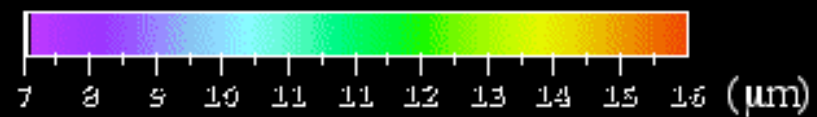
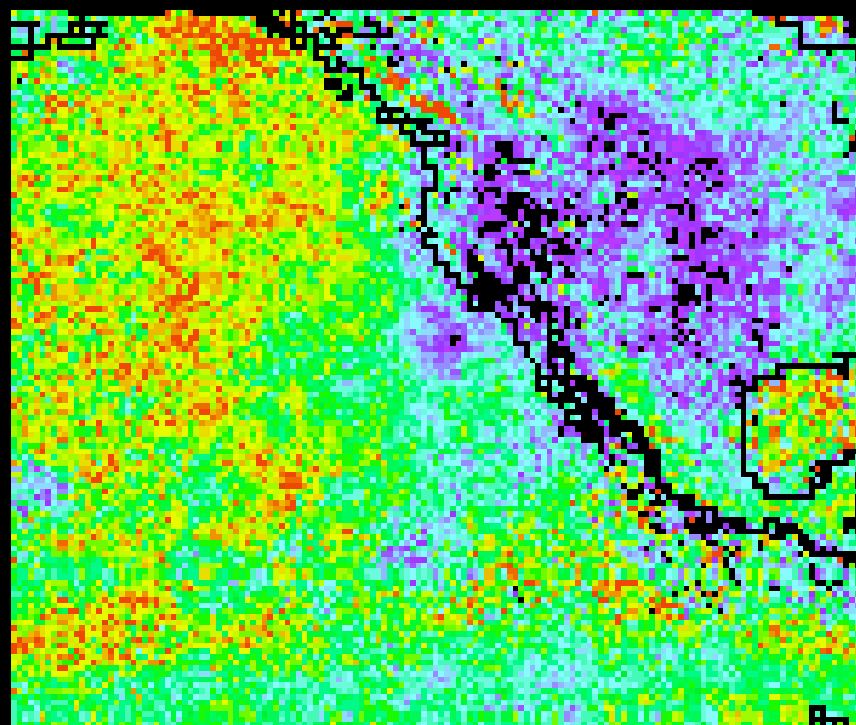
Cloud effective particle size over East Asia

July in 1990



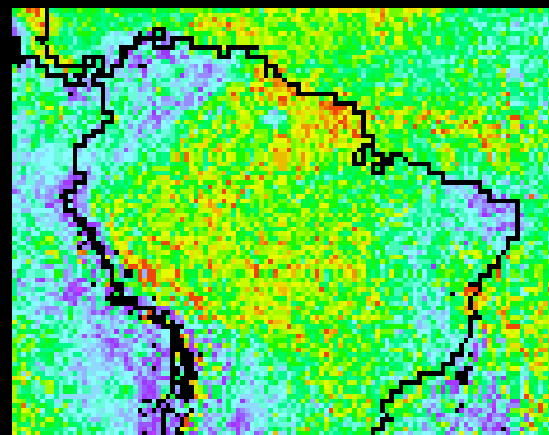
Cloud effective particle size off California

July in 1990

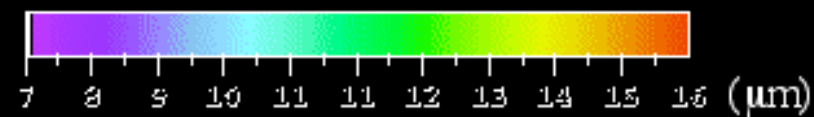
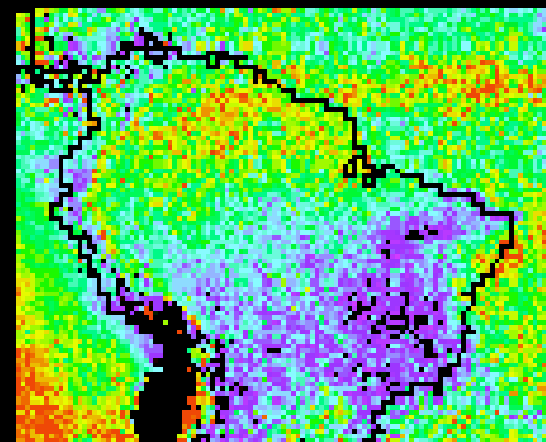


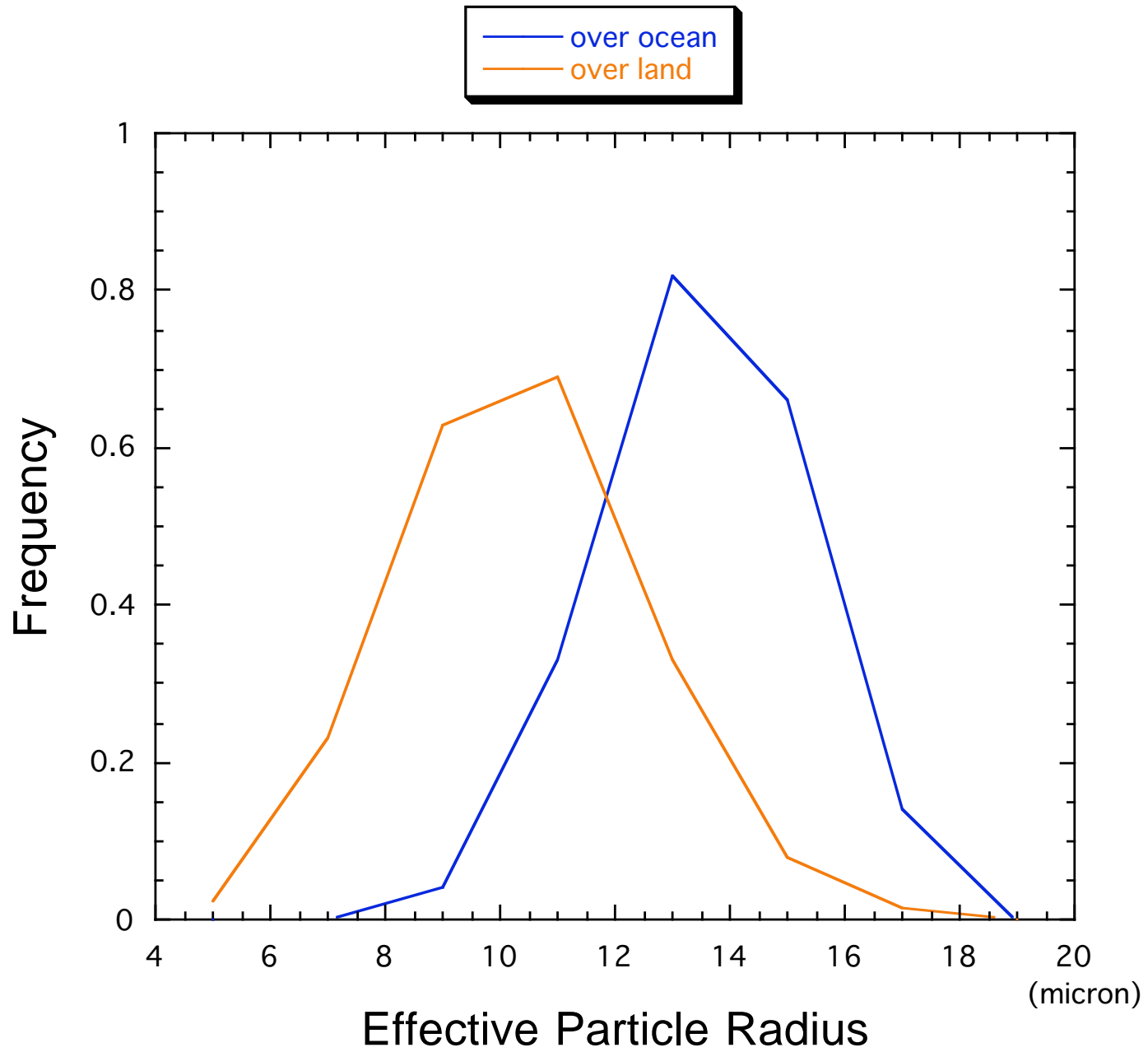
Cloud effective particle size over Amazon

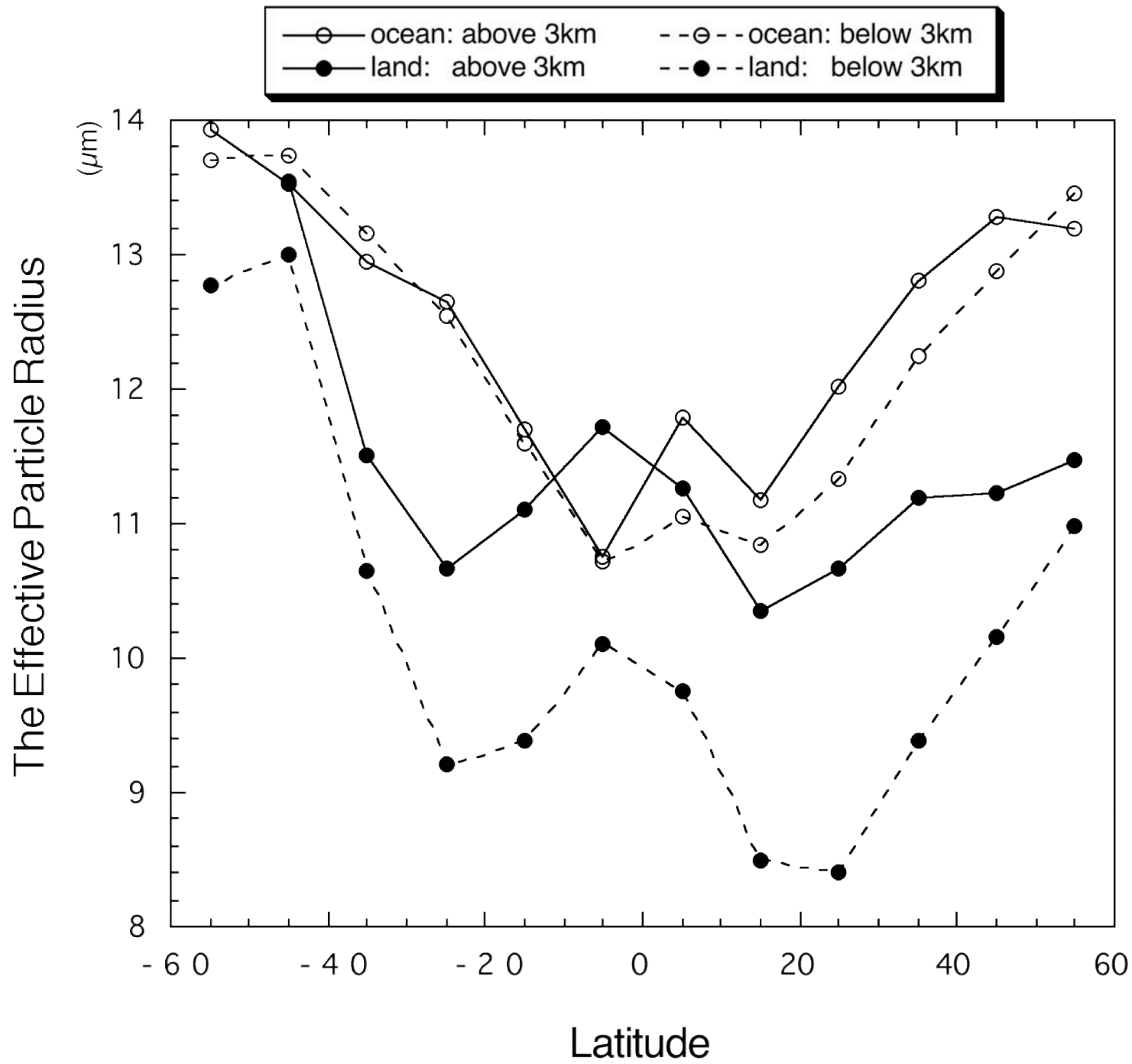
January in 1990



July in 1990







Climate Applications:

Relationships of clouds
with aerosols and precipitation

Datasets used here

Aerosol amount

Numerical simulation SO_4 , NH_4 , NO_3 , EC, OC by I. Uno (Kyushu U.)
inputting the emission inventory

Low cloud properties ($T_c > 273\text{K}$)

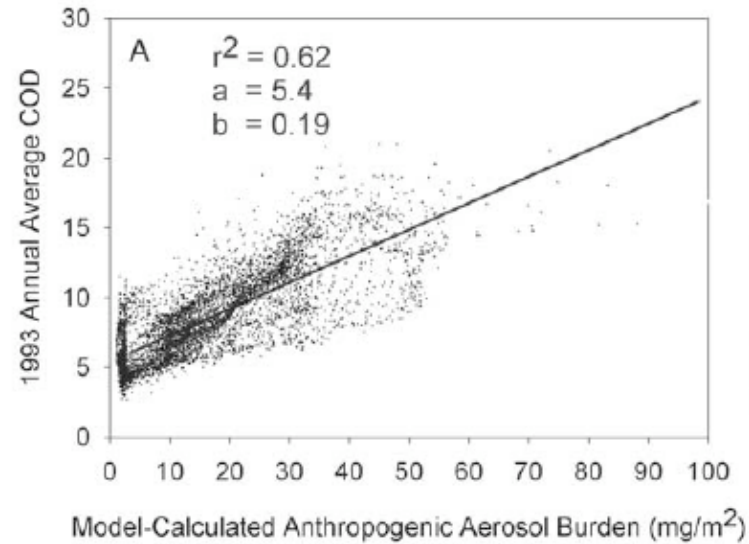
(optical depth and effective particle size)

AVHRR remote sensing by Kawamoto et al. (2001)

Preceding studies on aerosol-cloud relationships over China

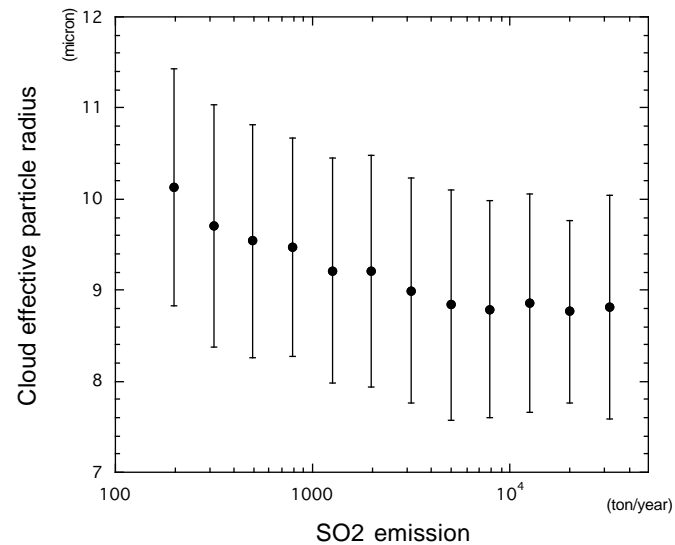
model aerosol vs. ISCCP tau

Chameides et al. 2002, *JGR*

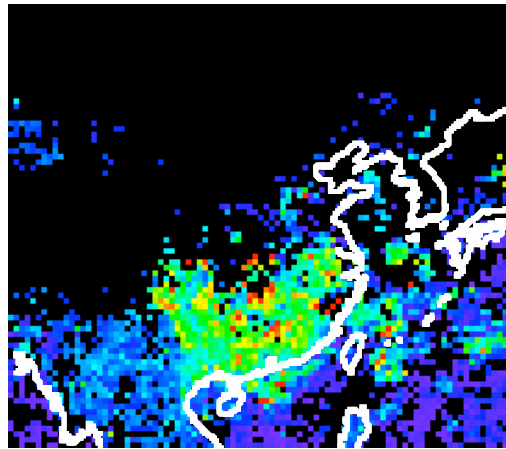


SO₂ emission and r_e

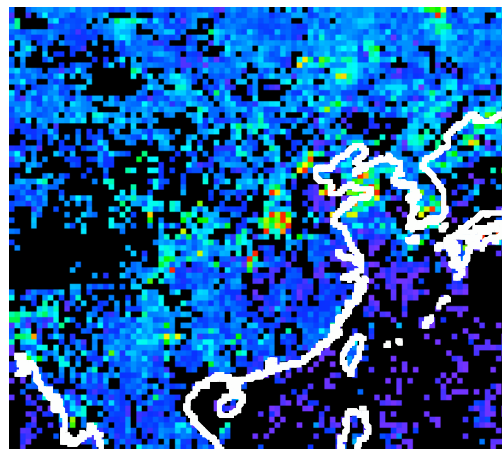
Kawamoto et al. 2004, *Atmos. Res.*



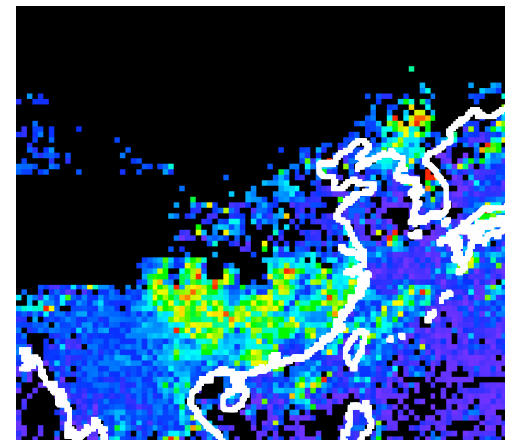
Map of τ in April, July and October in 1995



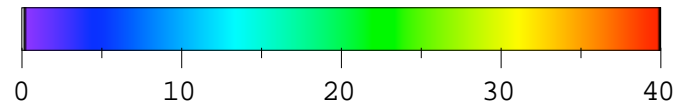
Apr.



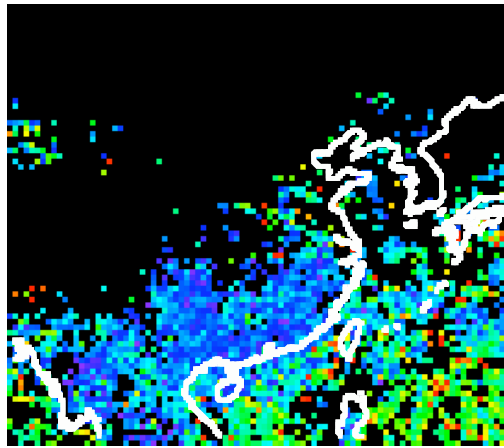
July



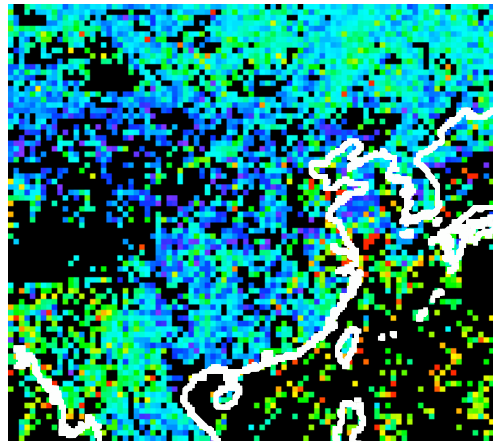
Oct.



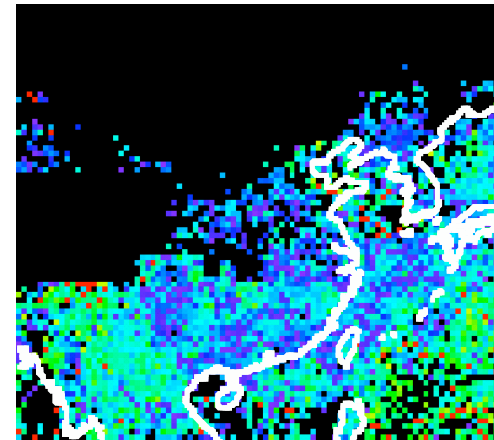
Map of r_e in April, July and October in 1995



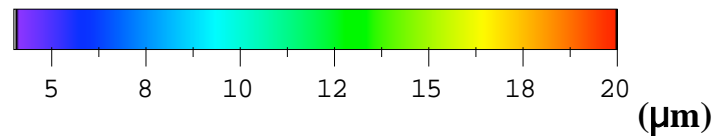
Apr.

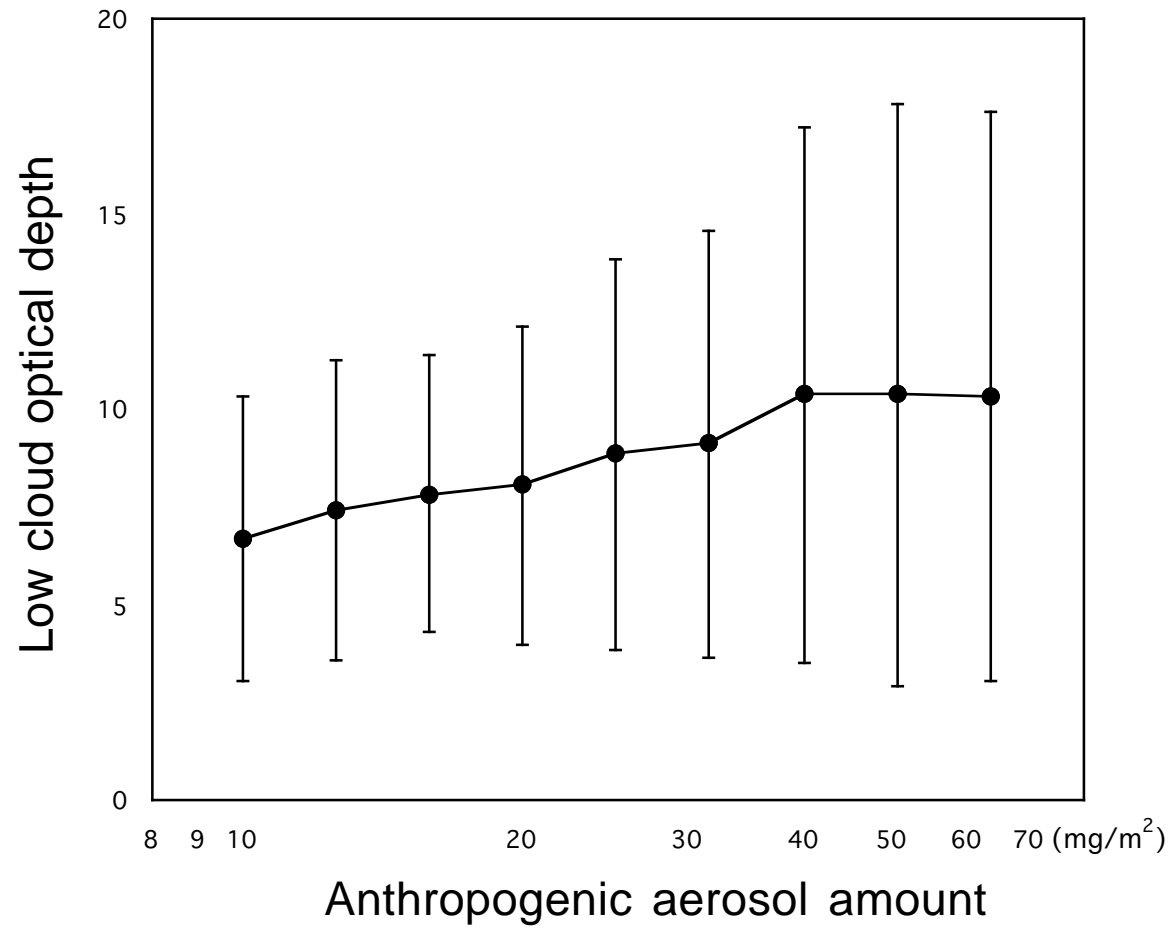


July

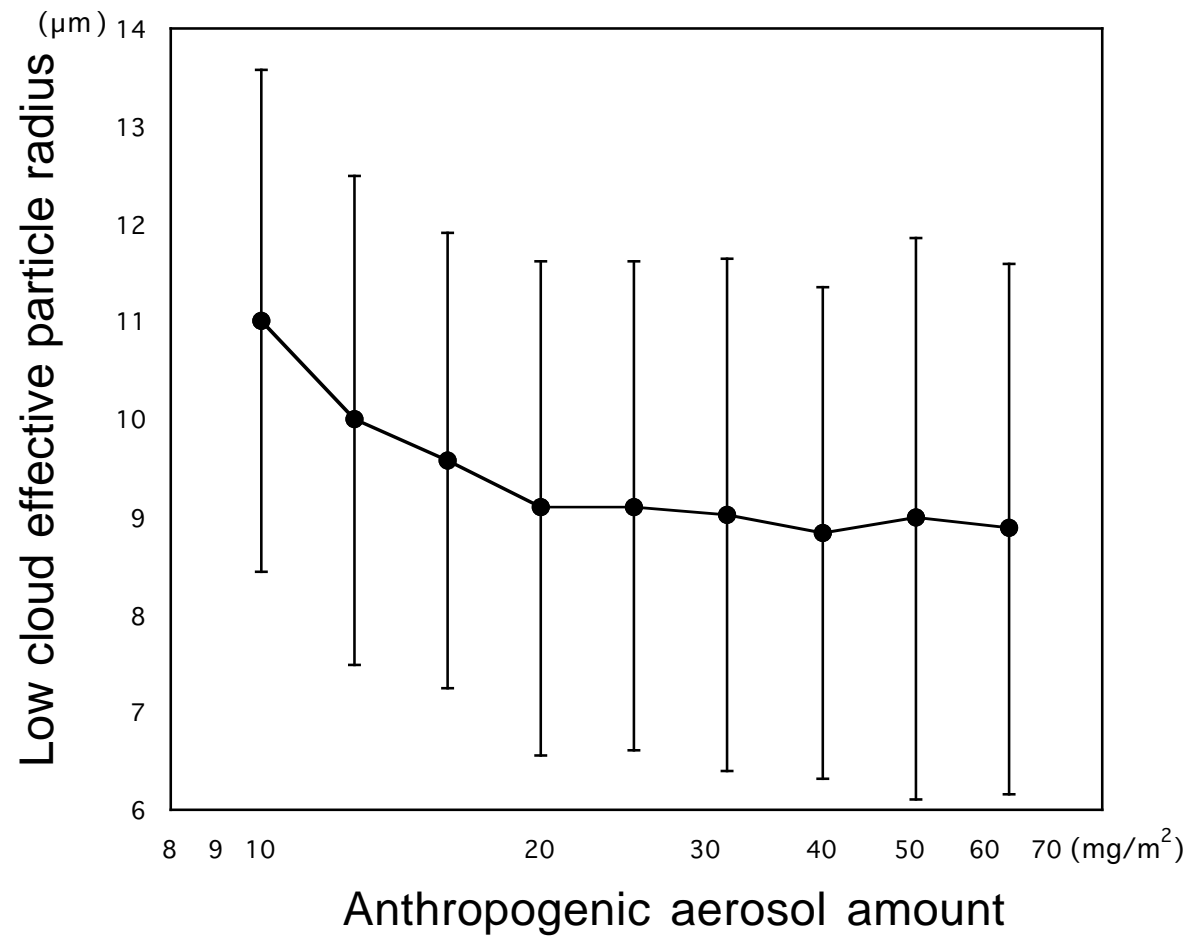


Oct.

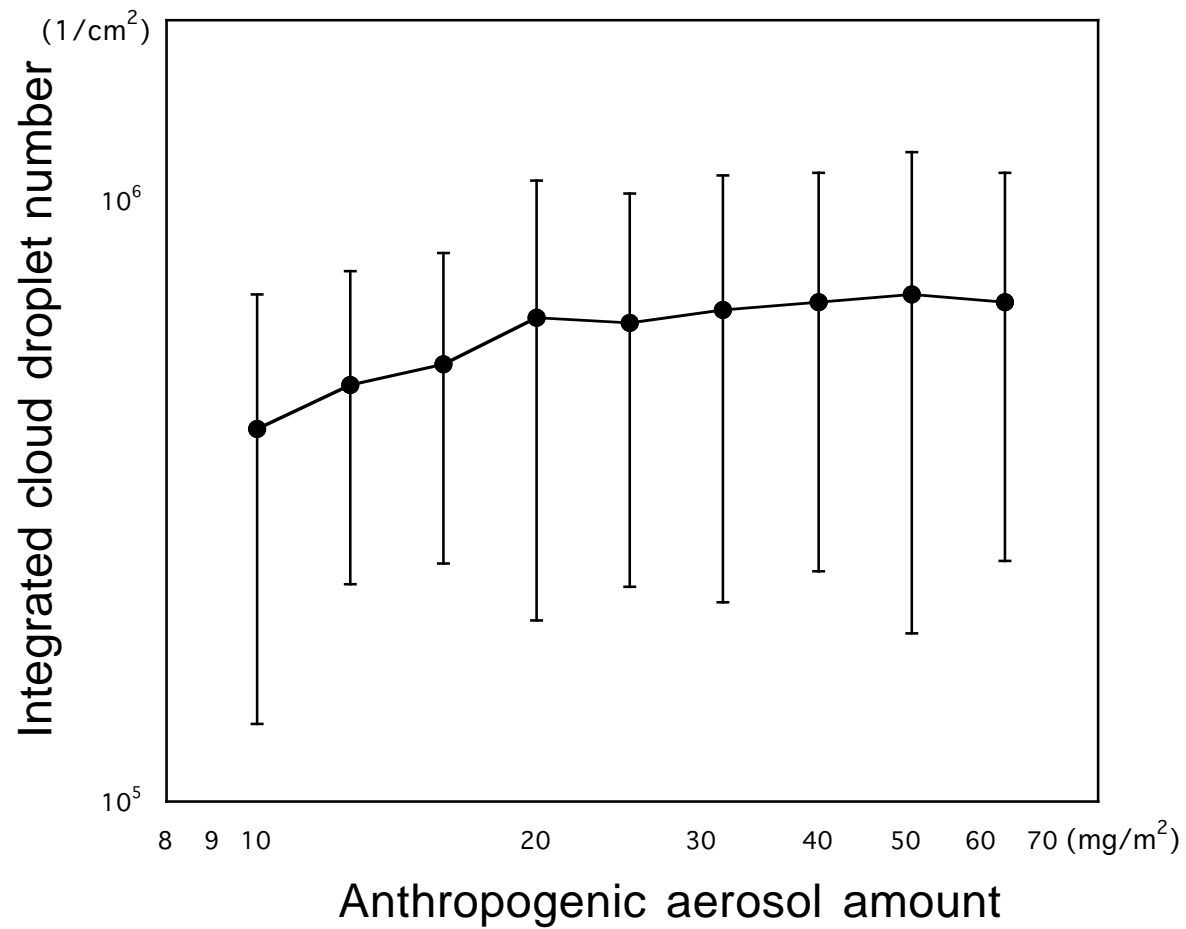




Relationship between M_a and τ in July in 1995



Relationship between M_a and r_e in July in 1995



Relationship between M_a and N_c in July in 1995

Datasets used here

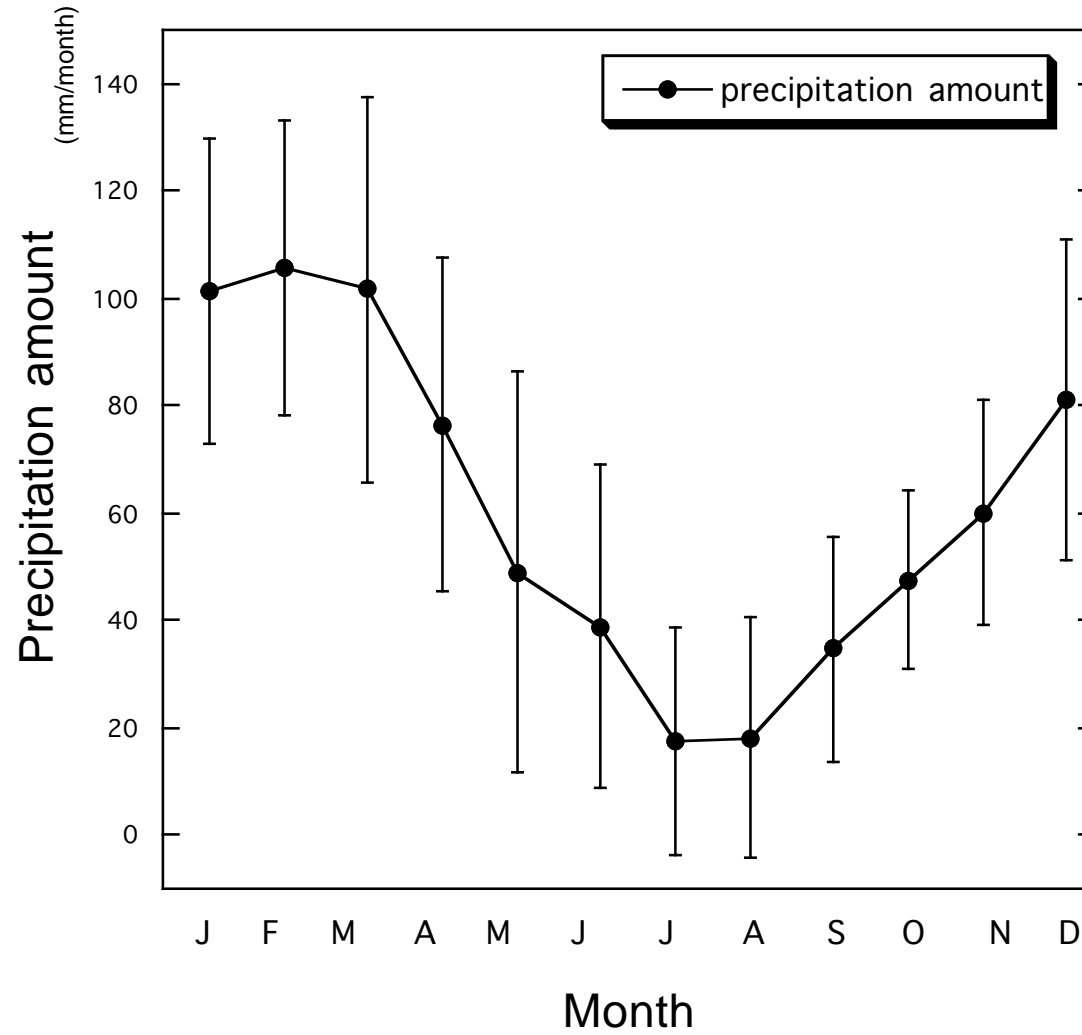
Precipitation amount

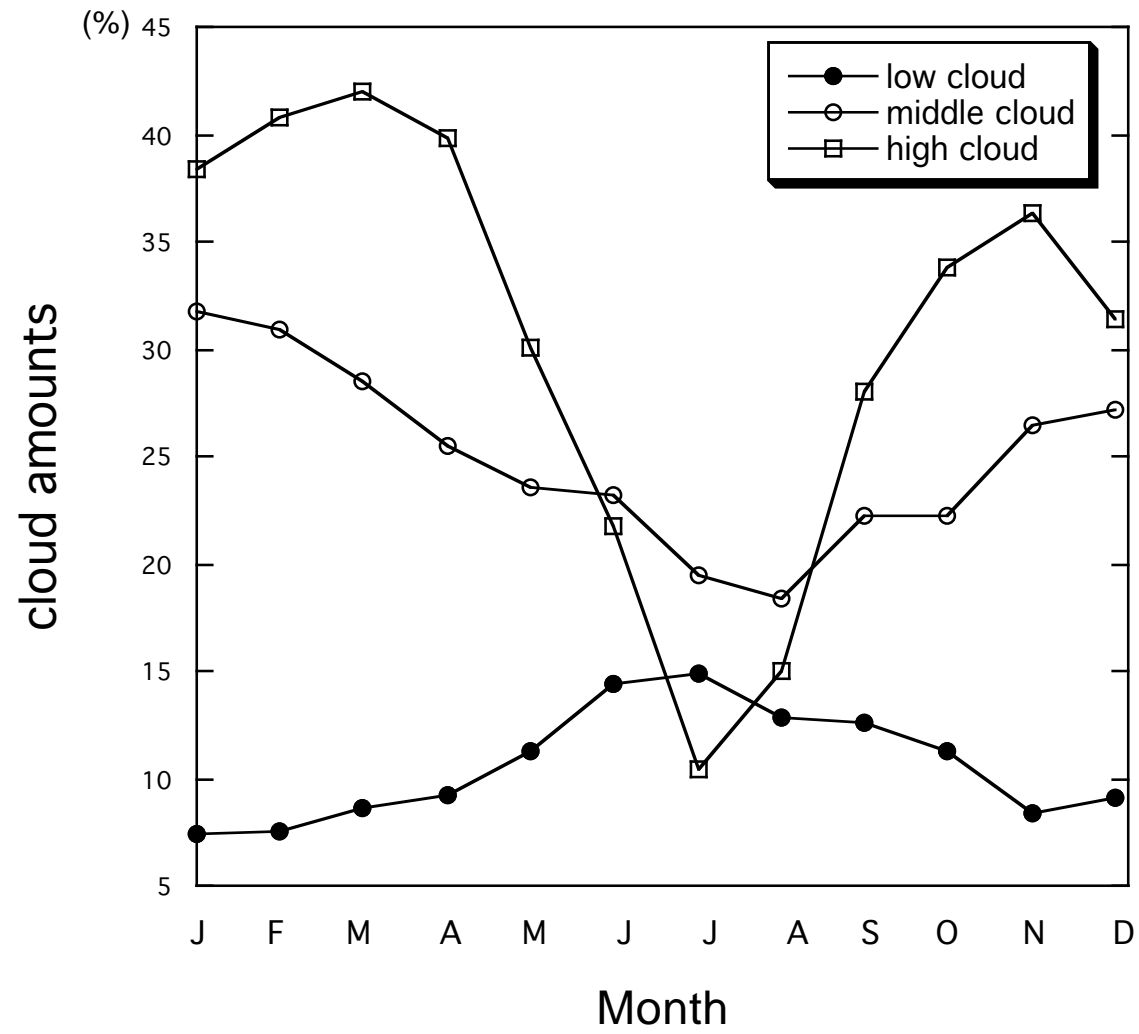
a merged algorithm based on Xie and Arkin (1997)
using gauges and satellites, 0.5-degree coverage

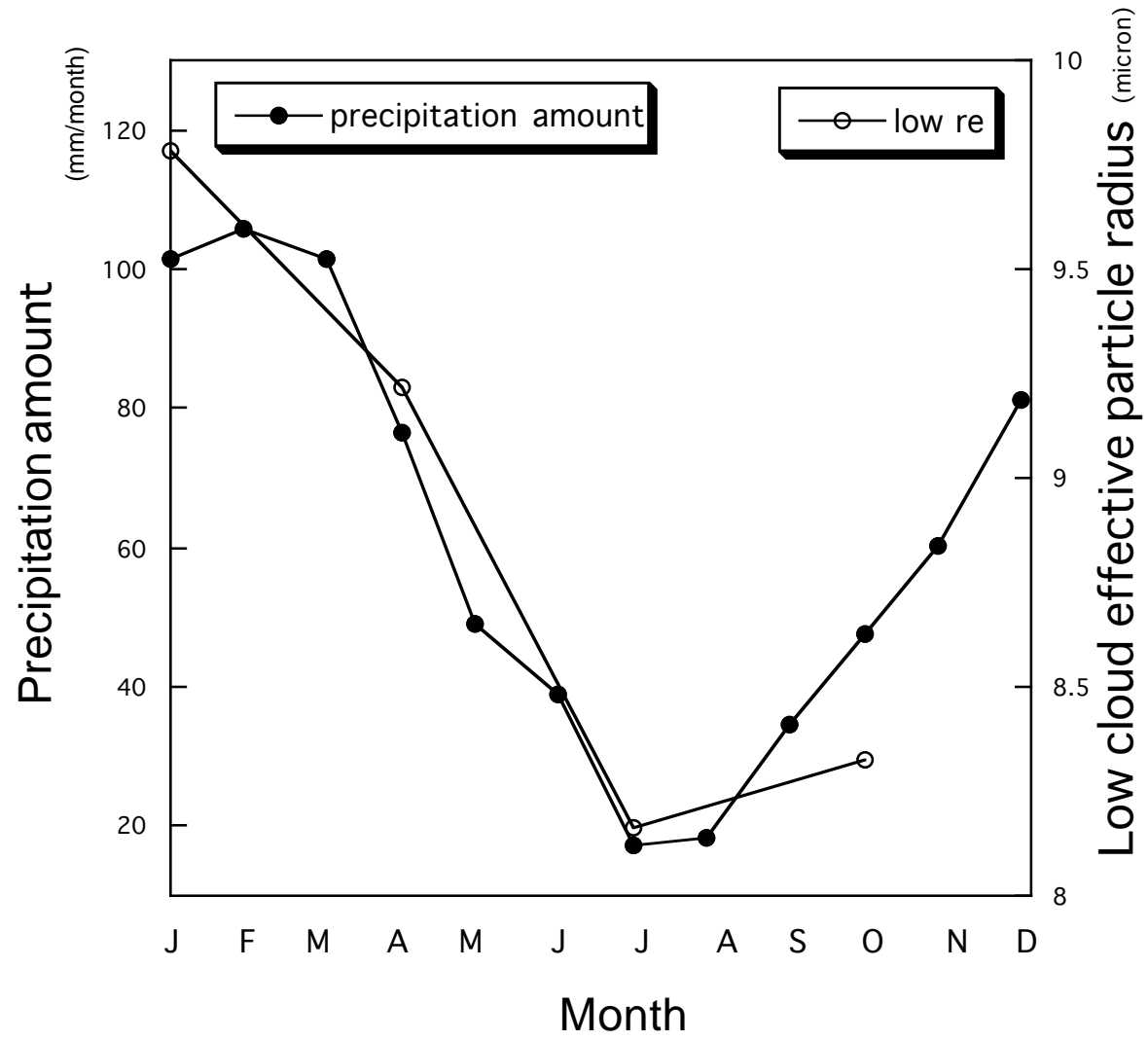
Low cloud properties ($T_c > 273\text{K}$)

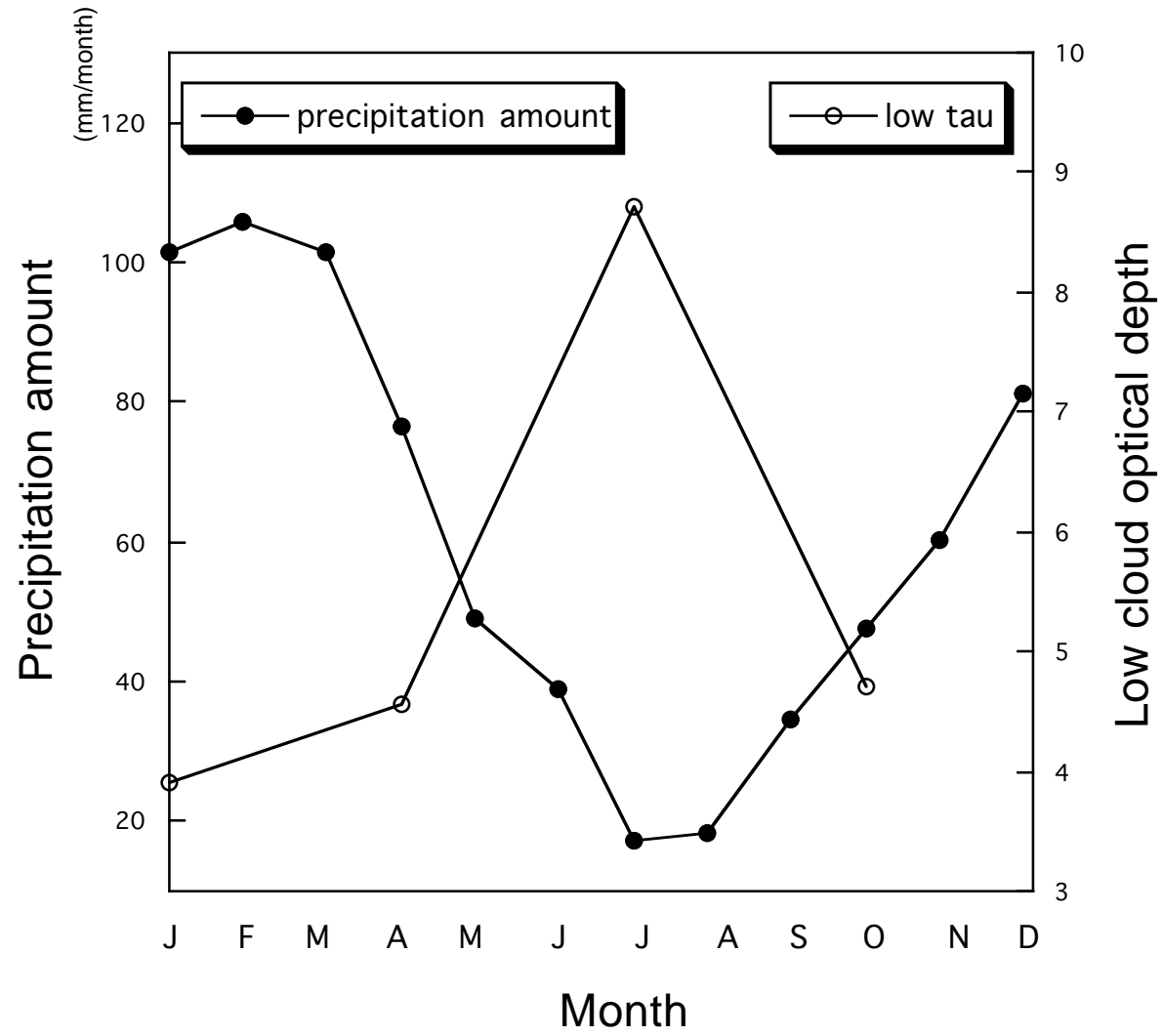
Optical depth and effective particle size
AVHRR remote sensing by Kawamoto et al. (2001)
0.5-degree coverage

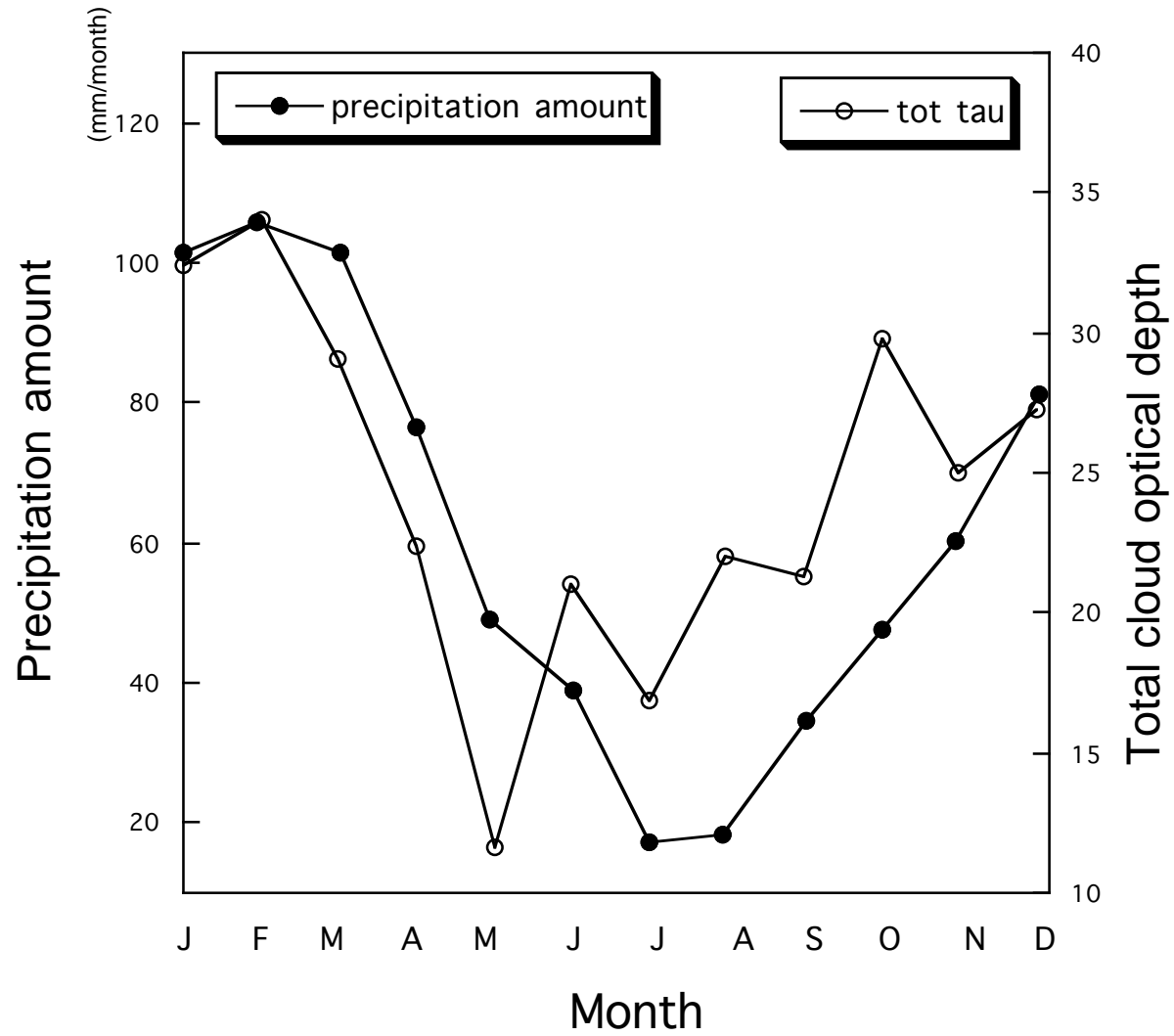
Amazon basin (W50-W70, EQ-S15) monthly-mean

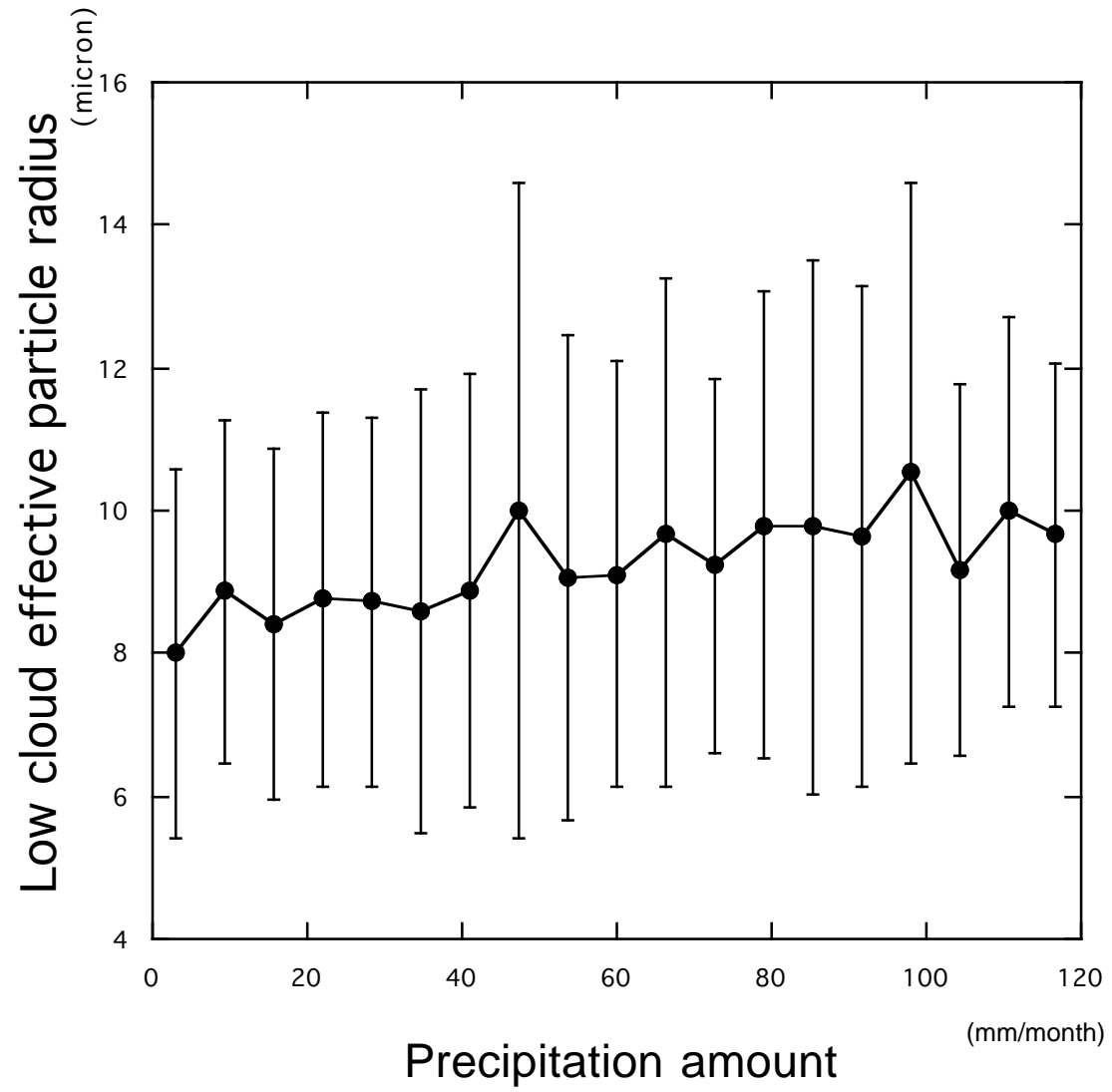


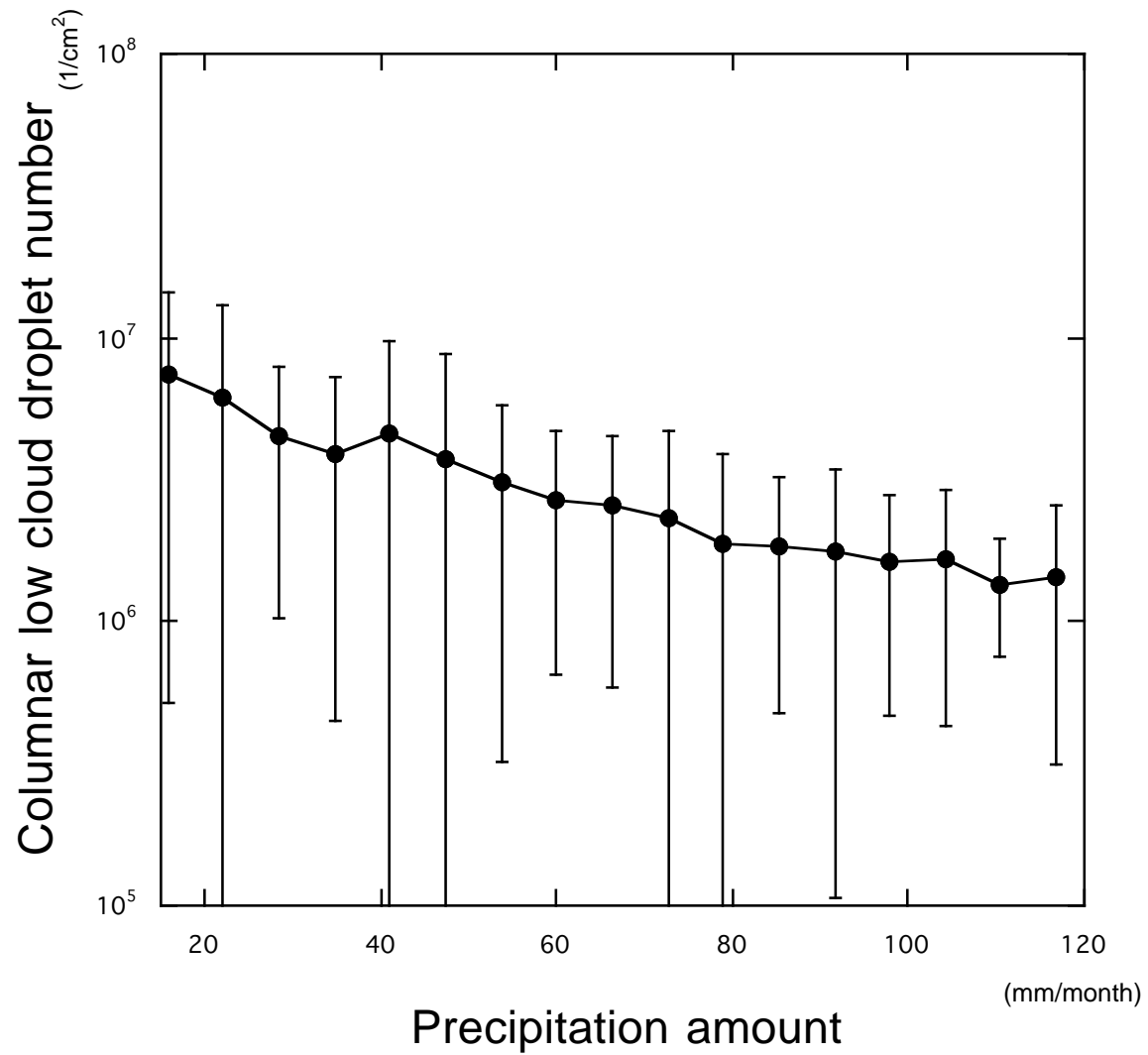




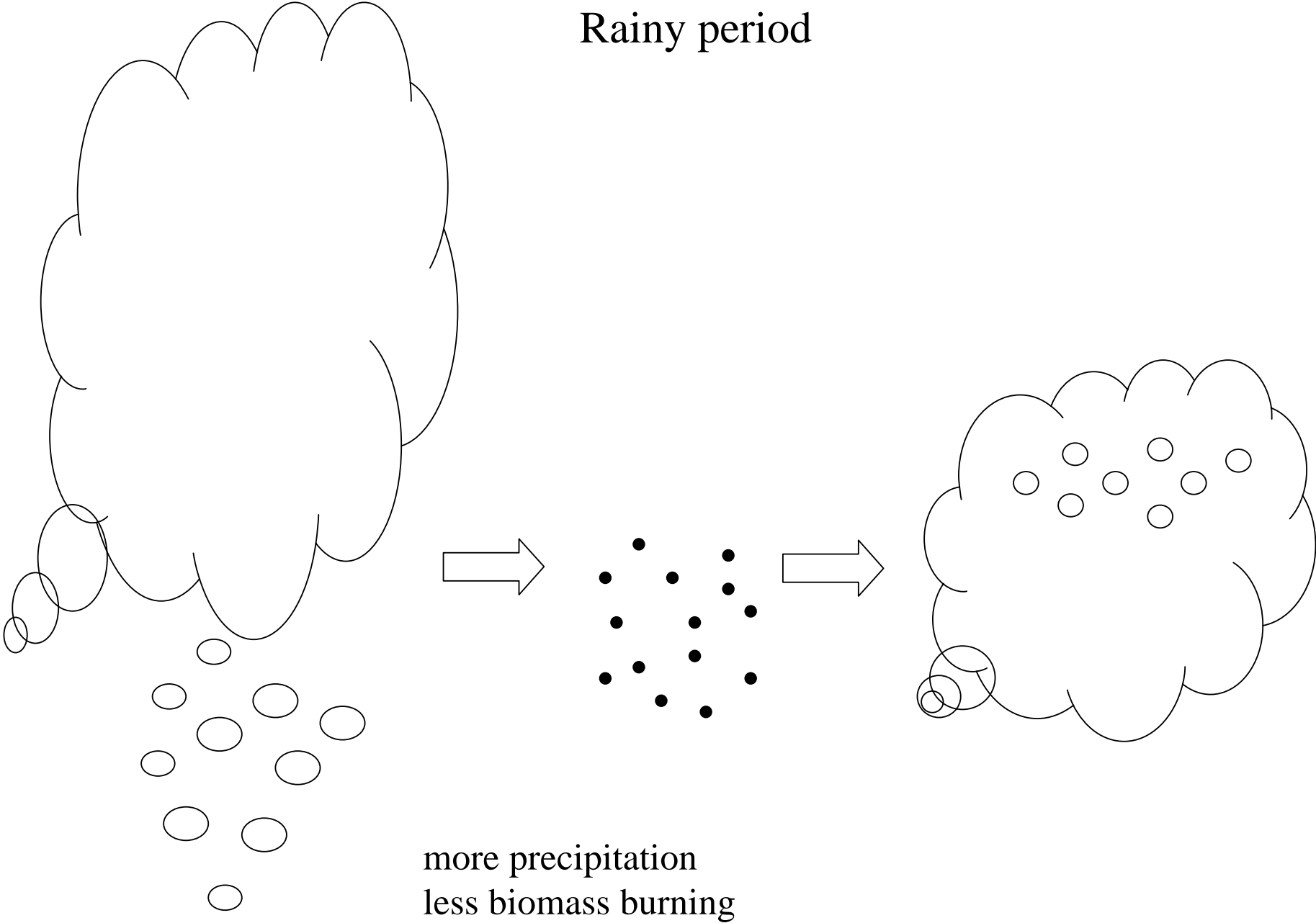






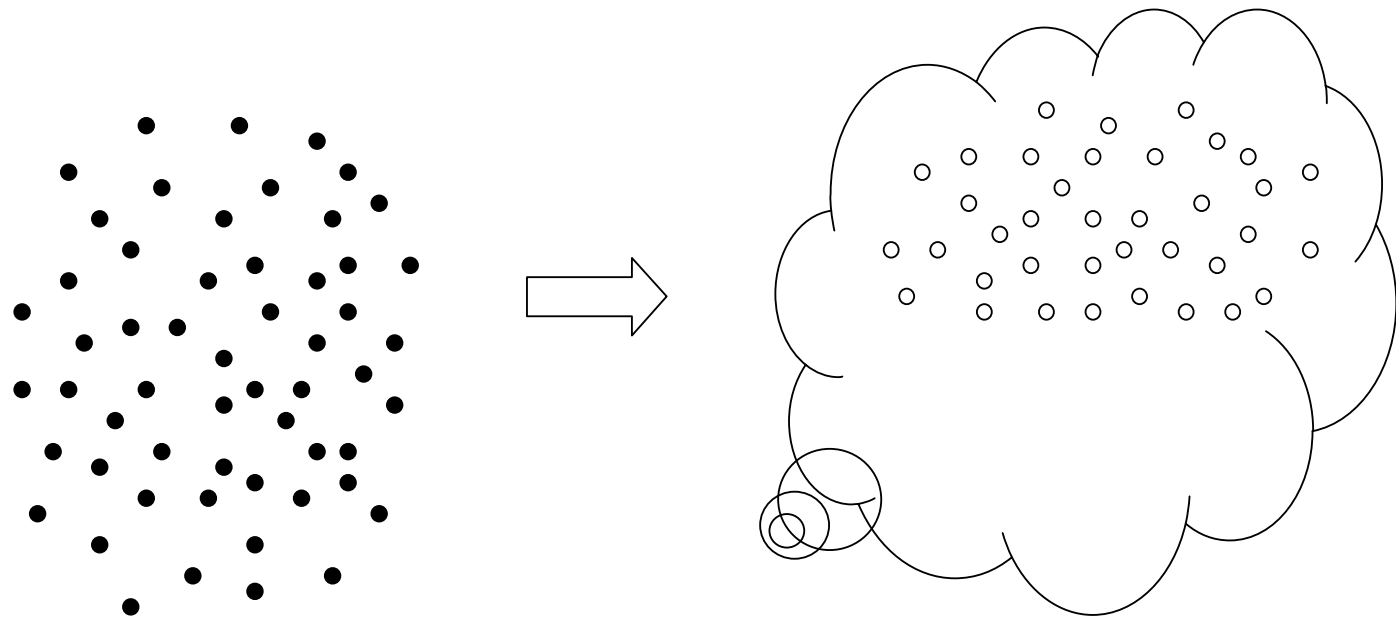


Rainy period



more precipitation
less biomass burning

dry period



less precipitation
active biomass burning

Summary

Retrieval principles using passive remote sensing of cloud properties

Visible => negligible absorption, NIR => moderate absorption

Comparisons between aerosol amount and low-level water cloud properties over the East Asia are performed.

Results support the Twomey effect.

(If more aerosols, cloud optical depth increases.

effective particle radius decreases
through aerosol - cloud interactions.)

Cloud-precipitation relationships are examined.

Low clouds generate little rain generally.

If precipitation (CCN scavenging) , then
 low cloud droplet size
 low cloud optical depth

Precipitation scavenging would be an important factor for
determining cloud properties

Low cloud properties are controlled by aerosols and precipitation.

Lecture in the 18th IHP Training Course in
Nagoya Univ., Nov.5, 2008

Satellite remote sensing of clouds by active sensors

Hajime Okamoto
(Tohoku University)

Contents

1. What is active remote sensing
2. About Scattering and absorption by particles
3. Lidar and radar equations
4. Why clouds are important.
5. Observations of clouds from radar and lidar
6. Evaluation of the Clouds from the Atmospheric General Circulation Model
7. Retrieval of ice microphysics by synergy use of CloudSat and CALIPSO data
8. Future satellite mission with radar

I. What is active remote sensing

Passive sensing relies on measuring natural levels of radiation, e.g., the radiation emitted from the sunlight reflected by the clouds.

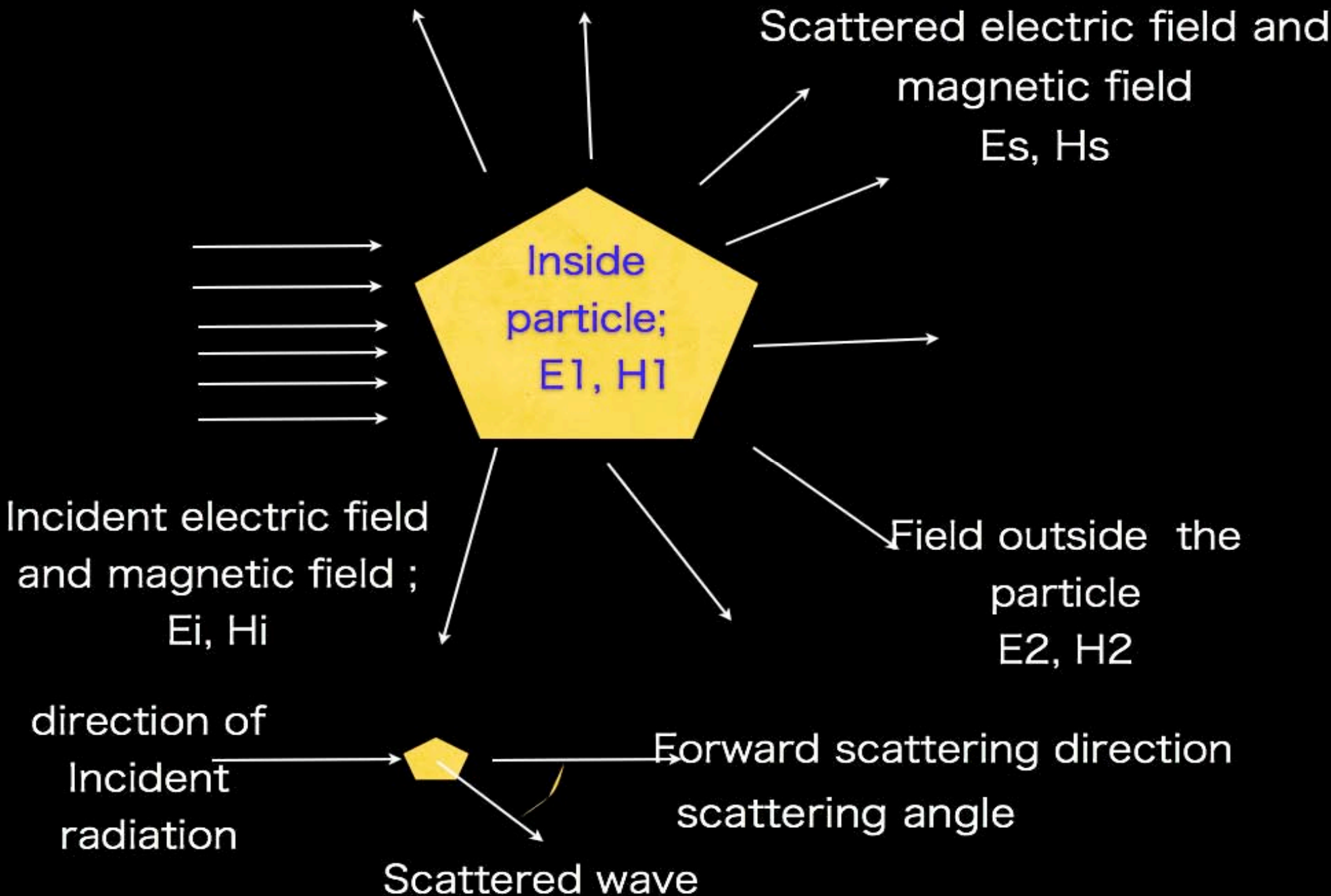
Active sensing makes use of electromagnetic energy transmitted from a specially chosen source to some target (clouds) and then monitoring the interactions between the target and the radiation.

(Stephens 1983)

2. About Scattering and absorption by particles

Scattering problem by spherical particle has been analytically solved from Maxwell equations by Lorentz and Mie in early 1900, (Mie theory). According to the recent development of computer resources the Mie theory has been widely used.

Scattering properties depend on size, wavelength, refractive index (real and imaginary part).



Definition of Extinction and Poynting vector

$\mathbf{E}_2, \mathbf{H}_2$: Electric and magnetic fields outside particle

$$\mathbf{E}_2 = \mathbf{E}_i + \mathbf{E}_s$$

$$\mathbf{H}_2 = \mathbf{H}_i + \mathbf{H}_s$$

$$\mathbf{E}_i = \mathbf{E}_0 \exp(i\mathbf{k} \cdot \mathbf{x} - i\omega t)$$

$$\mathbf{H}_i = \mathbf{H}_0 \exp(i\mathbf{k} \cdot \mathbf{x} - i\omega t)$$

\mathbf{S} : Poynting outside the particle

$$\mathbf{S} = \frac{1}{2} \text{Re}\{\mathbf{E}_2 \times \mathbf{H}_2\}$$

$$= \frac{1}{2} \text{Re}\{(\mathbf{E}_i + \mathbf{E}_s) \times (\mathbf{H}_i + \mathbf{H}_s)^*\}$$

$$= \frac{1}{2} \text{Re}\{\mathbf{E}_i \times \mathbf{H}_i^*\} + \frac{1}{2} \text{Re}\{\mathbf{E}_s \times \mathbf{H}_s^*\}$$

$$+ \frac{1}{2} \text{Re}\{\mathbf{E}_i \times \mathbf{H}_s^* + \mathbf{E}_s \times \mathbf{H}_i^*\}$$

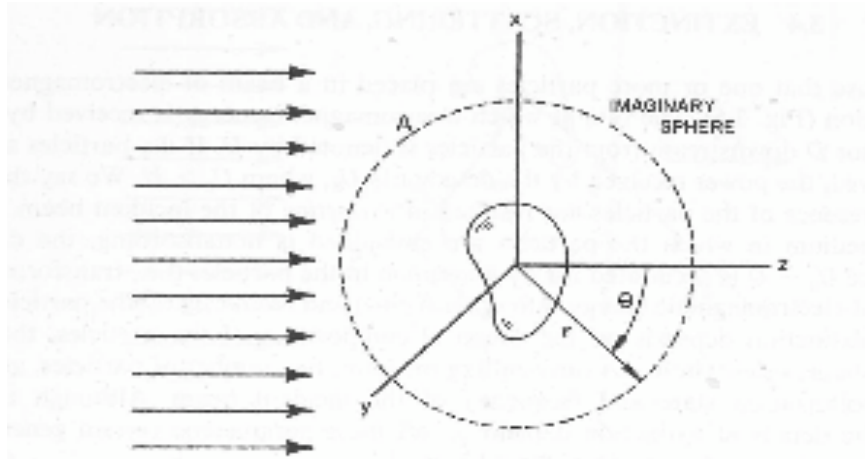
$$S_i = \frac{1}{2} \text{Re}\{\mathbf{E}_i \times \mathbf{H}_i^*\},$$

$$S_s = \frac{1}{2} \text{Re}\{\mathbf{E}_s \times \mathbf{H}_s^*\},$$

$$S_{ext} = \frac{1}{2} \text{Re}\{\mathbf{E}_i \times \mathbf{H}_s^* + \mathbf{E}_s \times \mathbf{H}_i^*\}.$$

$$S = S_i + S_s + S_{ext}$$

Particle embedded in imaginary sphere



(Bohren and Huffman 1983)

$$W_a = - \int_A \mathbf{S} \cdot \mathbf{e}_r dA$$

$$W_a > 0;$$

$$W_a = W_i - W_s + W_{ext}$$

$$W_a = - \int_A (\mathbf{S}_i + \mathbf{S}_s + \mathbf{S}_{ext}) \cdot \mathbf{e}_r dA$$

$$W_i = - \int_A \mathbf{S}_i \cdot \mathbf{e}_r dA$$

$$W_s = \int_A \mathbf{S}_s \cdot \mathbf{e}_r dA$$

$$W_{ext} = - \int_A \mathbf{S}_{ext} \cdot \mathbf{e}_r dA$$

$$\therefore W_a = W_i - W_s + W_{ext}$$

$$W_i = 0$$

$$W_{ext} = W_a + W_s$$

Extinction = absorption + scattering

$$C_{ext} = \frac{W_{ext}}{I_i}$$

Extinction cross section

$$C_{abs} = \frac{W_{abs}}{I_i}$$

Absorption cross section

$$C_{sca} = \frac{W_{sca}}{I_i}$$

Scattering cross section

$$\therefore C_{ext} = C_{abs} + C_{sca}$$

Extinction cross section

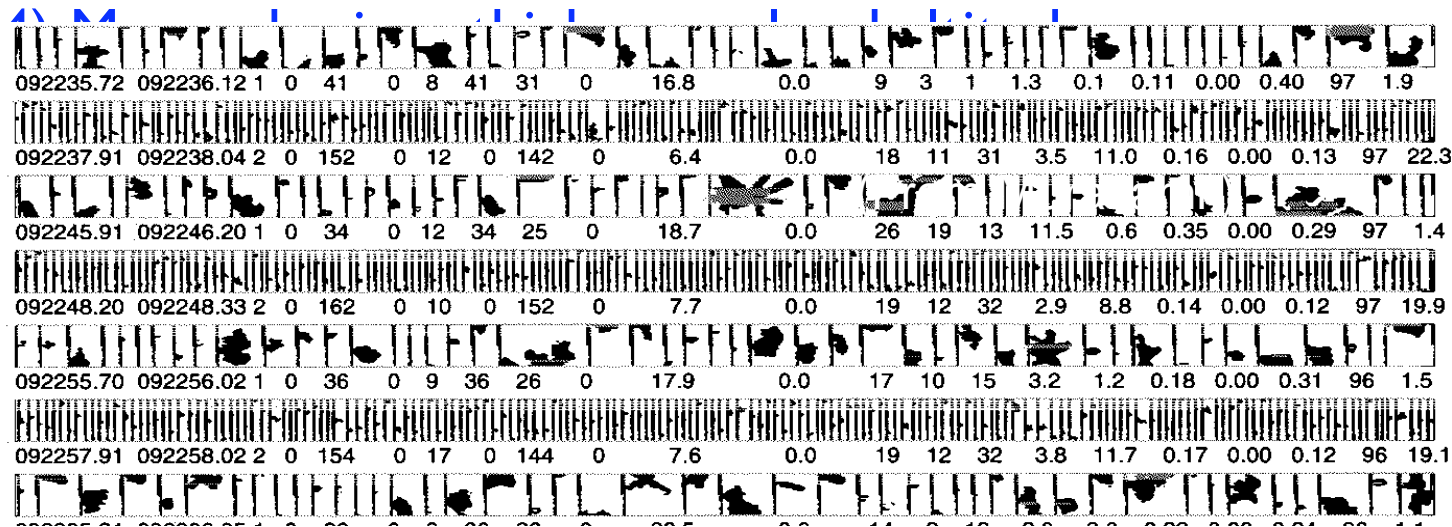
= Scattering cross section + Absorption cross section

Electromagnetic properties of particles depend on

1) Shape

2) Size distribution

3) Chemical composition/phase ; refractive index
(wavelength dependence)



From Murakami

For small particles compared with the wavelength, Rayleigh scattering theory is applicable.

For large particles compared with the wavelength, geometrical optics can be used.

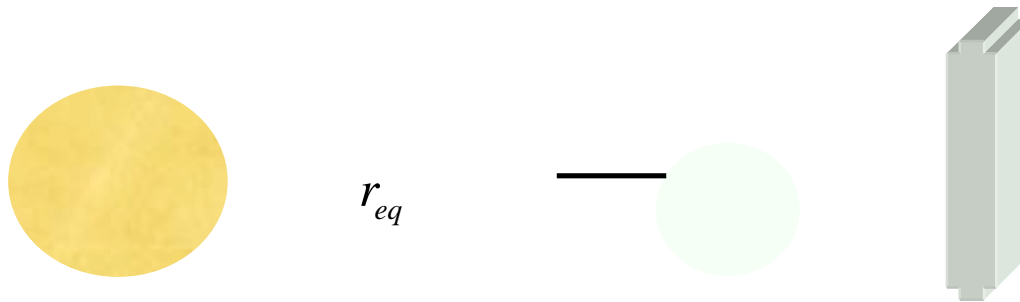
Approximations of scattering theories for arbitrary shaped particles have been also developed, e.g., discrete dipole approximation.

Treatment of non-sphericity

We need to define radius for non-spherical particle.

We introduce mass equivalent radius r_{eq}

$$\frac{4}{3}\pi r_{eq}^3 \rho = m \quad r_{eq} = \left(\frac{3m}{4\pi\rho} \right)^{1/3}$$



When the two particles have the same radius , it means both have the same mass.

Using a scattering theory, e.g., Mie theory,
the following physical quantities can be obtained.

Backscattering cross section [$\mu\text{m}^2/\text{ster}$] $C_{bk,p}(r)$

Extinction cross section [μm^2] $C_{ext,p}(r)$

Size distribution function [$1/\mu\text{m}/\text{m}^3$] $\frac{dn(r)}{dr}$

Lidar backscattering coefficient
[$1/\text{m}/\text{ster}$]

$$\beta_{true,p} = \frac{1}{4\pi} \int \frac{dn(r)}{dr} C_{bk,p}(r) dr$$

Extinction coefficient [$1/\text{m}$]:

$$\sigma_{ext,p} = \int \frac{dn(r)}{dr} C_{ext,p}(r) dr$$

Effective radius [μm] :

$$R_{eff} = \frac{\int \frac{dn(r)}{dr} r^3 dr}{\int \frac{dn(r)}{dr} r^2 dr}$$

3. Lidar and radar equations

Lidar equation

Lidar uses laser beam where the wavelength is in visible or infrared regions.

Relation between received power P_r and backscattering coefficient is described by Lidar equation.

$$P_{r,li}(R) = \frac{C_L P_{in,li} \Delta R}{R^2} \beta_{obs}(R)$$

$$\beta_{obs}(R) = (\beta_{true,P}(R) + \beta_{true,Ray}(R)) \\ \times \exp(-2\tau(R))$$

$$\tau = \int_0^R (\sigma_{ext,P}(R') + \sigma_{ext,Ray}(R')) dR'$$

R : distance between the particle and the lidar

Radar equation :

Radar equation is similar to lidar equation.

Radar wavelength is in microwave region,

e.g., mm- to cm.

$$P_r(R) = \frac{C \Delta R}{R^2} |K|^2 Z_e(R) \exp \left[-2 \int_0^R \sigma_{ext,i}(R_i) dR_i \right]$$

$$Z_e = \frac{\lambda^4}{\pi^5 |K|^2} \int \frac{dn(r)}{dr} C_{bk}(r) dr$$

Radar reflectivity factor
: Z_e

$$|K| = \left| \frac{(m^2 - 1)}{(m^2 + 2)} \right|$$

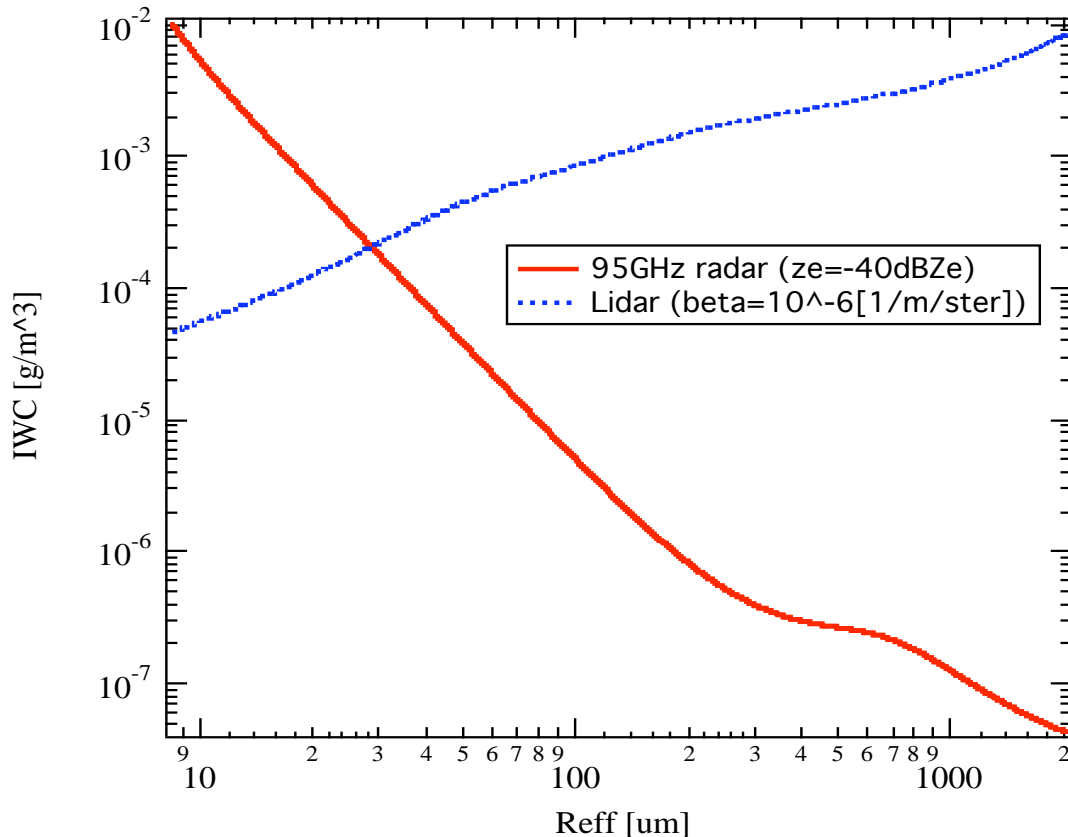
$$dBZ_e = 10 \log_{10} Z_e$$

Radar signal; $Z_e \propto r^6$
for one particle

Lidar signal ; $\beta \propto r^2$

$Z_e \sim r_{eff}^3$
for a IWC

$\beta \sim r_{eff}^{-1}$



Differences between lidar
and radar.

Radar is sensitive to large
particles.

Lidar is sensitive to small
particles.

Minimum IWC as a function of
effective radius

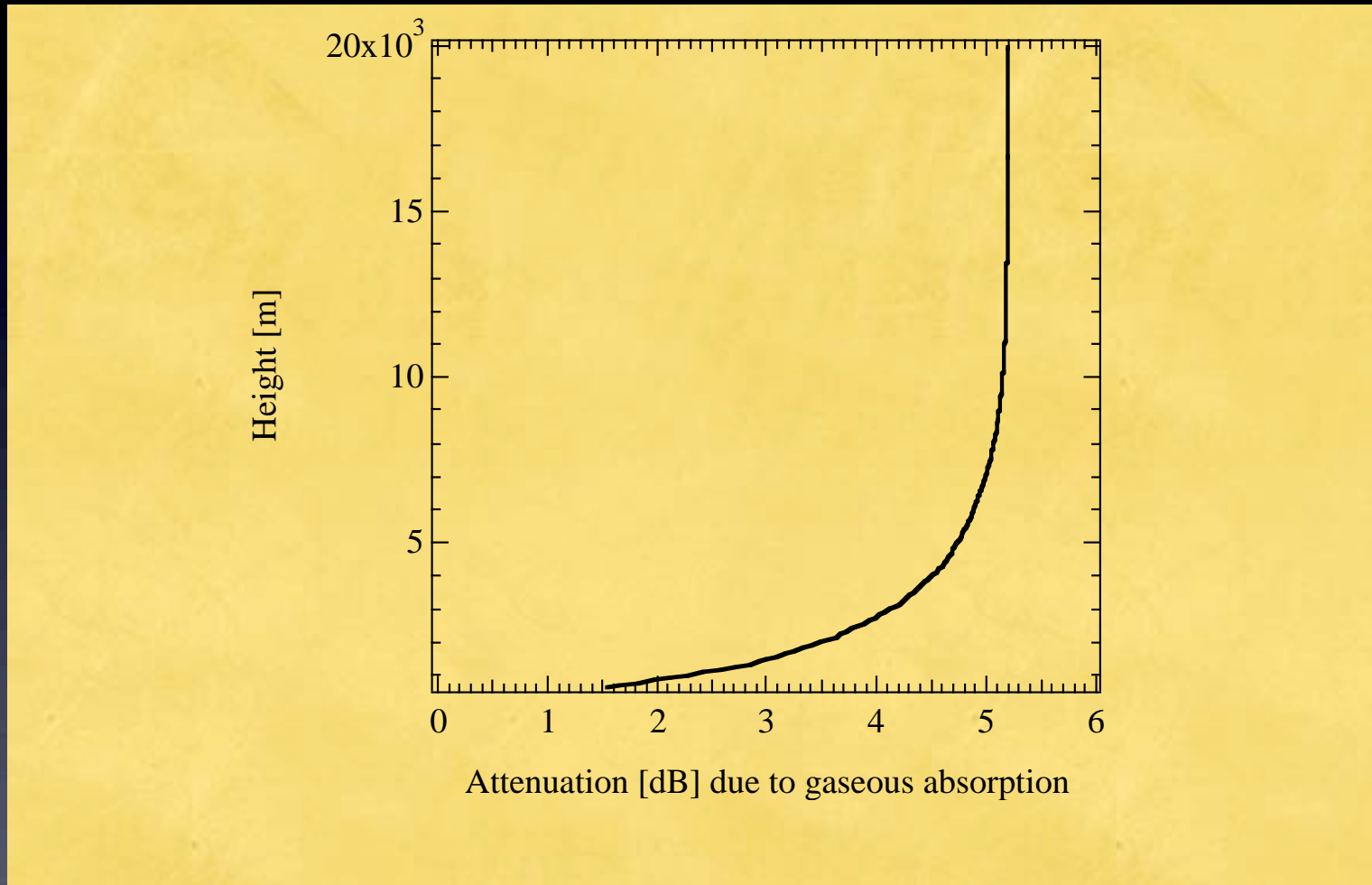
Attenuation (extinction) should be taken into account for interpretation. attenuation due to clouds, precipitation, gasses

$$dBZe_{atte} = dBZe_{true} - dB_{cl} - dB_{gas} - dB_{redome} - dB_{precip}$$

$$\beta_{atte}(R) = (\beta_{aero}(R) + \beta_{cl}(R) + \beta_{gass}(R)) \exp(-2\tau(R))$$

$$\tau(R) = \int_0^R (\sigma_{aero}(R) + \eta(R)\sigma_{cl}(R) + \sigma_{gass}(R)) dR$$

Attenuation due to gas in tropics



4. Why clouds are important.

Issues and motivation

Cloud microphysics is a key component; radiation and these leads to the change in atmospheric dynamics and this generates cloud and aerosols (cloud-aerosol feedback loops).

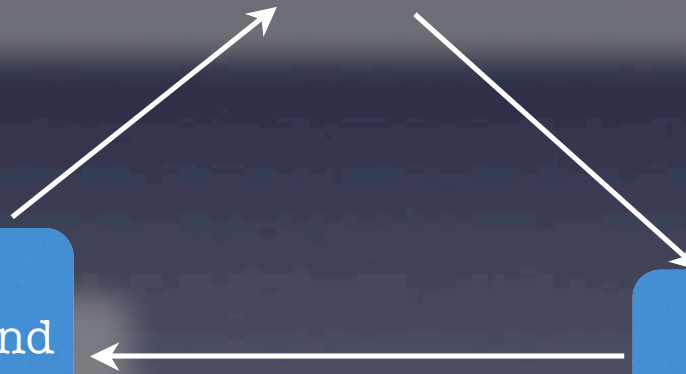
Difficulties in the studies of cloud feedback exist. Passive instruments on current satellites provide integrate quantities since they measure radiation from column. Large uncertainties exist in the distribution of clouds and aerosols, e.g., cloud vertical structure and microphysics, i.e., phase, size, ice/liquid water content and types and scattering characteristics of aerosols.

Towards the evaluation of the role of clouds and aerosols on the climate system.
Cloud feedback process

distribution of cloud, aerosol, precipitation

circulation of atmosphere and
water
convection; horizontal and
vertical transport

Energy distribution
(radiation and latent
heat)

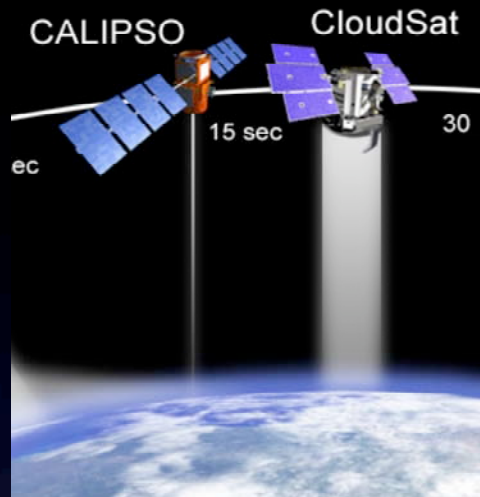


To validate the numerical models, we also need knowledge of cloud distribution and cloud microphysics.

Another way is the direct comparisons of signals where physically-based simulation of signals of satellite sensors can be used from the output of numerical models (in order to take into account observation conditions). For the purposes, we need sophisticated treatment in the modeling, e.g., scattering models of clouds and aerosol particles from visible to mm-wavelength.

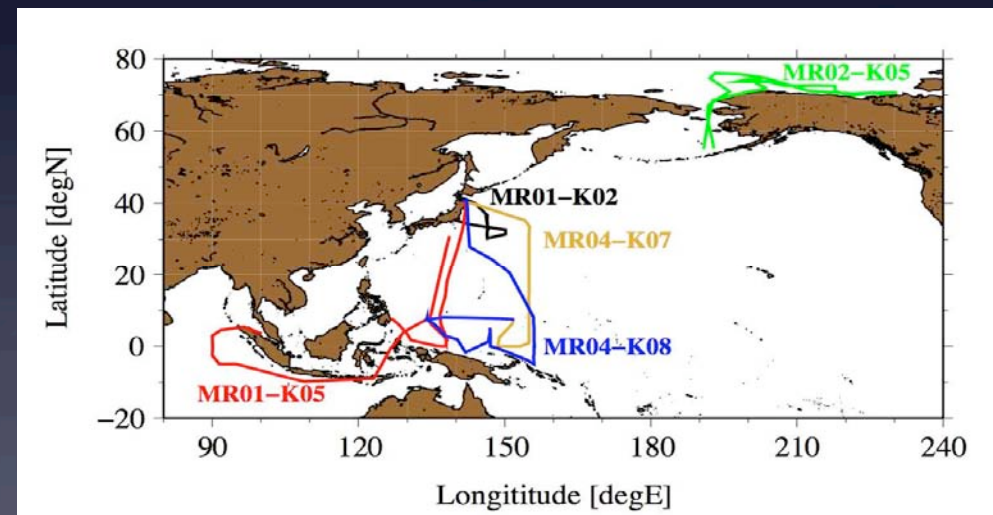
5. Observations of clouds from radar and lidar

data sources



(I) Ship-borne cloud radar/lidar experiments using R/V Mirai since 2001; The radar has the same frequency as CloudSAT And the lidar is the same as CALIPSO.

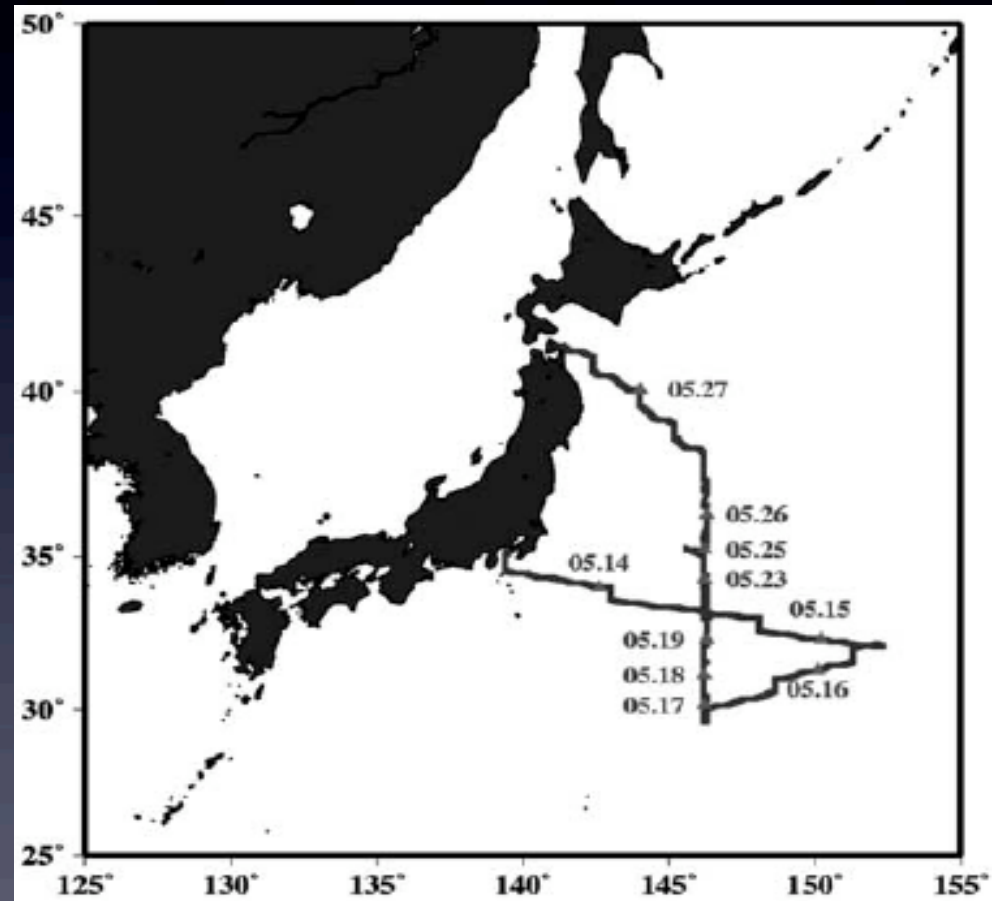
(II) CloudSAT and CALIPSO were successfully launched in April 2006.
CloudSAT : 95GHz cloud profiling radar
CALIPSO : 532nm/1064nm lidar



Cruise tracks of R/V Mirai

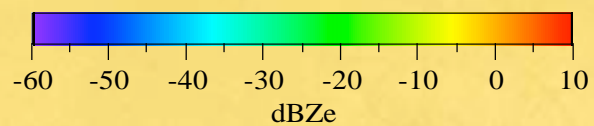
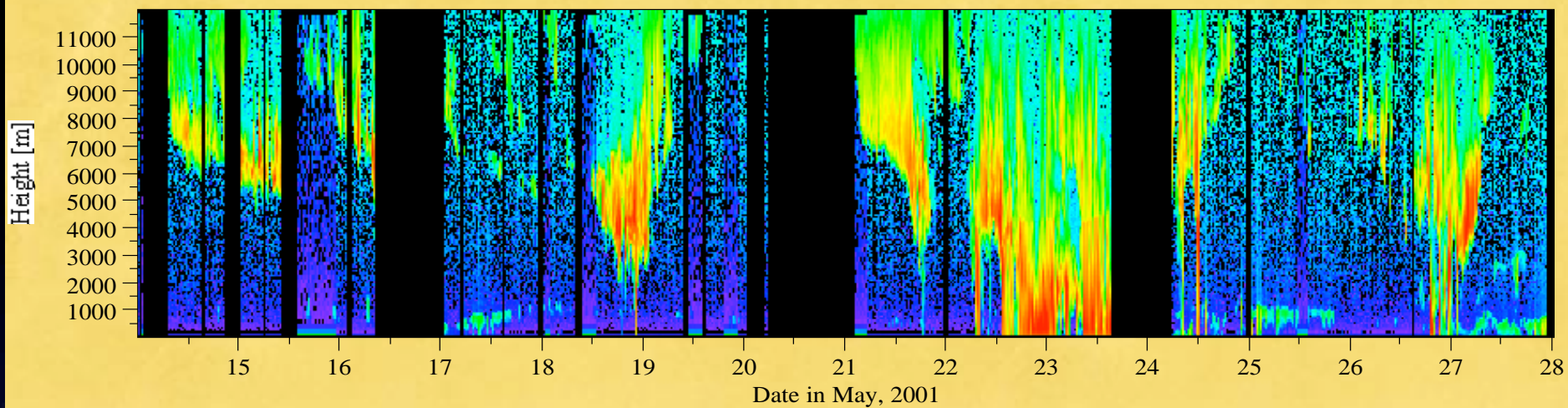
5-1. Analysis of radar/lidar data during R/V Mirai cruise

5-1-1 mid-latitude case

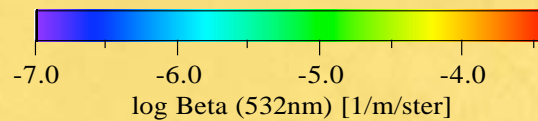
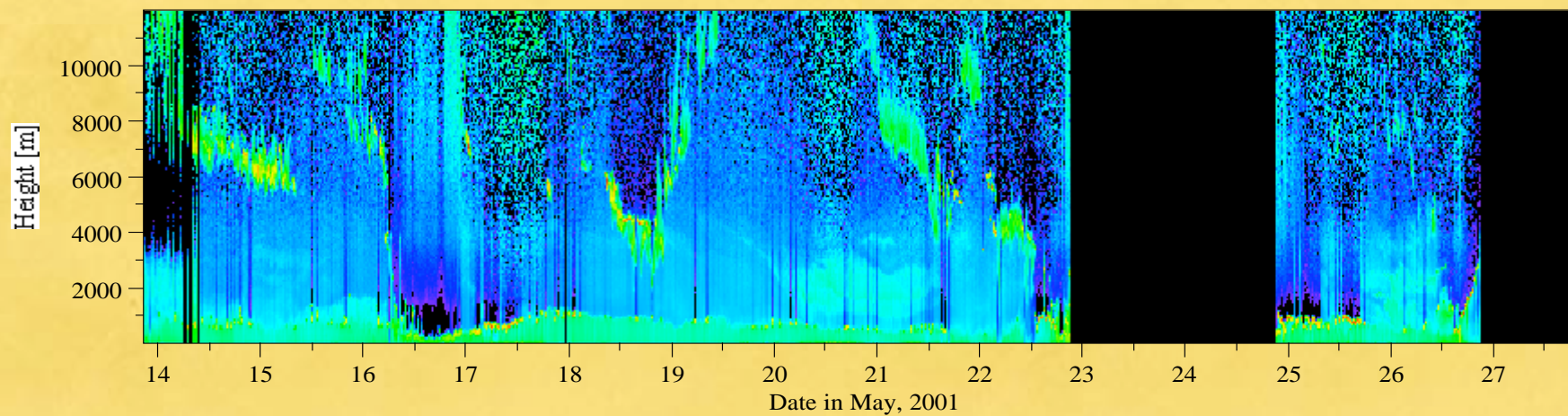


Mirai cruise track in MR01-K02 from May 14-
27, 2001

lidar

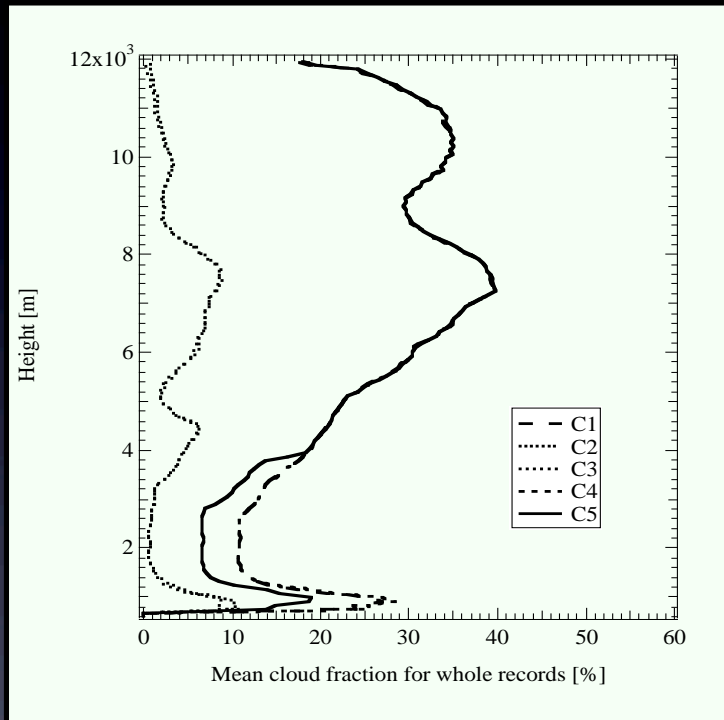


Radar



Lidar

Cloud vertical structures obtained from radar/lidar in Western Pacific Ocean near Japan in 2001



Triple peaks in cloud fractions.

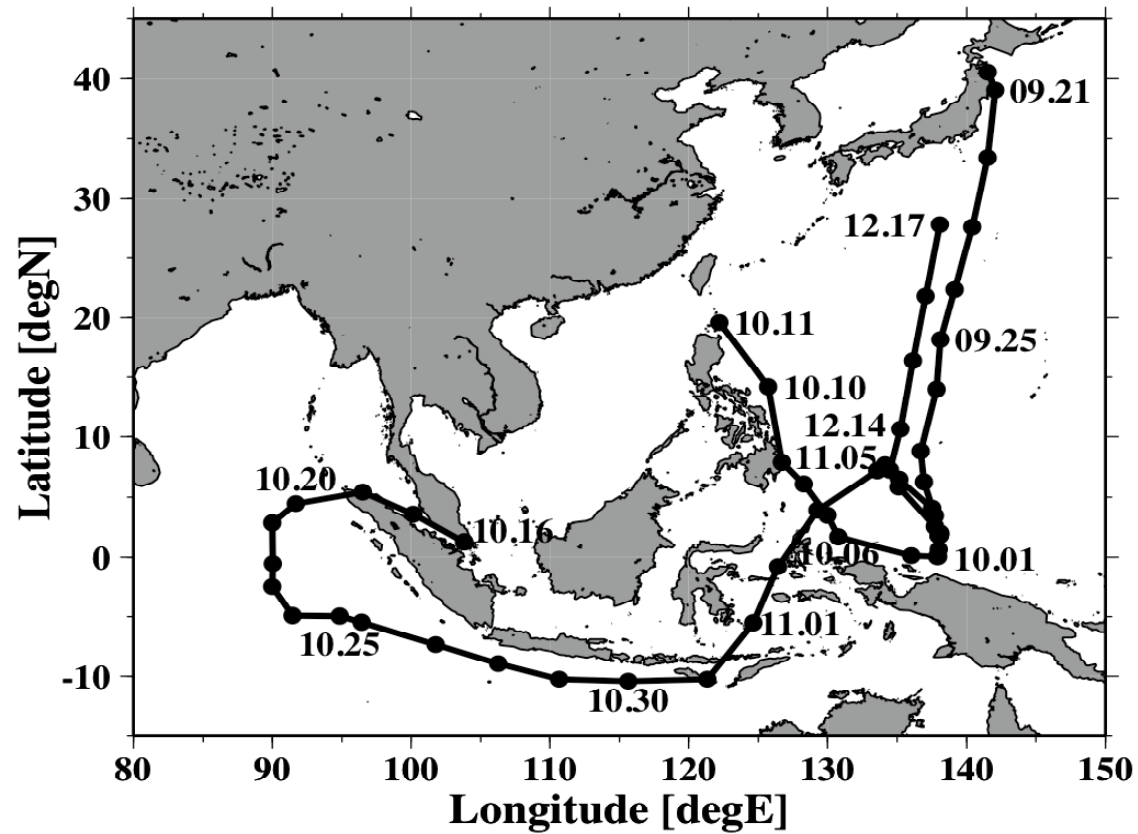
Cloud and hydrometeor fraction
in May 2001 (Okamoto et al., JGR 2007)

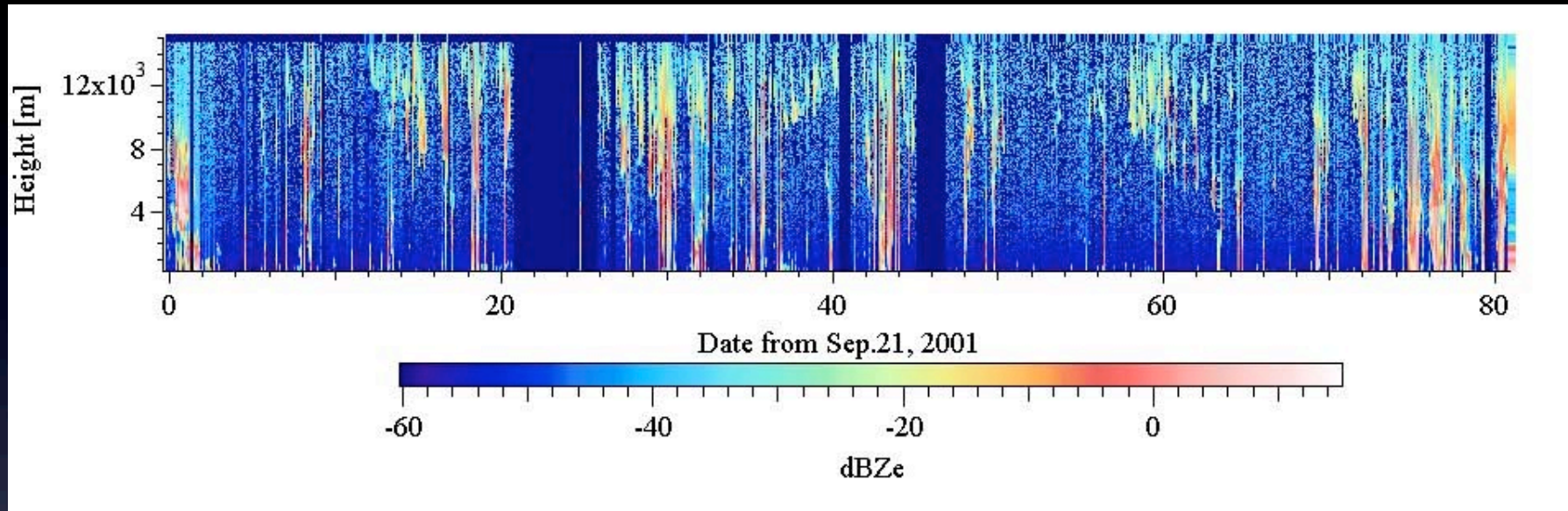
C1 : radar only :

Radar signal is contaminated by drizzle and precip.

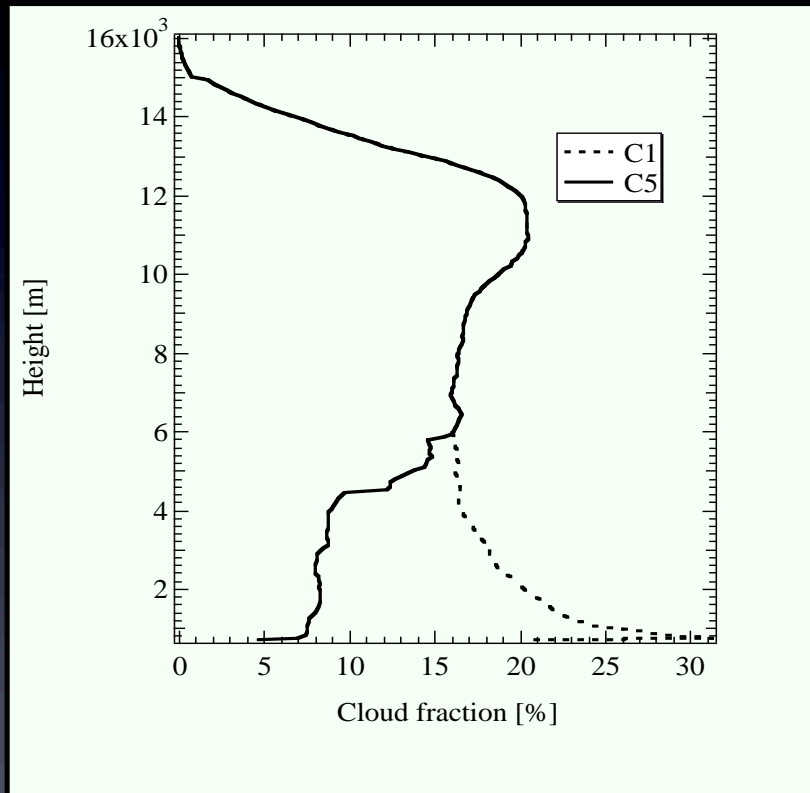
C5 : C1 +lidar cloud bottom

5-1-2 Tropical Western Pacific Ocean case in Sep.21-Dec. 17, 2001





Cloud vertical structures obtained from radar/lidar in Tropical Western Pacific Ocean in 2001

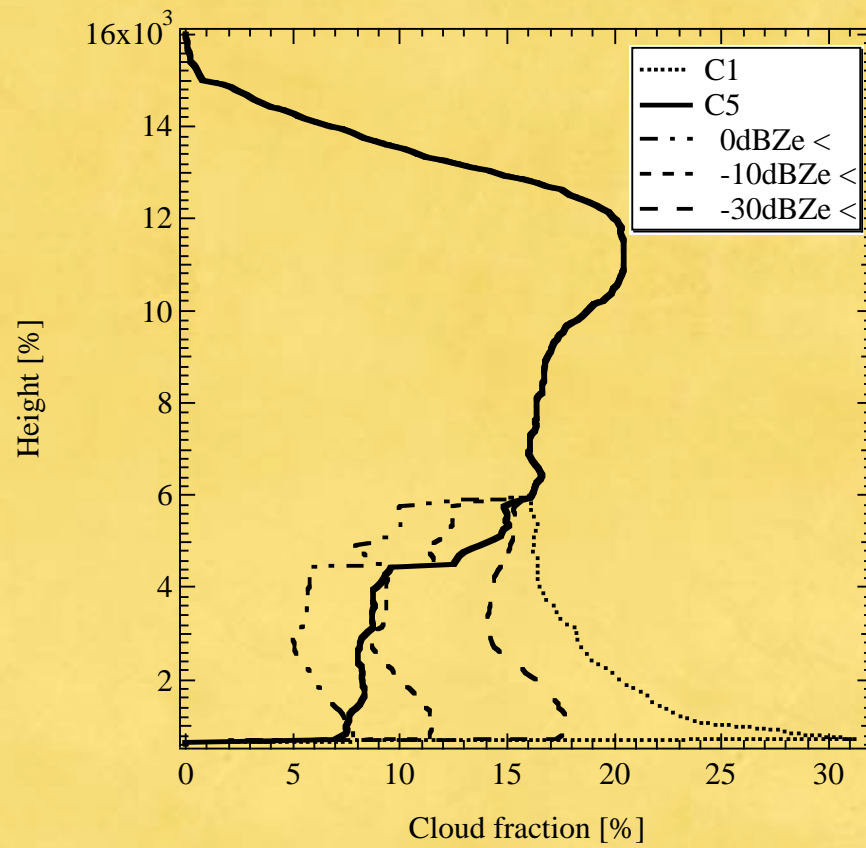


More homogeneous structure in vertical
direction compared with mid-latitude.

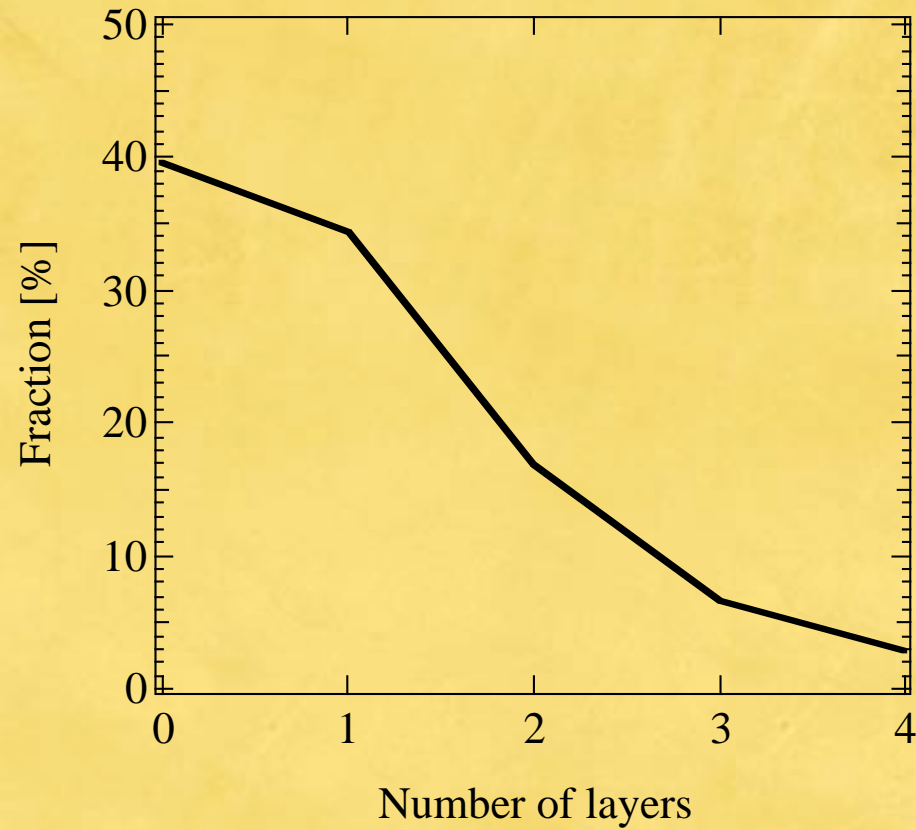
Maximum of cloud fraction
is 20% (smaller) and is located at 12km.

Tropical Western Pacific Ocean
near Japan, 2001)

Precipitation frequency



Number of cloud layers



6. Evaluation of the Clouds from the Atmospheric General Circulation Model

: Simulation of cloud radar and lidar signals from model outputs and validations of the GCM.

1. Model: CCSR-NIES-FRCGC GCM, T106(~100km) L20
NCEP/NCAR reanalysis data is used to nudge the GCM for each 6 hours. Four aerosols are treated in SPRINTARS (Takemura et al., JGR 2005) to simulate lidar signals.

To compare, sampling of the clouds for the grid along the cruise track is performed. Time resolution of output is 6 hours/40 minutes for comparison with observations.

2. Parameters used for the comparisons;

Large scale condensation (CF_{ls} : cloud fraction, grid mean liquid water content LWC_{ls} /ice water content IWC_{ls} (3d))

Cumulus convection parameterization (Cf_{cu} : cloud fraction (2d), LWC_{cu} , IWC_{cu})

$$CF_{total} = 1 - (1 - CF_{ls})(1 - Cf_{cu})$$

Radar reflectivity factor dBZe

Lidar backscattering coefficient

Simulation of CPR and lidar signals

Simulator of CPR and lidar signals (Okamoto et al., 2007,2008) for validation of numerical models.

CPR:

model output from GCM or JMA-NHM : cloud microphysics, precipitation (2D or 3D), cloud fraction. Attenuation of gas is included. (~5dB in tropics).

Lidar signals:

cloud part: consistent to CPR.

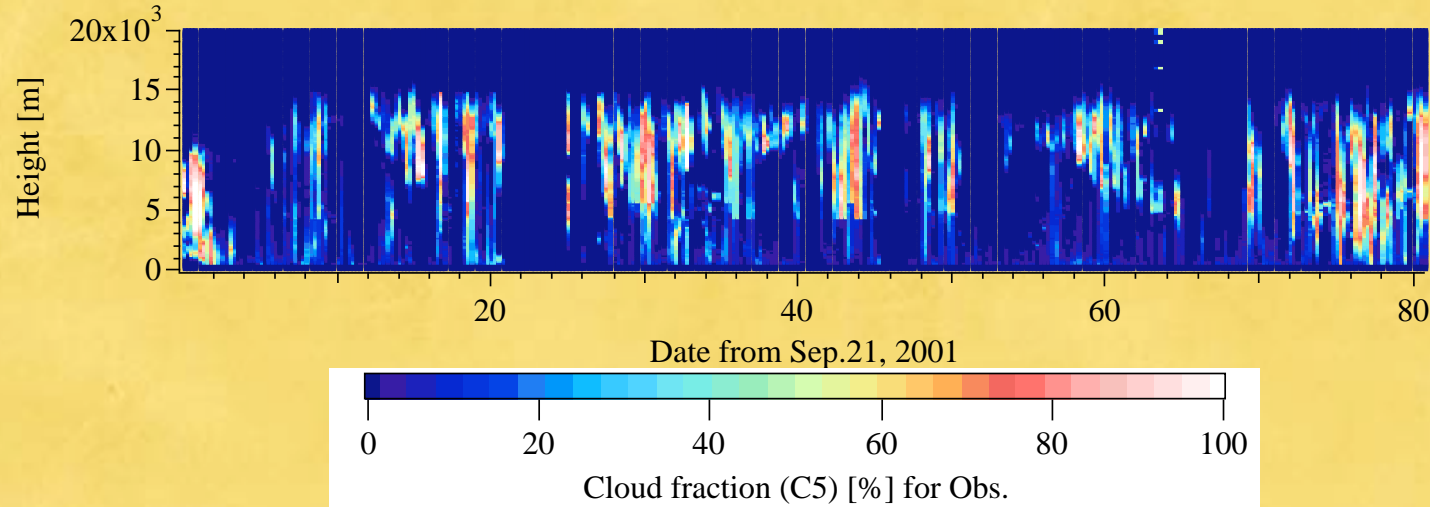
model out from SPTRINTARS (Takemura et al., 2005):

Four types of aerosols, sulfate, carbonaceous, sea-salt and dust are treated. Each extinction is produced and converted to backscattering coefficient.

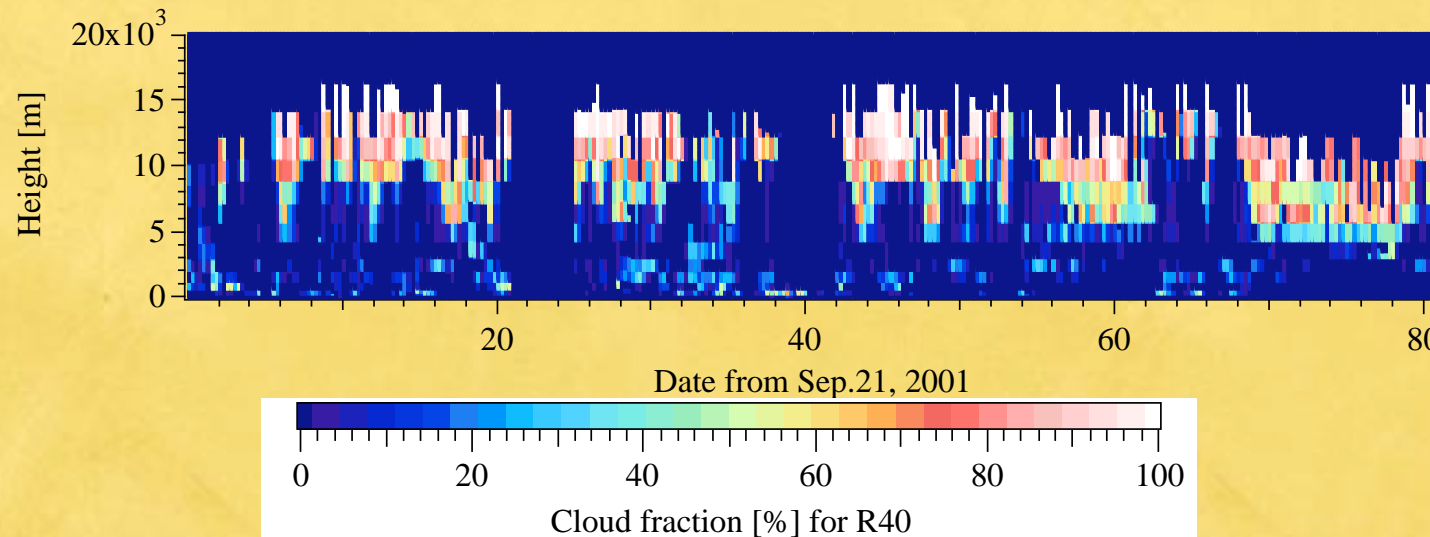
Use look up tables. (see also Nishizawa et al., 2007, 2008)

***CloudSAT/CALIPSO simulators are also developed.

Comparison of observed and simulated cloud fraction

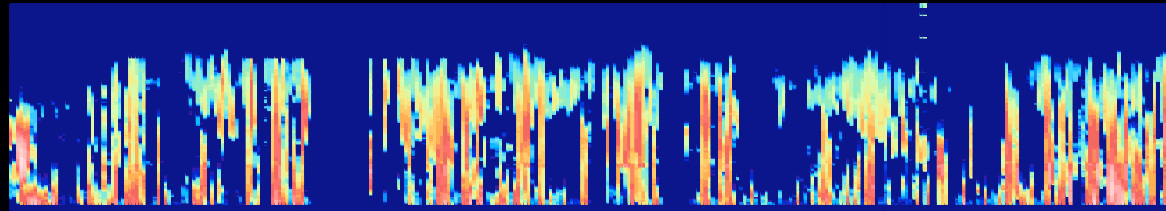


Observation

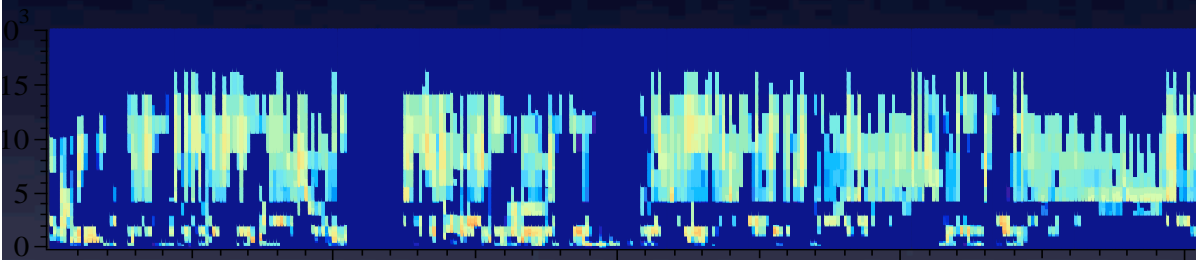
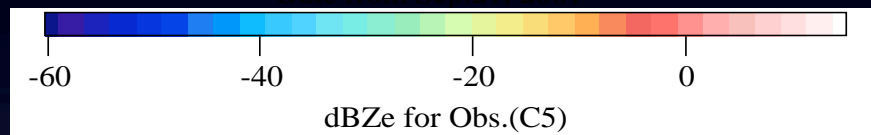


GCM

Example in Tropics, comparison of observed and simulated Ze in CCSR-NIES-FRCGC GCM



Observed Ze



Simulated Ze

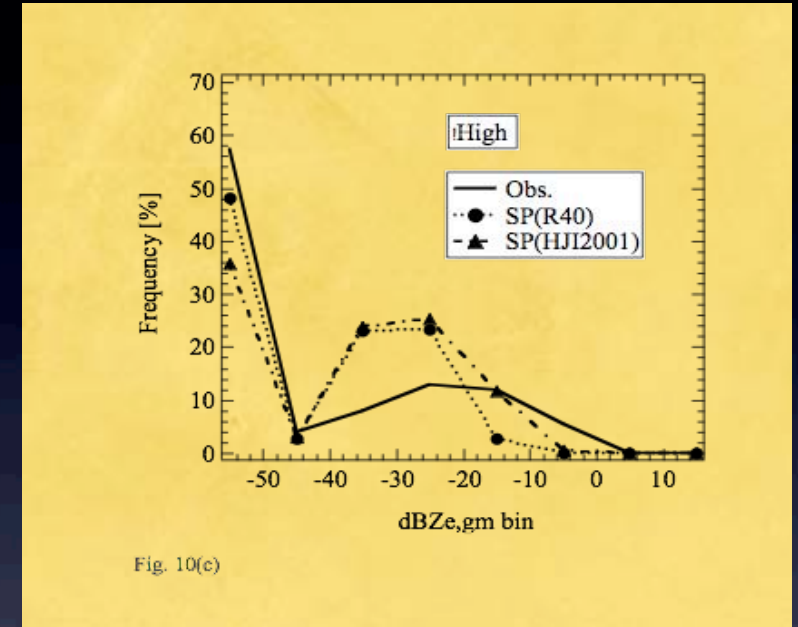
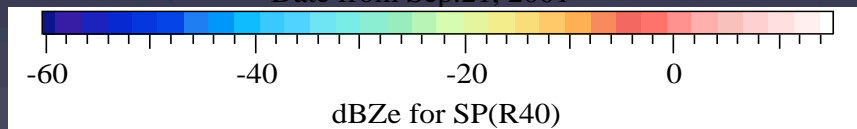
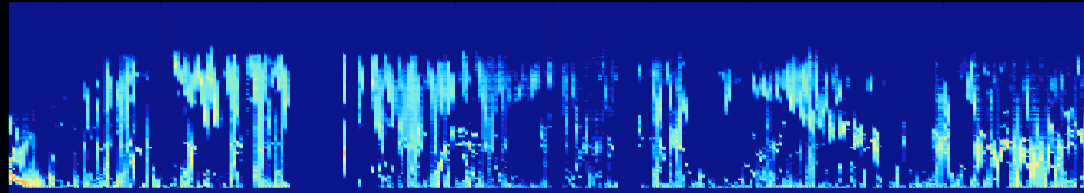


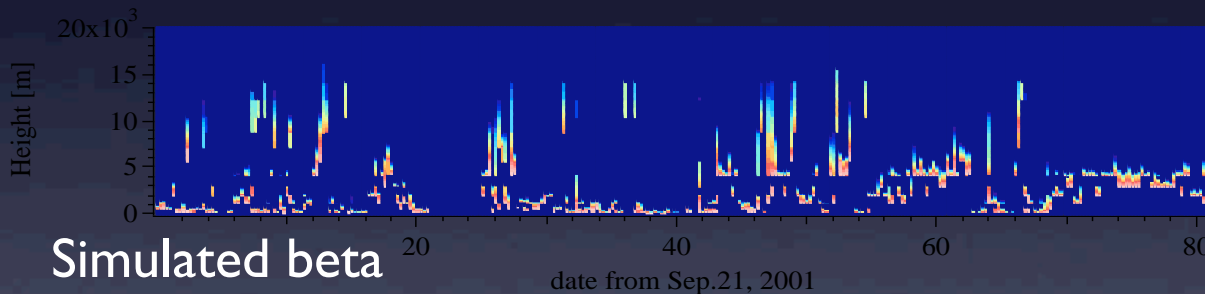
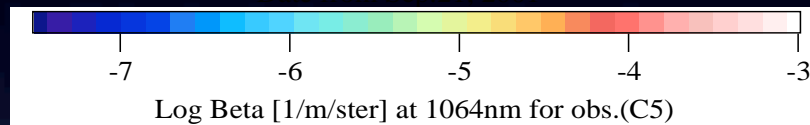
Fig. 10(c)

Simulated Ze has narrower distribution in high clouds and smaller signals.

Example in Tropics, comparison of observed and simulated beta in due to clouds



Observed beta



Simulated beta

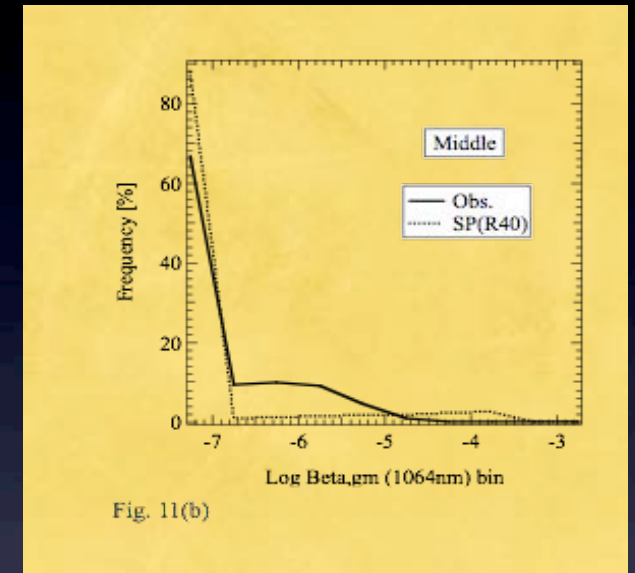
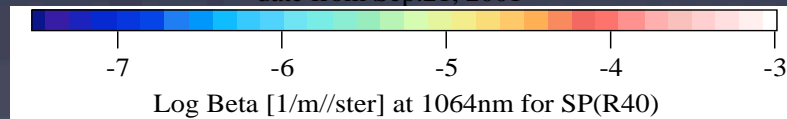
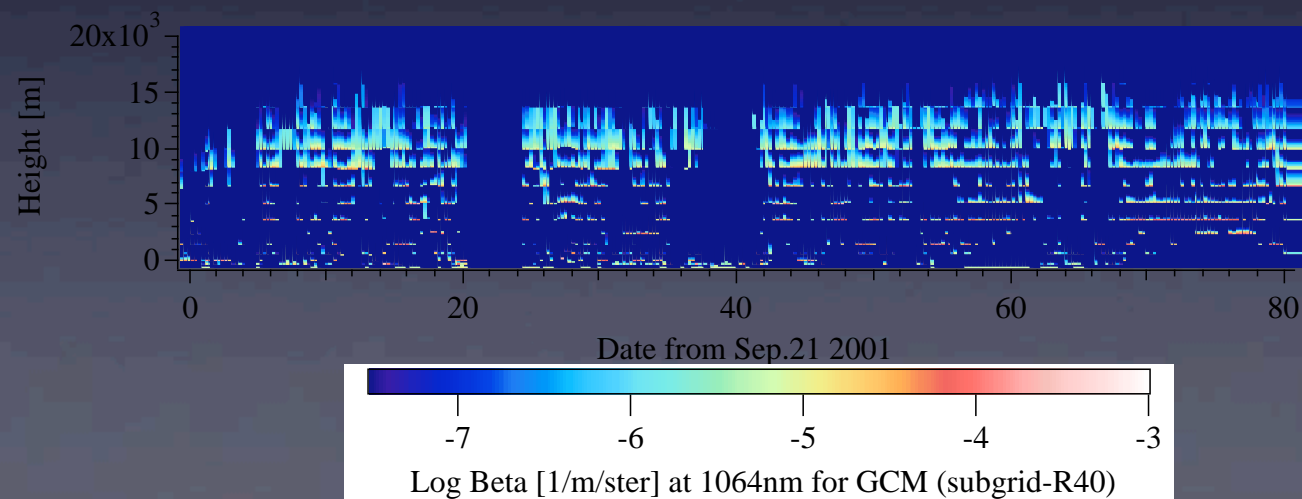
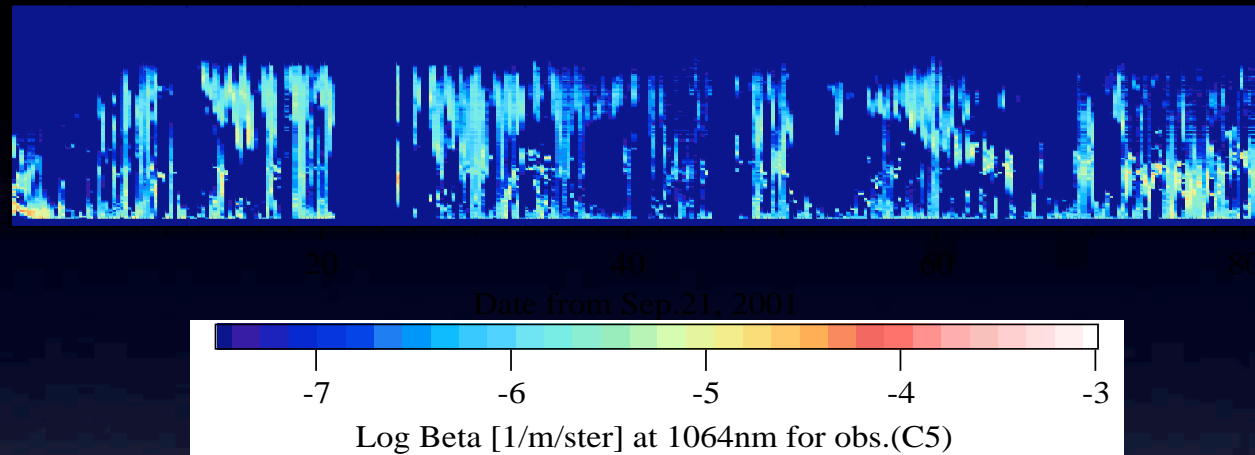


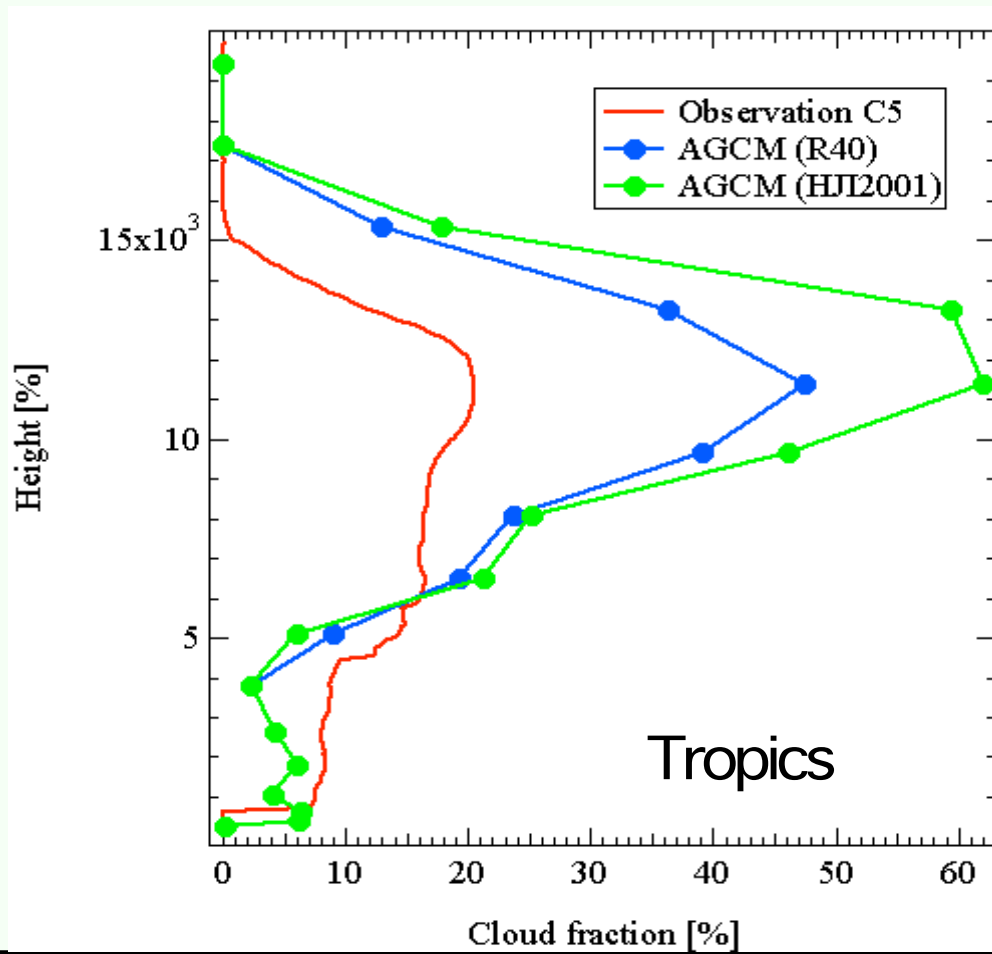
Fig. 11(b)

Simulated beta has larger beta in mid-level clouds.

Treatment of sub-grid scale clouds in the model



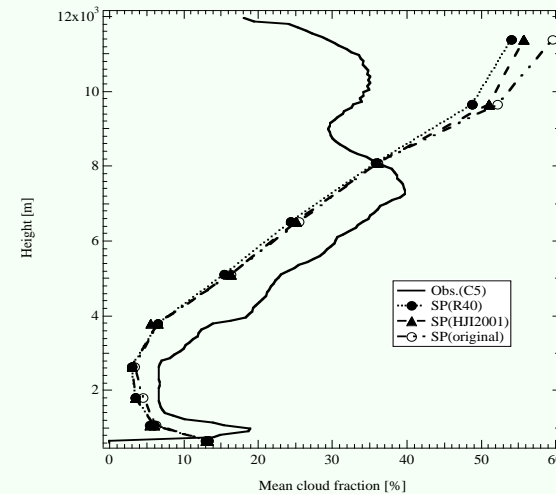
Comparison of cloud fraction between observation and GCM in Tropical Western Pacific Ocean In 2001.



Okamoto et al., 2008, JGR)

Problem in Upper/low-level cloud fraction

1. Cumulus convection parameterization?
2. Life cycle: dissipation process (terminal velocity and air motion)?



In mid-latitude

Okamoto et al., 2007, JGR)

7. Retrieval of ice microphysics by synergy use of CloudSat and CALIPSO data

Acknowledge: CloudSat science team and CALIPSO team

1. Motivation

Study of global distribution of ice microphysics from CloudSat and CALIPSO Synergy.

2. Problem.

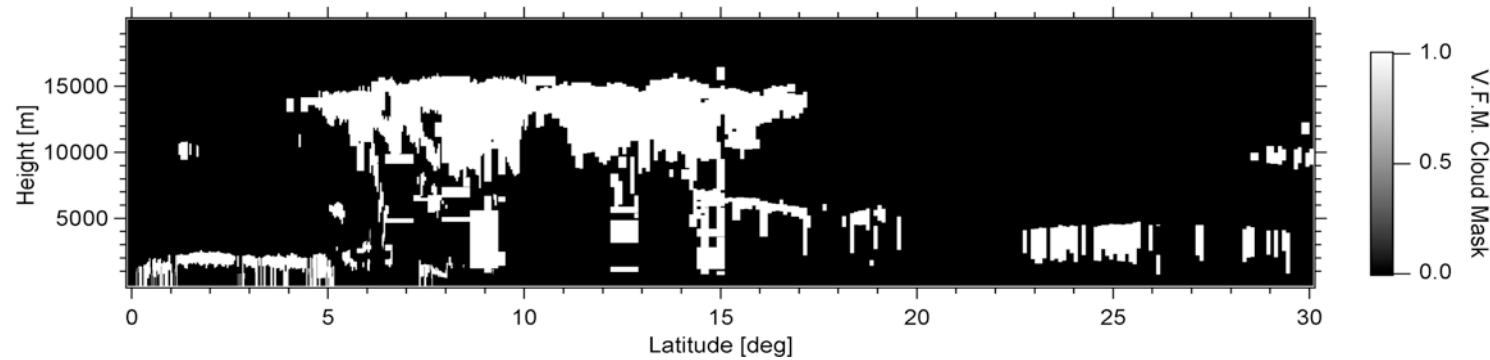
There are two issues in the analyses.

- 1) Vertical Feature mask (VFM) has some problem for the detection of clouds.
- 2) Specular reflection in CALIPSO is often observed (Winker). This turns out to be obstacle for the radar-lidar retrievals, i.e., not possible to find results or may contain large errors.

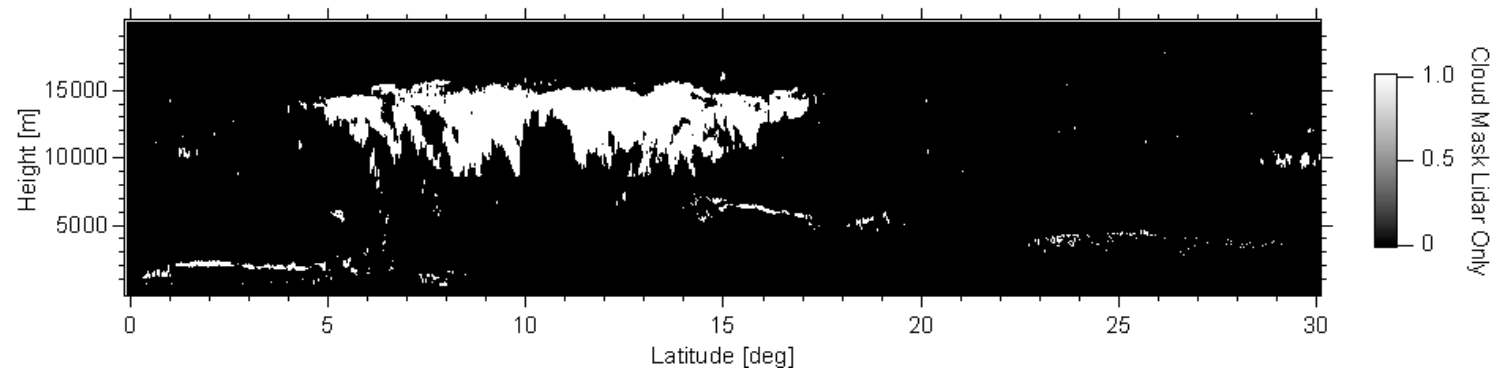
3. Efforts.

We develop cloud mask scheme for CALIPSO.

The radar-lidar algorithm (Okamoto et al., 2003 JGR) is modified in order to treat specular reflection.

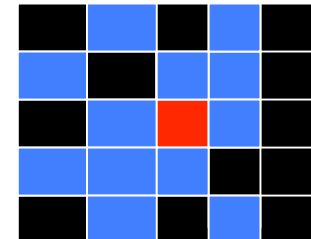


NASA Langely's Vertical Feature mask (VFM)

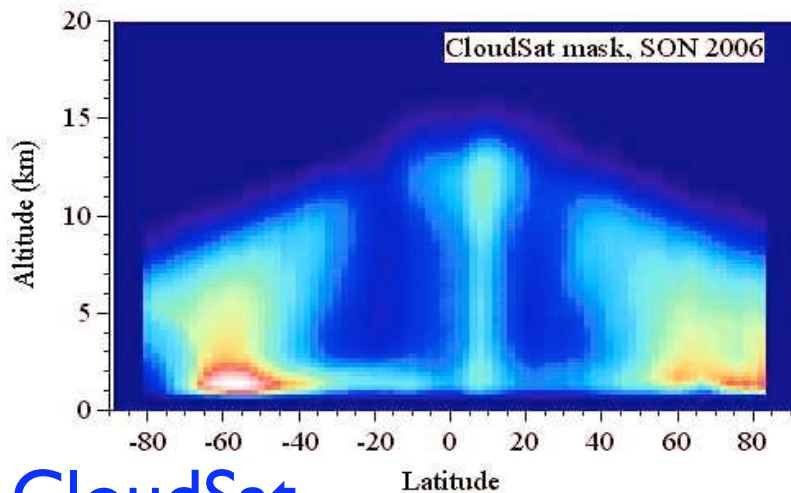


Cloud mask for CALIPSO (TU mask)

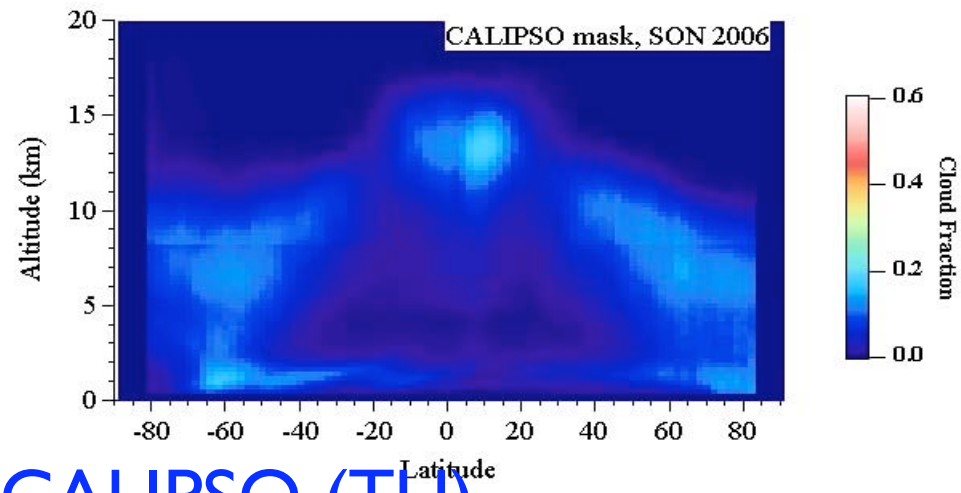
- (1) Signal > threshold value
- (2) More than 13 pixels satisfy the criterion (1) among surrounding 5*5 (=25) pixels.



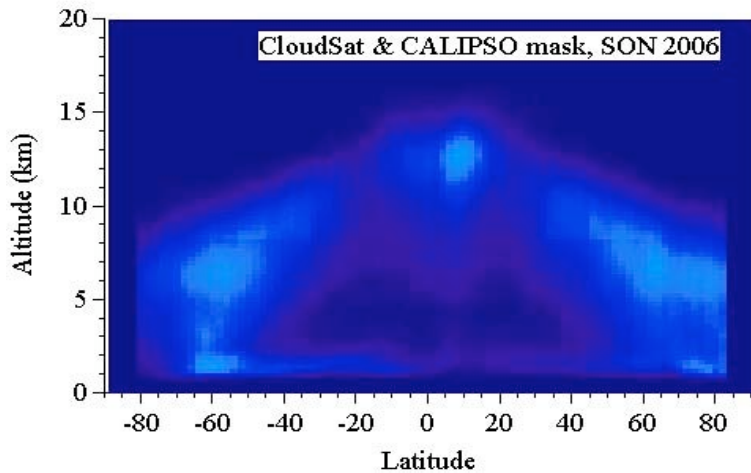
Zonal mean cloud frequency of occurrence from CloudSat and CALIPSO in September to November 2006



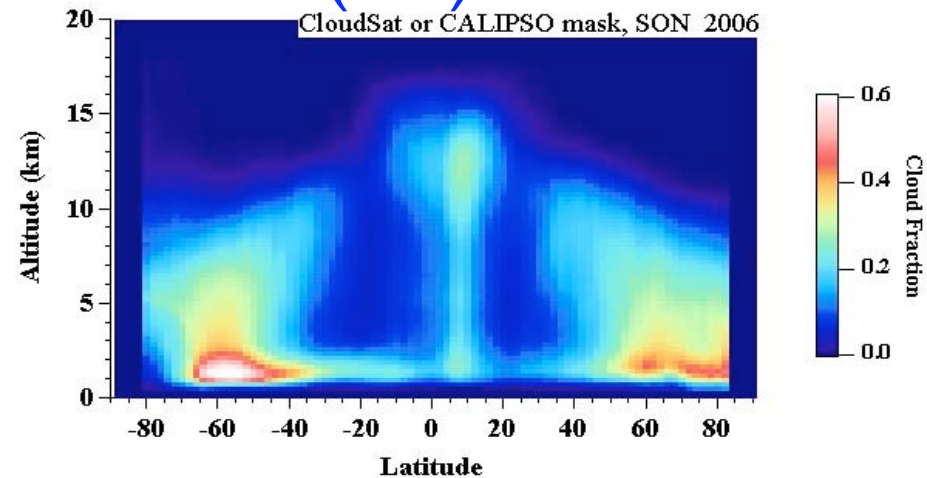
CloudSat



CALIPSO (TU)



CloudSat&CALIPSO



CloudSat or CALIPSO(TU)

(Hagihara et al., 2008)

I. Characteristic of the radar-lidar algorithm

modified from Okamoto et al., 2003 JGR.

- (1) Input observables are Z_e , β and depolarization ratio.
- (2) Forward type algorithm.

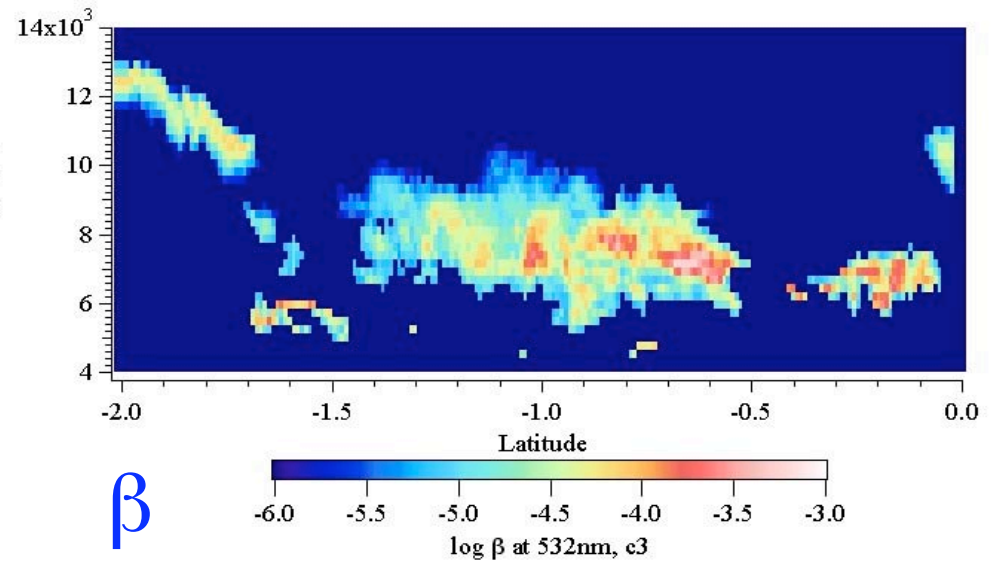
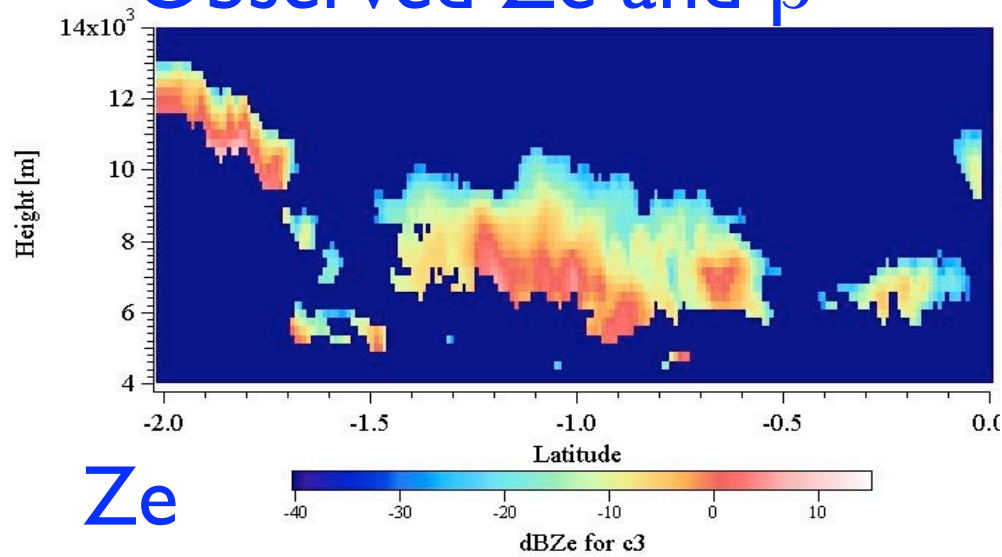
Extinction to backscattering ratio is not assumed to be constant as in Klett type one.

New feature is that the ratio of horizontally oriented crystals to the total number is also retrieved. In addition to the former look up tables, new LUTs introduced for oriented crystals, i.e., two radar (Z_e , extinction for 10000 reff bins) and two lidar (beta and extinction for 10000 reff bins).

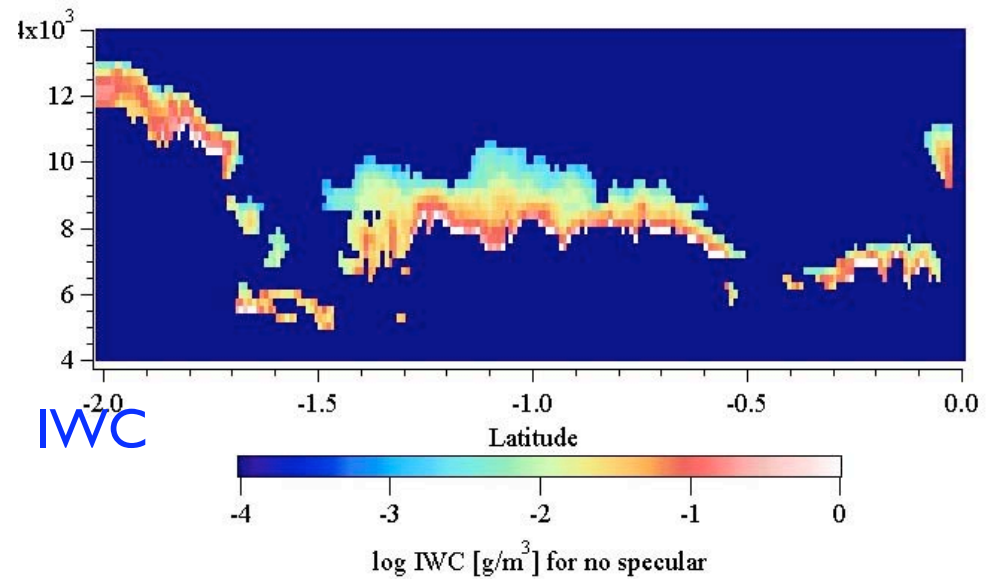
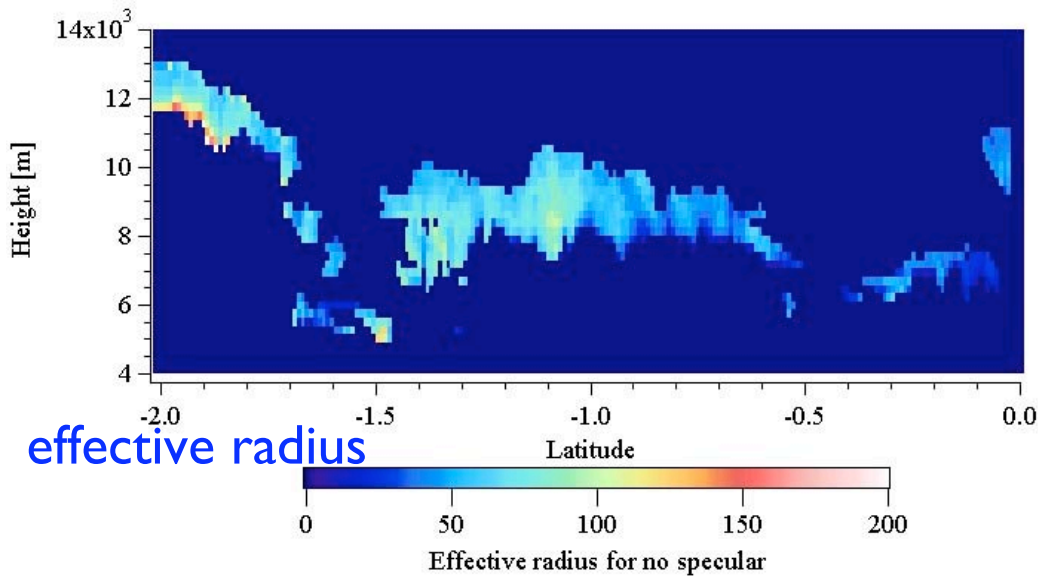
The algorithm retrieves effective radius and IWC that match observables. Z_e and extinction for oriented crystals are calculated by the discrete dipole approximation (Sato and Okamoto 2006 JGR). β and extinction are estimated by the modified Kirchhoff approximation (Iwasaki and Okamoto 2001, Appl. Opt.)

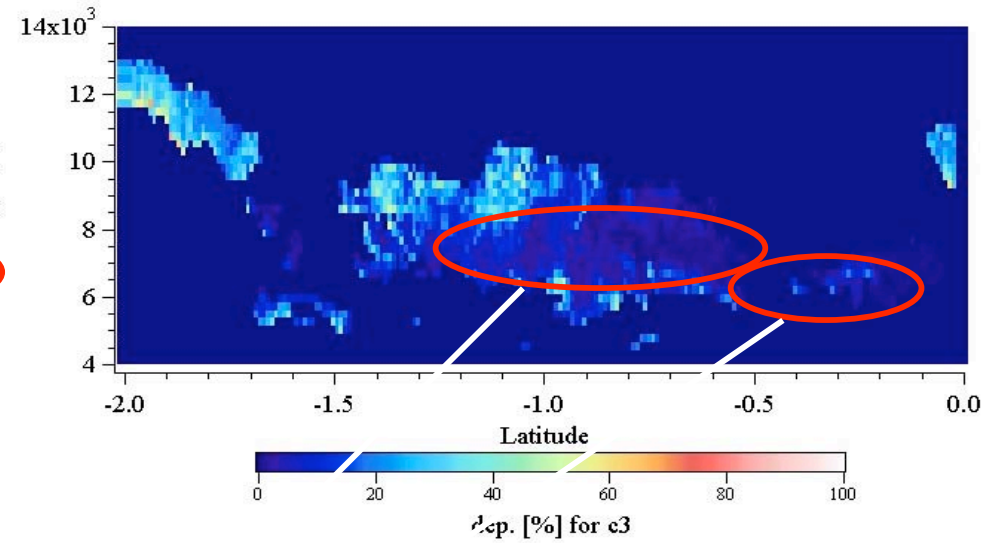
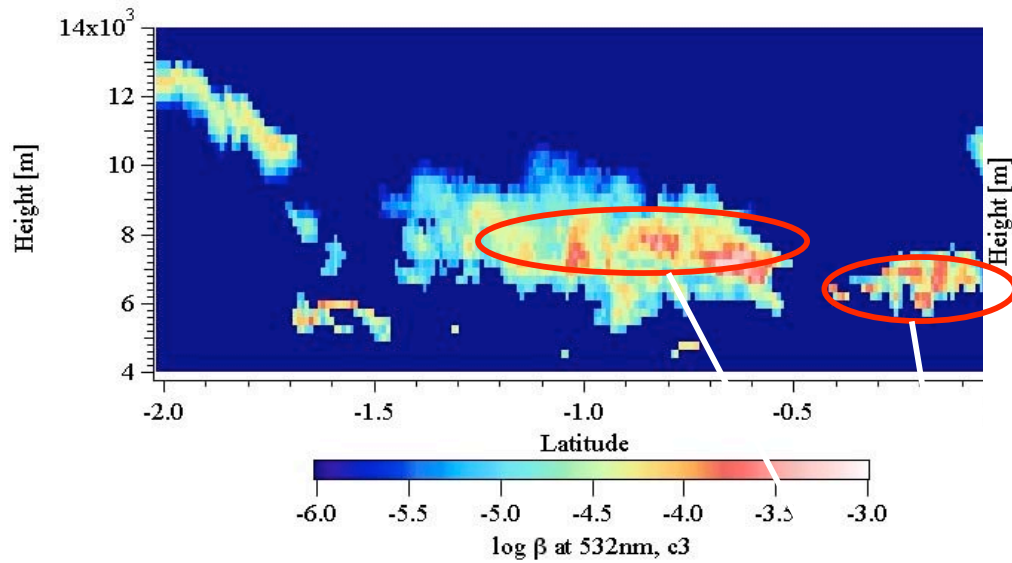
- (3) Attenuation correction is carried out by the retrieved microphysics.

Observed Ze and β



Retrieved effective radius and IWC from our conventional algorithm

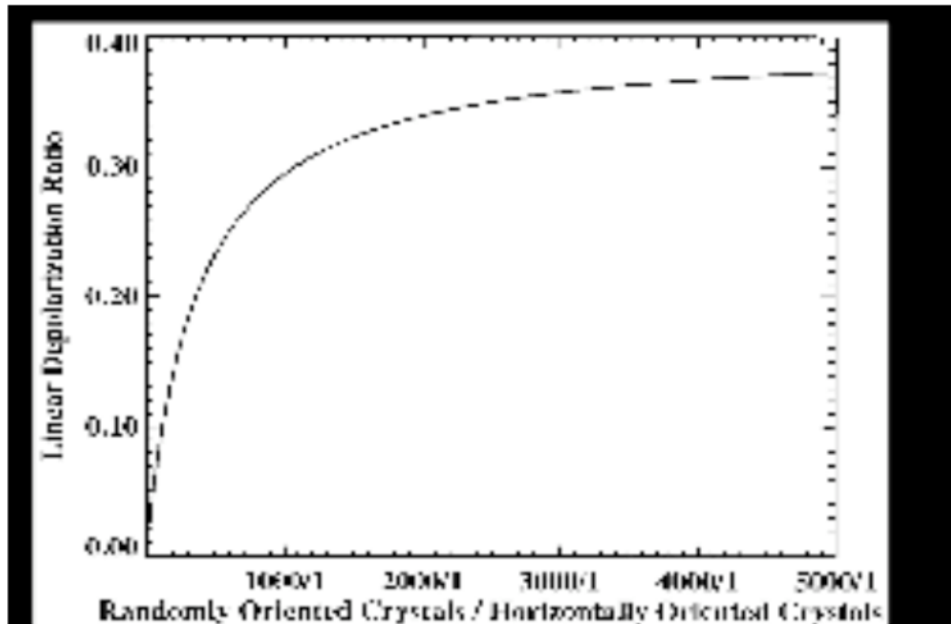




Large backscattering and low depolarization ratio denote specular reflection.

We found difficulties in the retrieval of microphysics
 In these regions when our conventional algorithm is applied .

How to treat specular reflection in lidar signals.

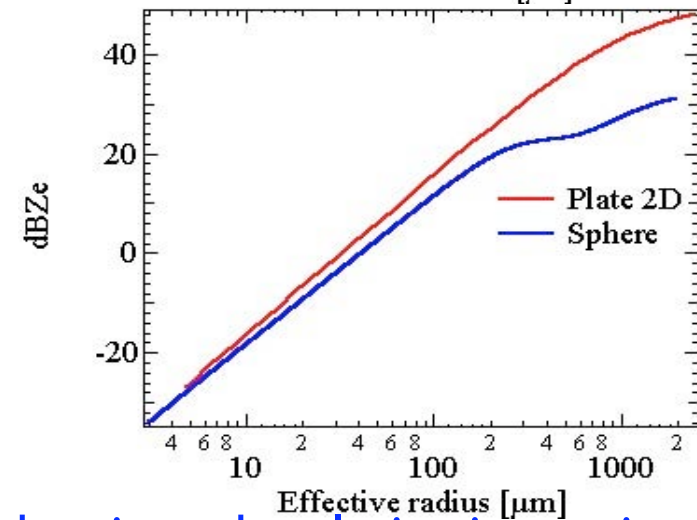
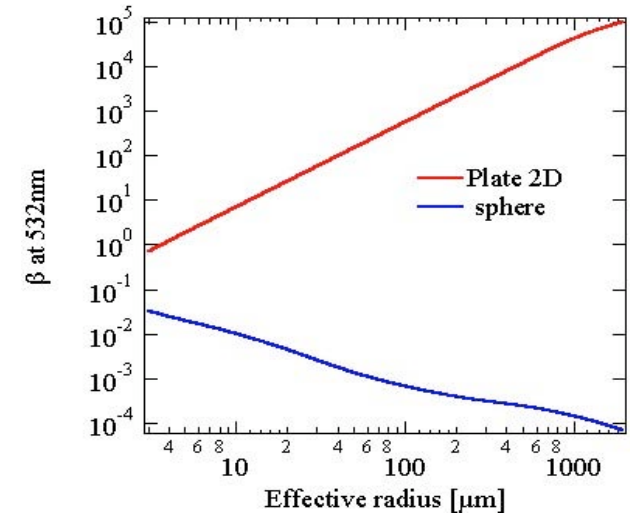
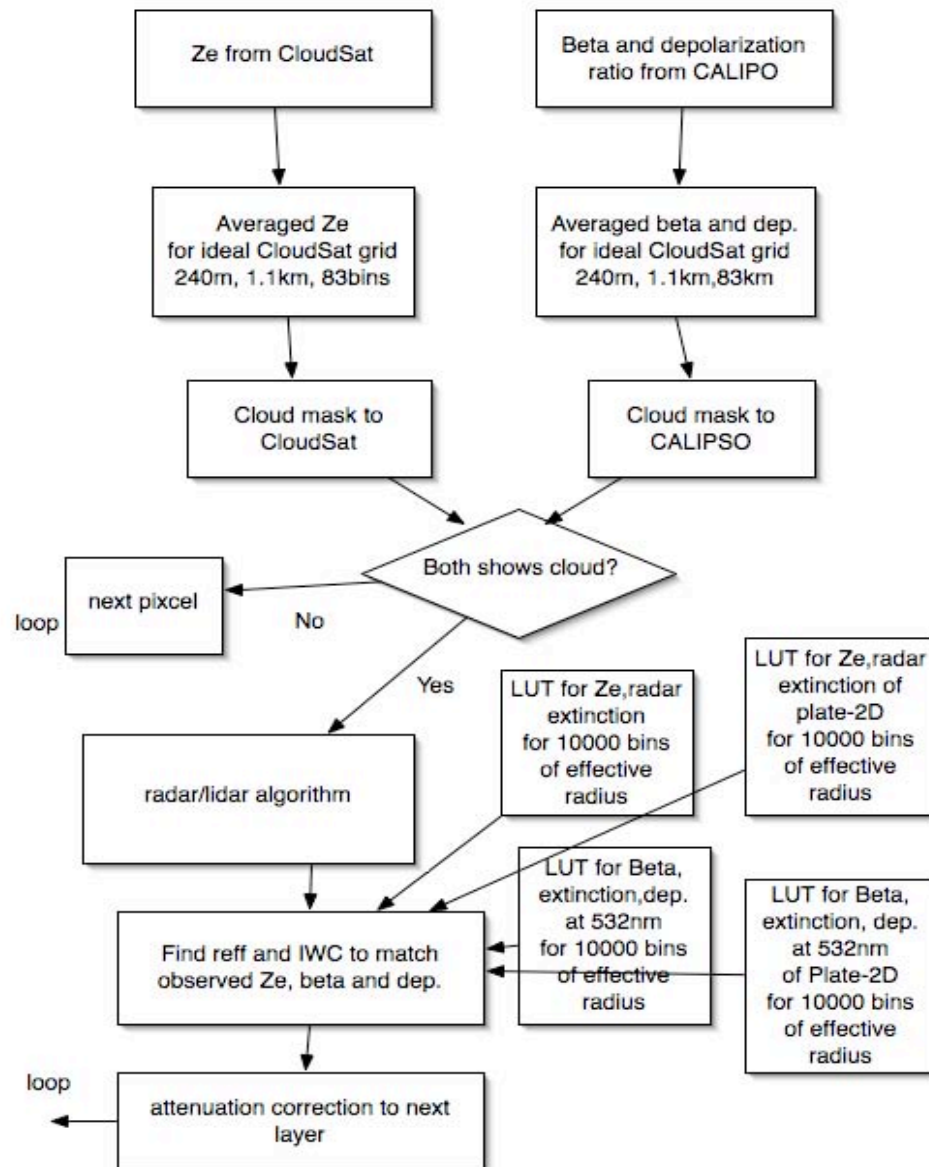


Sassen and Benson (2001, JAS)

Sassen and Benson (2001, JAS) estimated the ratio X of number concentration of randomly oriented crystals and that of horizontally oriented crystals from depolarization ratio, assuming the randomly oriented crystals have $dep.=0.4$ and that for horizontally oriented crystal $=0$. $\beta(2d) / \beta(3d) = 360$.

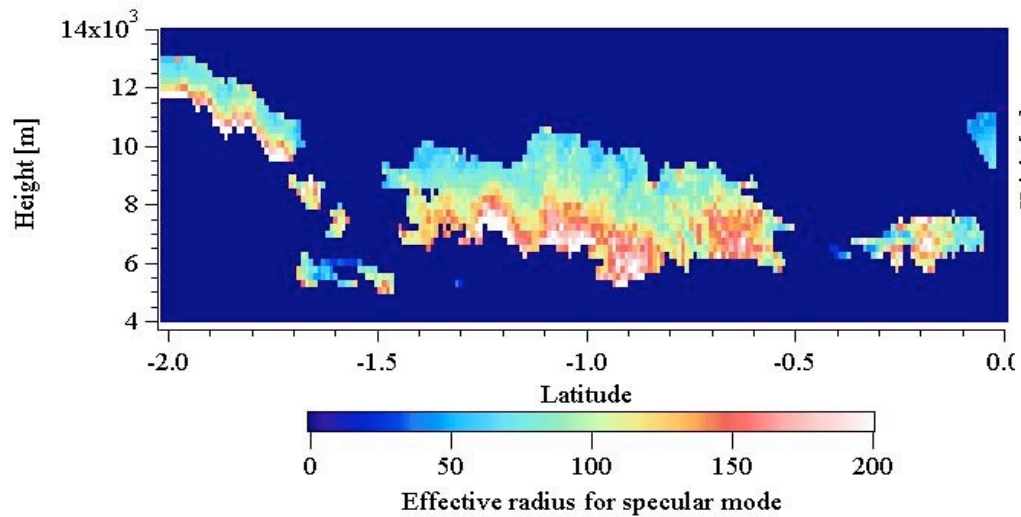
(They stated 360 might be lower than actual).

Algorithm flow

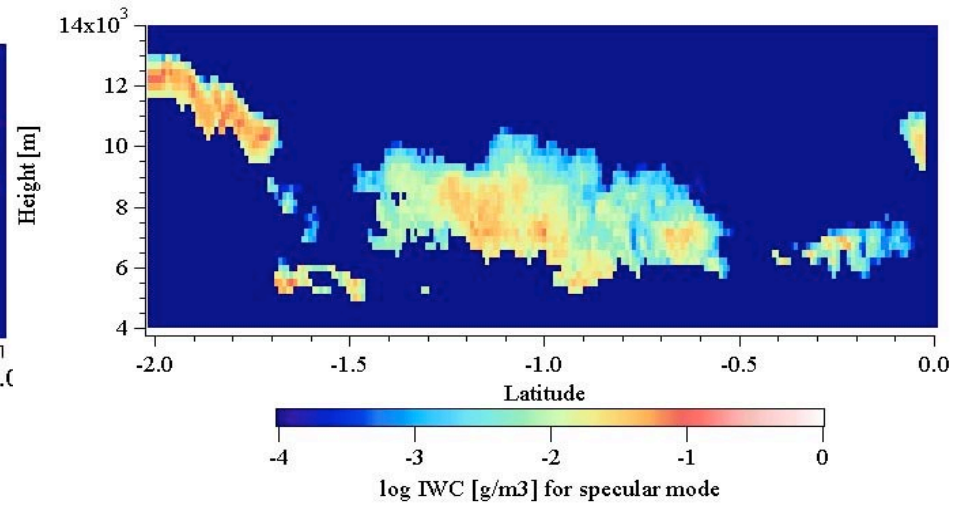


The ratio $\beta(2d) / \beta(3d)$ depends on size. Thus for the given depolarization ratio, $N(2d)/N_t$ depends on size.

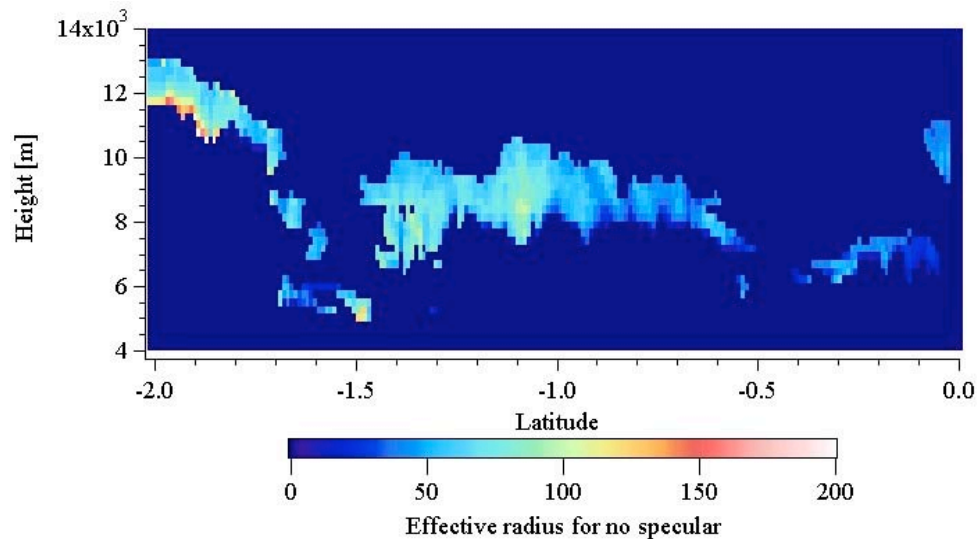
Results from the new radar-lidar algorithm



effective radius from new algorithm

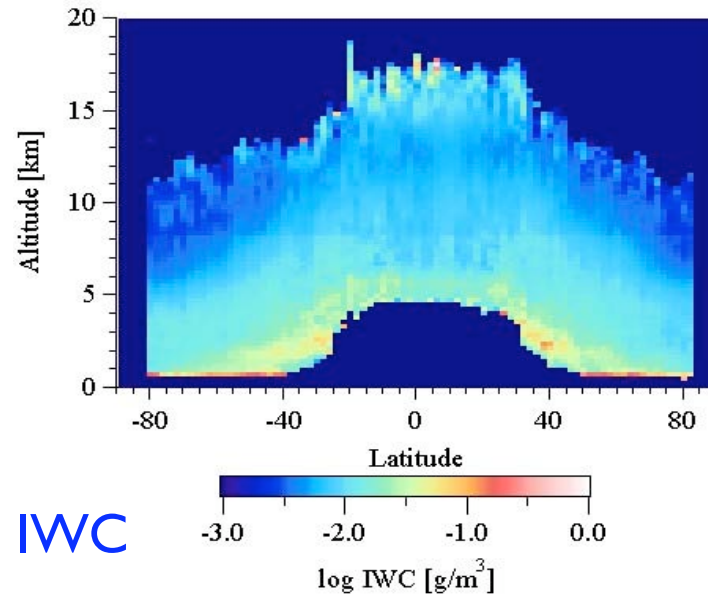
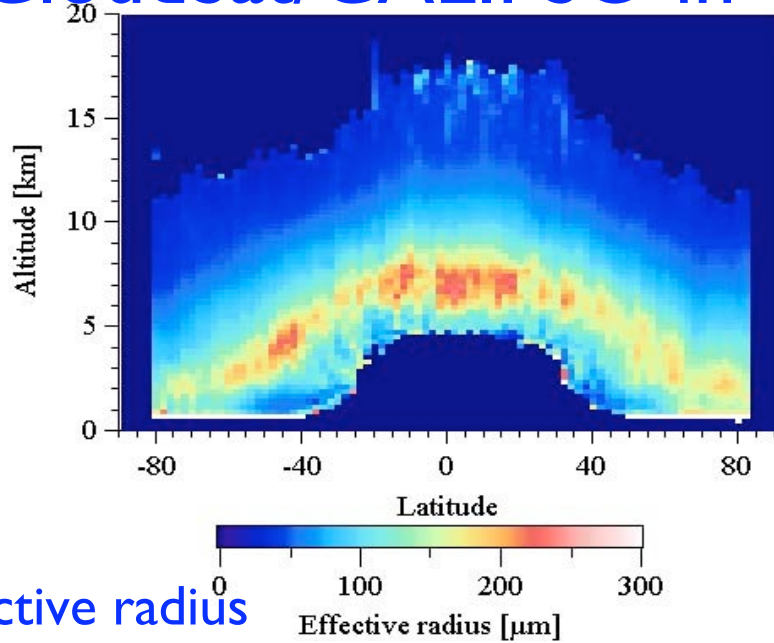


IWC from new algorithm



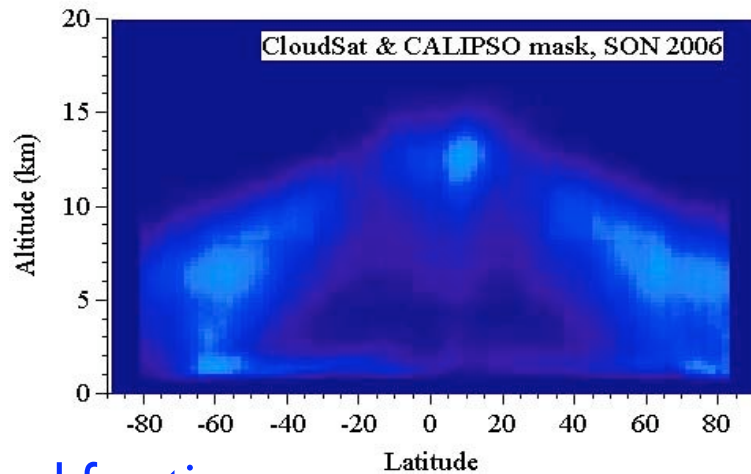
effective radius from conventional algorithm

Zonal mean of ice microphysics from CloudSat/CALIPSO in Oct.2006



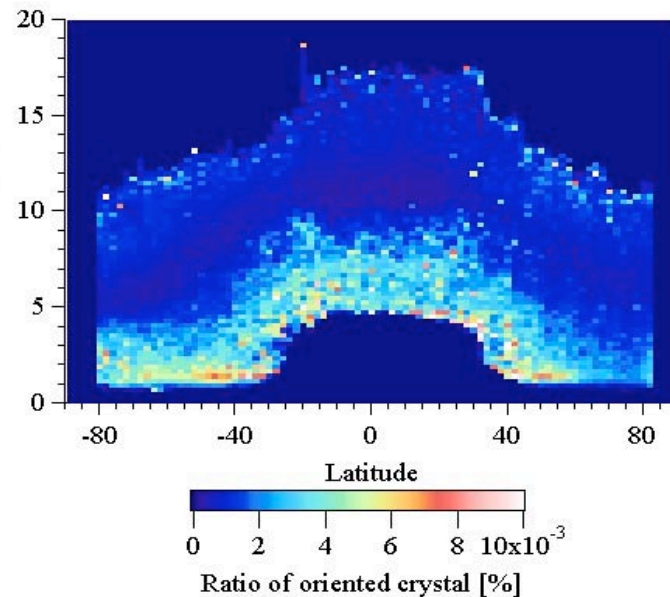
IWC

Effective radius



Cloud fraction

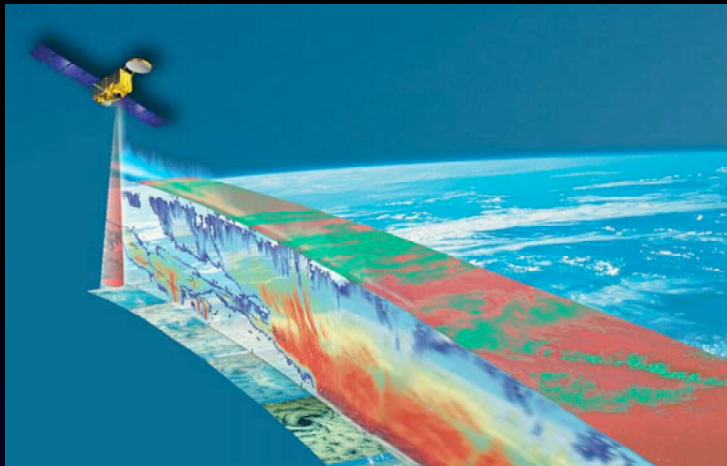
$N(2d)/N_t$



Summary

0. VFM seems to overestimate cloud fraction and new cloud mask for CALIPSO is developed.
1. We develop new radar-lidar retrieval algorithm that can treat the mixture of oriented crystals and random ones.
2. We use the modified Kirchoff approximation for lidar specular reflection and discrete dipole approximation for Z_e for scattering signatures of oriented crystals.
3. Unless look up tables of oriented crystals are implemented, it is not possible to analyze specular region.
4. Zonal mean of ice cloud microphysics is derived. There are small particles ($\sim < 50\mu\text{m}$) in the upper layers. The size in specular region is large $\sim 200\mu\text{m}$.
5. Z_e -IWC relation applied to CloudSat is carried out and compared with this study.

7. Future satellite mission with radar

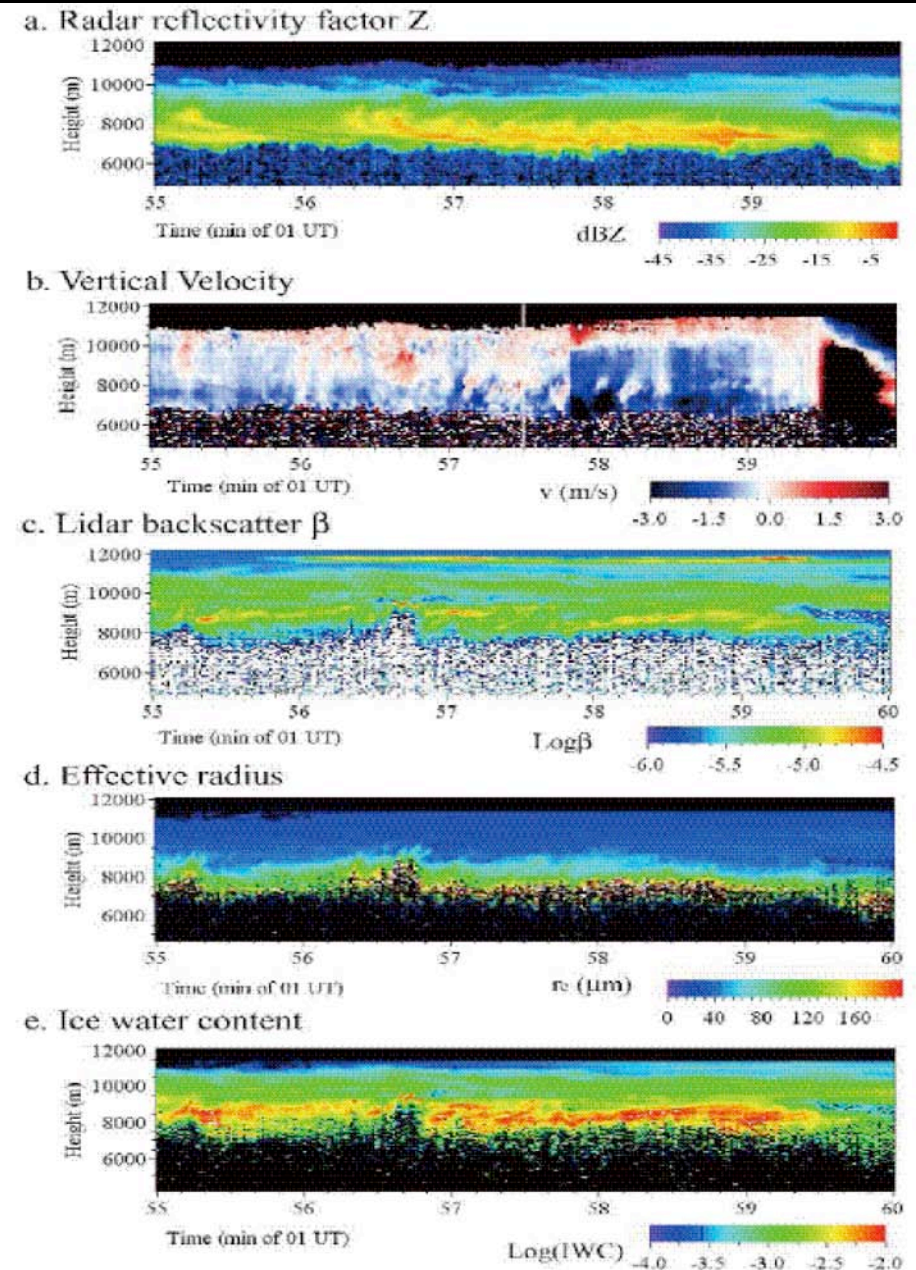


Beyond CloudSAT/CALIPSO

EarthCARE in 2013 (ESA-JAXA mission)

- Cloud radar with Doppler function,
- High spectral resolution lidar
- Broad Band Radiometer
- Multi spectral Imager

We develop algorithms for clouds and aerosols for EarthCARE with JAXA.



Summary

- 1) We performed shipbased radar and lidar observations in Tropics, mid-latitude and polar regions from 2001 to present.
- 2) We develop the radar and lidar signal simulator for shipbased radar/lidar and for CloudSAT and CALIPSO from the model outputs. We tested the cloud fields from the ship- and satellite-borne with those simulated from SPRINTARS (GCM).

Findings are;

General pattern of clouds and aerosols is reasonably reproduced in mid-latitude and less agreements in the tropics. Overestimation of high level clouds in simulation than in observations, due to the over-prediction of frequency of deep convection.

The effective radius is too small in mid- and high level clouds.

The simulated low clouds tend to be too thick.

The Mirai data are distributed via ftp server from us.

2) Several retrieval algorithms have been developed for microphysics of clouds and aerosols from synergy use of radar/lidar data. Our radar/lidar and radar-Doppler algorithms show the smallest errors (bias/dispersion) among teams through blind tests (Heymsfield et al., JAMC 2007 in press).

3) Correction of specular reflection is implemented and seems to improve the applicability of the radar/lidar method.

4) Validation of the algorithms of CloudSAT/CALIPSO against the in-situ measurements are tried. Some agreements and some under-estimation.

References

Heymsfield, A. J., A. Protat, R. Austin, D. Bouniol, R. Hogan, J. Delaue, H. Okamoto, K. Sato, G. Zadelhoff, D. Donovan, Z. Wang, Testing and Evaluation of Ice Water Content Retrieval Methods using Radar and Ancillary Measurements, *J. Appl. Meteor.Clim*, 2007 (in press)

Nishizawa, T., H. Okamoto, N. Sugimoto , I. Matsui, A. Shimizu , K. Aoki, An algorithm that retrieves aerosol properties from dual-wavelength polarized lidar measurements, *J. Geophys.Res.*, 112, D06212, doi:10.1029/2006JD007435, 2007

Nishizawa, T., H. Okamoto, N. Sugimoto , I. Matsui, A. Shimizu, Aerosol retrieval from dual-wavelength polarization lidar measurements taken during the MR01K02 cruise of the RV Mirai and validation of a global aerosol transport model (*J. Geophys. Res.*, (2008 in press)

Okamoto, H., Information content of the 95GHz cloud radar signals: theoretical assessment of effect of non-sphericity by the discrete dipole approximation, *Geophys. Res.*, 107(D22), 4628, doi:10.1029/2001JD001386.

Okamoto, H., S. Iwasaki, M. Yasui, H. Horie, H. Kuroiwa, and H. Kumagai, An algorithm for retrieval of cloud microphysics using 95-GHz cloud radar and lidar. *J. Geophys. Res.*, 108(D7), 4226, doi:10.1029/2001JD001225, 2003

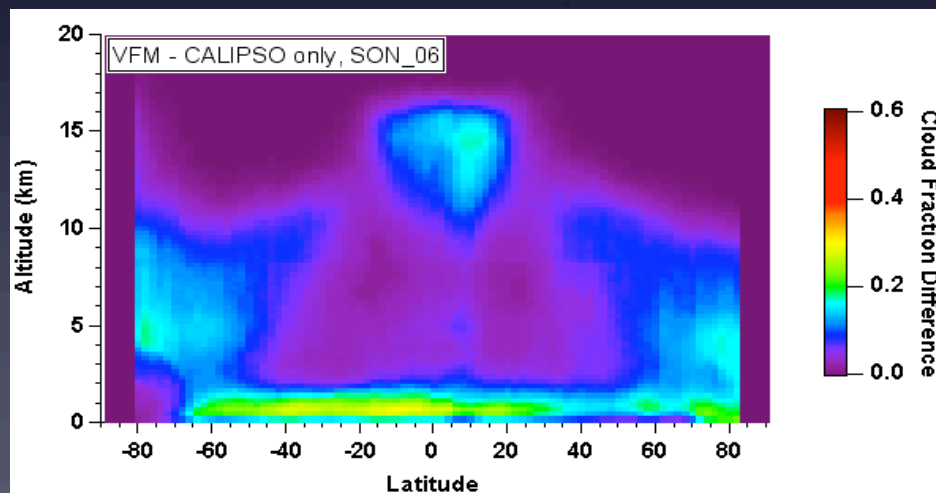
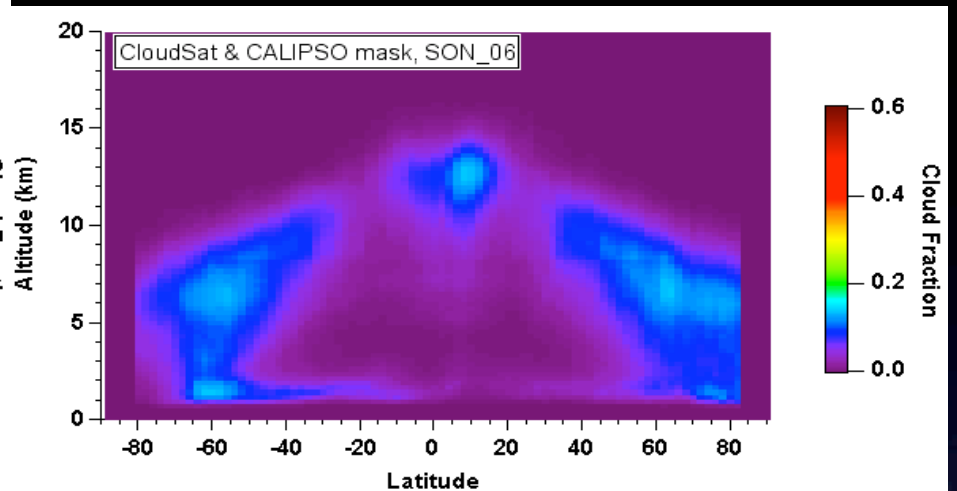
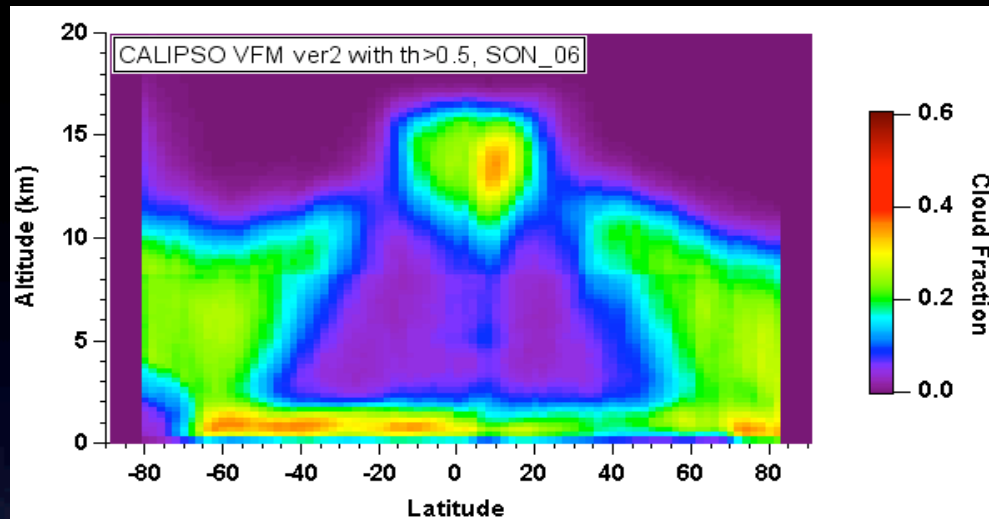
Okamoto, H., T. Nishizawa, T. Takemura, H. Kumagai, H. Kuroiwa, N. Sugimoto, I. Matsui, A. Shimizu, A. Kamei, S. Emori, and T. Nakajima, Vertical cloud structure observed from shipborne radar and lidar, Part (I) : mid-latitude case study during the MR01/K02 cruise of the R/V Mirai, *J. Geophys. Res*, 112, D08216, doi:10.1029/2006JD007628, 2007

Okamoto, H., T. Nishizawa, T. Takemura, K. Sato, H. Kumagai, Y. Ohno, N. Sugimoto, I. Matsui, A. Shimizu, and T. Nakajima, Vertical cloud properties in Tropical Western Pacific Ocean: Validation of CCSR/NIES/FRCGC GCM by ship-borne radar and lidar, *J. Geophys. Res.*, (2008 in press)

Sato, K., and H. Okamoto (2006), Characterization of Ze and LDR of nonspherical and inhomogeneous ice particles for 95-GHz cloud radar: Its implication to microphysical retrievals, *J. Geophys. Res.*, 111, D22213, doi:10.1029/2005JD006959.

Sato, K., Okamoto, M. Yamamoto, H. S. Fukao, Kumagai, Y. Ohno, H. Horie, and M. Abo 95-GHz Doppler radar and lidar synergy for simultaneous ice microphysics and in-cloud vertical air motion retrieval. *J. Geophys. Res.*, (2008, in press)

Backup



Mirai MR06-05 cruise from Oct.4, 2006 to Jan 17, 2007 test cases: CloudSat/CALIPSO in Oct.-Nov. 2006



CloudSAT/CALIPSO overpasses
close to Mirai cruise track.

In the leg1. (Oct.4-Nov. 27,
2006), there are 7 overpasses;
Oct.4, 3:35UTC (40.6°N, 141.5°E)

Oct. 24, 20:15UTC (0°N, 79°E)

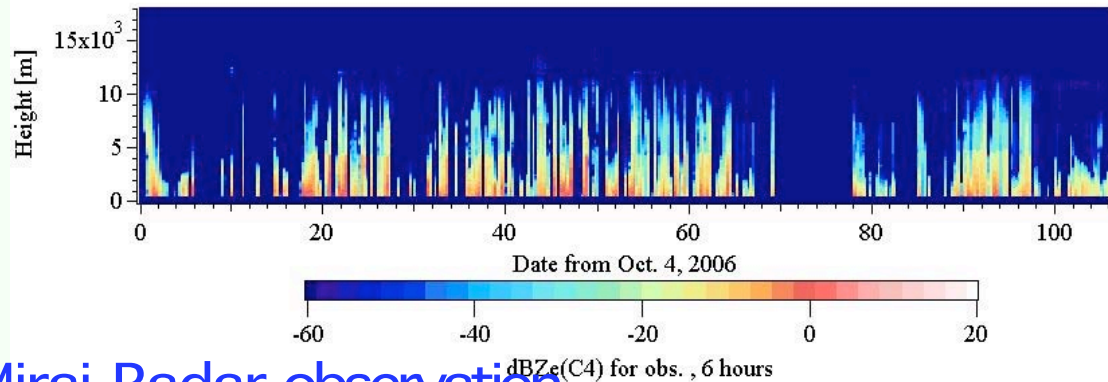
Oct. 29, 8:15 (0°N, 80.5°E)

Nov. 5, 8:20 (0°N, 80.5°E)

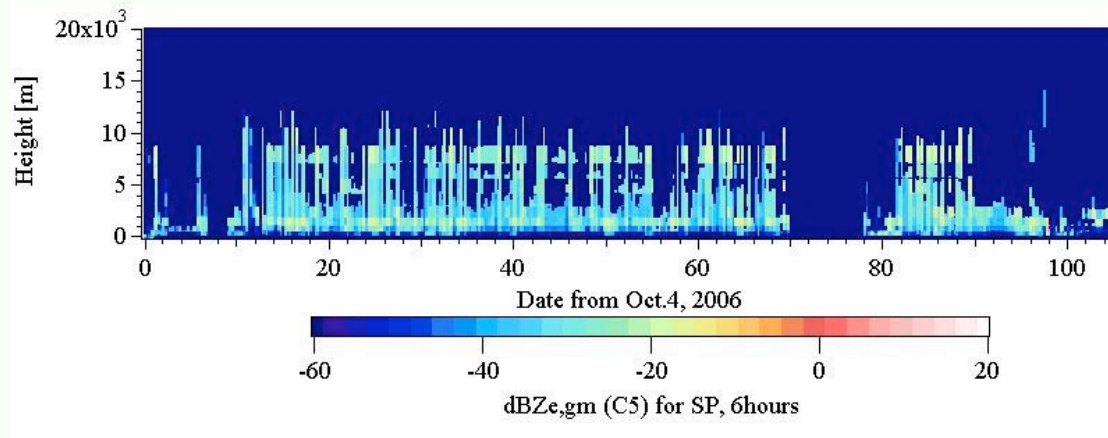
Nov.21, 8:20 (0°N, 80.5°E)

Nov. 25, 20:15 (0°N, 80.5°E)

Comparison of radar reflectivity factor Z_e by Mirai-radar observation and simulated one from SPRINTARS.

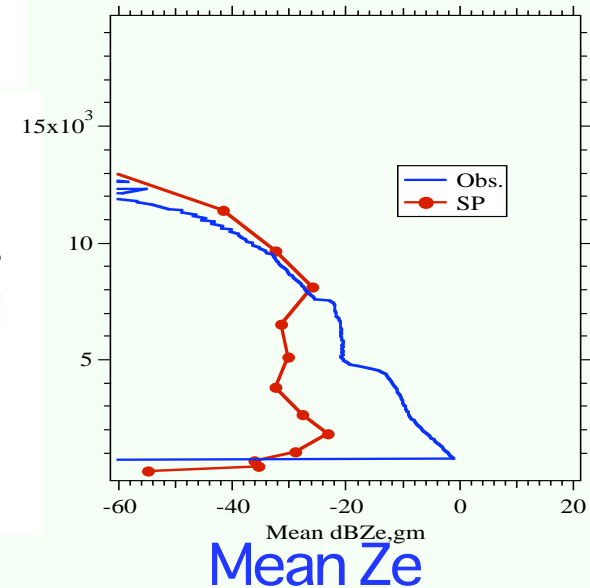


Mirai-Radar observation



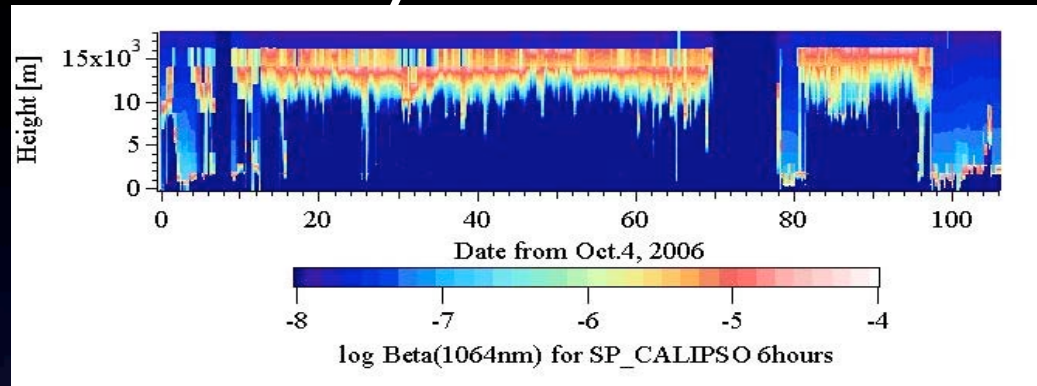
Simulated signal for Mirai-radar based on SPRINTARS

General pattern is reasonably simulated. Z_e is larger above 10km and smaller at 5-8km. Above 10km, sensitivity is not sufficient? Uncertainties!

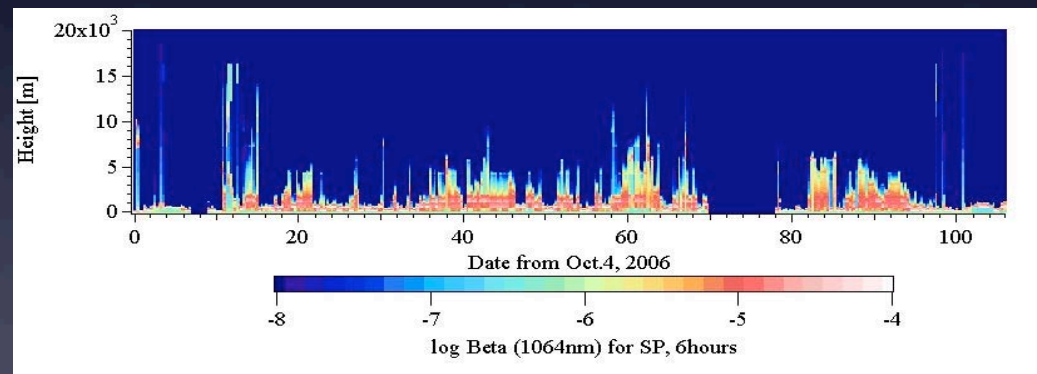


Mean Z_e

Differences between space-borne and ground or ship-borne systems: based on AGCM-SPRINTARS

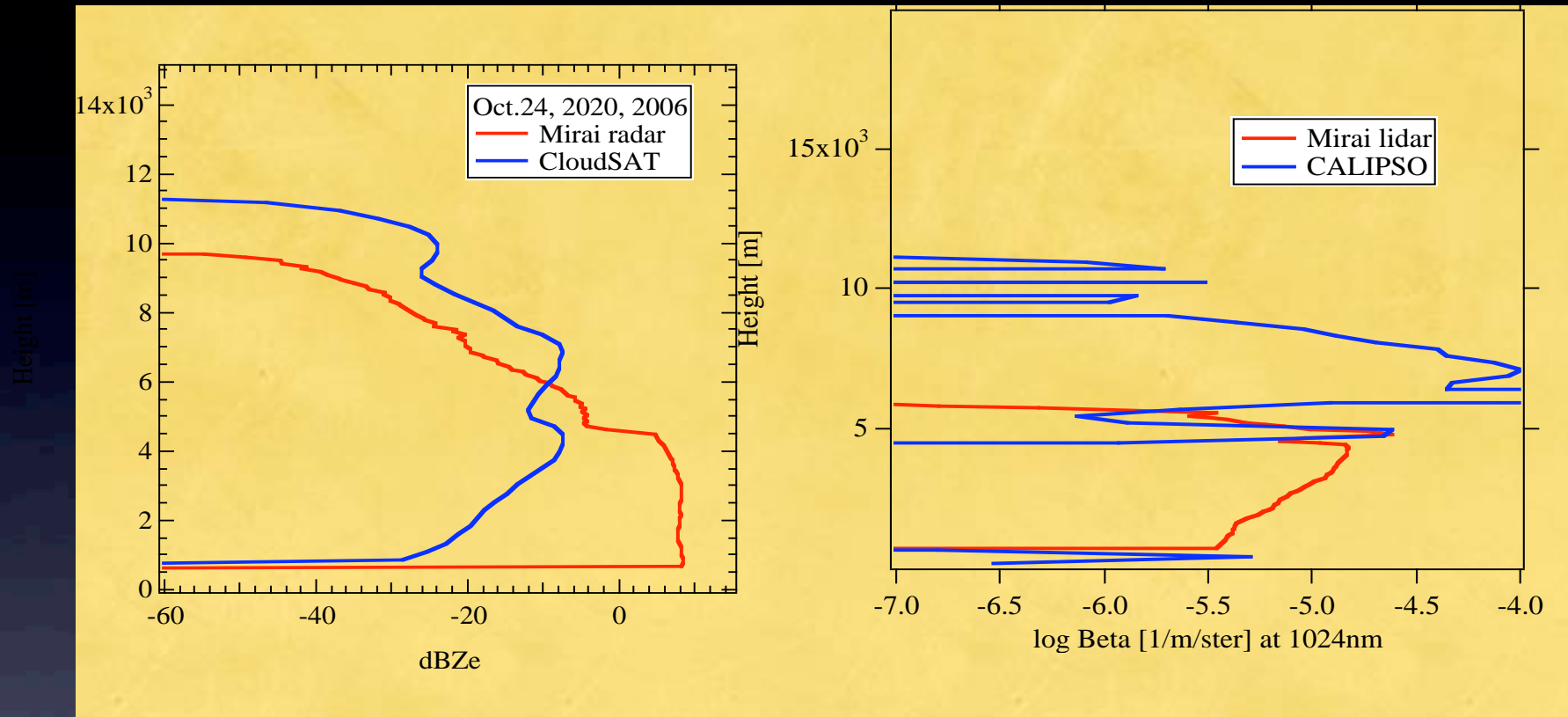


CALIPSO case (similar to ATLID)



Ground-base lidar case

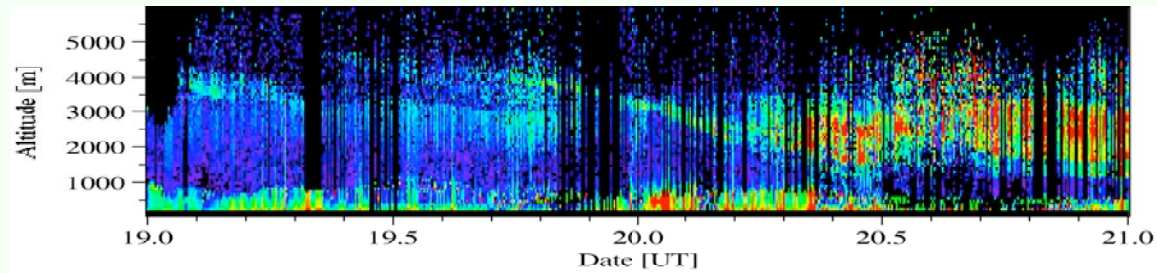
Overpass on Oct.24, 20:20 UTC



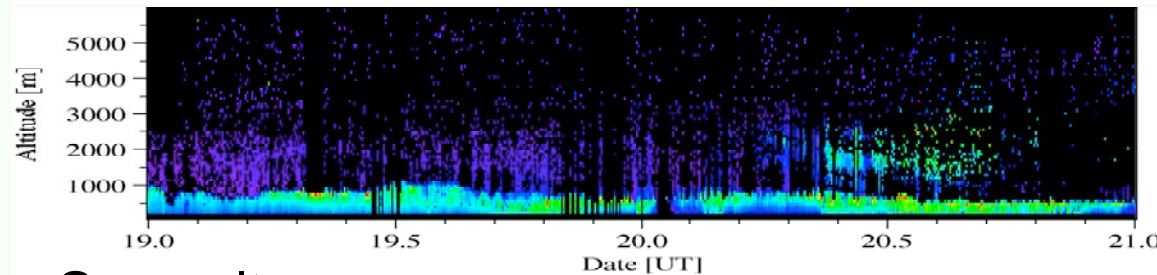
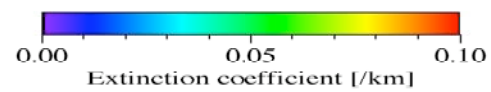
Comparisons of Mirai radar
and CloudSAT

Comparisons of Mirai radar
and CloudSAT

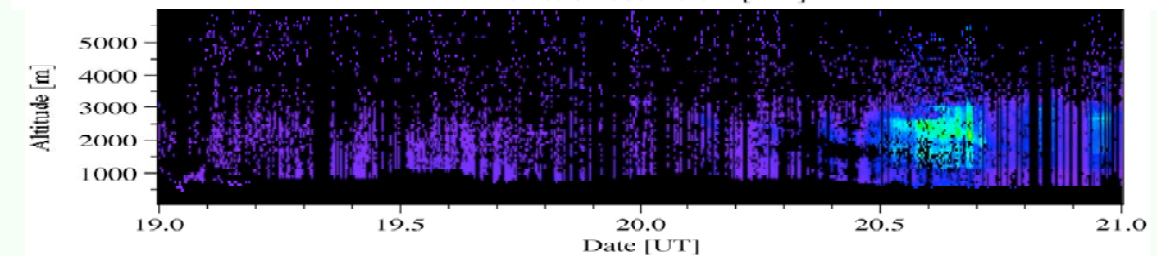
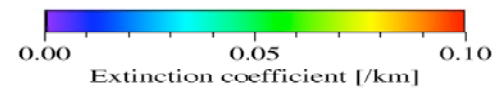
Aerosol properties in MR01-K02



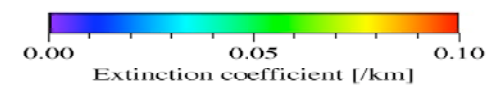
Water soluble



Sea-salt



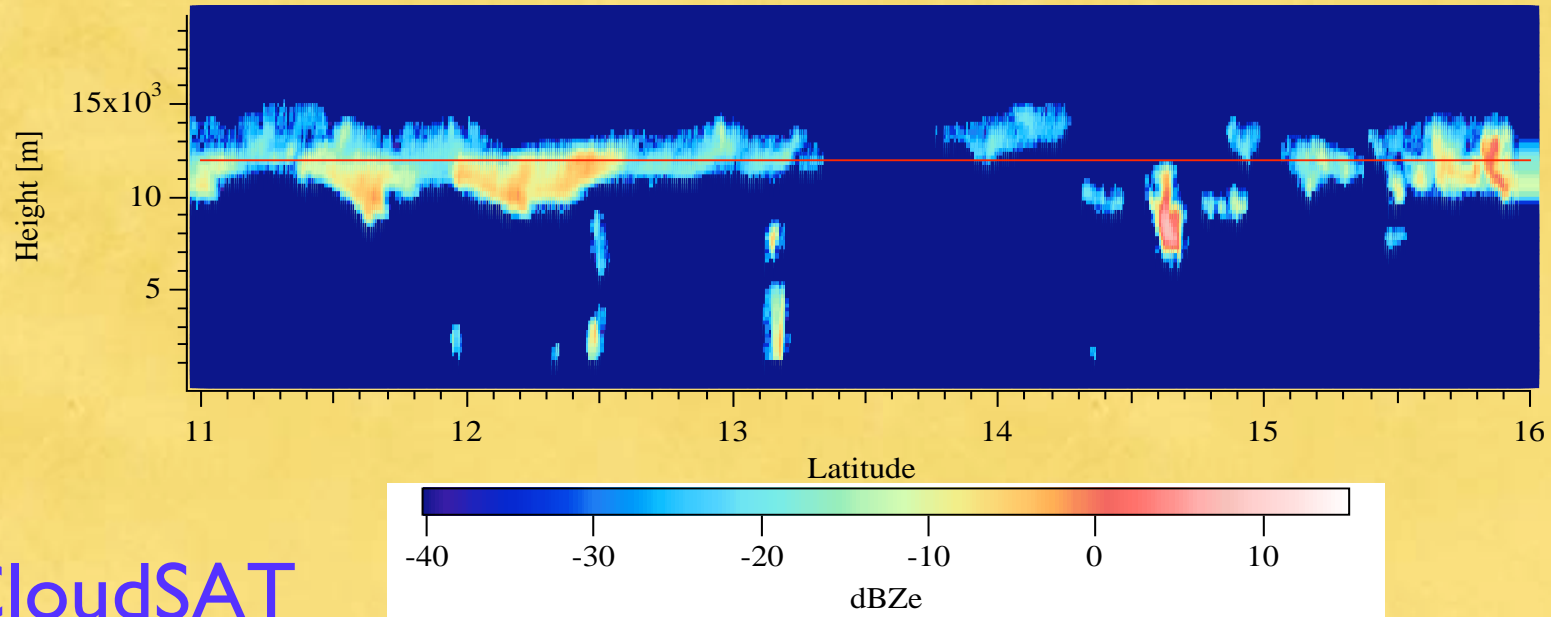
dust



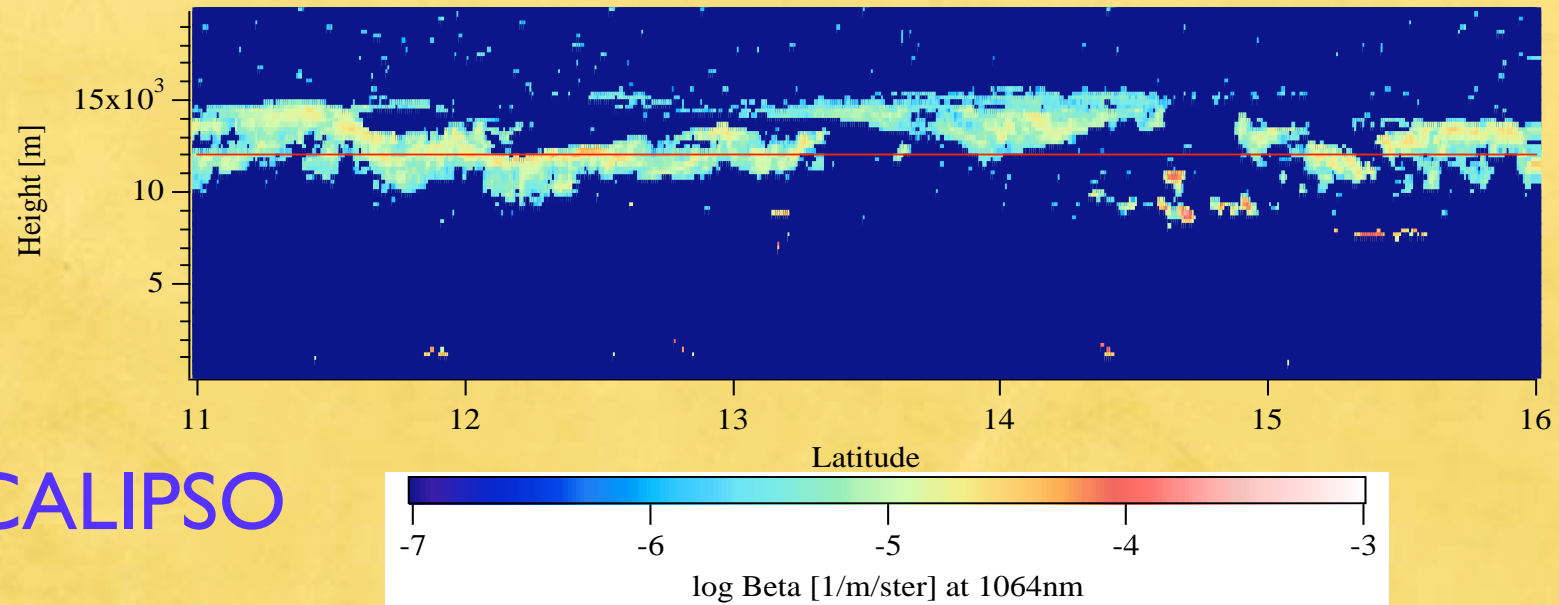
(Nishizawa et al., 2007, JGR)

Validation of CloudSAT/CALIPSO algorithms (collaborate with J. Mace)

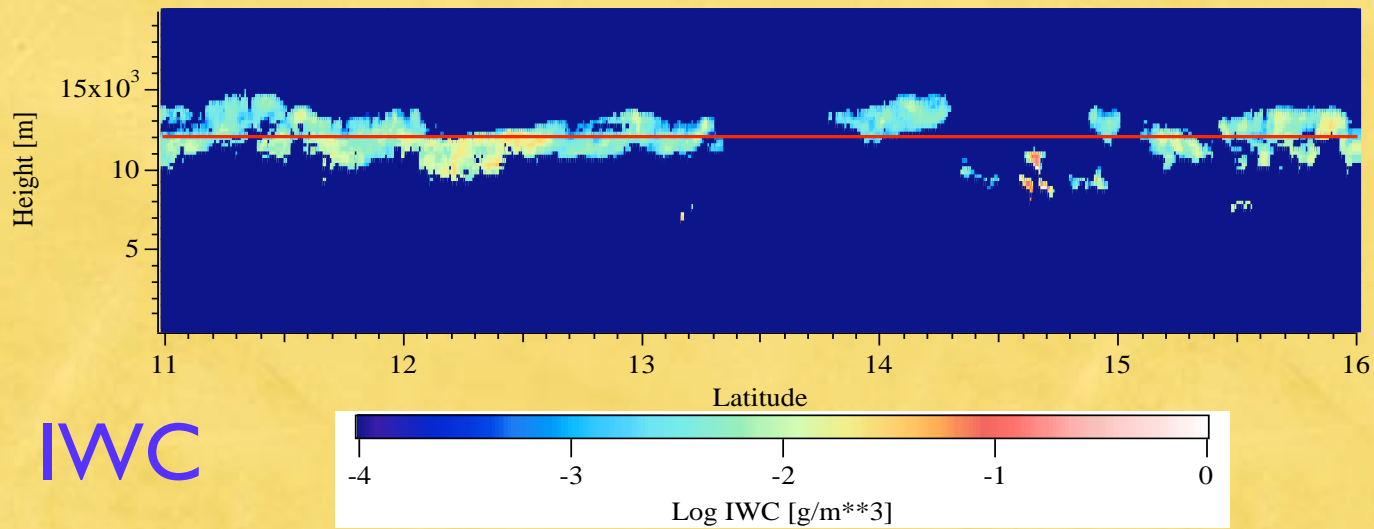
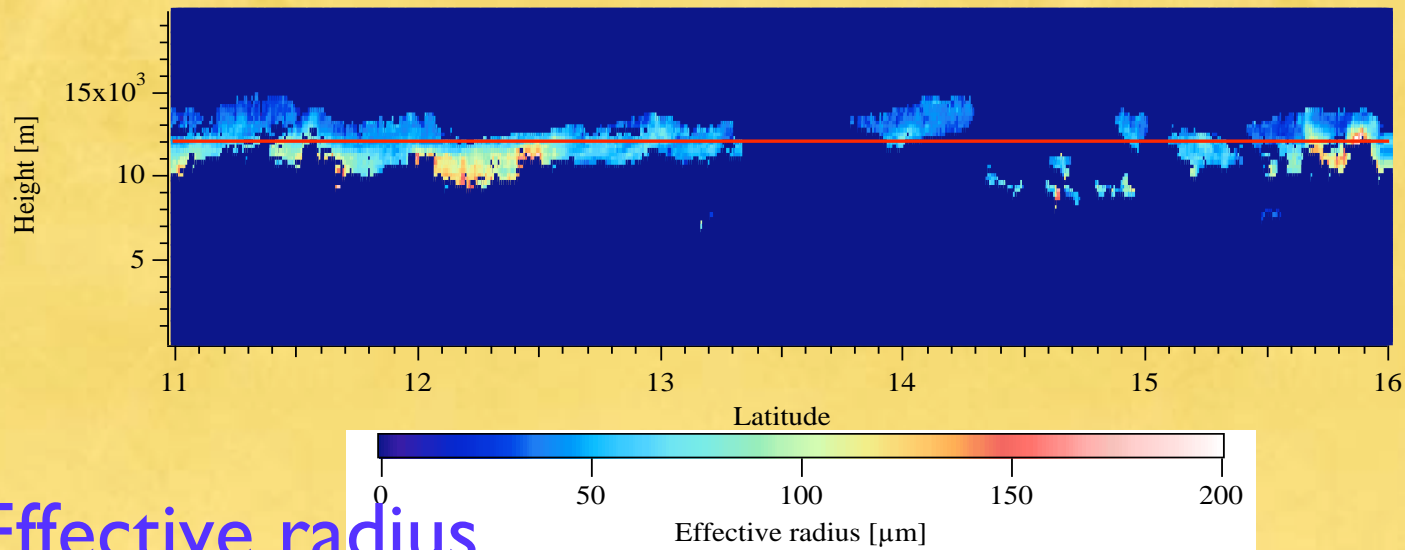
Retrieval results from CloudSAT/CALIPSO is compared with Condensed Water Content from DC-8 (NCAR) CVI--Counterflow Virtual Impactor



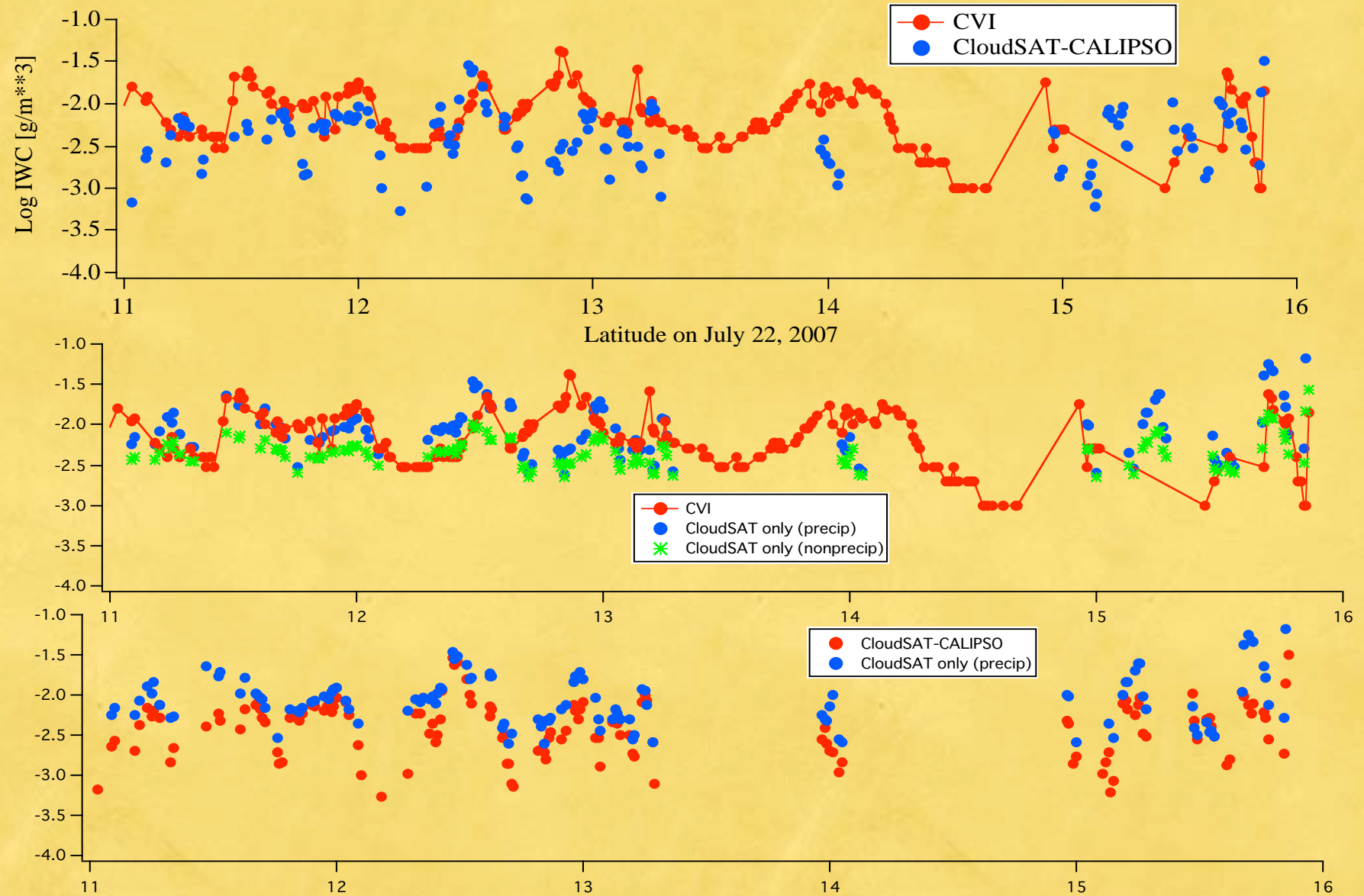
CloudSAT



CALIPSO



CVI vs radar/lidar algorithm, Ze-T algorithm





Aerosol Remote Sensing

Itaru Sano (Kinki University)



contents

1. Introduction
2. Satellite aerosol remote sensing
 - 2.1 Basic concept
 - 2.2 Light scattering by aerosols
 - 2.3 Satellite aerosol retrieval
3. Validation of aerosol remote sensing
 - 3.1 Ground-based sun photometry
 - 3.2 Model simulation
4. Future satellite sensors

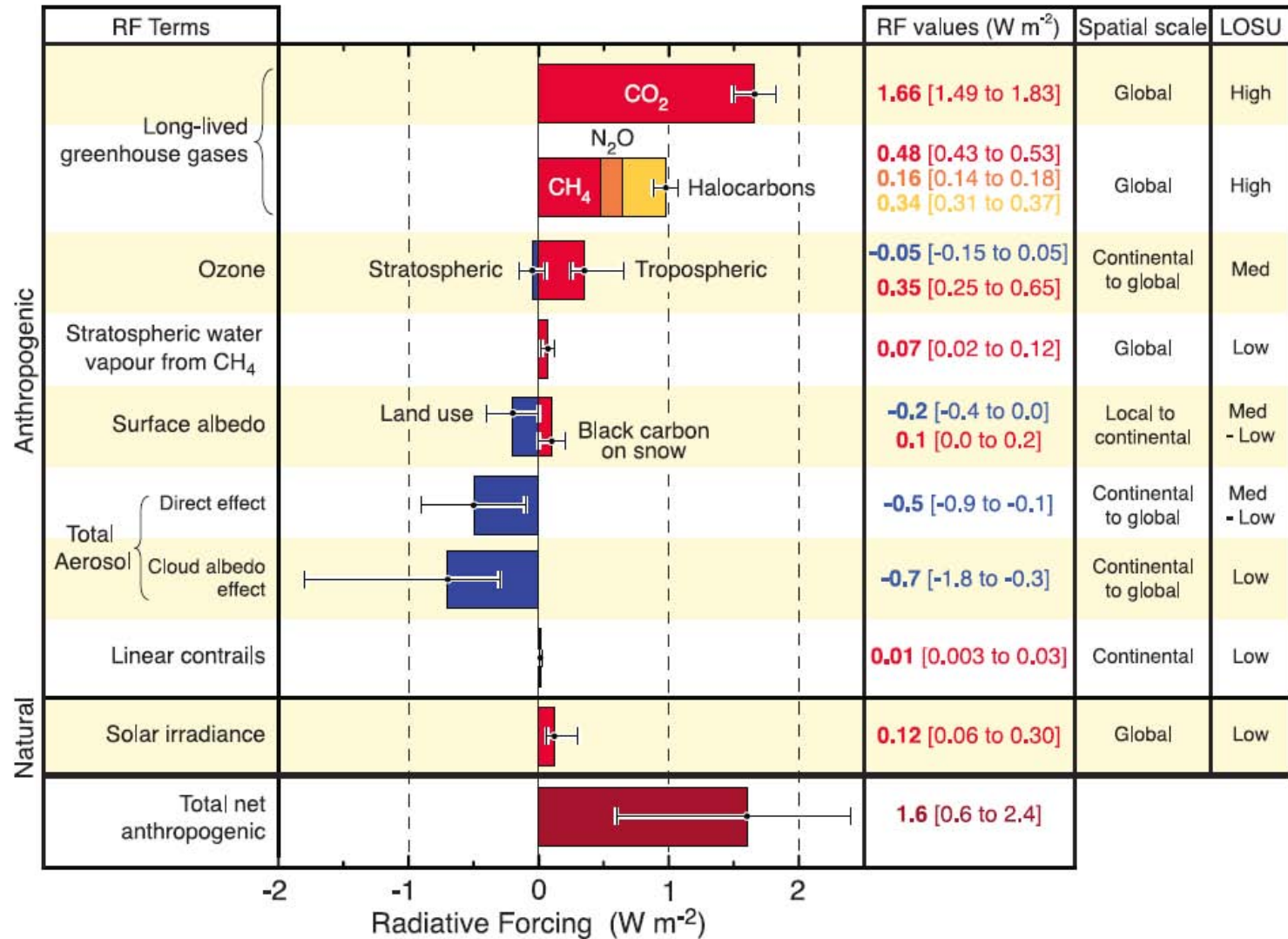
Contents

1. Introduction
2. Satellite aerosol remote sensing
 - 2.1 Basic concept
 - 2.2 Light scattering by aerosols
 - 2.3 Satellite aerosol retrieval
3. Validation of aerosol remote sensing
 - 3.1 Ground-based sun photometry
 - 3.2 Model simulation
4. Future satellite sensors

Role of aerosols shown in 4th-IPCC report

RADIATIVE FORCING COMPONENTS

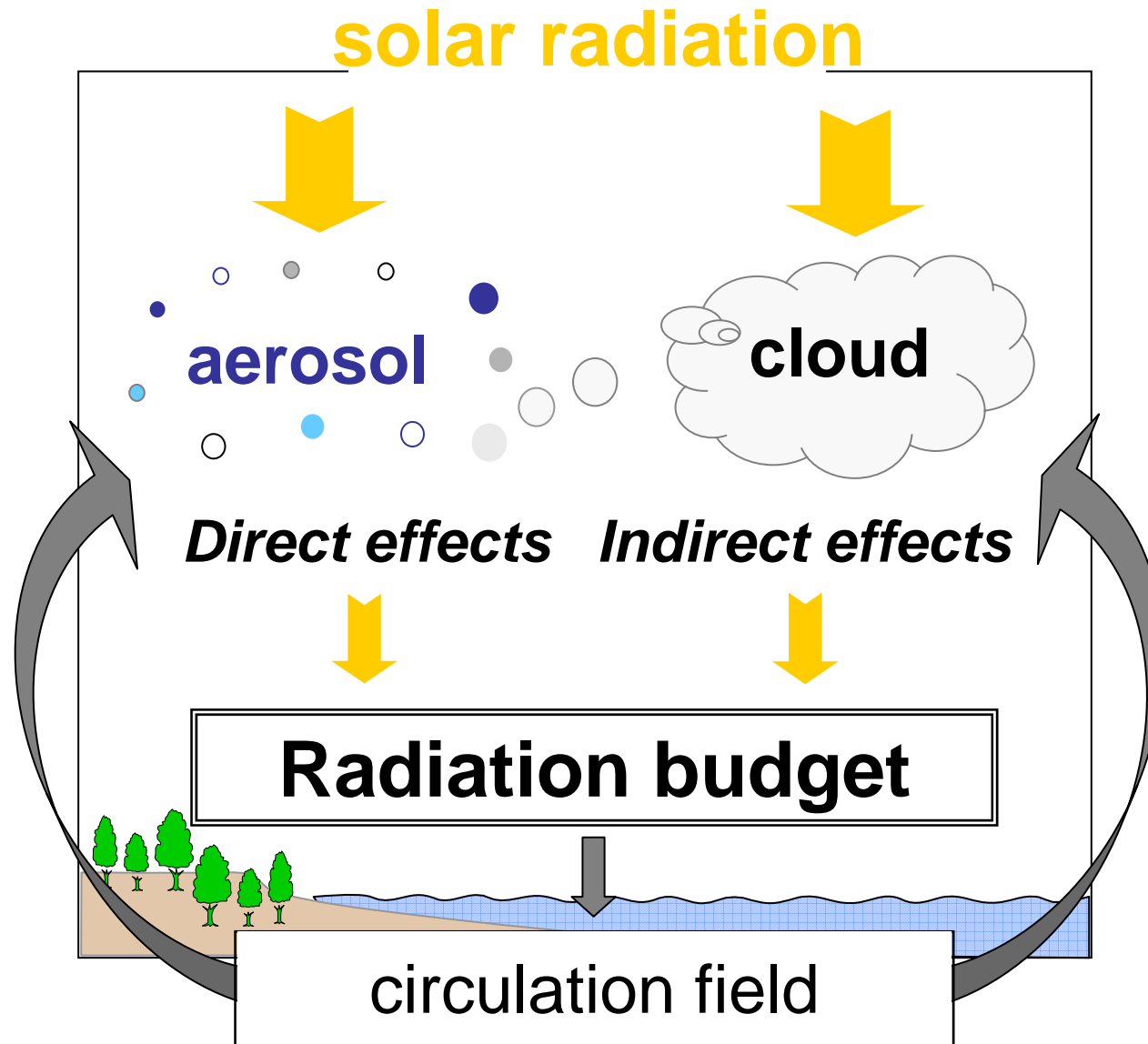
Aerosols



©IPCC 2007: WG1-AR4

IPCC, 2007: Summary for Policymakers.
In: Climate Change 2007: The Physical Science Basis.

Radiation forcing of aerosols



courtesy of Dr. M.Mukai

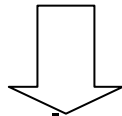
Role of aerosol study

Long standing climate need

- # Negative and/or positive forcing of magnitude in the radiation budget
- # Exact magnitude with sign is currently still poor

Variable component of the atmosphere

- # Aerosols are highly variable and shows complicated phenomena.



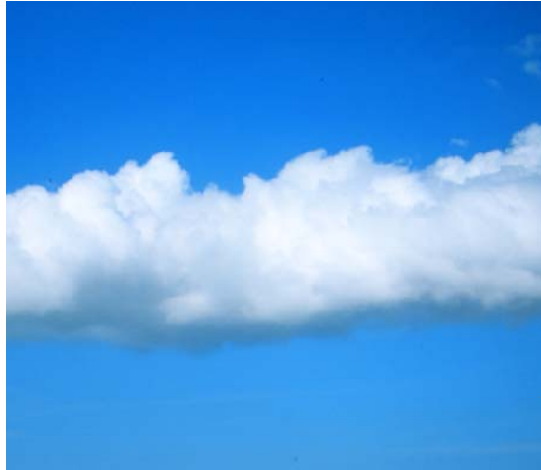
Aerosols should be precisely retrieved

- # for radiative transfer models (Atmos. Corr.)
- # for GCM models
- # for $PM_{2.5}$, PM_{10} (Air quality, health care etc.)

Contents

1. Introduction
2. Satellite aerosol remote sensing
 - 2.1 Basic concept
 - 2.2 Light scattering by aerosols
 - 2.3 Satellite aerosol retrieval
3. Validation of aerosol remote sensing
 - 3.1 Ground-based sun photometry
 - 3.2 Model simulation
4. Future satellite sensors

Color of sky



Sun light scattering
by atmospheric ptls.

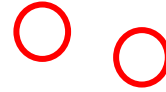


atmospheric particles

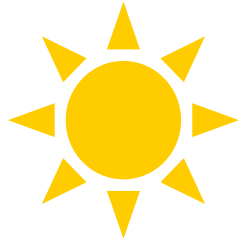
gas molecules



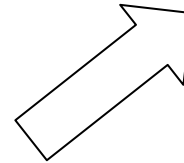
aerosols



solar radiation



sunset glow



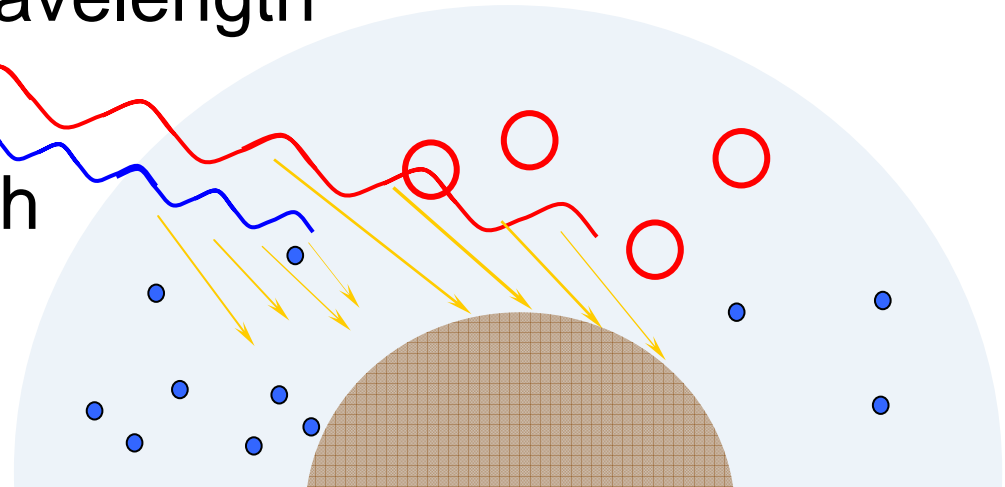
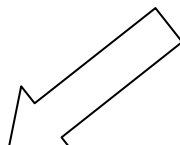
long wavelength



short wavelength



blue sky

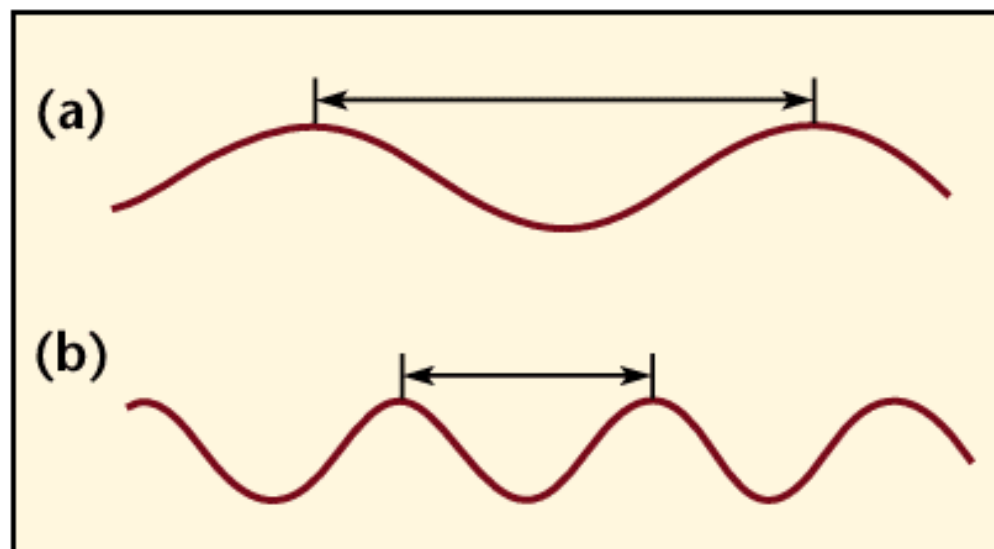


Wavelength (usually symbolized by λ)

wavelength is the distance between 2 consecutive peaks in a wave

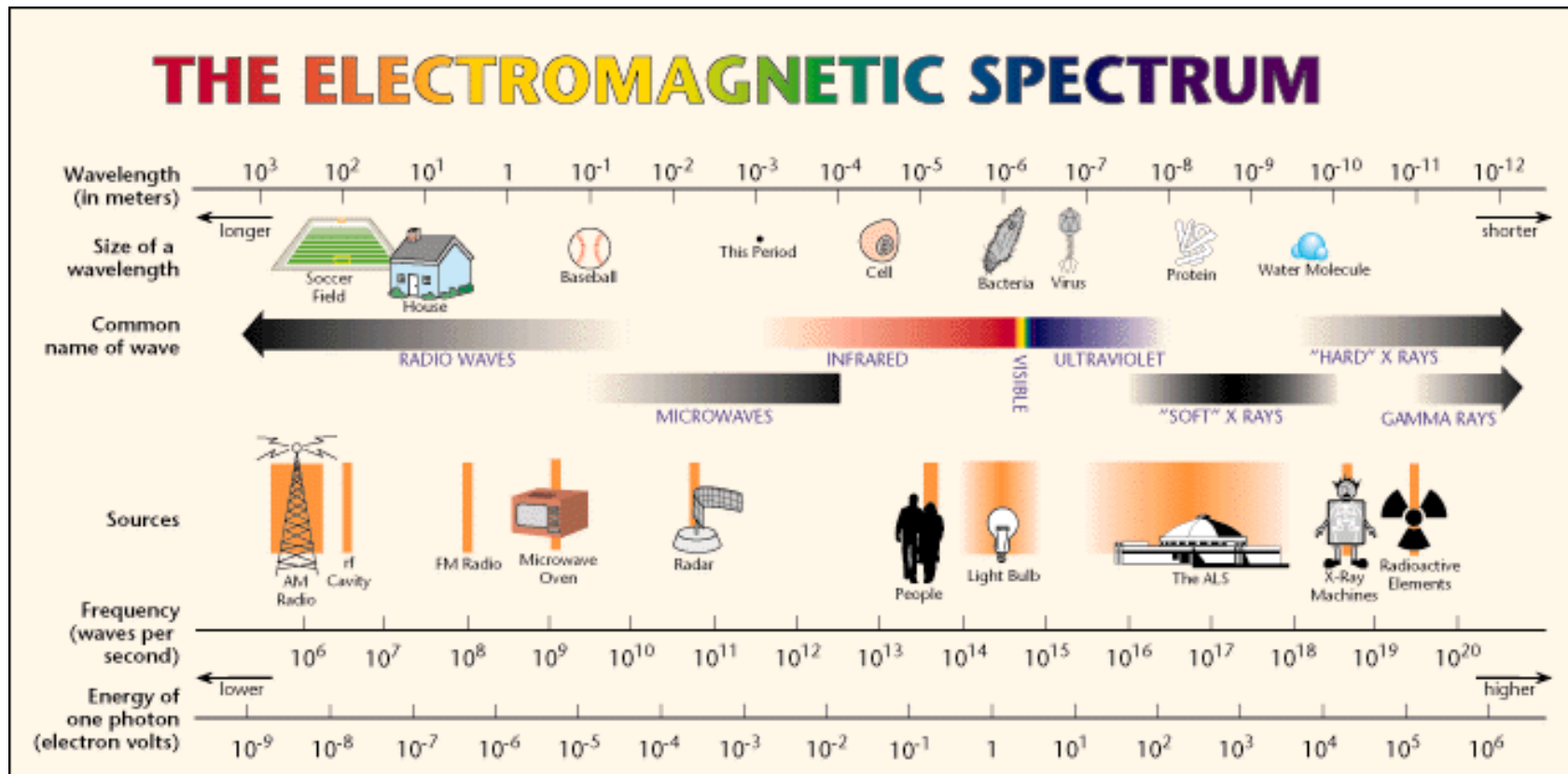
long wavelength ;

short wavelength ;

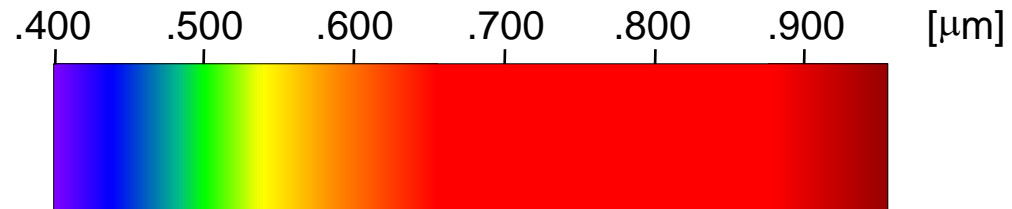
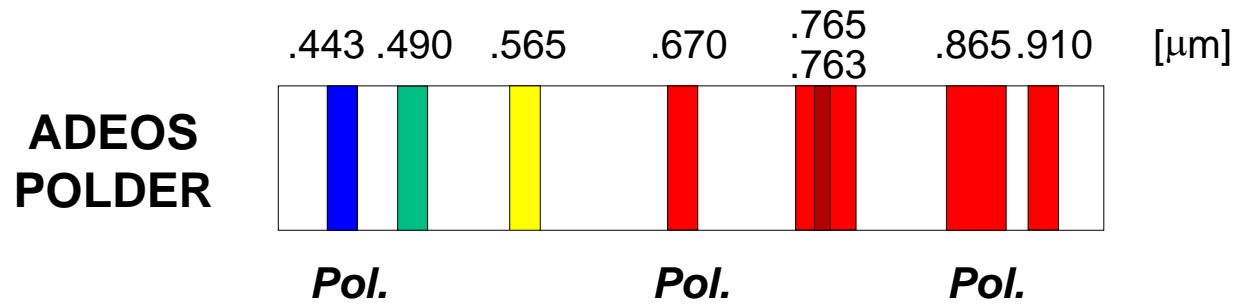


Spectrum of electromagnetic radiation

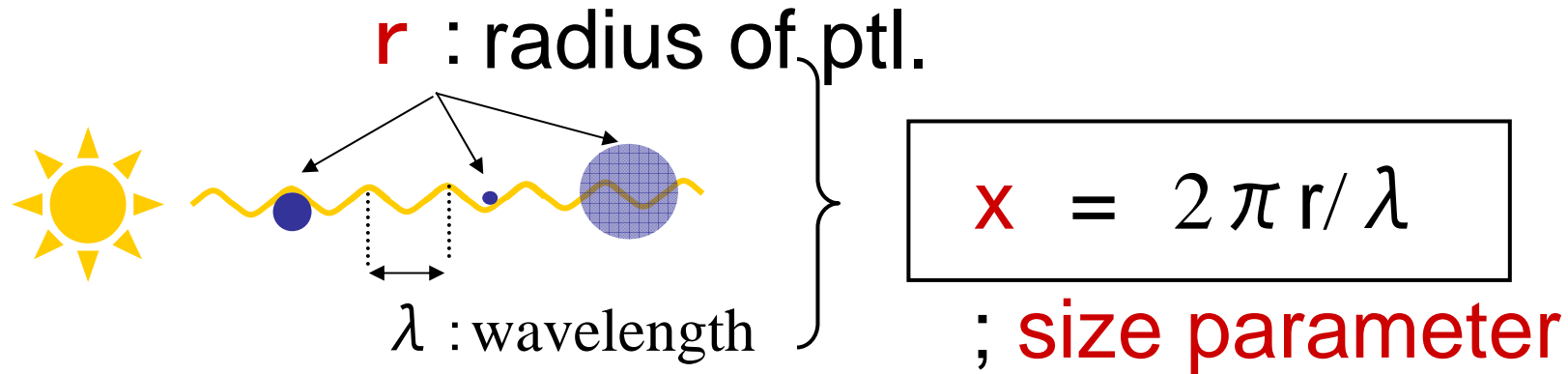
The spectrum is the distribution of radiation according to the wavelength



Observing wavelength of POLDER sensor equipped on the satellite ADEOS



Light scattering by ptls.



Light scattering is most effective at $x \approx 1$

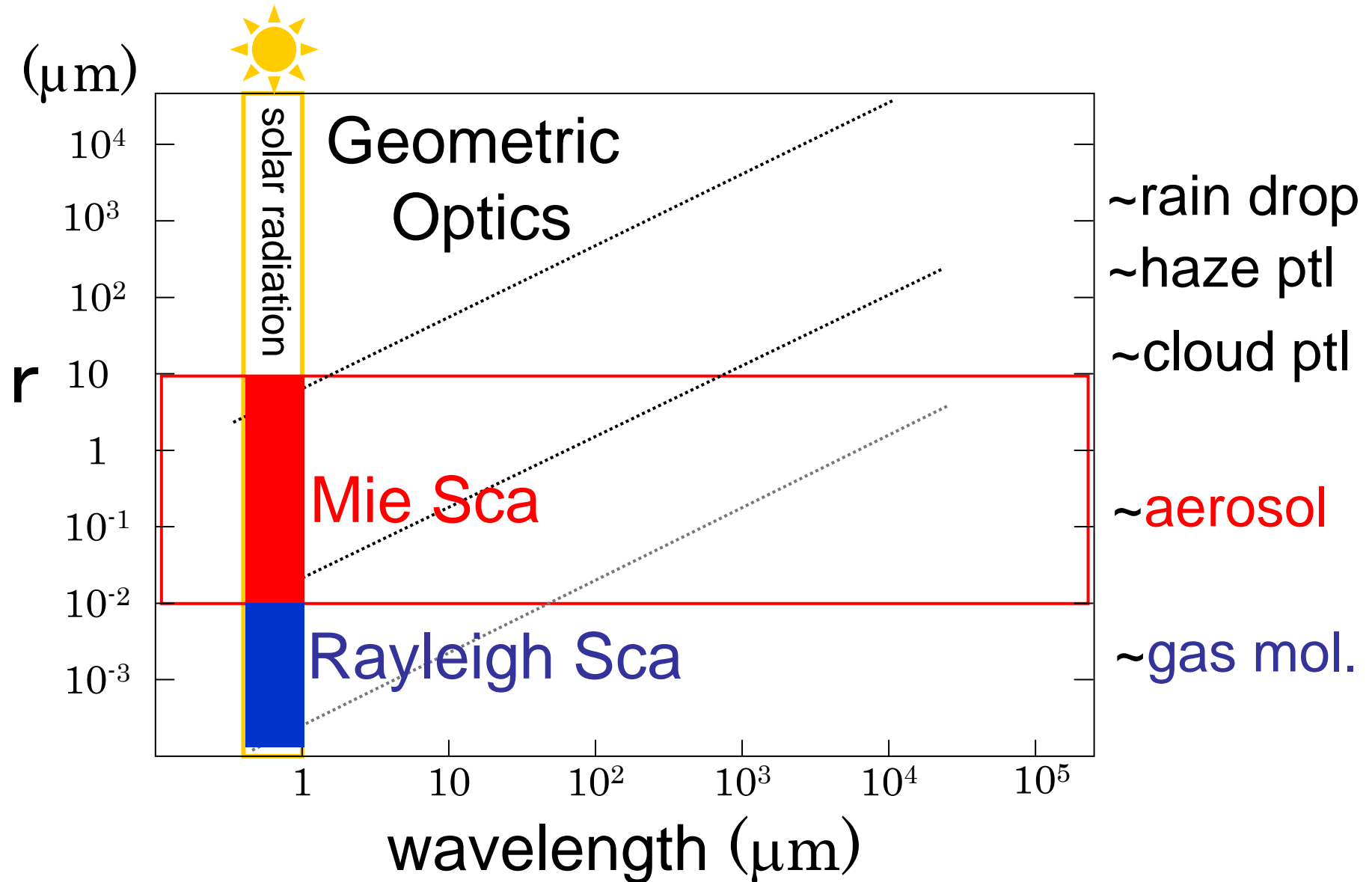


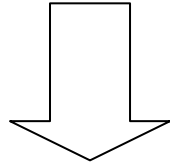
small ptl. \approx short wavelength light
large ptl. \approx long "



gas molecules provide **blue sky**
aerosols " **sunset glow**

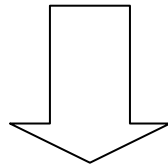
Classification of light scattering by atmospheric ptls.





Aerosols ($X \approx 1$)
accord to the Mie scattering

Gas molecules ($X \ll 1$)
" Rayleigh scattering



The spectrum information by satellite
provides characteristics of atmospheric ptl.

Contents

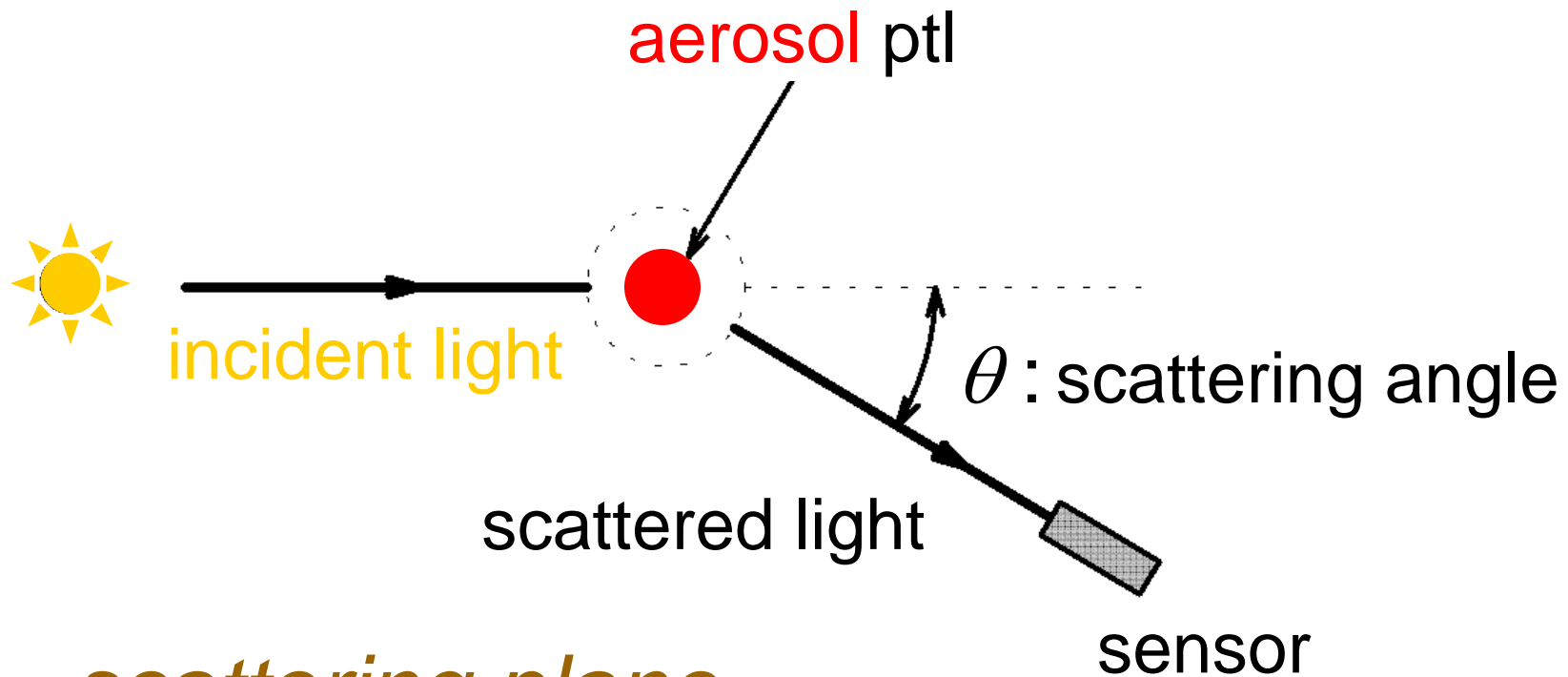
1. Introduction
2. Satellite aerosol remote sensing
 - 2.1 Basic concept
 - 2.2 [Light scattering by aerosols](#)
 - 2.3 Satellite aerosol retrieval
3. Validation of aerosol remote sensing
 - 3.1 Ground-based sun photometry
 - 3.2 Model simulation
4. Future satellite sensors

2.2.1 Single scattering

single scattering pattern (phase function)

(usually symbolized by P)

P is the angular distribution of scattered light. ; $\int P(\theta) d\theta / 4\pi = 1$



- *scattering plane* -

$X \ll 1$: Rayleigh scattering

Ref.S.Chandrasekhar(1960)

$$P(\cos \theta) = \frac{3}{4} (1 + \cos^2 \theta)$$

- In the Rayleigh scattering approximation, a molecule (or a small particle) is considered as an individual dipole.
- Because the sizes of atmospheric molecules are much smaller than the wavelengths of solar and IR radiation, the scattering by atmospheric gases is the Rayleigh scattering.

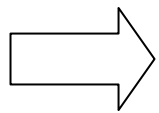
Rayleigh single scattering cross section : σ

$$\sigma = \frac{128\pi^5}{3\lambda^4} \alpha^2$$

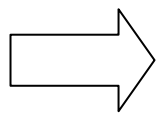
where α represents the polarizability

$$\alpha = \frac{3}{4\pi N} \left(\frac{m^2 - 1}{m^2 + 2} \right)$$

N: number of mols
m : ref idx



The Rayleigh scattering cross section and hence optical depth are inversely proportional to the fourth power of the wavelength.



blue color of the sky

$$I_\lambda \sim \frac{1}{\lambda^4}$$

$X \approx 1$: Mie scattering ref. Lorentz-Mie (~ 1900)

1. Ptl is a **sphere**,
2. Ptl is **homogeneous**
(therefore it is characterized by a **single refractive index $m=n - ik$** at a given wavelength)

⇒ Mie theory requires refractive index of ptl / **medium**.

⇒ **$m \approx 1$** for air

⇒ **refractive index of ptl**
(i.e. composition of ptl)

- on Mie scattering calculation -

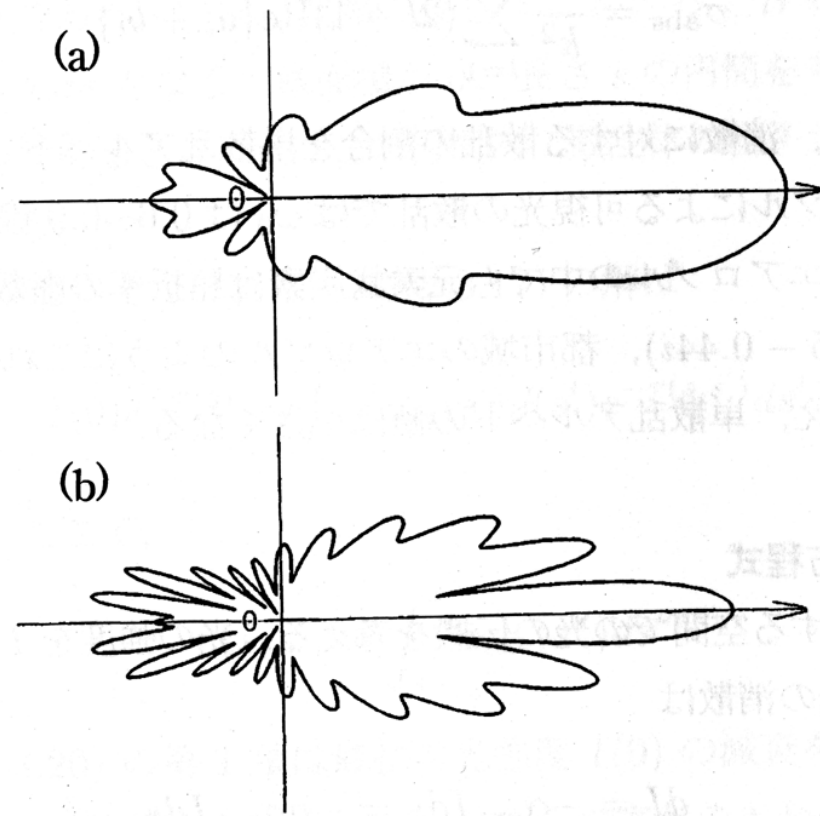
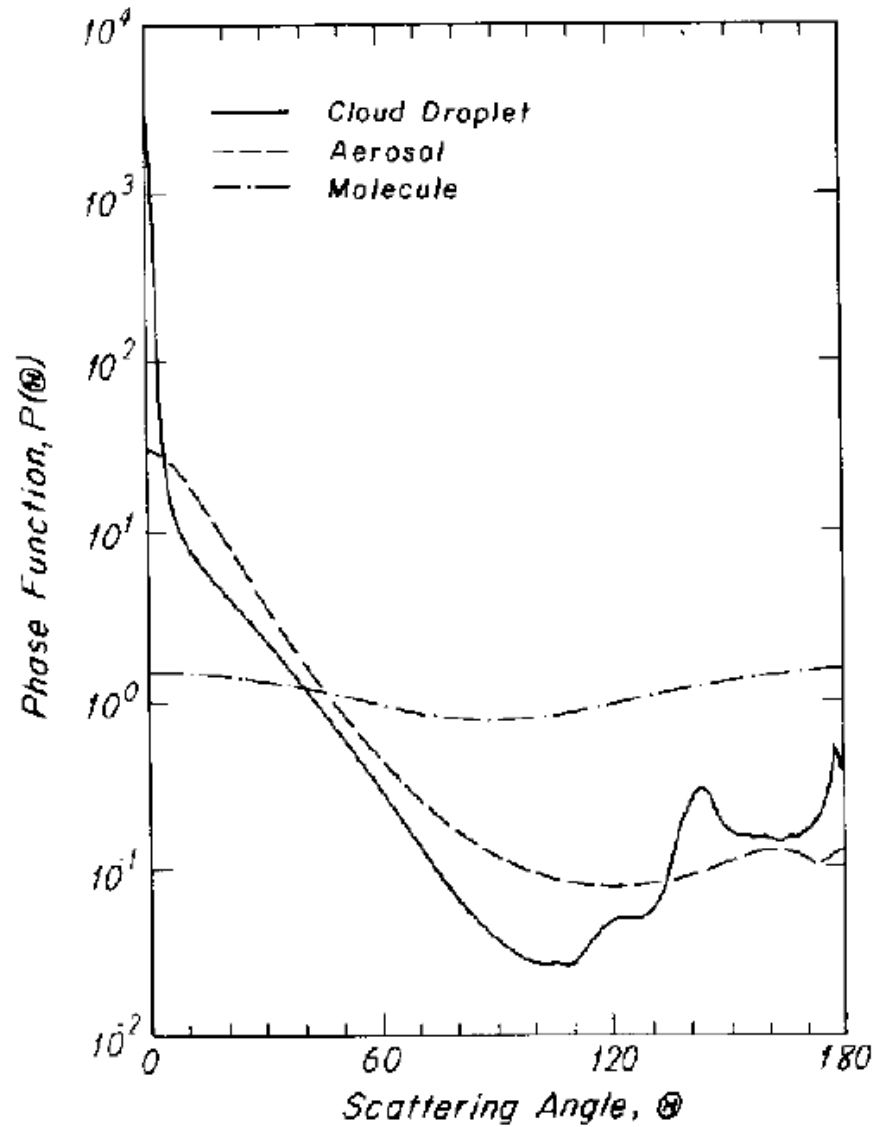
Size parameter; $X(r, \lambda)$ and refractive index $m(n, k)$
with Mie theory gives :

Efficiency factors,
 $Q_{\text{ext}}, Q_{\text{sca}}, Q_{\text{abs}}$

Amplitude function
phase matrix (phase function)

- on Mie scattering calculation 2 -

forward scattering is dominant in usual.



Shape of scattering ptl

sphere



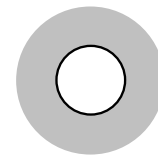
.....

Lorentz-Mie (~ 1900)

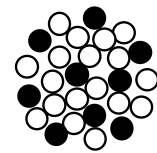
Mie scattering

infinite cylinder

coated sphere/core mantle

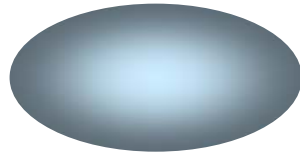


cluster of spheres



.....Asano & Yamamoto(1973)

spheroid



cluster of spheroid

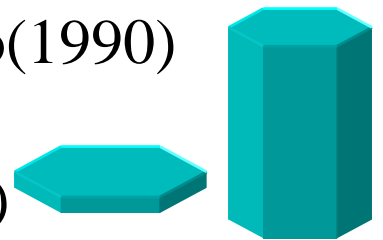
Non-spherical

DDA..... Purcell & Pennypacker(1973)

Drain & Flatau

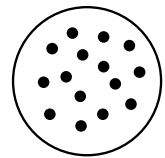
T-matrix.....M.Mishchenko(1990)

Hex. clm..... A.Macke(1993)



Heterogeneous sphere

Maxwell-Garnett
mixing rule

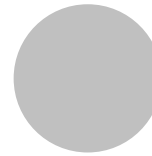
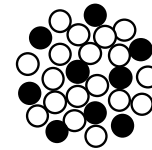


WS



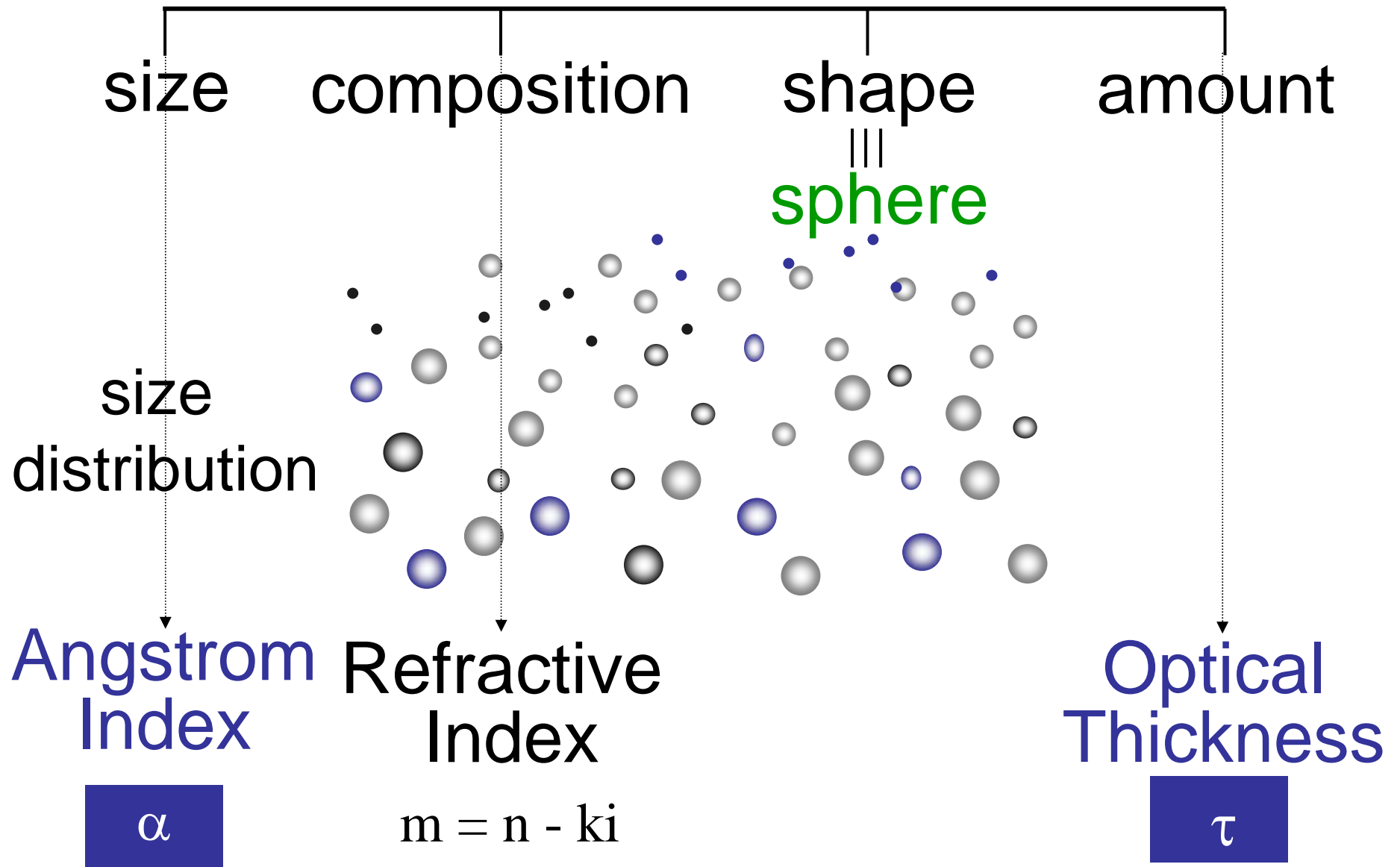
OC

Bruggeman
mixing rule



$$m = n - ik$$

Parameters of aerosols



Composition of scattering ptl. (complex refractive index)

$$m = n - ik$$

n : refractive index (0.55 μm)

1.38 : oceanic

1.43 : sulfate

1.53 : mineral dust

1.75 : soot

k : index for absorption

3.7 E-9 : oceanic

1.0 E-8 : sulfate

5.5 E-3 : mineral dust

4.4 E-1 : soot

ref. Shettle & Fenn (1979)
d'Almeida(1991)

Size distribution of scattering ptl

Mode of aerosol particles

nucleation mode (0.001 to 0.1 μm)

gas to particle condensation

accumulation mode (0.1 to 1 μm)

coagulation and heterogeneous condensation

coarse mode (> 1 μm)

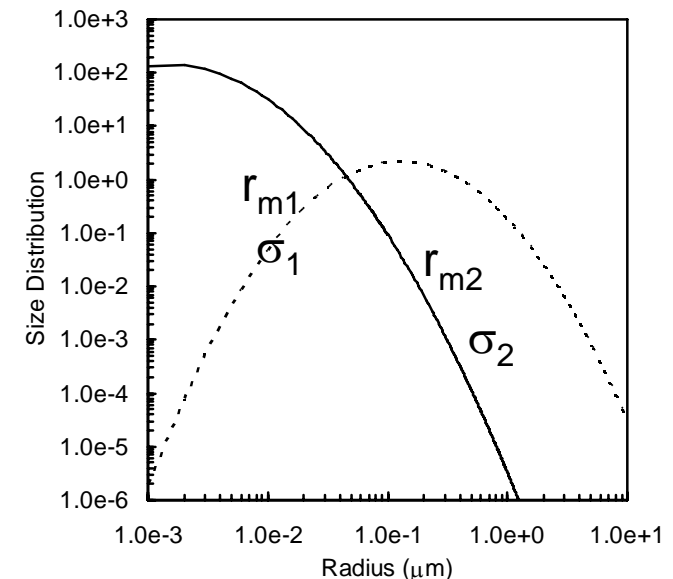
origin in mechanical process, dust, sea-salt

log-normal distribution

$$n(r) = \frac{dN(r)}{dr} = \frac{N}{\sqrt{2\pi} r \ln \sigma} \exp\left\{-\frac{(\ln r - \ln r_m)^2}{2 \ln^2 \sigma}\right\}$$

sum of log-normal dist.

$$n(r) = \frac{dN(r)}{dr} = \sum_i^n \frac{dN_i(r)}{dr}$$



Size dist.

Number size distribution

$$n(r) = \frac{dN(r)}{dr}$$

Volume size distribution

$$\frac{dV(r)}{dr} = \frac{4}{3} \pi r^3 n(r) \quad \text{for total amount of particulate matter}$$

Surface size distribution

$$\frac{dS(r)}{dr} = 4\pi r^2 n(r) \quad \text{for heterogeneous chemistry}$$

2.2.2 Multiple scattering

Light scattering in the atmosphere

The solar radiation field (denoted by I) is traditionally considered as a sum of two distinctly different components:

direct and **diffuse** : $I = I_{dir} + I_{dif}$

The direct radiation I_{dir} is expressed by **Beer-Bouguer-Lambert law**, which states that the extinction process is linear in the intensity of radiation and amount of matter.

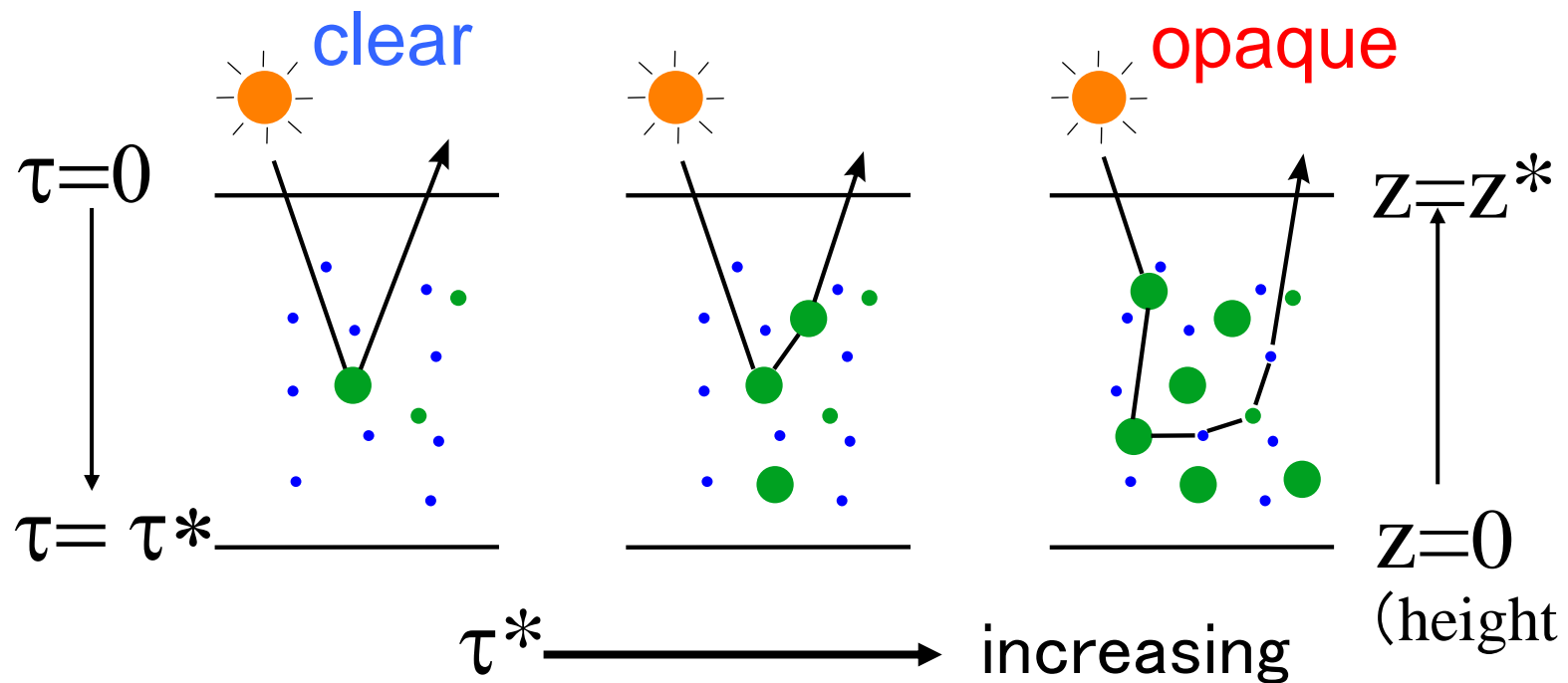
$$I_{dir} = I_0 \exp(-\tau^*)$$

τ^* : optical thickness of atmosphere

τ^* : optical thickness ← transmittance

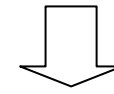
$$\tau^*(\lambda) = \int \kappa_{\text{ext}}(\lambda) dz$$

τ^* depends on the wavelength
⇒ Angstrom exponent (N.B.)

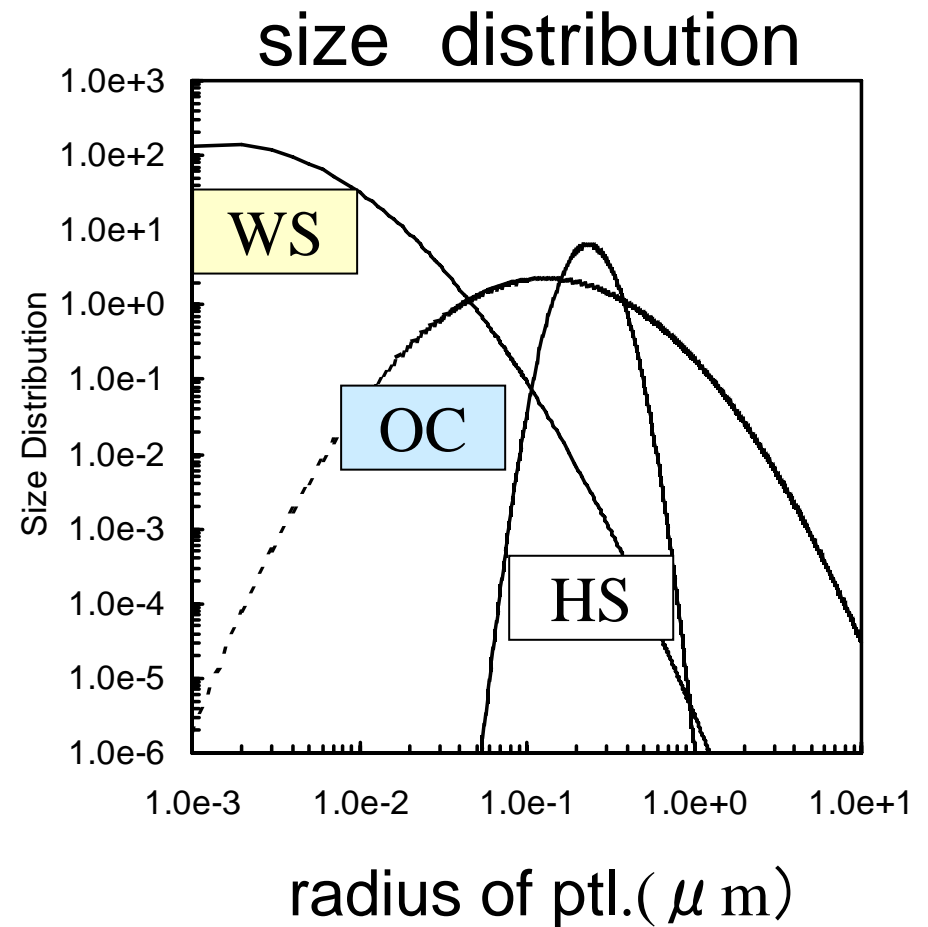
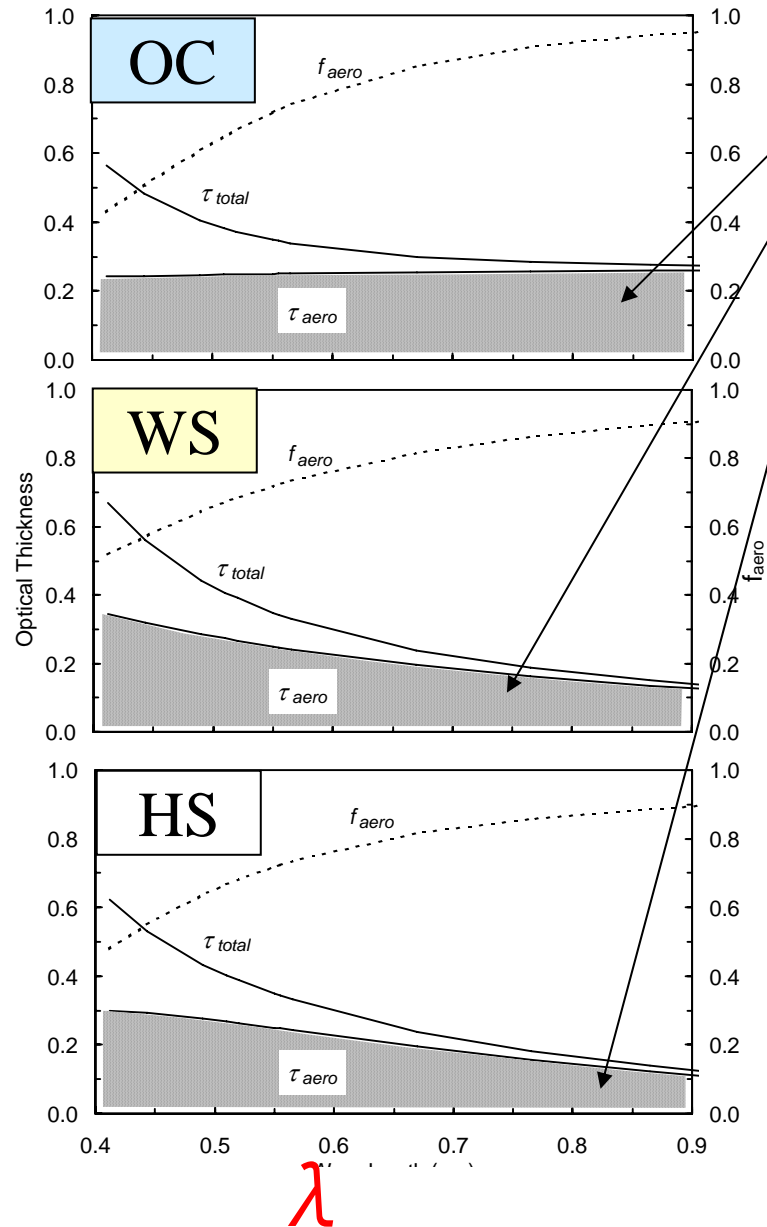


N.B.

$\tau^*(\lambda)$ by Mie cal.



size of aerosol $\sim 1 / \alpha$



N.B. Angstrom exponent (α)

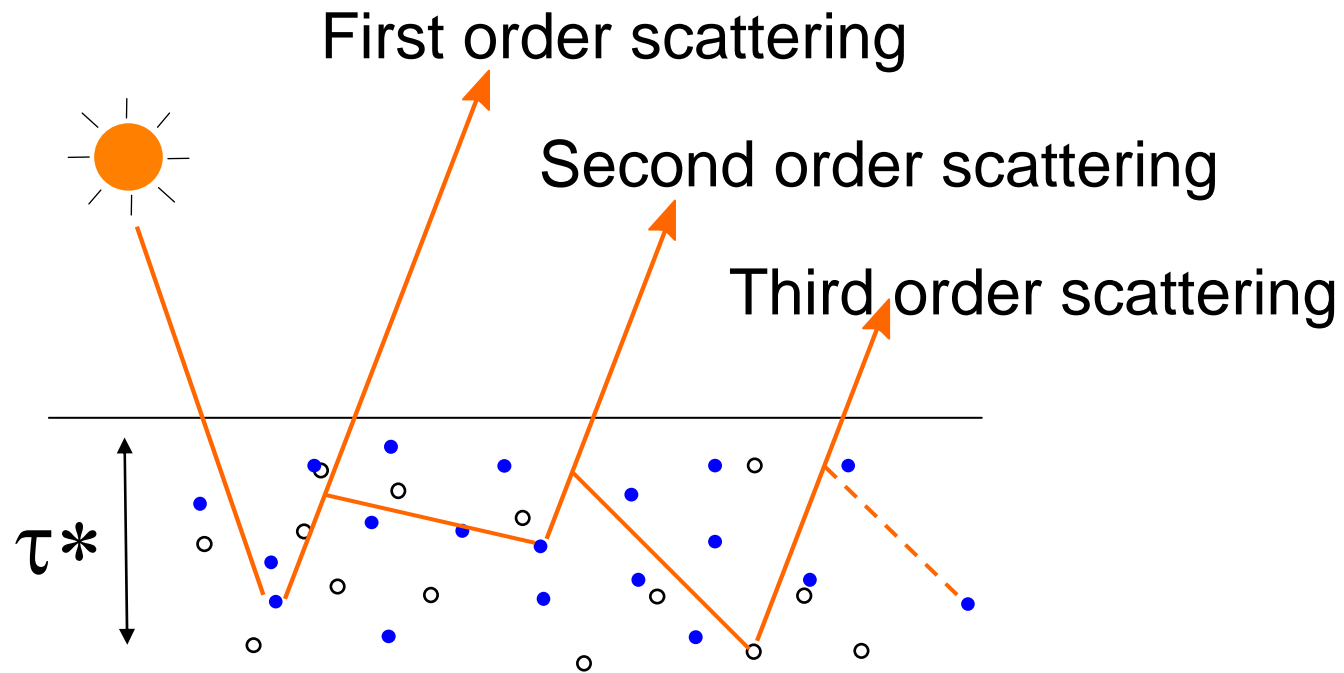
$$\alpha = -\ln(\tau_{\lambda_1} / \tau_{\lambda_2}) / \ln(\lambda_1 / \lambda_2)$$

Spectral aerosol optical thickness are used to retrieve the Angstrom exponent and particle size distribution :

size of aerosol $\sim 1 / \alpha$

Diffuse radiation field

Diffuse radiation arises from the light that undergoes one scattering event (**single scattering**) or many (**multiple scattering**).

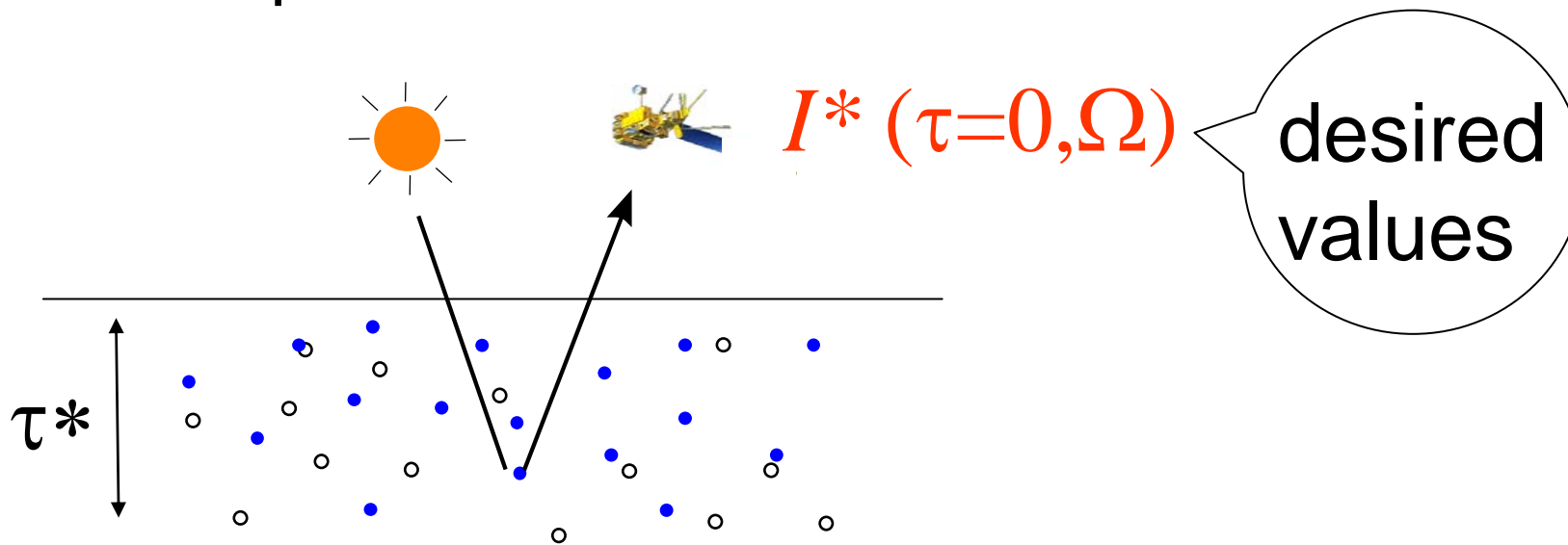


Radiative transfer equation

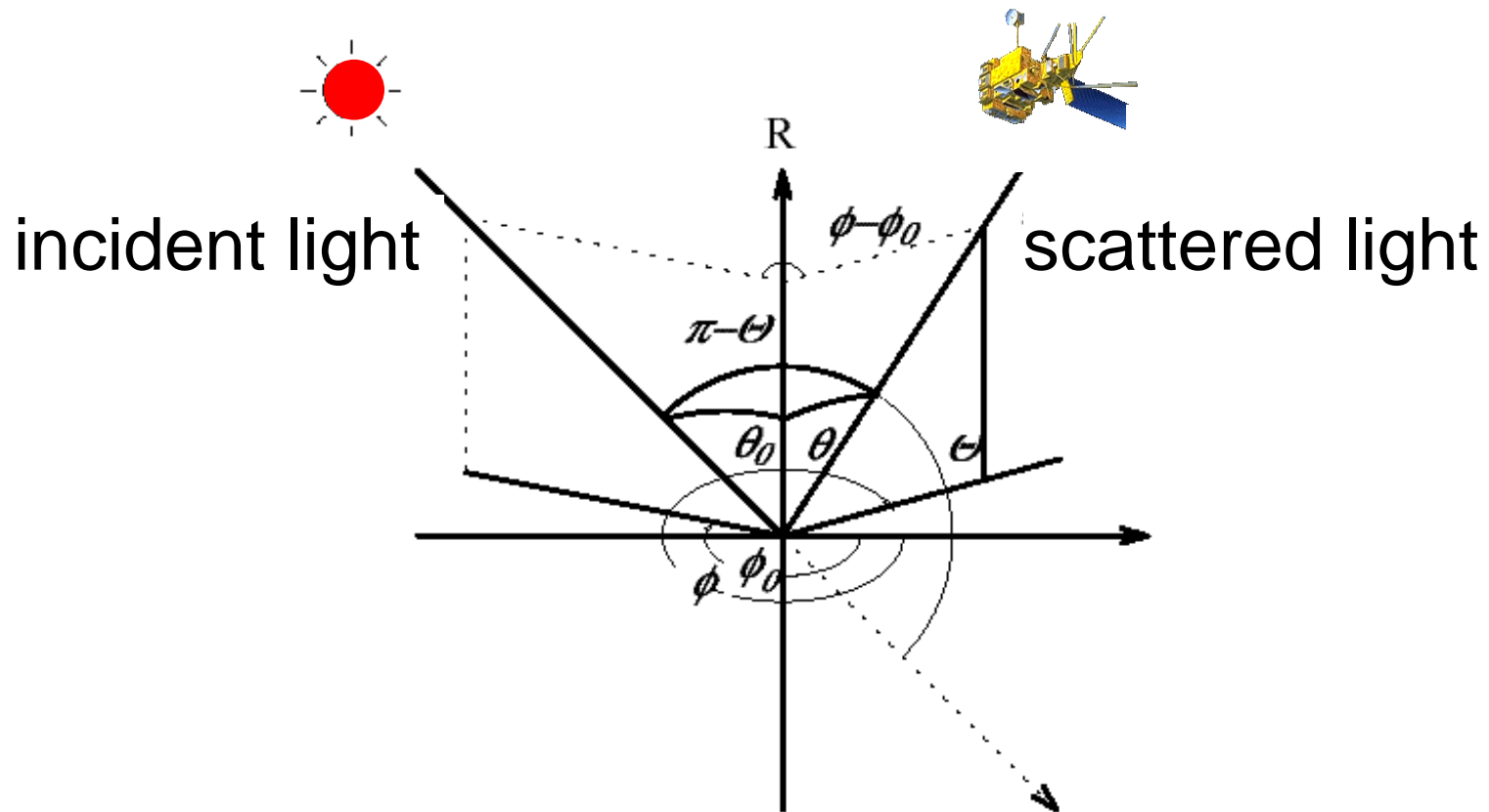
describes the diffuse radiation field: ref. S.Chandrasekhar "Radiative Transfer"

$$\mu \frac{\partial I}{\partial \tau} = I(\tau, \Omega) - \frac{1}{4\pi} \int_{4\pi} P(\Omega, \Omega') I(\tau, \Omega') d\Omega'$$

Satellite observes the upward radiation at the top of atmosphere:



Change of coordinate for multiple scattering calculations



$$\cos\Theta = \cos\theta_0 \sin\theta \mp \cos\theta \sin\theta_0 \cos(\phi - \phi_0)$$

To get the numerical values of $I^*(\tau=0, \Omega)$ for aerosol remote sensing, Radiative Transfer Equation is solved based on the adding-doubling method with boundary conditions:

example :

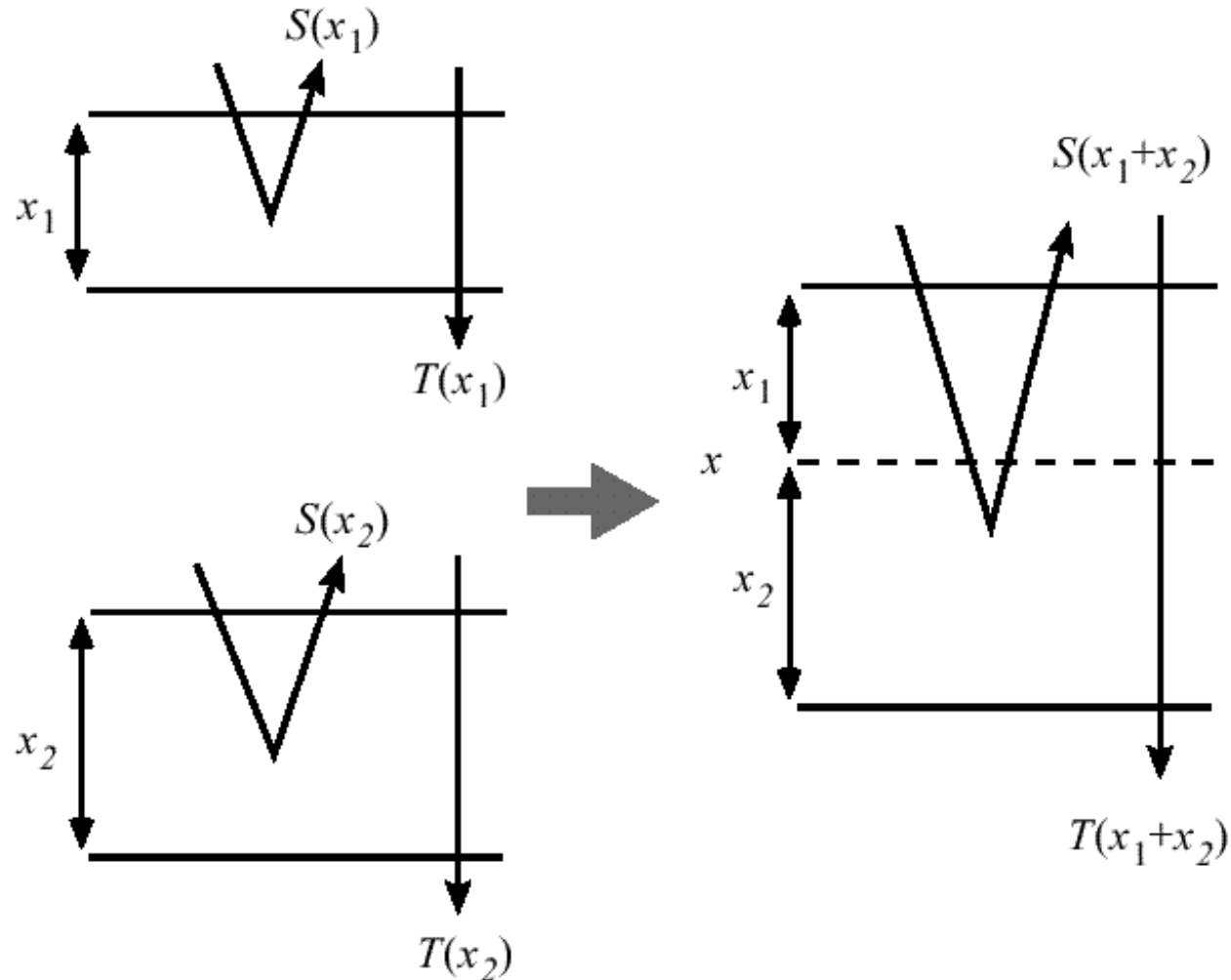
solar light incidence

$$I^-(0, \Omega) = \pi F_0 \delta(\Omega - \Omega_0)$$

Lambert ground

$$I^+(\tau, \Omega) = A / \pi \int_{2\pi} I^-(\tau, \Omega') \mu' d\Omega$$

Adding-doubling Method



$S(\tau^*) \rightarrow I^*(\tau^*) \rightarrow$ satellite aerosol retrieval

contents

1. Introduction
2. Satellite aerosol remote sensing
 - 2.1 Basic concept
 - 2.2 Light scattering by aerosols
 - 2.3 Satellite aerosol retrieval**
3. Validation of aerosol remote sensing
 - 3.1 Ground-based sun photometry
 - 3.2 Model simulation
4. Future satellite sensors

Algorithm for aerosol retrieval

- Total intensity
 - two channel method over ocean (Red, NIR)
 - AVHRR
 - four channel method over ocean (Vi, Bi, Red, NIR)
 - GLI, (SeaWiFS, MODIS)
 - dark target method over (veg.) land (Bi, Red, SWIR)
 - MODIS
 - deep blue method over bright target (desert) (Vi, Bi)
 - MODIS
 - UV method over land and ocean (UV)
 - TOMS, OMI
- Polarization
 - two channel polarization method over land (Red, NIR)
 - POLDER

Retrieval algorithm for aerosols (over ocean)

1. Four-channel algorithm

(by Higurashi and Nakajima):

- Retrieval of τ , α , and absorptivity in blue over ocean:
- 0.412, 0.443, 0.670, and 0.865 μm
(Violet, Blue, Red, NIR)
- Species
; soil dust, carbonaceous, sulfate, and sea salt

Retrieval algorithm for aerosols (ocean/land)

2. Two-channel method (by R. Hoeller et al.);

- Retrieval of τ and ω on a global scale
(land and ocean)
- 0.380 and 0.412 μm
(UV-absorbing and Violet);

Species

; soot and dust (absorbing) and
sulfate (non-absorbing)

Retrieval algorithm for aerosols (land)

3. Two-channel Polarization method

- Retrieval of τ , and α , on a global scale

- 0.678 and 0.865 mm

(Polarization and Directionality)

4. Two-channel Polarization method with UV-V channel method

2.3.1 Aerosol retrieval for POLDER-1 & -2

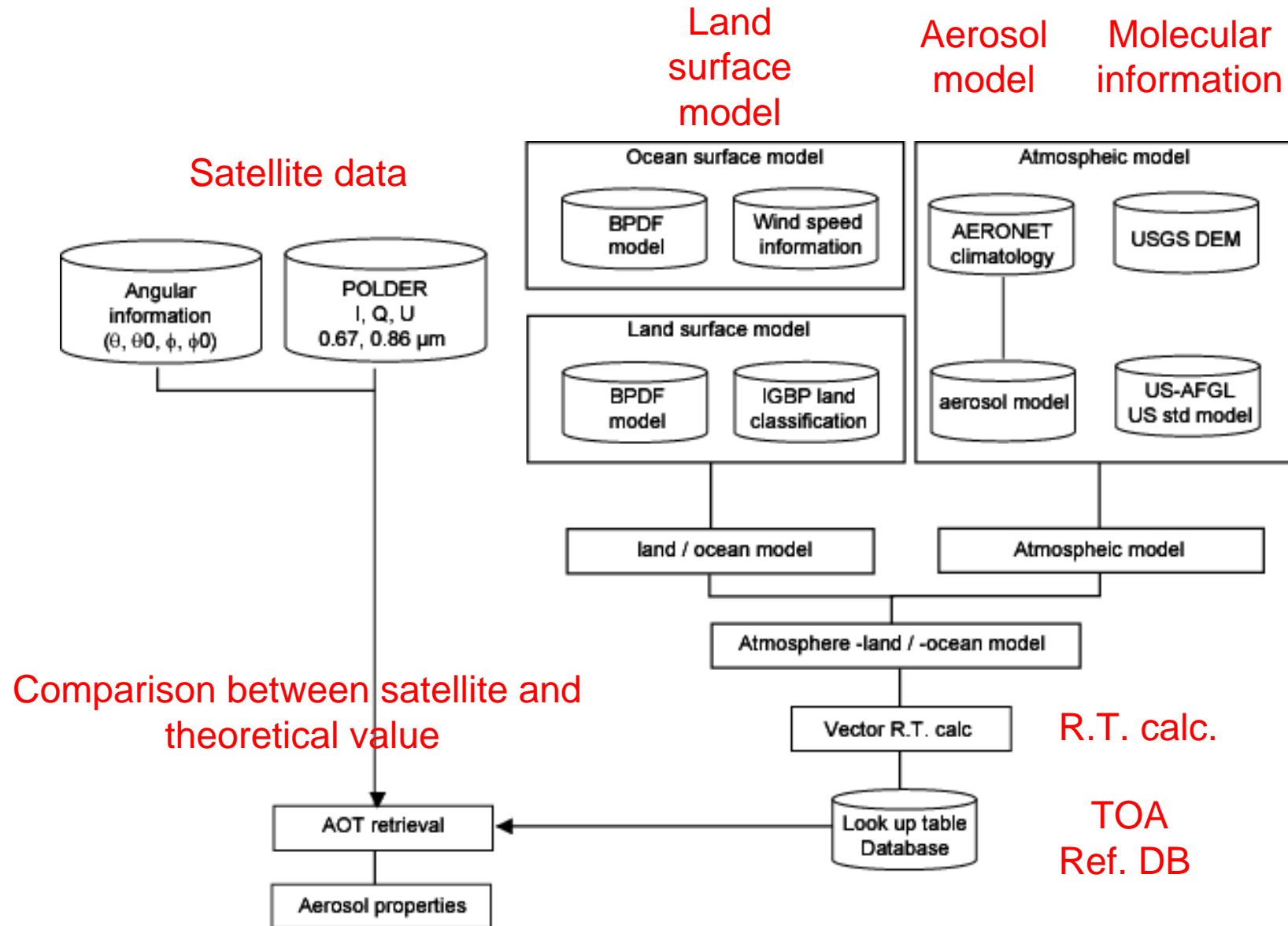
Example of aerosol retrieval

- Satellite data
 - POLDER on ADEOS-1 (1996 to 1997)
 - POLDER-2 on ADEOS-2 (2003)
 - POLDER-3 on PARASOL (2005- in operation)

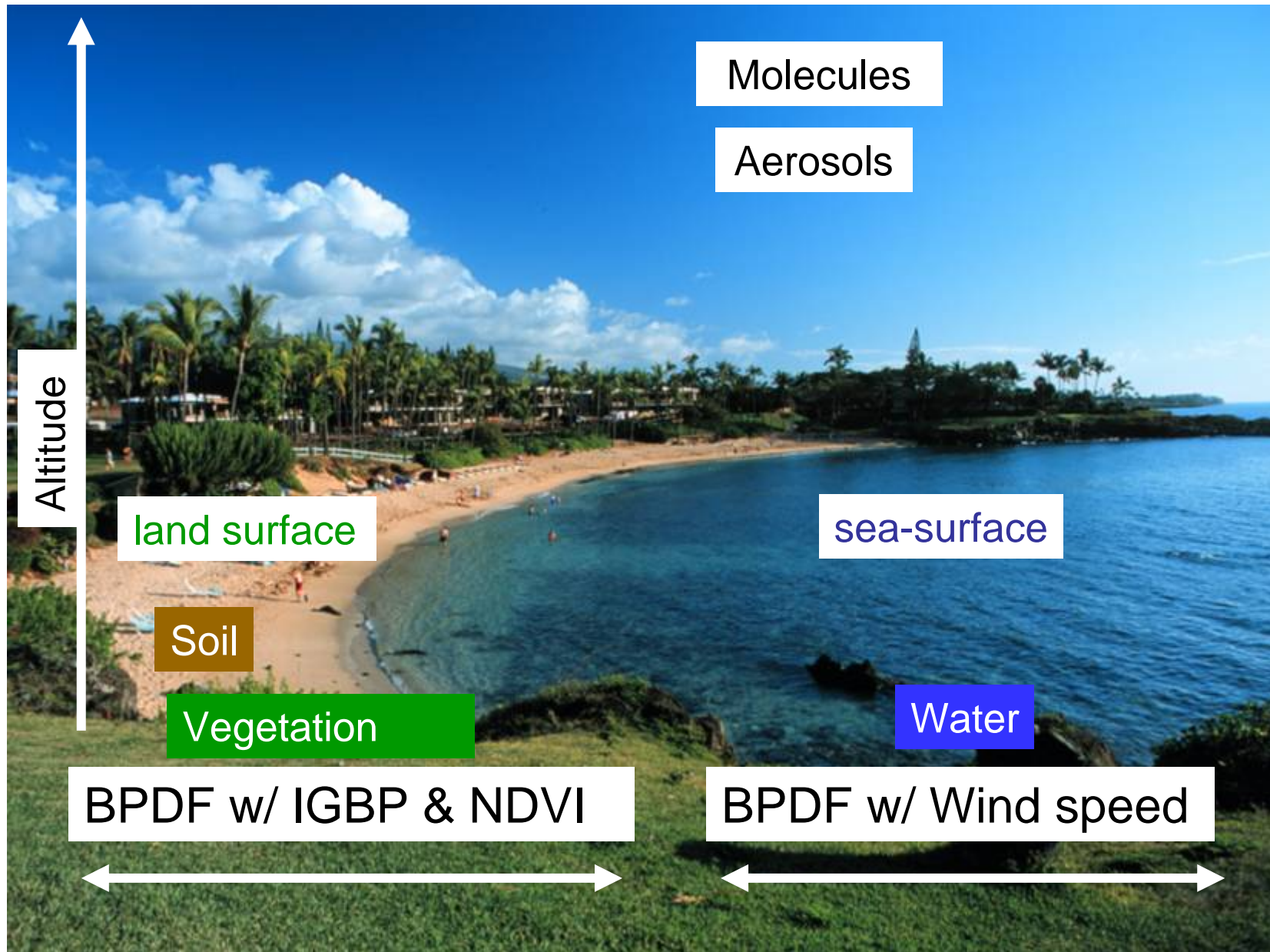
 - developed by CNES (France)

 - multi-angle viewing (up to 14 dir. = 14 scat. ang.)
 - polarization (Q, U) at 0.44, 0.67 and 0.87 μm
 - large FOV (global obs. / 1 day)
 - coarse resolution 6 by 7 km^2 at nadir

Processing line for POLDER



Atmosphere-surface model



Model description

Table 1. Atmosphere-Earth surface system.

Models	Descriptions
Aerosol models	
1. concentration :	Optical thickness of aerosols (τ_a),
2. size :	Angstrom exponent (a), which is calculated from Mie-scattering theory assuming log- normal size distribution
3. chemical composition	Complex refractive index (m).
Molecular information	AFGL US standard by Kneizys et al. (1988)
Ocean surface model	Cox and Munk (1954) model with 5 m/s wind speed, for the clear day.
Ocean model	completely absorbent in the near infrared wavelength.
Land surface model	Bi-directional polarization distribution functions by Nadal and Breon (1999) is adopted for soil, vegetated, and mixed of both, which is selected by land surface condition at target area.
Land classification	IGBP land classification map (Loveland et al., 2000) and NDVI values from POLDER Vis.- NIR measurements.
Land altitude	5 cases; sea level, 1, 2, 3, 4 km height

Aerosol models

- Spherical aerosols
- Size distribution (Bi-modal log-normal)
 - Modal radius of fine and coarse are chosen from aerosol climatology based on AERONET (Dubovik, 2002).
 - Fine mode $(rg_f, \ln \sigma_f) = (0.135, 0.430 \mu\text{m})$
 - Urban, Industrial and Biomass burning aerosols
 - (GSFC, Paris, Mexico, and Maldives)
 - Coarse mode $(rg_c, \ln \sigma_c) = (2.365, 0.630 \mu\text{m})$
 - Dust and Oceanic aerosols
 - (Bahrain, Solar-Village, Cape Verde, and Lanai Island)
- Complex Refractive Index (n, k)
 - 1.40-0.000i, 1.45-0.0005i, 1.50-0.001i, 1.55-0.010i

Sensitivity of aerosol properties

- Based of Mie calculation

λ : 0.670 μm , 0.870 μm

Size distribution: Single model log-normal (r_g , σ)

r_g : 0.05, 0.1, 0.2, 0.4 μm

σ : 2.0 μm (fixed)

Refractive index (m)

Real : 1.40, ^{sulfate} 1.45, 1.50, ^{dust} 1.55

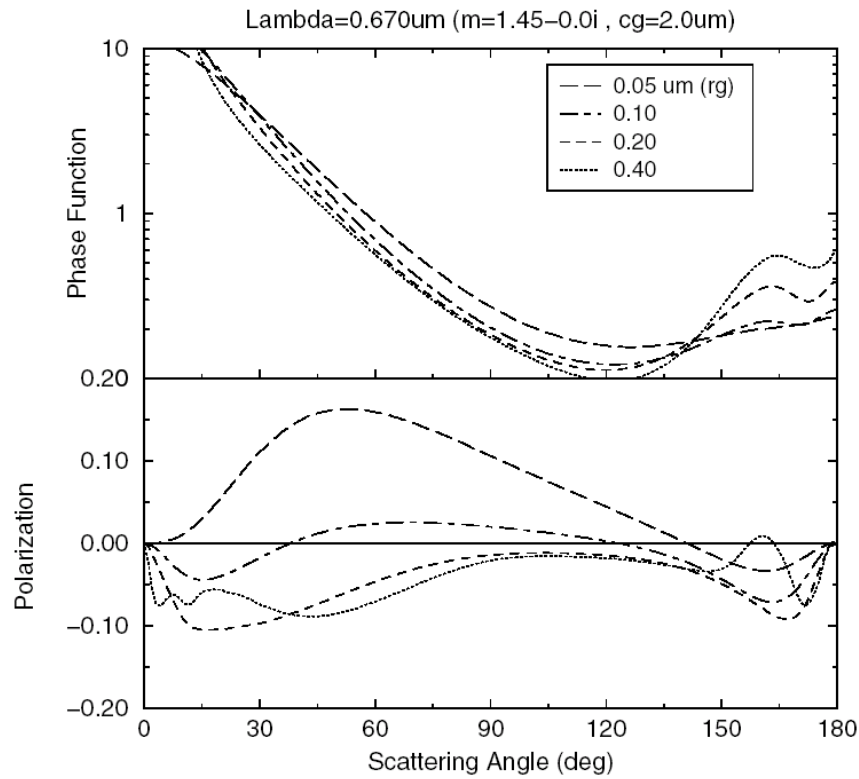
Imag: 0.0, 0.0005, 0.001, 0.002, 0.004

Dust aerosols by AERONET Ref.Img = 0.001 @ 0.87 μm

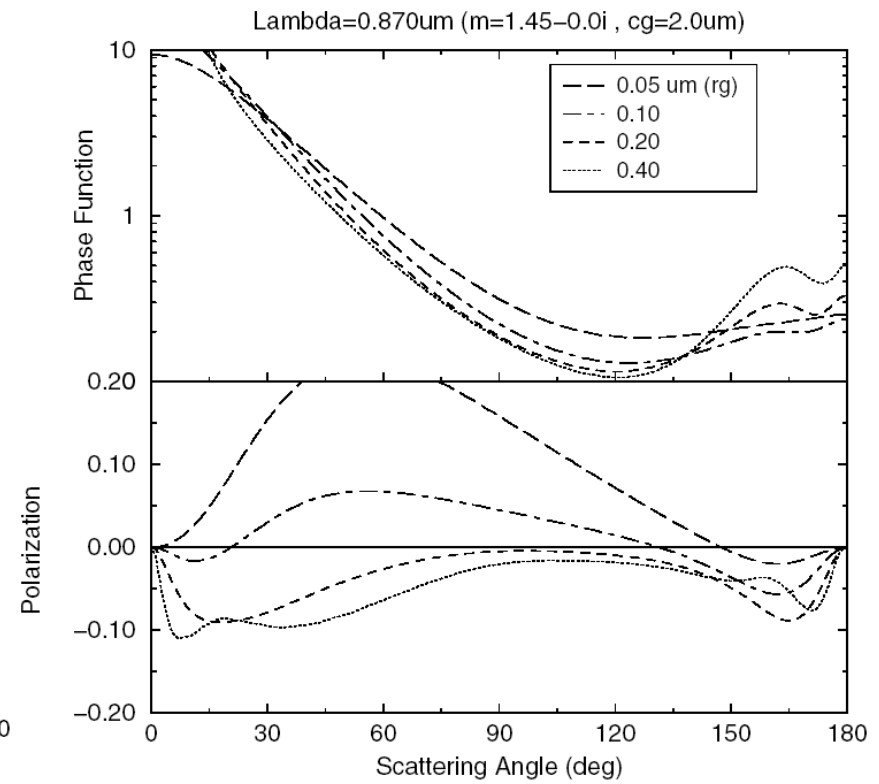
Sensitivity for size

($r_g = 0.05, 0.1, 0.2, 0.4 \mu\text{m}$, $\sigma = 2.0 \mu\text{m}$ (fixed))
 $m = 1.45 - 0.0i$ (fixed)

0.67 μm



0.87 μm

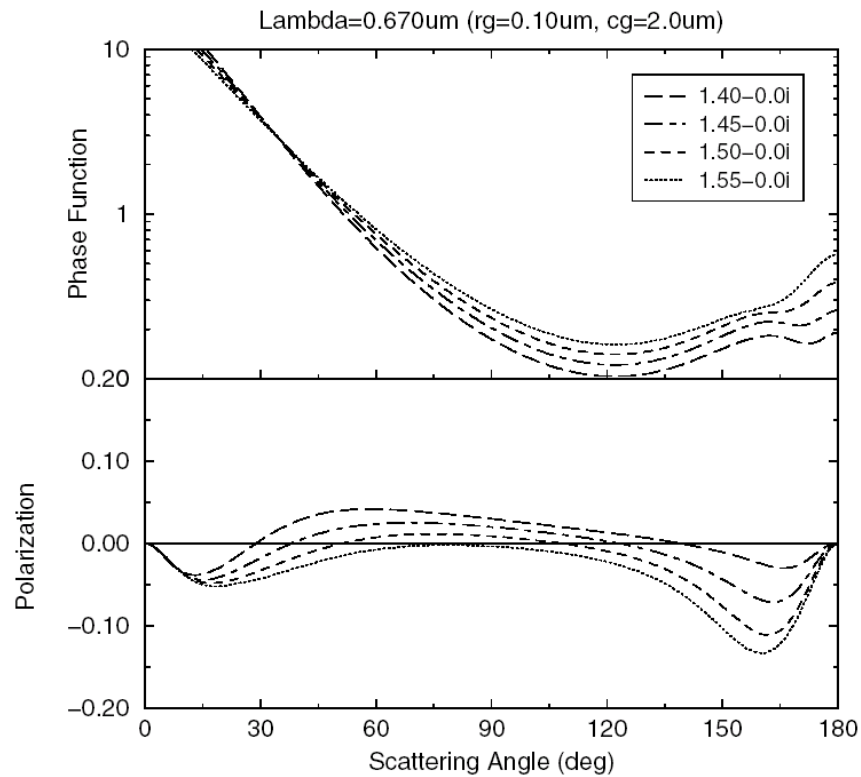


Sensitivity for Real part of Ref. Idx

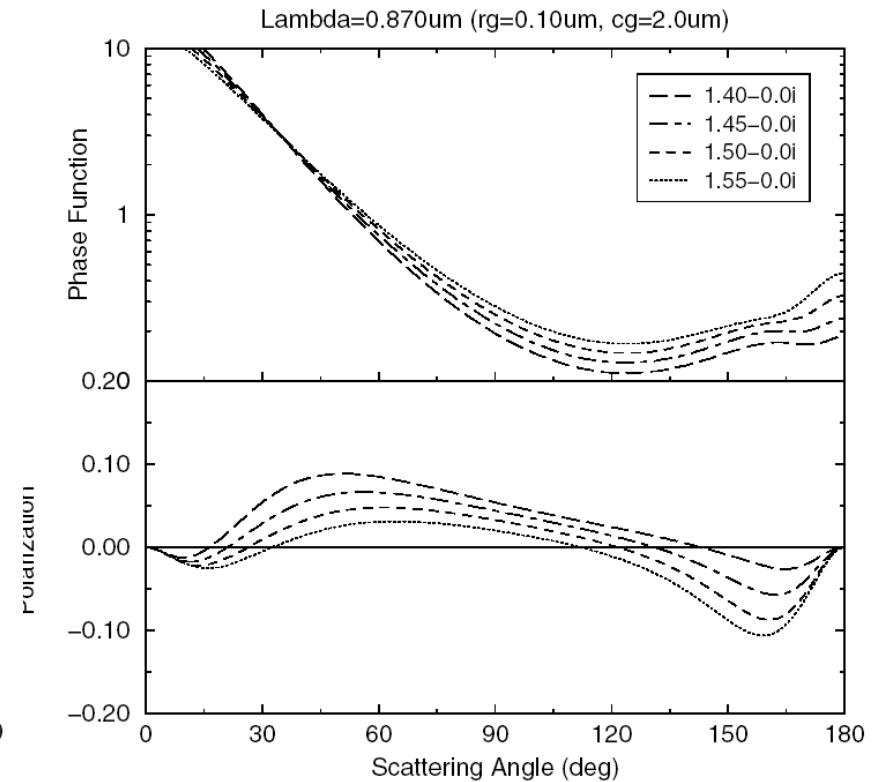
Size (Fixed): $r_g = 0.1 \mu\text{m}$, $\sigma = 2.0 \mu\text{m}$

$r_{fr} = 1.40, 1.45, 1.50, 1.55$, $r_{fi} = 0.0$ (Fixed)

$0.67 \mu\text{m}$



$0.87 \mu\text{m}$

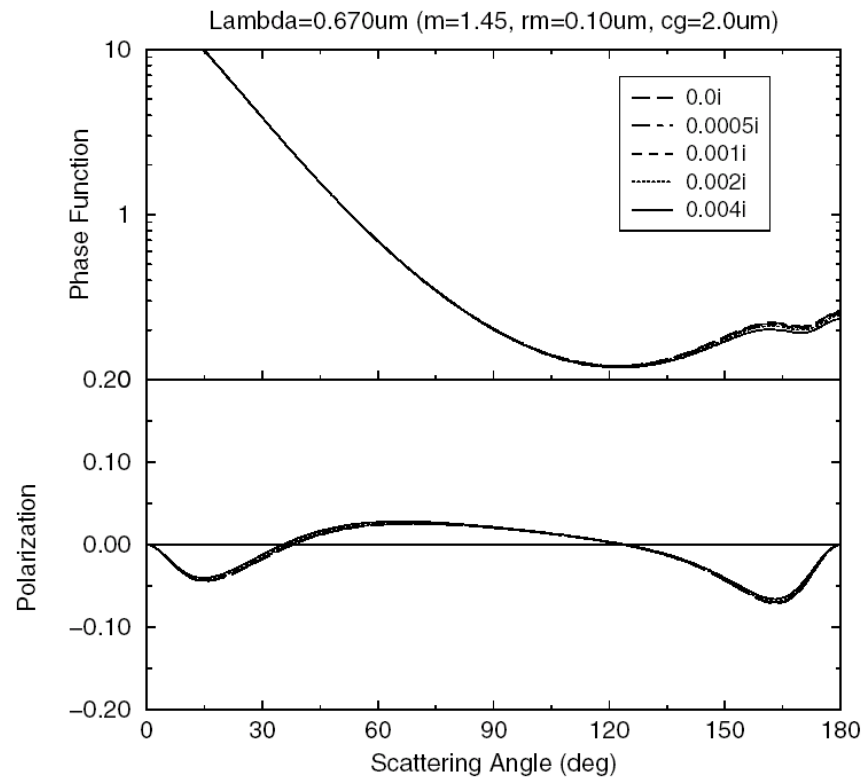


Sensitivity for Imag part of Ref. Idx

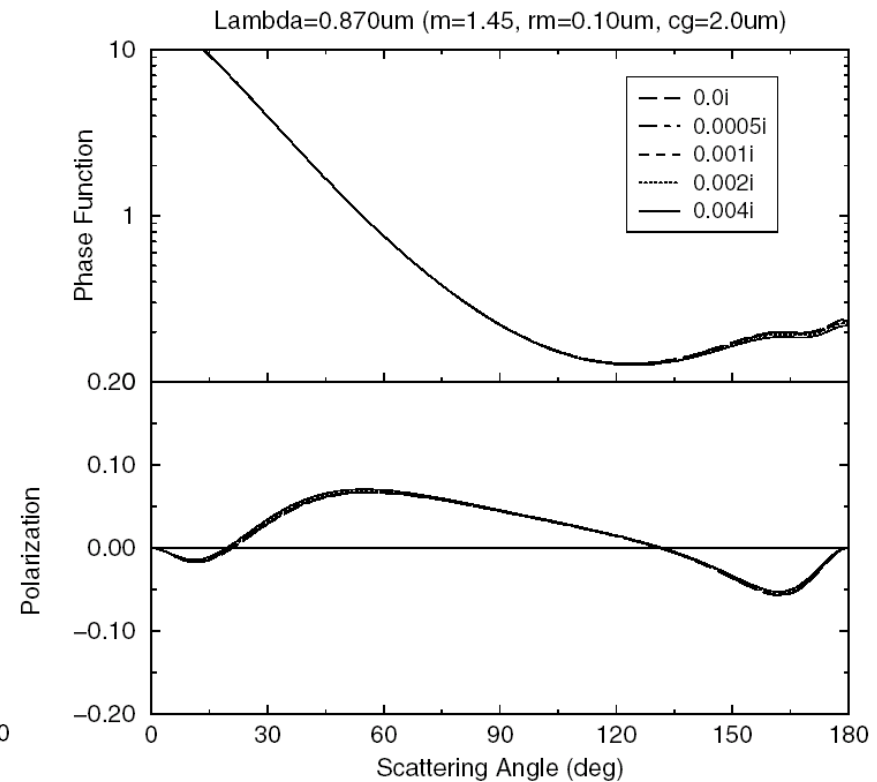
Size (fixed) : $r_g = 0.1 \mu\text{m}$, $\sigma = 2.0 \mu\text{m}$

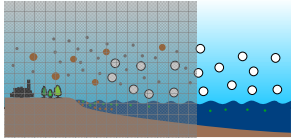
$r_{fr} = 1.45$ (fixed), $r_{fi} = 0.0, 0.0005, 0.001, 0.002, 0.004$

$0.67 \mu\text{m}$



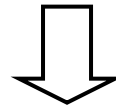
$0.87 \mu\text{m}$



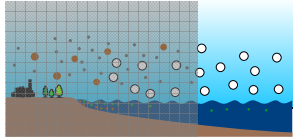


Aerosol retrieval over the ocean

radiance & polarization degree
at $0.670 \mu\text{m}$ and $0.865 \mu\text{m}$

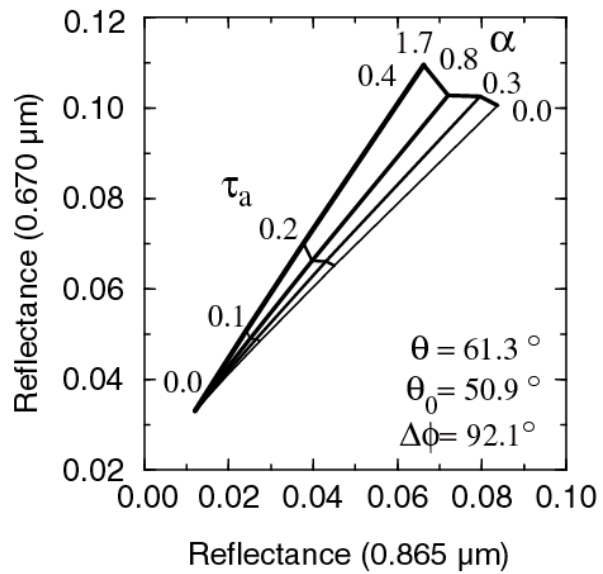


optical thickness (τ)
Ångström exponent (α)
refractive index (m ; real part)

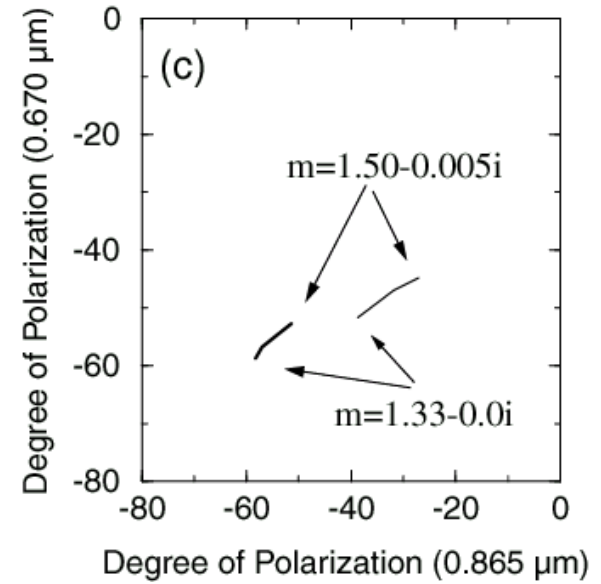
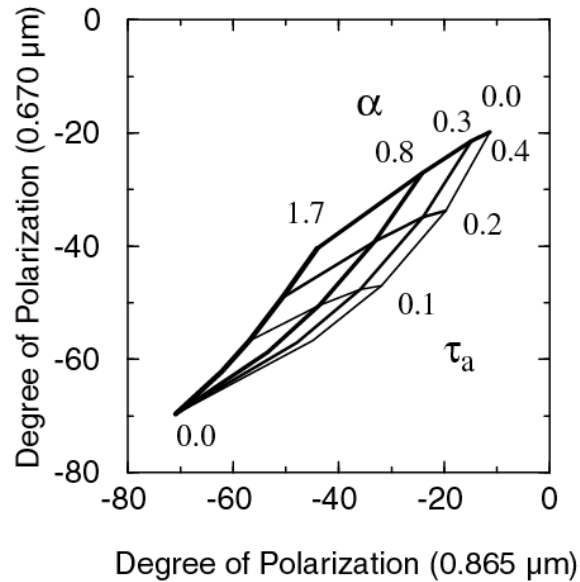


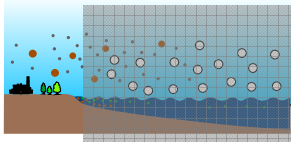
Aerosol retrieval over ocean

Intensity



Degree of Polarization

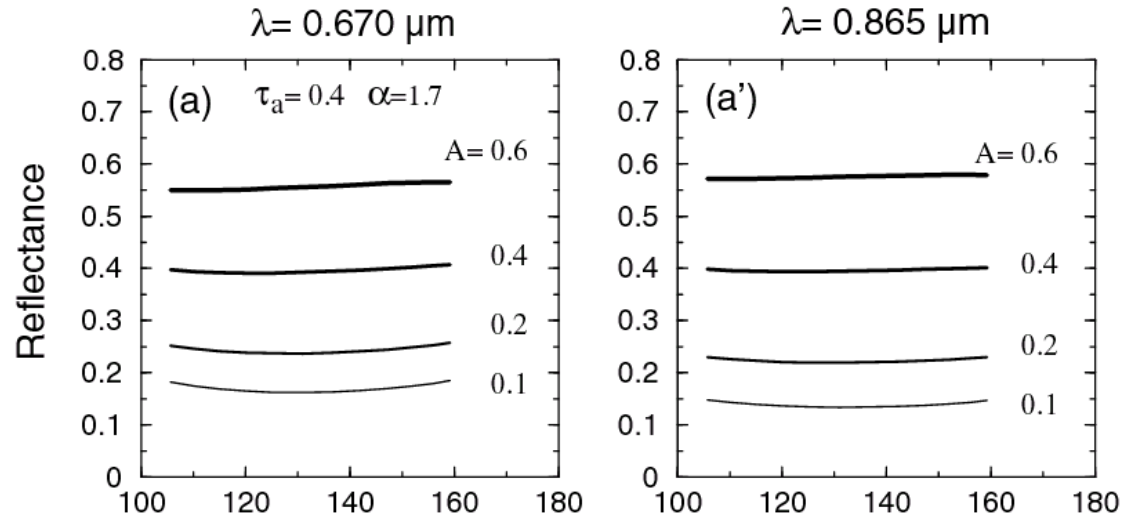




Aerosol retrieval over land

Intensity

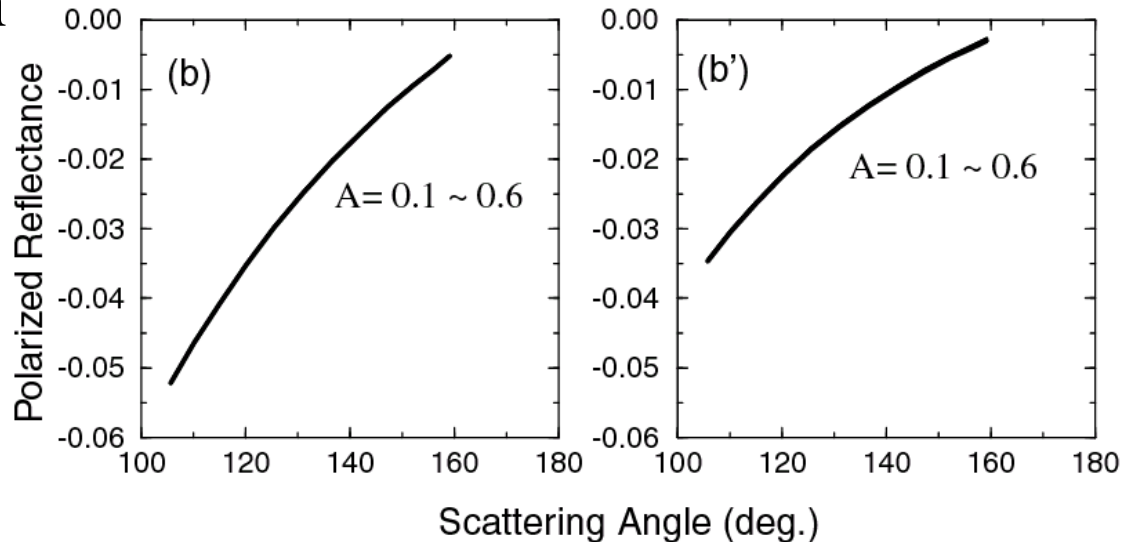
Lambertian surface



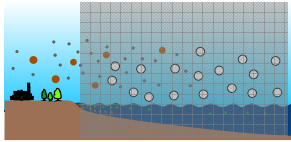
Large variability : Albedo dependent

Polarization

Lambertian surface

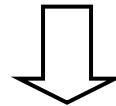


no variability : Albedo independent

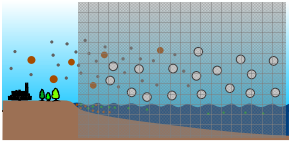


Aerosol retrieval over land

polarized radiance
at $0.670\mu\text{m}$ and $0.865\mu\text{m}$

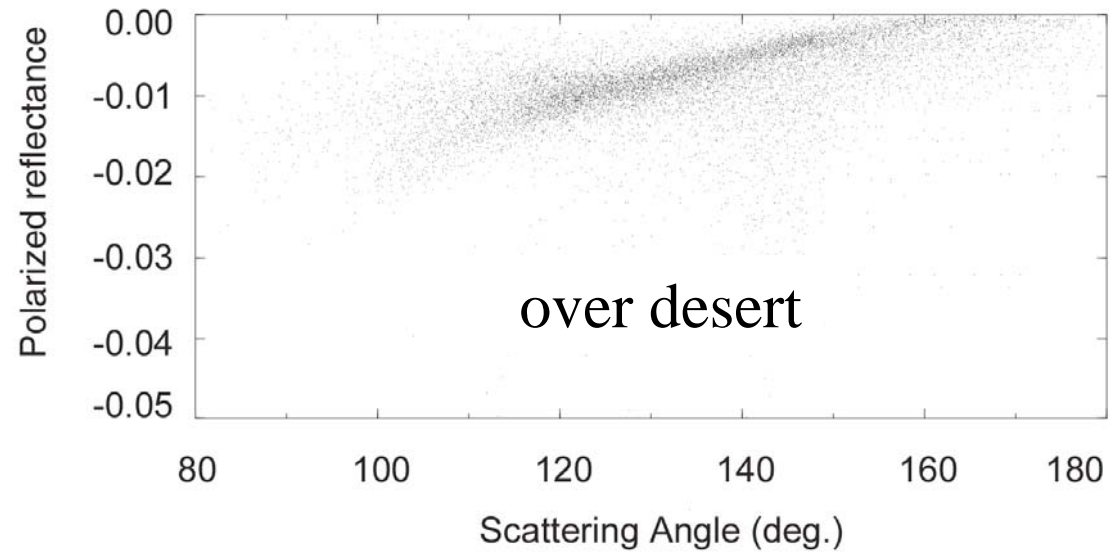


optical thickness (τ)
Ångström exponent (α)

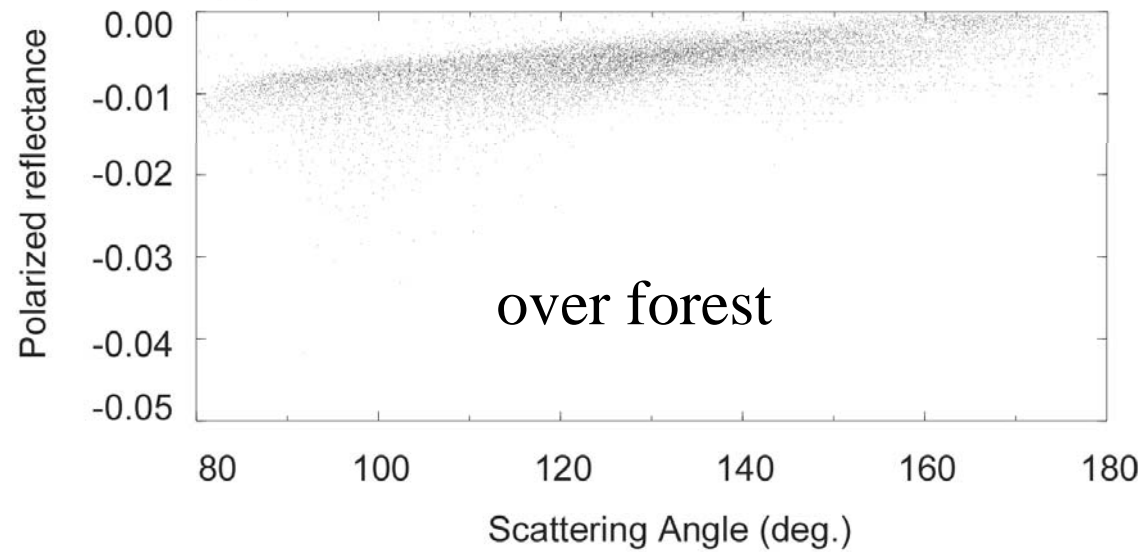


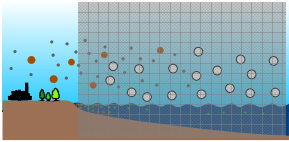
Surface model

(a) NDVI < 0.3

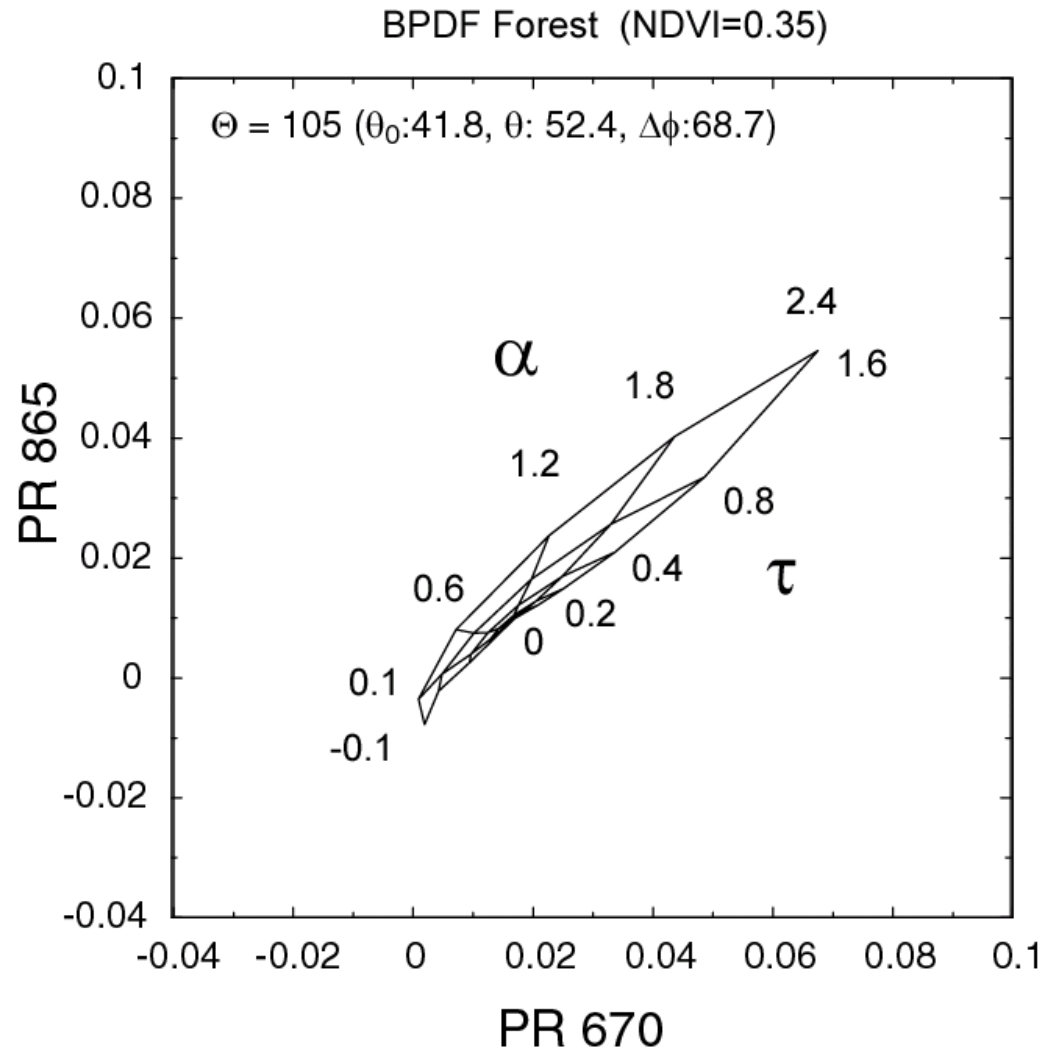


(b) NDVI > 0.6





Relationship between polarized reflectance at wavelength of 0.670 μm and that of 0.865 μm



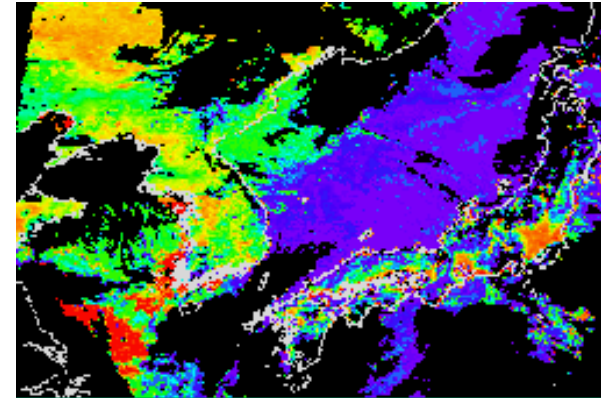
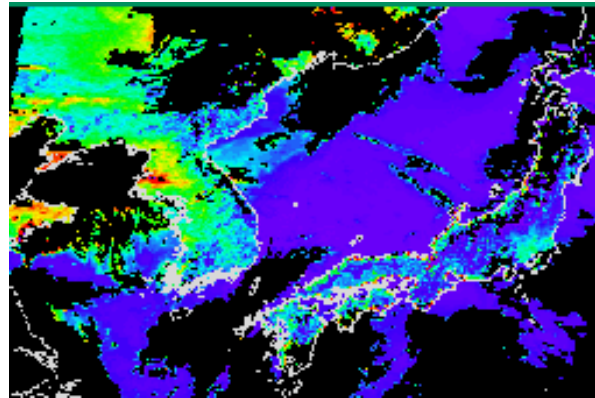
2.3.2 Retrieved aerosols from POLDER-1

Retrieved aerosol distribution over Japan

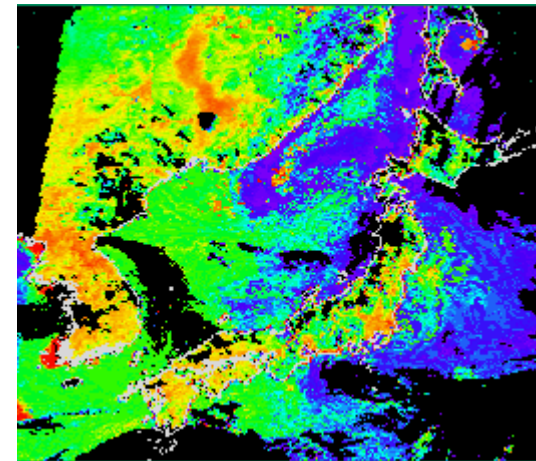
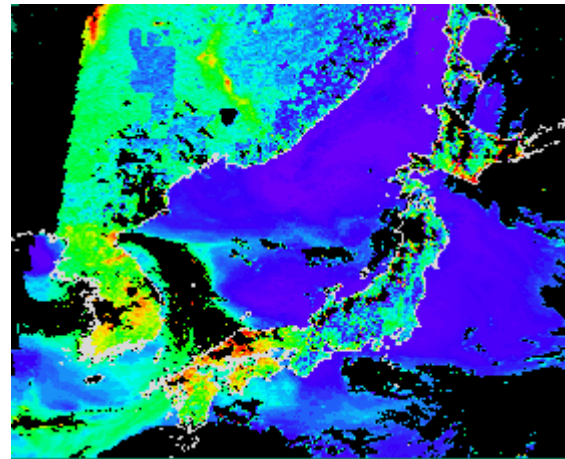
Aerosol optical thickness

Angstrom exponent

March 18, 1997

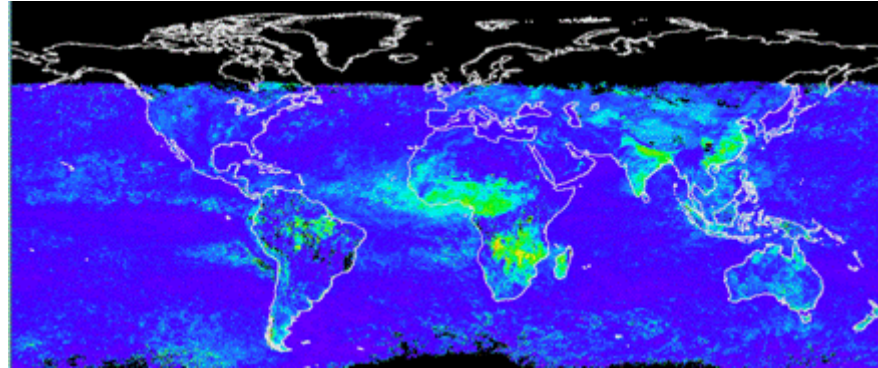


April 25, 1997

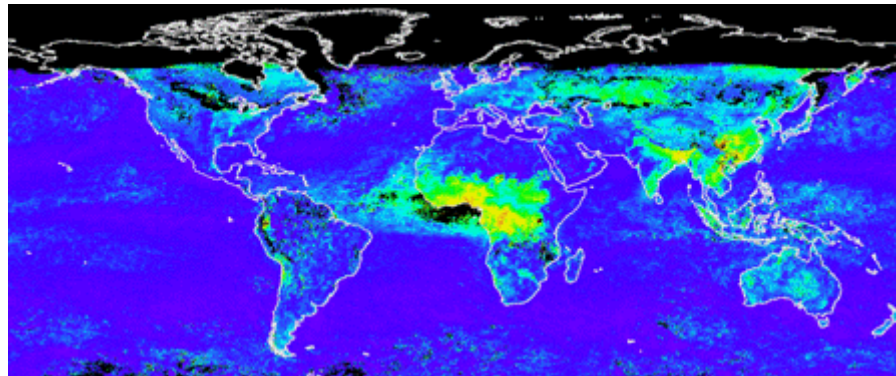


Retrieved global distribution of AOT(τ)

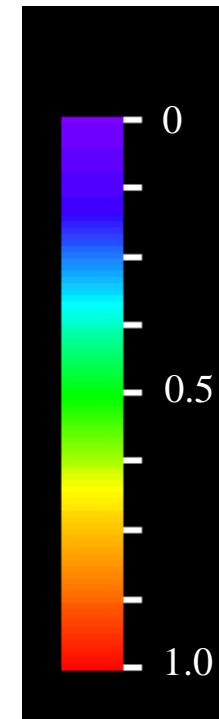
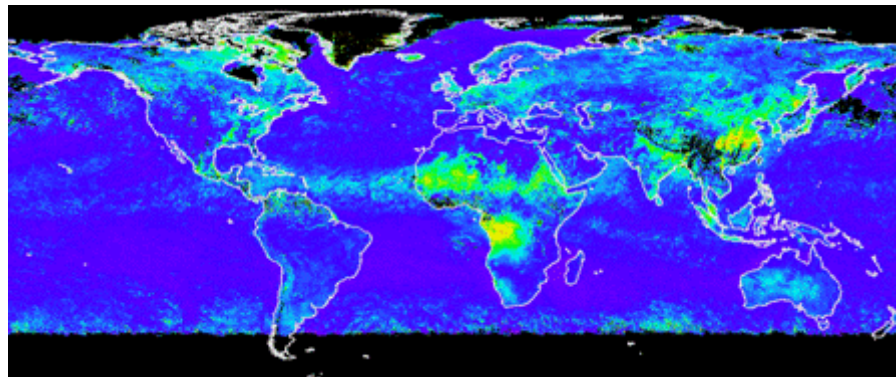
Nov. 1996



Feb. 1997



Jun. 1997



Retrieved anthropogenic aerosols on a global scale

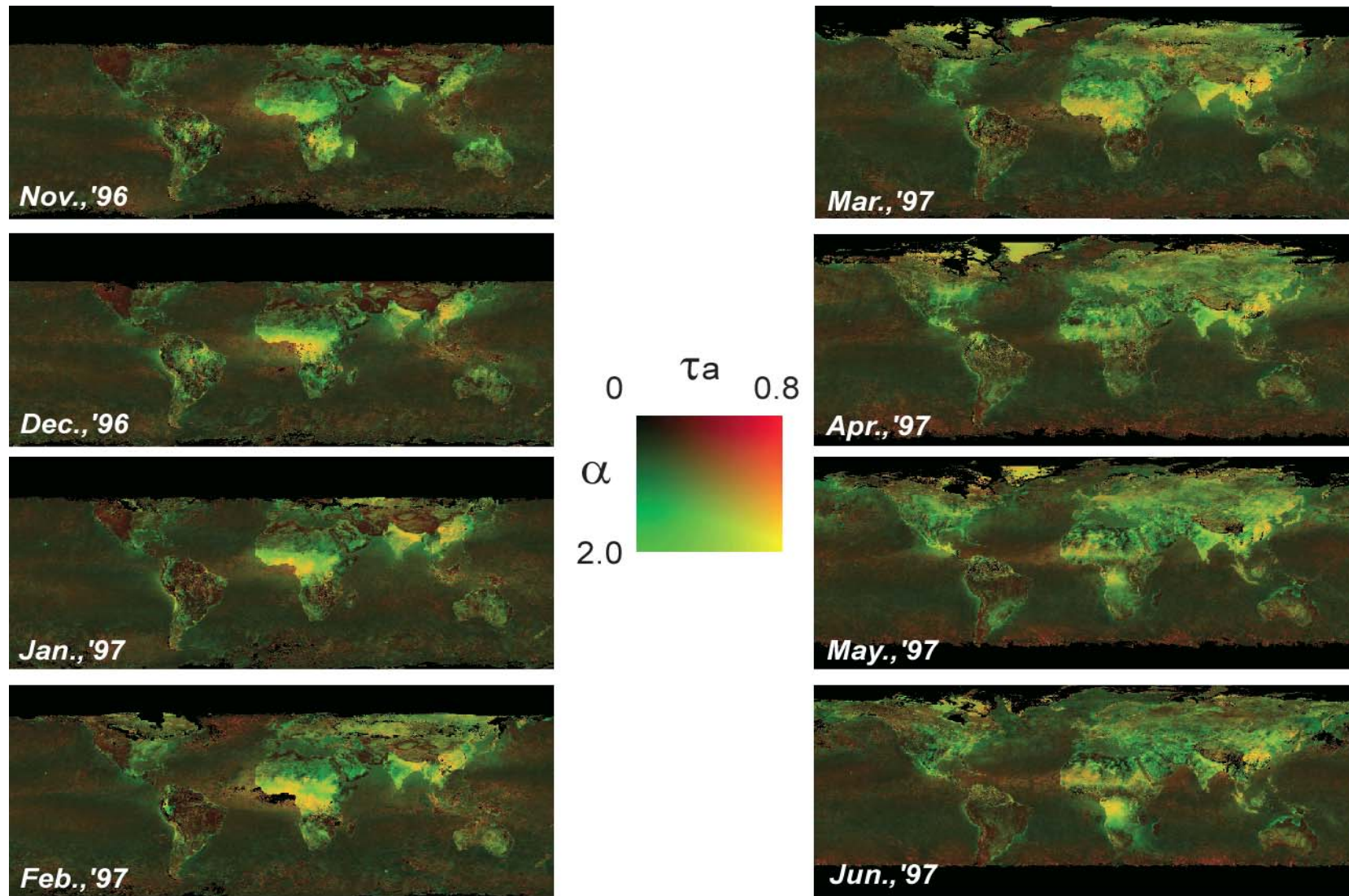
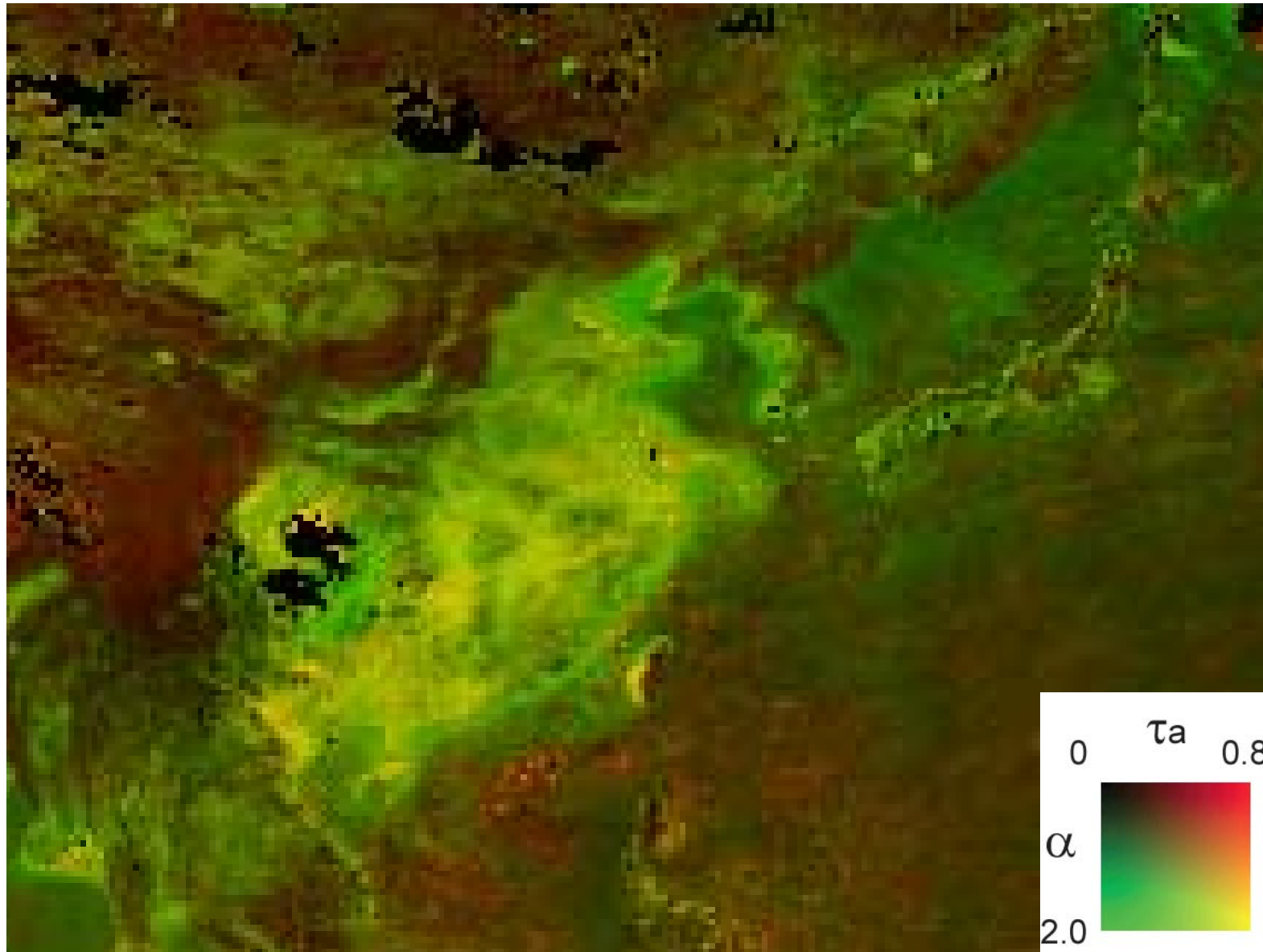


Figure 6. Composite images of aerosol optical thickness and Angstrom exponent from November, 1996 to June, 1997. The aerosol optical thickness and Angstrom exponent are assigned to red and green color, respectively.

Aerosols over East Asia : November, 1996



2.3.3 Retrieved aerosols from POLDER-2

Retrieved results derived from POLDER-2 data

1. Aerosol Events

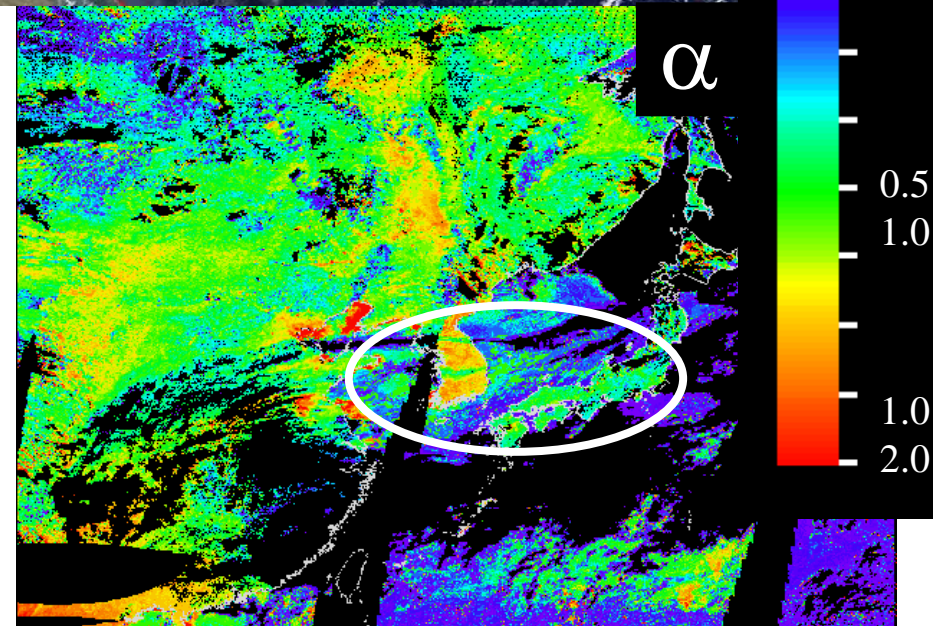
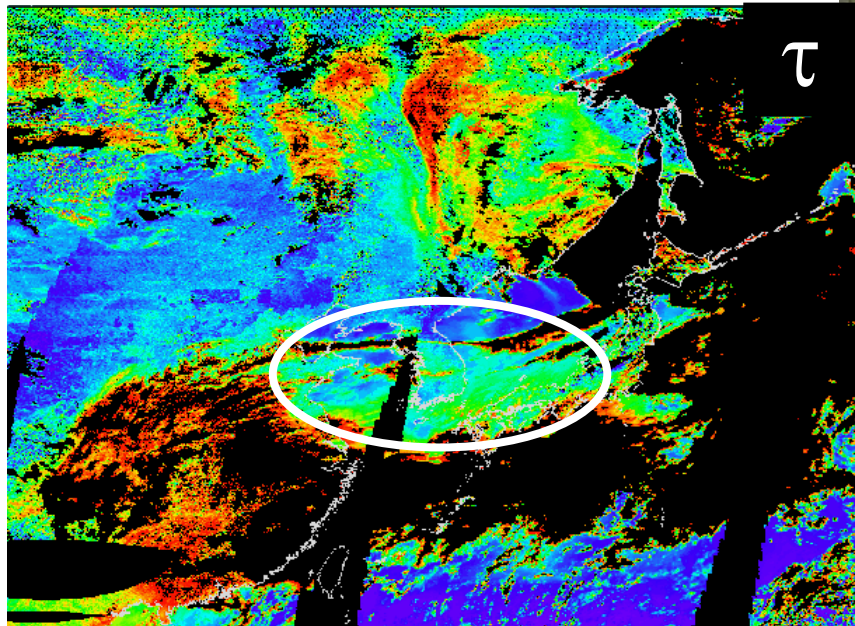
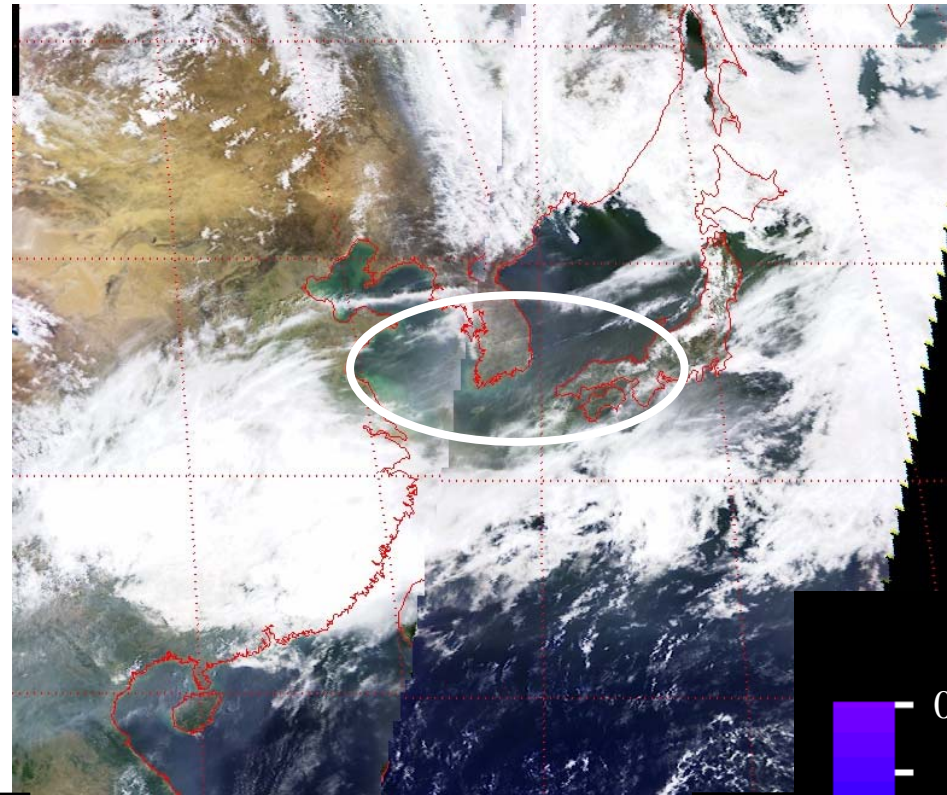
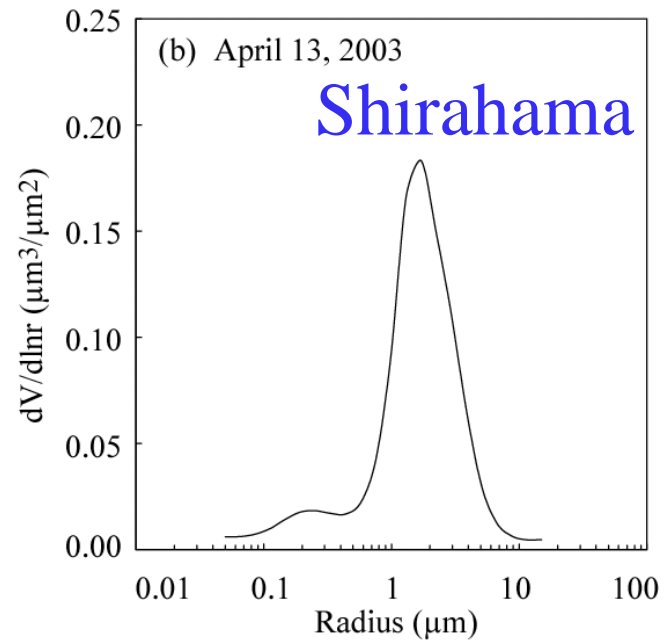
Dust event on April 13, 2003

Bio-mass burning on May 21, 2003

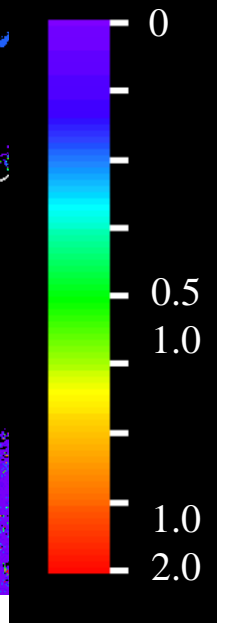
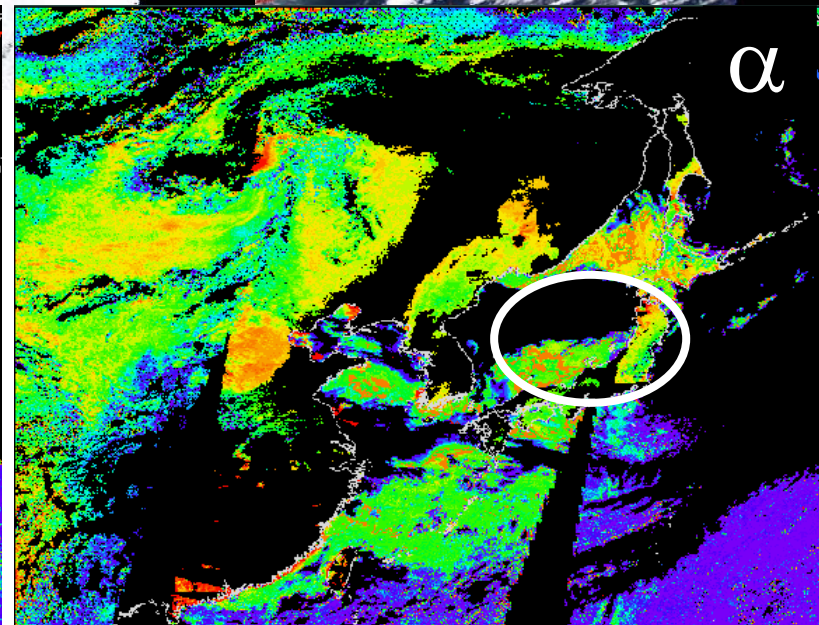
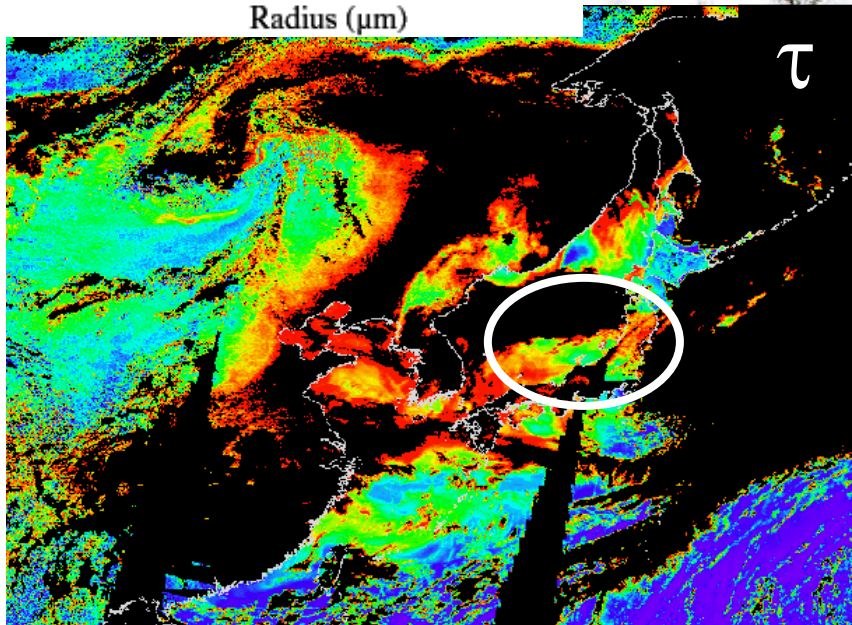
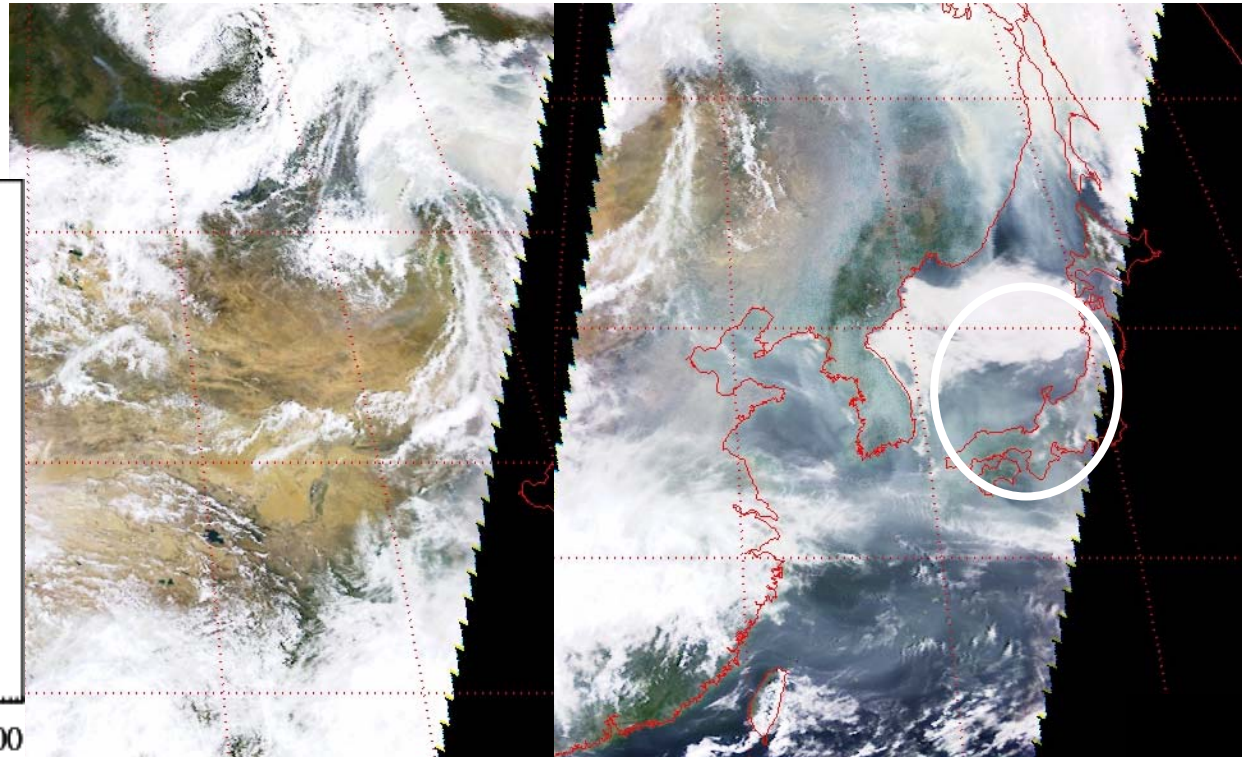
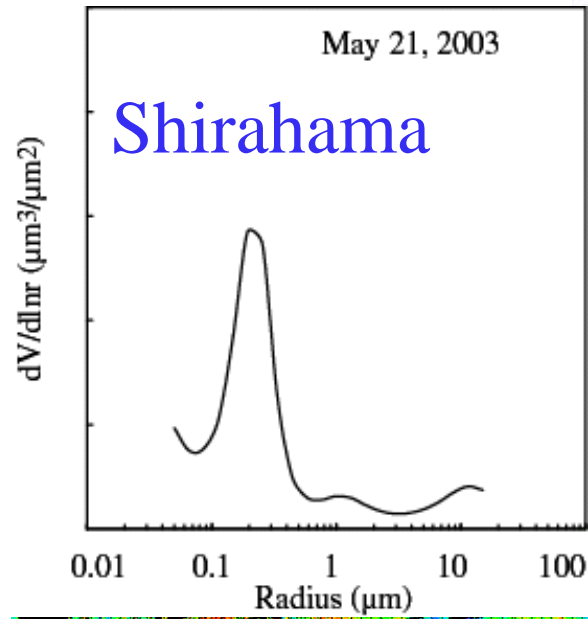
2. Global map in April, May, and June

3. Comparison of global map in AMJ, 1997 with that, 2003

Apr.13, 2003

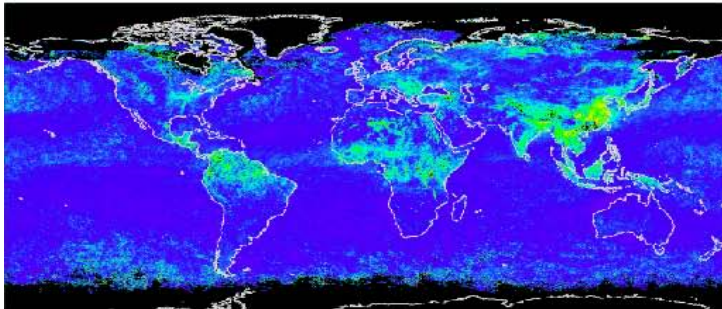


May 21, 2003

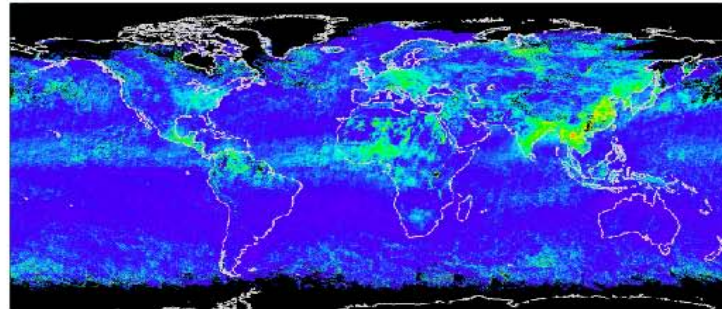


Inter-annual change in AOT (1997-2003)

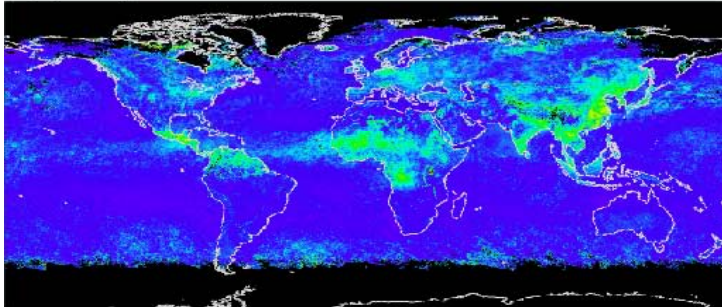
(a) April, 1997



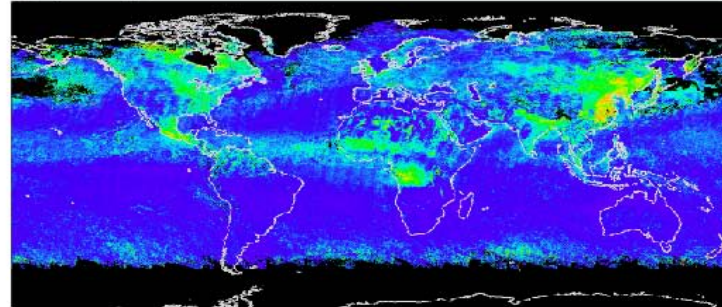
(a') April, 2003



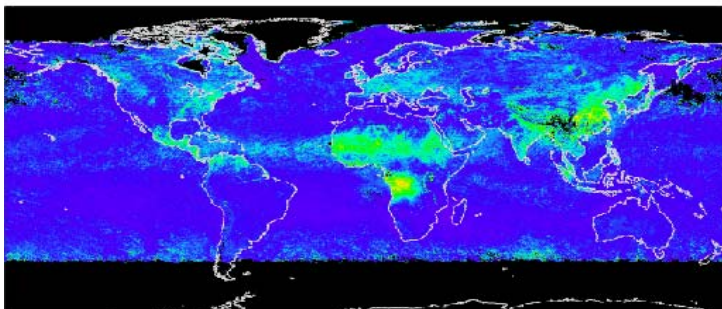
(b) May, 1997



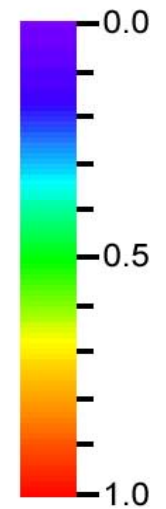
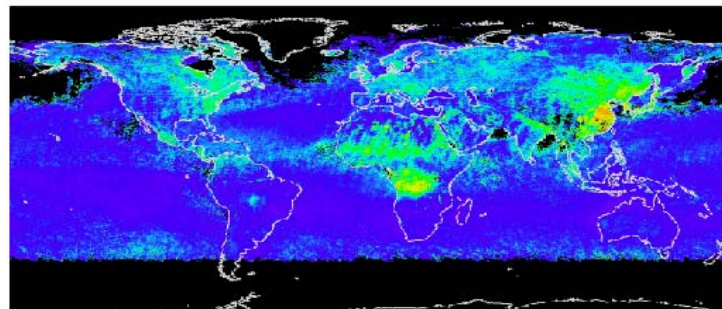
(c') May, 2003



(c) June, 1997

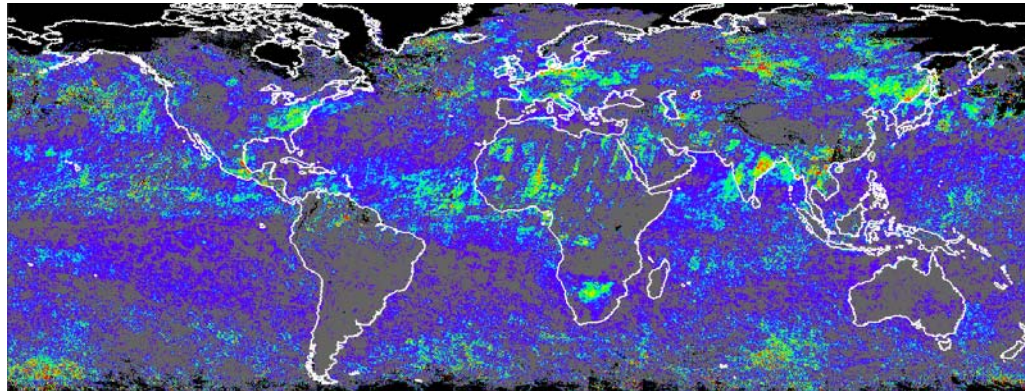


(c') June, 2003

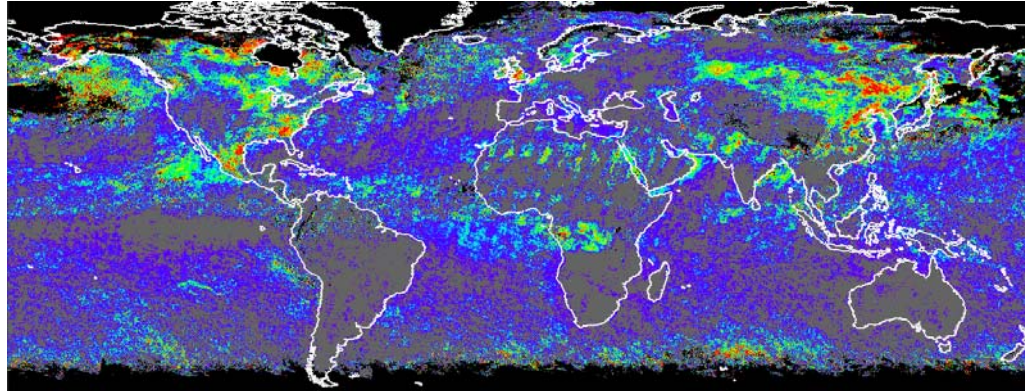


Inter-annual change in AOT (1997-2003)

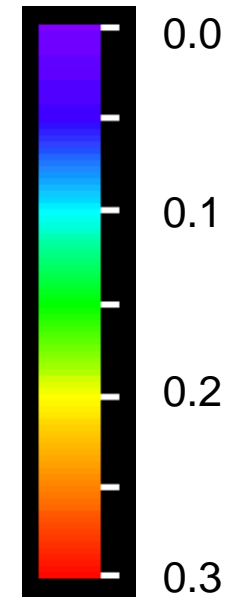
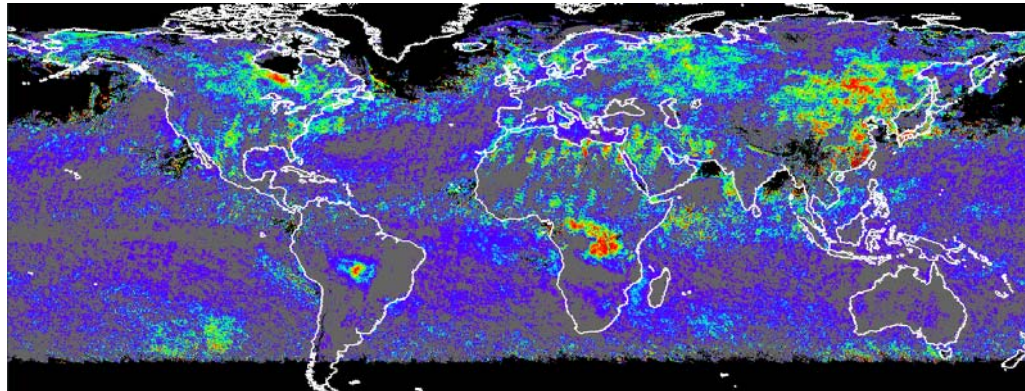
April



May



June



Contents

1. Introduction
2. Satellite aerosol remote sensing
 - 2.1 Basic concept
 - 2.2 Light scattering by aerosols
 - 2.3 Satellite aerosol retrieval
3. Validation of aerosol remote sensing
 - 3.1 Ground-based sun photometry
 - 3.2 Model simulation
4. Future satellite sensors

3.1.1. NASA/AERONET

Validation of aerosol remote sensing



Aerosol robotic network

GODDARD SPACE FLIGHT CENTER+ Visit NASA.gov



+ AEROSOL OPTICAL DEPTH	+ AEROSOL INVERSIONS	+ SOLAR FLUX	+ OCEAN COLOR	+ MARITIME AEROSOL
-------------------------	----------------------	--------------	---------------	--------------------

Web Site Feature **AERONET Data Synergy Tool - Access Earth Science data sets for AERONET sites**

- Home
- Home**
- + AEROSOL/FLUX NETWORKS
- + CAMPAIGNS
- + COLLABORATORS
- + DATA
- + LOGISTICS
- + NASA PROJECTS
- + OPERATIONS
- + PUBLICATIONS
- + SITE INFORMATION

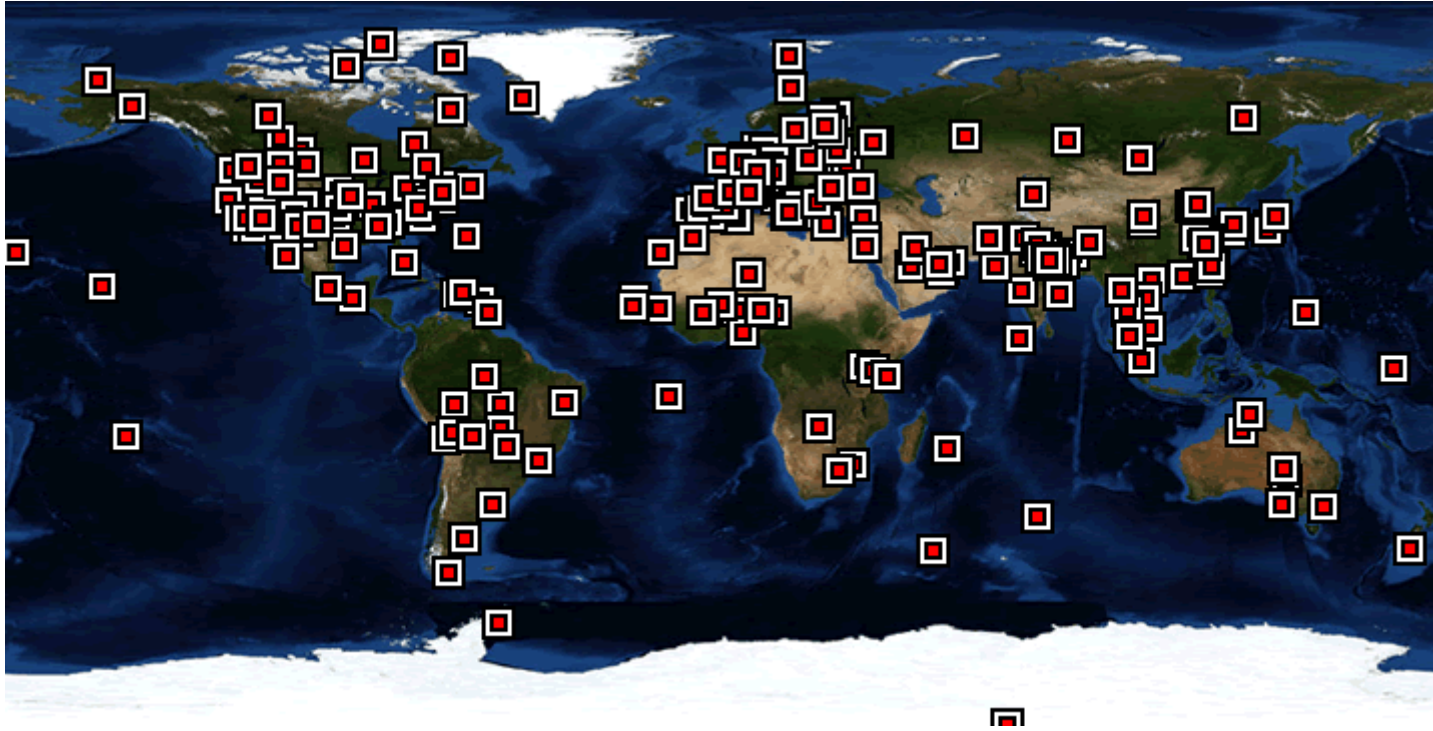
MISSION

The AERONET (**A**erosol **R**obotic **N**ETwork) program is a federation of ground-based remote sensing aerosol networks established by **NASA** and **LOA-PHOTONS (CNRS)** and is greatly expanded by **collaborators** from national agencies, institutes, universities, individual scientists, and partners. The program provides a long-term, continuous and readily accessible public domain database of aerosol optical, microphysical and radiative properties for aerosol research and characterization, validation of satellite retrievals, and synergism with other databases. The network imposes standardization of **instruments, calibration, processing and distribution**.

AERONET collaboration provides globally distributed observations of spectral aerosol optical depth (AOD), inversion products, and precipitable water in diverse aerosol regimes. Aerosol optical depth data are computed for three data quality levels: **Level 1.0 (unscreened)**, **Level 1.5 (cloud-screened)**, and **Level 2.0 (cloud-screened and quality-assured)**. Inversions, precipitable water, and other AOD-dependent products are derived from these levels and may implement additional quality checks.

The processing algorithms have evolved from Version 1 to Version 2.0 (fully released in July 2006) and are available from the AERONET and PHOTONS web sites. Version 1 data may be downloaded from the web site through 2006 and thereafter upon **special request**. New AERONET products will be released as new measurement techniques and algorithms are adopted and validated by the AERONET research community. The AERONET web site also provides AERONET-related news, a description of research and operational activities, related Earth Science links, and an AERONET staff directory.

World wide sun photometer network



200 sites
world wide

3 sites in Japan

Shirahama (2000~)

Osaka ('02, 2004~)

Noto ('01, '03, 2007~)

Instrument

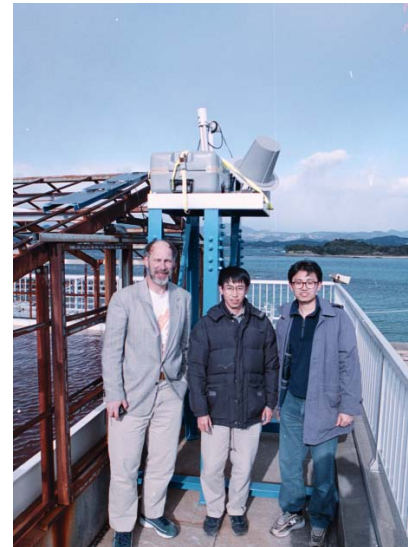
Cimel CE-318 sun/sky radiometer

0.34, 0.38, 0.44, 0.50, 0.67, 0.87, 0.94, 1.02 μm
(+polarization, +1.64 μm etc.)

Power: 12V Battery with solar panel

Controler: Water proof box

Data logger: Sat. Trans. GOES, Meteosat, GMS)



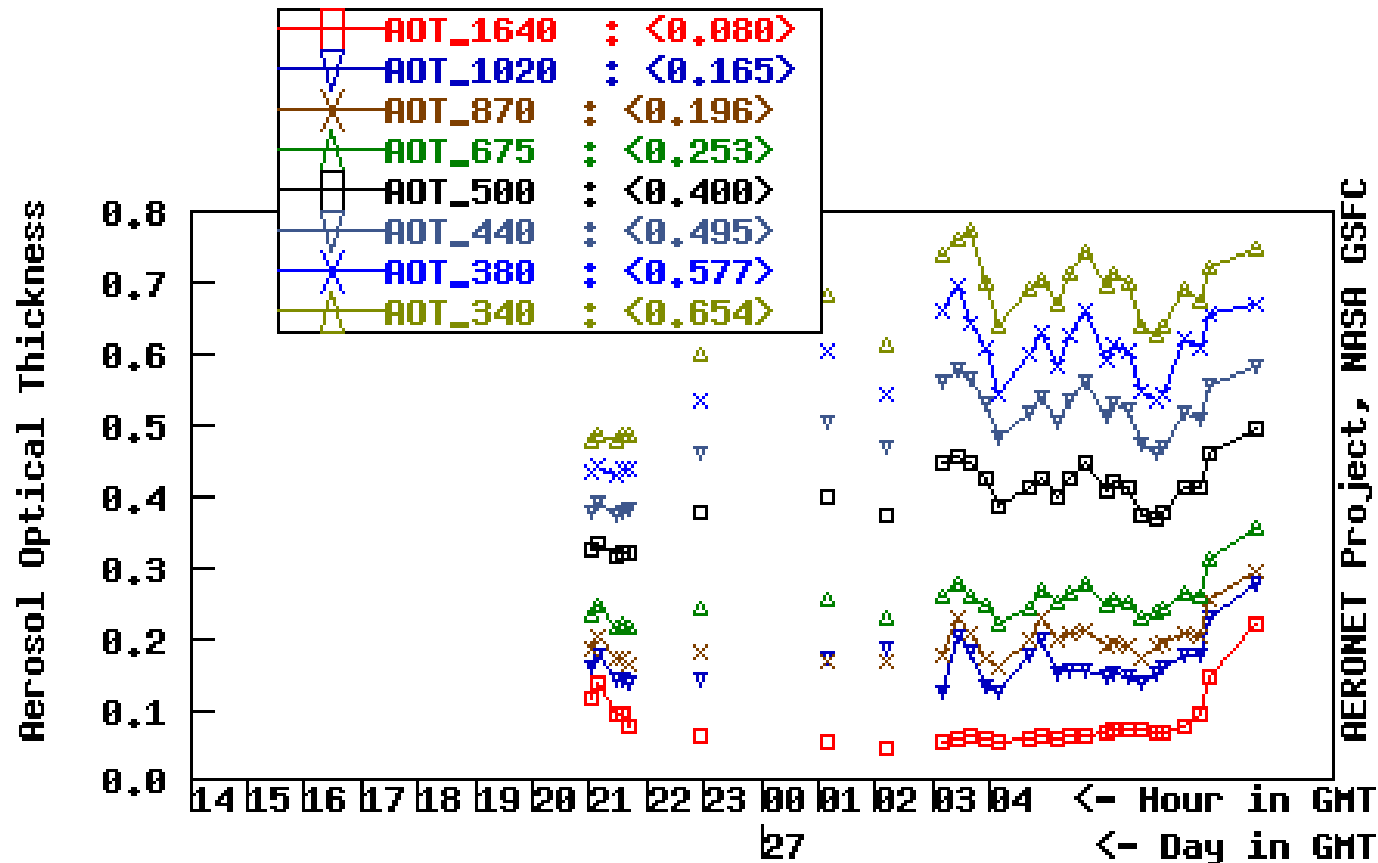
Swap out package

sensor head
collimator
cable
connectors brd.
control box



AOT measurements at Osaka

Osaka , N 34°39'03", E 135°35'27", Alt 50 m,
 PI : Itaru_Sano, sano@info.kindai.ac.jp
 Level 1.5 AOT; Data from 27 MAY 2008



AERONET Project, NASA GSFC

MAY
2008

Version 2 DS

Data quality

Quality assured AOT

± 0.01 (all instruments)

± 0.003 (master inst.)

Calibration for direct light

Master instruments

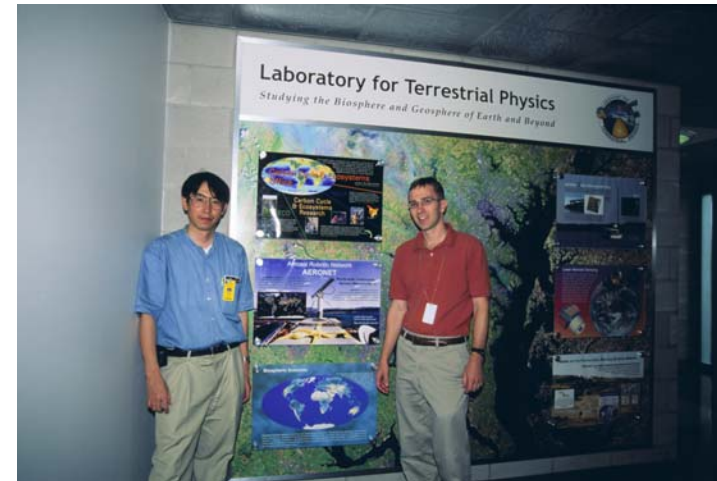
calibrated at Mauna Loa Observatory

Others

Inter calibration (trans. master to others,

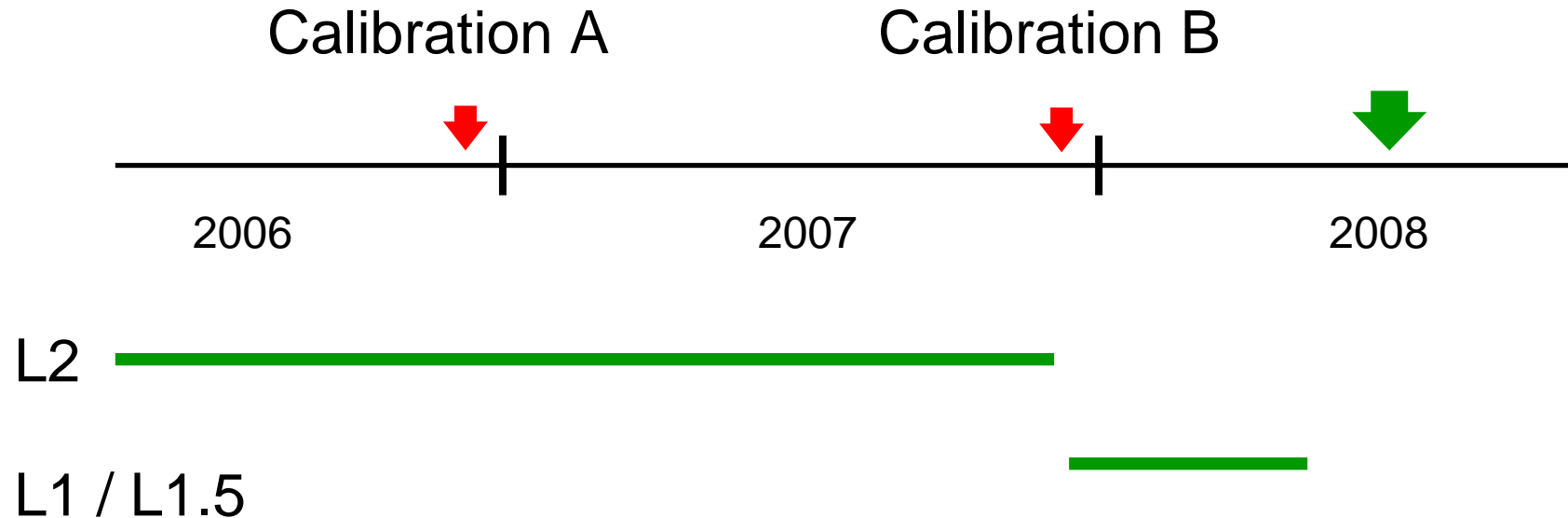
Calibrations for diffuse light

Integrated sphere (GSFC, LOA etc.)



Inter cal. at GSFC

Level 2 (quality assured) data



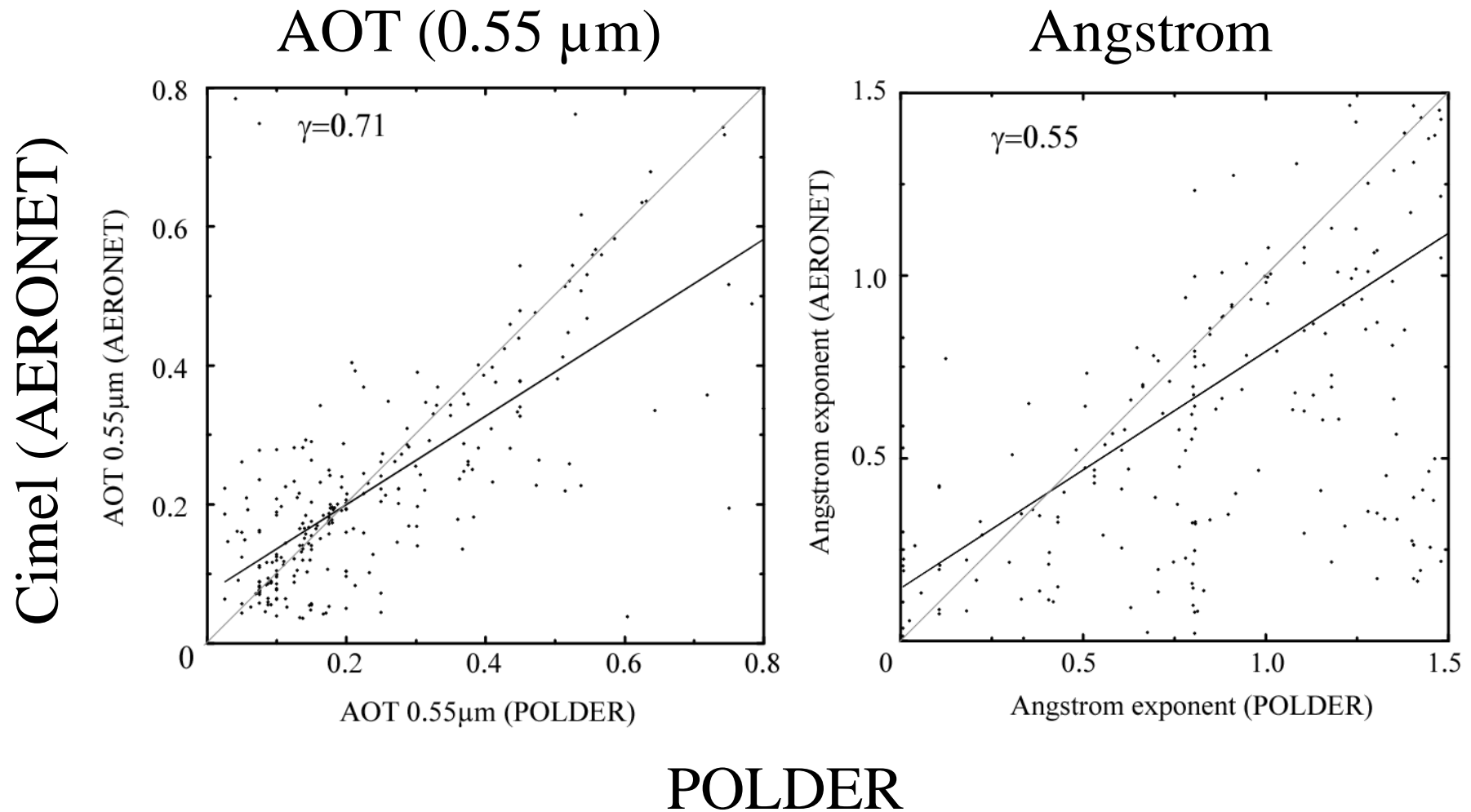
L1	Cal. B	w/o cloud screening
L1.5	Cal. B	w/ cloud screening
L2	Cal. A/B	w/ cloud screening and human check

Validation of POLDER results with sun photo (AERONET) data

Eleven AERONET sites (Aire Adour, Banizoumbou, Bidi Bahn, Bondoukou, Dakar, Dalanzadgad, GSFC, Los Fieros, Mfuwe, and Zambezi) are selected for validating the retrieved results from POLDER-1 data according to the following rules:

- 1) The AERONET measurements are selected within the ± 30 minutes over flight ADEOS-1 satellite.
- 2) The values of AOT at wavelengths of 0.443, and 0.870 μm as ground based measurements are selected for calculating Angstrom exponent.
- 3) The AOT at wavelength 0.550 μm is estimated based on the Angstrom exponent and the measurement of 0.670 μm .
- 4) The POLDER results are selected within the $\sim 20\text{km}$ (3x3 POLDER grid) square around the AERONET site.

Validation of retrieved results over land



3.1.2 Aerosol properties from MODIS Level 2 product (MYD04)

MODIS Aerosol product

MOD04 (Terra) , MYD04 (Aqua)

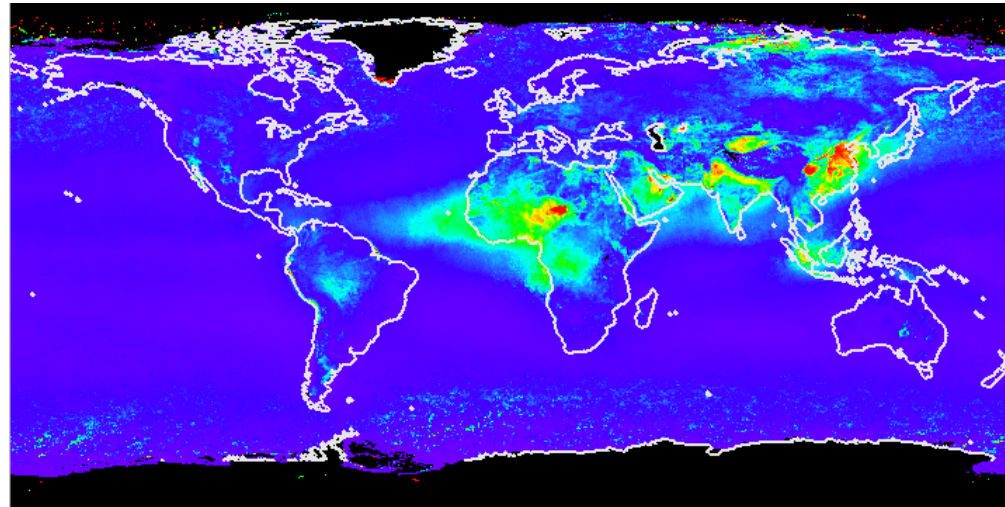
- L2 scene (10 by 10 km²)
- L3 monthly product

- AOT over ocean and land
- other aerosol properties are also available.

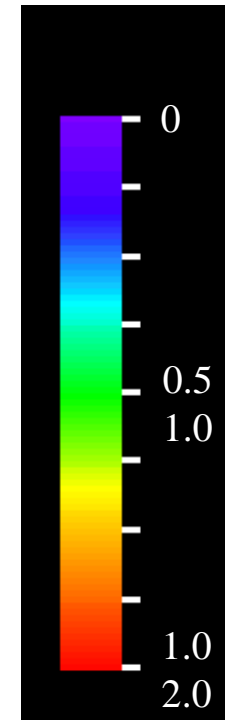
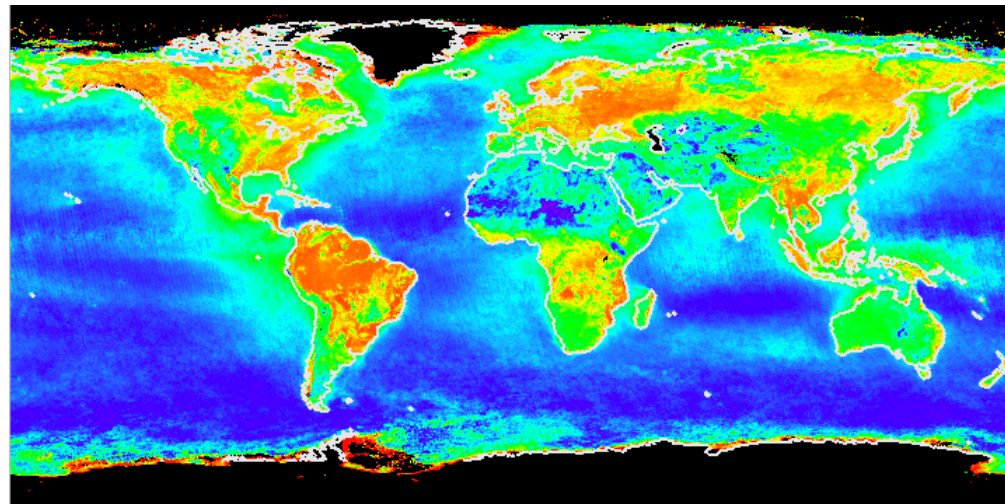
http://modis-atmos.gsfc.nasa.gov/MOD04_L2/index.html

Aerosols by MODIS/Aqua in 2006

Monthly mean of AOT (0.55 μm) (w/ deep blue algorithm)

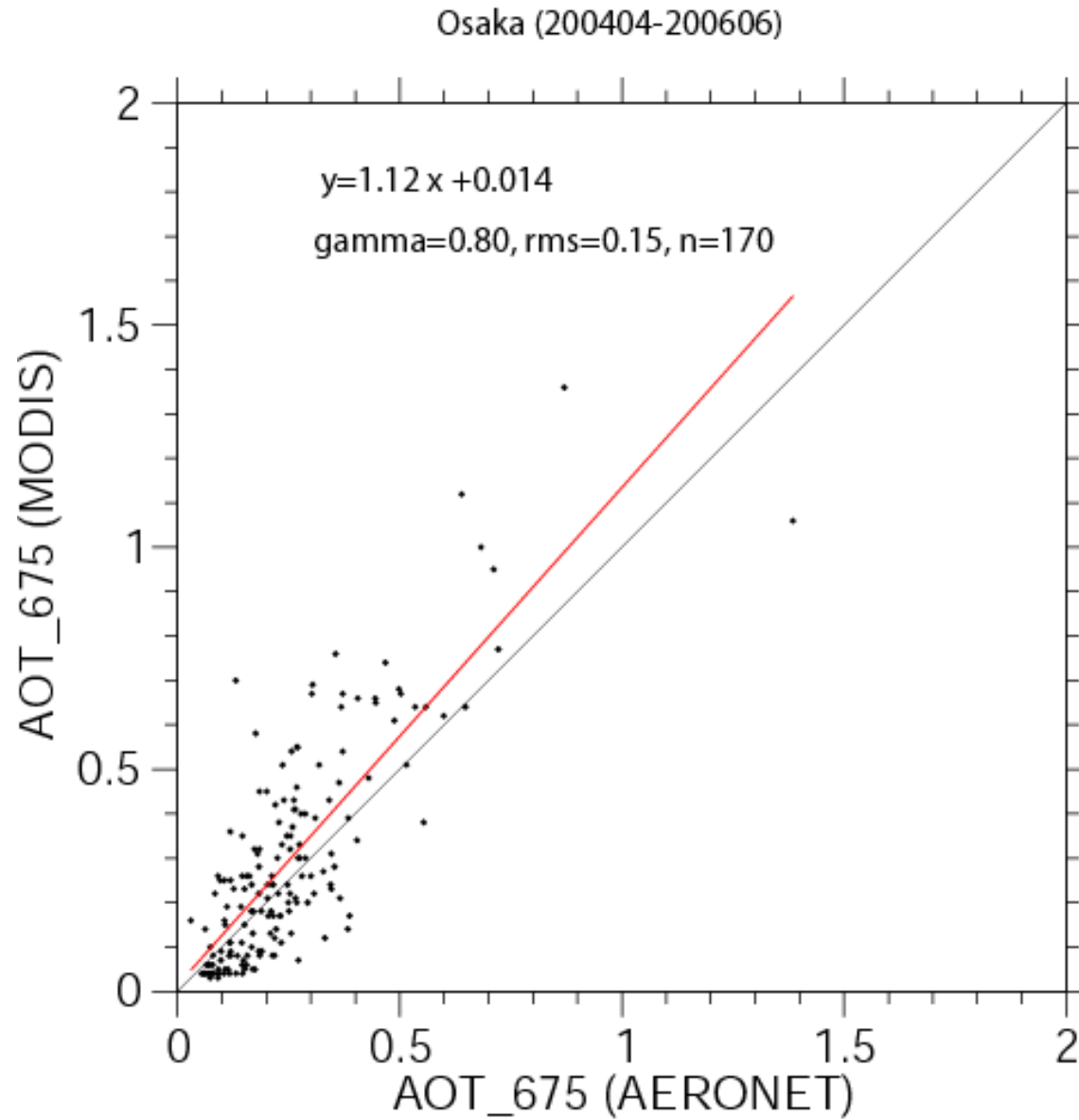


Angstrom exponent (w/ deep blue algorithm)



AOT
Ang.

Validation of MODIS AOT (Osaka,Japan)



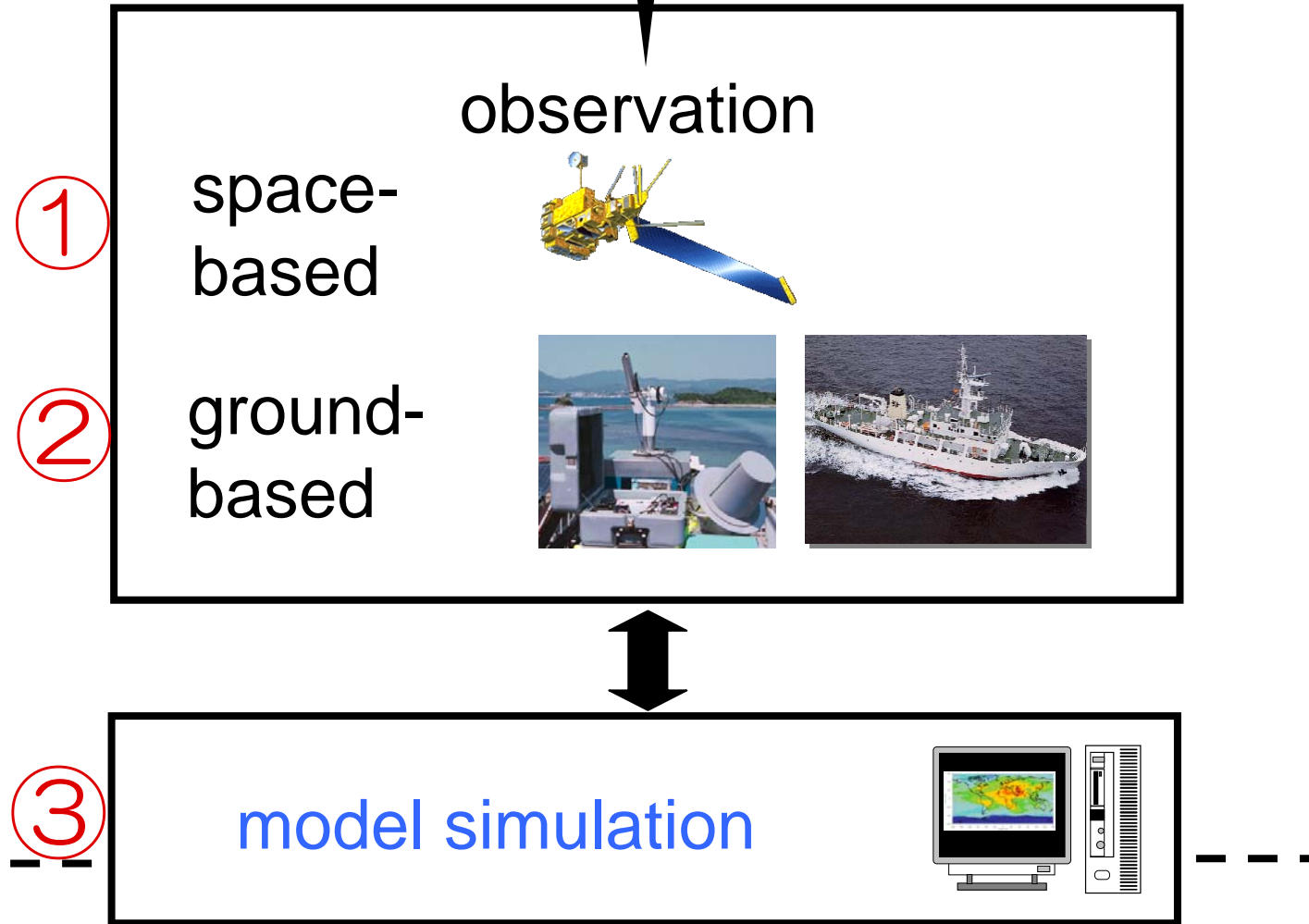
Contents

1. Introduction
2. Satellite aerosol remote sensing
 - 2.1 Basic concept
 - 2.2 Light scattering by aerosols
 - 2.3 Satellite aerosol retrieval
3. Validation of aerosol remote sensing
 - 3.1 Ground-based sun photometry
 - 3.2 Model simulation**
4. Future satellite sensors

Aerosol Study

evaluation

forecast



Aerosol simulation model

SPRINTARS

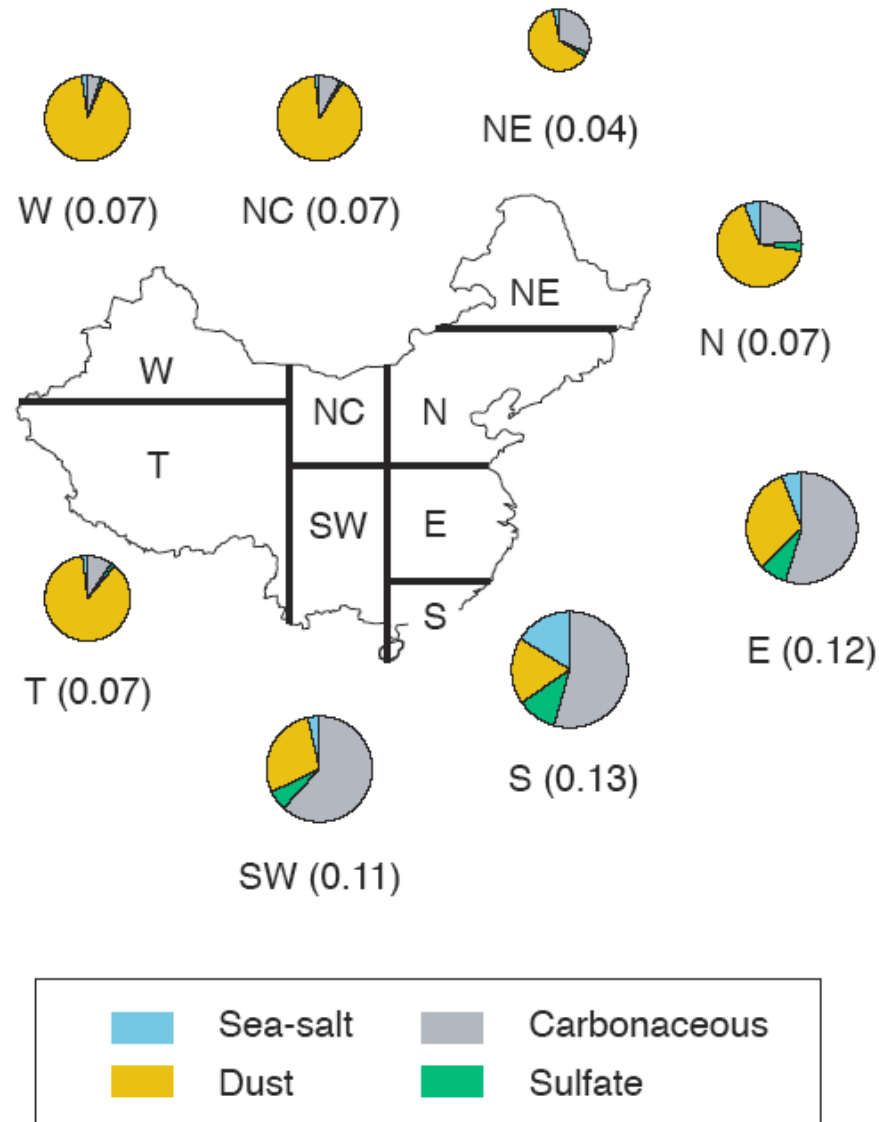
(Spectral Radiation-Transport Model for Aerosol Species)

[Takemura et al., 2000; Takemura et al., 2002; Takemura et al., 2005]

- combine with CCSR/NIES/FRCGC AGCM5.7.
- resolution: T42 and 20 levels
- aerosol species
 - **sulfate**: SO₂(fossil fuel, biomass burning, volcano),
DMS(Calculated by surface downward short wave radiation flux and
surface skin temperature and land vegetation)
 - **carbone** (BC, OC) : BC and OC (fossil fuel, biofuel,
agricultural activity,biomass burning), OC (terpen)
 - **dust**: Calculated by wind speed at 10m, soil water, snow amount
and land vegetation.
 - **oceanic**: Calculated by wind speed at 10m.
- **aerosol transport processes**:
emission, advection, diffusion, chemical reaction and deposition.

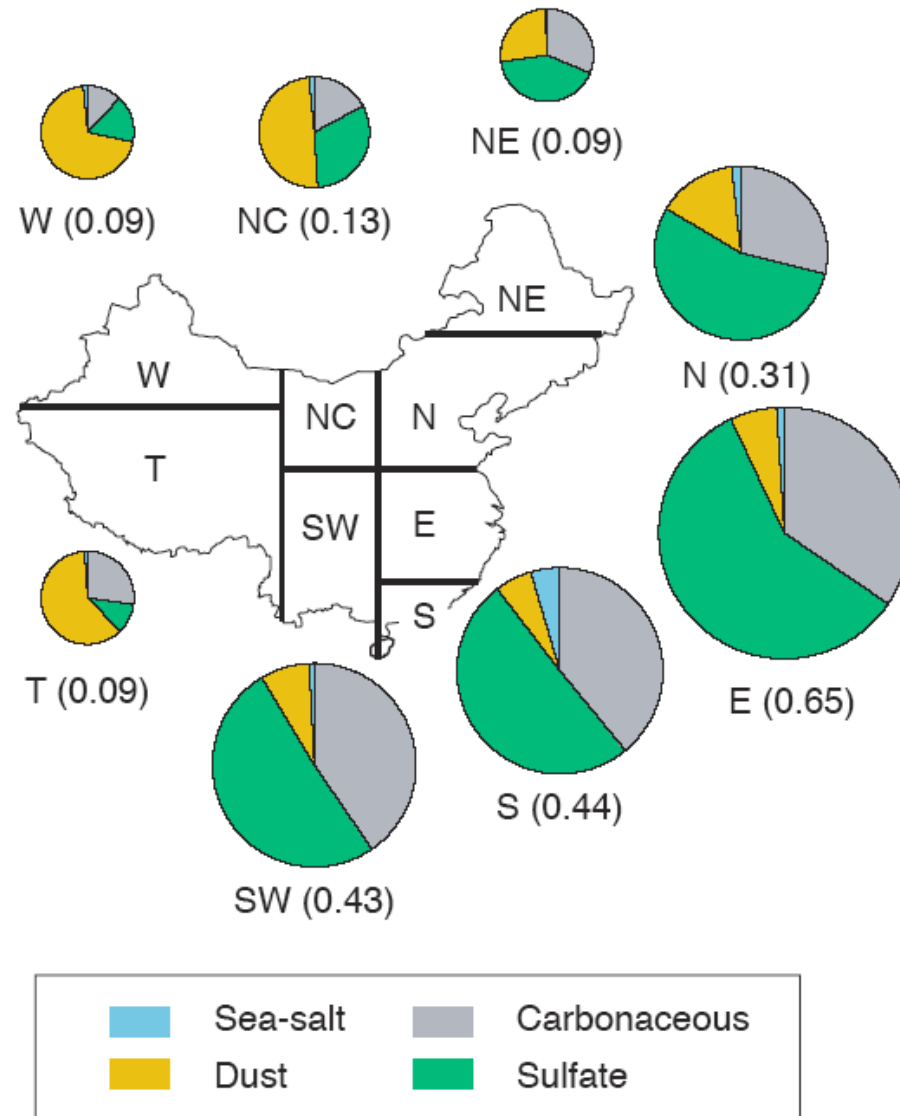
courtesy of Dr. M.Mukai

ex) simulated aerosol emission in 1850



courtesy of Dr. M.Mukai

ex) simulated aerosol emission in 2000



courtesy of Dr. M.Mukai

Contents

1. Introduction
2. Satellite aerosol remote sensing
 - 2.1 Basic concept
 - 2.2 Light scattering by aerosols
 - 2.3 Satellite aerosol retrieval
3. Validation of aerosol remote sensing
 - 3.1 Ground-based sun photometry
 - 3.2 Model simulation
4. **Future satellite sensors**

Future aerosol sensors (JP)

- CAI on GOSAT in Jan., in 2009 (JP)
0.38, 0.67, 0.87 and 1.6 μm for aerosols/ clouds
- APS (polarimetry) on GLORY in 2009 (US)
multi wavelength polarimetry for aerosols
- VIIRS on NPP (2010) and on NPOESS (201x) (US)
- SGLI (polarimetry) on GCOM-C in 2013 (JP)
two wavelength polarimetry for aerosols

Polarization measurements with SGLI
on GCOM-C1 (in 2013)

- Stokes parameter
I, Q, U (0 – 60 –120 position angles)
- Visible and near-infrared channels
0.670 and 0.865 μm (similar to POLDER chls)
- Large tilting angle
 ± 45 degrees about nadir in the along-track
direction
- Fine resolution 1 km (nadir)
- FOV ~1000 km swath (cross-track)

L5. Satellite Remote Sensing by Temperature and Humidity Sounders



Kozo Okamoto

Numerical Prediction Division, Forecast Department,
Japan Meteorological Agency

The Eighteenth IHP Training Course
Satellite Remote Sensing of Atmospheric Constituents
3-15 November 2008
Nagoya, Japan

Outline

1. What is sounder?
2. Example of sounder data
3. Principle of sounding
4. Retrieval process and products
5. Application to data assimilation
6. Summary
7. References

1. What is sounder?

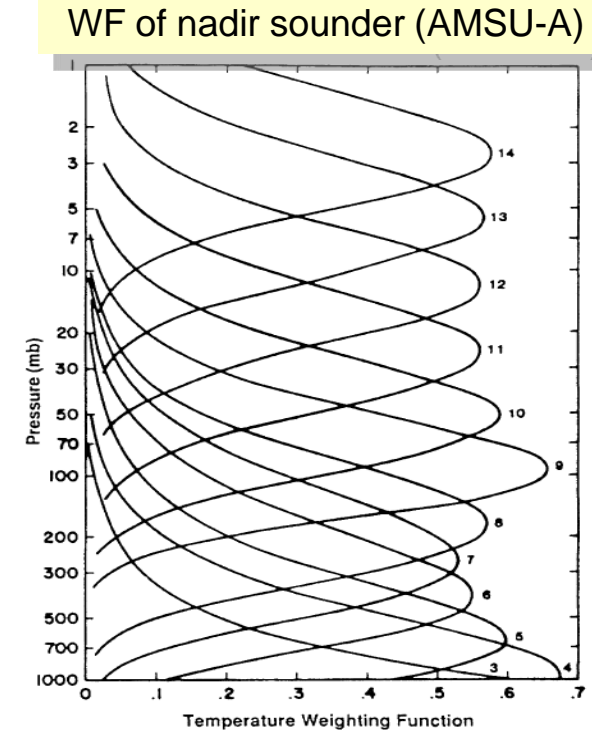
What is “sounding”?

- “Sounding” is the process to derive (vertical) distributions of temperature, atmospheric constituents (e.g. humidity, ozone,...) , aerosols, and hydrometeors (clouds/precipitations)
- This lecture focuses on sounding of **temperature and humidity (T & H)** using **passive** sensors
 - Ref: Active sensors, such as radar and lidar, also measure high-resolved vertical distribution of parameters above.
- Sounders are passive sensors aiming at sounding profiles of, mainly, T & H.

What is "sounder"? (cont.)

- 3 types of T & H vertical sounding by passive sensors
 - (1) nadir sounding
 - ▣ Satellites measure upward radiation from the atmosphere and surface
 - ▣ Extract vertical distribution information from radiations at a number of wavenumbers
 - ▣ Fine horizontal resolution (10~km) but poor vertical resolution (1~5km), compared with limb sounding
 - ▣ e.g. AMSU, HIRS, AIRS, IASI

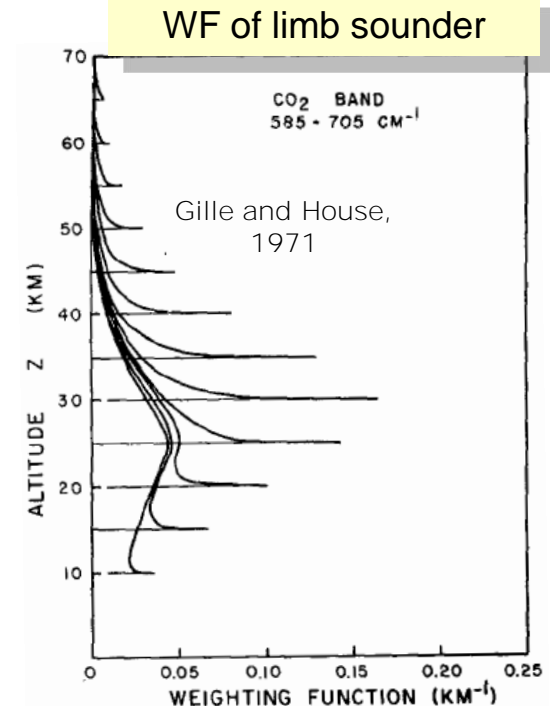
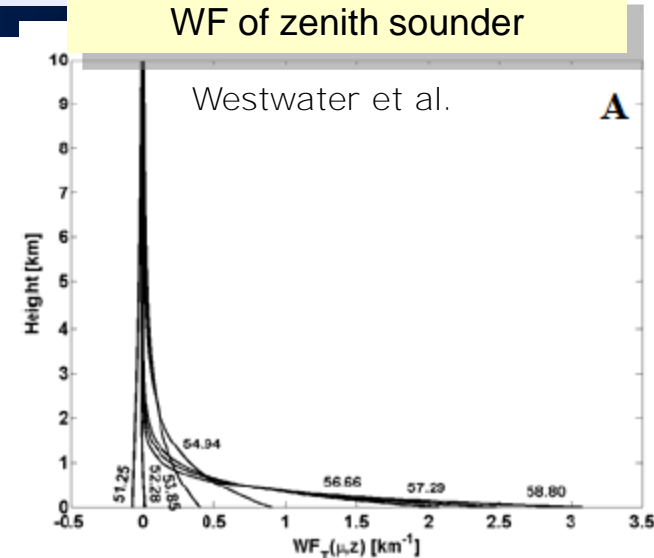
WF (Weighting Function) :
the contribution each atmospheric layer and surface make to the radiation measured



What is "sounder"? (cont.)

- (2) zenith sounding (from ground station)
 - Ground-based sensors measure downward radiation from the atmosphere
 - Extract vertical distribution information from radiation at a number of wavenumbers
 - Hard to extract vertical-resolved information due to the maximum sensitivity to the atmosphere adjacent to the ground

- (3) limb sounding
 - Satellites measure atmospheric radiation, sunlight, starlight and radio wave that cross atmosphere
 - Extract vertical distribution information using many paths of them
 - Fine vertical resolution (1-2km) but poor horizontal resolution (>100km) compared with nadir sounding.
 - No surface influence
 - e.g. ENVISAT/MIPAS, Aura/MLS, GPS radio occultation

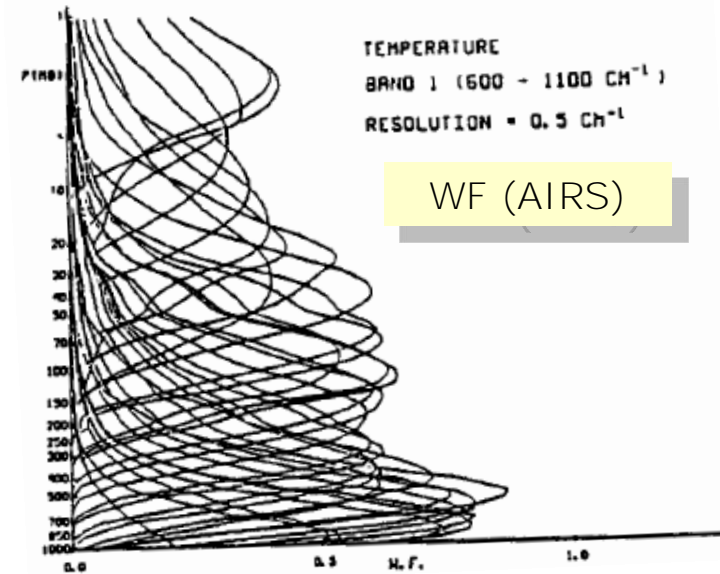
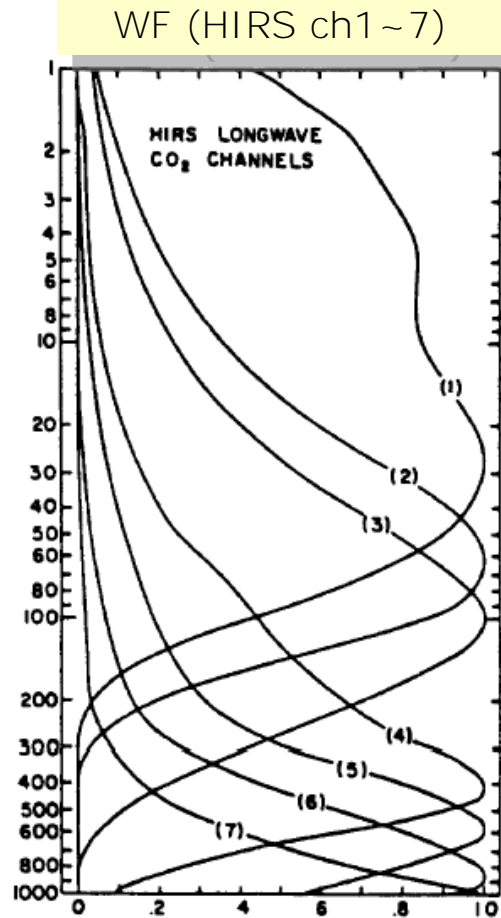


Nadir sounding in the IR/MW region

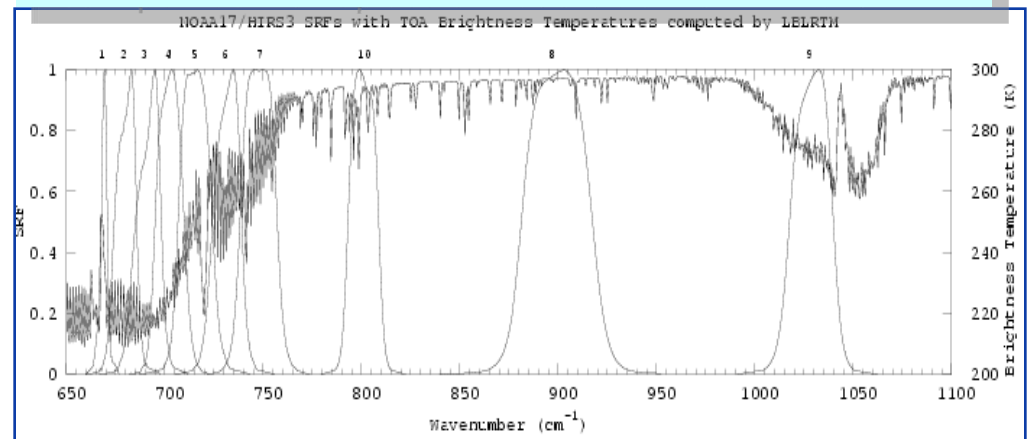
- Commonly used for operational meteorological observations
- IR (infrared) sounders
 - Less variable surface emissivity, higher spatial resolution
 - Sensitive to clouds => cannot see inside and under clouds
 - NOAA/HIRS(20ch), GOES/SOUNDER(19ch), FY3/IRAS(20~26ch)
 - Hyper-spectral sounders, such as FTS (Fourier Transfer Spectrometer), provide higher spectral resolution data
 - ▣ Higher vertically resolved information can be derived
 - Aqua/AIRS(2378ch), Metop/IASI(8461ch)
- MW (microwave) sounders
 - Less sensitive to clouds => much wider observation coverage
 - Lower horizontal resolution, more variable surface emissivity
 - NOAA/AMSU-A(15ch), AMSU-B(5ch), MHS(5ch), FY3/MWTS(4~17ch), MWHS(8ch), DMSP/SSMIS(24ch)
- ATOVS=HIRS + AMSU-A + AMSU-B (or MHS)

WF of IR sounder

- comparison of traditional IR sounder HIRS (20ch) with hyperspectral IR sounder AIRS (2378ch)
 - Longwave CO₂ band



comparison of spectral resolution of HIRS & AIRS

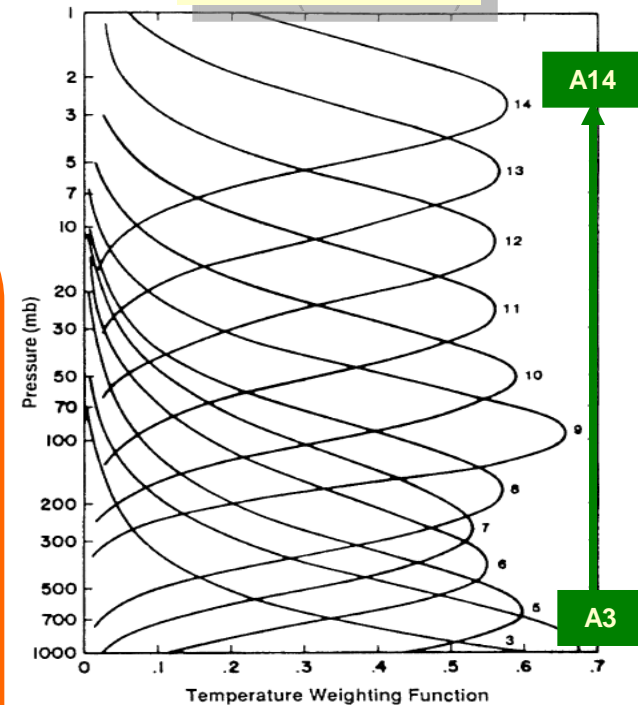


Ch characteristics & WF of AMSU-A

AMSU-A channel characteristics and specification

ch	Center Frequency	Bandwidth [MHz]	NE Δ T [K]	Polarization at nadir	characterization
1	23.800 GHz	270	0.30	V	window
2	31.400 GHz	180	0.30	V	window
3	50.300 GHz	180	0.40	V	window
4	52.800 GHz	400	0.25	V	T sounding
5	53.596 GHz \pm 115MHz	170	0.25	H	T sounding
6	54.400 GHz	400	0.25	H	T sounding
7	54.940 GHz	400	0.25	V	T sounding
8	55.500 GHz	330	0.25	H	T sounding
9	57.290 GHz ($=f_0$)	330	0.25	H	T sounding
10	$f_0 \pm 217$ MHz	78	0.40	H	T sounding
11	$f_0 \pm 322.2$ MHz \pm 48MHz	36	0.40	H	T sounding
12	$f_0 \pm 322.2$ MHz \pm 22MHz	16	0.60	H	T sounding
13	$f_0 \pm 322.2$ MHz \pm 10MHz	8	0.80	H	T sounding
14	$f_0 \pm 322.2$ MHz \pm 4.5MHz	3	1.20	H	T sounding
15	89.000 GHz	<6,000	0.50	V	window

WF (AMSU-A)



Ch characteristics & WF of AMSU-B & MHS

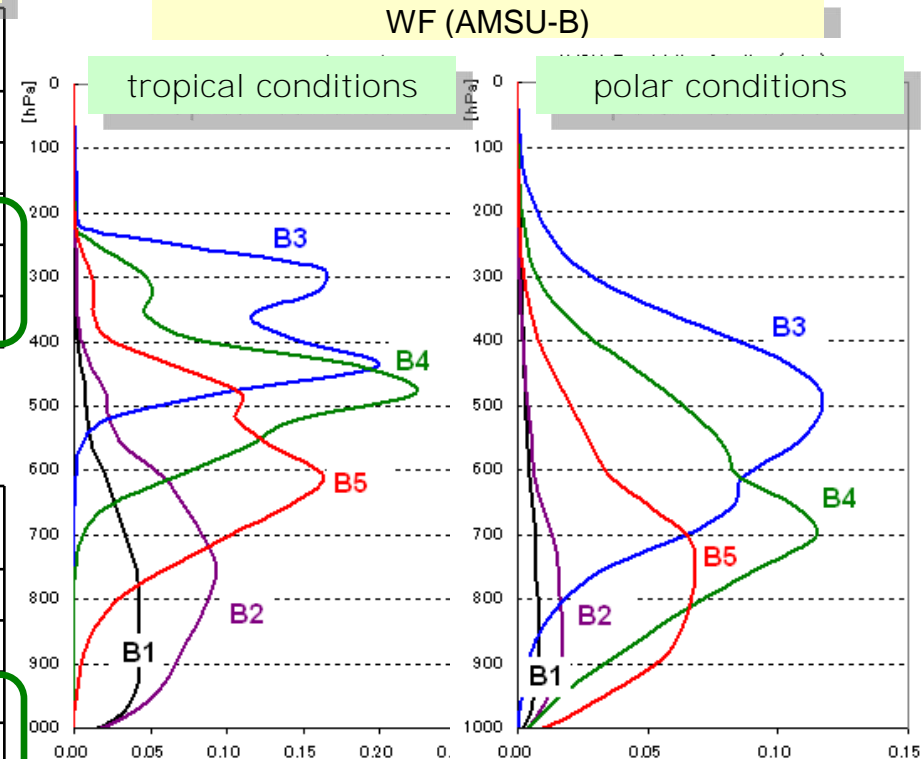
- Altitude of the WF peak for H-sounding is more variable than for T-sounding depending on absorber amount.
 - Increasing absorber makes WF peak higher.

AMSU-B channel characteristics and specification

ch	Center Frequency	Bandwidth [MHz]	NE Δ T [K]	Polarization at nadir	characterization
1	89.0 \pm 0.9 GHz	1000	0.37	V	window
2	150.0 \pm 0.9 GHz	1000	0.84	V	window
3	183.31 \pm 1.0 GHz	500	1.06	V	H sounding
4	183.31 \pm 3.0 GHz	1000	0.70	V	H sounding
5	183.31 \pm 7.0 GHz	2000	0.60	V	H sounding

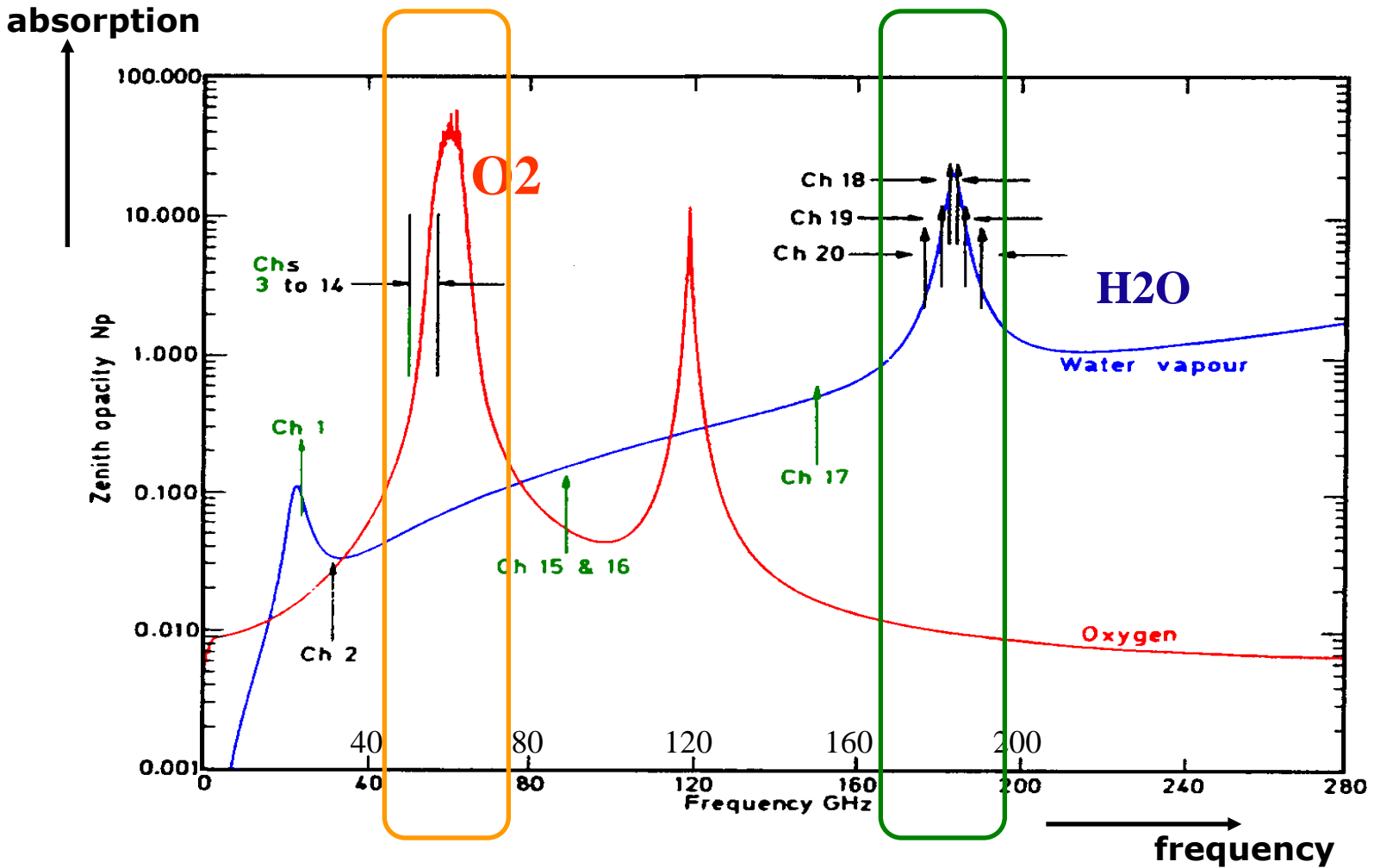
MHS channel characteristics and specification

ch	Center Frequency	Bandwidth [MHz]	NE Δ T [K]	Polarization at nadir	characterization
1	89.0 GHz	2800	0.22	V	window
2	157.0 GHz	2800	0.34	V	window
3	183.31 \pm 1.0 GHz	2x500	0.51	H	H sounding
4	183.31 \pm 3.0 GHz	2x1000	0.40	H	H sounding
5	190.31 GHz	2200	0.46	V	H sounding



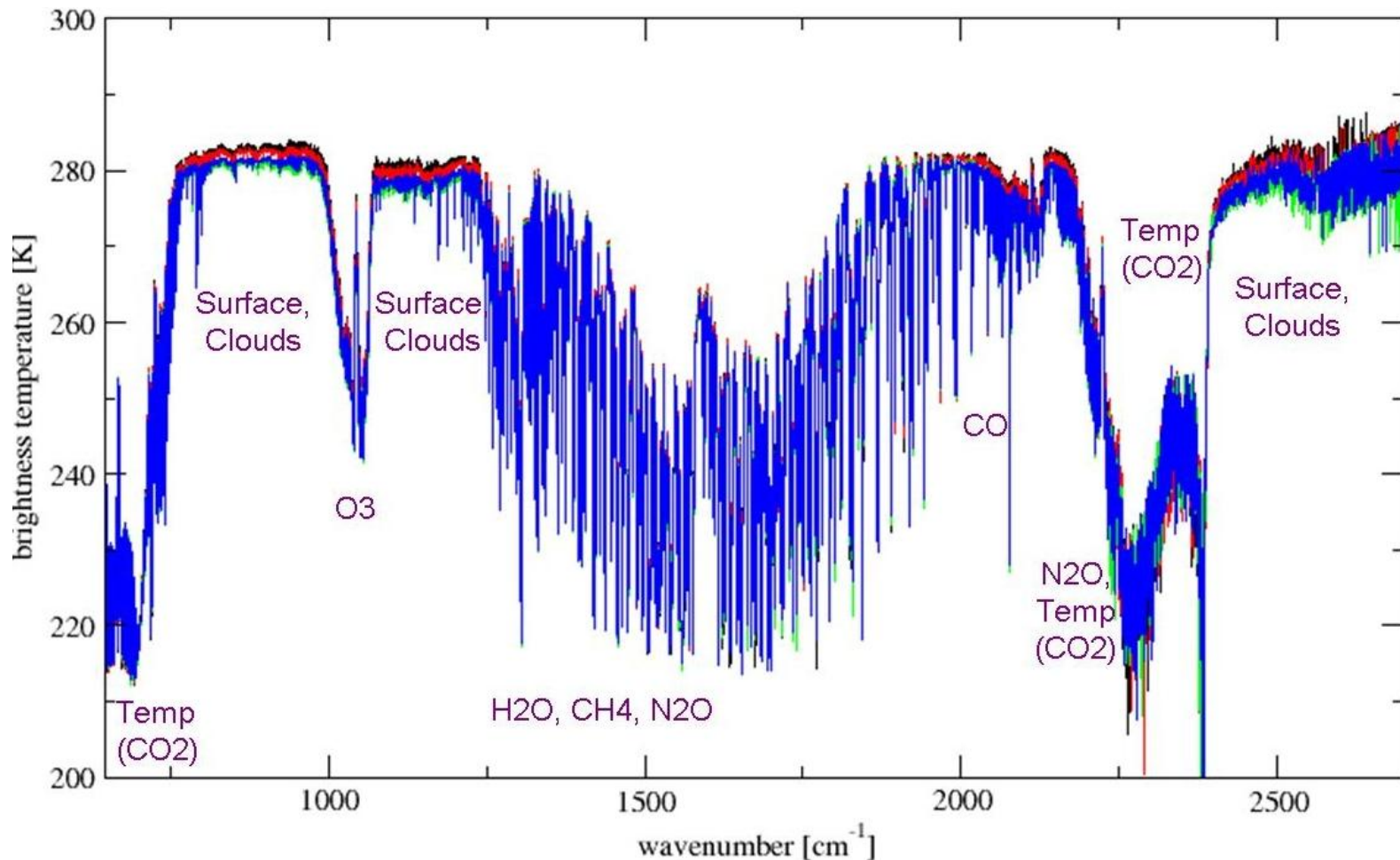
O2 & H2O absorption lines in MW region

- Bands where absorption is relatively strong and changes with frequency are used for T/H-sounding.



IASI spectra in the IR regions

- First IASI observation of brightness temperature (TB)
- Bands where TB gradually changes, or absorption changes, are mainly used for T/H-sounding.



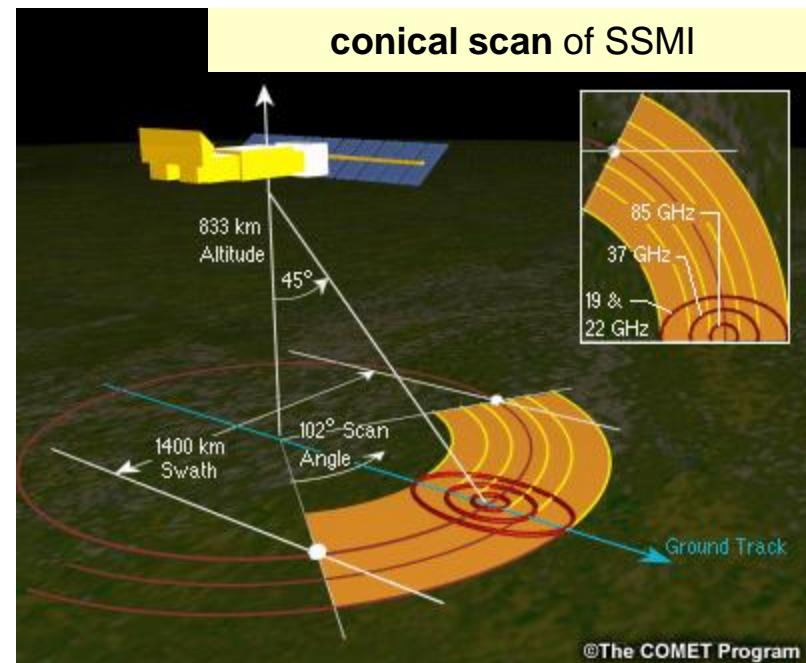
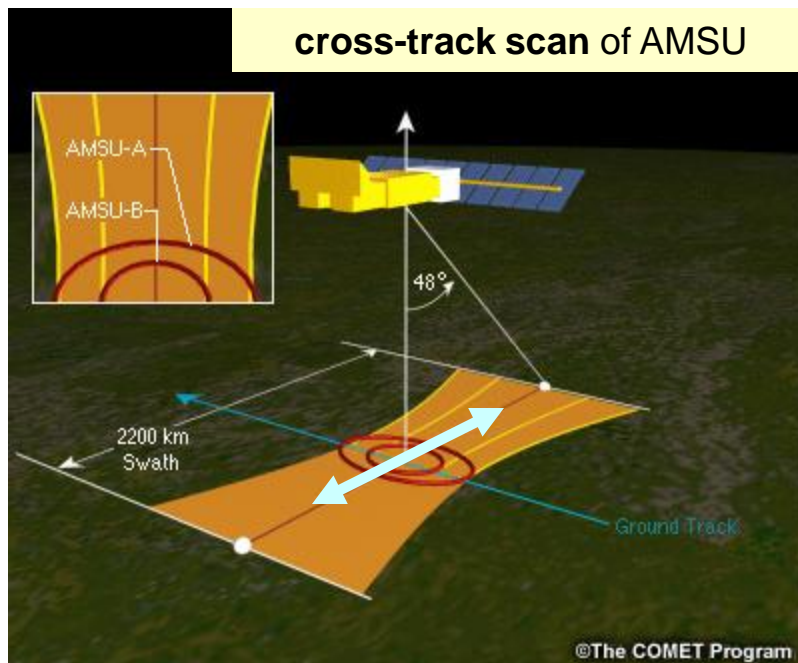
Scanning systems

■ Cross-track scan

- View angle varies to get wide swath
- ATOVS, AIRS, IASI, CrIS, ATMS
- Note spatial resolution degrades towards the edge
 - ▣ For AMSU-A, 48km at nadir and 79X149 km at edge

■ Conical scan

- View angle is fixed and rotates around the nadir direction
 - ▣ Spatial resolution does not vary with view angle
- SSMIS, MIS

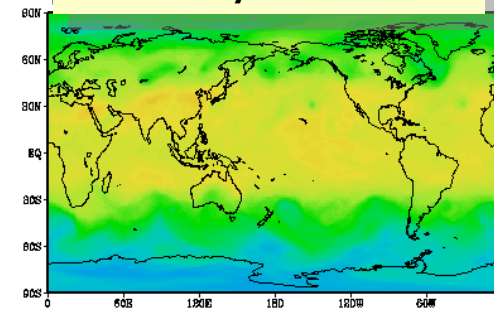


2. Example of sounder data

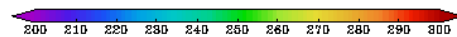
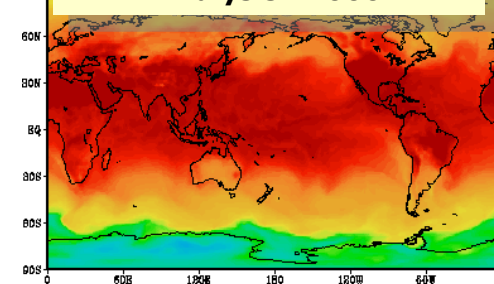
2-1. IR sounder : AIRS

- Brightness temperature (TB) of AIRS ch 168, 221 and 787
- As WF goes down, TB increases in the troposphere
- Window ch reflects SST
 - Highest TB (if inversion does not exist) because of surface emissivity is almost 1.0
- Upward radiation is absorbed by clouds
 - Lower TB in cloudy areas than in clear areas

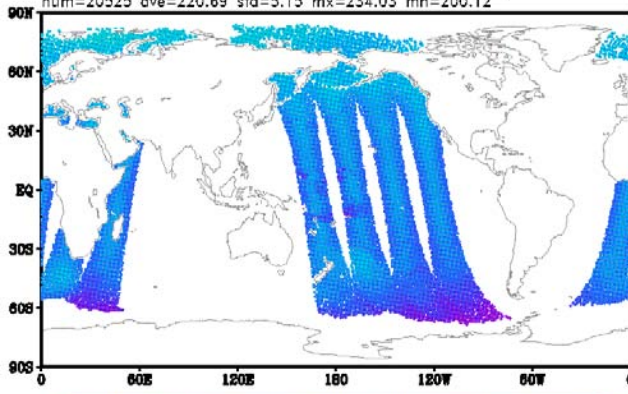
Analysis T500



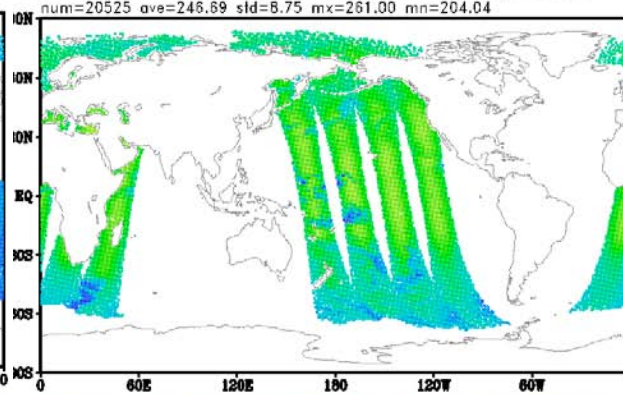
Analysis T1000

AIRS168 14.33 μ m 200hPa

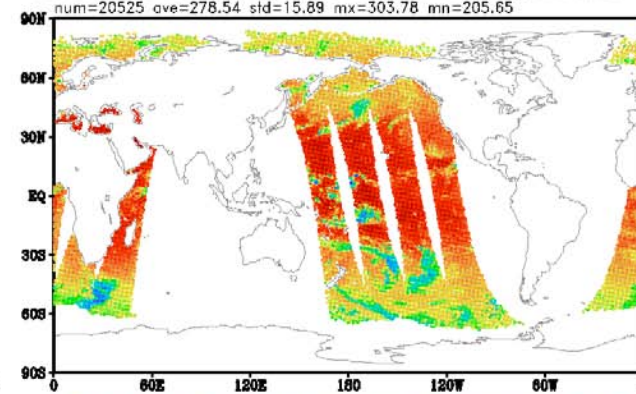
EOS2AIRS TB Obs [K] CH168(697.7cm⁻¹ 14.33 μ m) 200hPa
 num=20525 ave=220.69 std=5.15 mx=234.03 mn=200.12

AIRS221 14.03 μ m 600hPa

EOS2AIRS TB Obs [K] CH221(712.7cm⁻¹ 14.03 μ m) 600hPa
 num=20525 ave=246.69 std=8.75 mx=261.00 mn=204.04

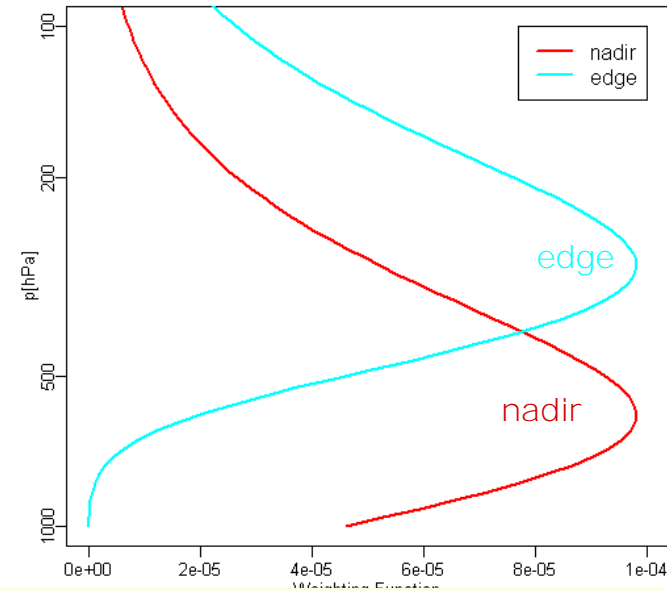
AIRS787 10.90 μ m window

EOS2AIRS TB Obs [K] CH787(917.3cm⁻¹ 10.90 μ m) 1100hPa
 num=20525 ave=278.54 std=15.89 mx=303.78 mn=205.65



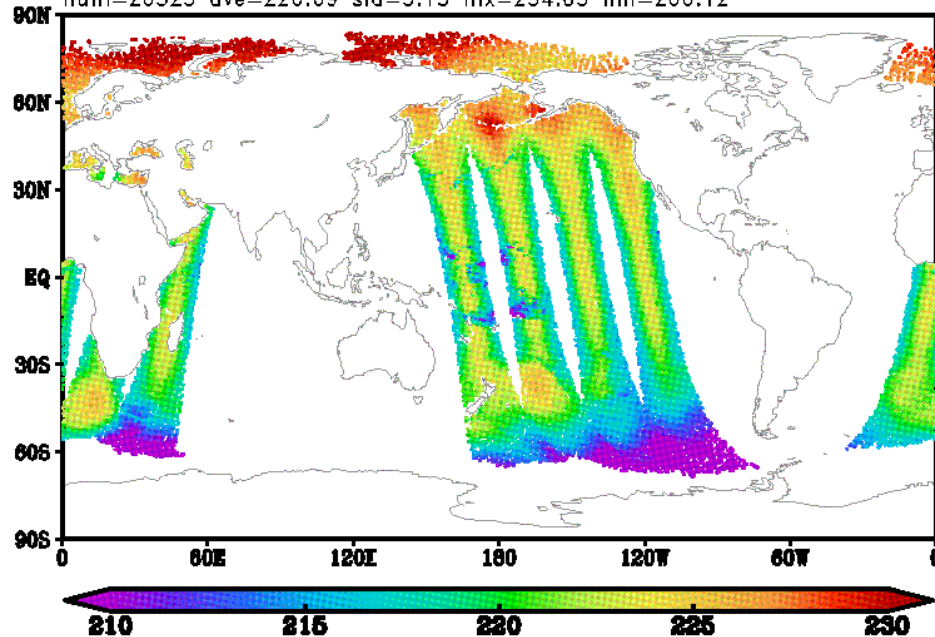
IR sounder : AIRS (cont.)

- limb darkening and brightening
 - Inherent in cross-track scan sounders
 - TB decreases toward scan edges in the troposphere where temperature is down with altitude
 - TB increases toward scan edges in the stratosphere where temperature is up with altitude



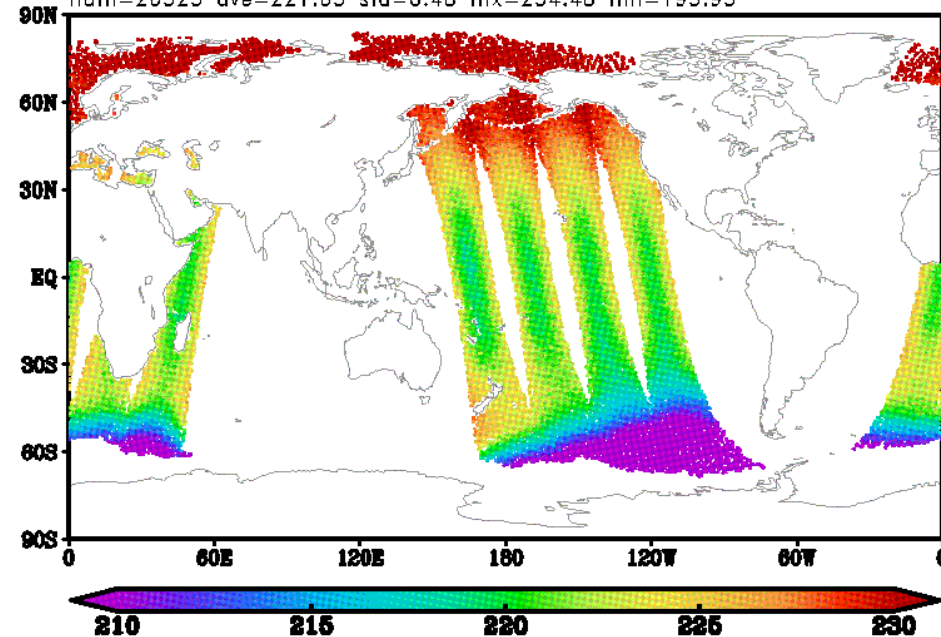
AIRS168 14.33 μ m : 200hPa **limb darkening**

EOS2AIRS TB Obs [K] CH168(697.7cm⁻¹ 14.33 μ m) 200hPa
num=20525 ave=220.69 std=5.15 mx=234.03 mn=200.12



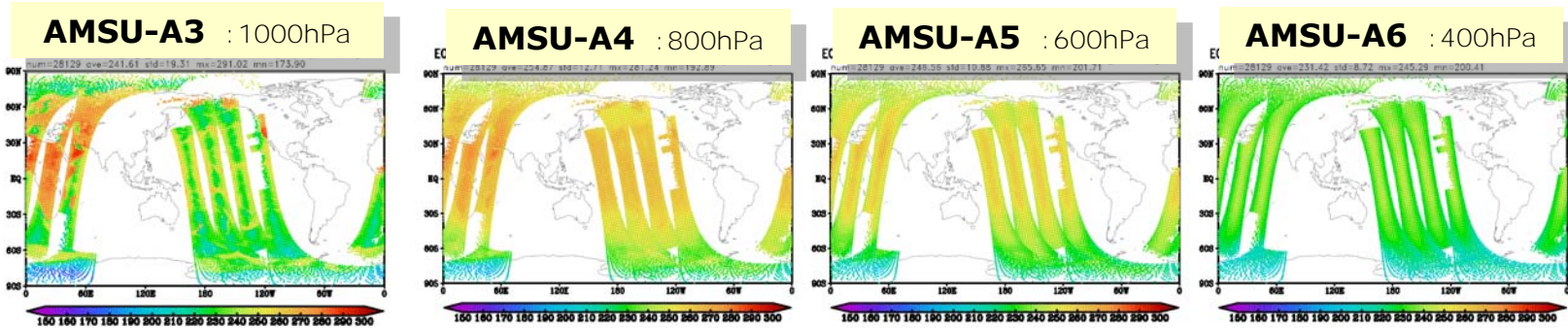
AIRS72 14.99 μ m : 50hPa **limb brightening**

EOS2AIRS TB Obs [K] CH72(667.0cm⁻¹ 14.99 μ m) 50hPa
num=20525 ave=221.65 std=6.48 mx=234.48 mn=193.93

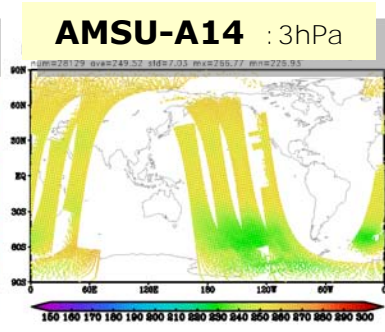
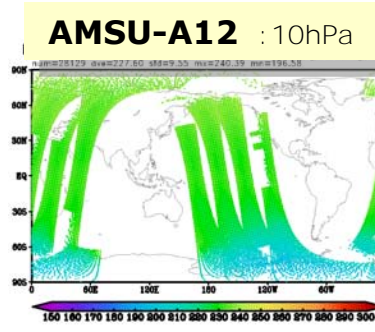
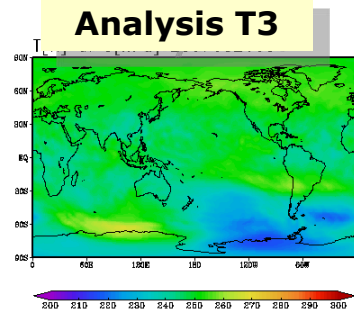
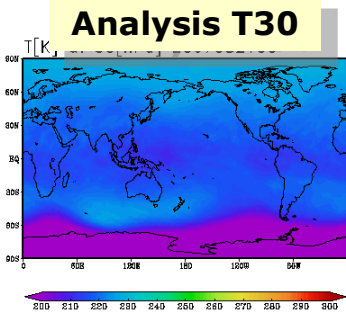
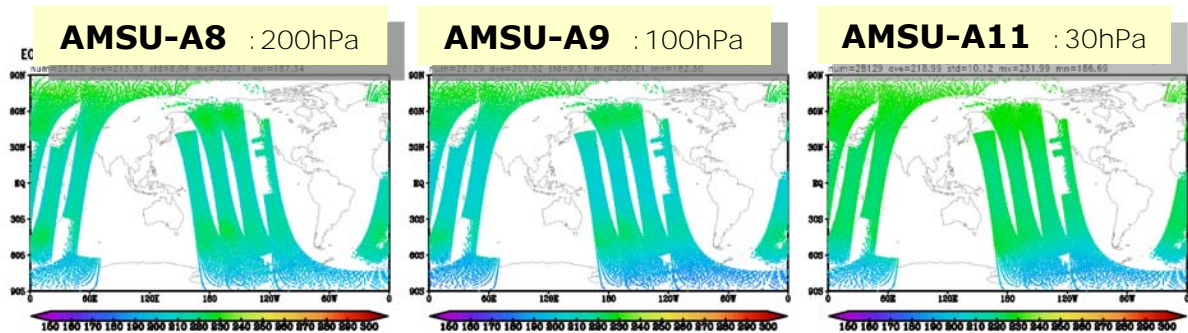


2-2. MW sounder : AMSU-A

- TB decreases (increases) with altitudes in the troposphere (stratosphere), as IR sounders



- However, TB of window channel is not highest over the sea because of low emissivity

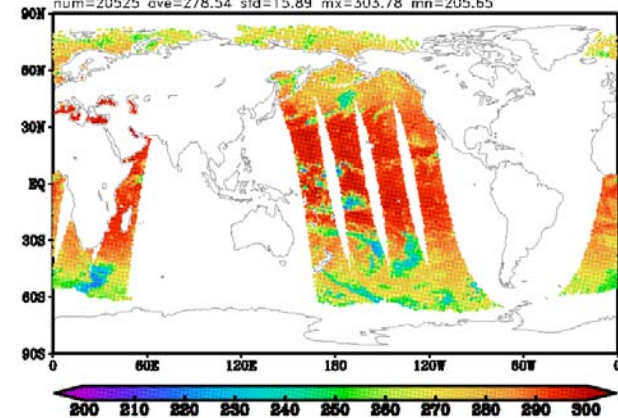


MW sounder : AMSU-A (cont.)

- TB increases in areas with dense water vapor and cloud over the sea where the surface contribution is small unlike IR observations
- Limb darkening/brightening can be seen as IR sounder
 - However, surface sensitive channels in MW can show limb brightening in the troposphere too.

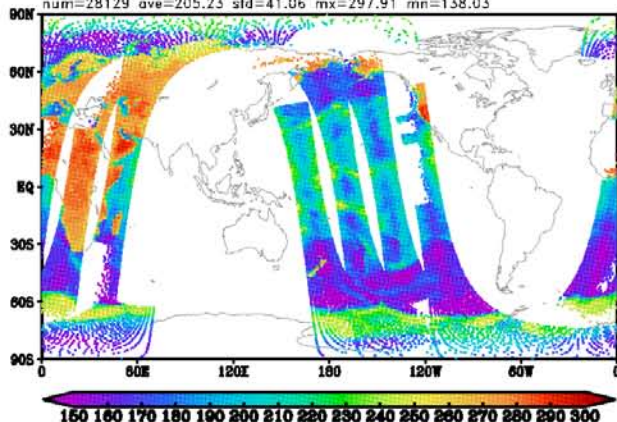
AIRS787 : surf

EOS2AIRS TB Obs [K] CH787(917.3cm⁻¹ 10.90um) 1100hPa
num=20525 ave=278.54 std=15.89 mx=303.78 mn=205.65



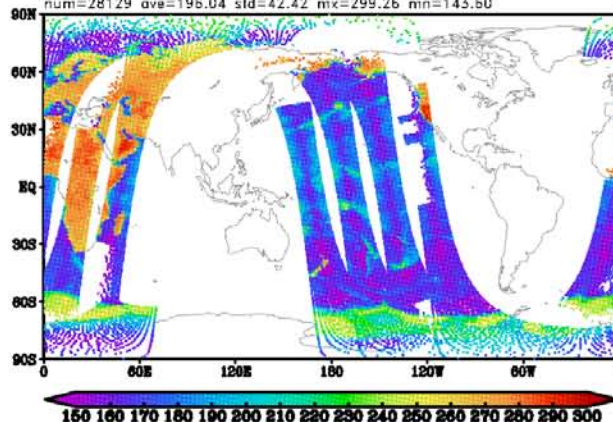
AMSU-A1 : surf,TPW

EOS2AMSUA TB Obs [K] CH1(23.8GHz) 1000hPa
num=28129 ave=205.23 std=41.06 mx=297.91 mn=138.03



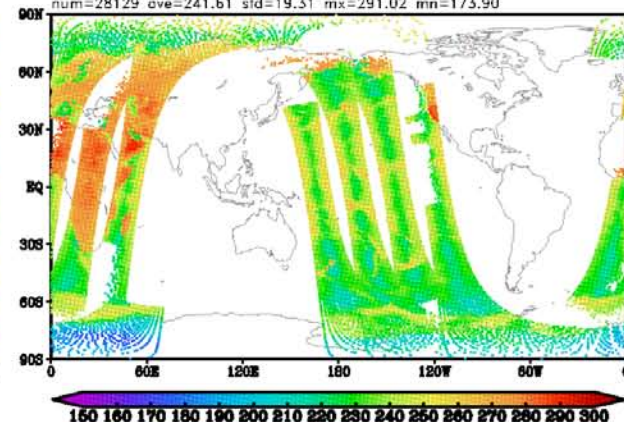
AMSU-A2 : surf,TCCLW

EOS2AMSUA TB Obs [K] CH2(31.4GHz) 1000hPa
num=28129 ave=196.04 std=42.42 mx=299.26 mn=143.60



AMSU-A3 : surf

EOS2AMSUA TB Obs [K] CH3(50.3GHz) 1000hPa
num=28129 ave=241.61 std=19.31 mx=291.02 mn=173.90



3. Principle of sounding

Conditions of (simple) temperature sounding

- (1) The emitting/absorbing constituent should be uniformly mixed (constant mixing ratio with altitude)
 - (2) The absorption strength should be appropriate
 - (3) The absorption band in question should not be overlapped by bands of other constituents
 - (4) LTE (local thermodynamic equilibrium) should apply
- These conditions determine the absorber gas, wavenumber (frequency) and target altitude range for temperature sounding
 - CO₂: 15 & 4.3 μ m, O₂: 60, 118GHz
 - O₂: 60GHz \leq 100km, CO₂: 15 μ m \leq 80km, CO₂: 4.3 μ m \leq 35km
 - Humidity sounding usually uses
 - H₂O: 6.3 μ m, 183GHz
 - The stronger absorption, the higher WF peak.

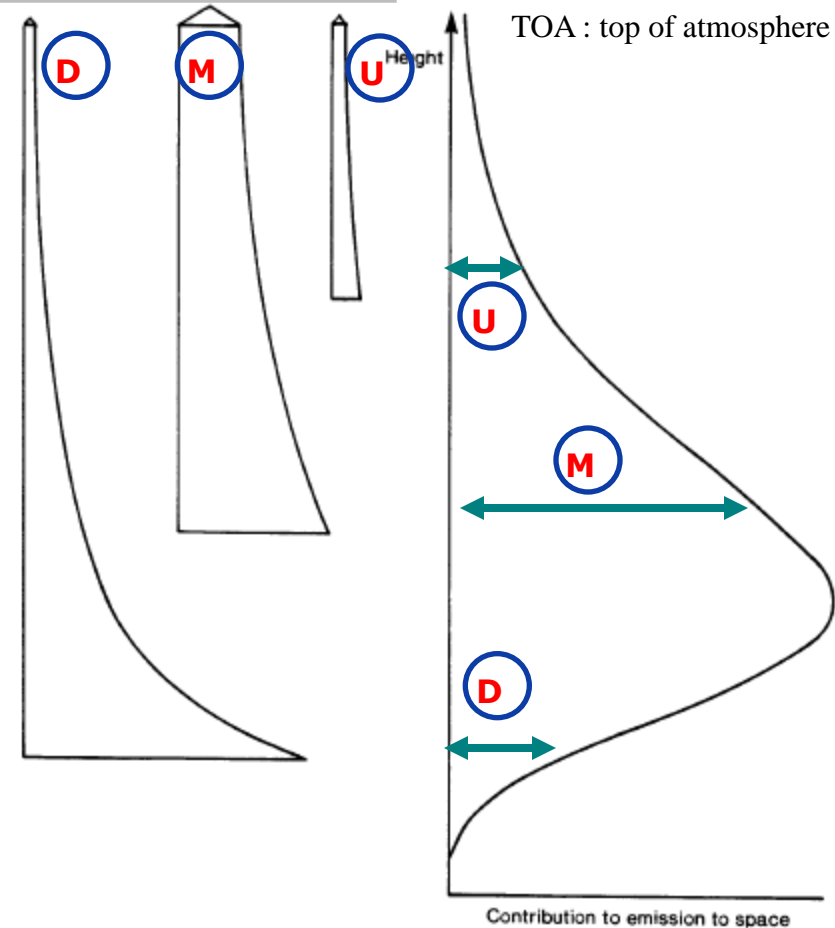
Bell-shape of WF

Why WF has a peak at a particular altitude?

- Lower atmosphere
 - ▣ Strong radiation is emitted because of high atmospheric density
 - ▣ But, almost all is absorbed by the upper atmosphere
- Upper atmosphere
 - ▣ Little radiation is absorbed by the further upper atmosphere
 - ▣ But, little radiation is emitted because of low density.
- As a result, radiation from the atmosphere at an intermediate altitude has a maximum contribution.

upward radiation from three heights in the atmosphere

profiles of contribution to radiance at TOA



Eyre (1991)

What is WF? (1)

- Radiative transfer model for upward radiance

$$I = I_s + I_{air} = I_s + I_{up} + (1 - \varepsilon_s) T_{rs} I_{down}$$

$I_s = \varepsilon_s T_{rs} B(T_s)$: upward radiance from the surface

$I_{up} = \int_0^{\tau_s} B(T) T_r(\tau) d\tau = - \int_0^{\tau_s} B(T) \frac{dT_r}{d\tau} d\tau$: upward radiance from atmosphere

$$I_{down} = \int_0^{\tau_s} B(T) T_r(\tau_s - \tau) d\tau + B(T_c) T_{rs} = \int_0^{\tau_s} B(T) \frac{T_{rs}}{T_r} d\tau + B(T_c) T_{rs}$$

: downward radiance from atmosphere and cosmic background

, where ε , T , T_c , $B(T)$ are emissivity, atmospheric temperature, cosmic background temperature ($\sim 2.7\text{K}$), and Planck function. τ and $T_r(\tau)$ are optical depth and transmittance from the satellite or top of atmosphere (TOA). Suffix s indicates the surface (to TOA).

$$T_r = \exp(-\tau)$$

- Weighting function WF, when $\varepsilon_s = 1$, is described by

$$I_{air} = I_{up} = \int_{\tau_s}^0 B \frac{dT_r(\tau)}{d\tau} d\tau = \int_{p_s}^0 B \frac{dT_r(p)}{dp} dp = \int_0^\infty B \frac{dT_r(z)}{dz} dz = \int B \cdot WF(y) dy$$

- The most familiar form is $WF(z) = \frac{dT_r(z)}{dz}$

- WF determines contribution of $B(T)$ at each layer to radiation at TOA

What is WF? (2)

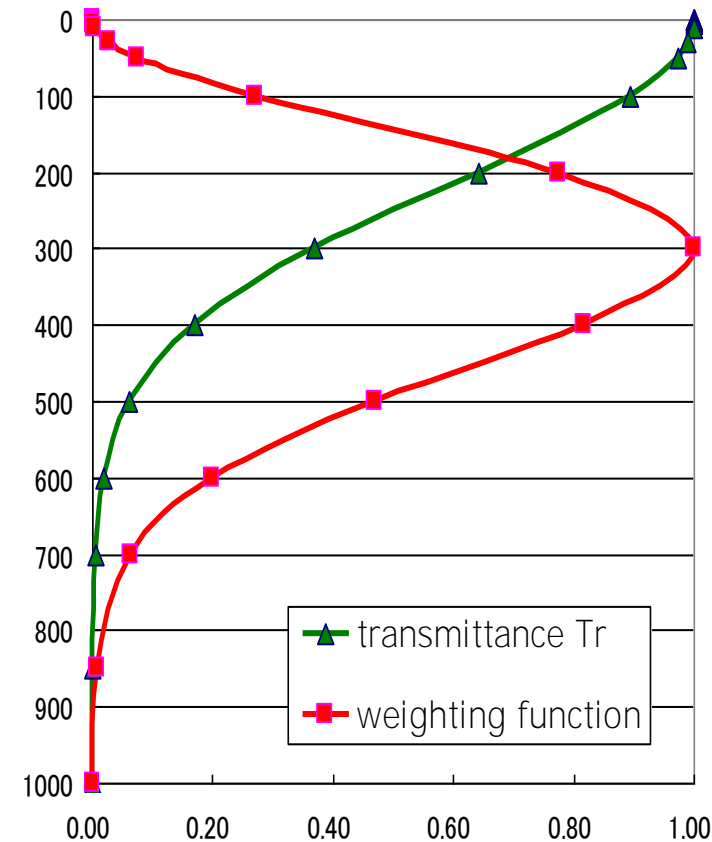
- $WF = dT_r/dz$
- WF has peak where T_r varies most with respect to altitude (right fig)
 - The greater T_r change, the shaper WF

Another perspective:

- $$WF = \frac{dT_r}{dz} = \frac{dT_r}{d\tau} \frac{d\tau}{dz} = T_r \cdot k\rho$$

$$\because T_r = \exp(-\tau), d\tau = -k\rho dz$$
 - k : absorption coefficient
 - ρ : absorber density
- WF has a peak where conflicting changes in T_r and $k\rho$ are balanced.
 - As altitude increases, transmission (T_r) generally increases and absorber (ρ) decreases.

Transmittance and WF



What is WF? (3)

- General weighting function takes I_{down} into account

$$I = I_s + I_{air} = I_s' + I_{air}'$$

$$I_s' = I_s + (1 - \varepsilon_s) B(T_c) T_{rs}^2, \quad I_{air}' = I_{up} + (1 - \varepsilon_s) T_{rs} I_{down}$$

$$\begin{aligned} T_{rs} I_{down} &= T_{rs} \int_0^{\tau_s} B(T) \frac{T_{rs}}{T_r} d\tau = \int_0^{\tau_s} B(T) \left(\frac{T_{rs}}{T_r} \right)^2 T_r d\tau \\ &= \int_{T_{rs}}^1 B(T) \left(\frac{T_{rs}}{T_r} \right)^2 dT_r = \int_0^\infty B(T) \left(\frac{T_{rs}}{T_r} \right)^2 \frac{dT_r}{dz} dz \end{aligned}$$

$$\therefore I_{air}' = \int_0^\infty B(T) \left\{ 1 + (1 - \varepsilon_s) \left(\frac{T_{rs}}{T_r} \right)^2 \right\} \frac{dT_r}{dz} dz = \int_0^\infty B(T) \cdot W F dz$$

- As a result, general weighting function GWF is

$$GWF = 1 + (1 - \varepsilon_s) \left(\frac{T_{rs}}{T_r} \right)^2 \frac{dT_r}{dz}$$

- However, we hereafter consider a simple WF ($= \frac{dT_r}{dz}$), not GWF, for clearer perspective.

Simple models of WF

- [1] Nadir sounding (for a single absorption line)
- [2] Zenith sounding (for a single absorption line)
- [3] Nadir sounding for a non-monochromatic band

- WF of nadir sounding in the pressure coordinate

$$WF = \frac{dT_r}{dz} = \frac{dp}{dz} \frac{dT_r}{dp} = -\frac{p}{H} \frac{dT_r}{dp}, \quad (1)$$

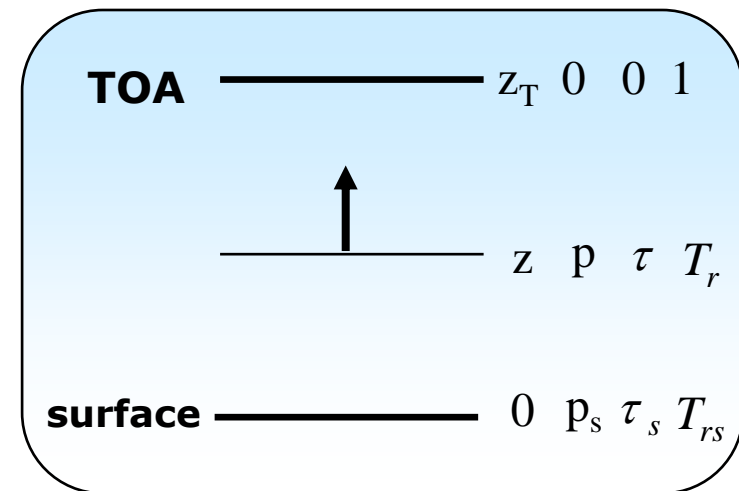
$$\text{where } p = p_s e^{-z/H}, \quad \frac{dp}{dz} = -\frac{p}{H}$$

- p : pressure, p_s : surface pressure,
 H : scale height

- optical depth τ

$$\tau = \int_z^{z_T} k \rho dz = -\int_p^0 k \frac{r}{g} dp = \frac{r}{g} \int_0^p k dp \quad (2)$$

- k : absorption coefficient, ρ : absorber density,
 r : mixing ratio of absorber, g : acceleration of gravity,
 z_T : satellite altitude at TOA ($p=0$)



Simple model of WF [1] : Nadir sounding

- Estimate τ for a absorption gas with **constant r** with altitude
 - Now we select observation wavenumber ν in the line **wing region** with large $\nu - \nu_0$. Absorption coefficient with the Lorentz line shape becomes

$$k = \frac{k_0 p}{(\nu - \nu_0)^2 + k_1 p^2} \approx k_0 p \quad (3)$$

- Insert (3) in (2),

$$\tau = \frac{k_0 r}{g} \int_0^p p dp = \frac{k_0 r}{2g} p^2 = \frac{p^2}{p_m^2}, \quad (4)$$

where $p_m^2 = 2g/k_0 r$.

- Transmittance T_r is derived by (4)

$$T_r = e^{-\tau} = \exp\left[-(p/p_m)^2\right] \quad (5)$$

- WF is finally obtained using (1) and (5),

$$WF = -\frac{p}{H} \cdot \exp\left[-(p/p_m)^2\right] \cdot \left(-\frac{2p}{p_m^2}\right) = \frac{2}{H} \left(\frac{p}{p_m}\right)^2 \exp\left[-(p/p_m)^2\right] \quad (6)$$

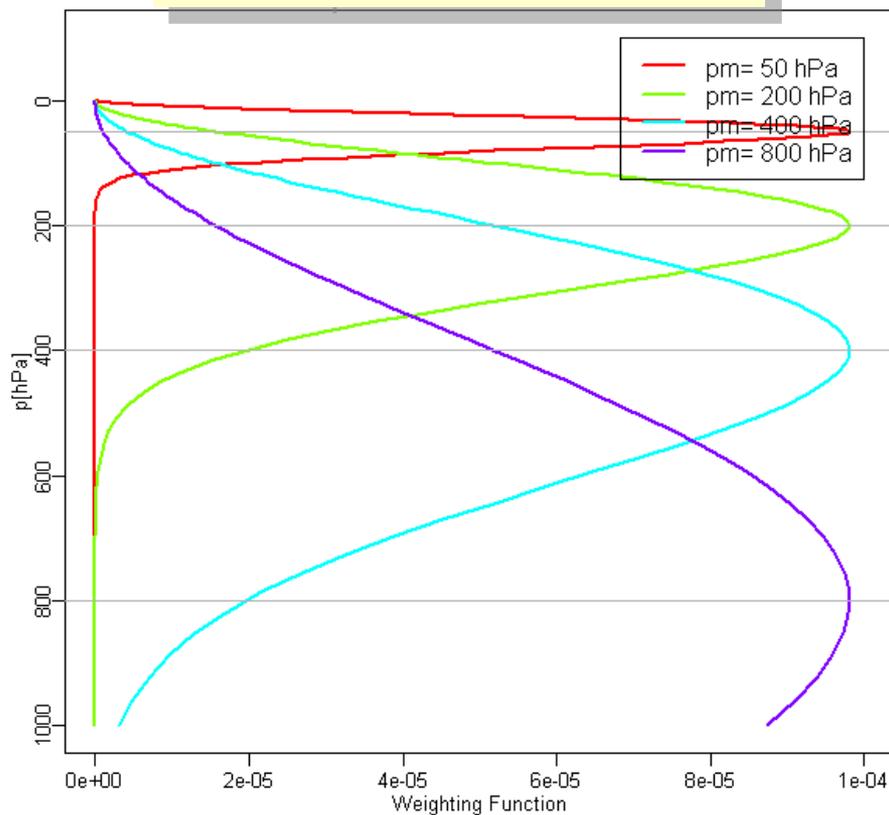
- Increase in absorber and decrease in transmission with p generate the bell-shape structure.
- Peak altitude of this WF is p_m by $dWF/dp=0$

Simple model of WF [1] (cont.)

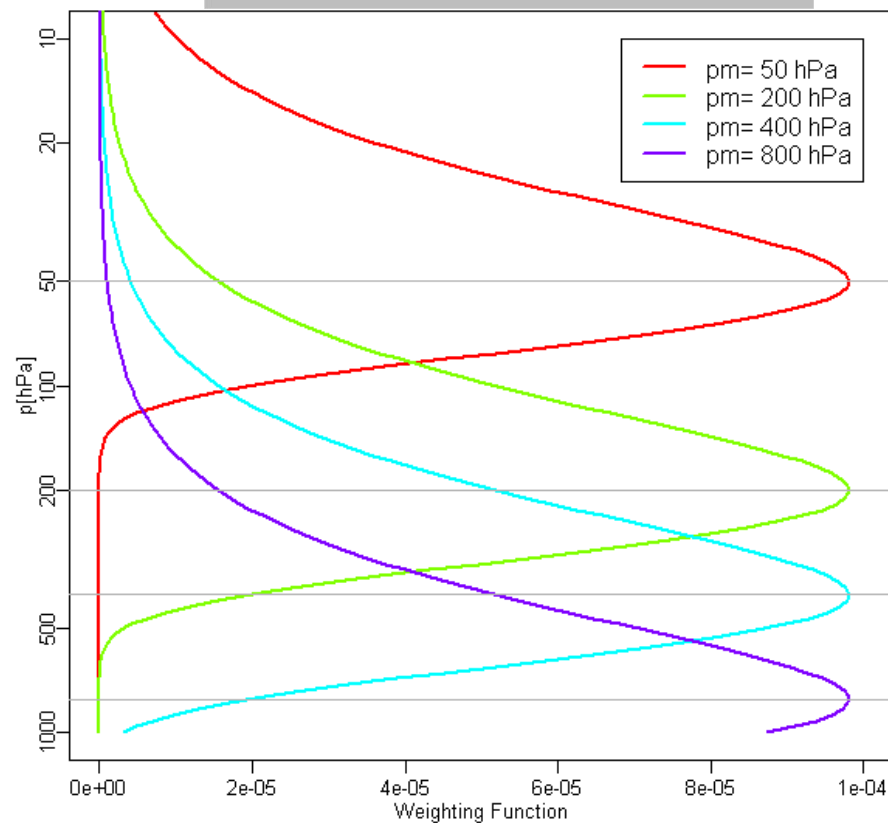
■ examples of WF

- peak position : $p_m = 50, 200, 400$ and 800 hPa

linear pressure coordinate



log pressure coordinate



Simple model of WF [2] : Zenith sounding

- Let's consider WF in the line wing for zenith sounding
- T_r for zenith sounding is described by (4)

$$T_r = e^{-(\tau_s - \tau)} = e^{-\tau_s} \cdot \exp\left[\left(\frac{p}{p_m}\right)^2\right] \quad (5)'$$

- WF is obtained, as (6), from (1) and (5)'.

$$WF = \frac{2}{H} e^{-\tau_s} \left(\frac{p}{p_m}\right)^2 \exp\left[\left(\frac{p}{p_m}\right)^2\right] \quad (6)'$$

- Increase in both absorber and transmission with p cannot generate the bell-shape structure, but a maximum at surface.

Simple model of WF [3]:

Nadir sounding for non-monochromatic band

- The previous models [1] & [2] have been based on a single absorption line.
- Because, however, real instruments have a wide spectral response function, many lines should be considered.
- T_r for a number of absorption lines can be calculated using a strong Elsasser band model.

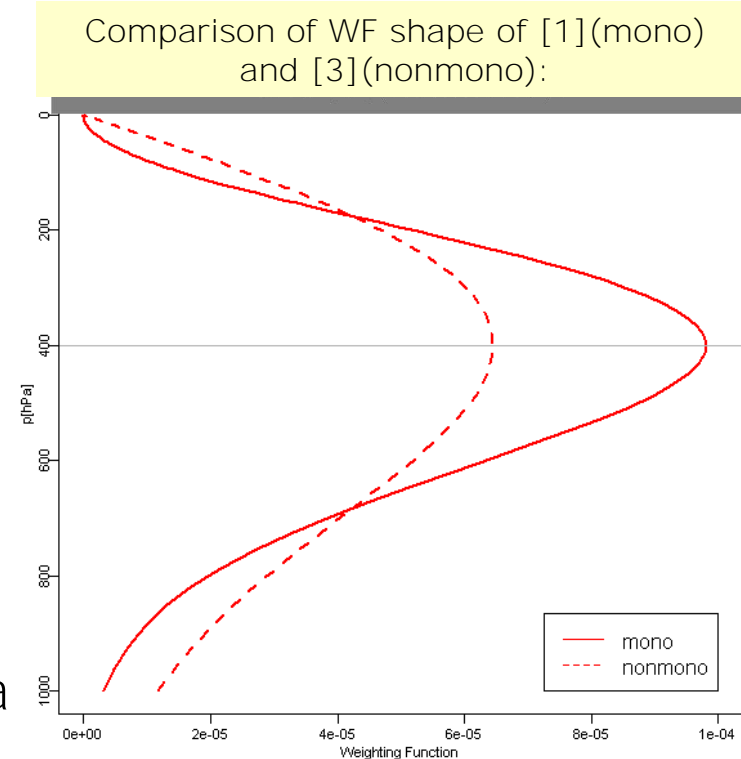
$$T_r = 1 - \frac{2}{\sqrt{\pi}} \int_0^{\beta' p} e^{-x^2} dx = 1 - \text{erf}(\beta' p) \quad (5)''$$

- $\text{erf}()$: error function, β' : constant and depends on the local line strengths

- WF is given by differentiating (5)'' with respect to p , as (1)

$$WF = \frac{1}{H} \sqrt{\frac{2}{\pi}} \frac{p}{p_m} \exp\left[-\left(\frac{p}{2p_m}\right)^2\right] \quad (6)''$$

- WF is broader than one from wing of a single absorption. (see right figure)



4. Retrieval process and products

Retrieve T/H profiles

- RT equation : $y=H(x)$
 - x : temperature/humidity profiles we want to infer
 - y : radiance observation of all channels
 - H : radiative transfer (RT) model
- Retrieval process: $x=H^{-1}(y)$
 - This is called “inversion problem”
 - “forward problem” is to calculate y from x (RT calculation itself)
- Methods of retrieval
 - Statistical method: $\Delta x=C\Delta y$
 - Δa means deviation from the average of a
 - C can be obtained from training dataset: a match-up of radiosondes (Δx_s) and corresponding radiances (Δy_s)
 - $\Delta x_s=C \Delta y_s \Rightarrow C=\Delta x_s \Delta y_s^T (\Delta y_s \Delta y_s^T)^{-1}$
 - Computationally cheap and need no RT calculation nor first-guess, but vulnerable to sampling error
 - MAP (maximum a posteriori) method
 - * Almost equivalent to ML (maximum likelihood) method
 - More sophisticated: hybrid of statistical and physical method
 - Not need huge training dataset, more stable and easier extension
 - But need a RT model and first-guess

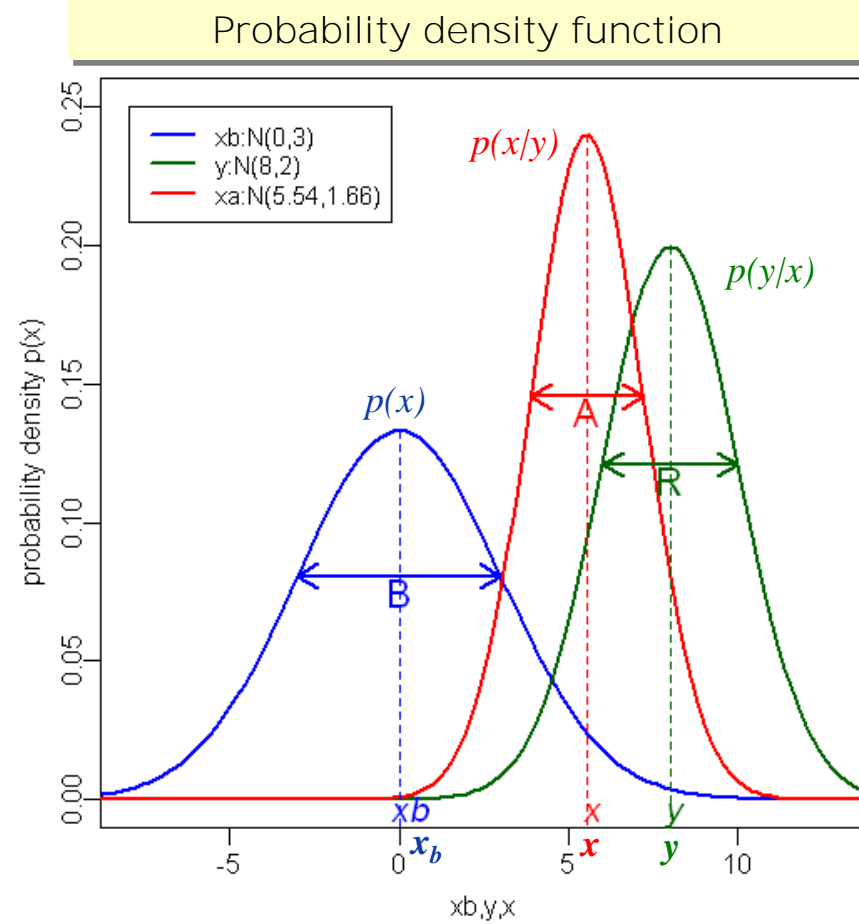
Retrieval process : MAP method

- Estimate the state that maximizes conditional probability $p(x/y)$
 - $p(x/y)$ means the probability that x will occur when y occurs (or measurements are given)
- Bayes theorem and the assumption of Gaussian probability gives

$$p(x | y) = p(y | x) \cdot p(x) / p(y)$$

$$\propto \exp\left[-1/2 \{y - H(x)\}^T \mathbf{R}^{-1} \{y - H(x)\}\right] \times \exp\left[-1/2 (x - x_b)^T \mathbf{B}^{-1} (x - x_b)\right]$$

- x_b : a priori state or background profile (first-guess)
 - e.g. NWP, climate, nearby radiosonde profiles, ...
 - \mathbf{B} : error covariance of x_b
 - \mathbf{R} : error covariance of observation y and its operator H



MAP method (cont.)

- This problem is equivalent to estimating the state that minimizes the cost function $J(x)$

$$J(x) = -\ln\{p(x/y)\} = 1/2(x-x_b)^T \mathbf{B}^{-1}(x-x_b) + 1/2[y-H(x)]^T \mathbf{R}^{-1}[y-H(x)]$$

- This is also called variational problem.
 - ▣ 1D-Var : x is one dimensional variable (e.g. vertical T/H profile)
- The optimal solution of x_a (the most probable profile) is obtained by $dJ(x)/dx=0$

$$x_a = x_b + \mathbf{W}(y - H(x_b)) = x_b + \mathbf{BK}^T (\mathbf{KBK}^T + \mathbf{R})^{-1} (y - H(x_b))$$

\mathbf{K} is linearized $H(x) : y - H(x_b) = \mathbf{K} \cdot (x - x_b)$

- Error covariance of retrieval x_a

$$\mathbf{A} = (\mathbf{K}^T \mathbf{B}^{-1} \mathbf{K} + \mathbf{R}^{-1})^{-1} = (\mathbf{I} - \mathbf{WK}) \mathbf{B}$$

Other retrieval processes

- Pre-processing needed for T/H-retrieval
 - cloud screening for IR T/H-sounding
 - rain screening for IR/MW T/H-sounding
 - limb correction for cross-track scan sounders (if necessary)
 - bias correction (if necessary)
 - create first-guess (if necessary)
 -

- Various products, in addition to T/H profiles, can be derived

Products of operational sounders

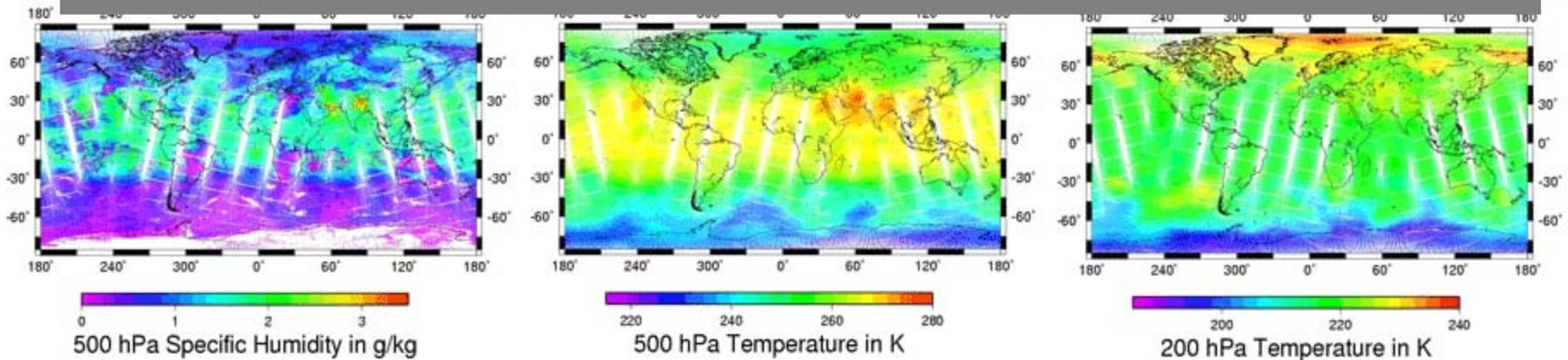
- EUMETSAT : European Organisation for the Exploitation of Meteorological Satellites
 - Metop/ATOVS products
 - ▣ T/H profiles at 40/15 pressure levels, Ts, CTH, CTT, CC, TCCLW, TPW
 - ▣ http://www.eumetsat.int/Home/Main/What_We_Do/Highlights/SP_1218437114837?l=en
 - Metop/IASI products
 - ▣ T/H profiles, Ts, CTH, CTT, CC, cloud phase, integrated ozone, total column of N2O, CO, CH4 and CO2
 - ▣ http://www.eumetsat.int/Home/Main/Access_to_Data/Metop__amp__NOAA_Services/Global_Data_Service/SP_1119366824888?l=en
- NOAA : National Oceanic and Atmospheric Administration
 - GOES SOUNDER products
 - ▣ TPW, Ts, CTH, CAPE, LI
 - NOAA/ATOVS products
 - MSPPS : Microwave Surface and Precipitation Products System
 - ▣ TCCLW, TPW, RR, sea ice concentration, ice water path, snow cover, land Ts, snow water equivalent, surface emissivity
 - ▣ <http://www.star.nesdis.noaa.gov/corp/scsb/mspps/main.html>

CTH: cloud top height, **CTT**: cloud top temperature, **CC**: Cloud Cover, **RR**: rain rate, **TCCLW**: total column cloud liquid water, **TPW**: total precipitable water
CAPE: convective available potential energy, **LI**: lifted index

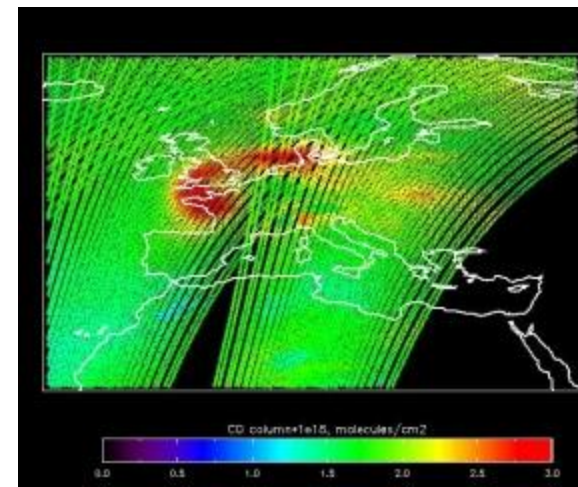
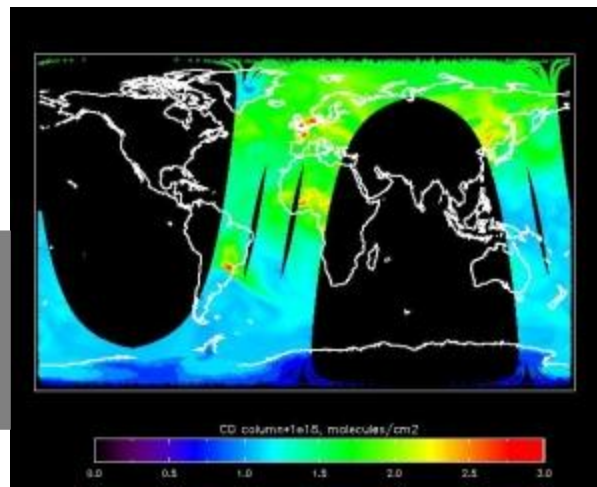
Examples : Products from Metop/ATOVS & IASI

- EUMETSAT products on 11. July 2008
 - Both ascending and descending orbits data

Specific Humidity [g/kg] at 500hPa (left), Temperature [K] ant 500 hPa (center) and at 200hPa (right) from ATOVS

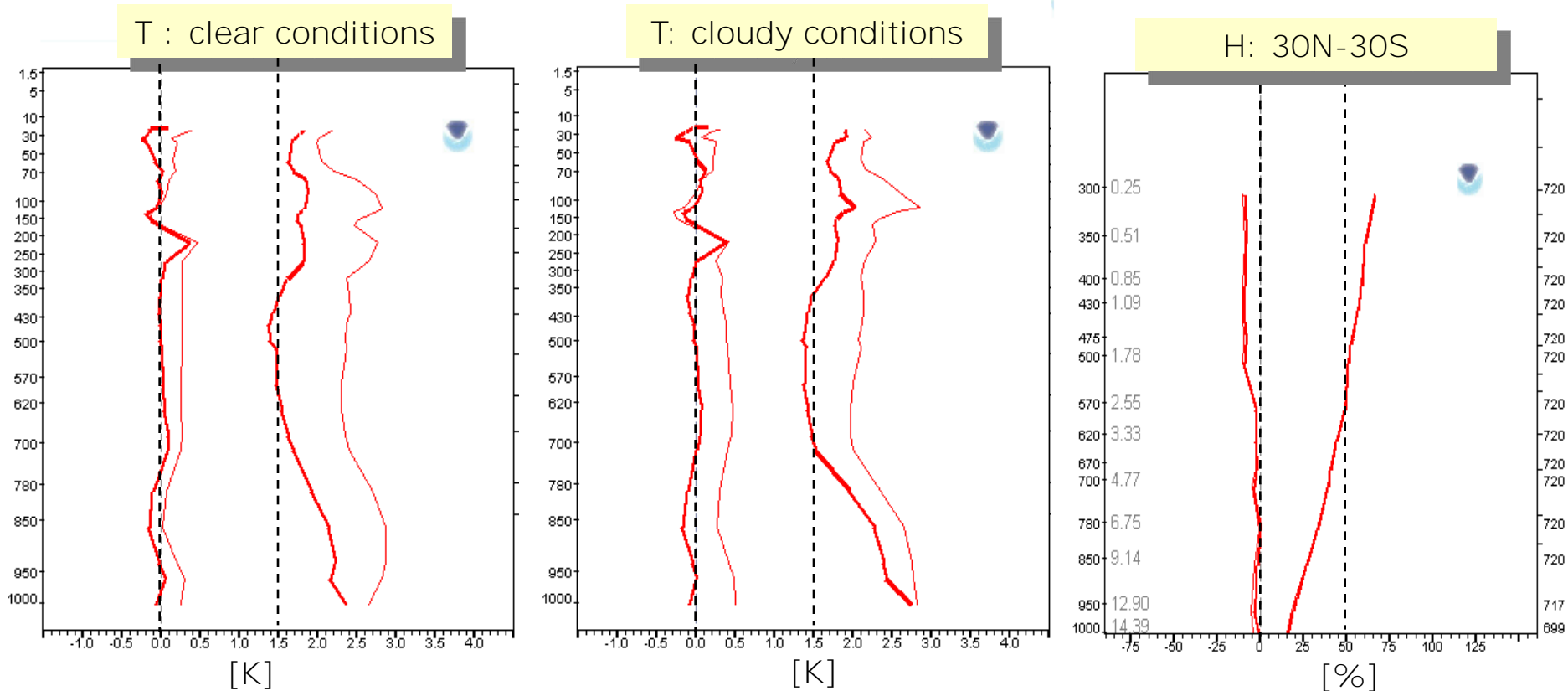


columnar amounts
of CO in 10^{18}
molecules/cm²,
from IASI



Examples : Products from NOAA16/ATOVS

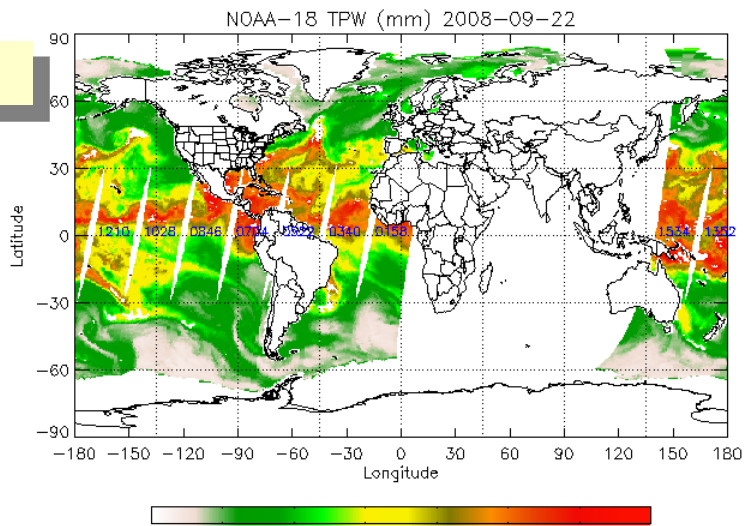
- NOAA/NESDIS operational product
 - Bias and RMSE of ATOVS temperature/humidity sounding retrieval (heavy lines) and first-guess (light lines)
 - NOAA-16; September 2001



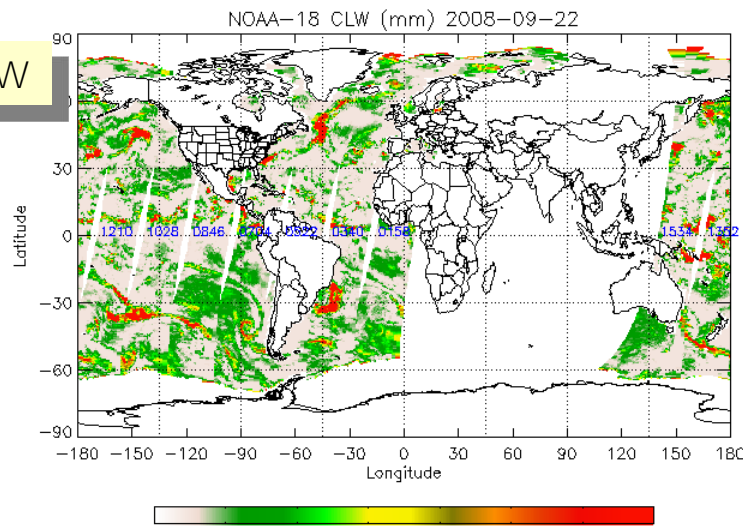
Examples : MSPPS Products from ATOVS

- NOAA MSPPS products on 22 Sep. 2008 from ATOVS
 - http://www.star.nesdis.noaa.gov/corp/scsb/mspps/realTime_n18.html

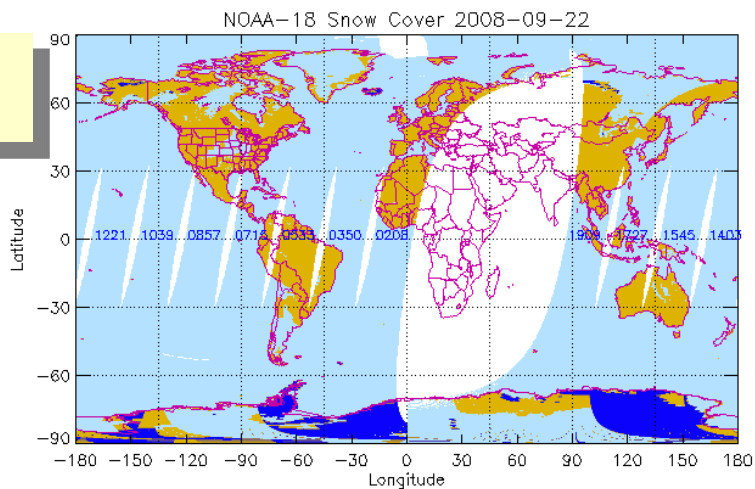
TPW



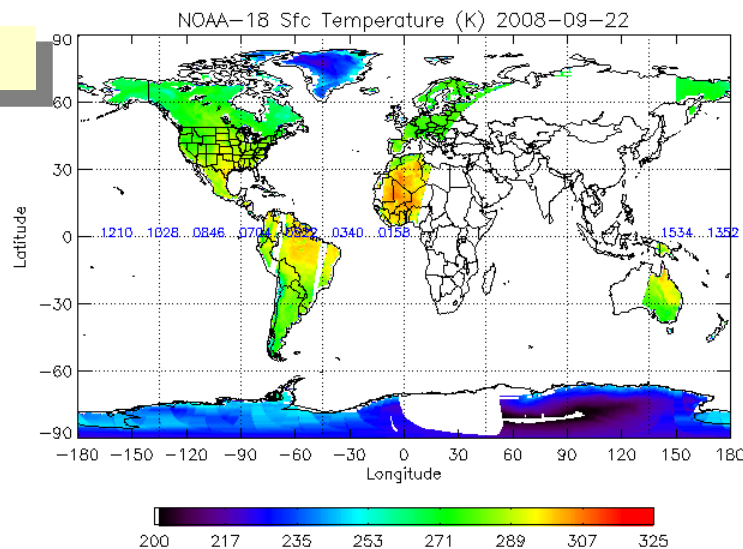
TCCLW



Snow Cover



Ts



Blue is snow, yellow is land without snow, light blue is undetermined (rain, desert, water, etc.)

Tools for retrieval

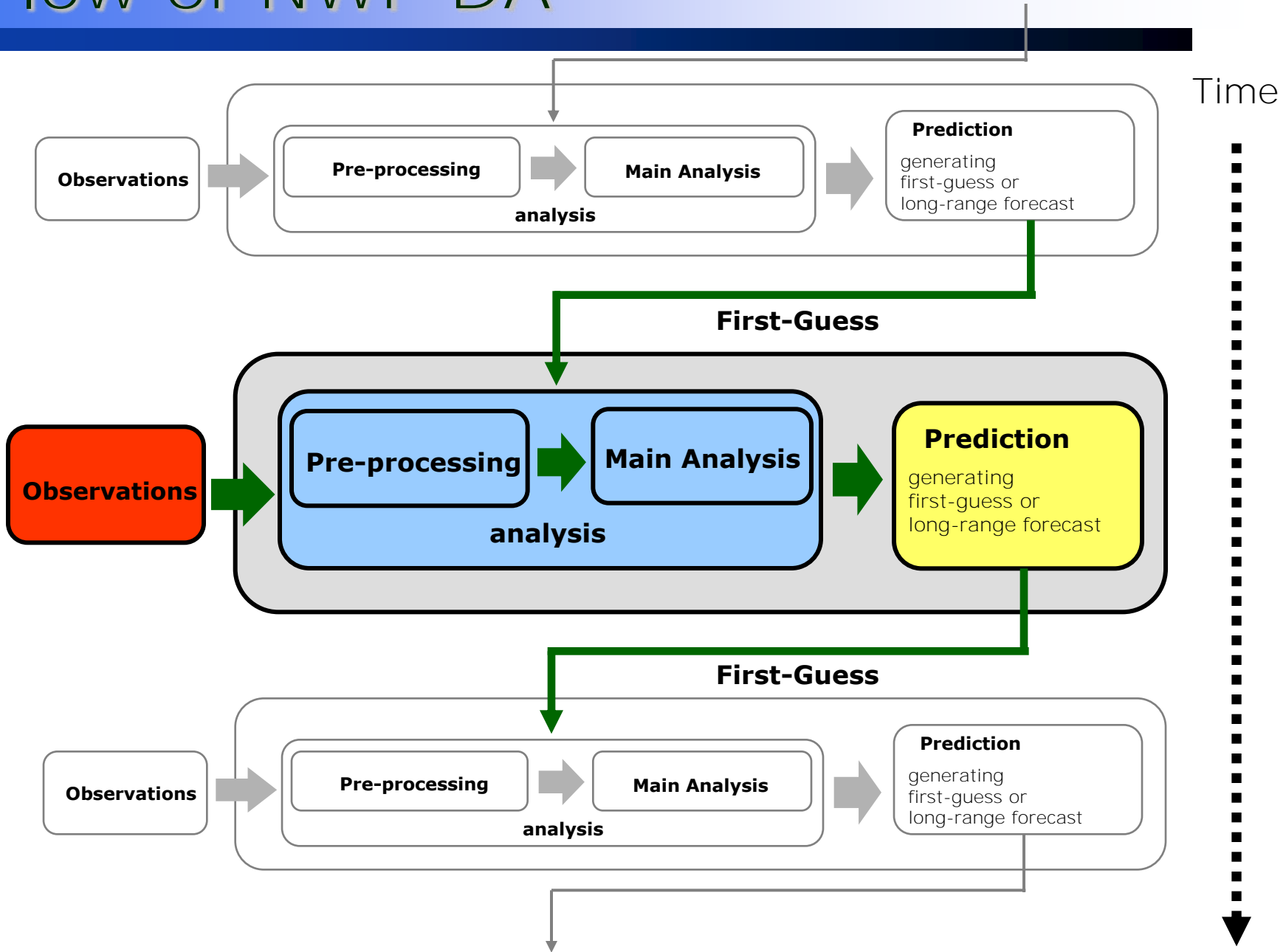
- Pre-processing package
 - AAPP The ATOVS and AVHRR Processing Package
- Radiative transfer model
 - RTTOV : Radiative Transfer for TOVS
 - <http://www.metoffice.gov.uk/research/interproj/nwpsaf/rtm/index.html>
 - CRTM : Community Radiative Transfer Model
 - http://www.jcsda.noaa.gov/projects_crtm.php
 - SDSU : Satellite Data Simulator Unit
 - <http://precip.hyarc.nagoya-u.ac.jp/sdsu/sdsu-main.html>
- Retrieval package
 - IAPP : International ATOVS Processing Package
 - 1D-Var: e.g. NWP SAF (organized by EUMETSAT)
 - <http://www.metoffice.gov.uk/research/interproj/nwpsaf/1dvar/index.html>
 - NWP SAF : Numerical Weather Prediction Satellite Application Facility
- ref : <http://cimss.ssec.wisc.edu/itwg/sssp/>

5. Application to data assimilation

What is Data Assimilation (DA)?

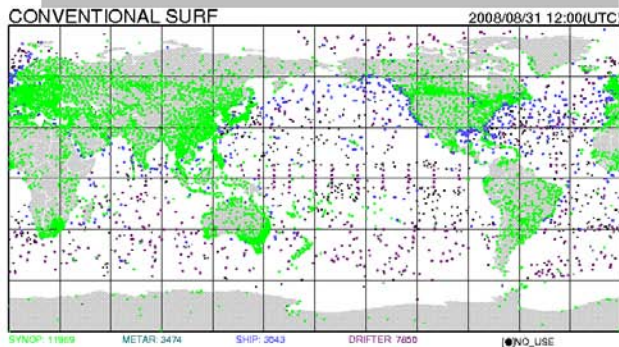
- Data Assimilation (DA)
 - Blend observations and numerical models to create more reliable state using the theory of statistical estimation
 - Accurate observations can still have errors and are irregularly distributed in time and space
 - Models based on physical laws can still have inaccuracy.
 - E.g. Improve models using reliable observations
 - E.g. Estimate 3D/4D state from limited observations using physical models
- DA is applied to data integration to understand the earth system and creating initial conditions of NWP (numerical weather prediction)

Flow of NWP DA

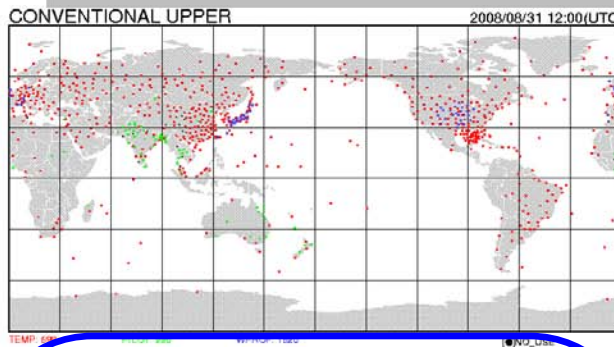


Data used in the JMA global DA system

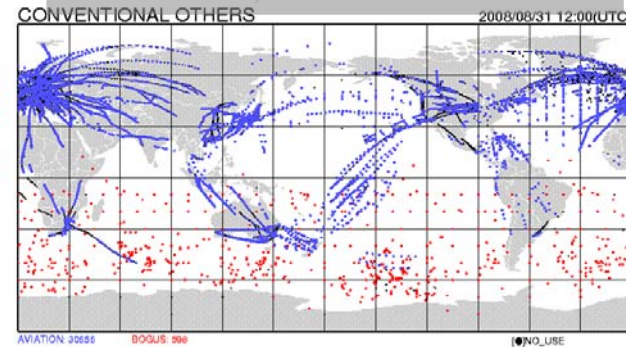
SYNOP, Ship, Buoy



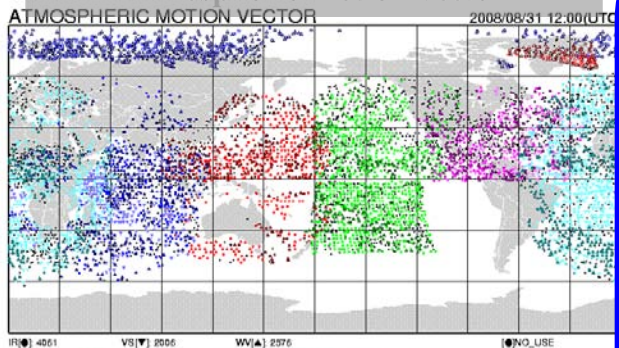
Radiosondes and Wind Profilers



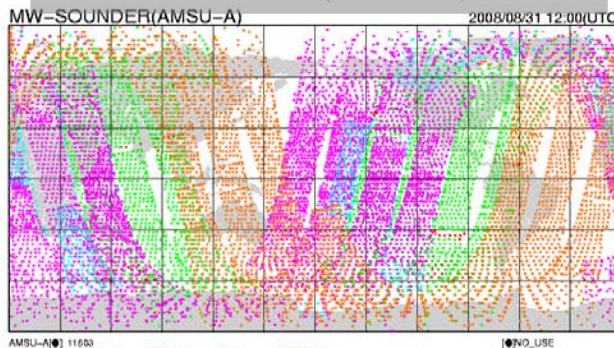
Aviation, Australian BOGUS



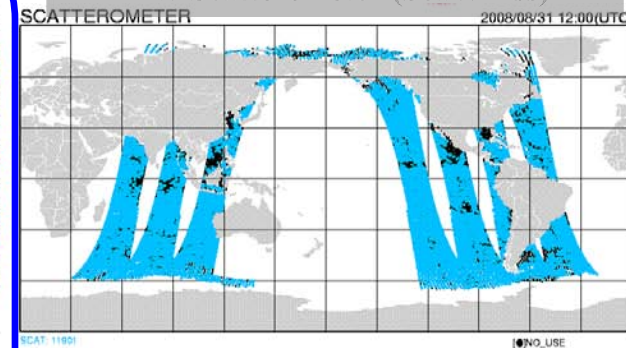
Atmospheric Motion Vector



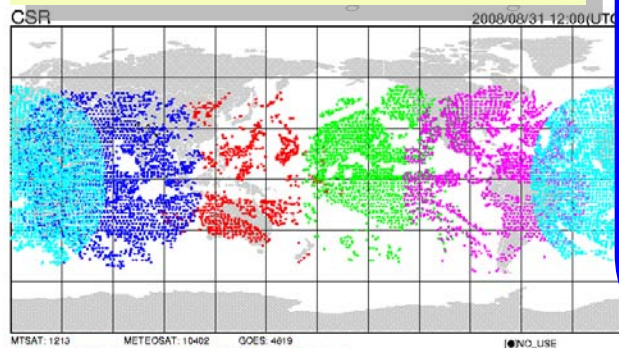
T-Sounder (AMSU-A)



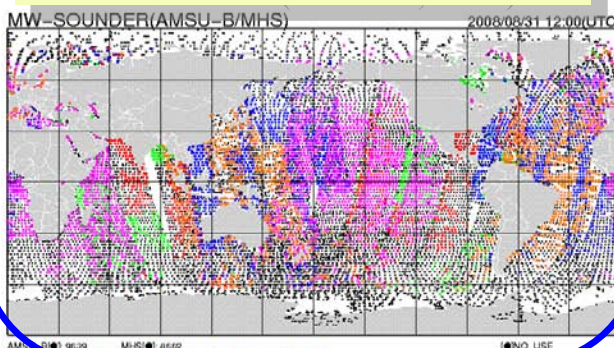
MW Scatterometer (SeaWinds)



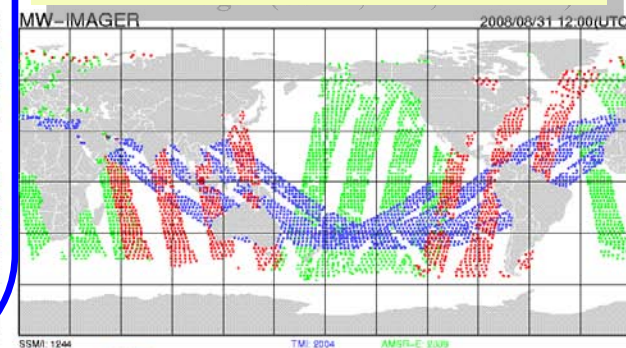
WV ch radiances of geo.sat. imagers



H-Sounder (AMSU-B, MHS)



MW imager (SSM/I, TMI, AMSR-E)



Satellite data operationally used in JMA

■ Imager

- AMV: Atmospheric Motion Vector (G/M)
 - ▣ MTSAT-1R, GOES-11,12, Meteosat-7,9
 - ▣ Aqua/MODIS, Terra/MODIS
- (WV-ch) radiance (G)
 - ▣ MTSAT-1R, GOES-11,12, Meteosat-7,9

satellite/sensor

G: global analysis
M: meso-scale analysis

■ MW scatterometer

- Ocean surface winds from QuikSCAT/SeaWinds (G/M)

■ GPS radio occultation (RO)/ground station

- Reflectivity (T/H) from GPS-RO (G)
 - ▣ CHAMP/BlackJack, GRACE/Black Jack
- Zenith tropospheric delay from GPS ground based station (M)

■ MW imager

- Radiance (G), TPW and RR (M)
- DMSP-13,14/SSMI, TRMM/TMI, Aqua/AMSR-E

■ Sounder

- Radiance (G) and Temperature profile (M)
- NOAA-15,16,17,18/ATOVS, Aqua/AMSUA, Metop/ATOVS

Analysis method

■ Typical analysis method

■ OI (Optimum Interpolation) :

$$\square x = x_b + \mathbf{BK}^T (\mathbf{KBK}^T + \mathbf{R})^{-1} \{y - H(x_b)\}$$

■ Used by many operational NWP centers in 1980s-1990s

■ Assimilate only observations linearly related to analysis variables

■ For sounders, assimilate T/H retrievals, not radiances

■ 3D-Var (3-Dimensional Variational)

$$\square J(x) = 1/2(x-x_b)^T \mathbf{B}^{-1}(x-x_b) + 1/2 \{y - MH(x)\}^T \mathbf{R}^{-1} \{y - MH(x)\}$$

■ 4D-Var : extend 3D-Var in time dimension

■ Currently adopted by many operational NWP centers

■ KF (Kalman Filter) :

$$\square x = x_b + \mathbf{BK}^T (\mathbf{KBK}^T + \mathbf{R})^{-1} \{y - H(x_b)\}$$

■ B is updated using linearized forecast model.

■ EnKF (Ensemble KF) : Merge KF and ensemble prediction systems

4D-Var

- $J(x) = J_B(x) + J_O(x)$

$$= 1/2(x-x_b)^T \mathbf{B}^{-1}(x-x_b) + 1/2[y-H(x)]^T \mathbf{R}^{-1}[y-H(x)]$$
- J_B : background term, J_O : observation term
 - $J_O = J_{O1} + J_{O2} + \dots$: sum of independent observations
- x : analysis variables (T, Q, U, V, Psrf, ...) in 3-dimension
- x_b : background or first-guess. Usually use short-range (e.g 6-hour) forecast from previous analysis
- y : all observations selected by pre-processing systems
- H : observation operator projecting analysis variables into observation variables
 - Interpolation of analysis variables at analysis grid points to observation points, RT model, TPW = $\int Q dz$, wind speed = $\sqrt{u^2 + v^2}$, ...
- M : forecast model
- \mathbf{B} : background error covariance (huge matrix!!)
- \mathbf{R} : observation error covariance
 - \mathbf{B} and \mathbf{R} give relative weights of background and observations

Assimilation of sounder data

- Sounders are essential for NWP DA
 - Provide vertical information of T/H
 - Installed in many satellites
 - MW sounders can see under (less) cloudy conditions
- Radiances are assimilated
 - Advantage over the assimilation of T/H retrievals
 - **Radiance assimilation, or “direct assimilation”** more accurately extract information from observation by including RT process.
 - Moreover it allows flexible data selection such as channel selection, easier error assignment and earlier data distribution after launch.
- However, the usage is limited to
 - **“clear” radiances**
 - RT model does not include cloud/rain effects in most NWP centers
 - radiances less sensitive to land surface, coast and sea-ice
 - Difficult to estimate accurate surface emissivities over the land/coast/sea-ice

Pre-processing for sounder data

- Main analysis (4D-Var) processes only high-quality and appropriate data.
- Pre-processing in DA system selects those data and, if necessary, correct them.

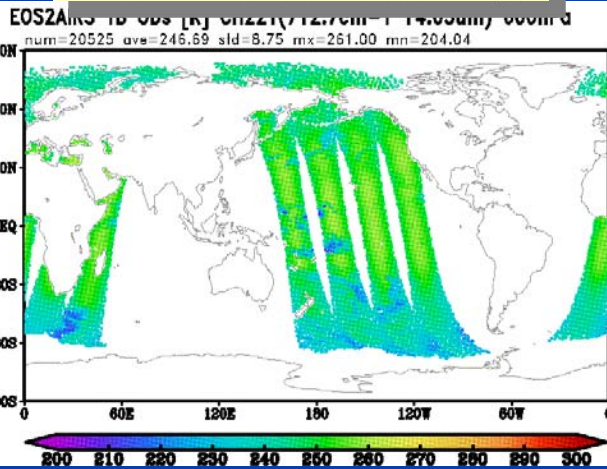
- Principal pre-processings
 - Quality control (QC)
 - ▣ Remove erroneous data
 - ▣ Remove data affected by clouds/rain, land surface and sea-ice.
 - Bias correction (BC)
 - ▣ Biases depend on scan, air-mass and instrumental conditions, and can temporally change.
 - Biases come from calibration, instrumental aging, orbit drift, inaccurate RT model, , ,
 - ▣ BC removes biases using a linear regression approach
 - Biases are usually estimated from $y-H(x_{sonde})$, $y-H(x_b)$ or $y-H(x_a)$
 - Thinning
 - ▣ Reduce data to match the resolution of DA system
 - ▣ Reduce computational costs
 - Assignment and modification of observation errors

Pre-processing : example of QC

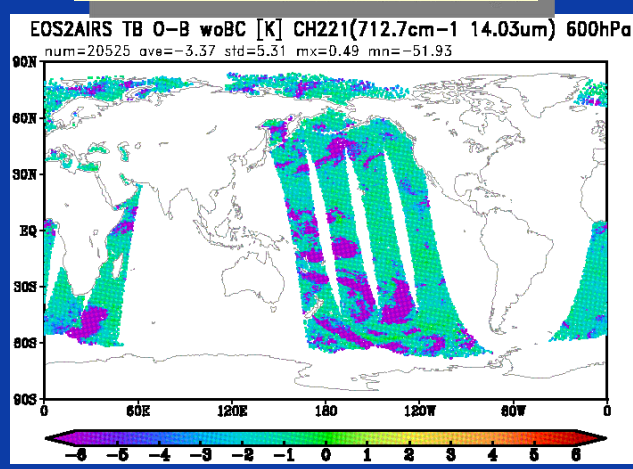
- Remove cloud/rain-affected radiances
- Remove radiances affected by land/coast/ice-sea surface.

$$O-B: y-H(x_b)$$

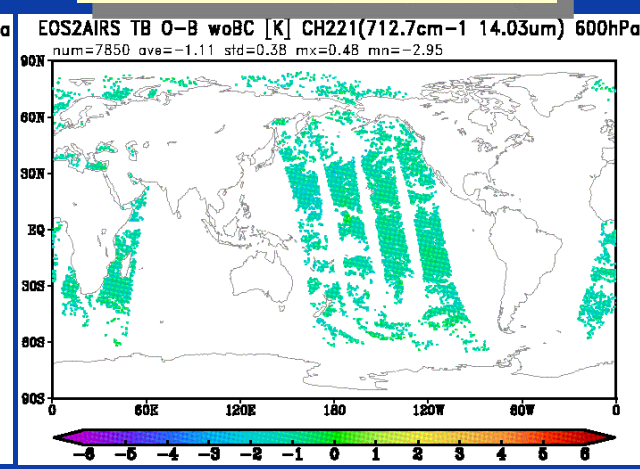
AIRS221 Obs before QC



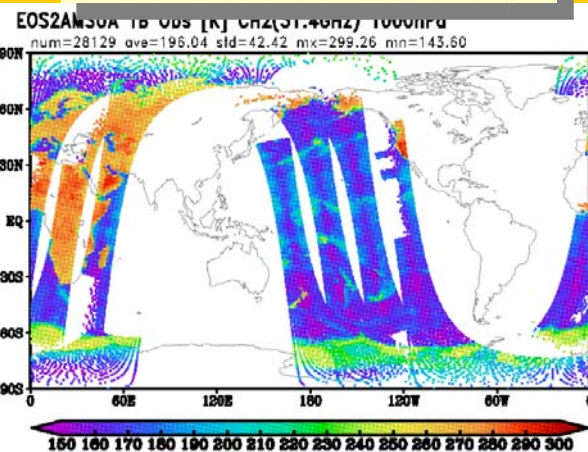
O-B before QC



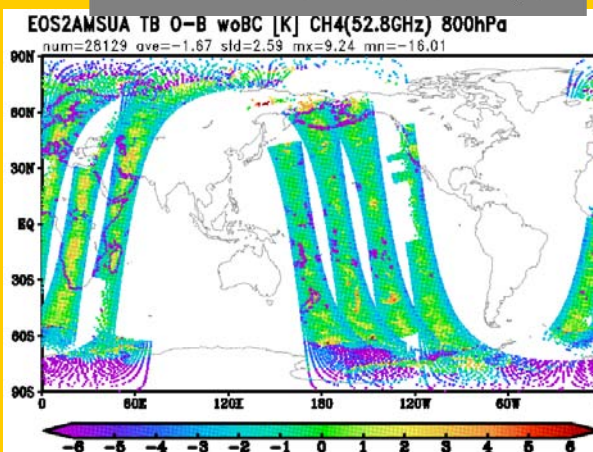
O-B after QC



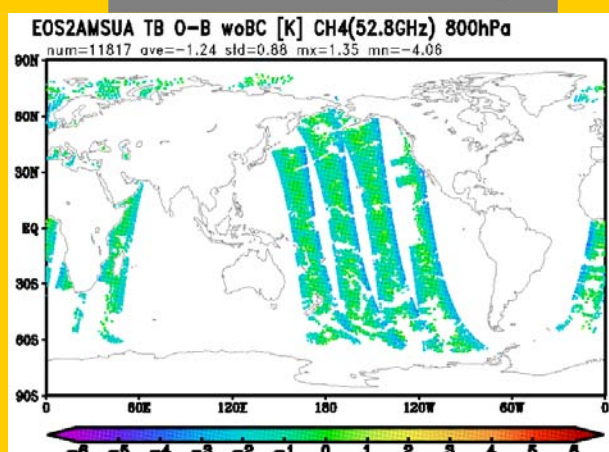
AMSU-A4 Obs before QC



O-B before QC



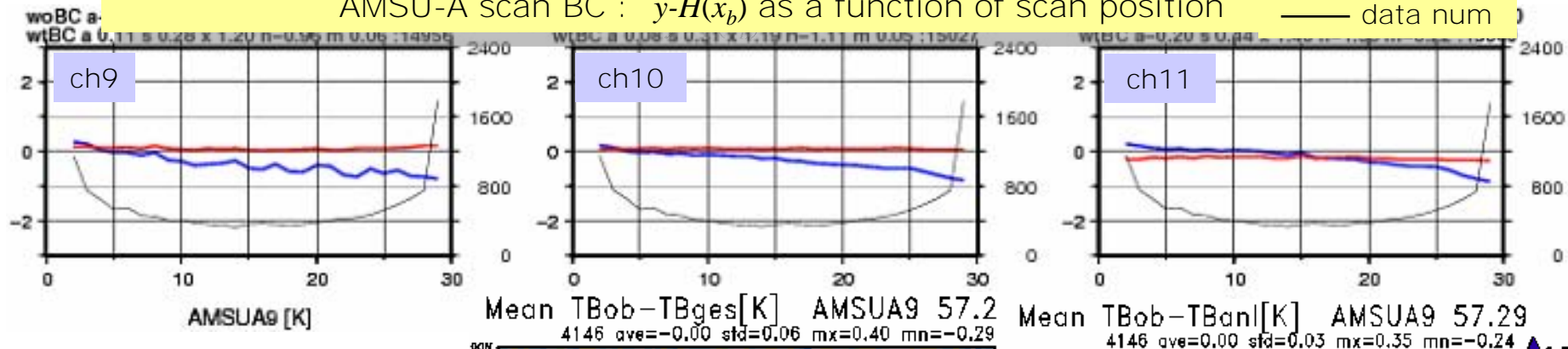
O-B after QC



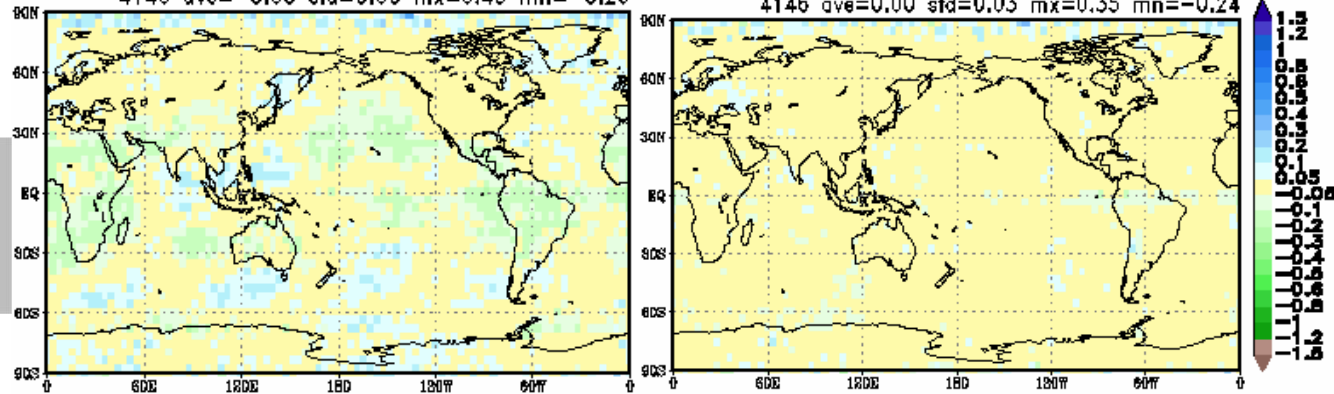
Pre-processing : Example of BC

- Scan bias correction
 - Bias is estimated by $y-H(x_b)$ averaged at each scan position
- Air-mass bias correction
 - Bias = $a_1 * IWLR + a_2 * TCCLW + a_3 * Ts + a_4 * 1/\cos(\text{scan}) + a_5 * \text{const}$
 - IWLR=integrated weighted lapse rate
 - Coefficients are updated at every analysis

AMSU-A scan BC : $y-H(x_b)$ as a function of scan position



AMSU-A air-mass BC:
 $y-H(x_b)$ before BC (left)
 and after BC (right)



Summary

- Sounders extract vertical distributions of temperature, atmospheric constituents using a number of wavenumbers with different radiative characteristics.
 - This lecture mainly aimed at passive nadir T/H sounders.
 - Radars, lidars and limb sounders also derive vertical information based on different principle.
- Sounders have been long and widely used by operational and research communities.
 - Diverse retrieval methods, such as MAP method, and products have been generated.
 - Essential data sources especially for NWP
 - ▣ Assimilation of (clear) radiances appropriately pre-processed substantially improves accuracy of NWP.
- Many new instruments are planned
 - IR sounders: NPP/CrIS (to be launched in 2010), NPOESS/CrIS (2013), MTG/IRS (2017)
 - MW sounders: Megha-Tropiques/SAPHIR(2009), NPP/ATMS (2010), NPOESS/ATMS (2013), NPOESS/MIS?, Geo.sat?

References

- ECMWF training course
http://www.ecmwf.int/newsevents/training/rcourse_notes/DATA_ASSIMILATION/INVERSION_METHODS/Inversion_methods.html
- Janssen, M.A. (editor), 1993: ***Atmospheric Remote Sensing by Microwave Radiometr.*** A Wiley-interscience publication, 592 pp.
- Kidder, S.Q. and T.H. Vonder Haar, 1995: ***Satellite Meteorology: An Introduction.*** Academic Press, 466 pp.
- Kalney, E., 2003: ***Atmospheric Modeling, Data Assimilation and Predictability.*** Cambridge University Press, 341 pp.
- MetEd Satellite Meteorology
http://www.meted.ucar.edu/topics_satellite.php
- Stephens, G.L., 1994: ***Remote sensing of the Lower Atmosphere: An Introduction.*** Oxford univ.press. 523 pp.

Lecture 6: Geostationary Meteorological Satellites

Atsushi Higuchi
Center for Environmental Remote Sensing
(CEReS)
Chiba University, Japan

The 18th IHP Training Course
“Satellite Remote Sensing of Atmospheric Constituents”
3-15 November 2008, Nagoya, Japan

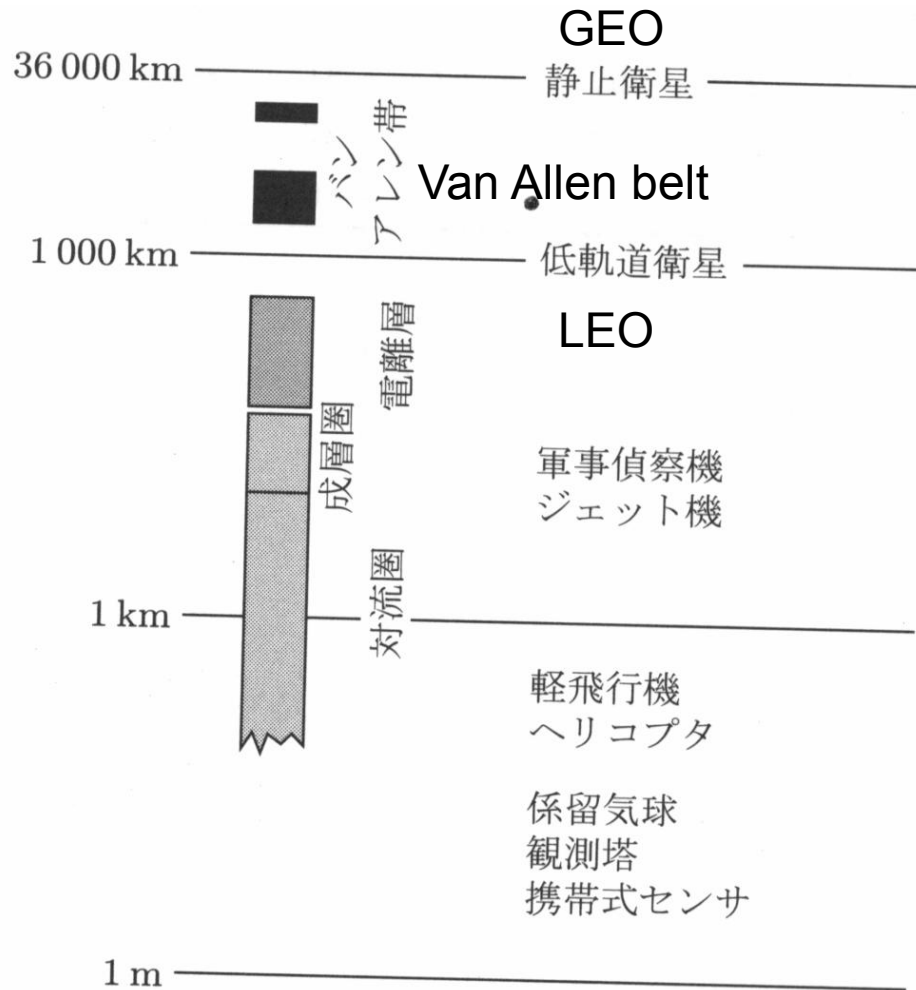
Today's Contents

- Introduction of Geostationary Meteorological Satellites platforms & Sensors:
 - GMS, MTSAT-1R, GOES, etc ..
 - Thermal-IRs, mid-IRs (water vapor, water droplet), Visible
- Applications for meteorological researches
 - Detection of Convective Activity (Ic), Traditional classification by a combination of several channels
 - More utilize of Geo-Satellites
- Recent Topics
 - Introduction of VL CEReS activity
 - Inter-calibration project (SAT GSICS), etc.

Advantage & Disadvantage of Geo. Sat.

- Advantages:
 - High-Time Frequent Observation: Most of Geo. Sat. capture hourly. (nothing to compare with them !)
 - Basic wavelength: Thermal-IR (one or two atmosphere's window [10-13 micron]), 7 micron (Water vapor), (3 micron: water droplet), and visible.
- Disadvantages:
 - Coarse spatial resolution: 4 or 5 km in IRs, 1 km in visible.
 - Indirect observation for internal-cloud: Due to principle of Optics (can not profiling like active sensor)

Spatial resolution (Altitude of platform)

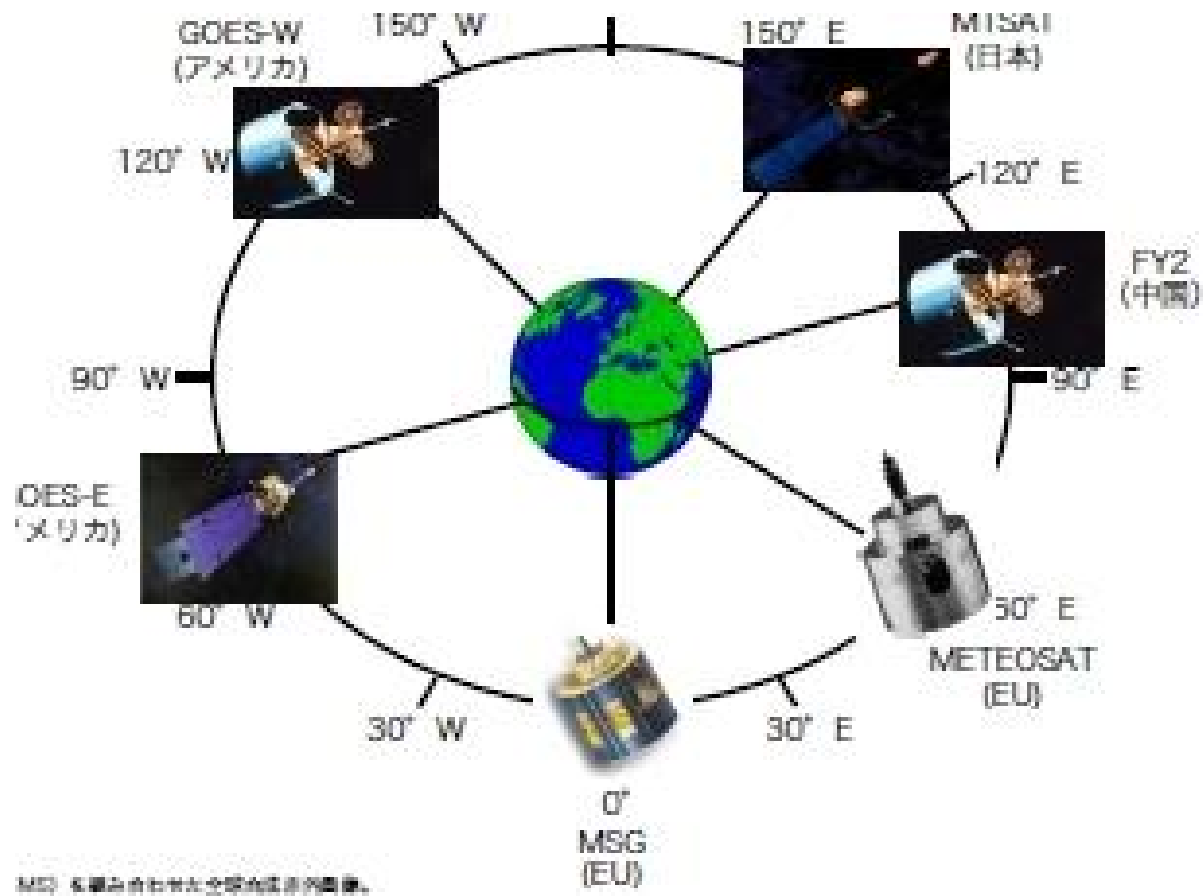


・ Polar orbit: 700-800km
-> Balance to gravity

・ Geostational: 36,000km
-> Also balanced with gravity

図 10.1 地上からの高度順に並べたリモートセンシングのプラットフォーム

Geo-Sat. Cover globe



Spin type (old style; old-GOES, GMS, FY2-X, Meteosat, MSG)



Meteosat

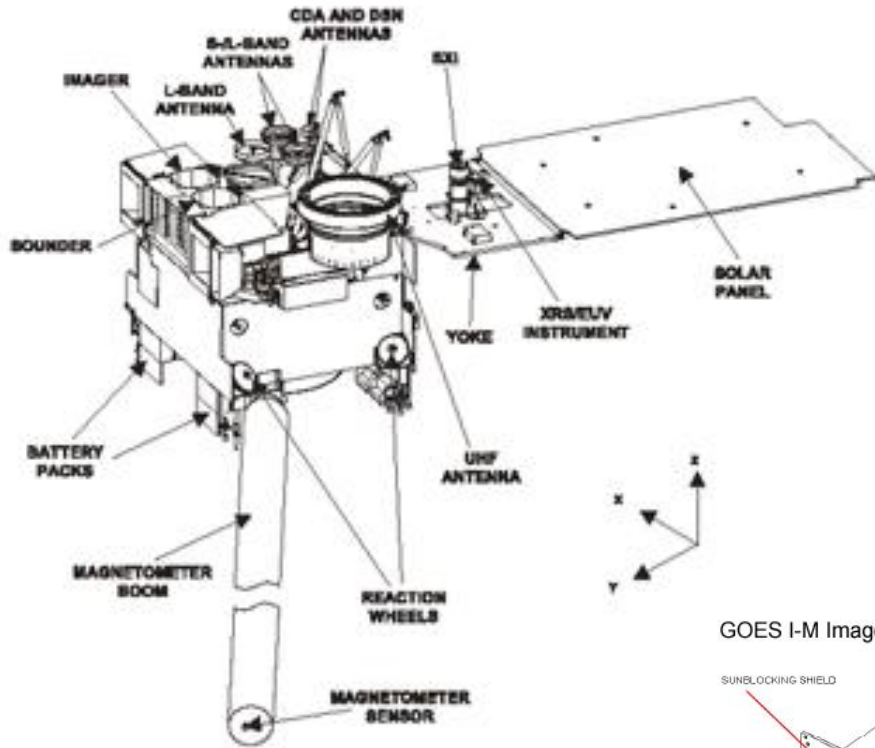


FY2-C(D),
GMS-5

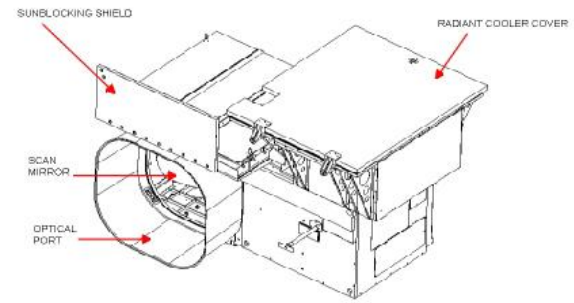


MSG
(Meteosat
Second
Generation)

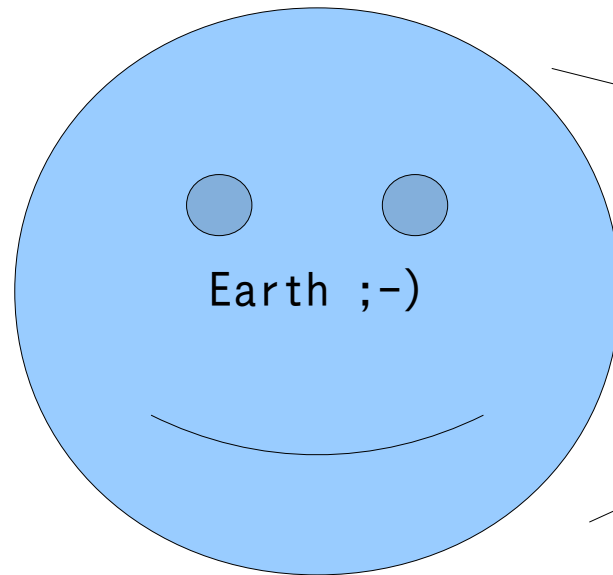
New type (three-axes control; new GOES, MTSAT-1R)



GOES I-M Imager

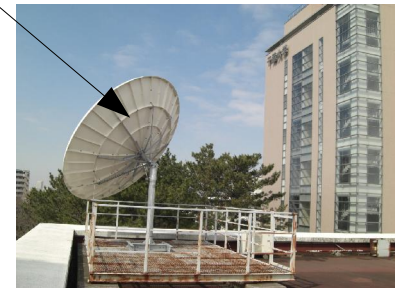


Geo-Sat operation (by in-situ Receiving station)



1. Scanning the Earth
by Geo-Sat.

Geo-Sat operation (by in-situ Receiving station)



Space Agency

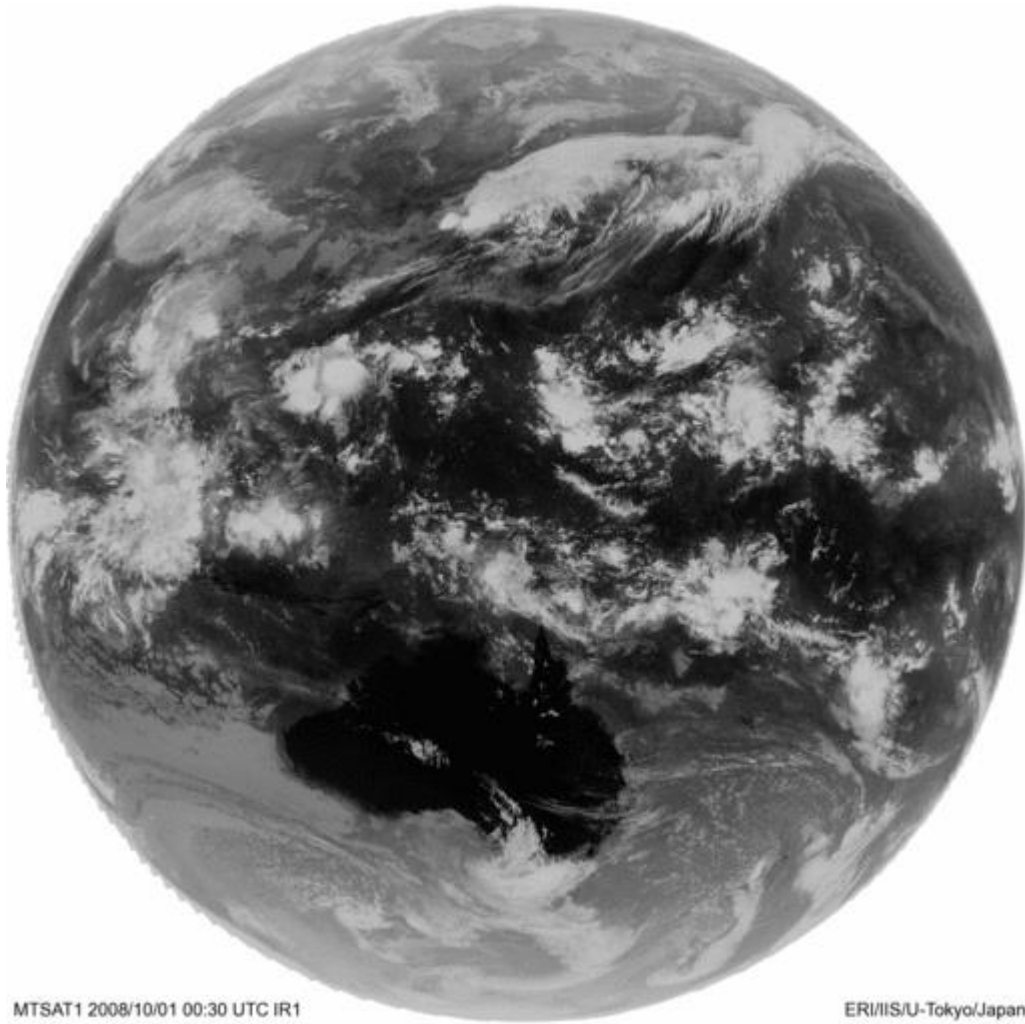
Space Agency

4. Then receive data by antenna

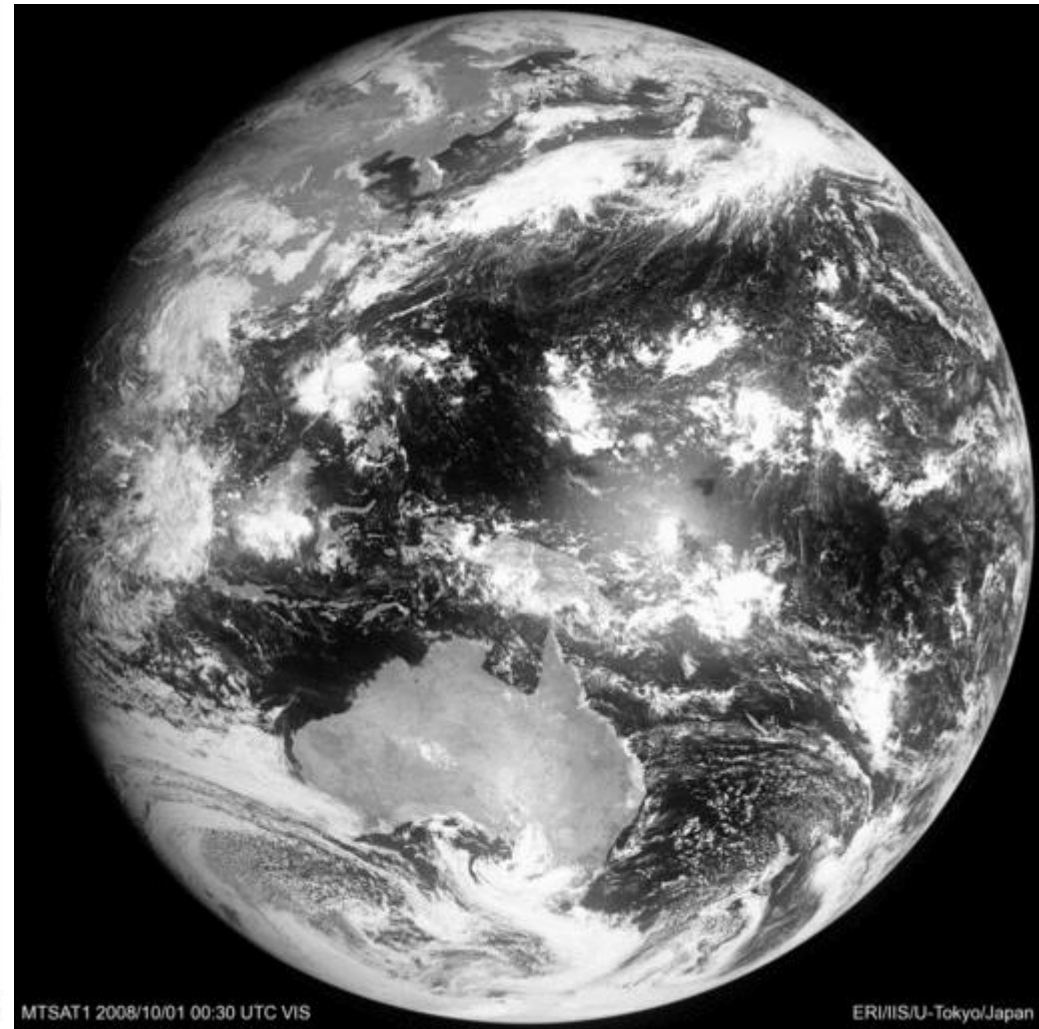
2. Send raw data into Space operational agency.

3. Send specified data to Geo-Sat

Full-disk Image example (MTSAT)



IR1



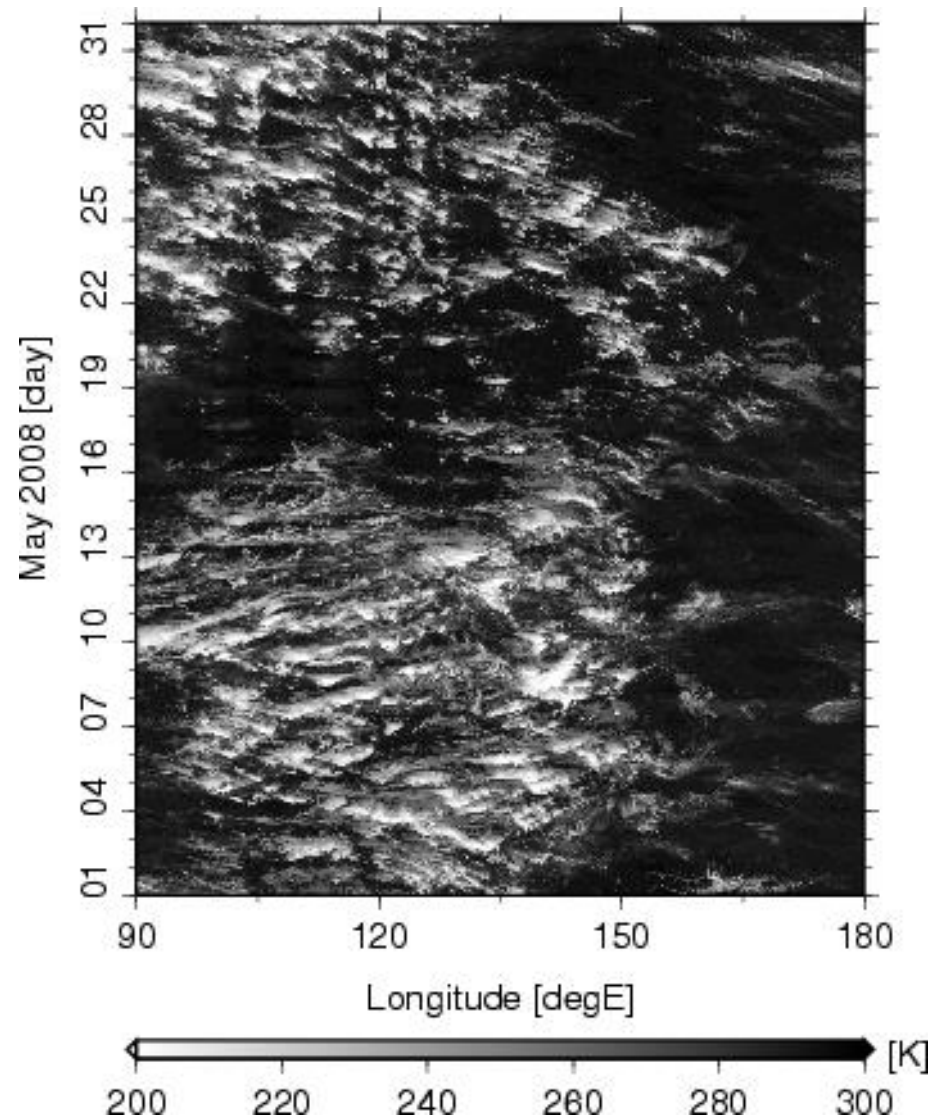
VIS

Here I will show several animations
derived from MTSAT-1R

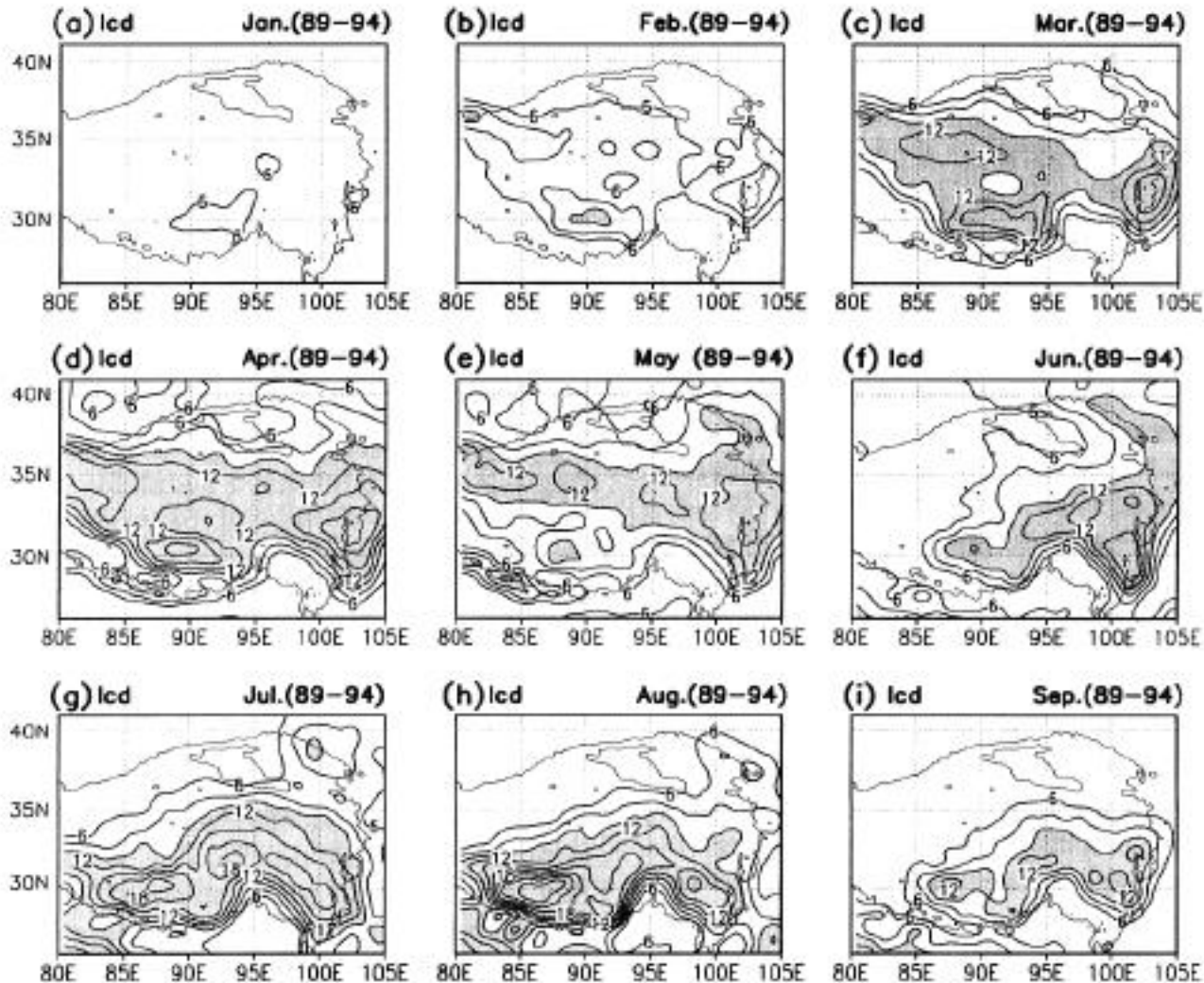
Analysis of Geo-Sat for Meteorology (1)

- Simple image analysis to diagnose a target situations
 - Detection of convective activity by thermal-IR
 - Detect low-level clouds by visible
 - Moving feature figure: Hovmoller diagram
- Multiple (combination) usage of several channels in Geo-Sat.
 - Combination of two thermal-IR (split window tech.)
 - Combination of visible and IR
 - Combination of water vapor and IR

Hovmoller Diagram (Equator's data)



Seasonal change in Ic over Tibet (Fujinami and Yasunari, 2001)

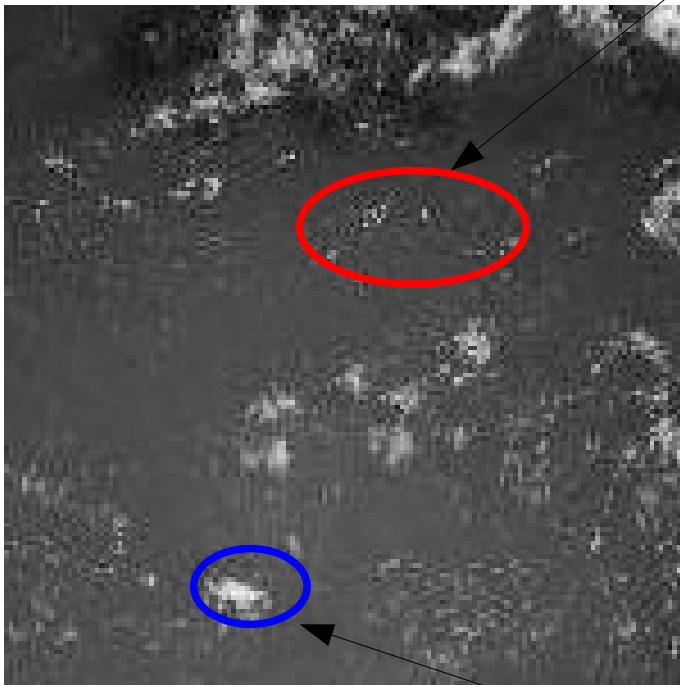


Convective Index (I_c)
(Nitta & Sekine, 1994)

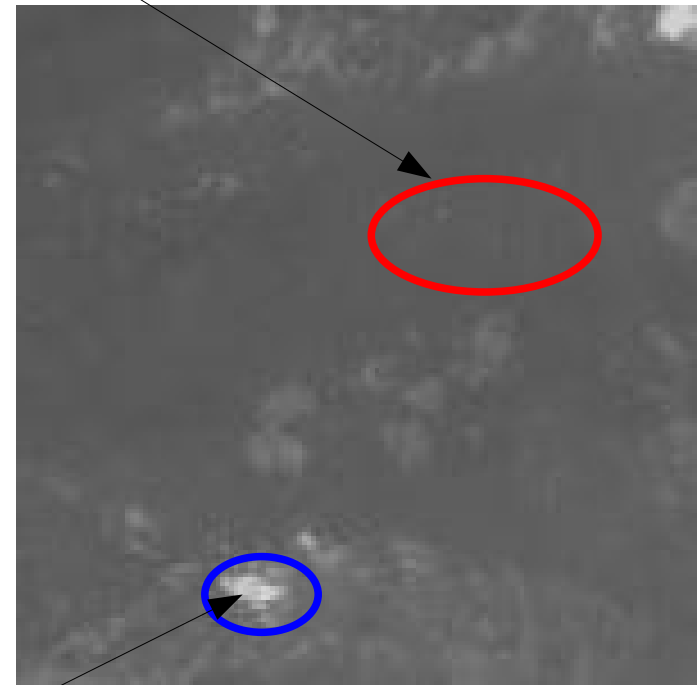
$$I_c = 250 - T_{bb} \quad (T_{bb} < 250K)$$
$$I_c = 0 \quad (T_{bb} \leq 250K)$$

Use of Visible (only daytime) for the detection of low-level cloud

Hard to detect clouds by thermal-IR



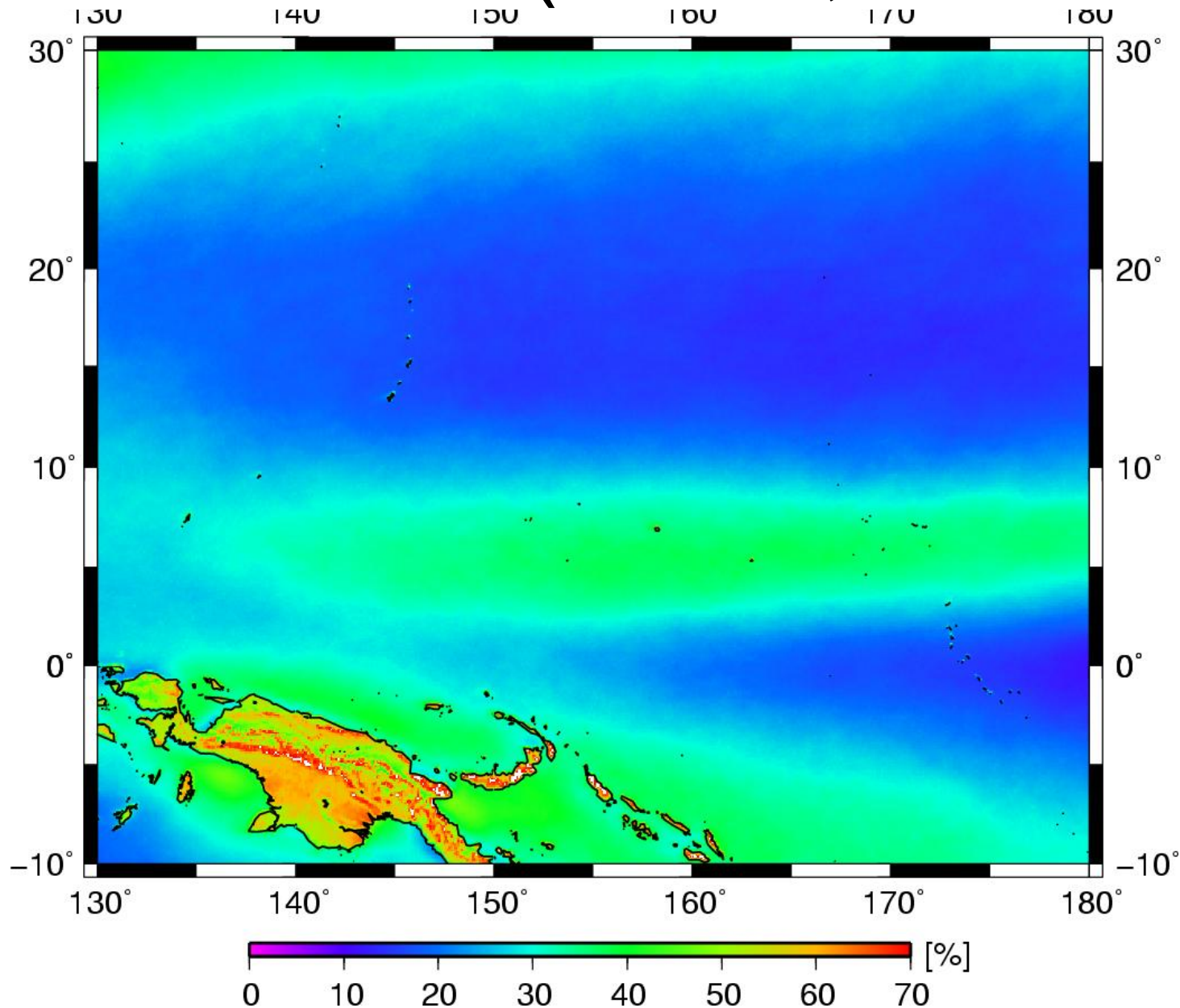
Visible



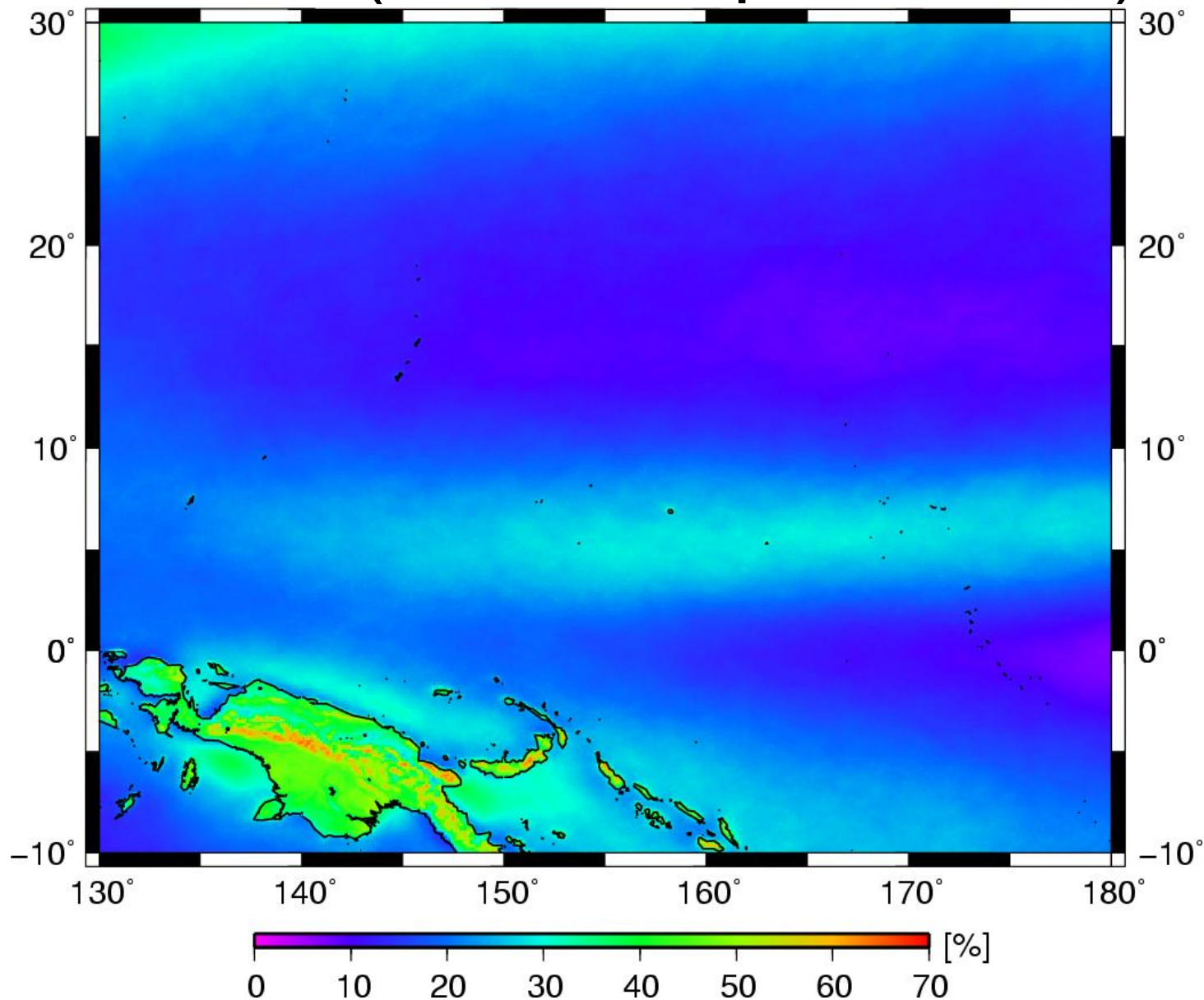
thermal-IR1

Detectable both channels

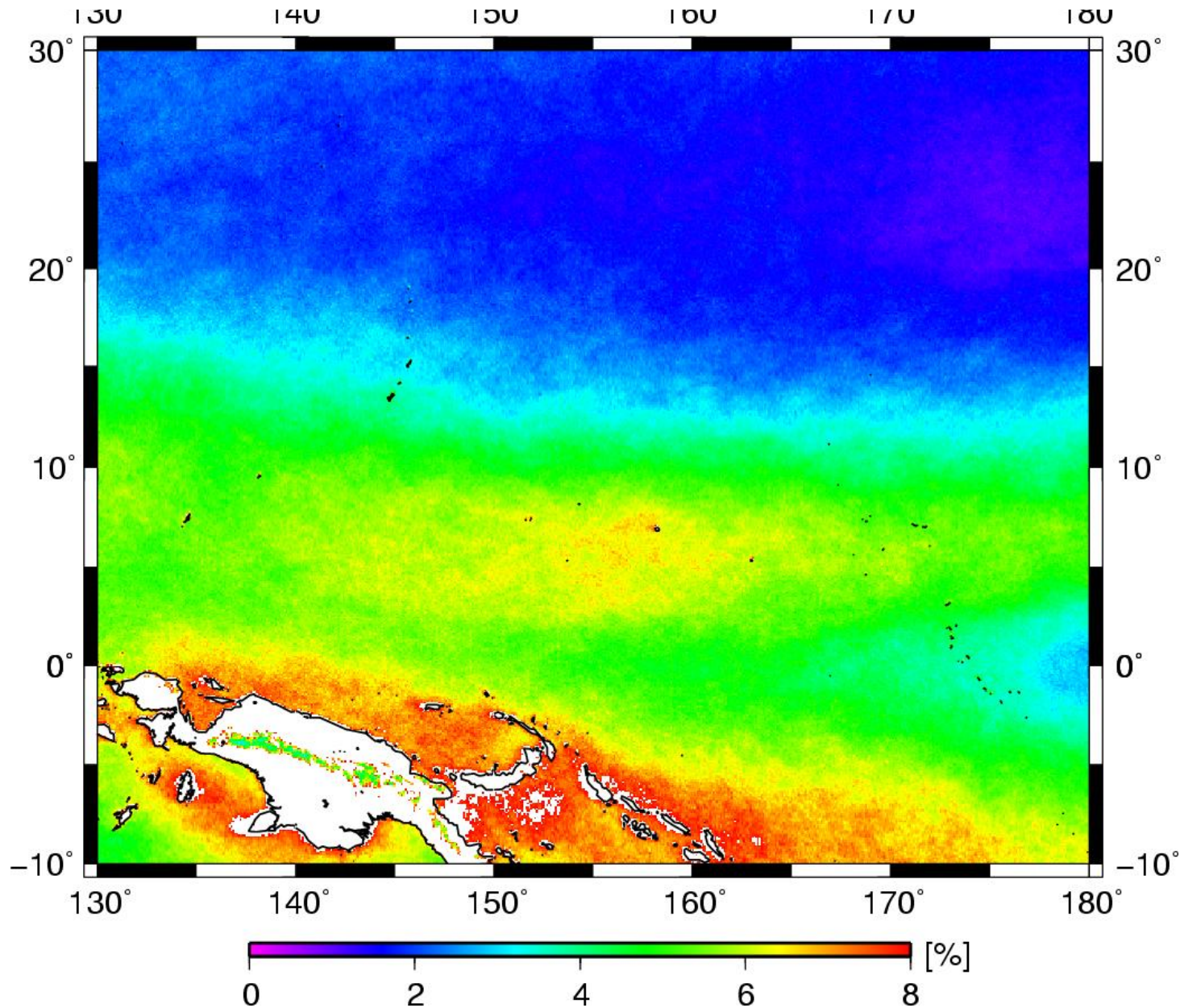
Amount of Cloud Map revealed by GMS 5 SVISSR (visible; 1998-2003)



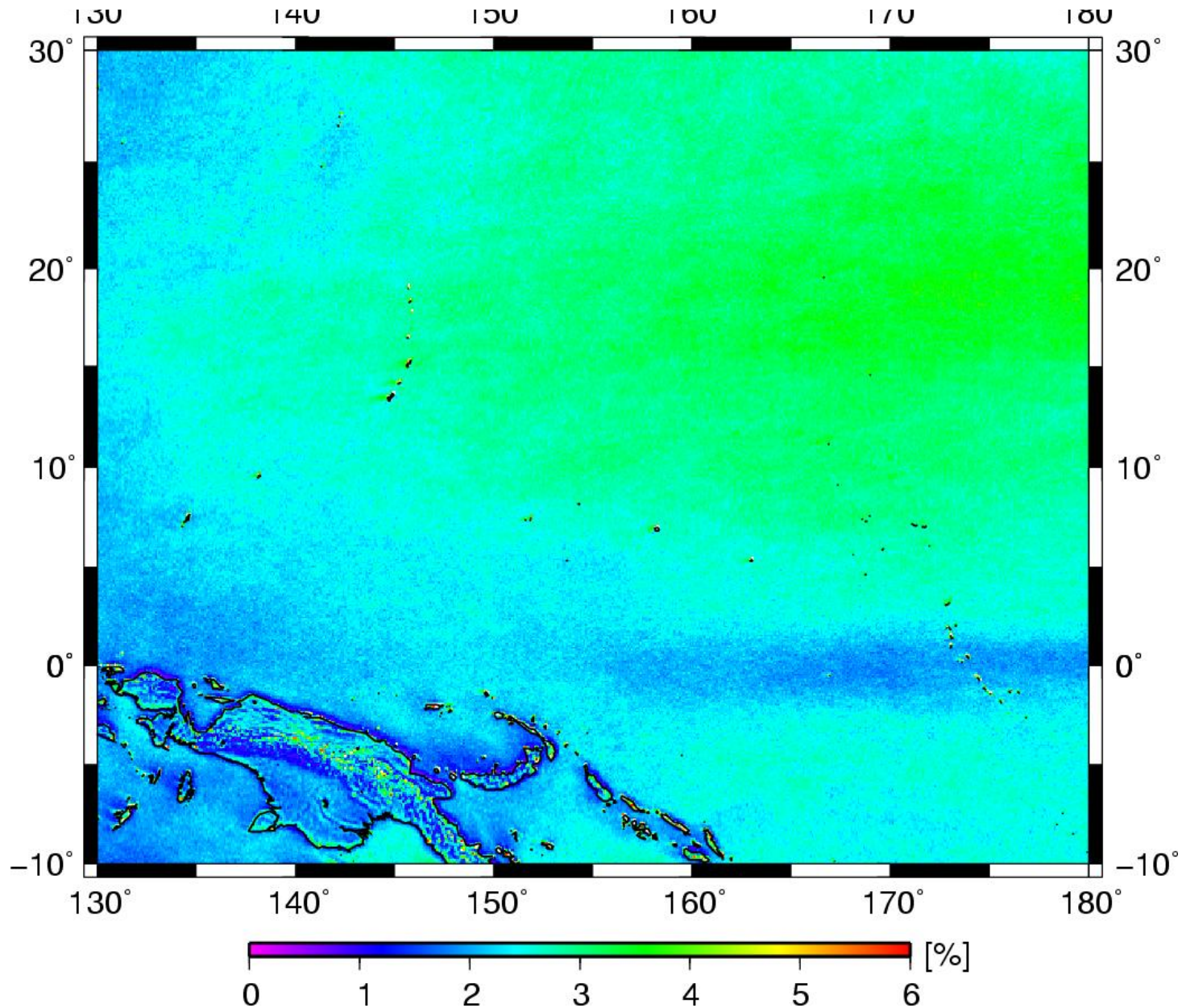
Amount of Cumulus, Cumulonimbus, Stratocumulus Map by GMS 5 (visible & split window)



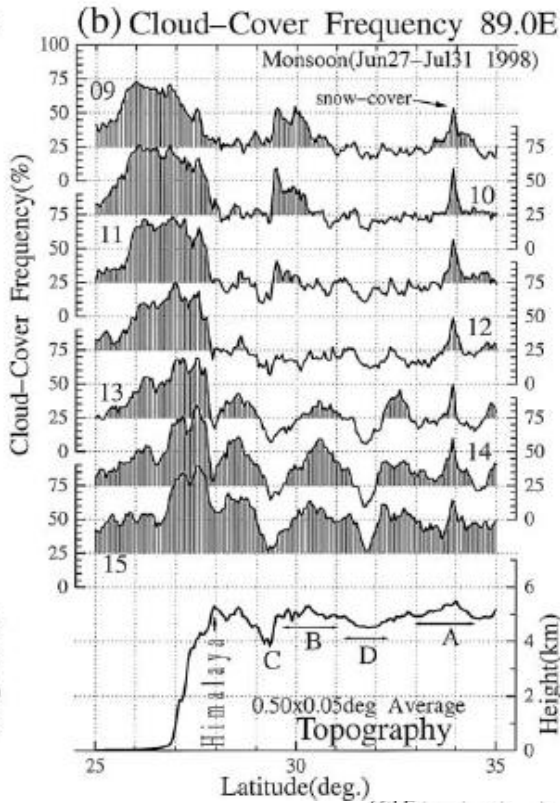
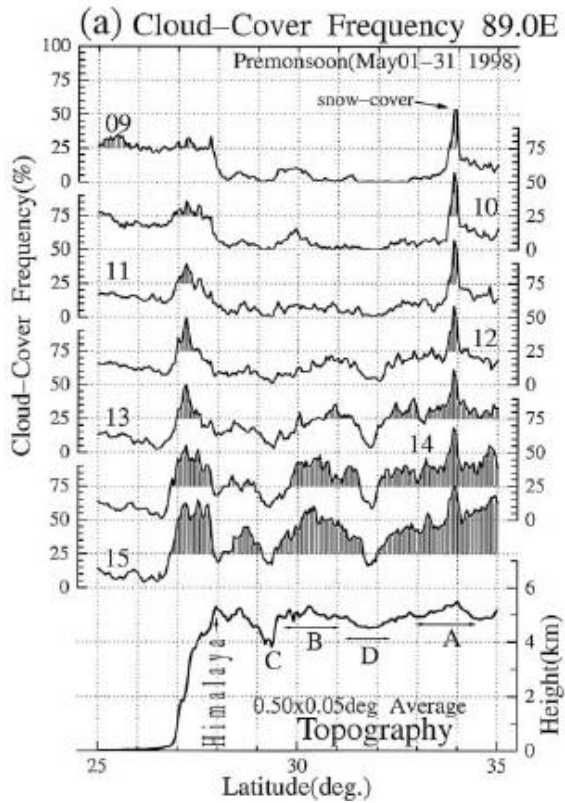
Amount of Cirrus (Anvil) Map by GMS 5 (visible & split window)



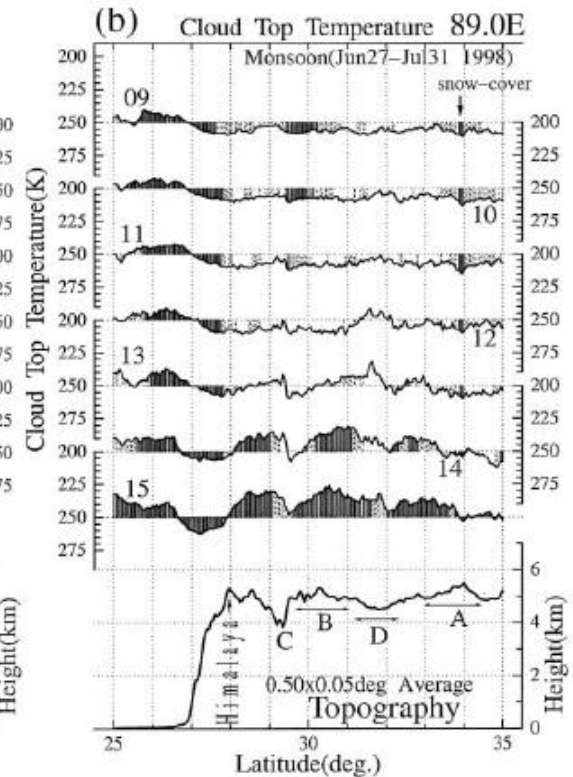
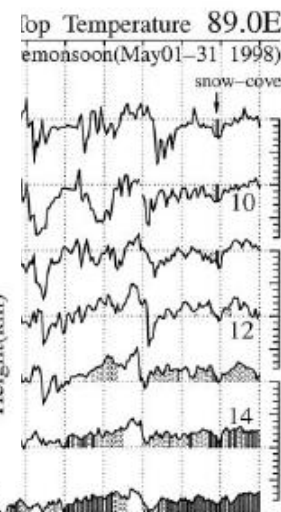
Amount of “Small” Cumulus Map



Utilize visible channel for the detection of orographic small cloud on Tibet (Kurosaki and Kimura, 2002)

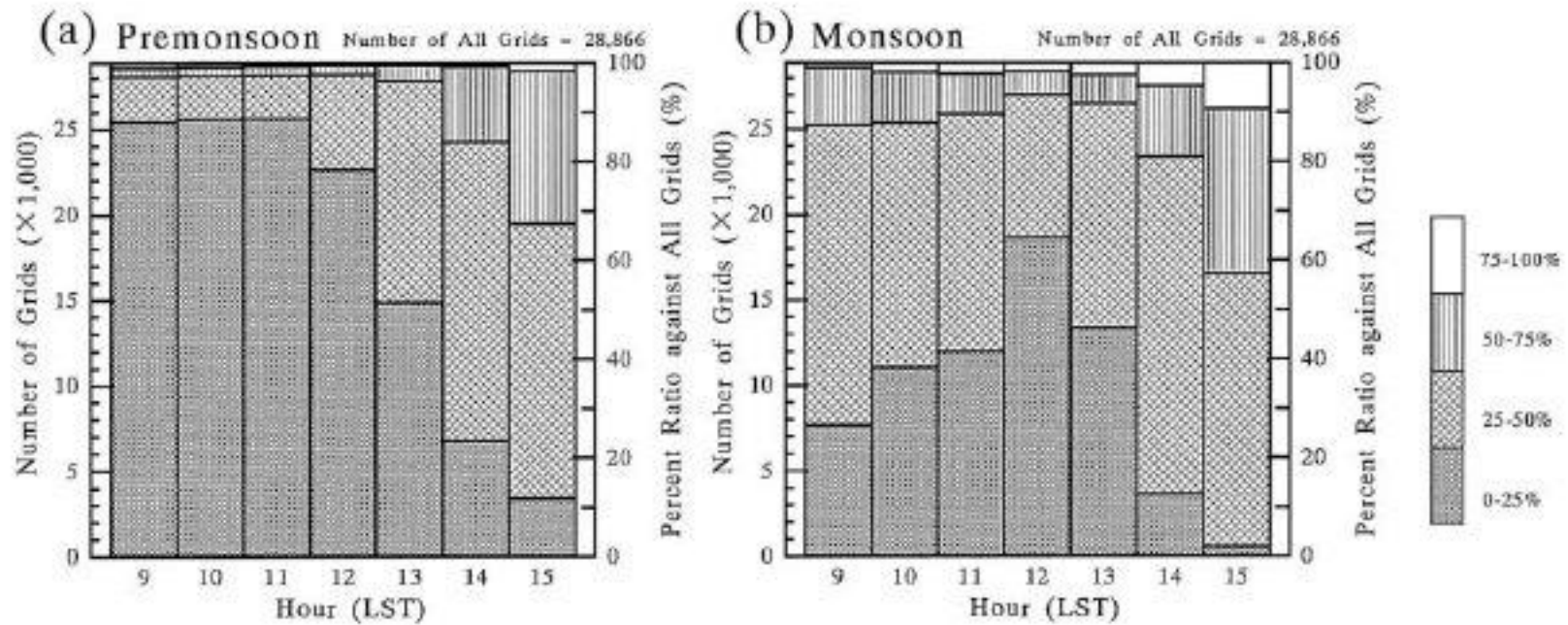


thermal-IR



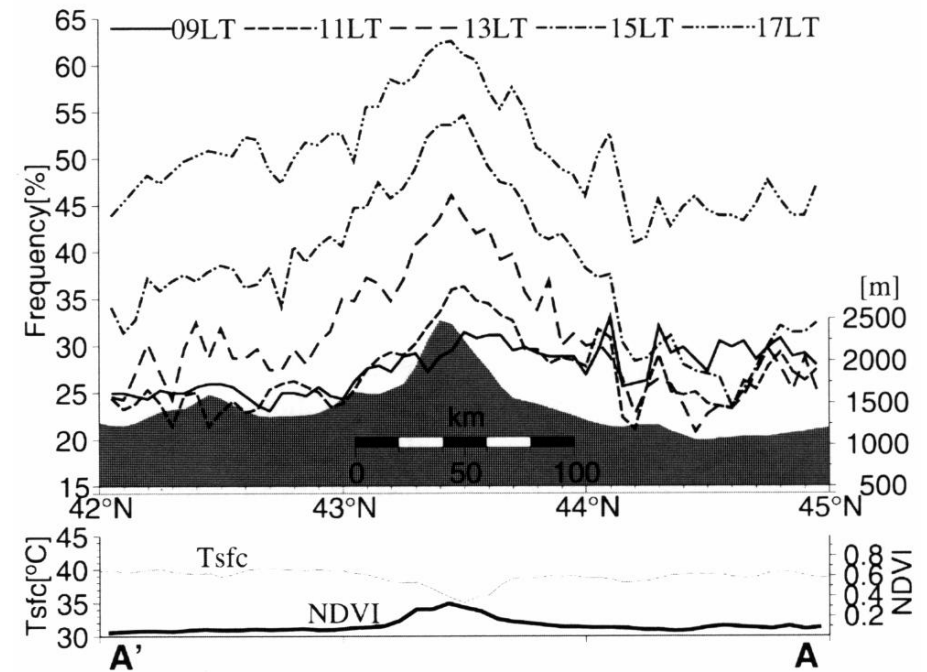
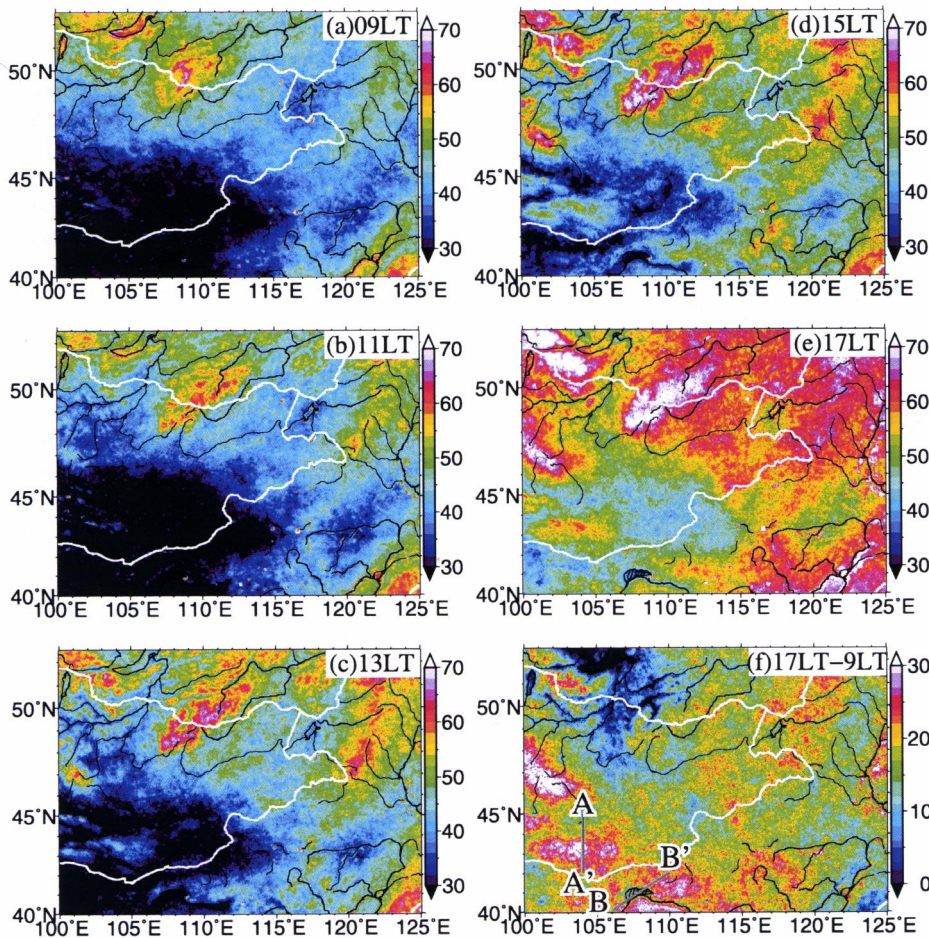
Visible

Cont. (Kurosaki Kimura, 2002)

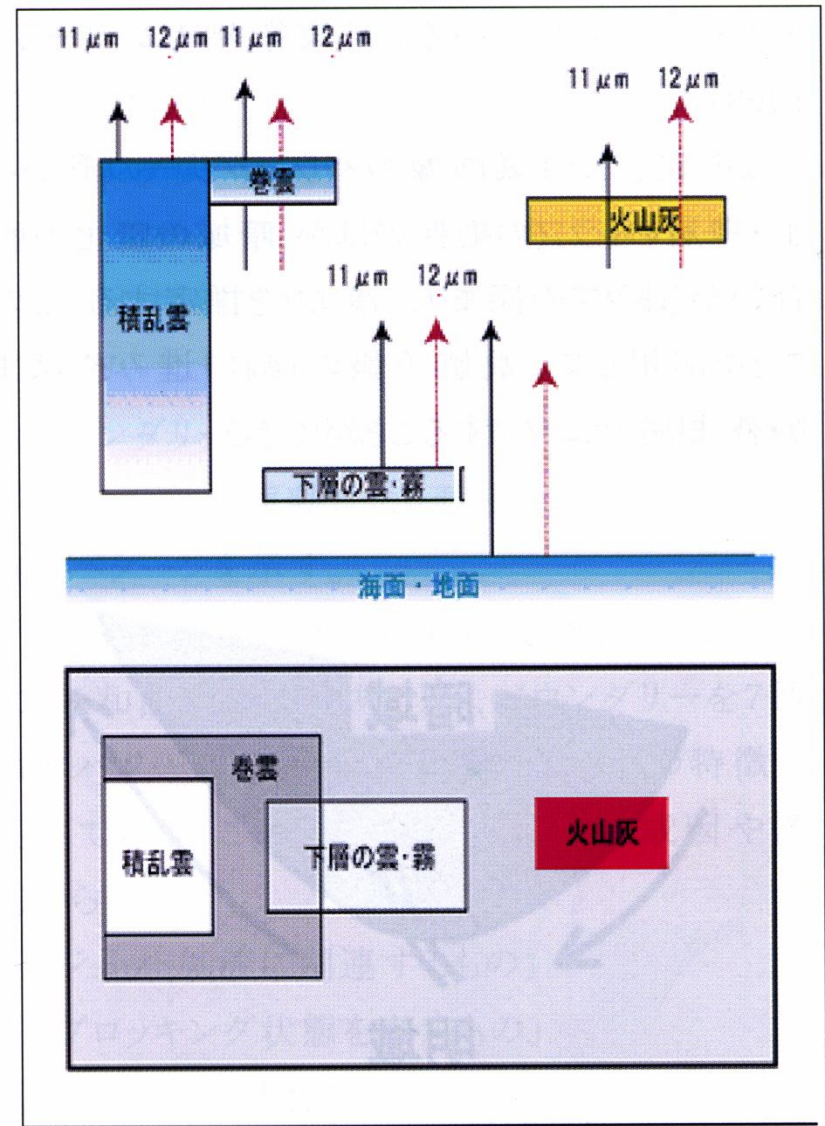
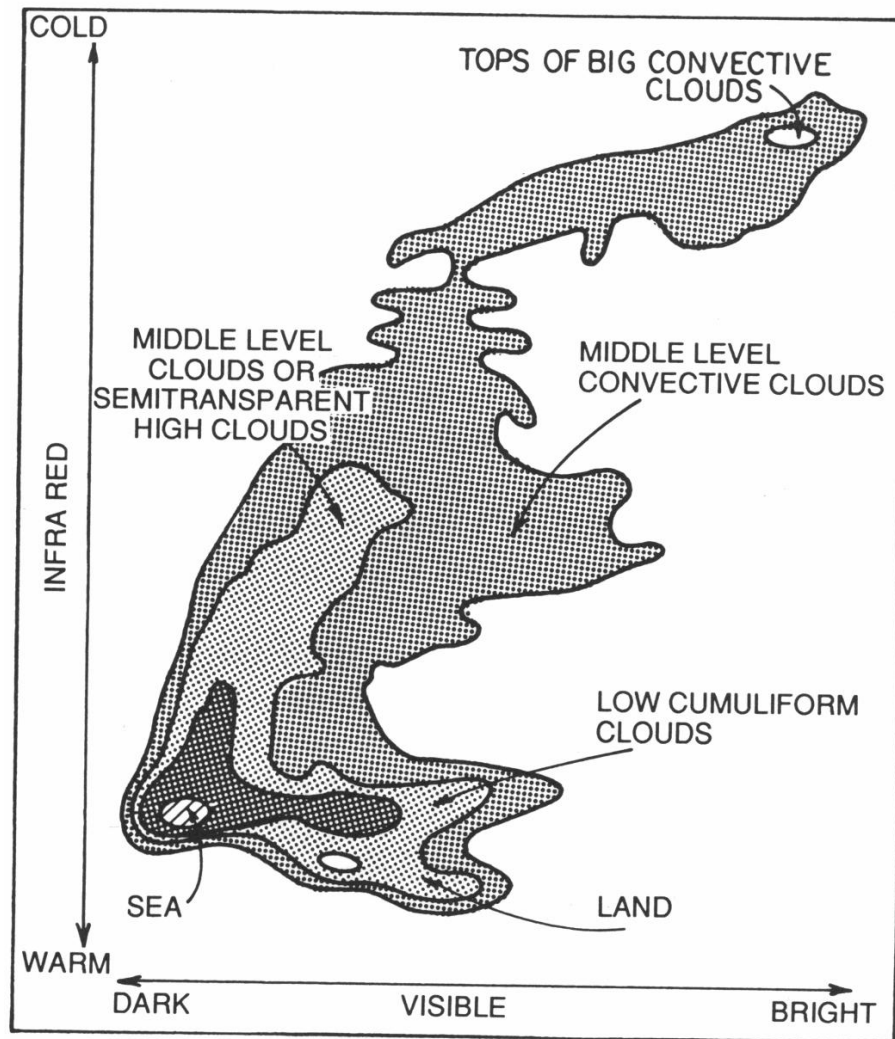


Use of Visible (2: Sato et al., 2006)

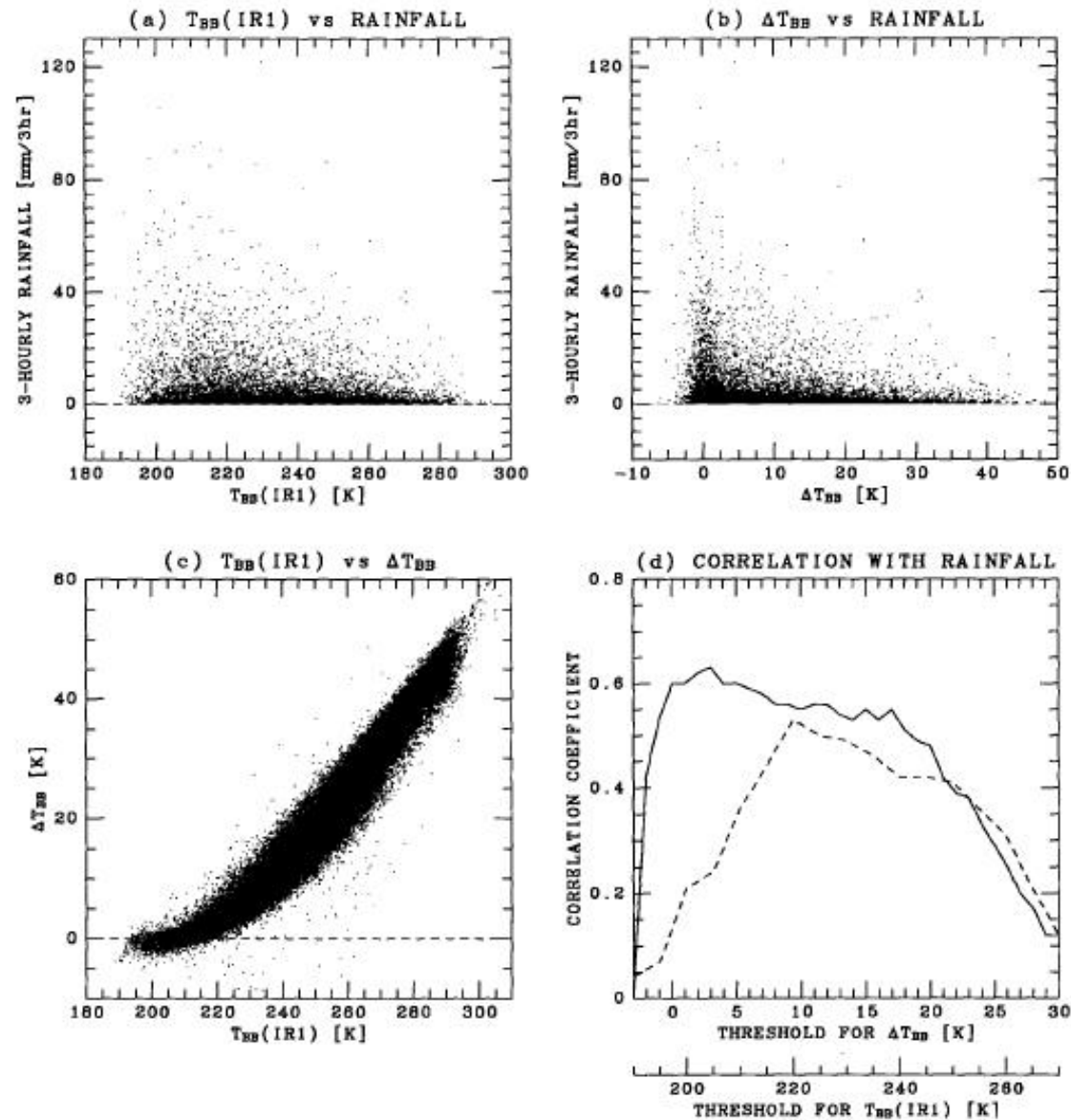
- Role of Vegetation and topography on Cloud Amount -



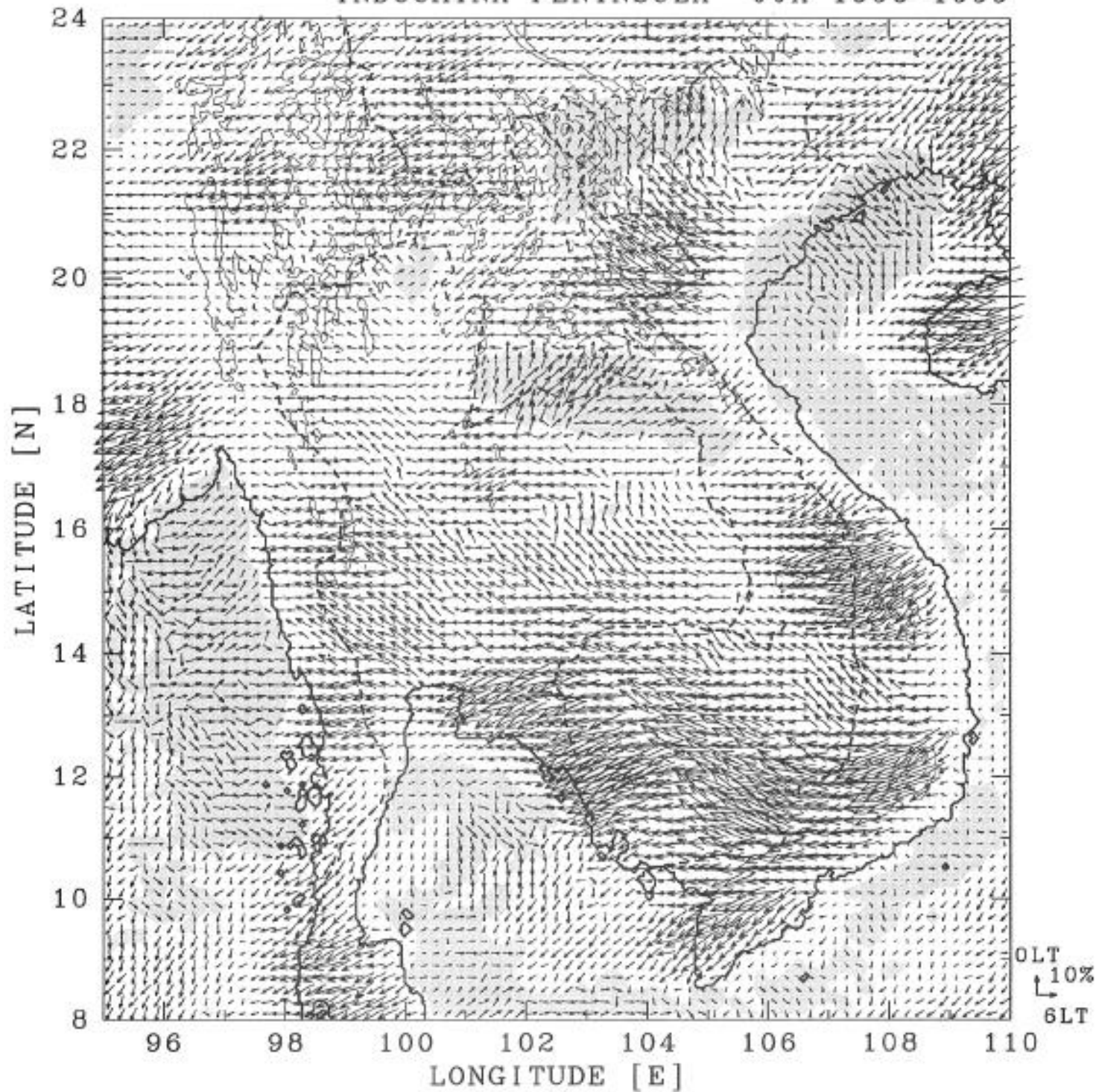
Combination Usage of Geo. Sat. Channels (visible, thermal-IRs, WV)



Example: Use of WV and thermal-IR (Ohsawa et al., 2001)

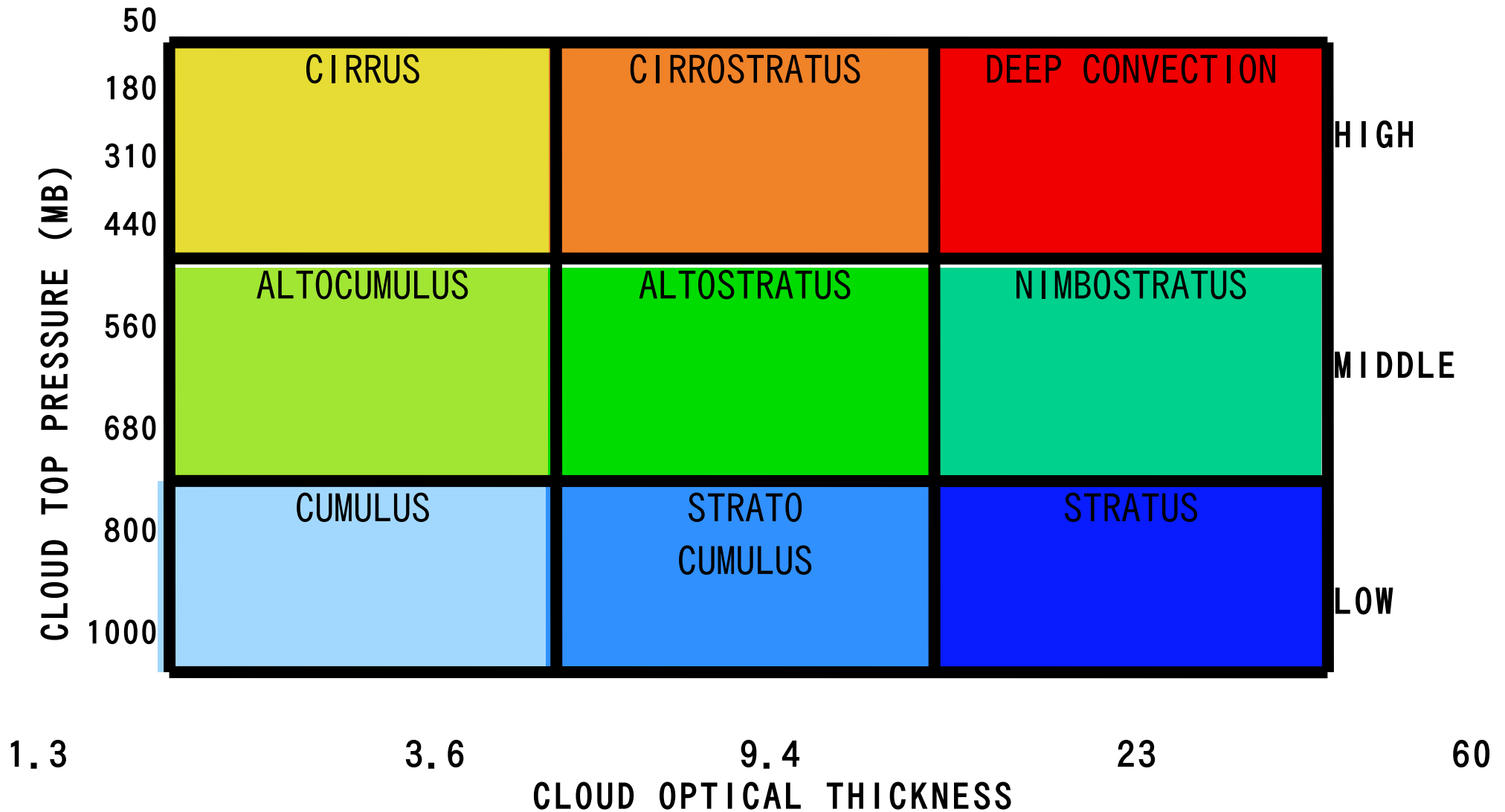


TIME OF MAXIMUM CONVECTIVE ACTIVITY
INDOCHINA PENINSULA JJA 1996-1999



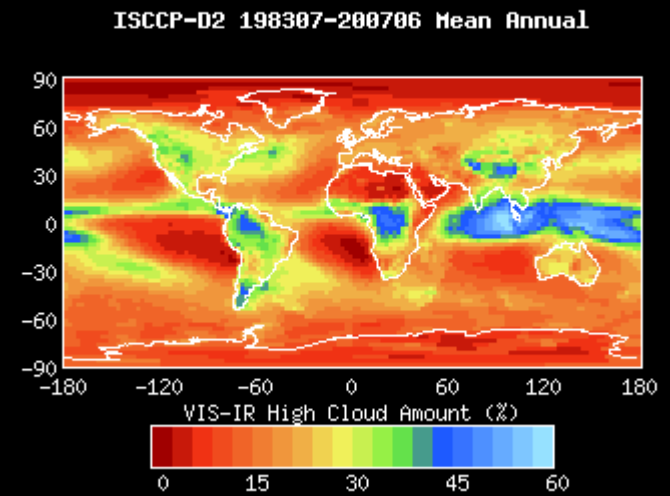
Cont.
(Ohsawa
et al.,
2001)

ISCCP CLOUD CLASSIFICATION

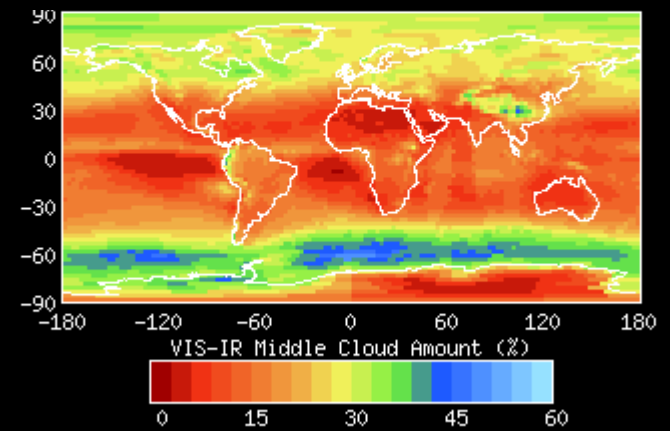


ISCCP-D2 1983-2007 mean annual

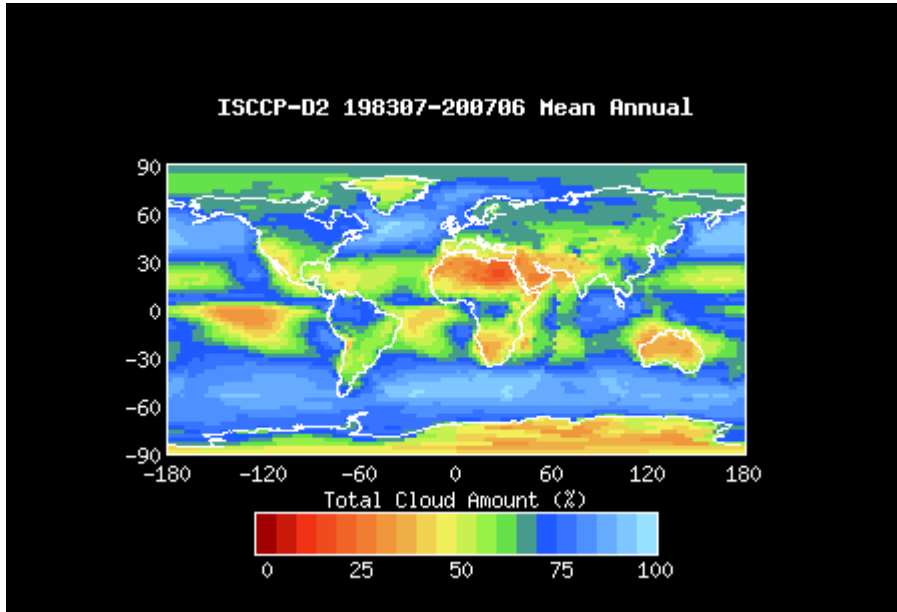
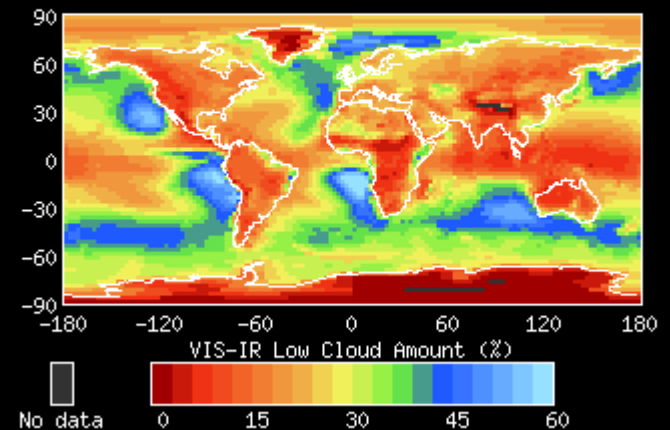
High



Middle



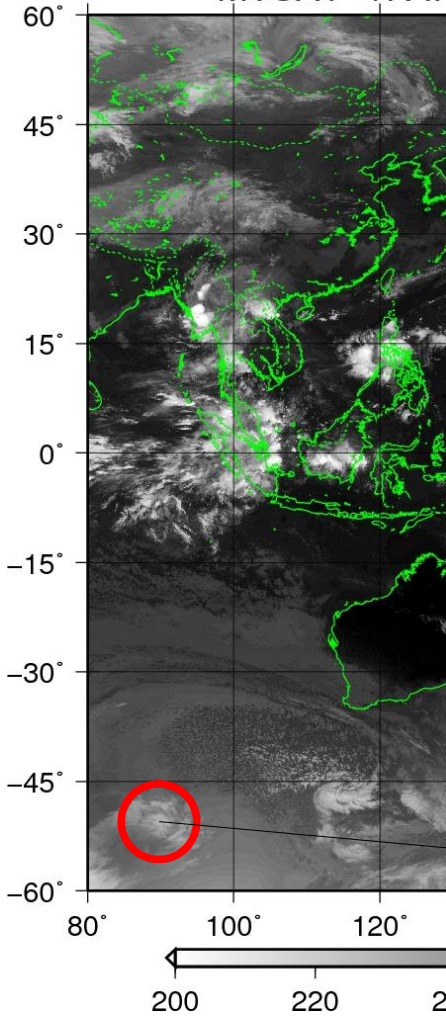
Low



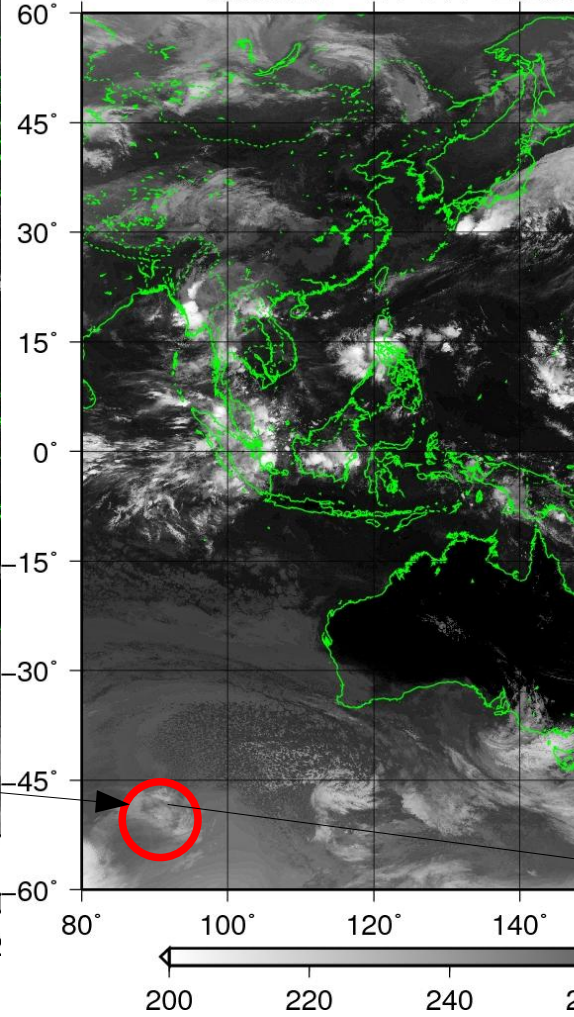
<http://isccp.giss.nasa.gov/products/onlineData.html>

Focus on time series (shape, tracking moving clouds)

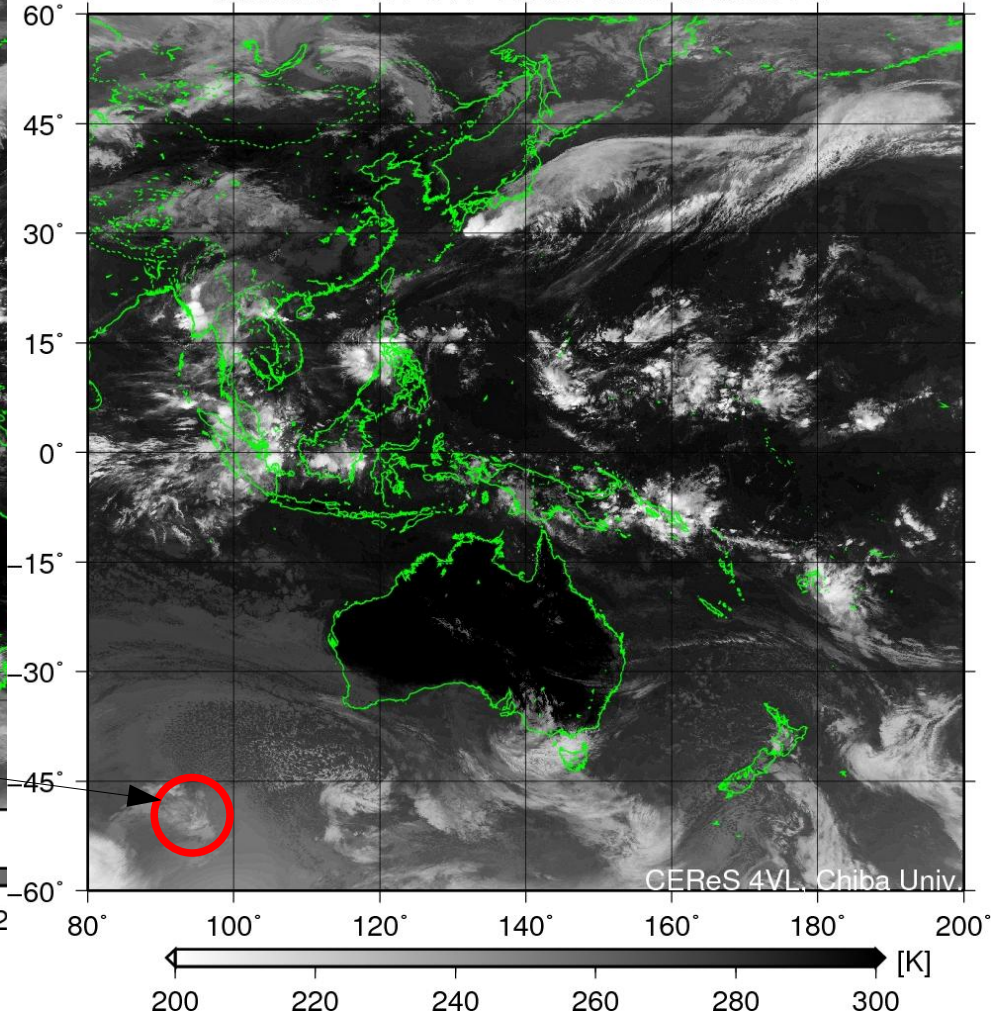
MTSAT-1R IR1 20081001 0030UTC

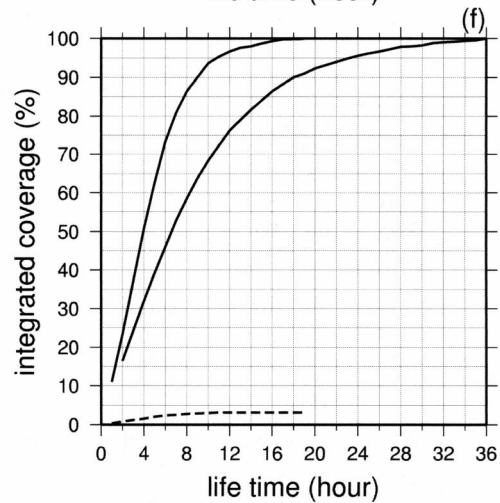
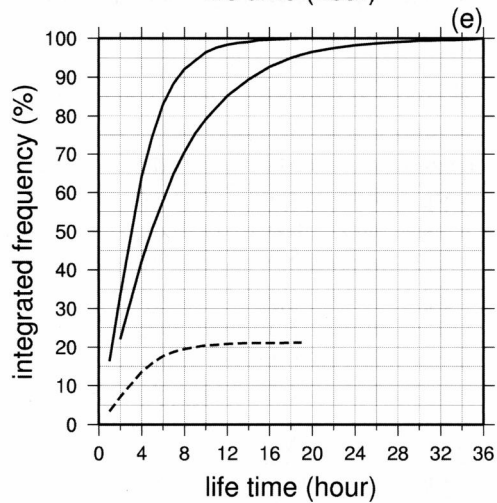
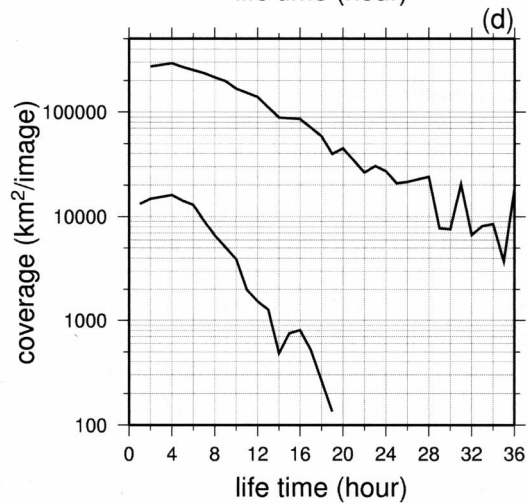
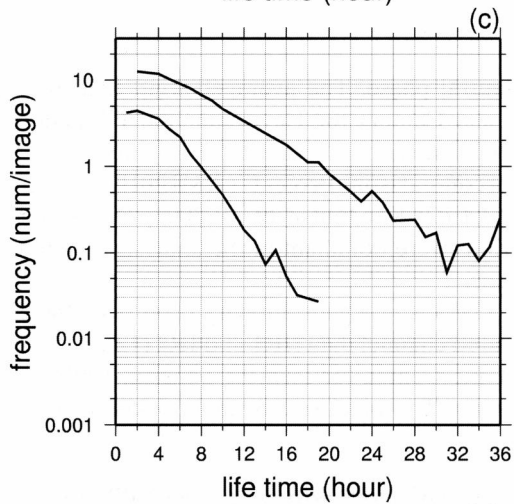
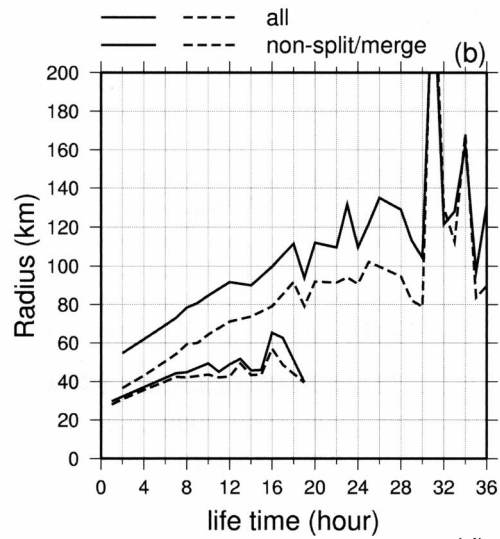
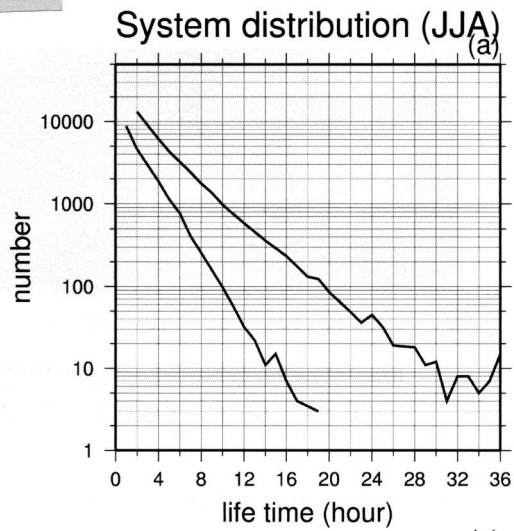


MTSAT-1R IR1 20081001 0130UTC



MTSAT-1R IR1 20081001 0230UTC

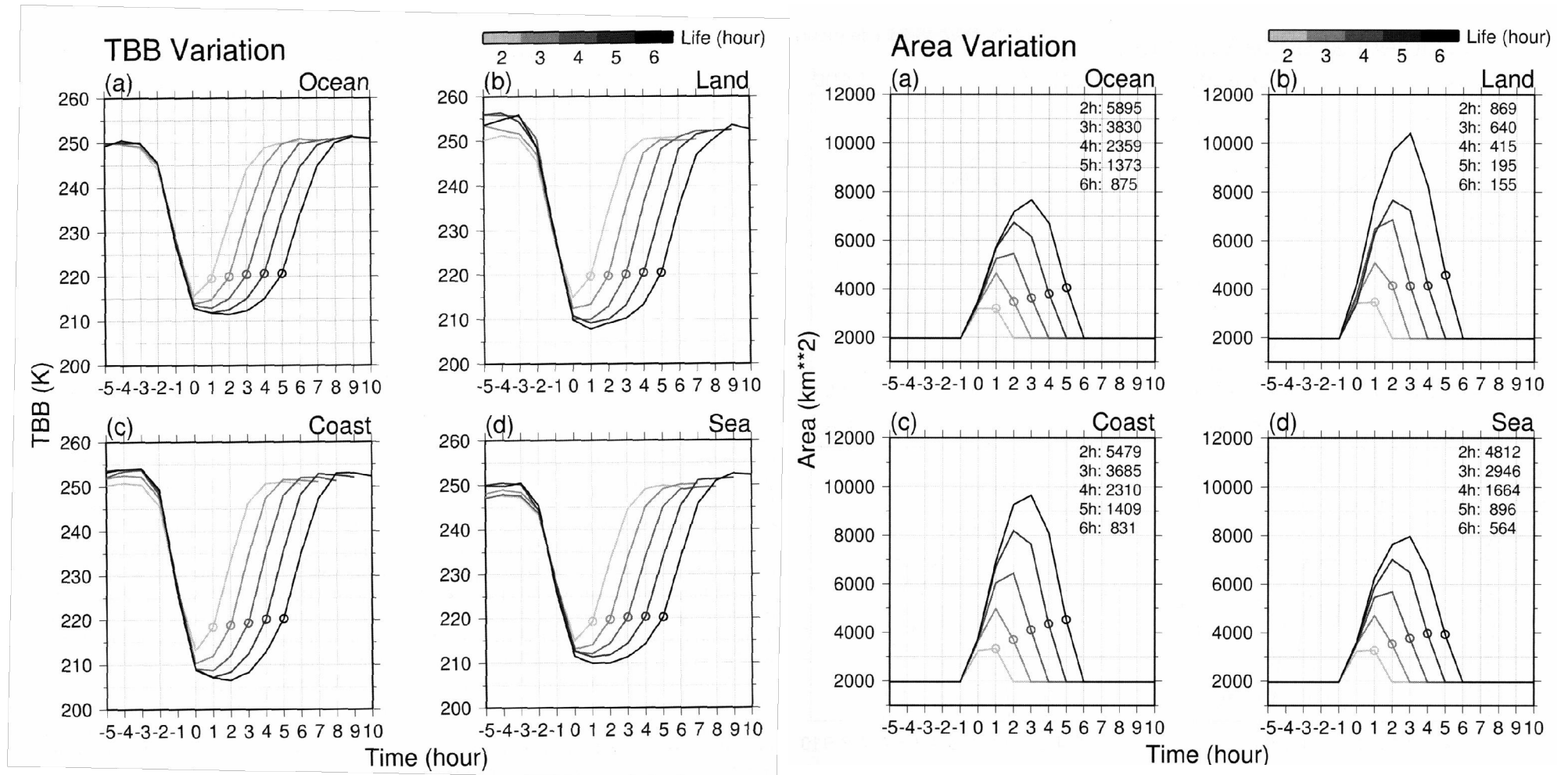




Example: Kondo et al., 2006

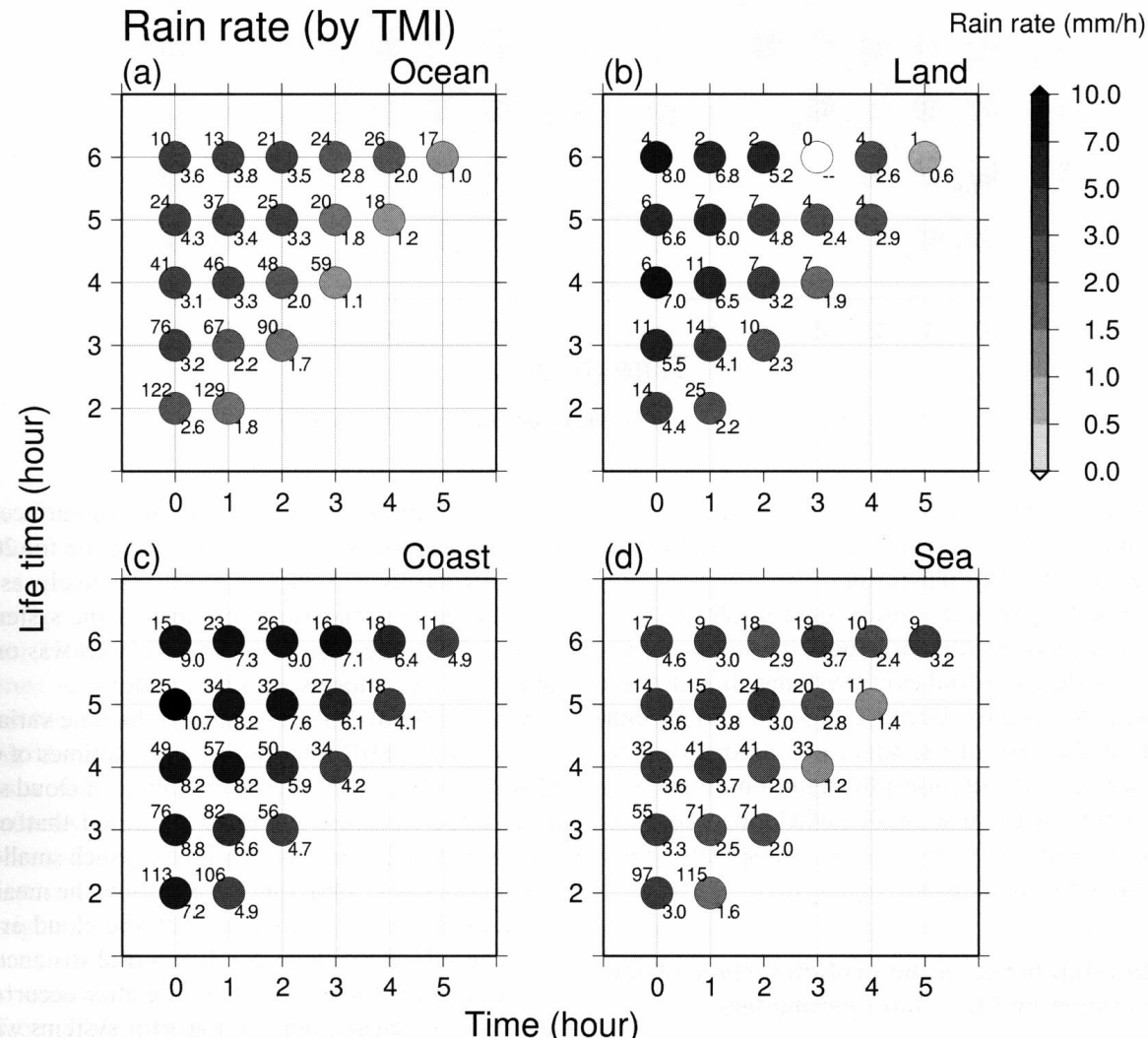
- Tracking statics
over Maritime
Continent -

(Count. Kondo et al., 2006)

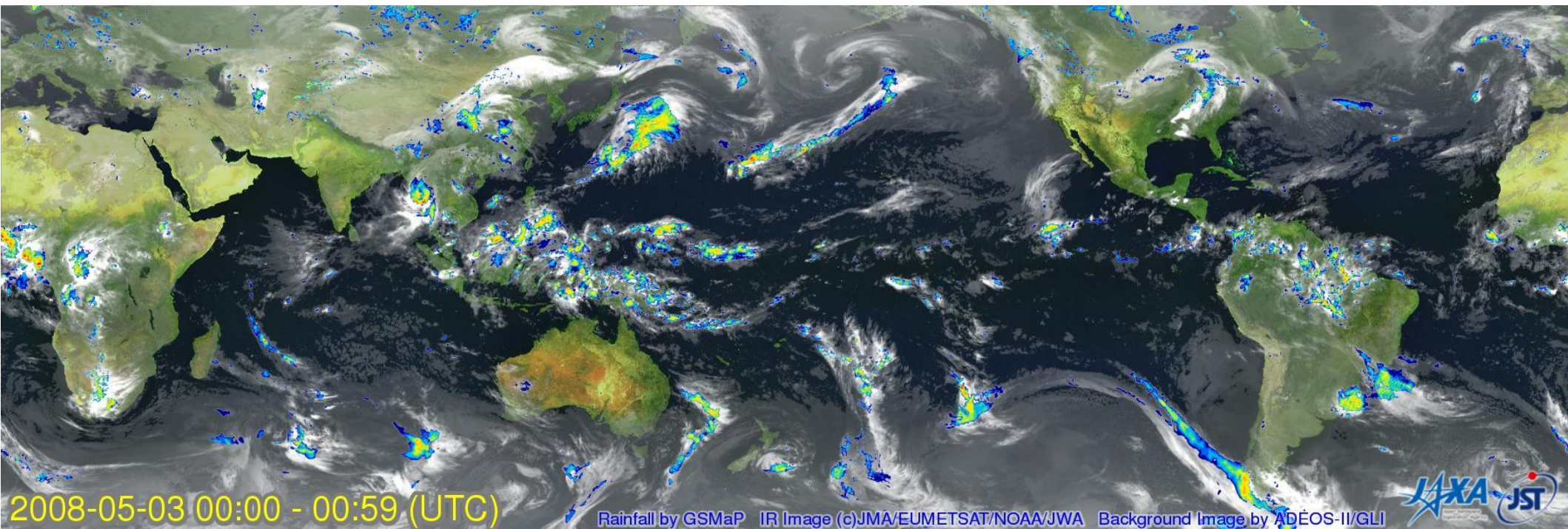


(Count. Kondo et al., 2006)

-Relation Life time vs rain rate by TRMM TMI -

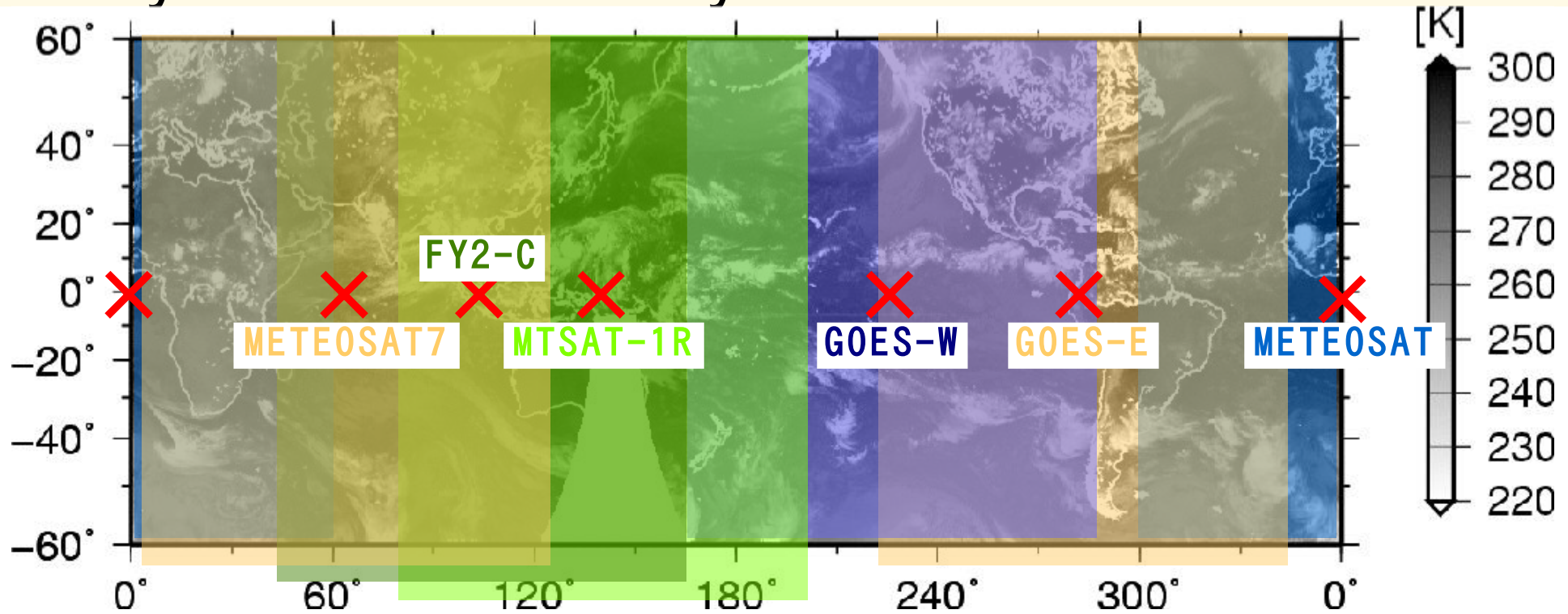
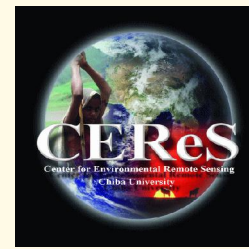


GSMaP (in detail, Lecture 10 by Prof. Ushio)



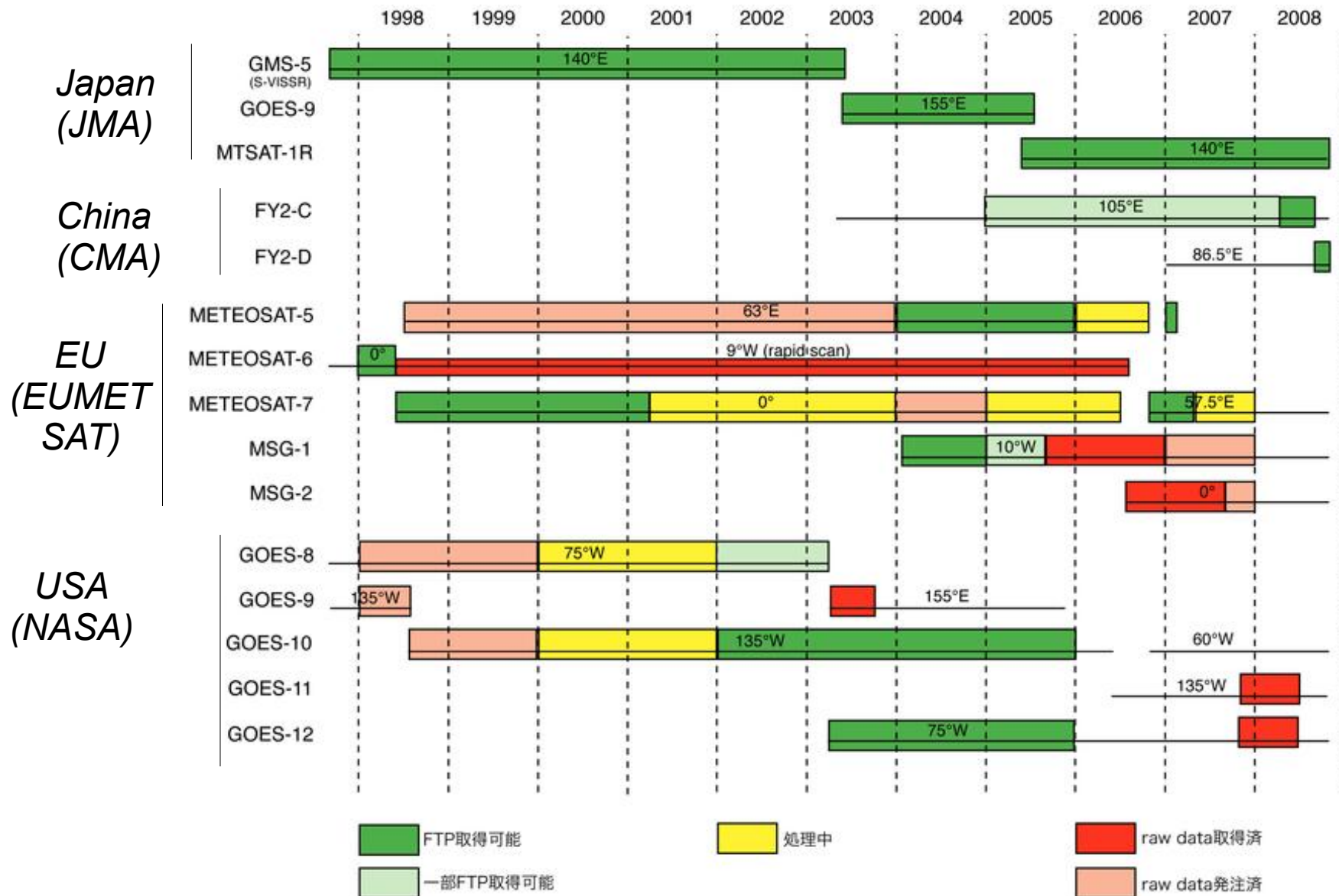
<http://sharaku.eorc.jaxa.jp/GSMaP/index.htm>

Global geostationary data by 4 Univ. VL activity

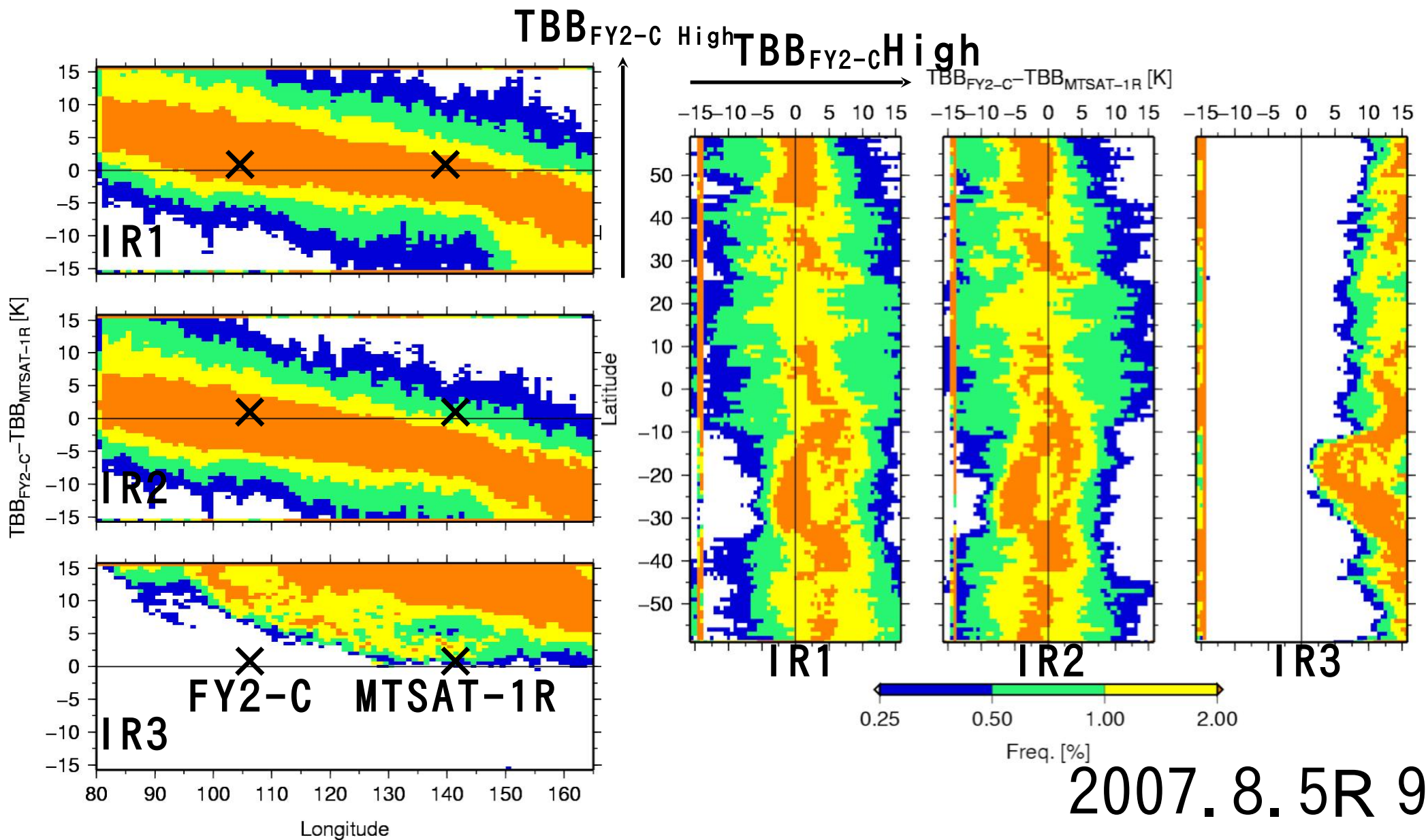


- *Under the formation of CCSR, HyARC, CAOS & CEReS (Virtual Labo.; VL), our team archive & publish “global” geostational satellite dataset.*
- *Not only IR, WV, VIS mid-IR channels dataset is target to archive & releasing (<http://www.cr.chiba-u.jp/~4vl/>)*

Operation Geo-Sat since 1998



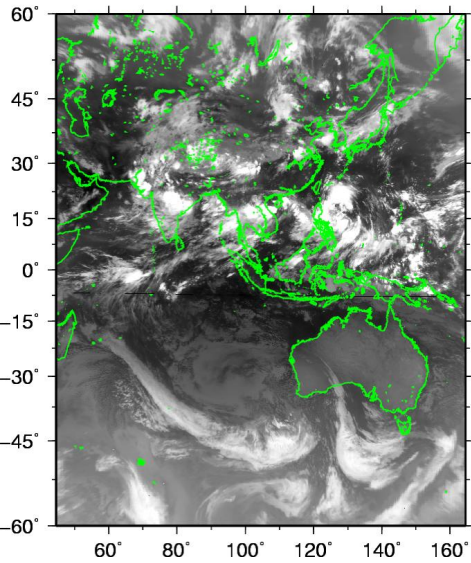
Inter-comparison of MTSAT-1R and FY-2C



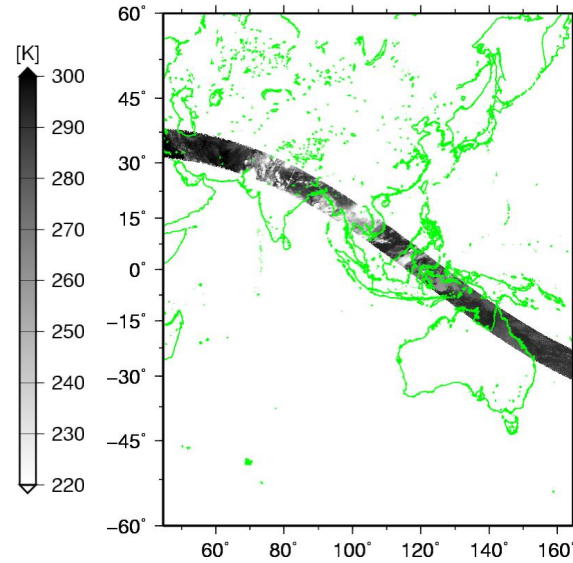
Comparison with TRMM VIRS

Yamamoto et al., 2007

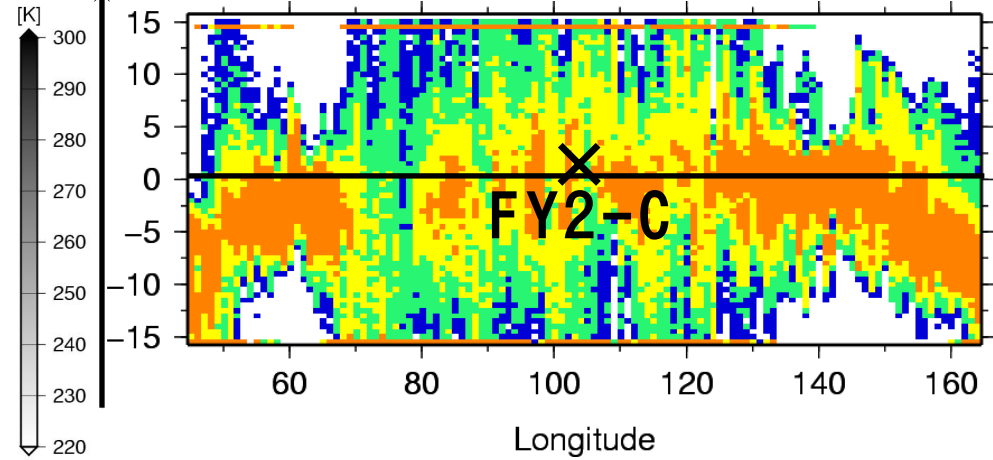
FY2-C: IR1 2007.08.06.17Z



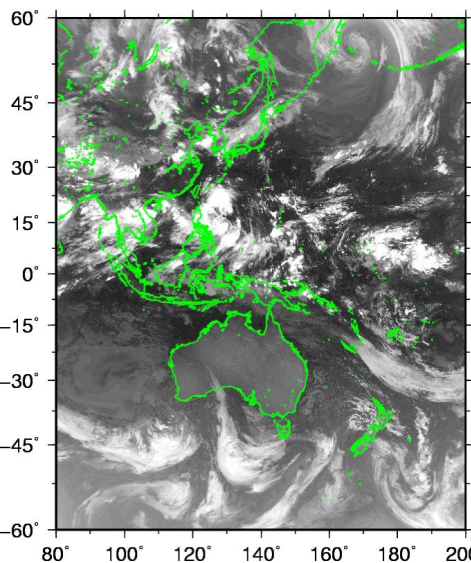
TRMM: CH4 2007.08.06.17:00



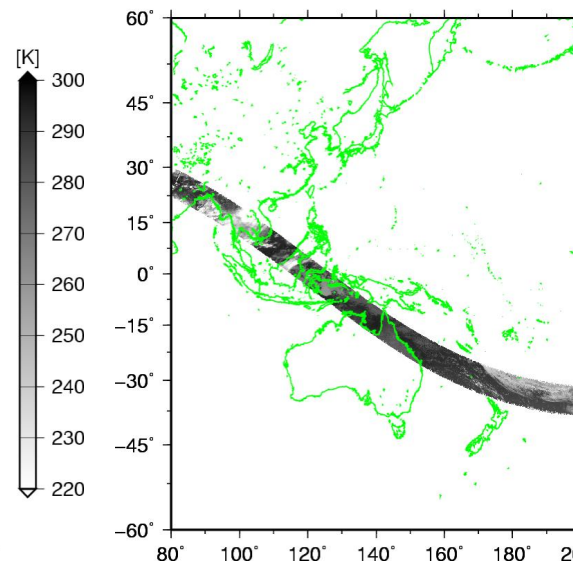
TBB_{FY2-C}^{High}



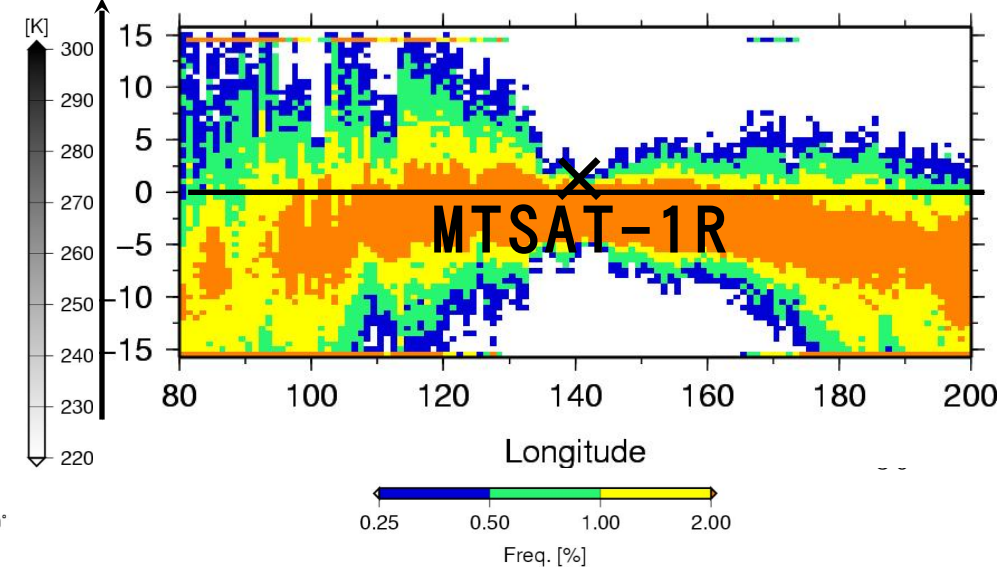
MTSAT-1R: IR1 2007.08.06.17Z



TRMM: CH4 2007.08.06.17:30Z



$TBB_{MTSAT-1R}^{High}$



GSICS

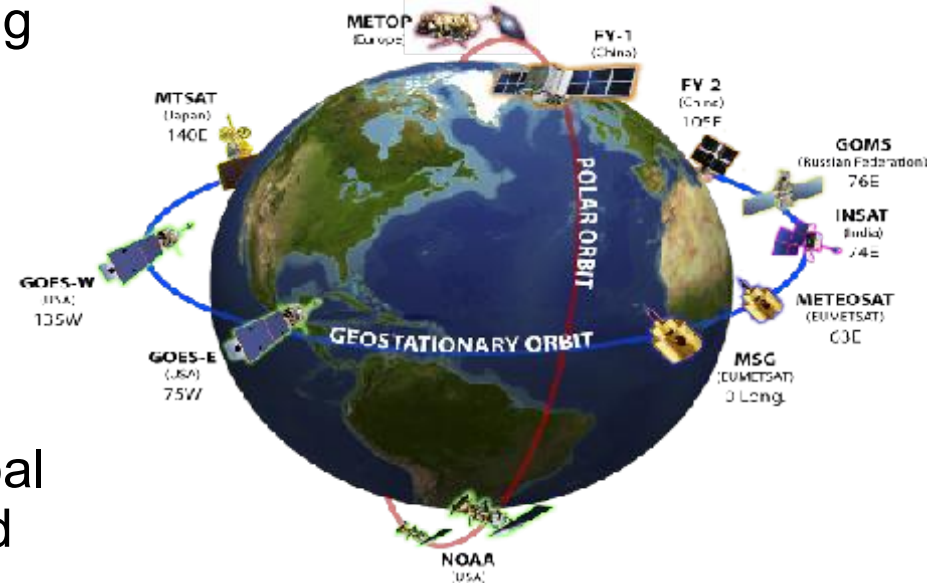
(Global Space-based Inter-Calibration System)

- Mission

- Assure high-quality, inter-calibrated measurements from the international constellation of operational satellites to support the GEOSS goal of increasing the accuracy and interoperability of environmental products and applications for societal benefit.

- Goals

- The primary goal of GSICS is to improve the use of space-based global observations for weather, climate and environmental applications through operational inter-calibration of the space component of the WMO World Weather Watch (WWW) Global Observing System (GOS) and Global Earth Observing System of Systems (GEOSS).



<http://www.star.nesdis.noaa.gov/smcd/spb/calibration/icvs/GSICS/>

(Hopefully) Useful Website

- JMA MTSAT: <http://www.jma.go.jp/en/gms/>
- GOES: <http://www.goes.noaa.gov/>
- EUMETSAT: <http://www.eumetsat.int/>
- CEReS VL website (most of them; in Japanese)
 - <http://www.cr.chiba-u.jp/~4vl/wiki/wiki.cgi>
 - MTSAT ftp: <ftp://mtsat-1r.cr.chiba-u.ac.jp/grid-MTSAT-1.01/>
 - FY-2X ftp: <ftp://fy.cr.chiba-u.ac.jp/disk1/grided/>
 - GOES-E, W ftp: <ftp://goes.cr.chiba-u.ac.jp/goes-e> (or -w) /grid-GOES-1.0/
- MTSAT at Kochi University: <http://weather.is.kochi-u.ac.jp/>
- Digital Typhoon: <http://agora.ex.nii.ac.jp/digital-typhoon/>
- ISCCP: <http://isccp.giss.nasa.gov/>
- GSICS: <http://www.star.nesdis.noaa.gov/smcd/spb/calibration/icvs/GSICS/>

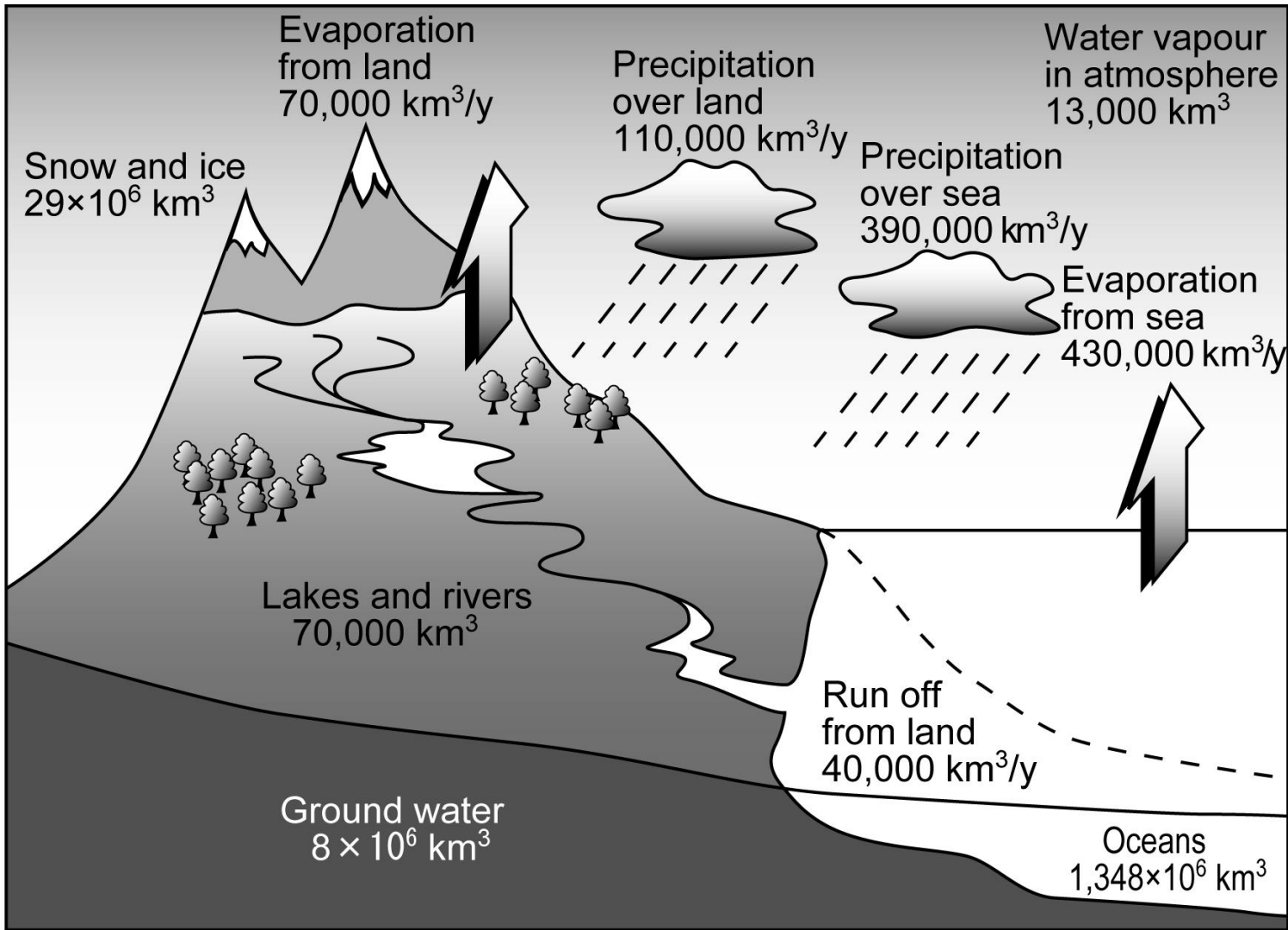
References

- Fujinami and Yasunari, JMSJ, 79, 1207-1227, 2001.
- Kato, 2006, Graduate Thesis, Chiba University
- Kato, 2008, Master Thesis, Chiba University
- Kurosaki and Kimura, JMSJ, 80, 1339-1355, 2002.
- Ohsawa et al., JMSJ, 79, 333-352, 2001.
- Kondo et al., MWR, 134, 1581-1599, 2006.
- Kidder and Haar, *Satellite Meteorology*, Academic Press, 466p, 1995.
- Sato et al., JGR, 112, D24109, doi:10.1029/2006JD008129, 2007.

Tropical Rainfall Measuring Mission (TRMM)

Kenji Nakamura
Hydrospheric Atmospheric Research Center
Nagoya University

The Eighteenth IHP Training Course
Nov. 11 (Tue) 2008



The amount of water

(Reference : ENCYCLOPEDIA of HYDROLOGY AND WATER RESORCES, 1998)

(b) SSMI LATENT HEAT FLUX (W/m2)**

AUG 1993

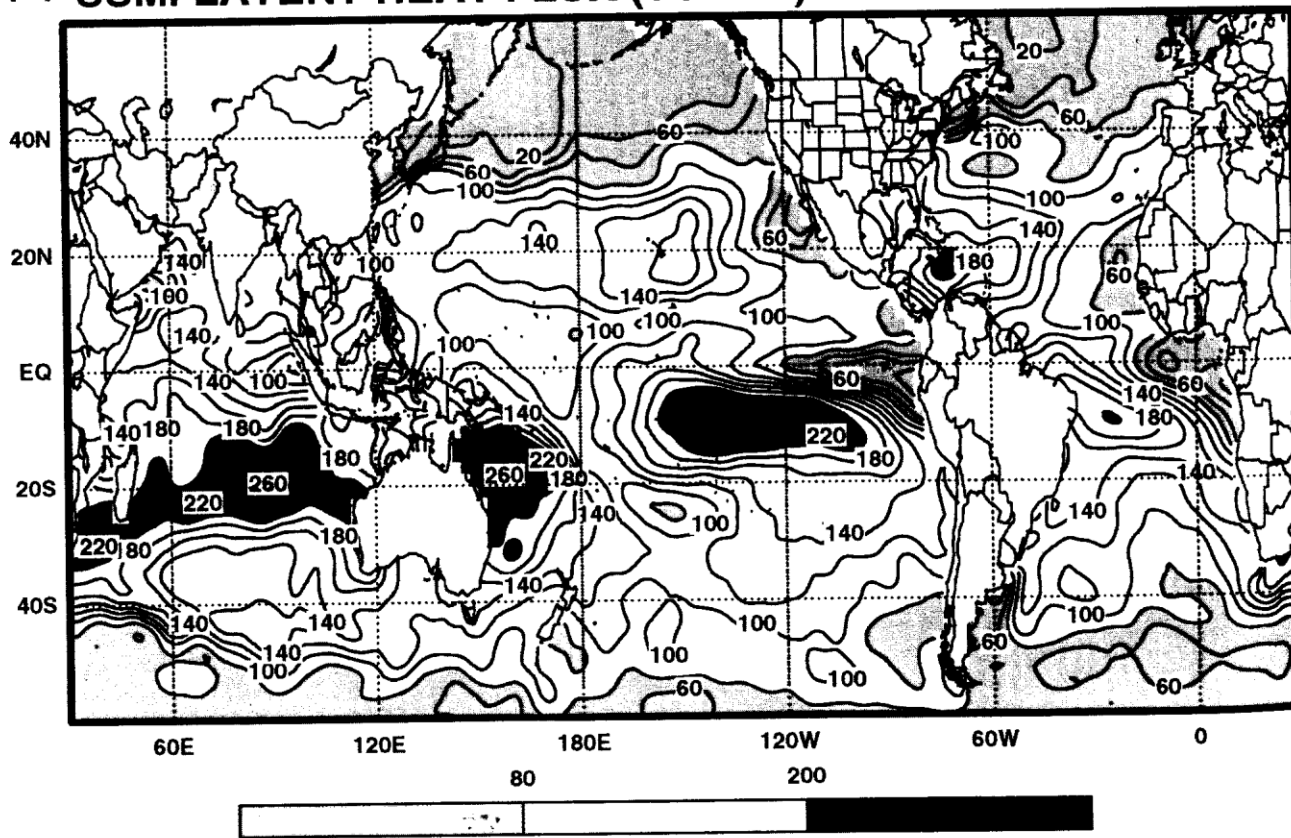


Figure 10. Monthly averages of daily SSM/I latent heat fluxes for (a) February and (b) August 1993. Daily flux is computed from daily values of SSM/I wind speed [Wentz, 1994], EOF-retrieved SSM/I surface humidity, NCEP SST, and SST minus 2-m temperature of ECMWF.

☒5(a)

Chou et al. JGR 1997

(b) SSMI SENSIBLE HEAT FLUX (W/m**2) AUG 1993

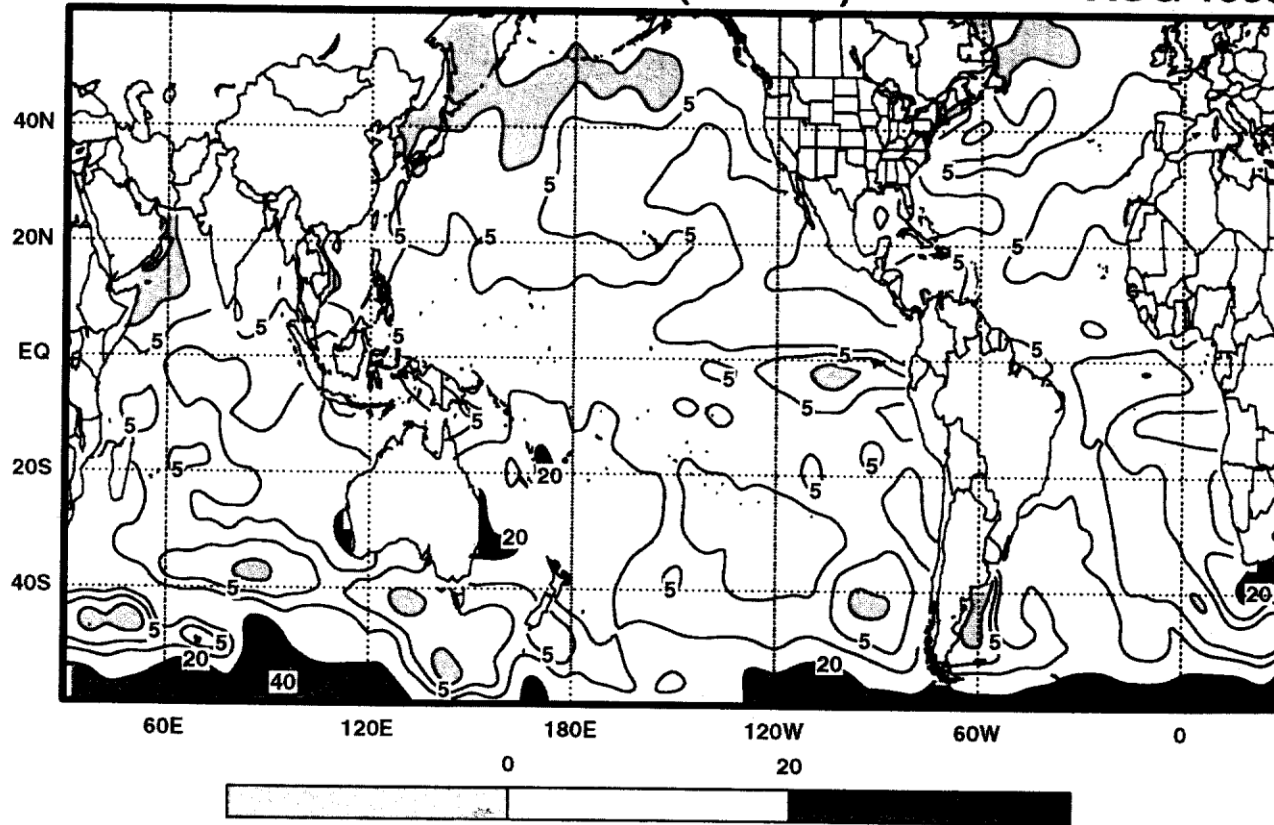


Figure 12. Monthly averages of daily SSM/I sensible heat fluxes for (a) February and (b) August 1993. Daily flux is computed from daily values of SSM/I wind speed [Wentz, 1994], EOF-retrieved SSM/I surface humidity, NCEP SST, and SST minus 2-m temperature of ECMWF.

図5(b) 顕熱フラックスの分布

Chou et al. JGR 1997

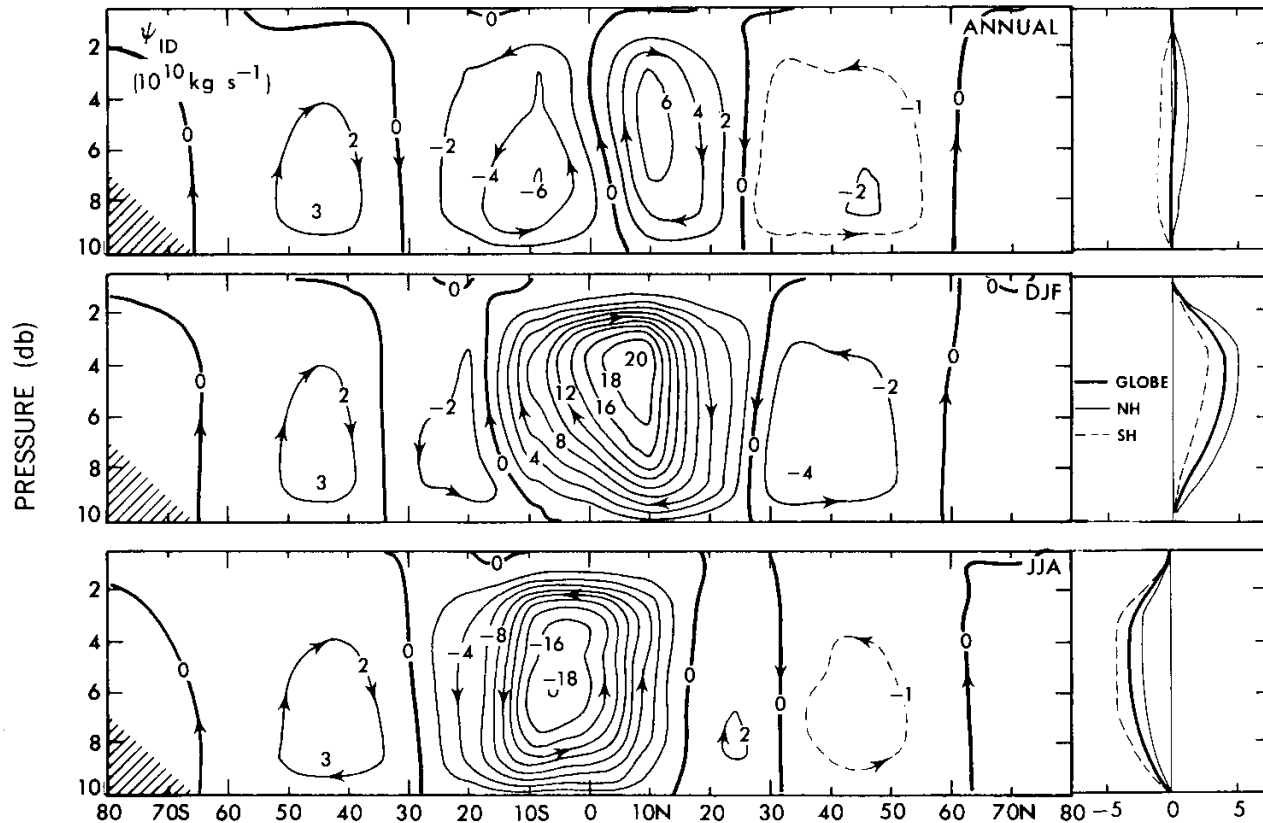


FIGURE 7.19. Zonal-mean cross sections of the mass stream function in $10^{10} \text{ kg s}^{-1}$ for annual, DJF, and JJA mean conditions. Vertical profiles of the hemispheric and global mean values are shown on the right.

Meridional circulation of the atmosphere (Peixoto and Oort, 1991)

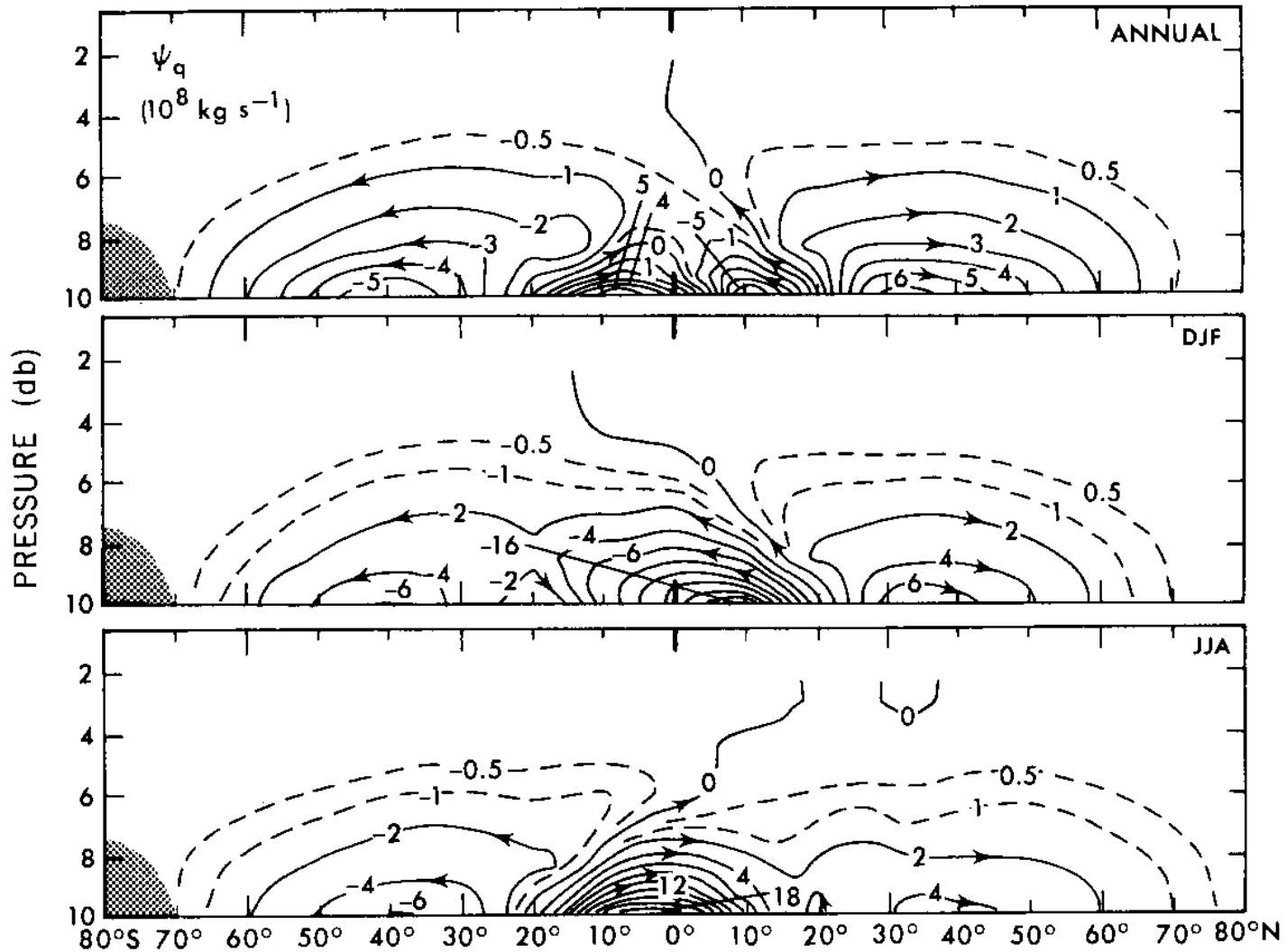


FIGURE 12.18. Streamlines of the zonal-mean transport of water vapor for annual, DJF, and JJA mean conditions in 10^8 kg s^{-1} (from Peixoto and Oort, 1983).

Meridional circulation of water vapor (Peixoto and Oort, 1991)

Zonal Mean Precipitation

1979–2001 Climatology

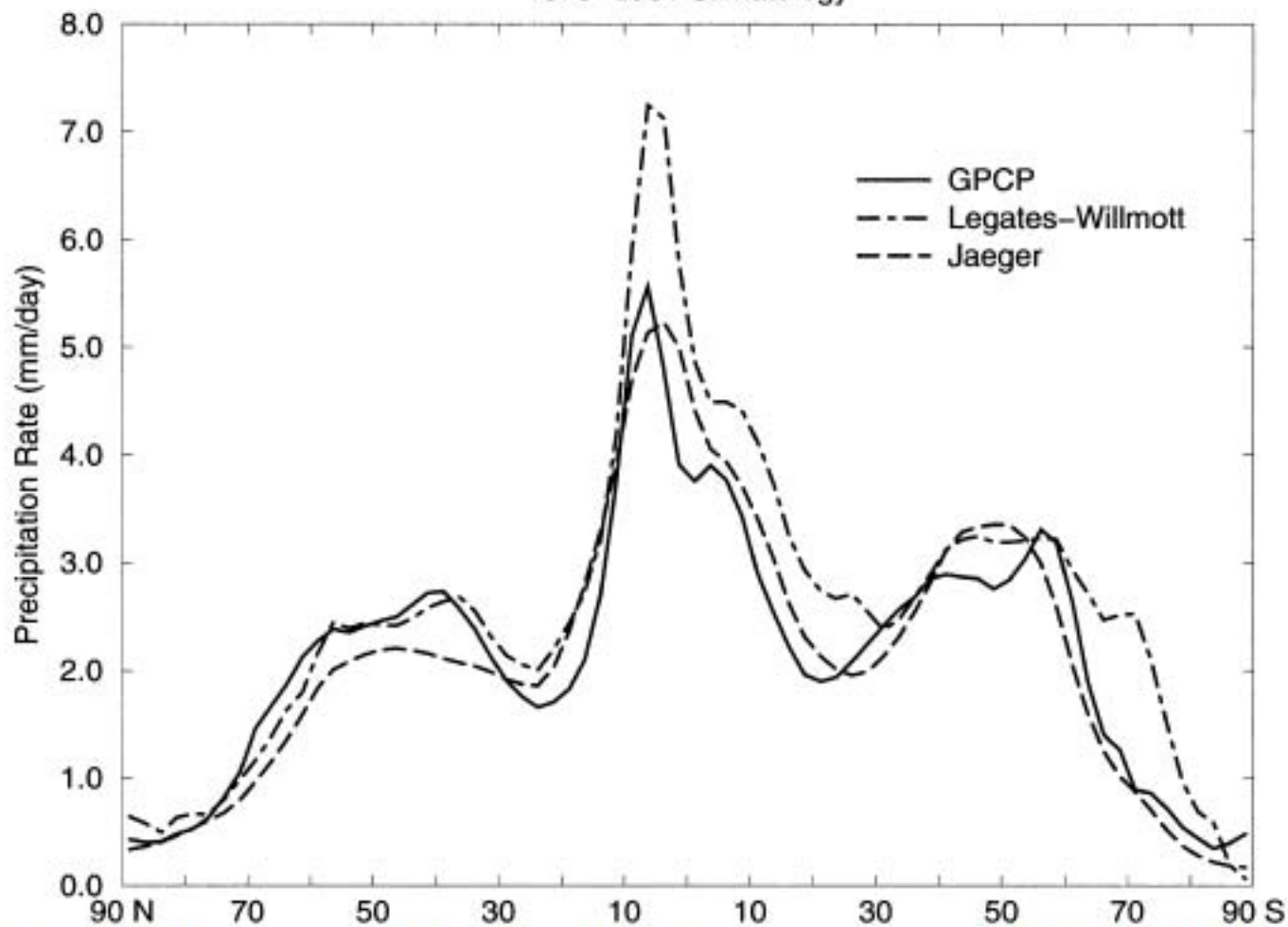


FIG. 5. Zonally averaged annual mean climatologies of precipitation (mm day^{-1}): the GPCP (solid line, see Fig. 4), Legates and Willmott (1990) (dot-dashed line), and Jaeger (1976) (long-dashed line).

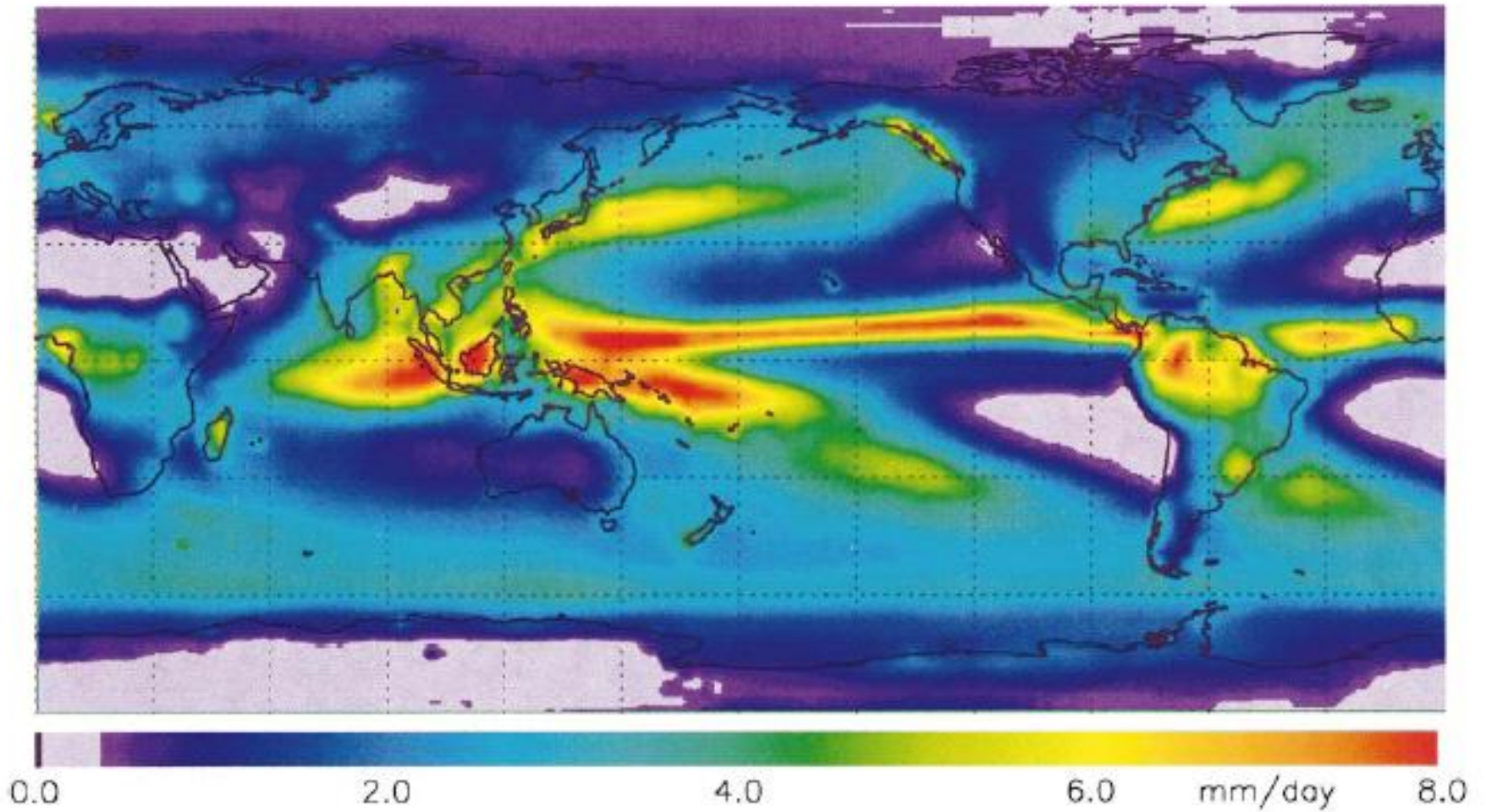


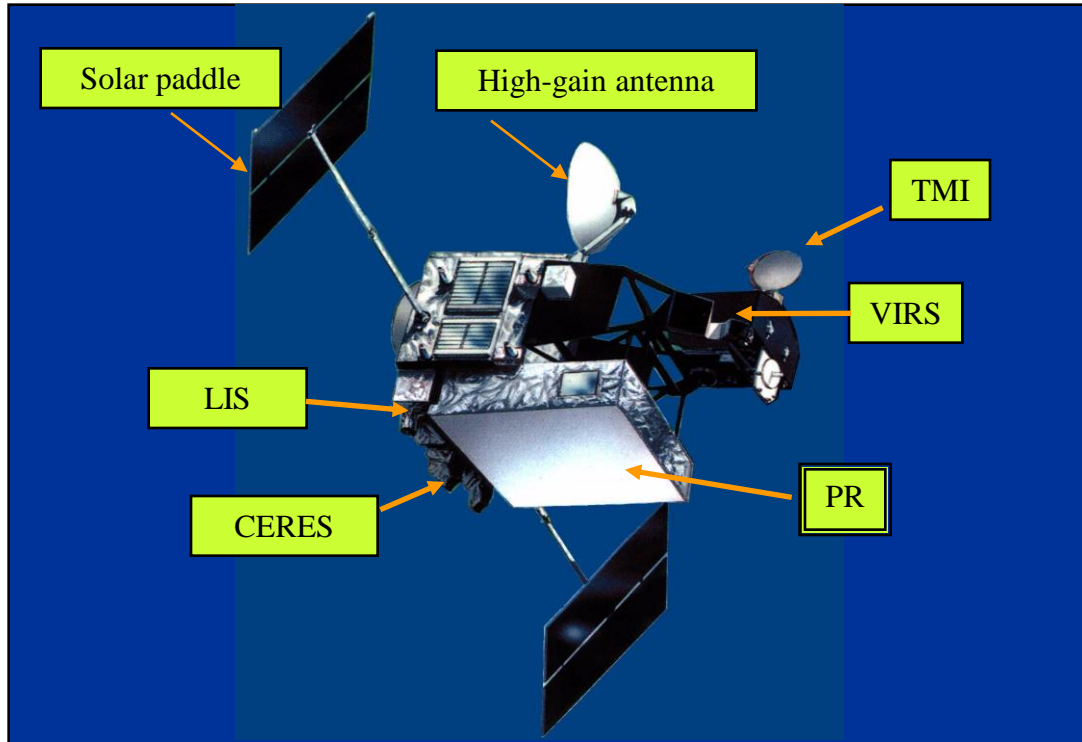
FIG. 4. The 23-yr (1979–2001) annual mean precipitation (mm day^{-1}).

(Adler et al., 2003)

図6 世界の降水の気候値



Tropical Rainfall Measuring Mission: TRMM



Observation of tropical rainfall (Driving engine of global atmosphere)

US-Japan joint mission (Japan: PR, Launch, US: Bus, 4 sensors, operation)

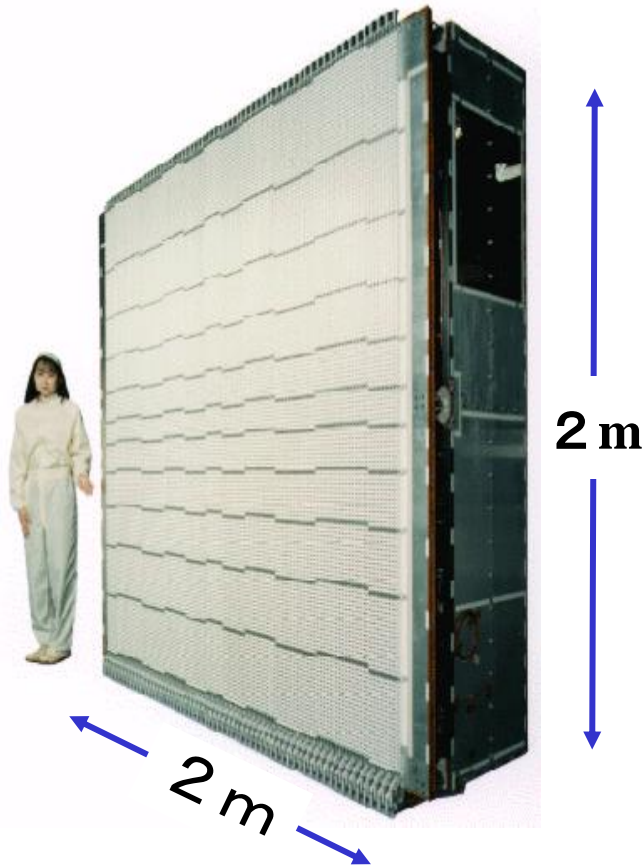
Launched in Nov., 1997. Still under operation

First space-borne precipitation radar developed by CRL and NASDA

Orbit	Circular (Non-Sun Synchronous)
Altitude	350km (402.5km since Aug. 2001) (± 1.25 km)
Inclination	35 deg.
Sensor	Precipitation Radar (PR) TRMM Microwave Imager (TMI) Visible and Infrared Scanner (VIRS) Clouds and the Earth's Radiation Energy System (CERES) Lightning (LIS)



TRMM Precipitation Radar



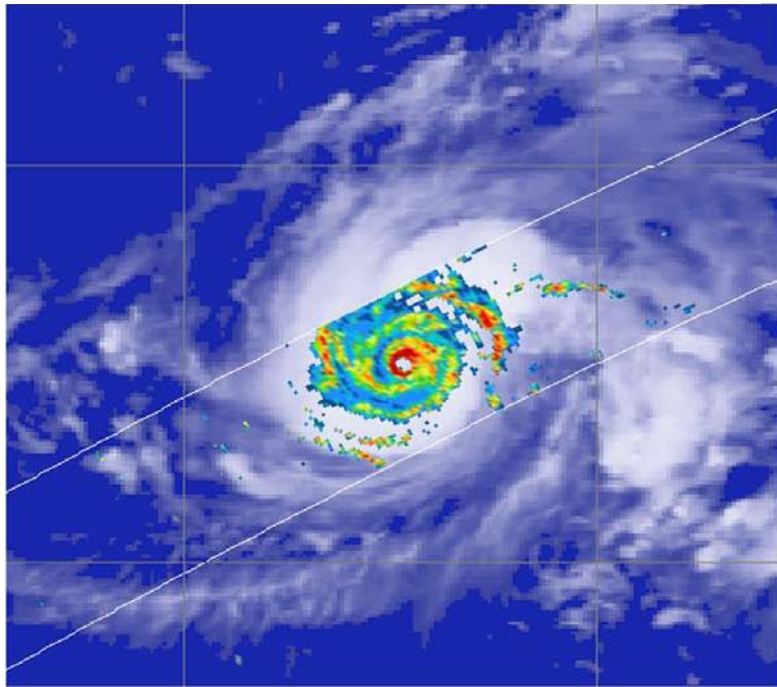
Radar type	Pulse radar
Antenna type	128-elem. WG slot array
Beam scanning	Active phased array
Frequency	13.796, 13.802 GHz
Polarization	Horizontal
TX/RX pulse width	1.57 / 1.67 μ sec
RX band width	0.6 MHz
Pulse rep. freq.	2776 Hz
Data rate	93.5 kbps
Mass	460 kg
Designed Life time	3 years
Sensitivity	< 0.5mm/h
Horizontal resolution	4.3 km (nadir)
Range resolution	250 m
# of indpdt samples	64 (fading noise < 0.7 dB)
Swath width	215km
Observable range	Surface to 15km

3-D Observation of a Typhoon by TRMM

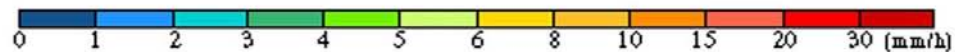
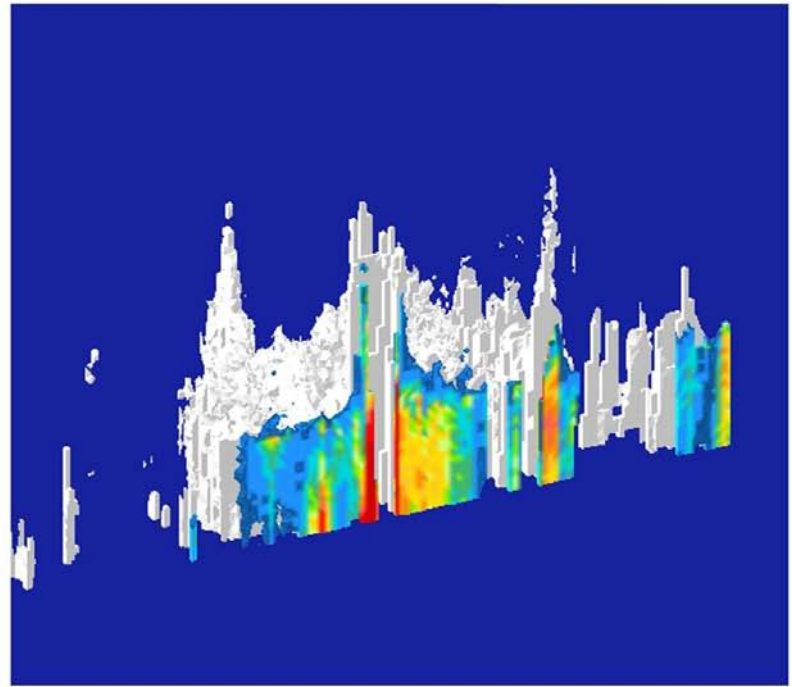
TRMM PR 2A25 Rain

Aug. 2, 2000, 20:49-20:53 (Japanese local time)

Rain intensity at H=2 km



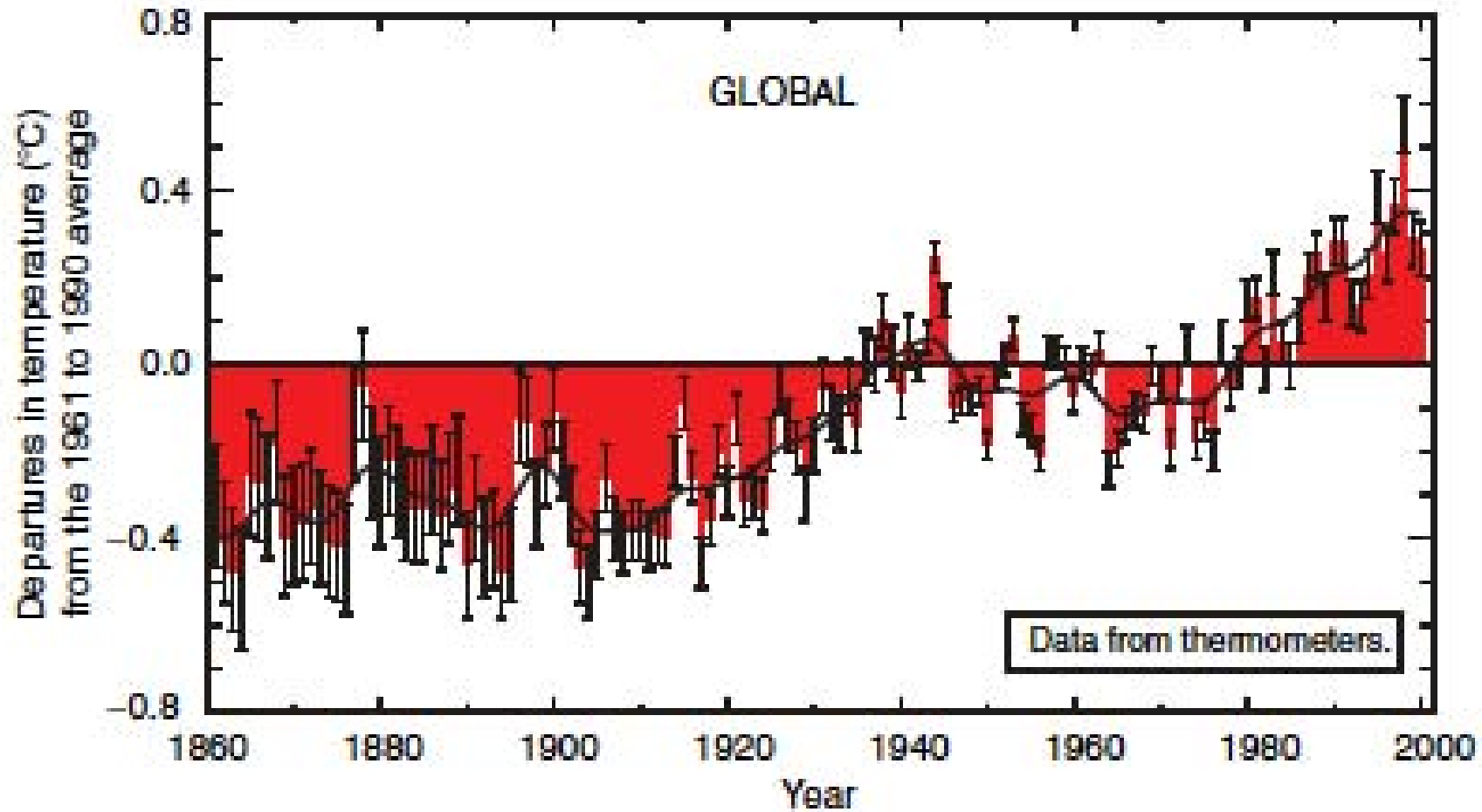
Vertical cross section through the eye and 3D structure



PR realized observation of 3D structure of rain over ocean where few observations had been available.

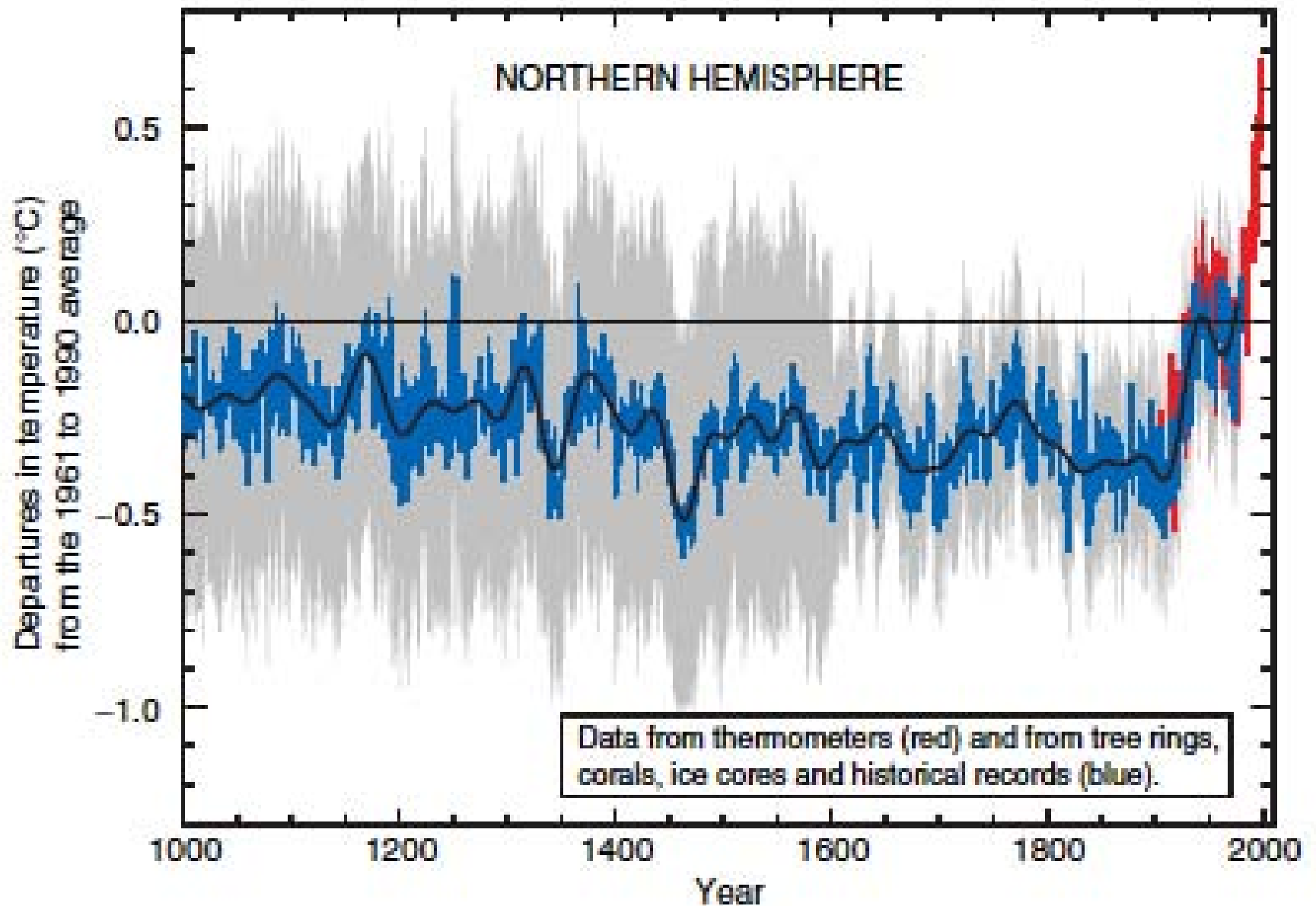
Variations of the Earth's surface temperature for:

(a) the past 140 years



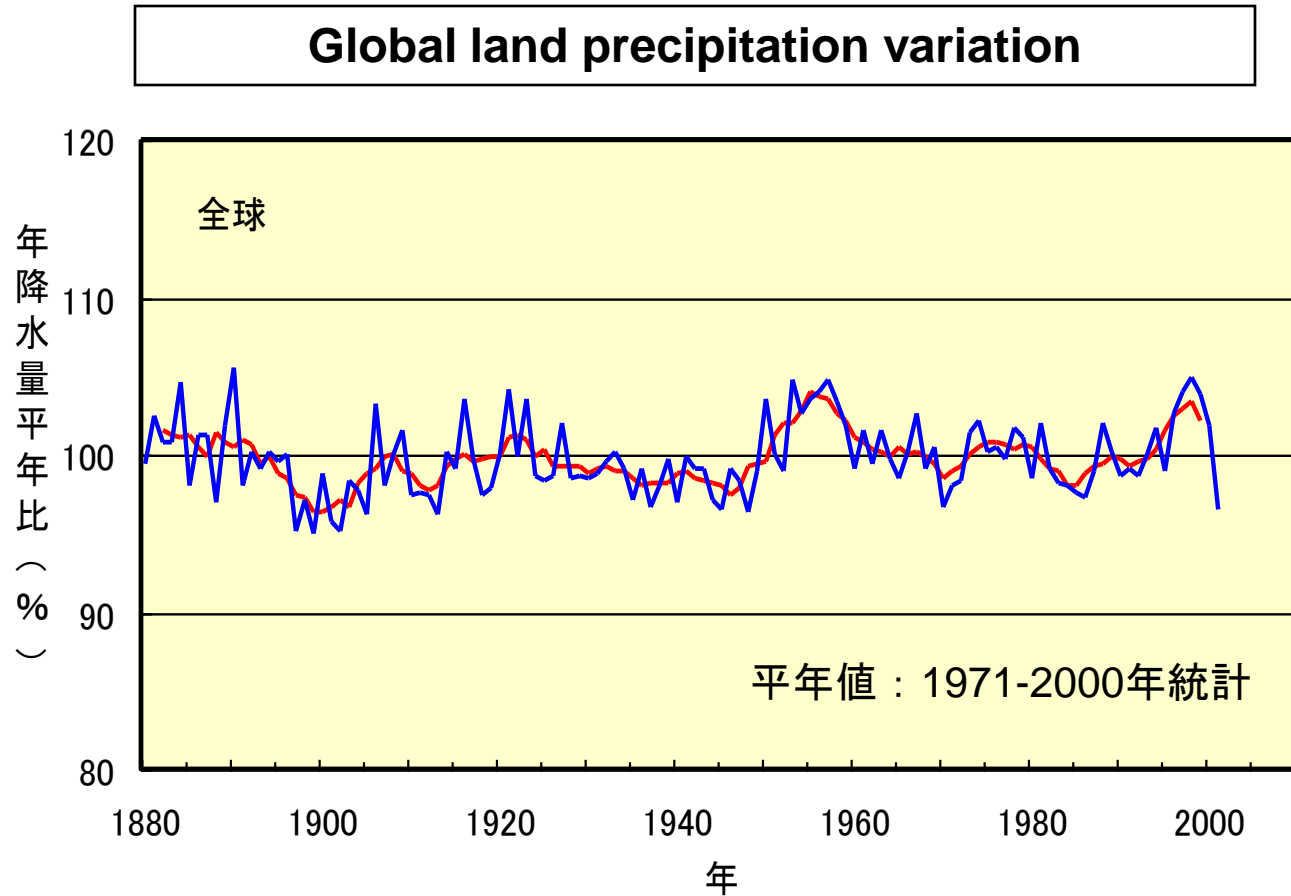
(IPCC3)

(b) the past 1,000 years



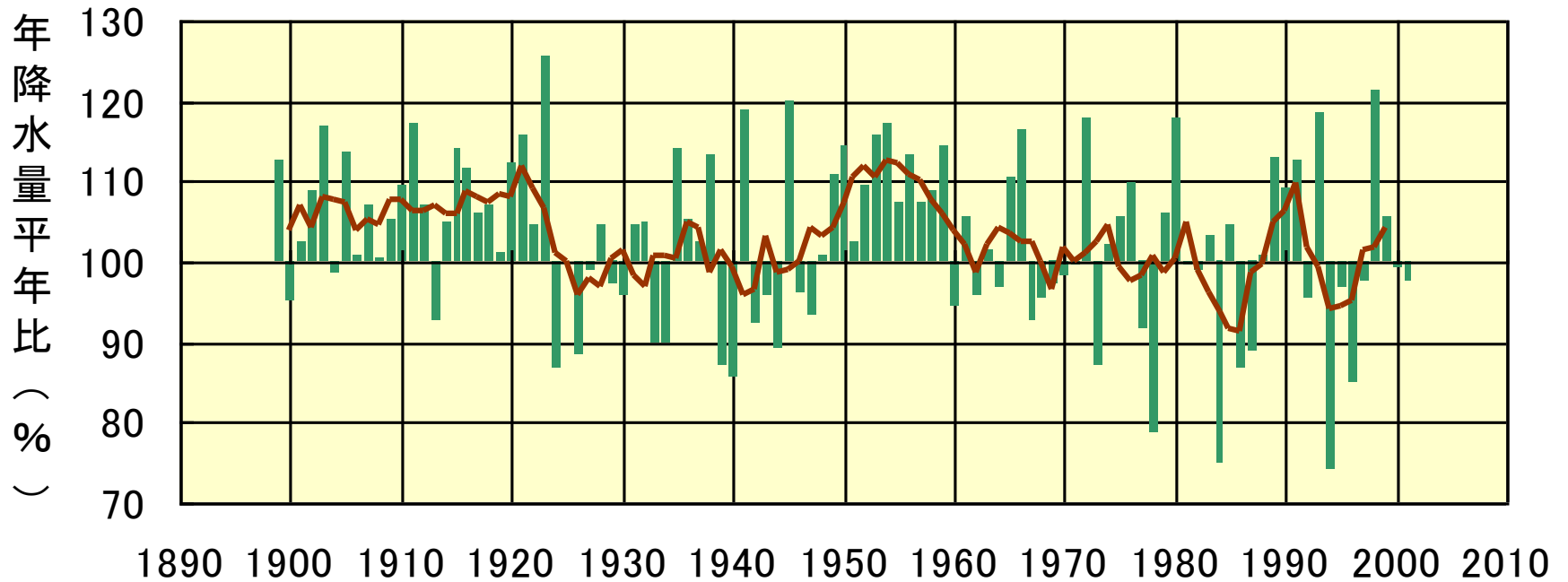
(IPCC3)

- Precipitation over land increased by about 2 % in the 20 th century, but with large variations.



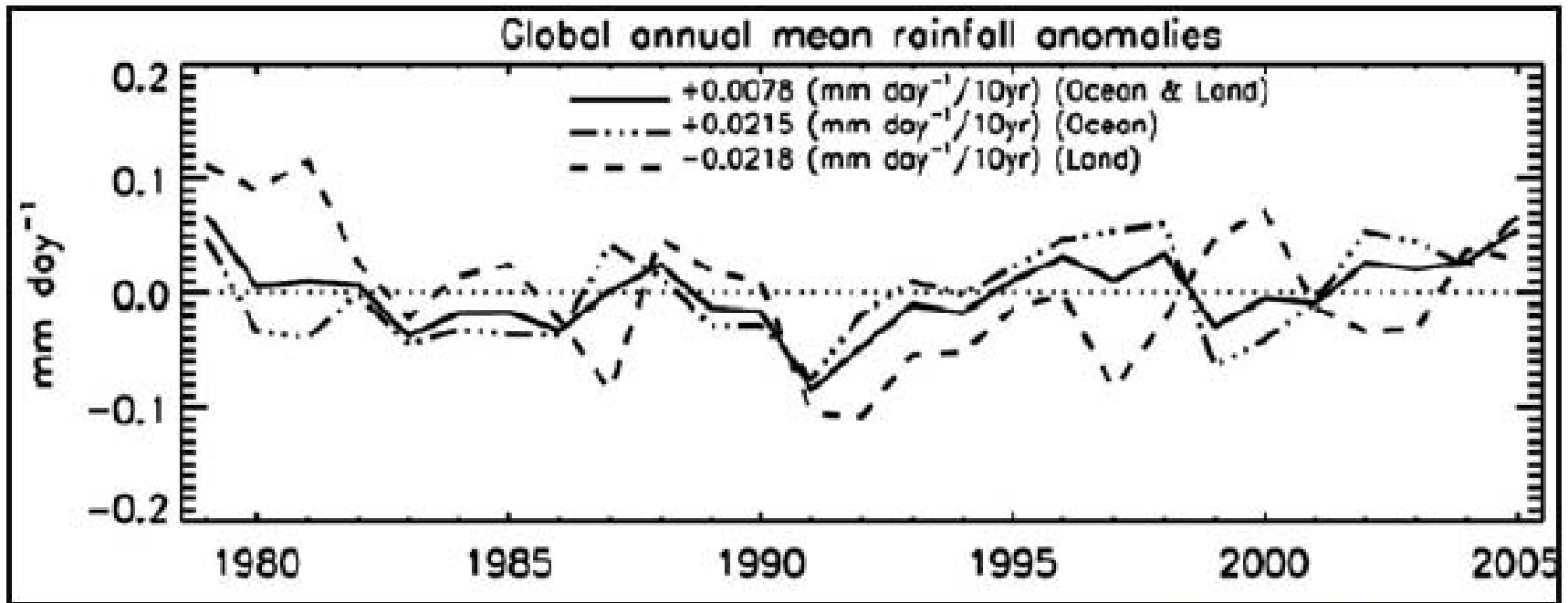
- In Japan, about 6 % decrease in precipitation with larger interannual variations.

Precipitation variation in Japan



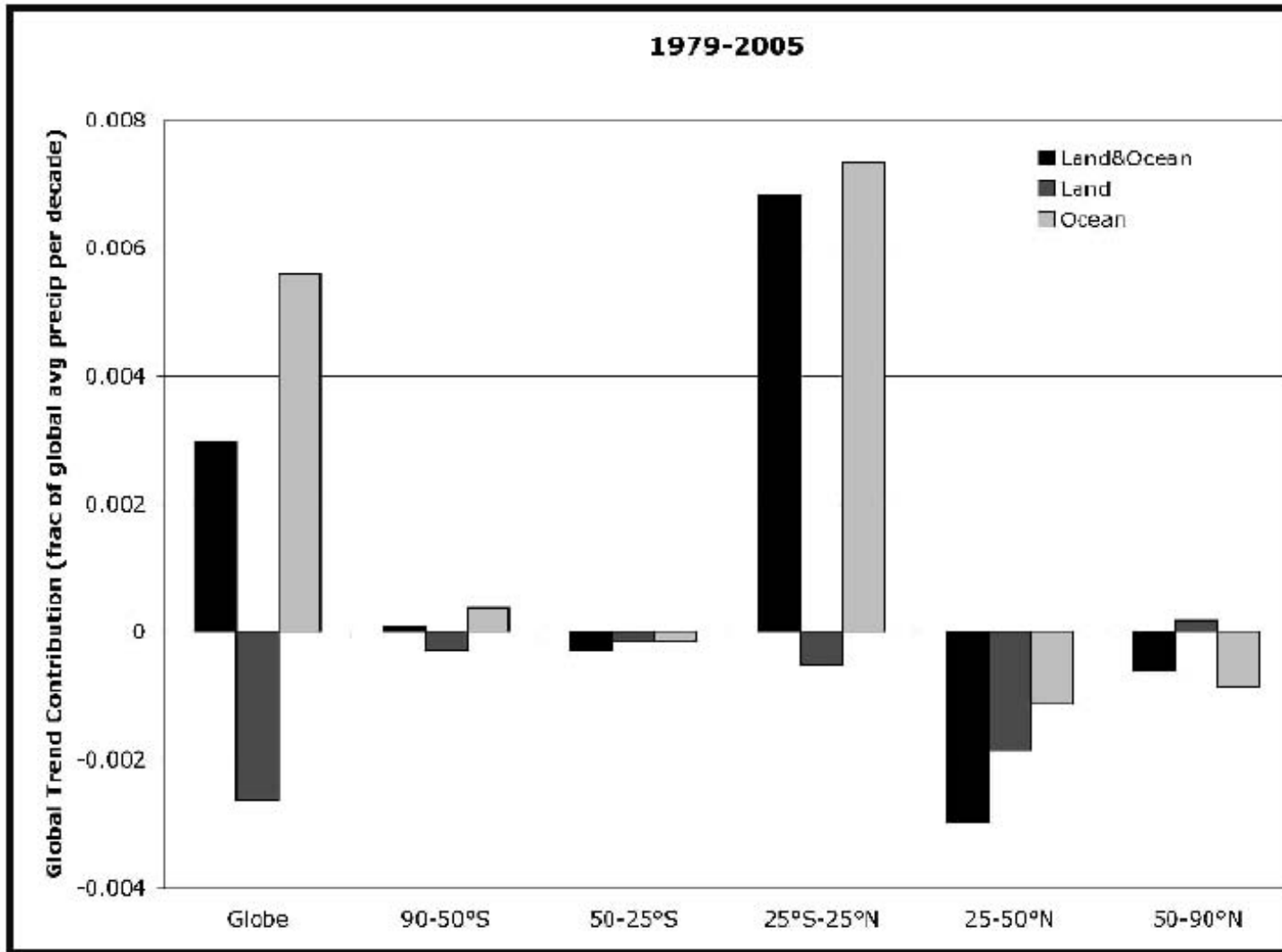
JMA Report

1898年以降の国内51地点における年降水量平年比の平均。平年値は1971～2000年統計値。実線は5年移動平均。



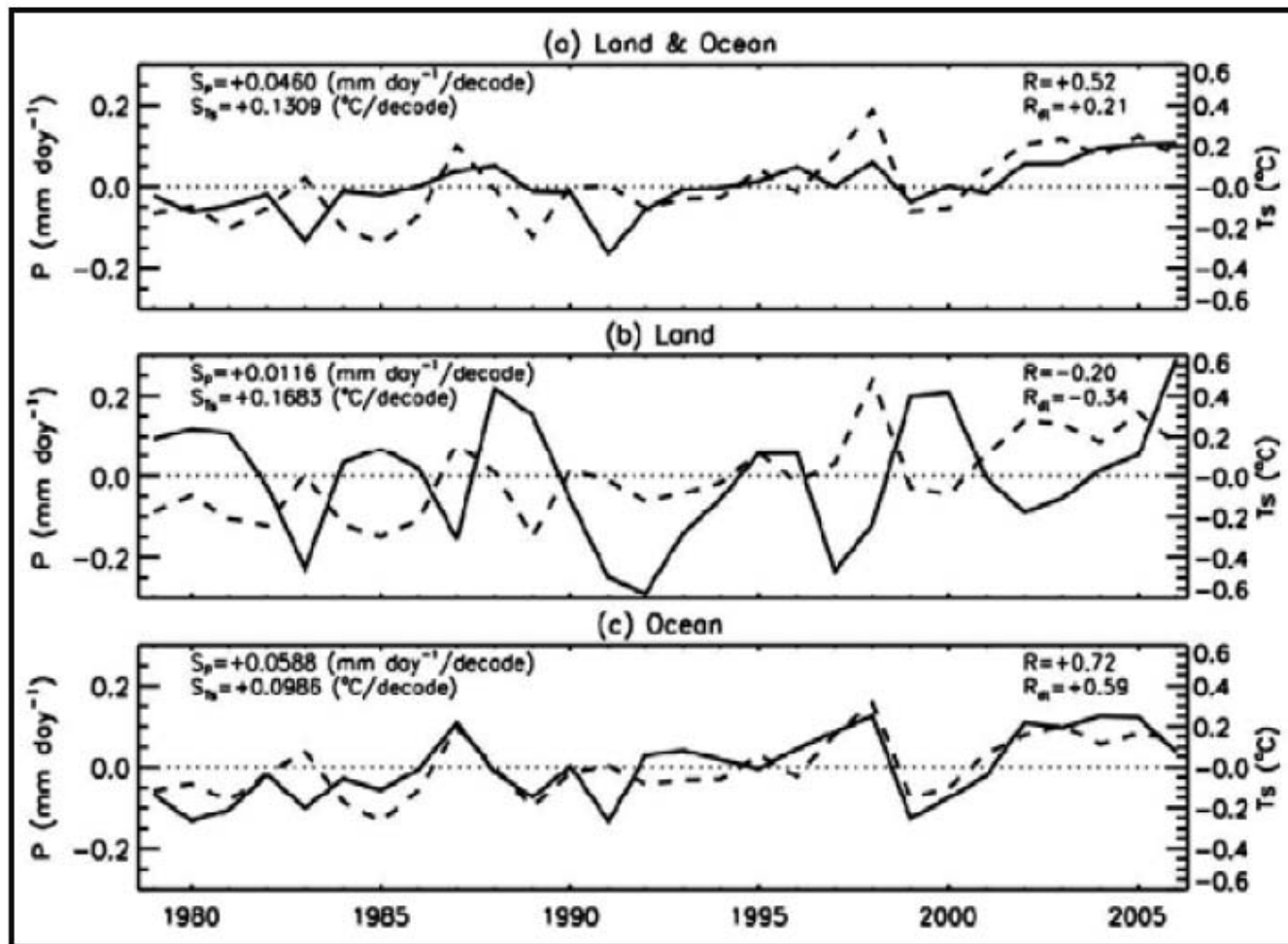
Annual mean global rainfall anomalies over ocean, land, and both ocean and land. Also shown are the estimated slopes of the linear fits.

(Adler et al., 2007)



Volume contributions to long-time change/linear fit during 1979–2005.

(Adler et al., 2007)



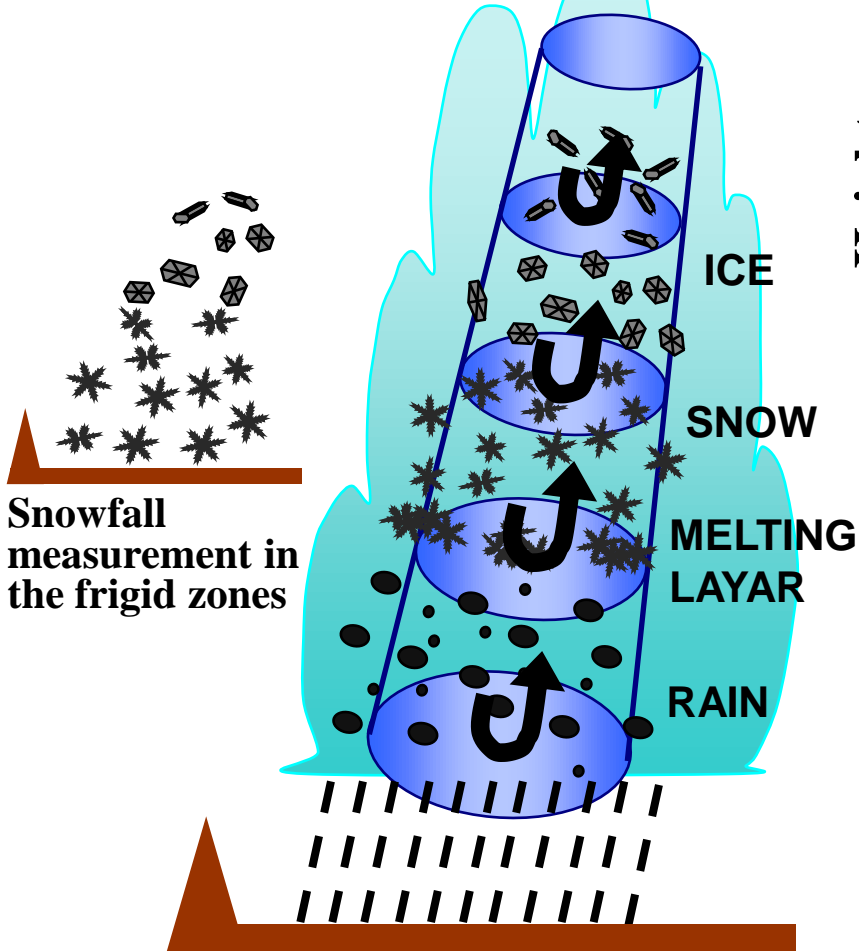
Tropical (25S–25N) annual mean precipitation (solid lines) and temperature (dashed lines) anomalies. S_p and S_{T_s} denote linear changes for precipitation and temperature anomalies, respectively. R and R_{dt} represent the correlations between precipitation and temperature anomalies with and without the respective linear changes.

(Adler et al., 2008)

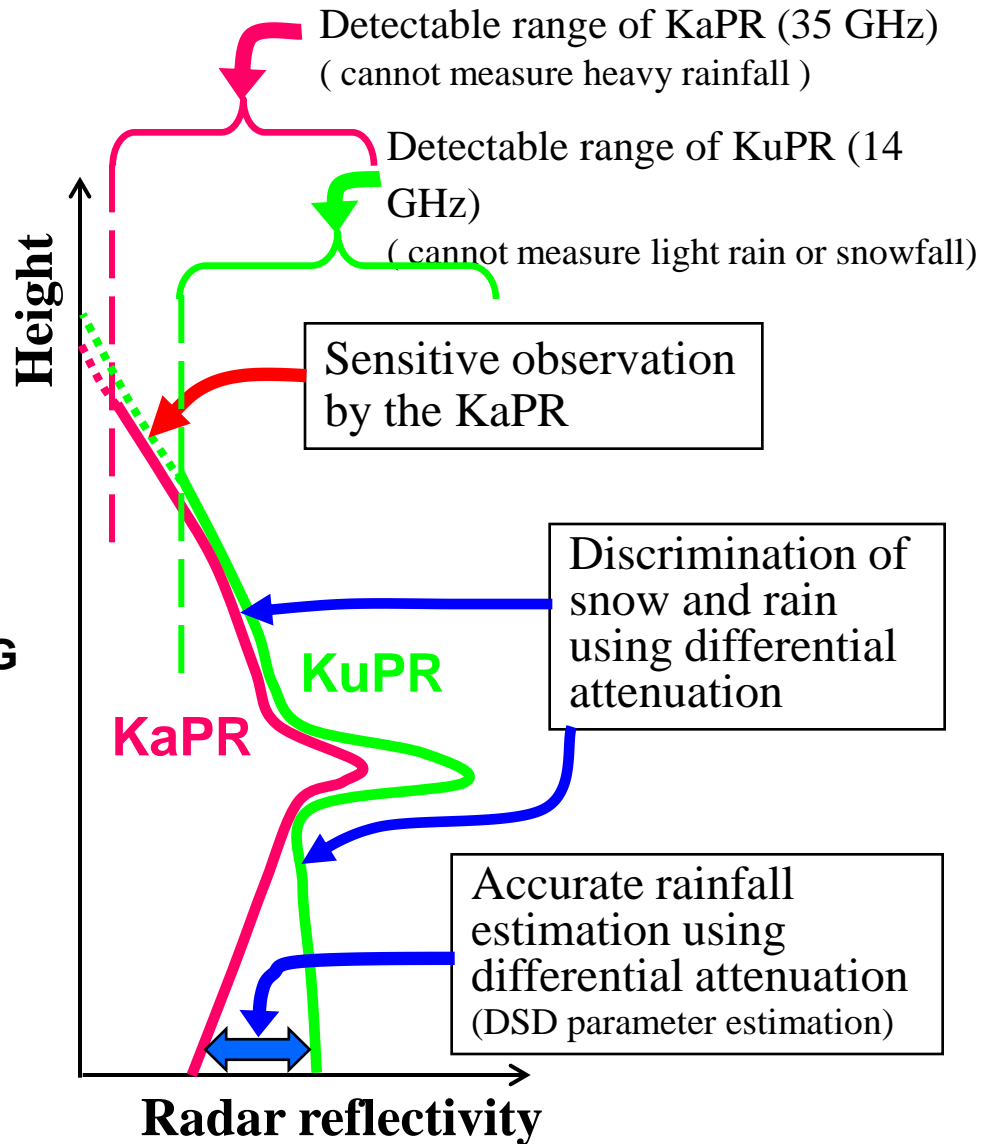


Precipitation measurement with DPR

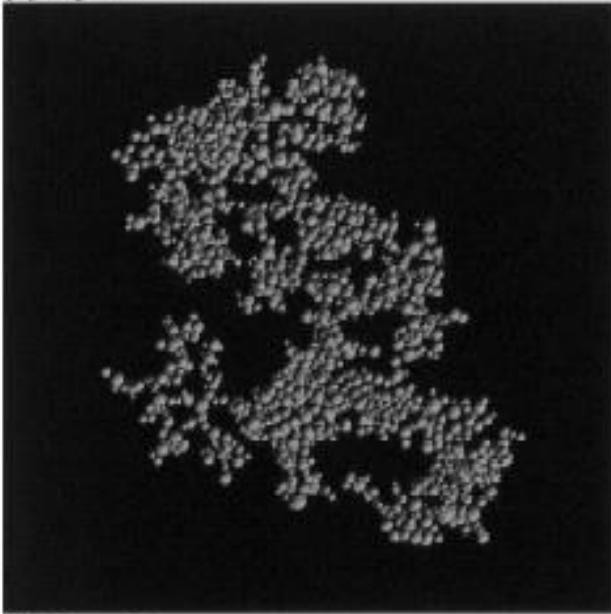
Matched beam of
KuPR and KaPR



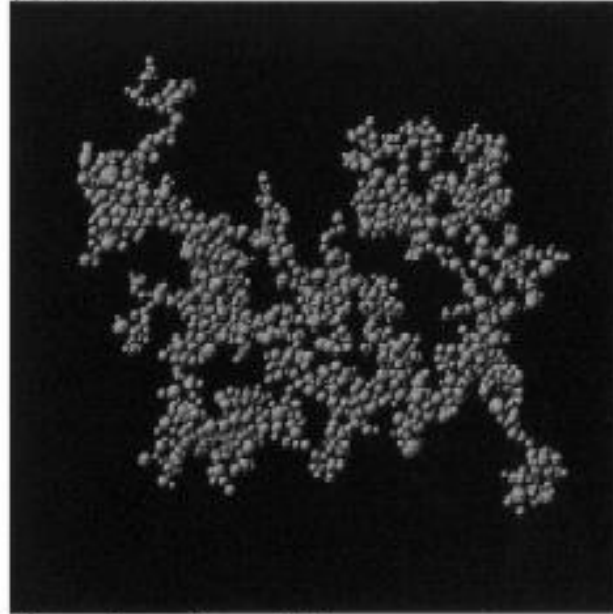
Accurate rainfall measurement in the tropics and the temperate zones



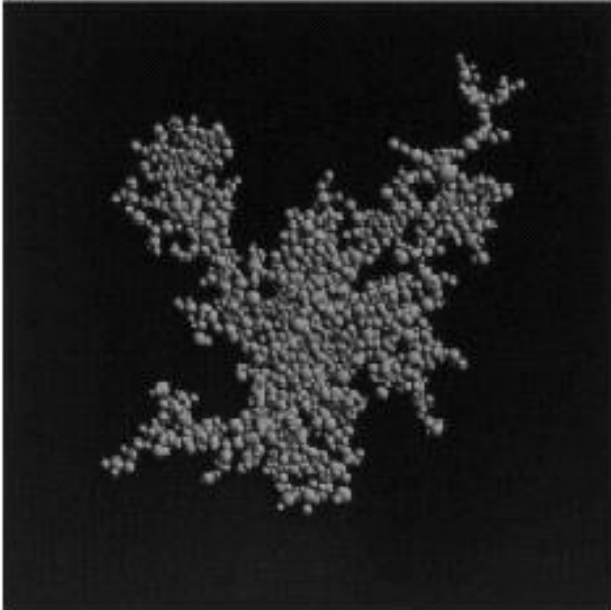
(a) top view



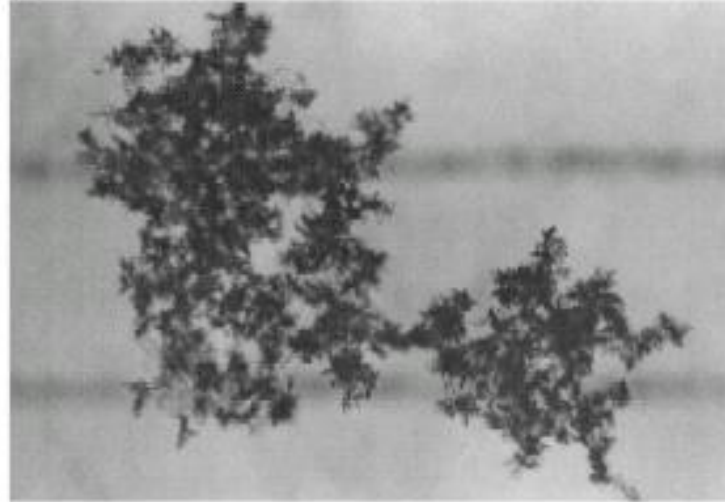
(c) side view



(b) front view



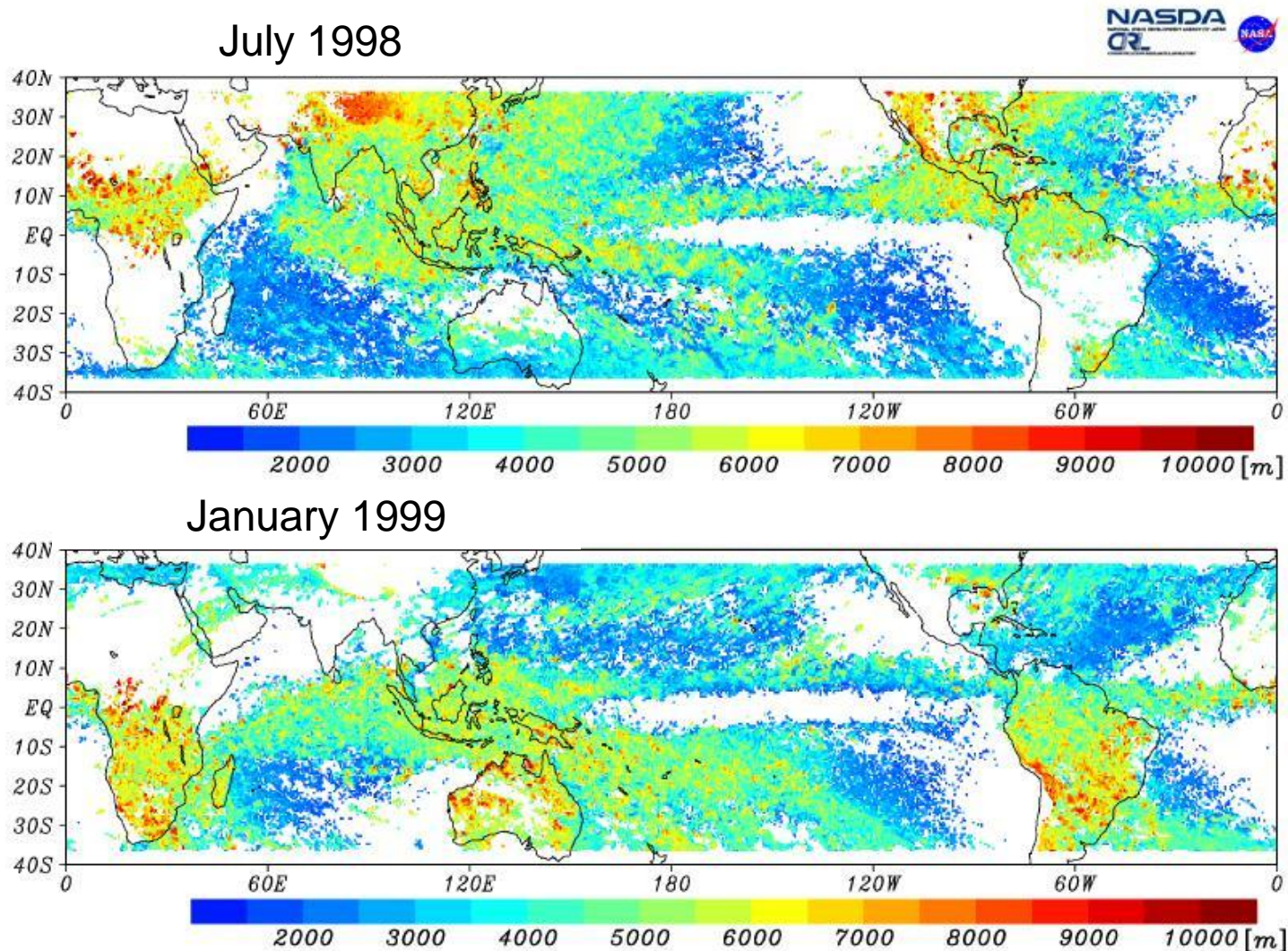
(d) an observed snowflake



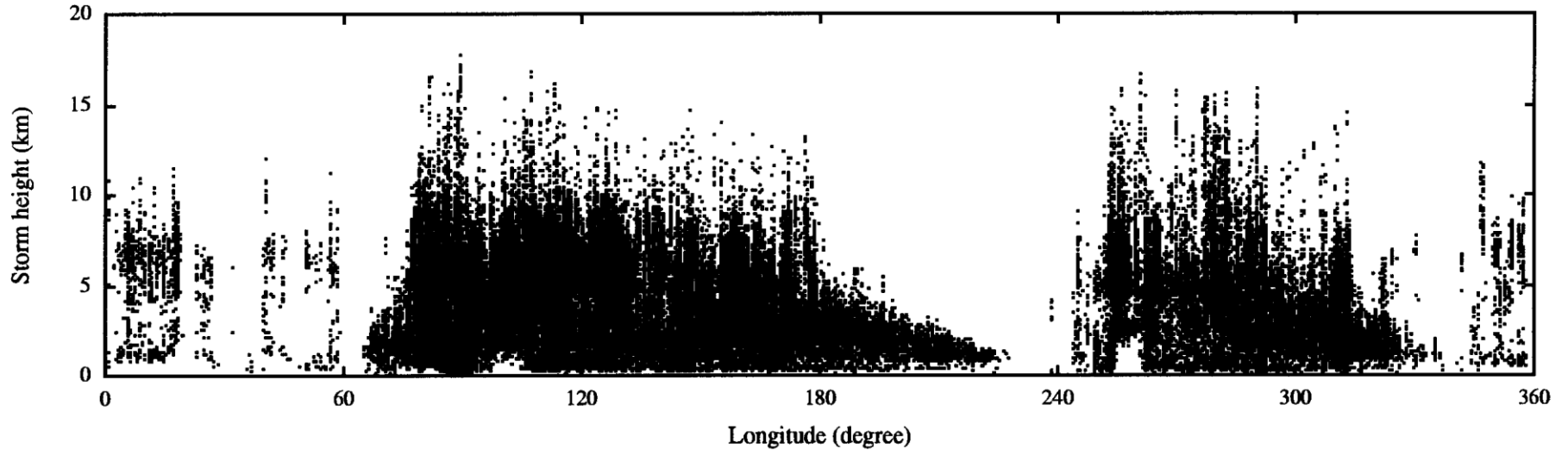
(Maruyama and Fujiyoshi, JAS, 2005)

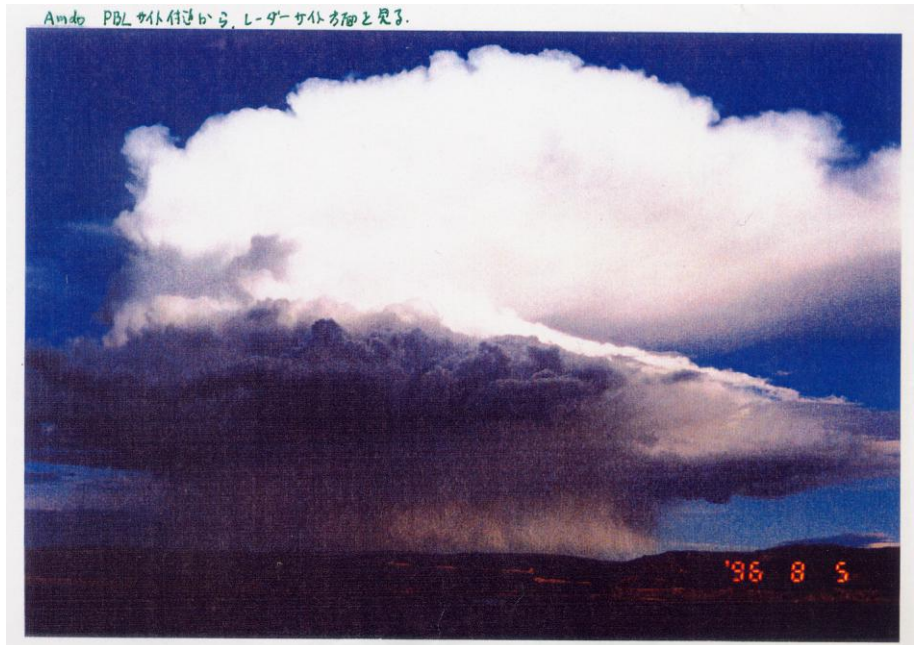
FIG. 2. Images in 3D of a generated snowflake consisting of 1760 particles: (a) top view and (b) front view. (c) A picture of an observed snowflake is also shown for comparison; the two faint lines behind the observed snowflake are separated by 5 mm.

Global Distribution of the Mean Storm Height Measured by the TRMM Precipitation Radar



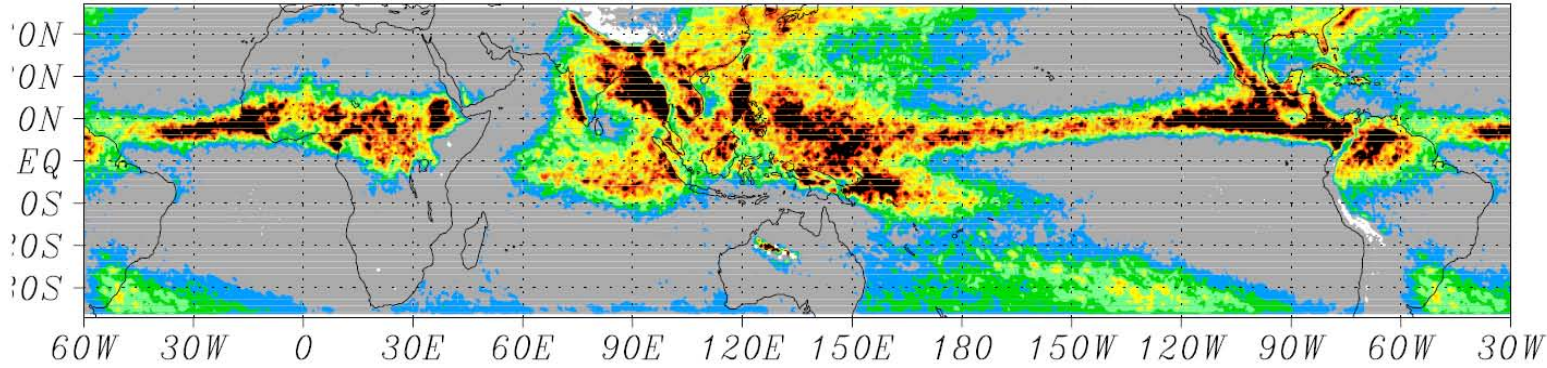
Storm height vs. longitude



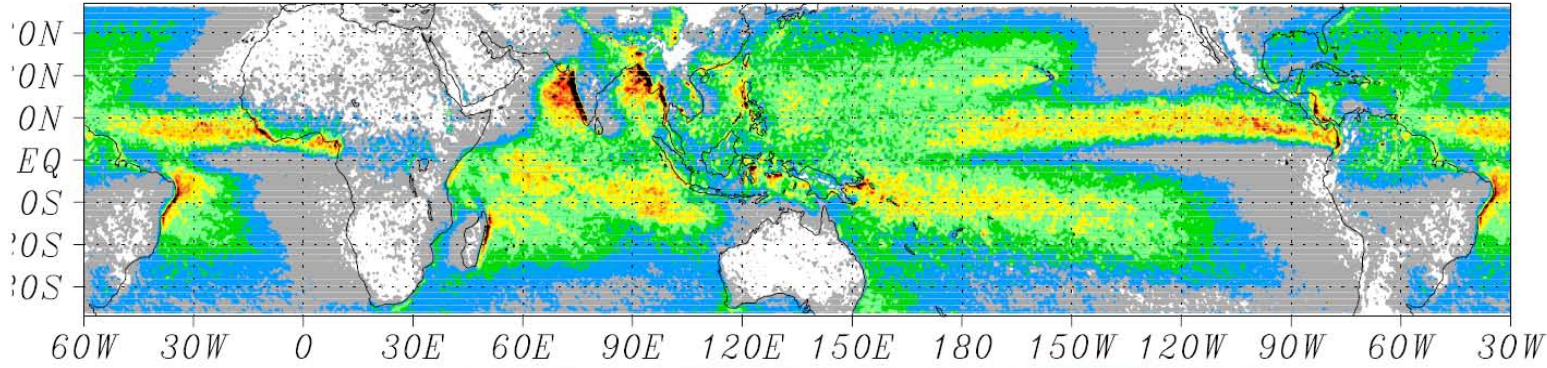


(by Endo and Koike)

7.5 km



2 km



Latent heating from TRMM PR for 1998-2000.

(Takayabu et al.)

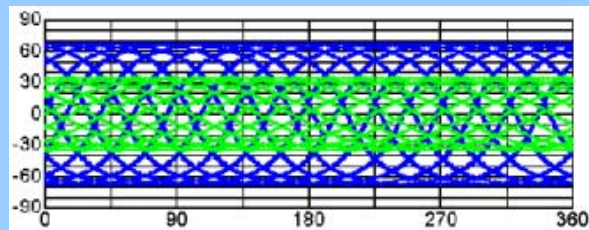


The Concept of Global Precipitation Measurement (GPM)

Core Satellite

- Dual-frequency Precipitation Radar (DPR)
- Microwave Radiometer
- ✧ High-sensitivity precipitation measurement
- ✧ Calibration for constellation radiometers

NASDA (Japan) :
DRP, H-IIA Launcher
NASA (US) :
Spacecraft, MWR



Blue: Inclination $\sim 65^\circ$ (GPM core)
Green: Inclination $\sim 35^\circ$ (TRMM)

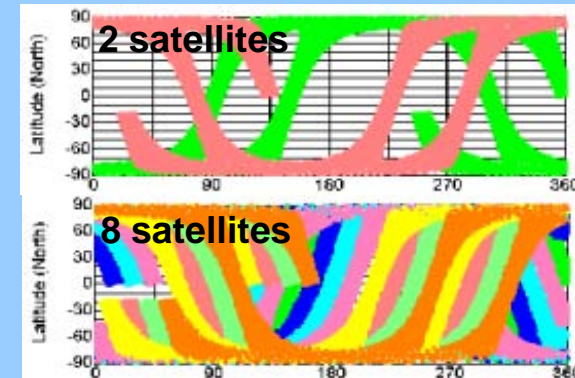


Constellation Satellites

- Microwave Radiometers installed on each country's satellite
- ✧ Frequent precipitation measurement

Expected Partners:
NASA, NOAA (US),
ESA (EU), NASDA,
China, Korea, others

**3-hourly
global
rainfall map**

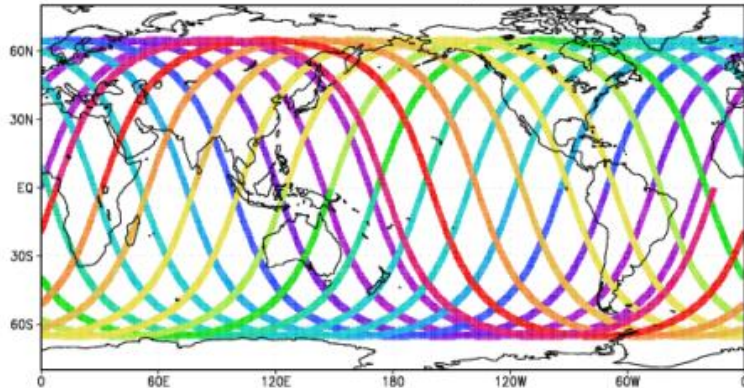


Time and space Interval of the DPR database

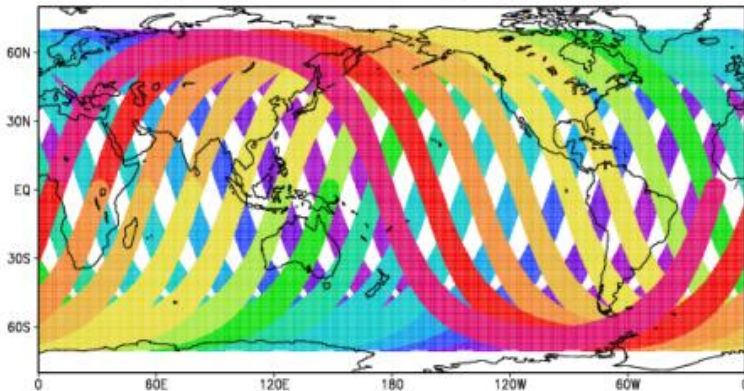
1-day orbit

Color: orbit num

GPM-Core DPR 1-day Obs Area



GPM-Core GMI 1-day Obs Area

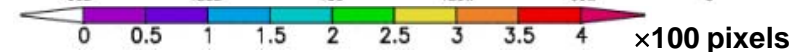
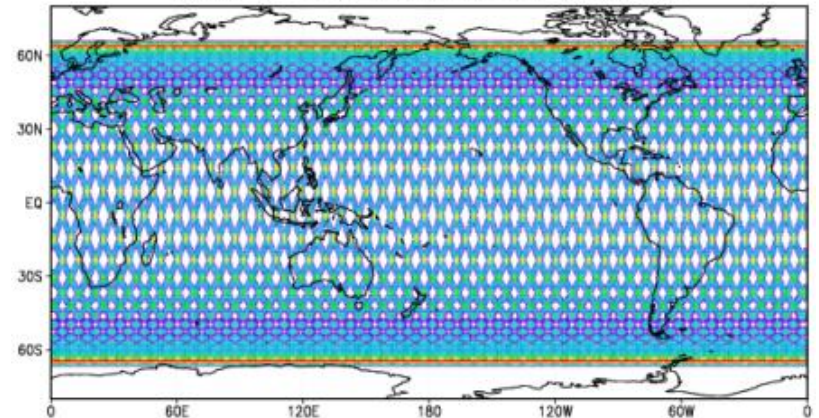


One-day orbit observations of DPR (upper) and GMI (lower)

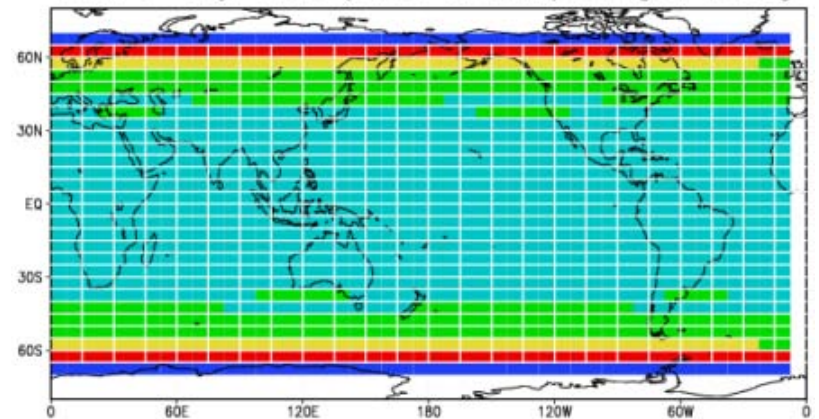
3-days orbit

Color: IFOV pixel num

DPR 3-day Orbit (Obs Pix Num) 0.5x0.5deg



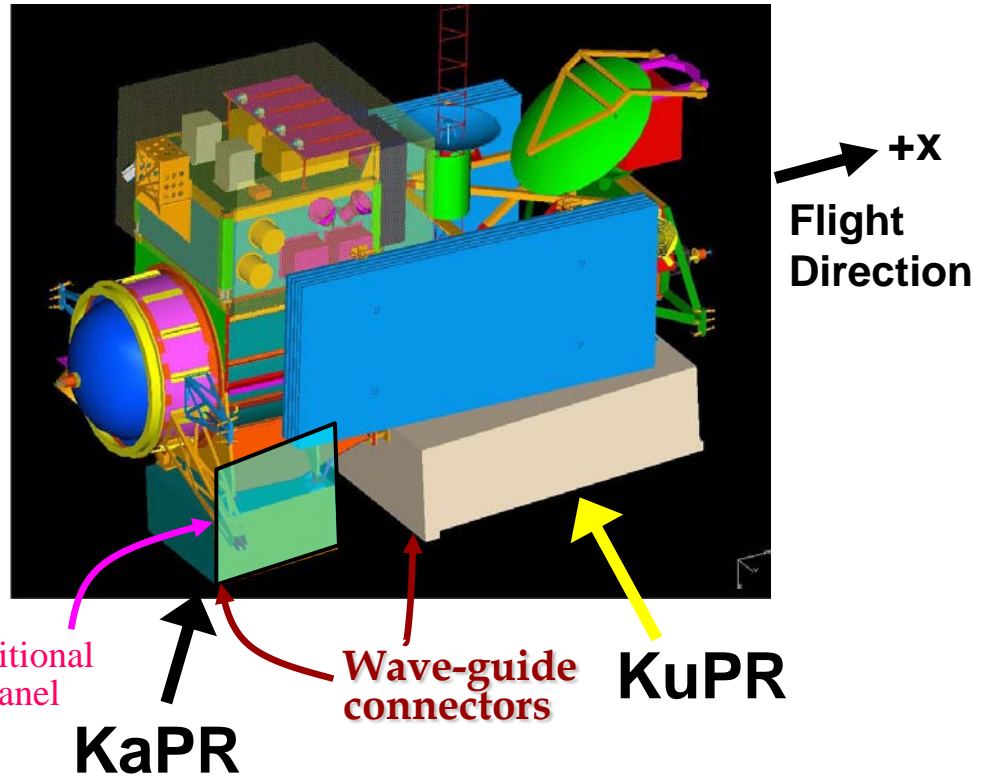
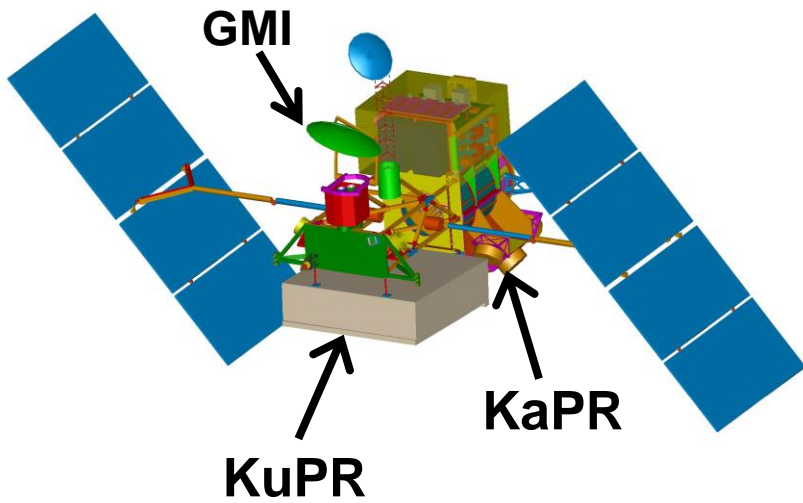
DPR 3-day Orbit (Obs Pix Num) 5deg x 15deg



DPR dynamic database will be renewed in 15 deg x 5 deg grids every 3-10 days



Design of the GPM Core Satellite and the DPR

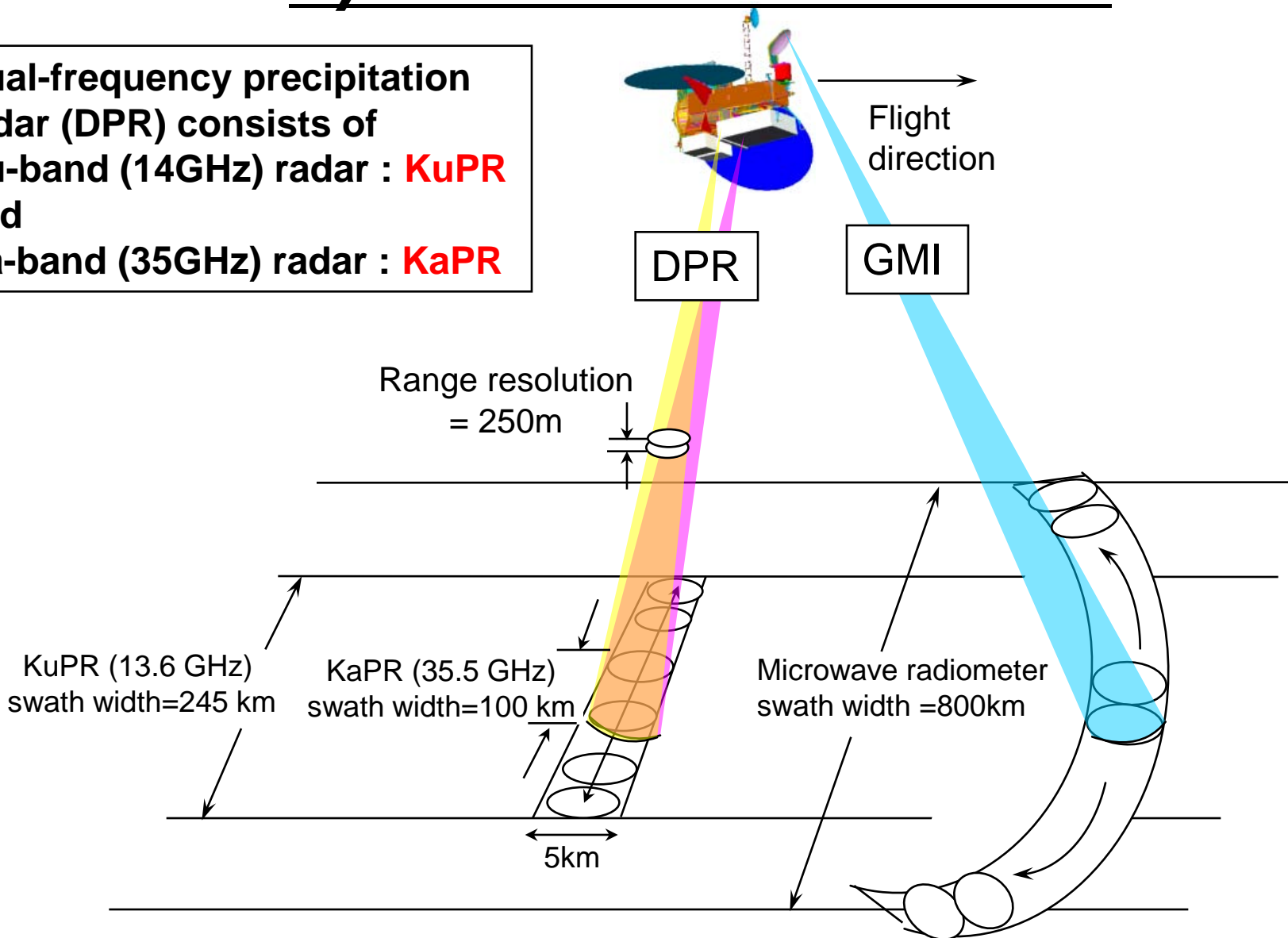


Basic design of KuPR and KaPR is the almost same as TRMM PR.

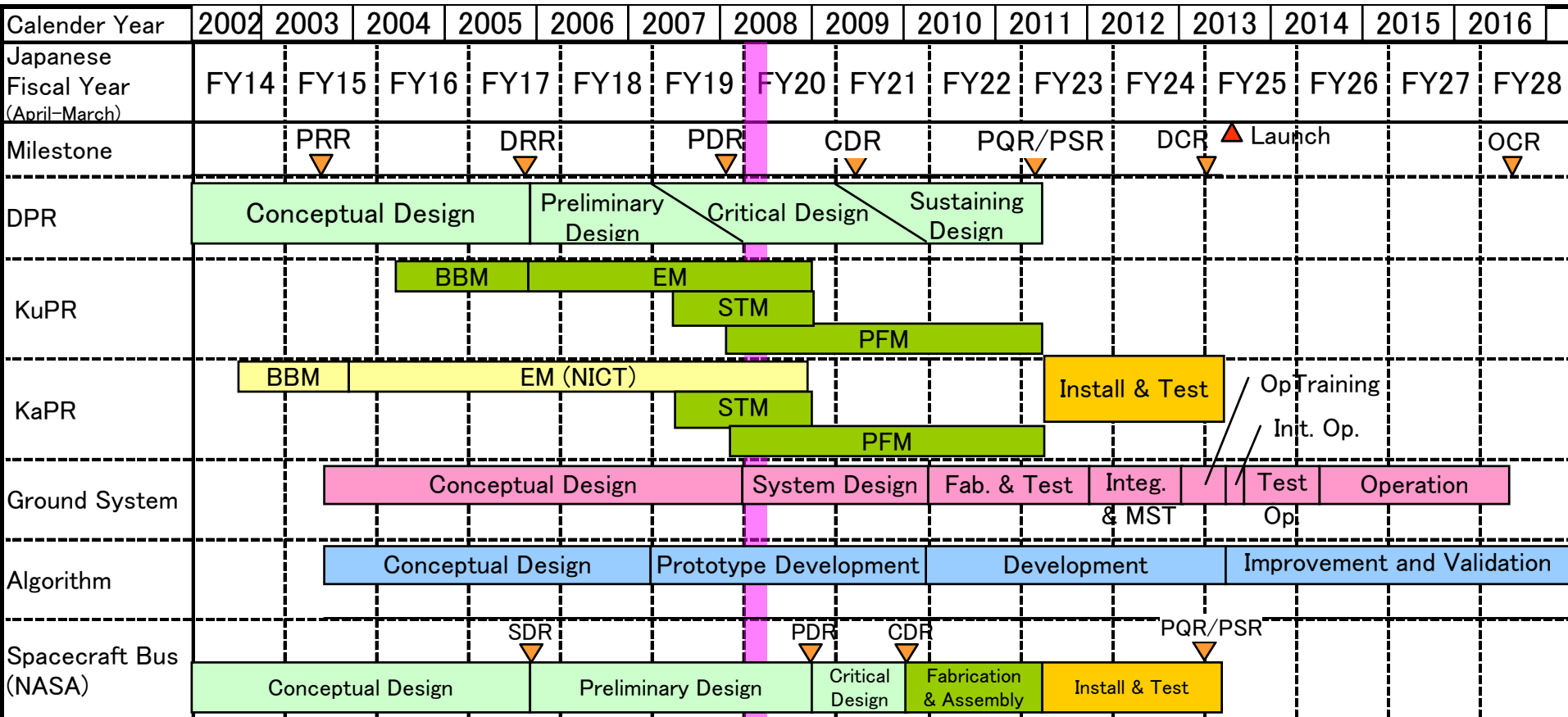


Concept of precipitation measurement by the GPM core satellite

Dual-frequency precipitation radar (DPR) consists of Ku-band (14GHz) radar : **KuPR** and Ka-band (35GHz) radar : **KaPR**



GPM/DPR Project Schedule



PRR : Project Readiness Review
 DRR : Development Readiness Review
 PDR : Preliminary Design Review
 CDR : Critical Design Review

PQR : Post Qualification–test Review
 PSR : Pre–Shipment Review
 DCR : Development Completion Review
 OCR : Operation–phase Completion

L8. Space borne Precipitation Radars

- Rainfall profiling by space borne K-band radars
- Current and future satellite missions carrying precipitation radars

Toshio Iguchi

Applied Electromagnetic Research Center,
National Institute of Information and Communications Technology

The Eighteenth International Hydrological Program (IHP) Training Course

Satellite Remote Sensing of Atmospheric Constituents

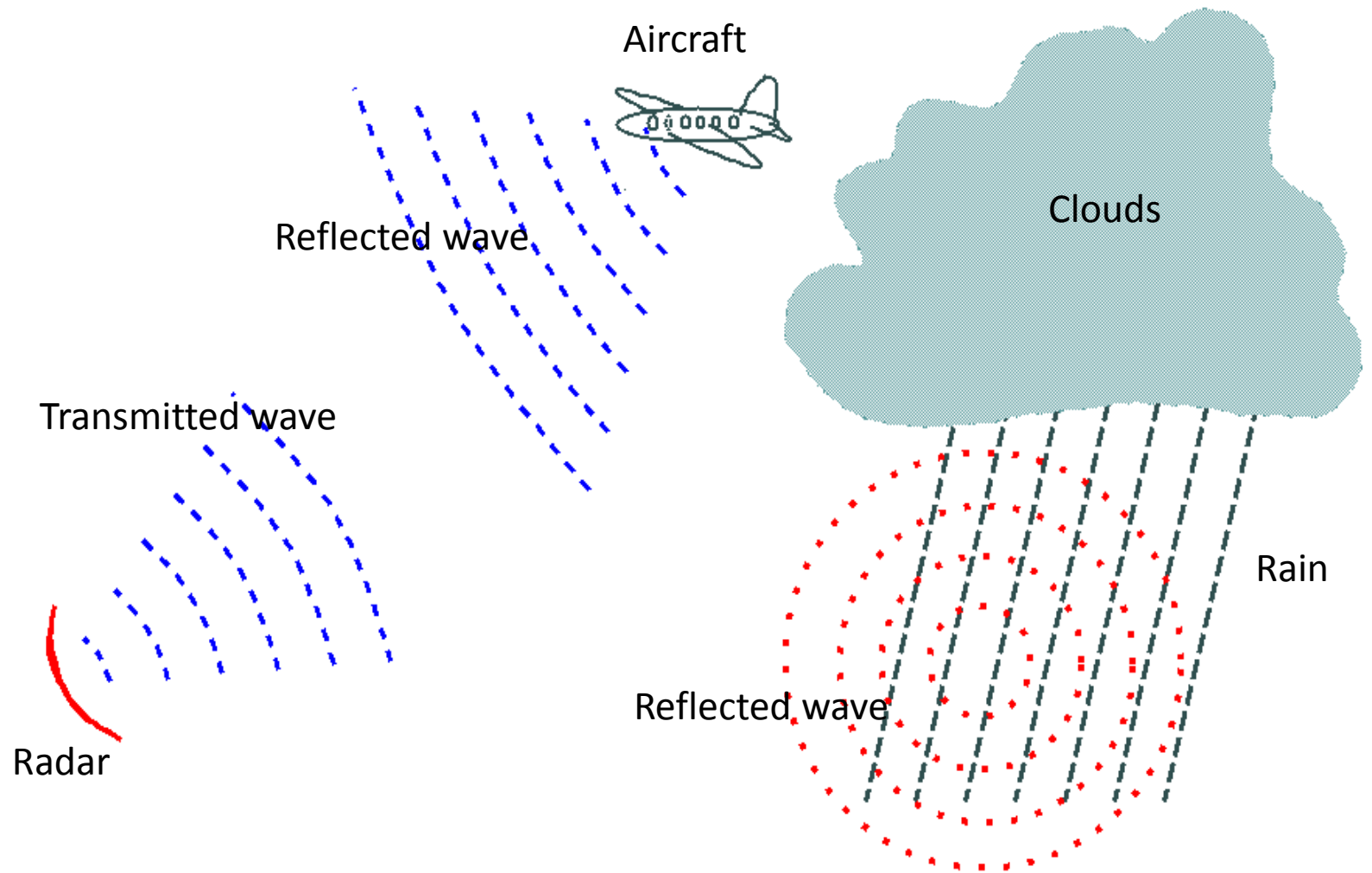
3-15 November 2008

Nagoya, Japan

Remote sensing of rain by radar

- Radar emits a known pulse of radio waves and measures its echoes from objects or targets.
- The time for the pulse to travel to the target gives the distance to the target.
- The direction of the radio waves gives the direction of the target.
- The echo power depends on the size and number of the targets.

RADAR: RAdio Detection And Ranging

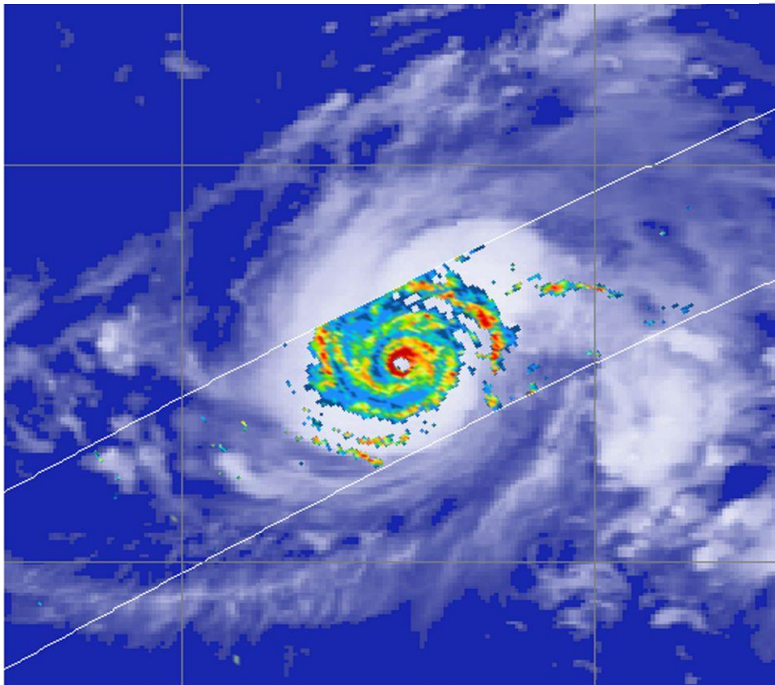


3-D Observation of a Typhoon by the PR

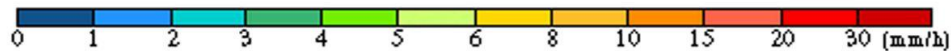
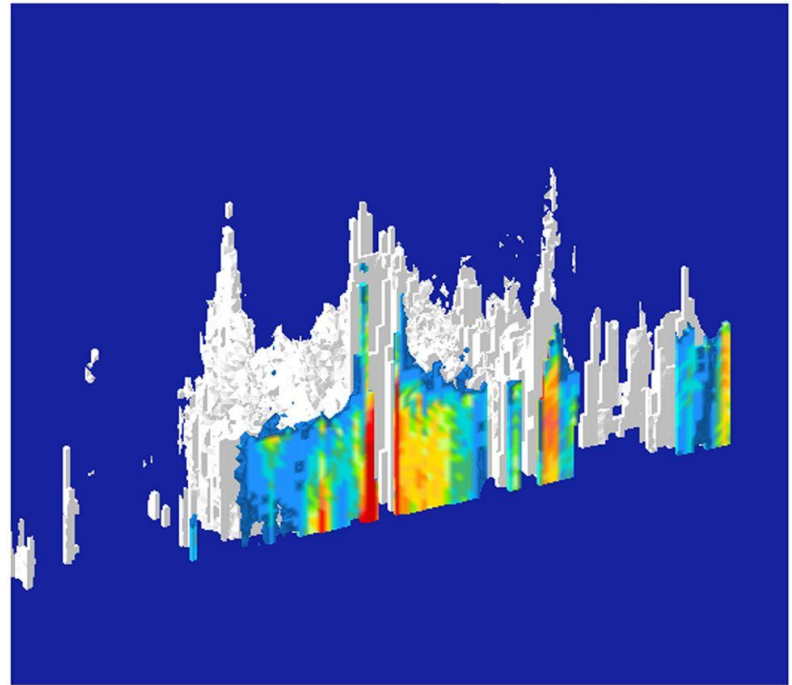
TRMM PR 2A25 Rain

Aug. 2, 2000, 20:49-20:53 (Japanese local time)

Rain intensity at H=2 km



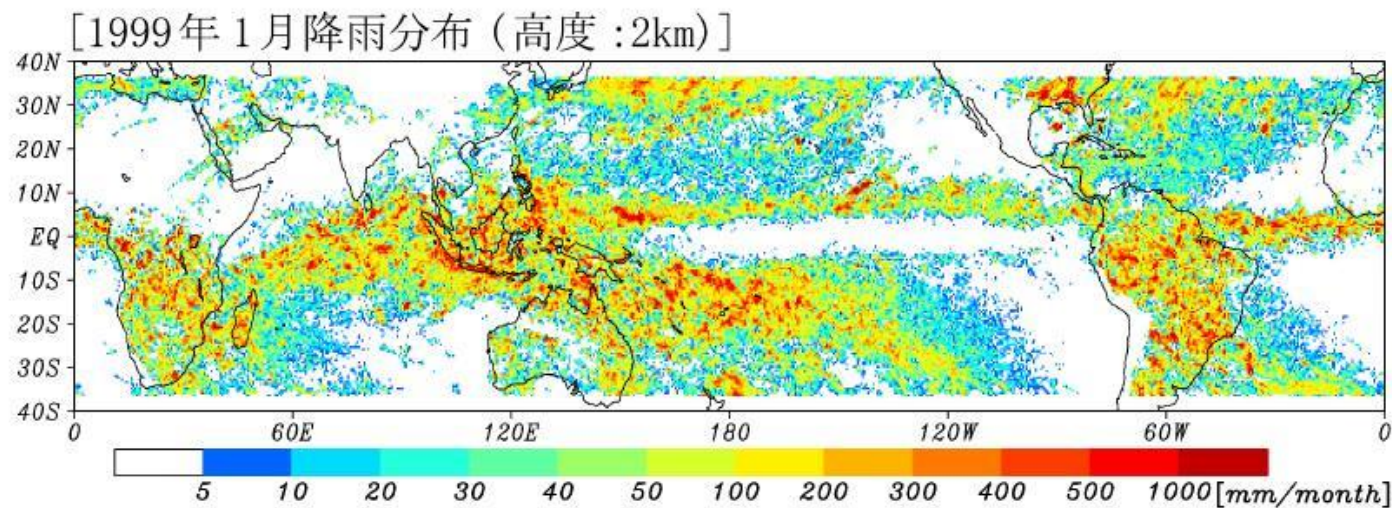
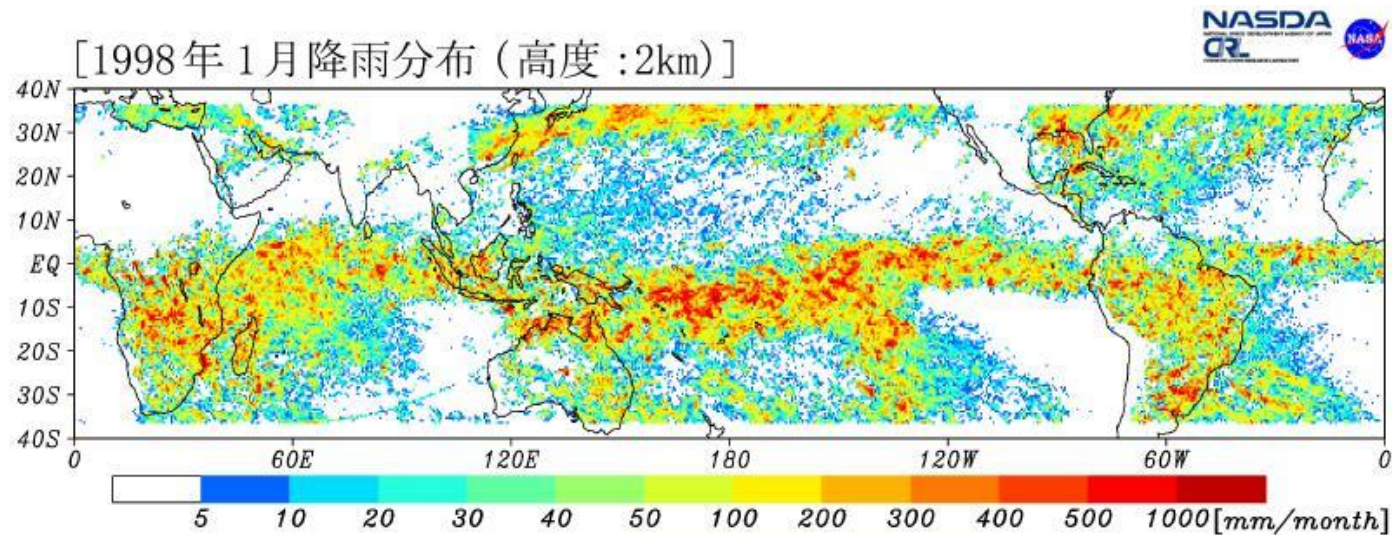
Vertical cross section through the eye and 3D structure



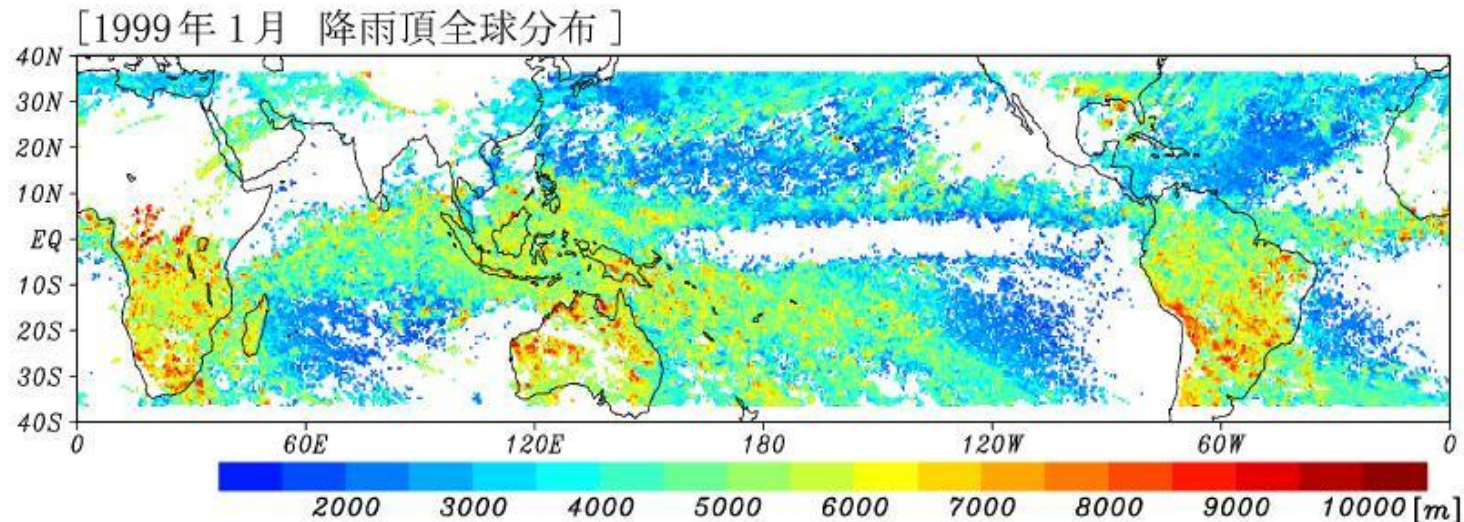
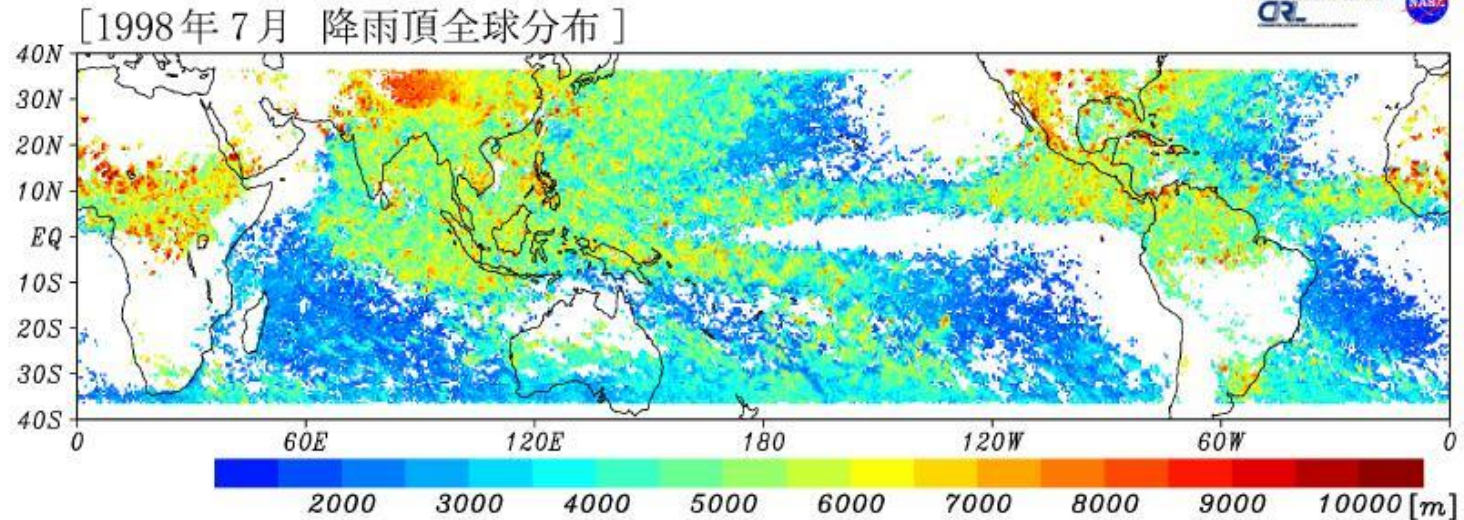
PR realized observation of 3D structure of rain over ocean where few observations had been available.



Monthly Rain Distributions estimated from the TRMM PR data in 1998 (El Nino year) and 1999



Strom Top Height Distribution measured with the TRMM Precipitation Radar



Radar Equation

$$P_r(r) = P_t \frac{G_t G_r \lambda^2 \theta_1 \theta_2 c \tau}{2^{10} \pi^2 \ln(2) r^2} \eta(r) \exp\left(-2 \int_0^r k(s) ds\right)$$

$$\eta = \frac{1}{V} \sum_V \sigma_b = \int \sigma_b(D) N(D) dD$$

$$k = \frac{1}{V} \sum_V \sigma_t = \int \sigma_t(D) N(D) dD$$

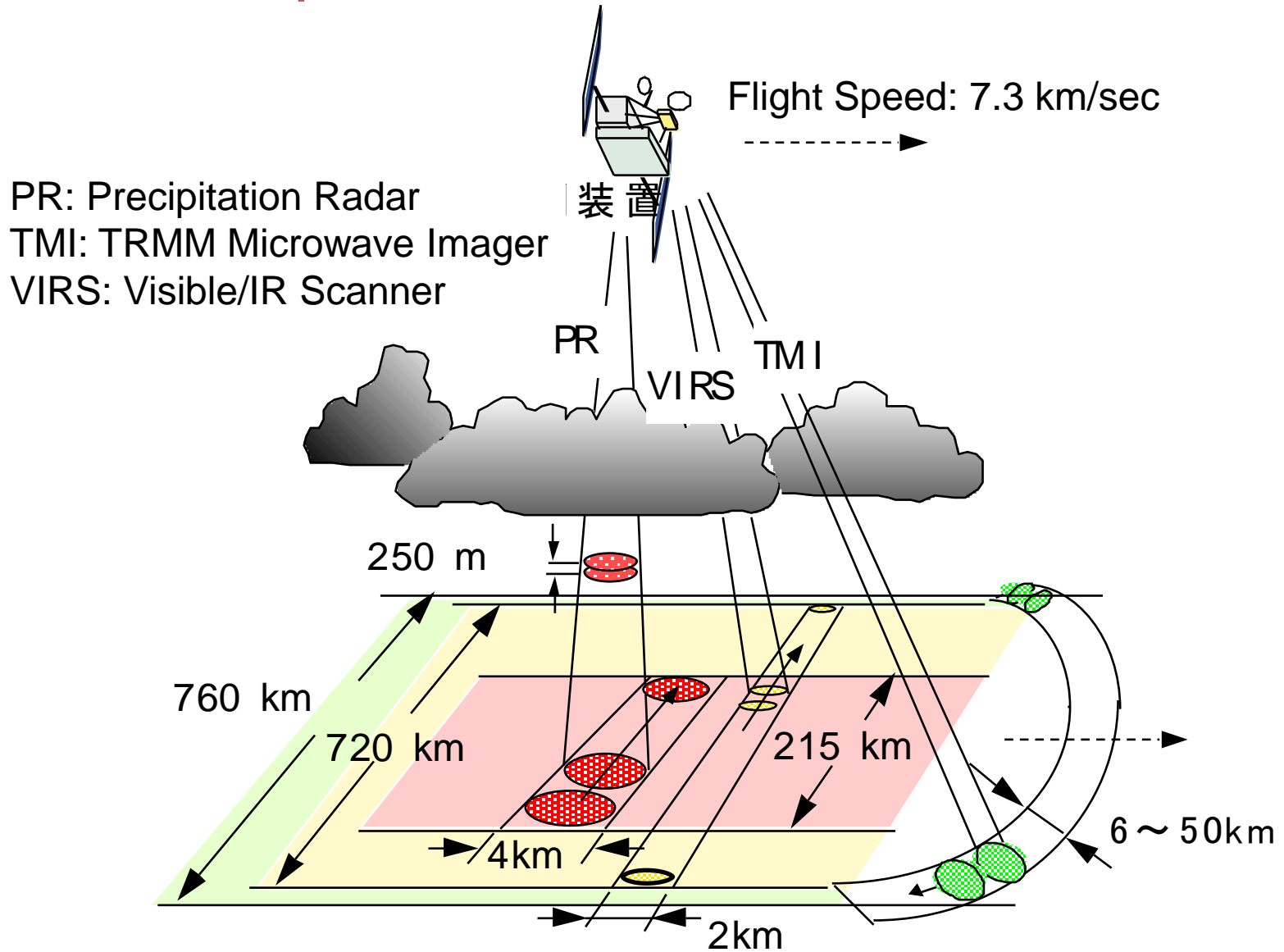
$$Z_e = \frac{\lambda^4}{\pi^5 |K_w|^2} \eta, \quad K = \frac{\epsilon_r - 1}{\epsilon_r + 2} = \frac{n^2 - 1}{n^2 + 2}$$

$$R = \frac{\pi}{6} \int D^3 v(D) N(D) dD \approx \int D^{3.67} N(D) dD$$

If $\lambda \gg \pi D$ (Rayleigh scattering),

$$\eta \propto \int D^6 N(D) dD = Z, \quad k \propto \text{Im}(-K) \int D^3 N(D) dD$$

Concept of TRMM Rain Observation



Factors that affect the Rain estimates from space-borne radar

- Type of precipitation
 - rain, snow, graupel, hail, etc.
- Drop size distribution (DSD)
- Flatness (non-sphericity) of rain drops
- Fall speed of rain drops
 - need this quantity to convert reflectivity into rain rate
- Influence from matters other than precipitation
 - Clouds, water vapor, other gasses
- Non-uniform distribution of precipitation
- Variation of surface radar cross sections
 - Surface reference method

Peculiarities of satellite-borne radar

Differences from ground-based radar

- Hardware constraints
 - size, mass, power consumption
 - use of short waves -> attenuation
 - sensitivity
 - reliability
- Observation geometry
 - distance, angle
 - sensitivity, resolution
 - surface behind rain
 - surface clutter
 - moving platform (unless from a geostationary satellite)
 - difficulty in Doppler measurement

Footprint size and wavelength

- Use of relatively high frequency (short wave) to realize a good horizontal resolution.
 - antenna beam width $\sim c_1\lambda/D$ (wavelength/diameter)
 - λ : wavelength of the electromagnetic wave
 - D : antenna diameter
 - c_1 : a constant that depends on the antenna illumination (~ 1.2)
 - footprint size $\sim c_1r\lambda/D$ (r : range to surface)
 - $D < 2\sim 3$ m unless the antenna is developed on orbit
 - $r > \sim 300$ km.
 - -> use a small λ to make the footprint size ($c_1r\lambda/D$) small.
 - to realize a 5 km footprint with a 2 m antenna from a 400km orbit, $\lambda \sim 5*2/(1.2*400)$ m = 2.08 cm (= 14.4GHz)

Issues associated with short waves

- Attenuation
 - rain, snow, water vapor, cloud liquid water (liquid cloud droplets), and oxygen molecules
 - Correction methods:
 - Hitschfeld-Bordan method, Surface reference method
- Non-Rayleigh scattering effect
 - scattering cross section does not change proportionally to D^6
 - Drop size distribution model

Attenuation by rain

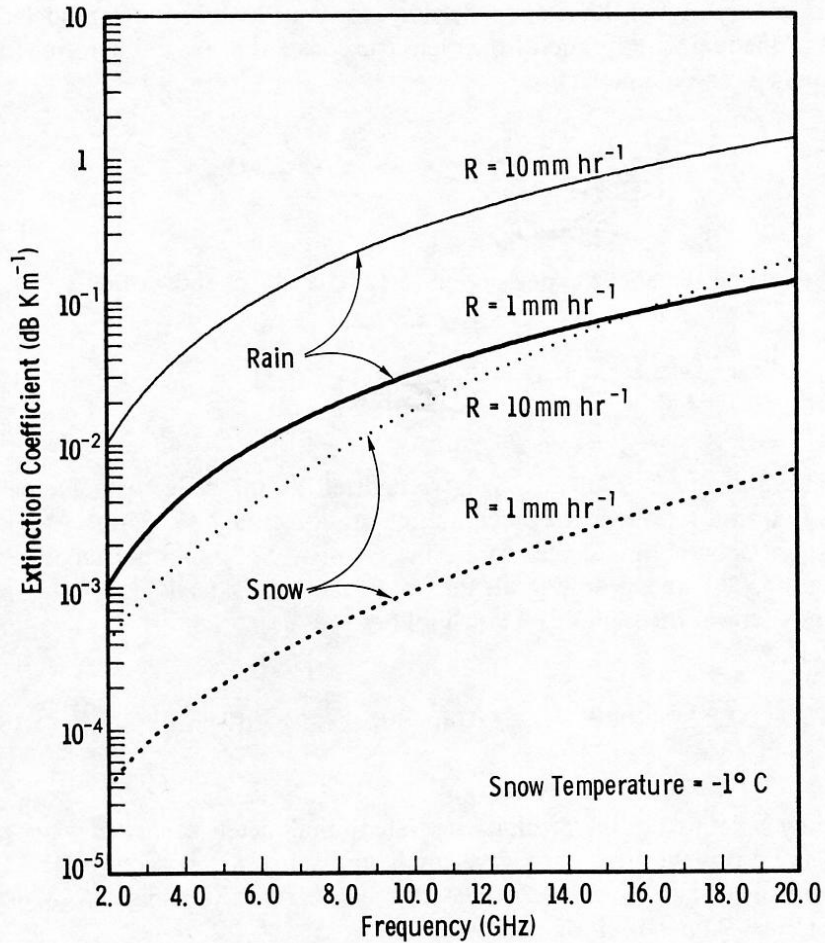


Fig. 5.31 Extinction coefficient of rain as a function of frequency, based on a summary of experimental data (adapted from Barton, 1974).

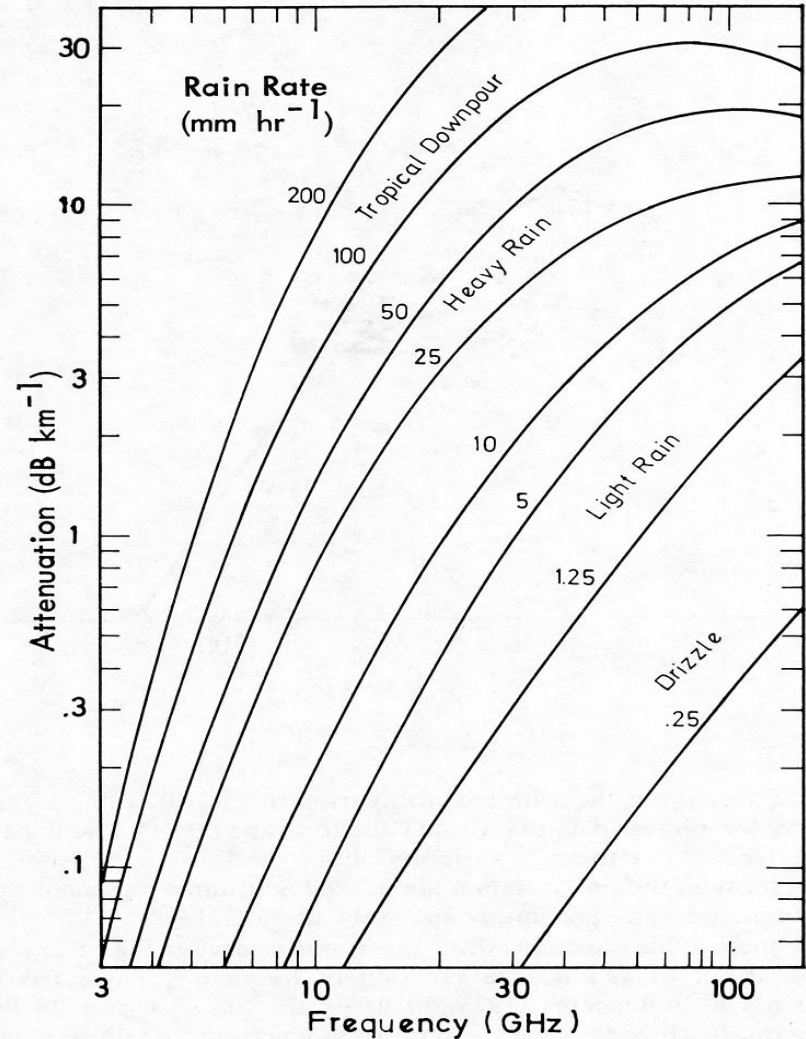


Fig. 5.29 Horizontal-path attenuation at various rain rates (compiled by Schanda, 1976, from data by Haroules and Brown, 1968; Treussart et al., 1970; and de Bettencourt, 1973).

Attenuation by H₂O and O₂

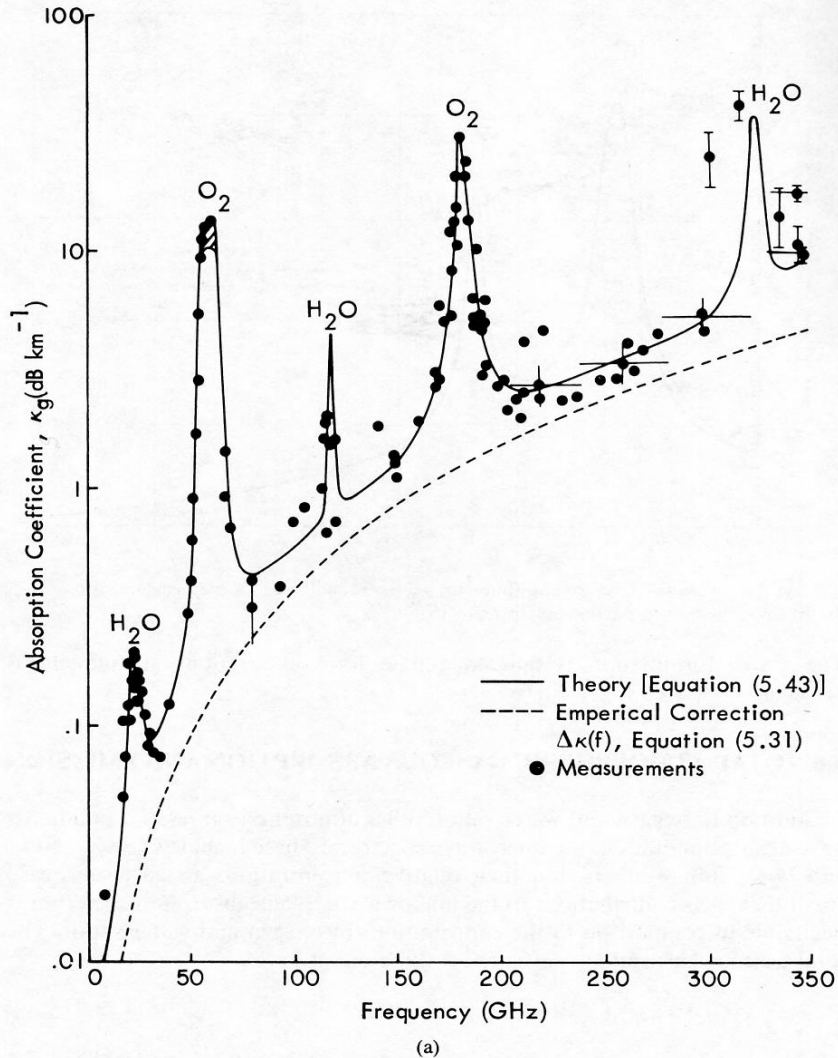


Fig. 5.7 Microwave absorption due to atmospheric gases: (a) gaseous absorption coefficient $\kappa_g(f)$ at sea level and (b) zenith opacity, both for the surface conditions $P_0 = 1013$ mbar, $T_0 = 293$ K, and $\rho_0 = 7.5$ g cm⁻³. Solid curves are calculated according to theory, and dots are measured values (Crane, © 1981 IEEE).

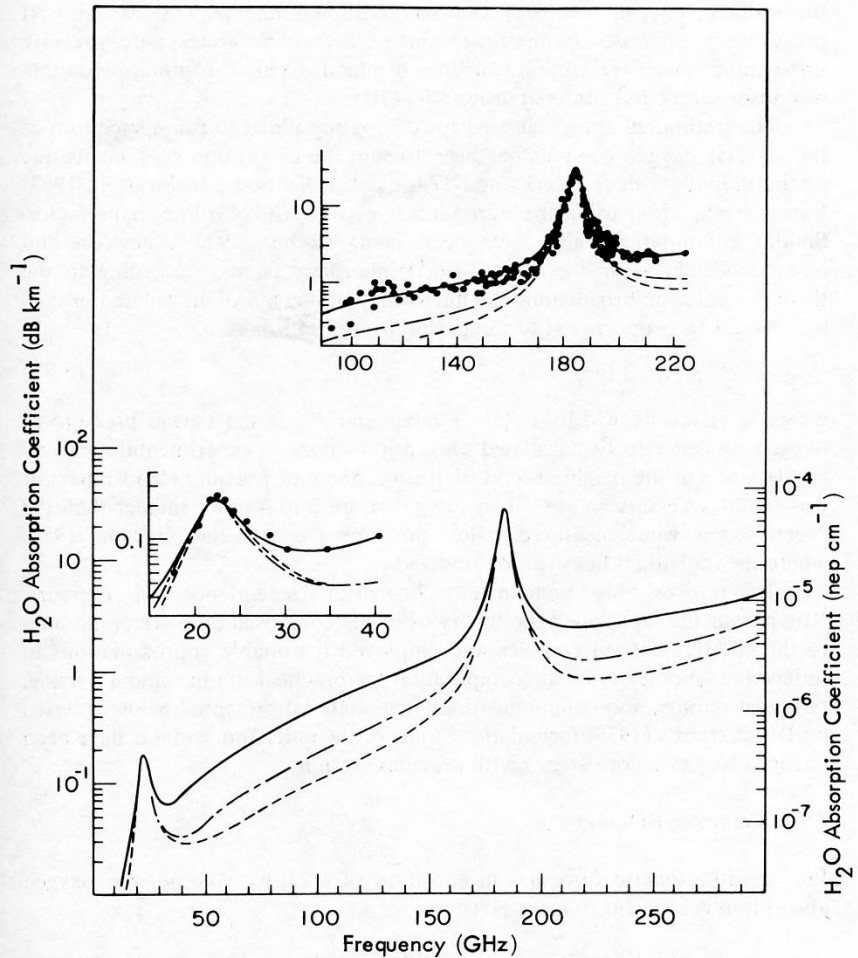


Fig. 5.5 Measured and calculated water-vapor absorption (from Waters, 1976). Calculations are shown for the Van Vleck-Weisskopf line shape (---), the Gross line shape (-.-.-), and the Gross line shape with the added empirical correction discussed in the text (-), with $T = 300$ K, $P = 1013$ mbar, and $\rho_v = 7.5$ g m⁻³. Points in the 20-40-GHz inset are measurements of Becker and Autler (1946), where $T = 318$ K, $P = 1013$ mbar, and $\rho_v = 10$ g m⁻³. Points in the 100-200-GHz inset are measurements quoted by Dryagin et al. (1966), where $T = 300$ K, $P = 1013$ mbar, and $\rho_v = 7.5$ g m⁻³.

Attenuation by O₂

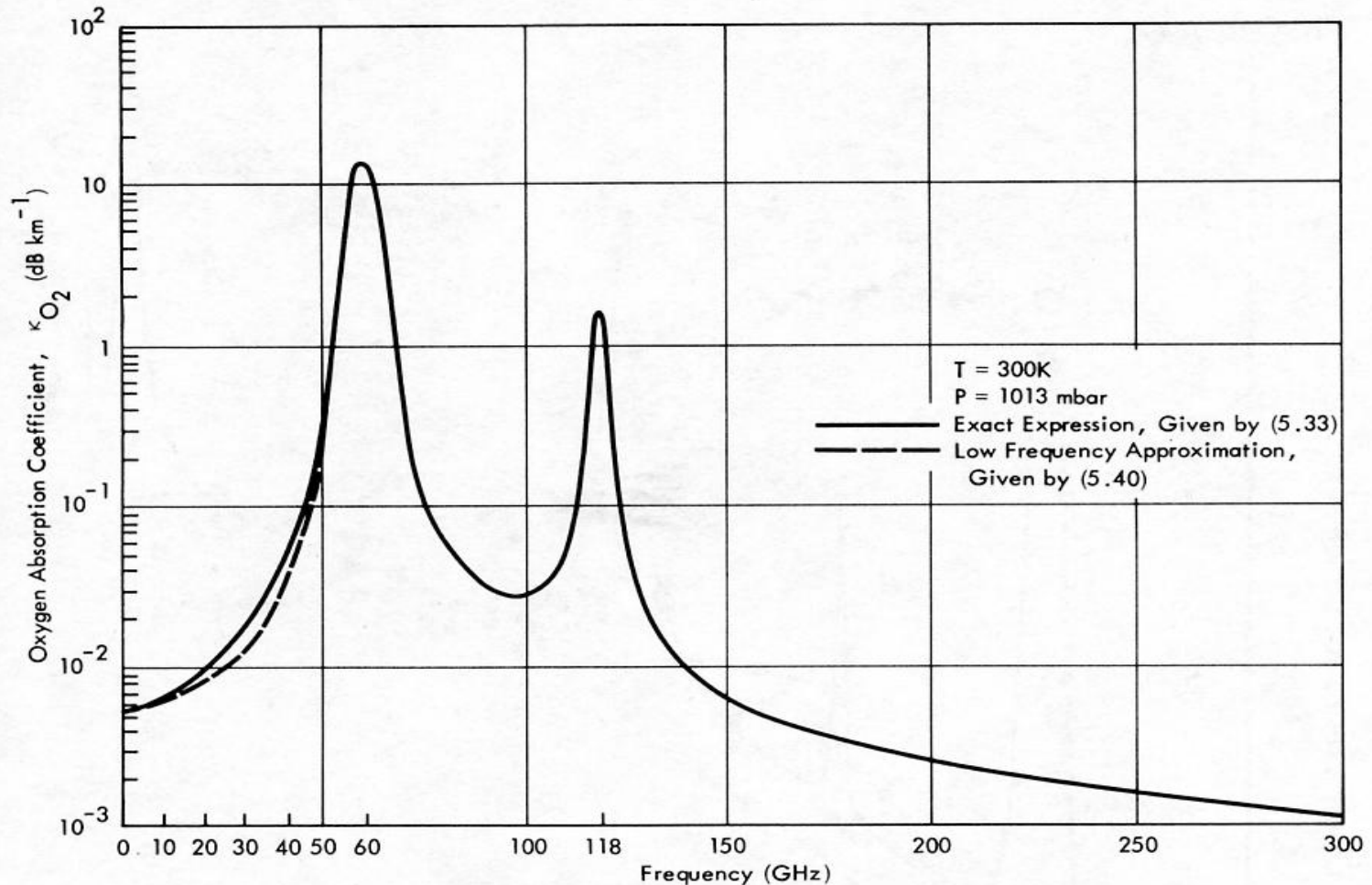


Fig. 5.6 Calculated oxygen absorption for sea-level conditions. The dashed curve is based on the low-frequency approximation given by (5.40).

Attenuation by H₂O

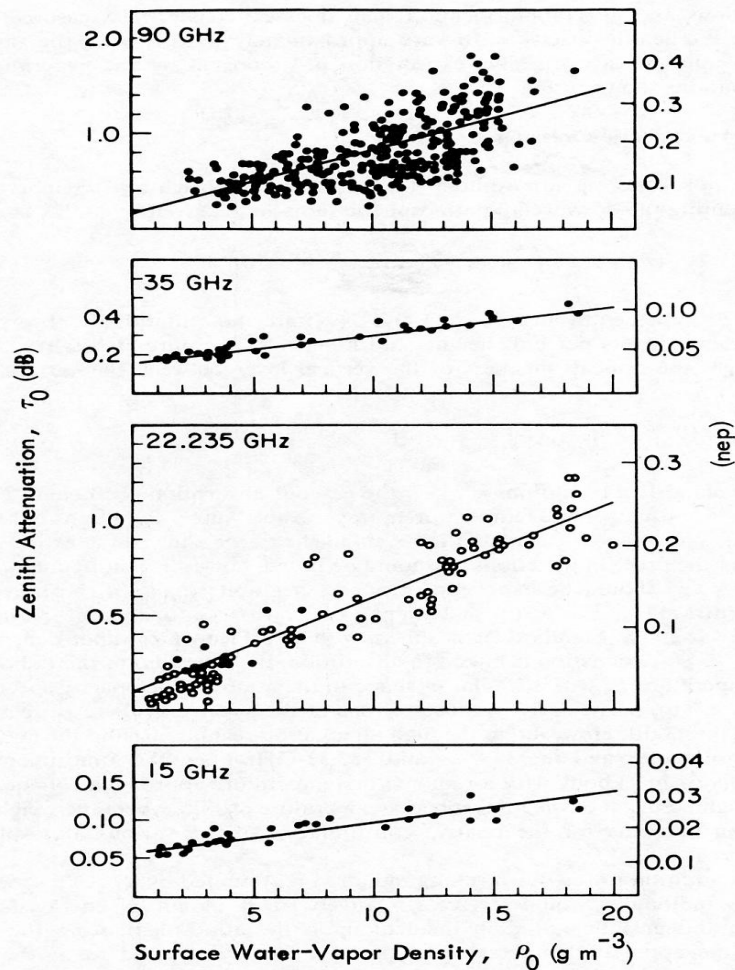
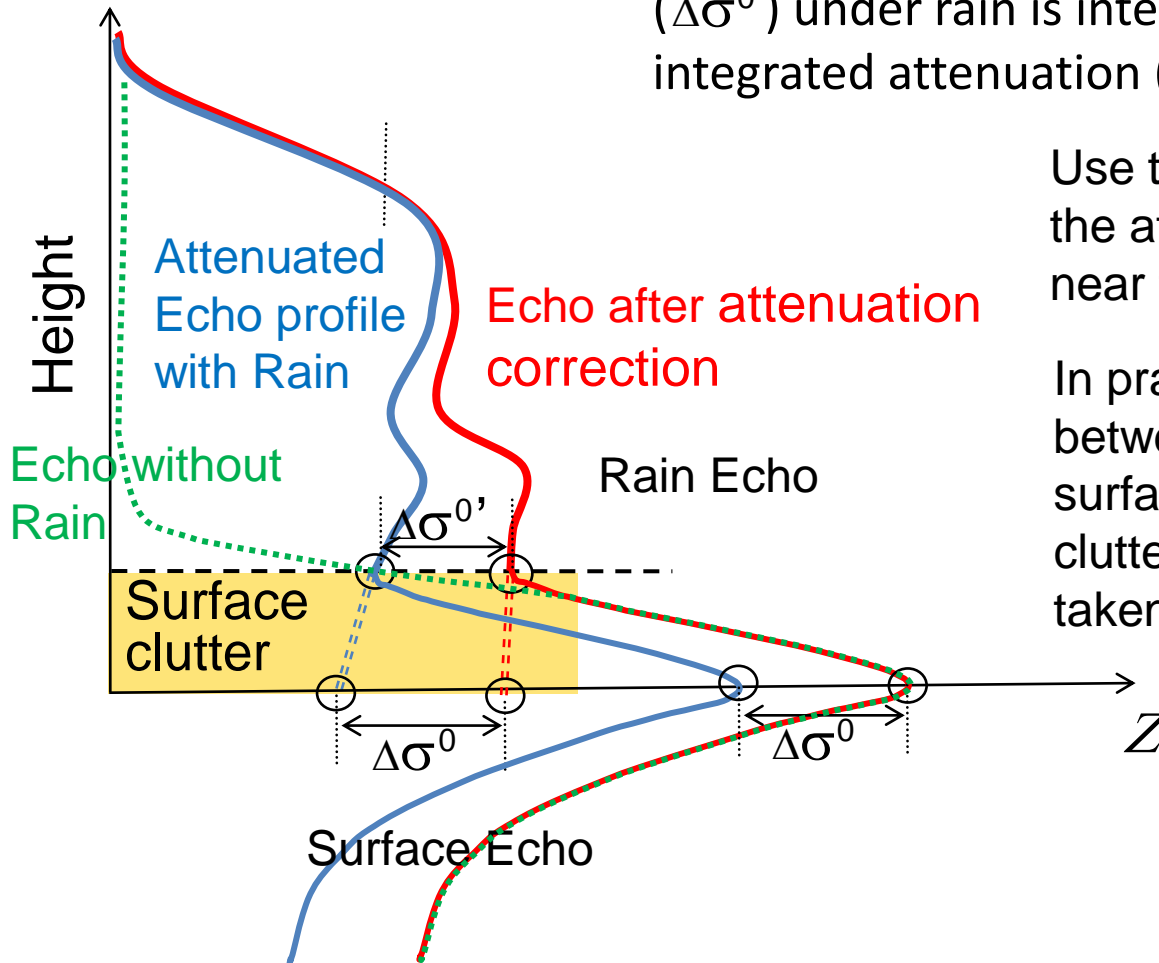


Fig. 5.8 Atmospheric zenith opacity versus surface water-vapor density (from Waters, 1976). The equations for the straight lines that best fit the points are: at 90 GHz, $\tau_0(\text{dB})=0.17+0.06\rho_0(\text{g m}^{-3})$; at 35 GHz, $\tau_0(\text{dB})=0.17+0.013\rho_0(\text{g m}^{-3})$; at 22.235 GHz, $\tau_0(\text{dB})=0.11+0.048\rho_0(\text{g m}^{-3})$; and at 15 GHz, $\tau_0(\text{dB})=0.055+0.004\rho_0(\text{g m}^{-3})$. Open points are values calculated by Waters, and closed points are measured values reported in the literature and summarized in the above form by Waters (1976).

Surface Reference Technique

Decrease of the apparent surface echo ($\Delta\sigma^0$) under rain is interpreted as the path-integrated attenuation (PIA) due to rain.



Use this PIA to correct for the attenuation of rain echo near the surface.

In practice, the difference between the PIA to the surface and the PIA to the clutter-free bottom must be taken into account.

Drop Size Distribution (DSD)

- Both k - Z_e and R - Z_e relations depend on DSD.
- Hitschfeld-Bordan's solution assumes a k - Z_e relation.
- When the SRT is not applicable, the initial DSD determines the attenuation correction and the Z_e -to- R conversion.
- When the SRT is applicable, α can be adjusted to match the H-B estimate of PIA to the SRT PIA. This in effect corresponds to adjusting the initial DSD.

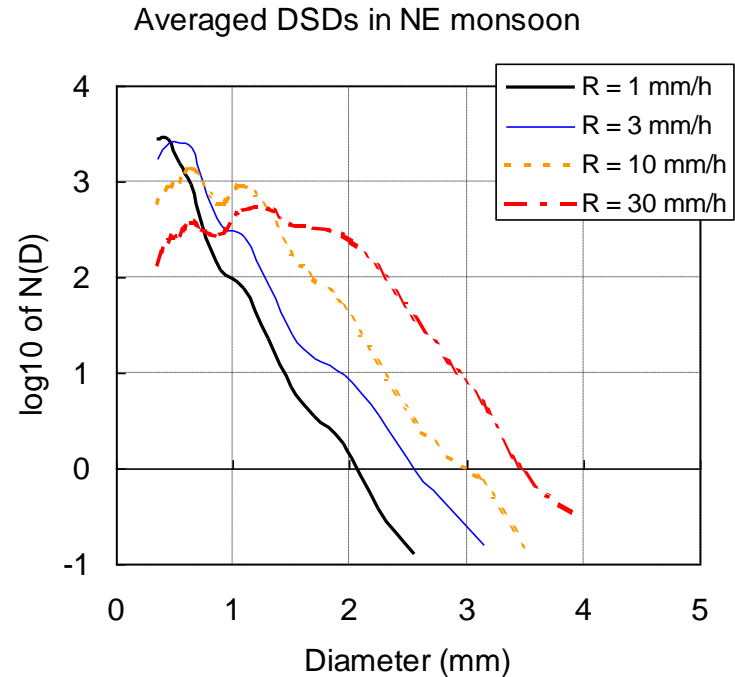
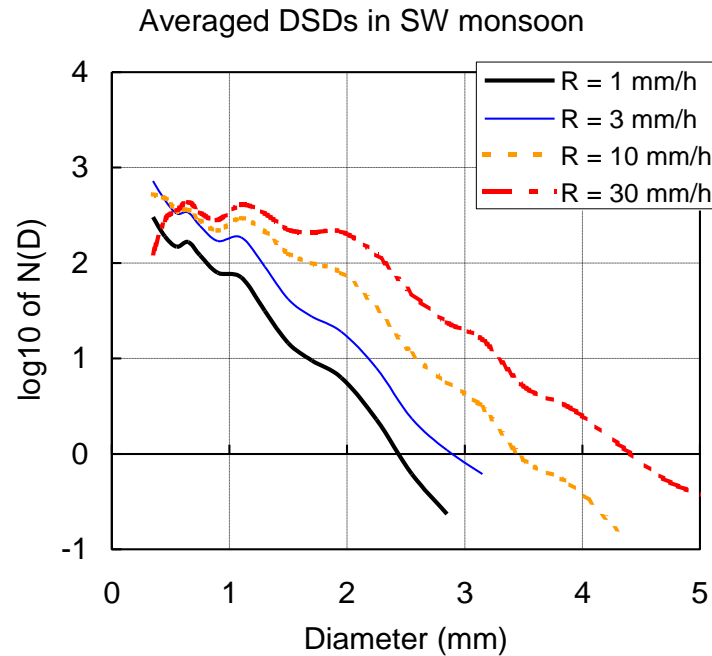
Hitschfeld-Bordan solution

$$Z_m(r) = Z_e(r) \exp \left(-0.2 \ln 10 \int_0^r k(s) ds \right)$$

If $k = \alpha Z_e^\beta$, then

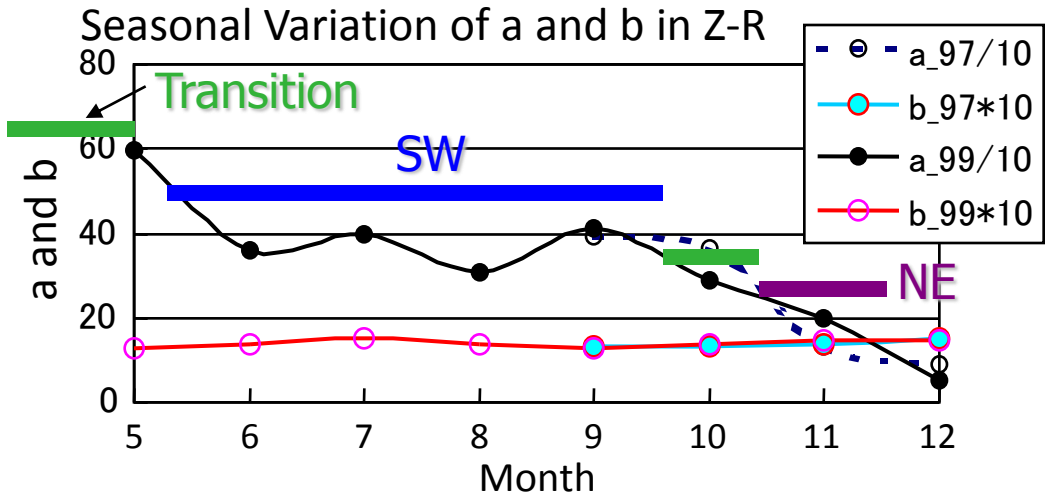
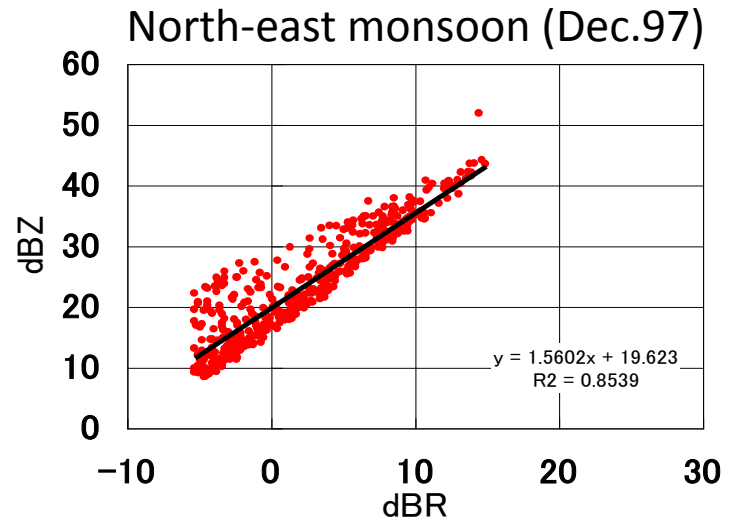
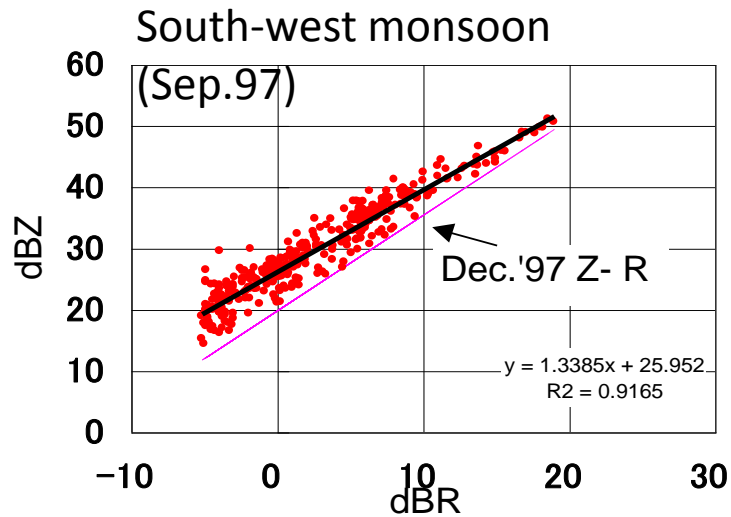
$$Z_e(r) = \frac{Z_m(r)}{\left(C_1 - 0.2 \ln(10) \beta \int_0^r \alpha(s) Z_m^\beta(s) ds \right)^{1/\beta}}$$

DSD variation in Indian rain



Averaged Dropsize Distribution during South-West (SW) and North-East (NE) monsoon seasons in Gadanki, south India in 1997 and 1999. SW and NE seasons are between May and October, and between November and December, respectively. DSDs within ± 1 dB centered at the rain rate specified are averaged.

Z-R relations in SW and NE Indian monsoon seasons



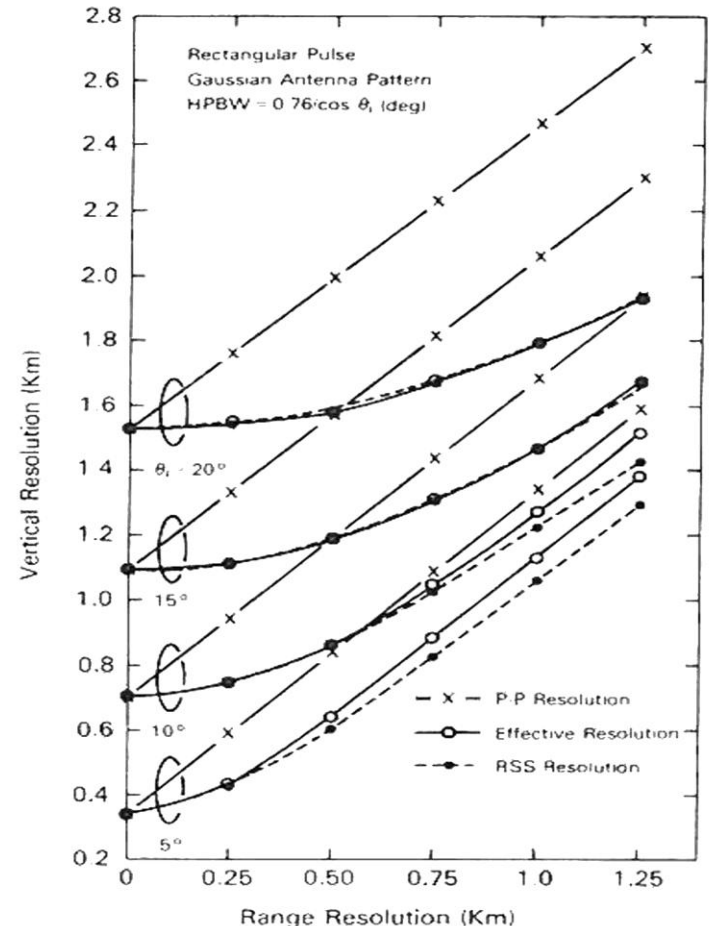
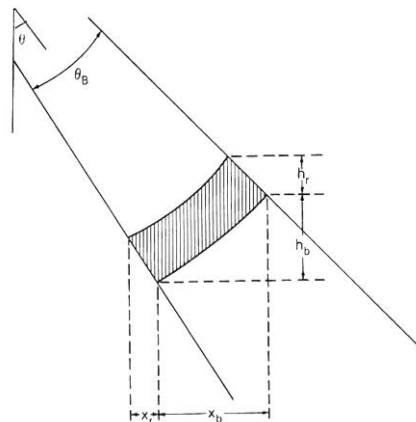
$$\text{SW } Z = 405R^{1.29}$$

$$\text{NE } Z = 144R^{1.38}$$

Strat/Conv separation:
Not significant

Off-nadir observations (1/2)

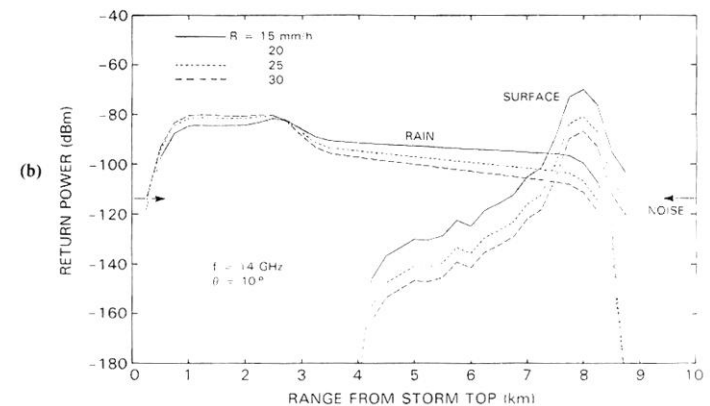
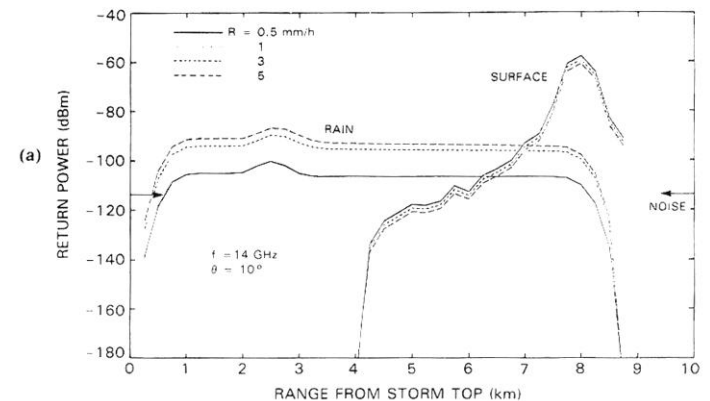
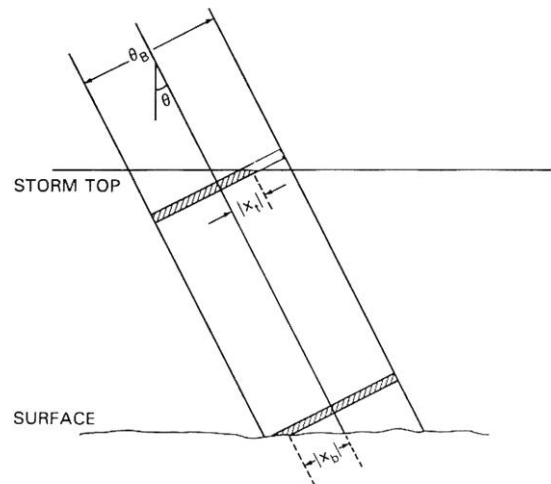
- Echo power consists of reflectivity distribution weighted by the antenna gain pattern and the pulse shape.
- Since the beam width near surface is much larger than the range resolution, the effective vertical resolution degrades with off-nadir angle.



(From Meneghini and Koizu)

Off-nadir observations (2/2)

- Surface echoes are generally much stronger than rain echoes.
- At off-nadir, surface echoes may contaminate rain echo near the surface. (Main-lobe problem)



(From Meneghini and Kozu)

Difference between radar and radiometer retrieval of rain

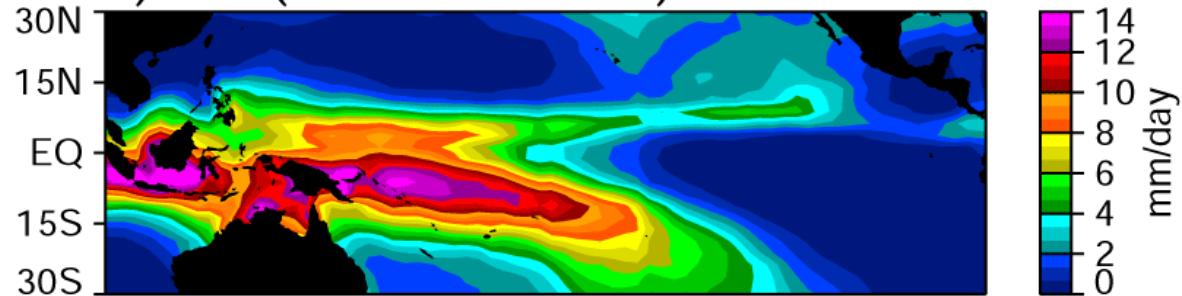
- Radar
 - well defined range information
 - Height information is very reliable.
 - Z-R relation scatters more than T_b -R relation
 - Echo power is more sensitive to DSD variation than T_b .
 - Number of wavelengths is very limited in practice.
- Radiometer
 - Needs to assume a vertical precipitation profile.
 - e. g., freezing height

Comparison of different satellite rainfall estimation algorithms

Mean DJF Rainfall (1987 – 1996)

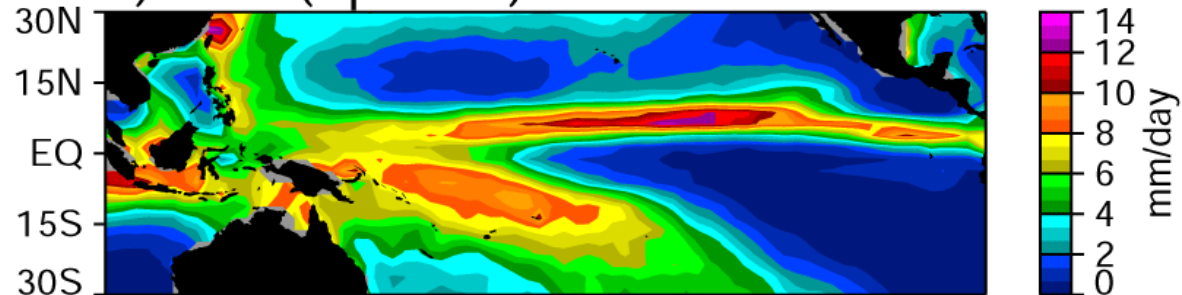
a) GPI (Arkin & Meisner)

Infrared



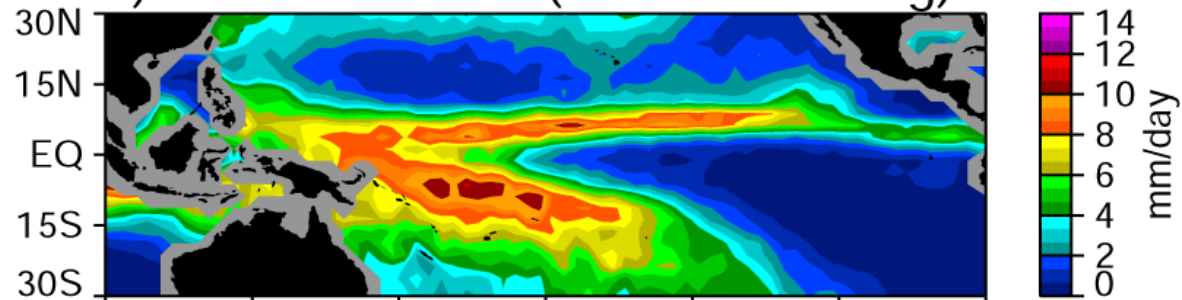
b) MSU (Spencer)

**Microwave Radiometer
(50GHz)**



c) SSM/I Emission (Wilheit & Chang)

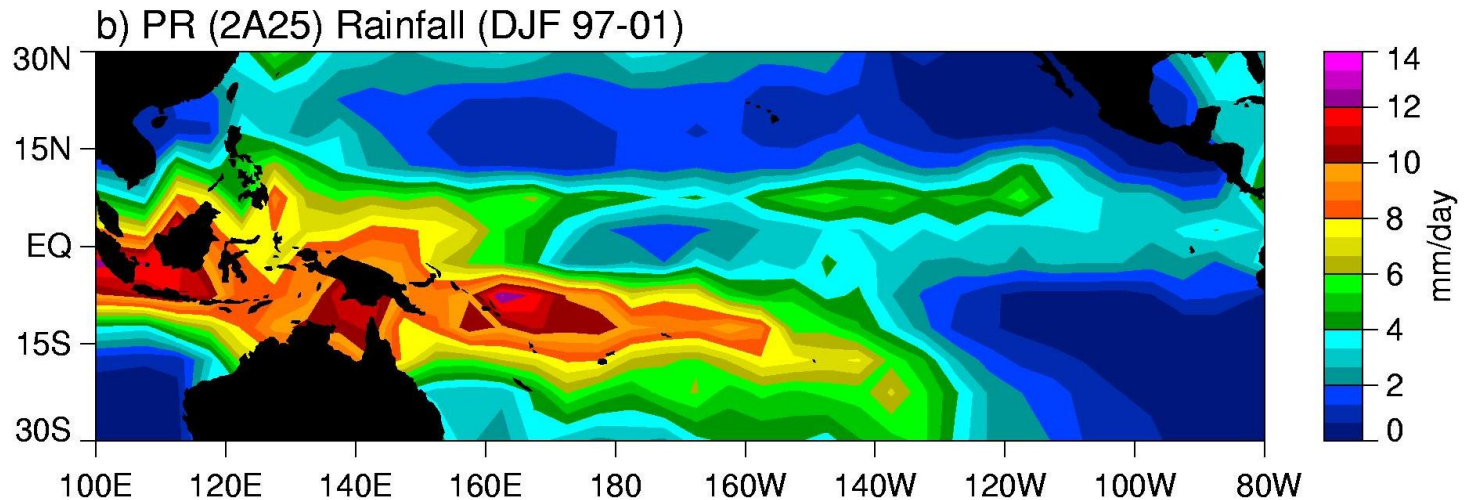
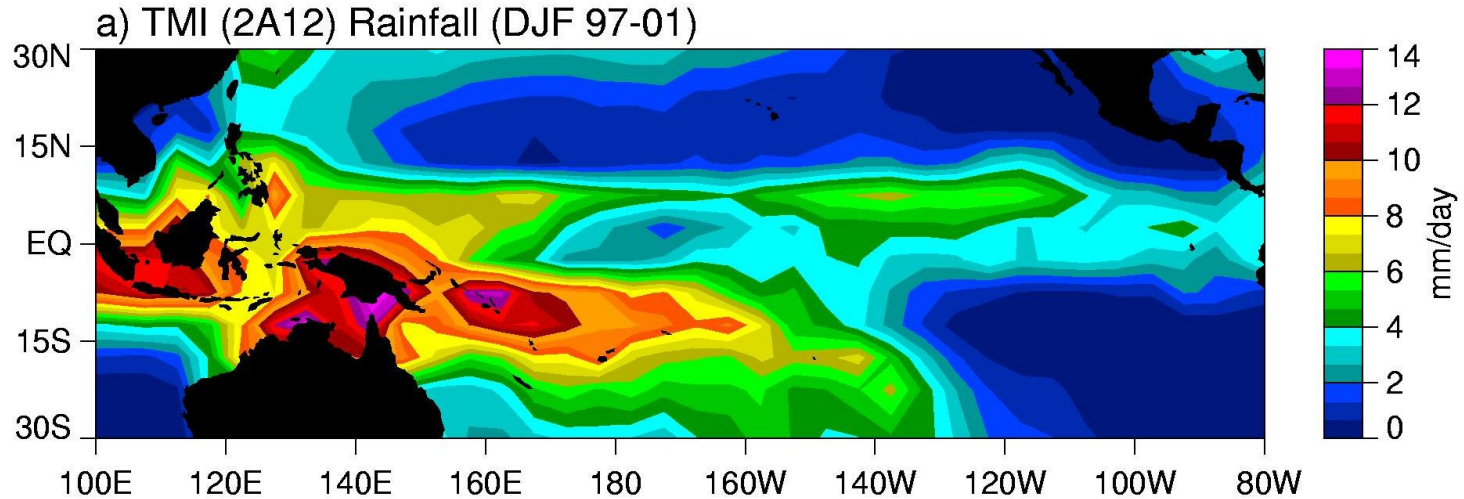
**Microwave Radiometer
(Multi-channel)**



100E 130E 160E 170W 140W 110W 80W

Comparison between TMI and PR rainfall estimates

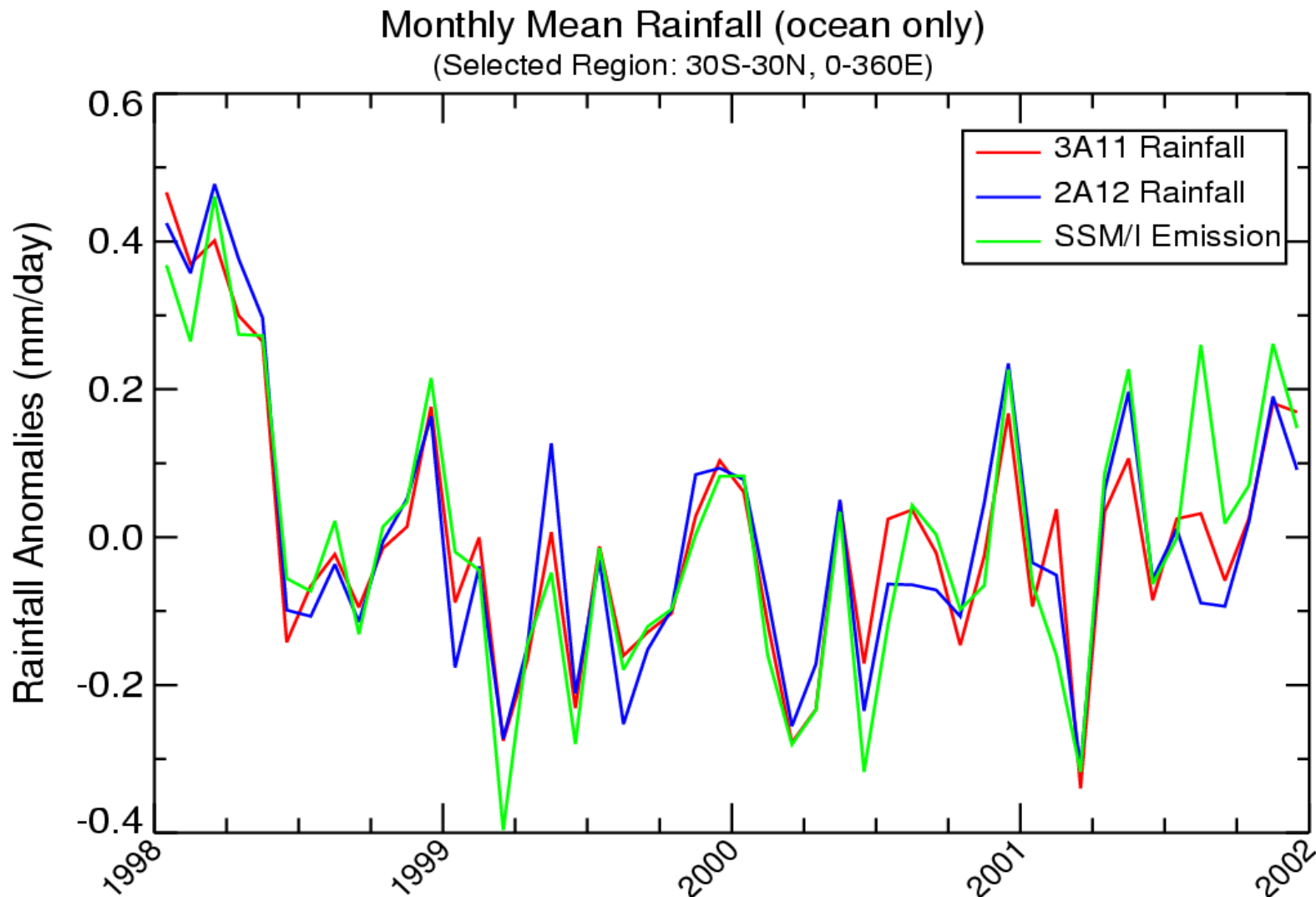
(Bias Adjusted TRMM Retrievals)



(W. Berg, et al.)

Time series of monthly mean rainfall anomalies over Tropical ocean

—Comparison among different passive microwave algorithms—



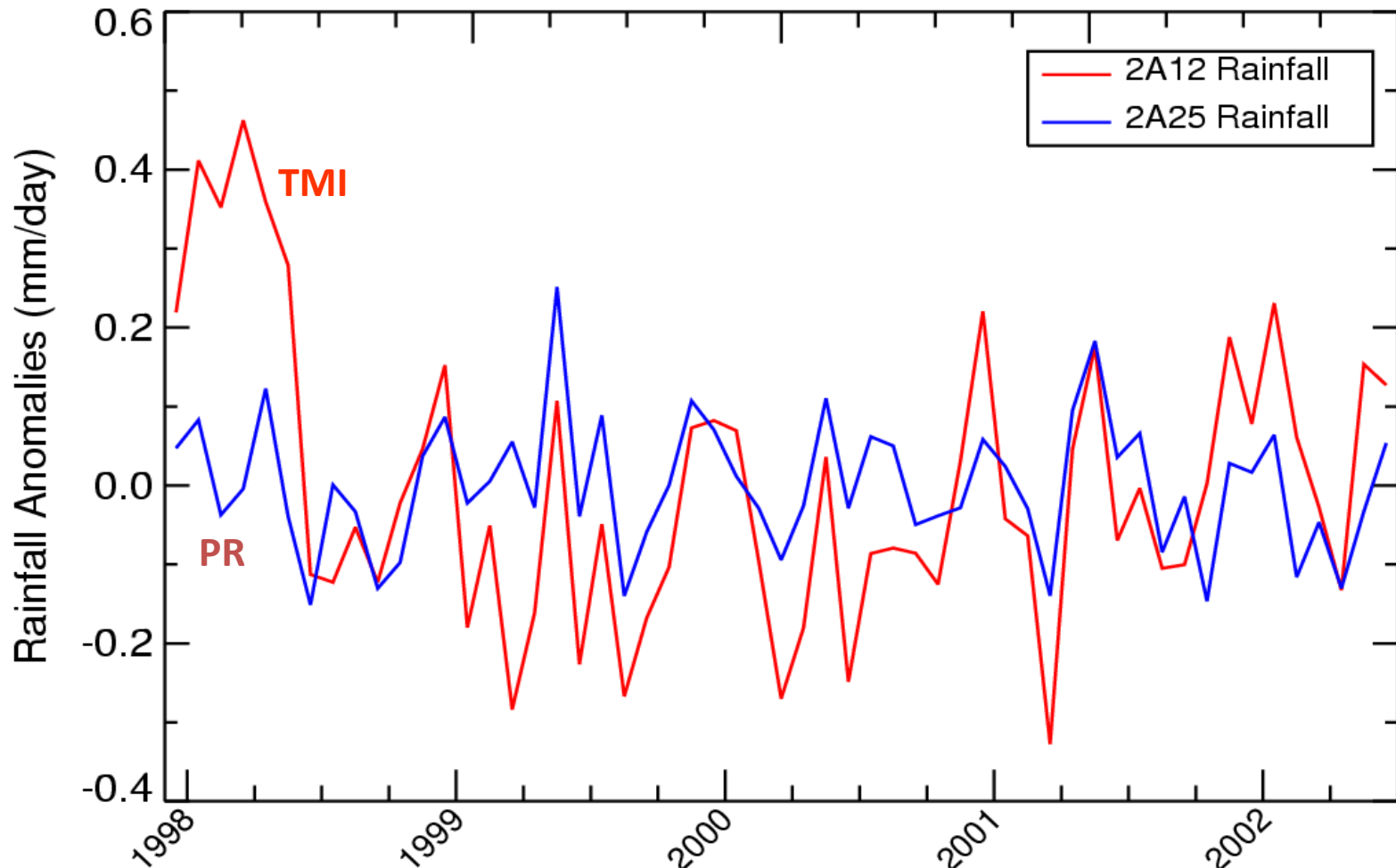
(W. Berg, et al.)

Time series of monthly mean rainfall anomalies over Tropical ocean

(TRMM Ocean Retrievals)

Monthly Mean Rainfall (ocean only)

(Selected Region: 30S-30N, 0-360E)

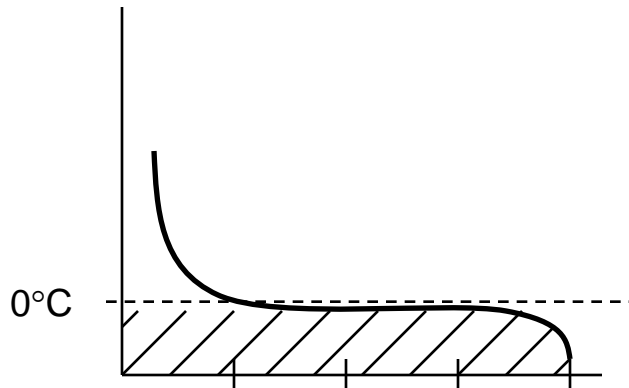


Passive Microwave Retrievals

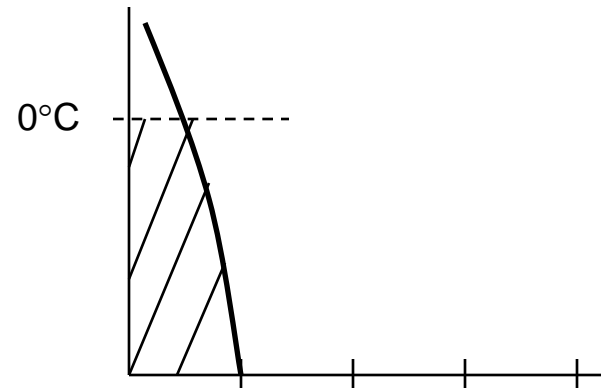
Column integrated water vs rainfall rate

Tb's in the low frequency channels of a microwave radiometer are proportional to the column integrated rain water content.

Freezing Level

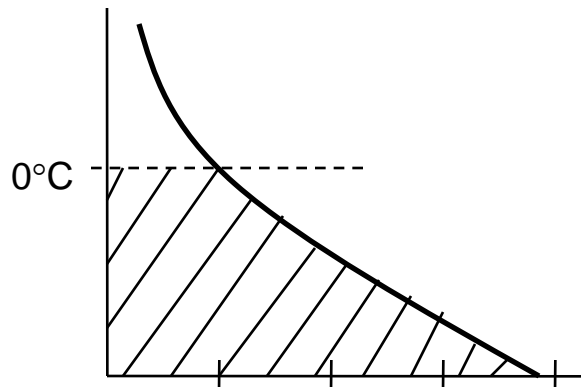


Surface Rainfall

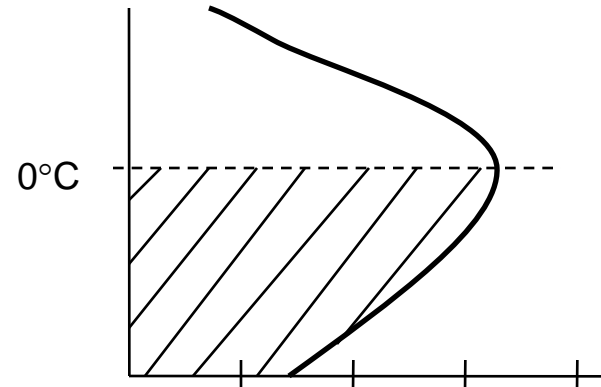


Surface Rainfall

Rain Profile



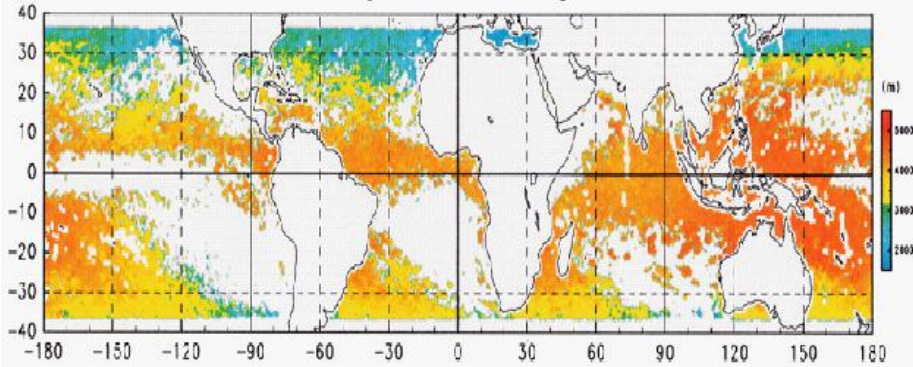
Surface Rainfall



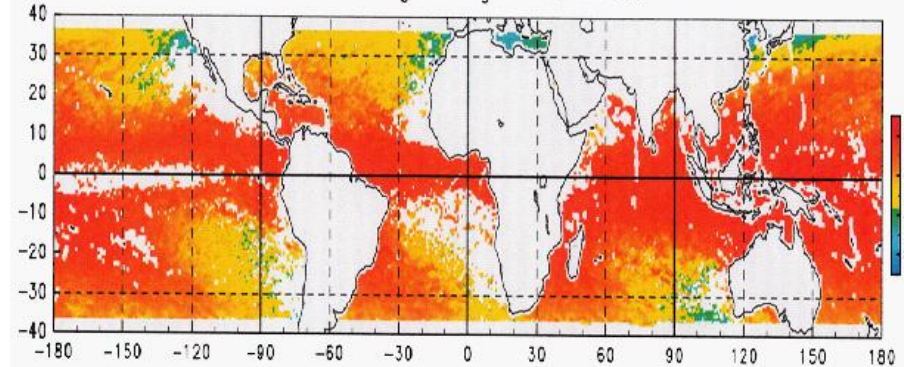
Surface Rainfall

PR Bright-Band Height and TMI Freezing Height

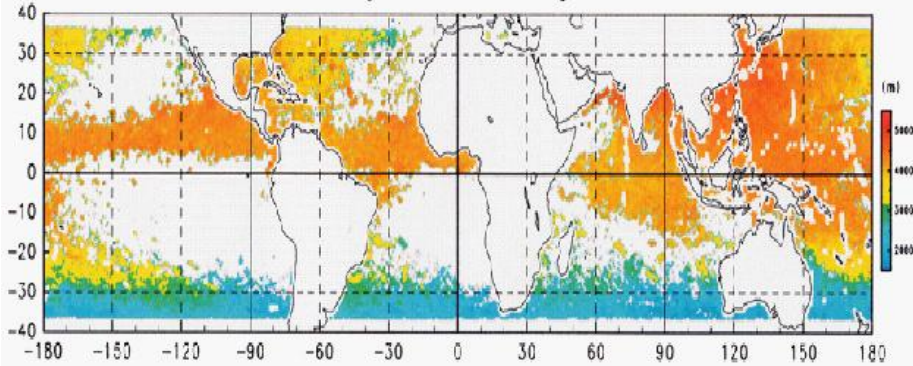
PR-3A25 bright band height DJF1999



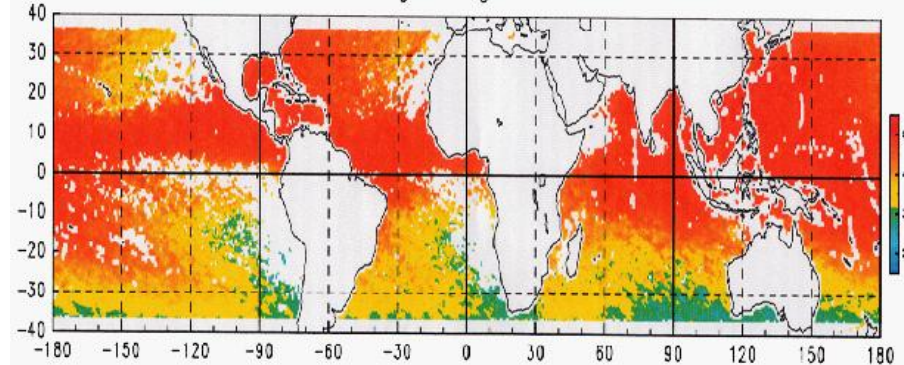
Freezing height DJF1999



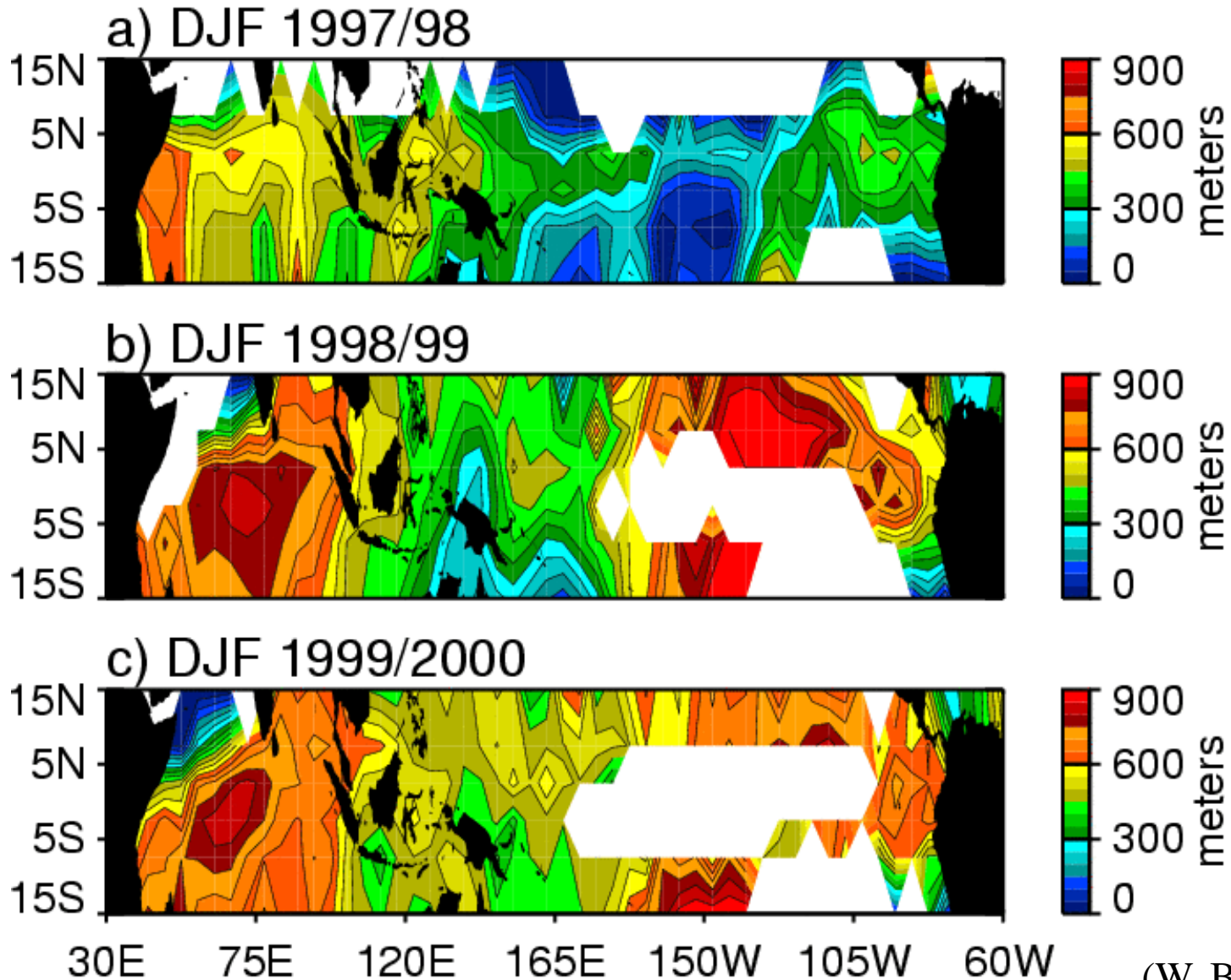
PR-3A25 bright band height JJA1999



Freezing height JJA1999



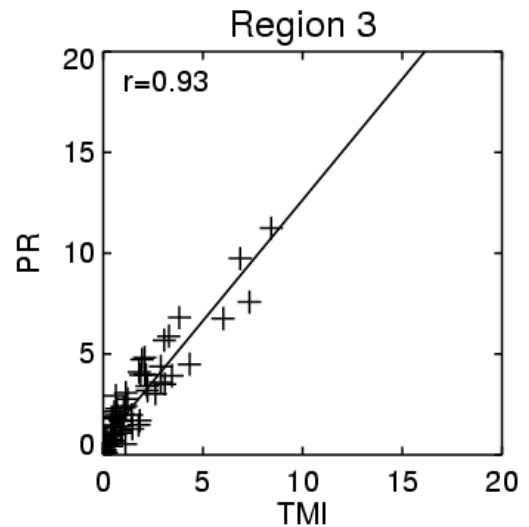
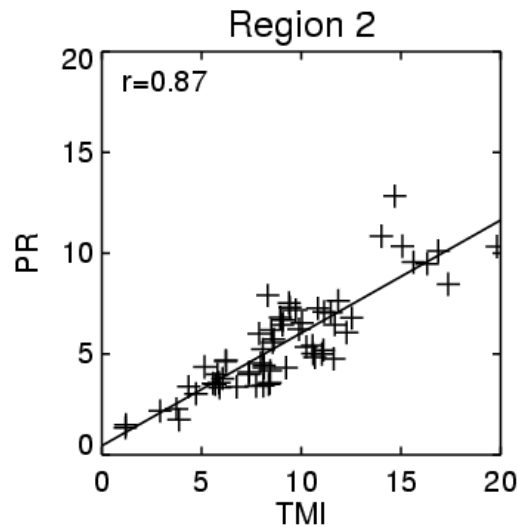
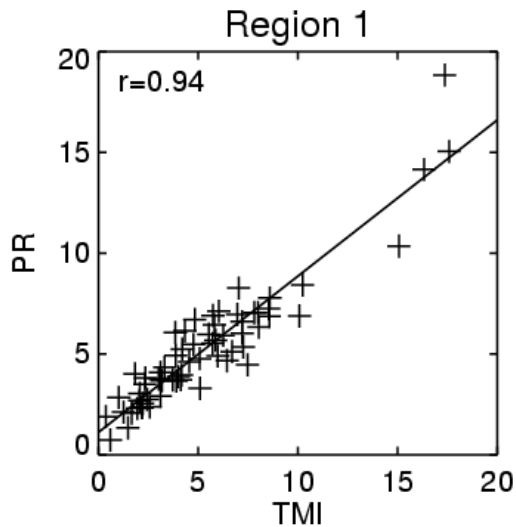
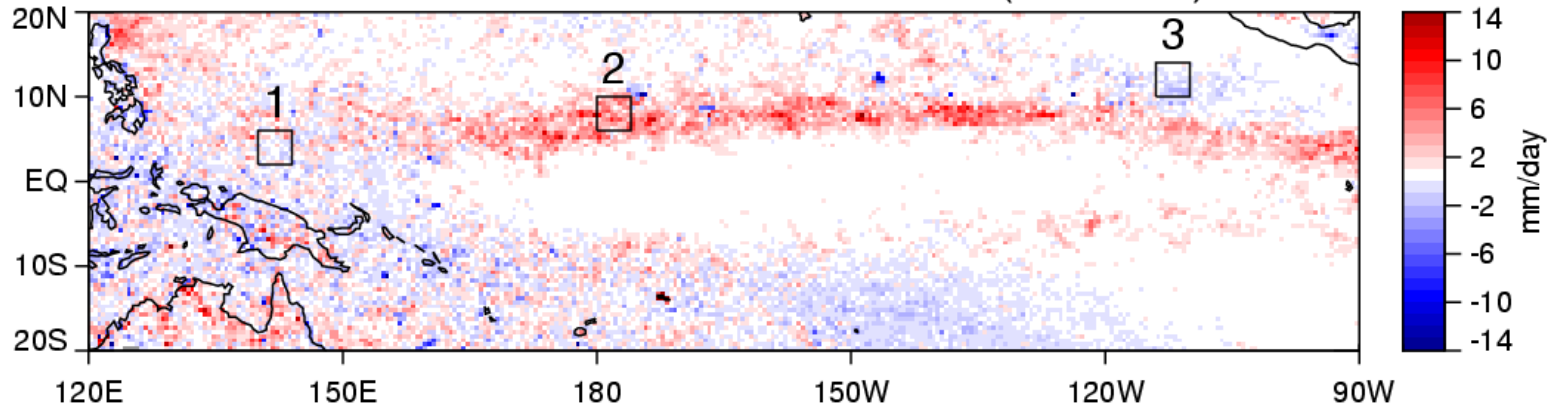
TMI Freezing Height – PR Bright Band Height



(W. Berg, et al.)

PR and TMI Regional Validation

Dec-Jan-Feb 1999/2000 Rainfall Bias (TMI - PR)

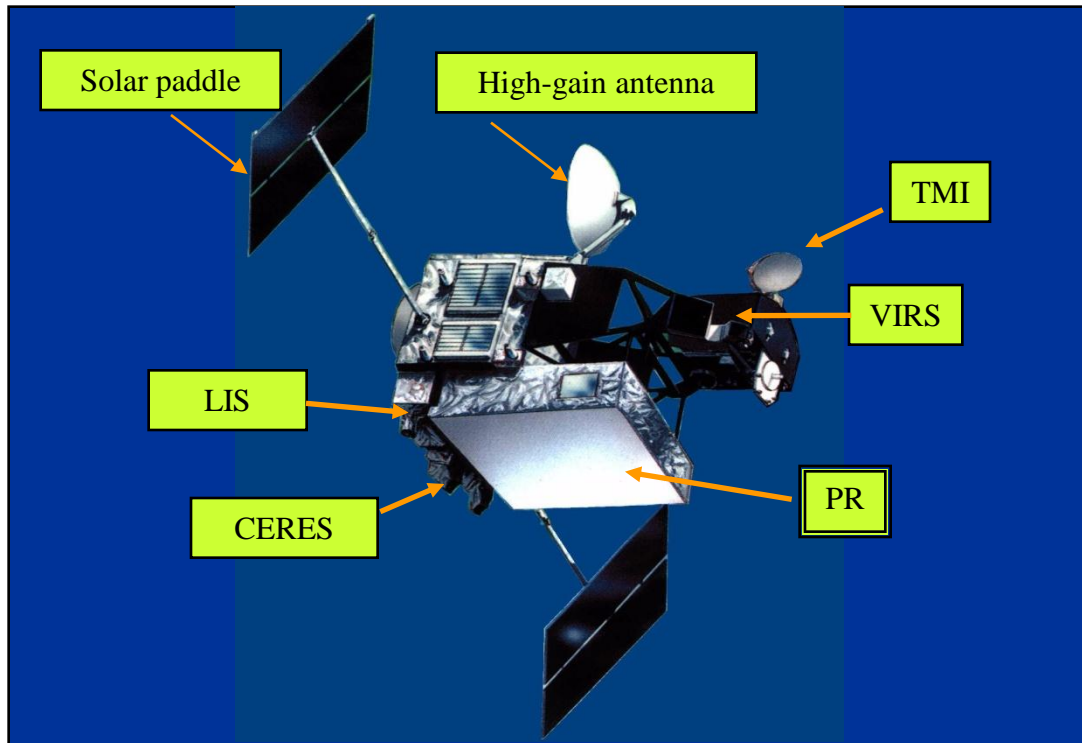


Current and future satellite missions carrying a precipitation or cloud radar

- Tropical Rainfall Measuring Mission (TRMM) / PR
 - November 1997 – present
 - Single frequency (13.8 GHz),
 - 250 km swath, >18 dBZ, 250 m v. res.
- Global Precipitation Measurement (GPM) / DPR
 - 2013 (launch)
 - Dual-frequency (13.6 GHz, 35.5GHz)
 - 250 km swath, >12dBZ (Ka, 125 km swath, 500 m vert. res)
- CloudSat/CPR
 - April 2006 – present
 - 94GHz, nadir only, > -30dBZ, 500 m vertical res.
- EarthCARE/CPR
 - 2013 (launch)
 - 94GHz, nadir only, > -35dBZ, 500 m vertical res.
 - Doppler



Tropical Rainfall Measuring Mission: TRMM



Observation of tropical rainfall (Driving engine of global atmosphere)

US-Japan joint mission (Japan: PR, Launch, US: Bus, 4 sensors, operation)

Launched in Nov., 1997. Still under operation

First space-borne precipitation radar developed by CRL and NASDA

Orbit	Circular (Non-Sun Synchronous)
Altitude	350km (402.5km since Aug. 2001) (± 1.25 km)
Inclination	35 deg.
Sensor	Precipitation Radar (PR) TRMM Microwave Imager (TMI) Visible and Infrared Scanner (VIRS) Clouds and the Earth's Radiation Energy System (CERES) Lightning (LIS)

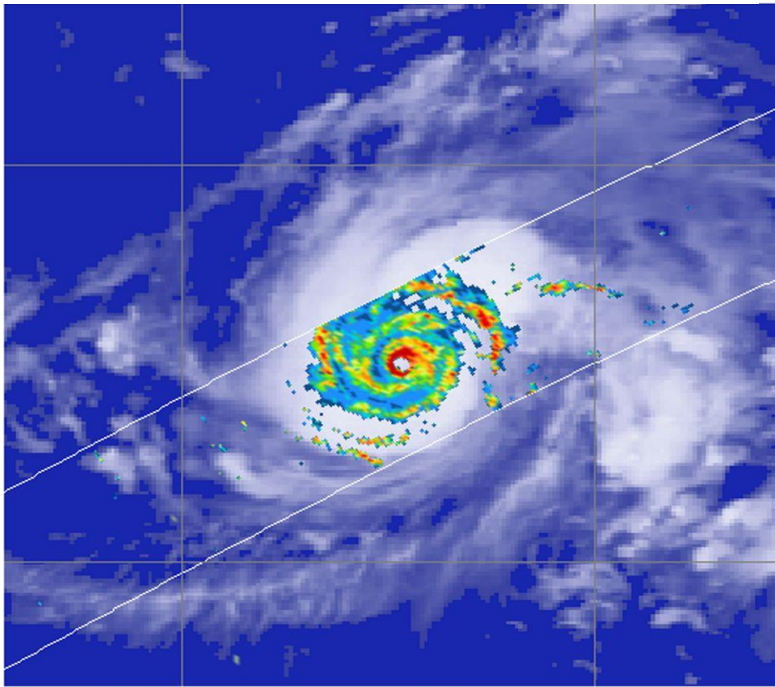


3-D Observation of a Typhoon by the PR

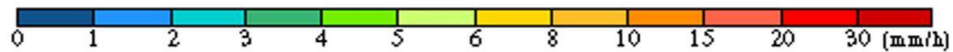
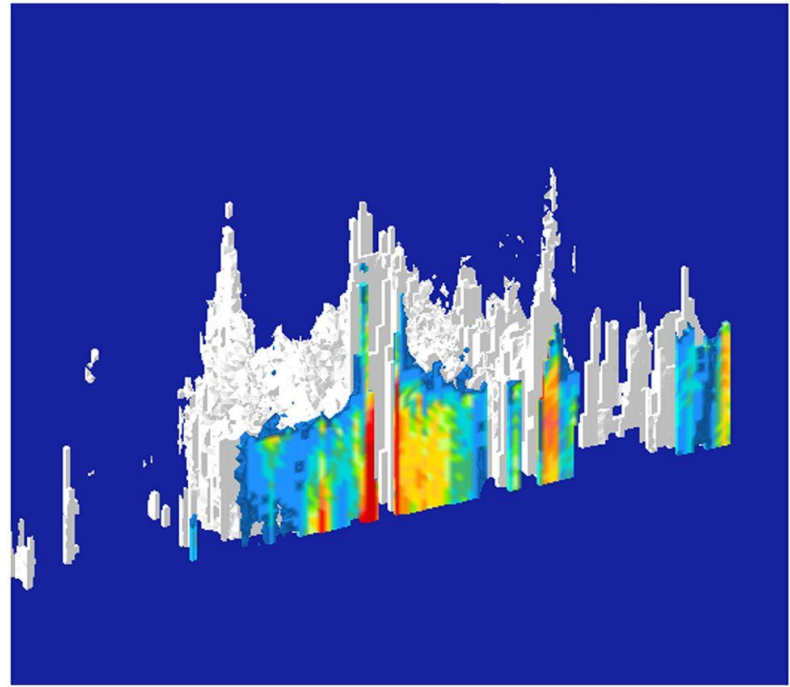
TRMM PR 2A25 Rain

Aug. 2, 2000, 20:49-20:53 (Japanese local time)

Rain intensity at H=2 km



Vertical cross section through the eye and 3D structure



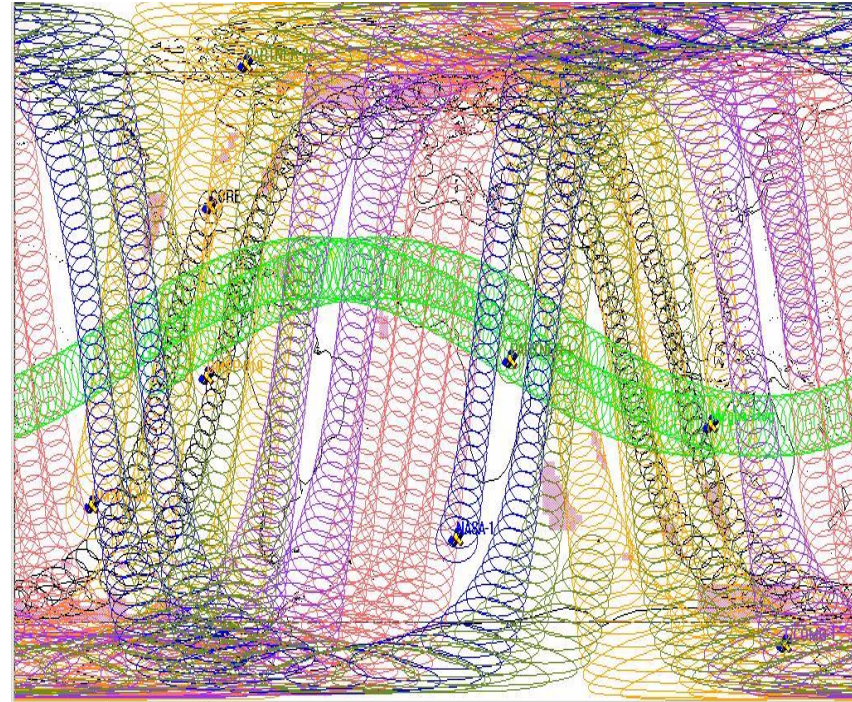
PR realized observation of 3D structure of rain over ocean where few observations had been available.



What's Next to TRMM? GPM

A Mission to:

- Measure a broader spectrum of precipitation (e.g. **light rain, snow**)
- Provide measurements in the tropics and mid-latitudes (e.g. **global**)
- Provide global precipitation products **every 3 hours** with 90% accuracy
- Further reduce uncertainty in precipitation **microphysics** and rainfall-radar reflectivity measurements
- Provide global precipitation measurements at temporal scales needed by **weather, climate, and hydrological models**
- Enable new **societal applications** in weather forecasting, flood prediction, freshwater resource management, public communications, and education



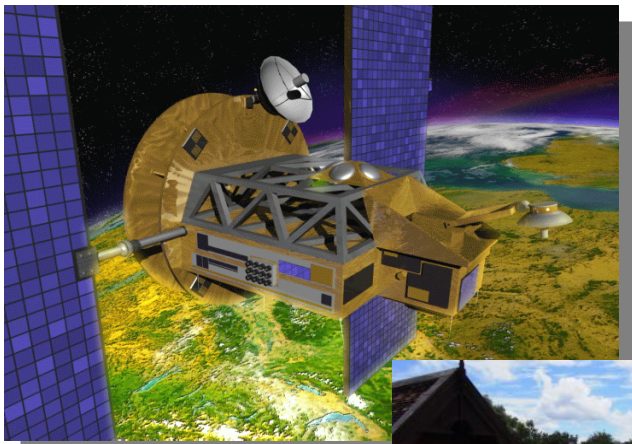
GPM Era Global Coverage

The Mission is Global Precipitation Measurement (GPM)

Scientific and Social Significance of GPM

Precision brought by DPR

- High sensitivity to detect weak rain and snow
- Accurate estimation of rainfall rate
- Separation of snow from rain
- Progress in cloud physics



Global rain map in every 3 hours by GPM

- Climate change assessment
 - monitor variations in rainfall and rain areas associated with climate changes and global warming
- Improvement in weather forecasts
 - Quasi-real-time assimilation of data in numerical prediction models,
 - Improved flood prediction
- Water resource management
 - river, dam, agricultural water, etc.
- Agricultural production forecasting

GPM Reference Concept

OBJECTIVE: Understand the Horizontal and Vertical Structure of Rainfall and Its Microphysical Element. Provide Training for Constellation Radiometers

OBJECTIVE: Provide Enough Sampling to Reduce Uncertainty in Short-term Rainfall Accumulations. Extend Scientific and Societal Applications.

Core Satellite

- Dual Frequency Radar
- Multi-frequency Radiometer
- H2-A Launch
- TRMM-like Spacecraft
- Non-Sun Synchronous Orbit
- ~70 deg. Inclination
- ~400 - 500 km Altitude
- ~5 km Horizontal Resolution
- 250 m Vertical Resolution

Constellation Satellites

- Small Satellites with Microwave Radiometers
- Aggregate Revisit Time, 3 Hour goal
- Sun-Synchronous Polar Orbits
- ~600 km Altitude

Precipitation Validation Sites

- Global Ground Based Rain Measurement

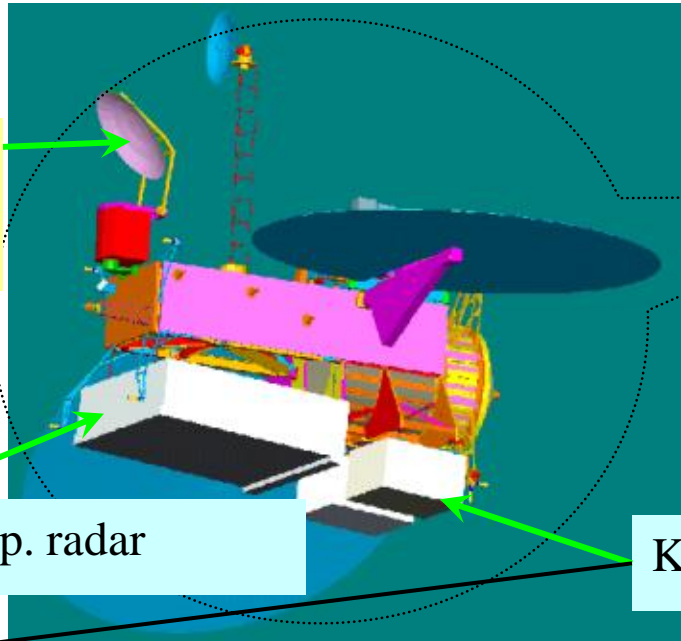
Global Precipitation Processing Center

- Capable of Producing Global Precip Data Products as Defined by GPM Partners



GPM Core Satellite

Microwave radiometer



Core



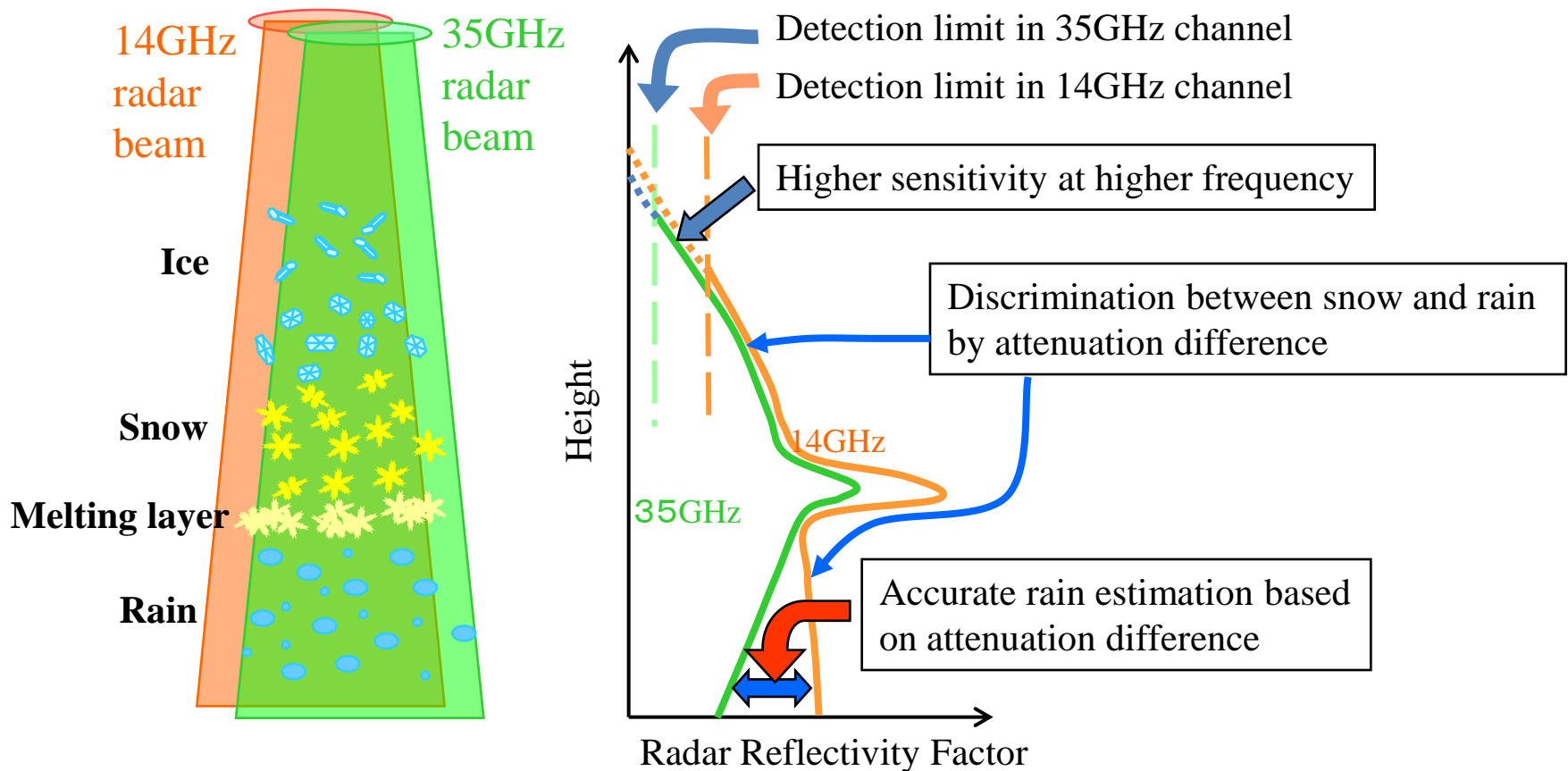
Ku-band precip. radar

Ka-band precip. radar

Frequency	Ku-band (13.6 GHz), Ka-band (35.5 GHz)
Sensitivity	Ku-band --- same as TRMM PR (18 dBZ, $\Delta z=250$ m) Ka-band --- same as Ku-band (18 dBZ, $\Delta z=250$ m) --- 6 dB better than Ku-band (12 dBZ, $\Delta z=500$ m)
Swath width	245 km (Ku), >100 km (Ka)
Footprint	5 km

Frequency	10 GHz --- 85 GHz (5 bands, 9 channels) --- similar to TMI
Swath width	Approximately 900 km (Conical scan)
Footprint	40 x 60 km (10 GHz) --- 5 x 8 km (85 GHz)

Dual Frequency Precipitation Radar



Measure 3-D structure of rain as TRMM, but with better sensitivity

Accumulate climatological precipitation data continuously since TRMM

Improve estimation accuracy with dual-frequency radar

Identification of hydrometer type

Estimation of DSD parameters

DPR Specifications (Tentative)

Item	13.6-GHz radar (Ku-PR)	35.5-GHz radar (Ka-PR)
Antenna Type	Active Phased Array	Active Phased Array
Beam Number	49	20+19+x
Swath Width	245 km	100 km
Pulse Width	1.67 micro sec. (x2)	1.67/3.34 micro sec. (x2)
Range Resolution	250 m	250 m / 500 m
Beam Width	0.7 deg.	0.7 deg.
Horizontal Resolution	5 km	5 km
PRF	VPRF (4000 Hz \pm 250 Hz)	VPRF (4500 Hz \pm 250 Hz)
Peak Power	1000 W	144 W [current]
Sensitivity	17 dBZ (0.4 mm/hr)	12 dBZ (0.2 mm/hr) [target]
Data Rate	95 kbps	95 kbps
Mass	370 kg	290 kg
Power Consumption	334 W [max 352 W]	306 W [max 331 W]
Dimensions	2.4 \times 2.4 \times 0.6 m	1.3 \times 1.0 \times 0.7 m

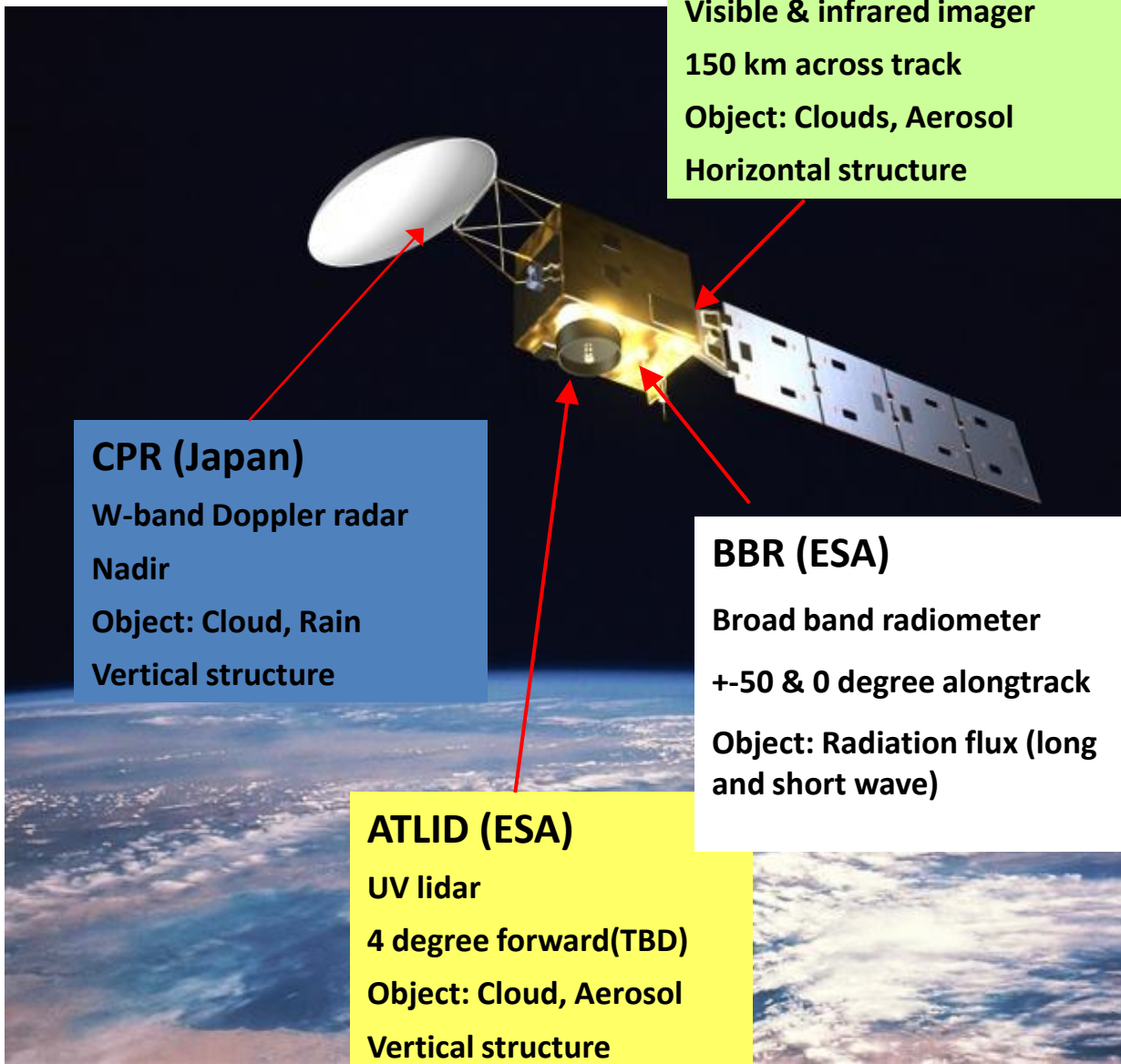
CloudSat CPR System Characteristics

- Nominal Frequency 94 GHz Pulse Width 3.3 μ sec
 - Minimum Detectable $Z^* < -29$ dBZ PRF 4300 Hz
 - Data Window 0-25 km Antenna Size 1.85 m
 - Dynamic Range 70 dB Integration Time 0.16 sec
 - Nadir Angle (since 15 Aug 2006***) 0.16°
 - Vertical Resolution 500 m Cross-track Resolution 1.4 km
 - Along-track Resolution** 1.7 km Data Rate 20 kbps
-
- *Equivalent radar reflectivity that gives a mean power equal to the standard deviation after integration and noise subtraction. Atmospheric attenuation is not included.
 - **The along-track resolution is based on averaging the instantaneous footprint over the integration time. Based on purely geometric arguments, the along-track resolution would be approximately 2.5 km. However, a more rigorous convolution calculation gives an along-track resolution of 1.7 km, as shown in the table.
 - ***Nadir angles were changed from approx. 1.71° to 0.0° on 7 July 2006 and from 0.0° to 0.16° on 15 August 2006

What is EarthCARE ?

EarthCARE (Earth Clouds, Aerosols and Radiation Explore)

- Satellite mission selected as the sixth Earth Explorer Mission in 2004 of ESA
- European Space Agency (ESA) and Japanese (JAXA, NICT) collaboration
- Objective: global clouds and aerosol vertical observation for global radiation budget
- Launch: 2013
- Instrument:
 - Cloud Profiling Radar (CPR)
 - Atmospheric Lidar (ATLID)
 - Multi-spectral Imager (MSI)
 - Broad Band Radiometer (BBR)



MSI (ESA)

Visible & infrared imager
150 km across track
Object: Clouds, Aerosol
Horizontal structure

CPR (Japan)

W-band Doppler radar
Nadir
Object: Cloud, Rain
Vertical structure

ATLID (ESA)

UV lidar
4 degree forward(TBD)
Object: Cloud, Aerosol
Vertical structure

BBR (ESA)

Broad band radiometer
+-50 & 0 degree alongtrack
Object: Radiation flux (long
and short wave)

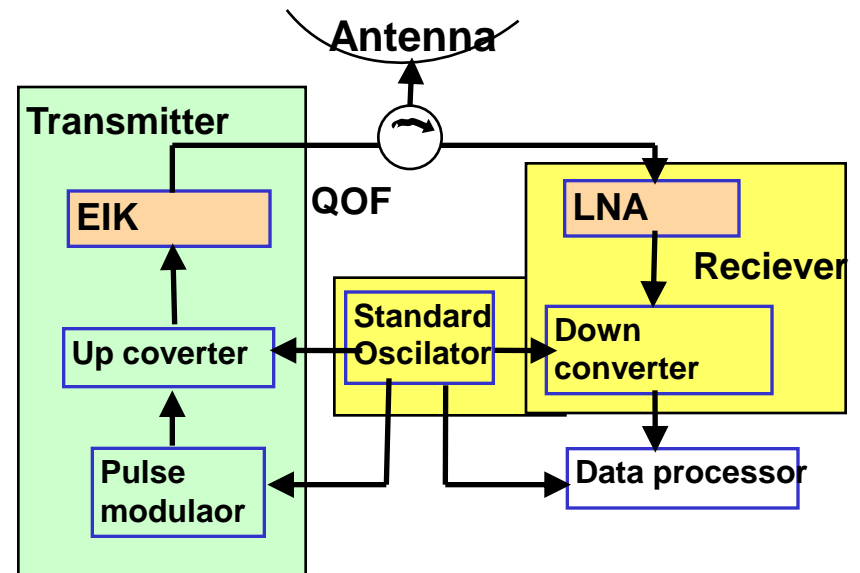
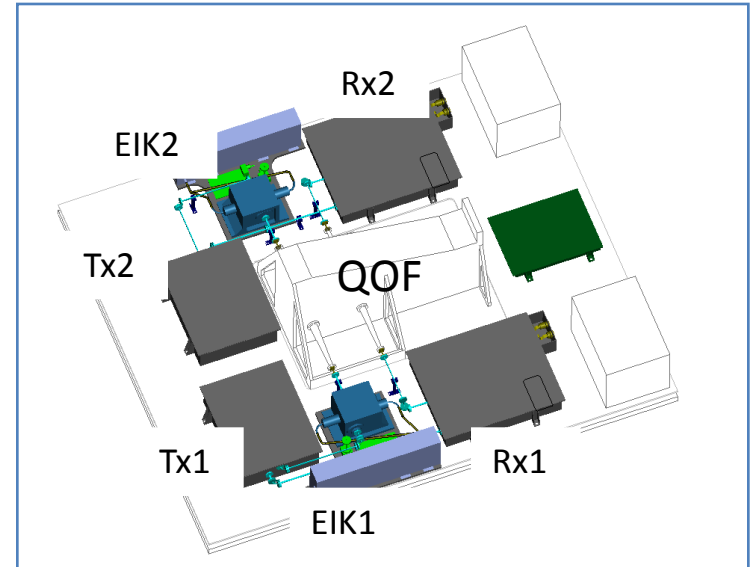
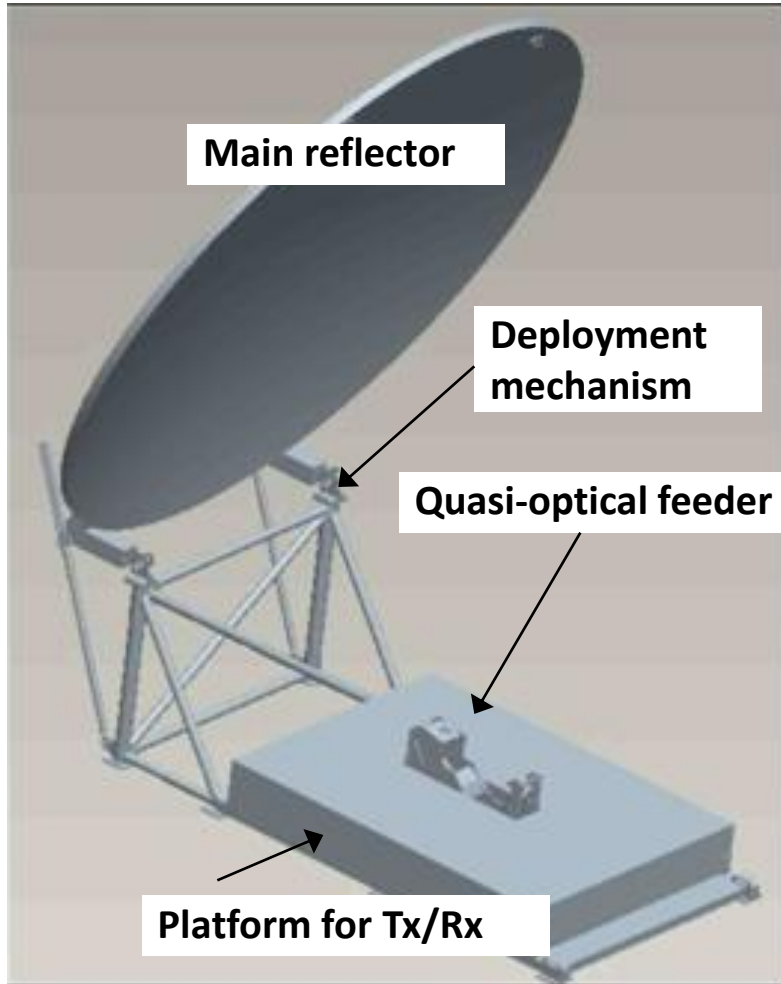
Orbit

- Sun-synchronous
- Inclination 97 degrees
- Altitude: 450 km (TBD)
- Local time: 13:30
descending node
- Period: 94 min
- Mission life: 3 years
- Revisit period: 10 - 30 days
(TBD)

Satellite

- Mass: 1300 kg
- Power: 1100 W
- Data rate: up to 1500
kbit/sec

CPR structure and function



CPR specifications

Tx frequency	94.05 GHz
Tx peak power	1.5 kW (EOL)
Pulse width	3.3 μ s
Polarization	Circular
Antenna diameter	2.5 m
Beam footprint size	700 m
Beam direction	Nadir
Minimum sensitivity	-35 dBZ (10km average)
Data sampling	100 m (Vertical) 500 m (Horizontal)
Doppler measurement	Pulse pair

Difference from CloudSat CPR

- Higher sensitivity (about 10 dB) from bigger antenna and lower orbit

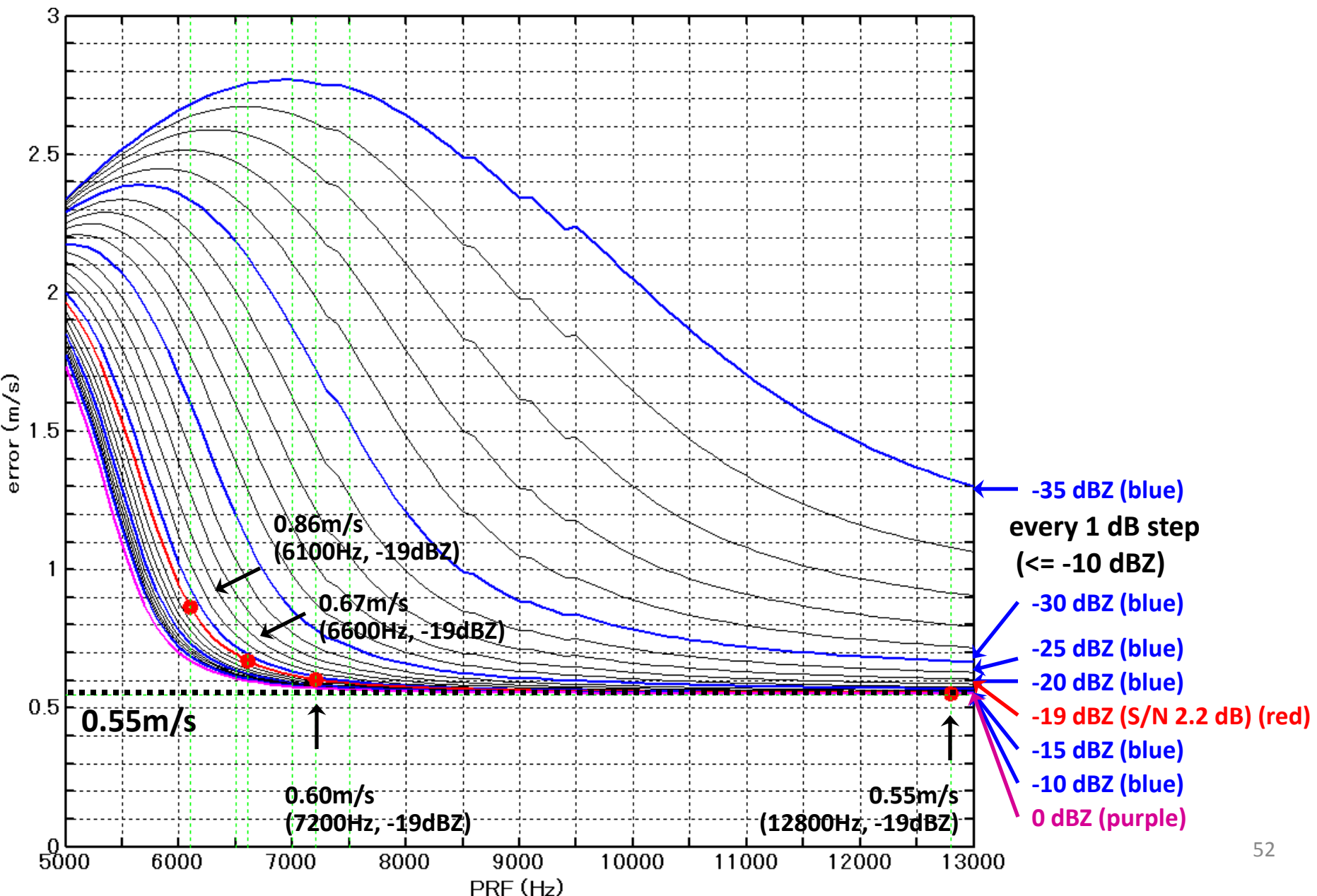
minimum detection: -35dBZ at TOA (10km integration)

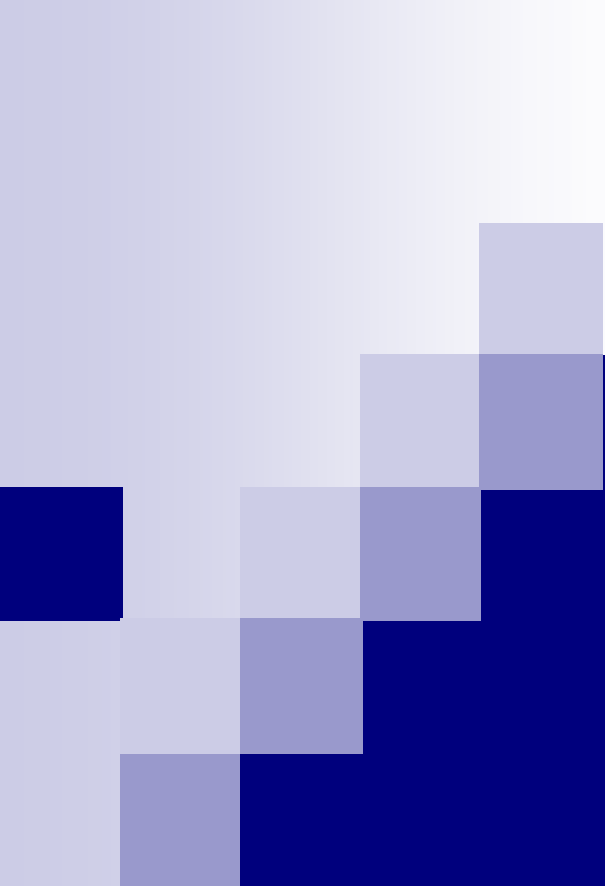
- Doppler function (pulse-pair method)
vertical velocity measurement

accuracy: 1 m/ s (10km integration -19dBZ echo)

- Variable PRF and height range
- Co-registration with Lidar and other sensors
- Circular polarization
- Less ground clutter effect
- Longer life transmit tube (EIK)

Error in Doppler measurement (10km integration error including antenna, satellite, etc.)





Global Precipitation Mapping

Tomoo Ushio

Osaka University, Osaka, Japan



INTRODUCTION

Scientific and Social Significance of the global precipitation map

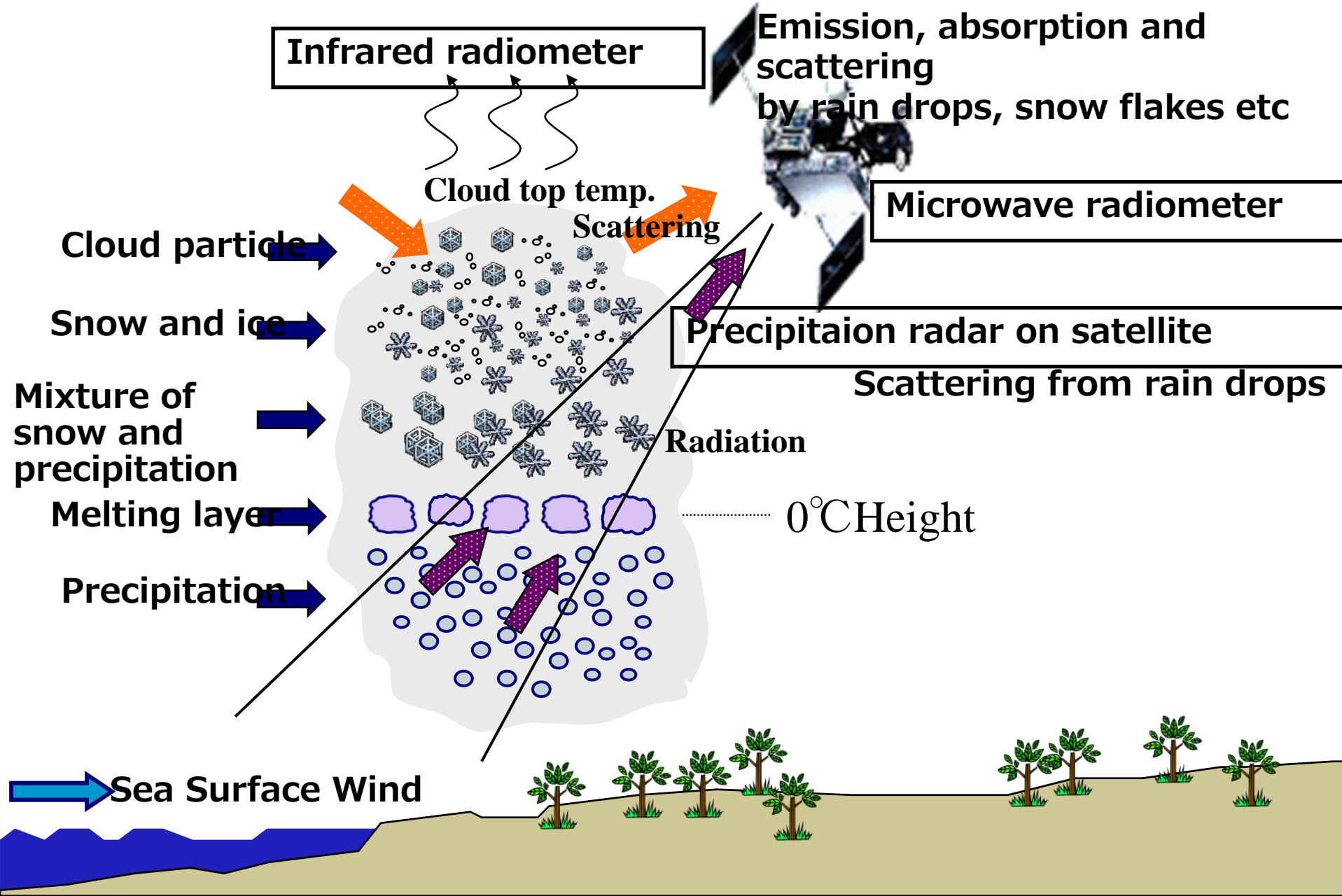
- Global rain map in daily to hourly scale
- Climate change assessment
 - Monitor variations in rainfall and rain areas associated with climate changes and global warming
- Improvement in weather forecasts
 - Data assimilation in numerical prediction systems
- Flood prediction
- Water resource management
 - River, dam, agricultural water, etc.
- Other applications
 - Agriculture, etc.



Precipitation measurement from space?

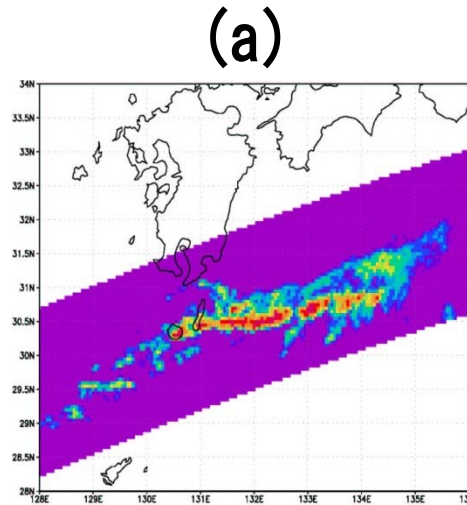


Remote Sensing from space using electromagnetic waves

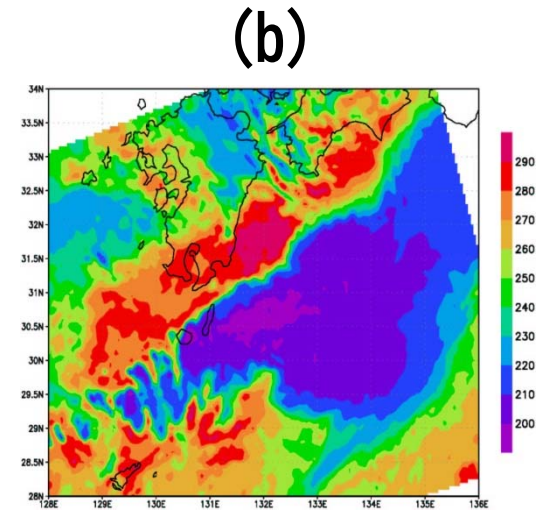


Precipitation characteristics observed by the space borne sensors

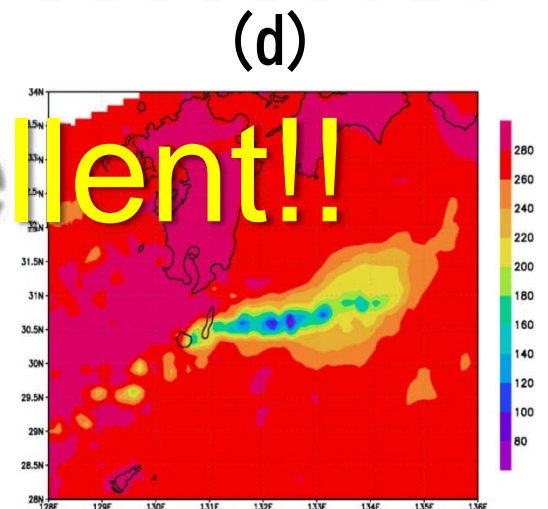
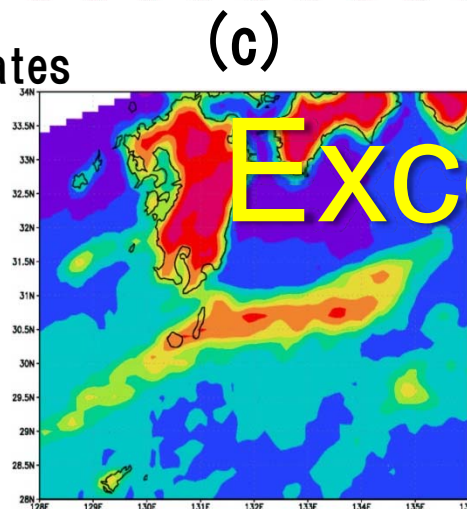
(a) Precipitation radar
Back scattering from rain drops
High accuracy
Narrow swath width



(b) Infrared radiometer:
Cloud top information
Not related to surface precipitation rates



(c) Microwave radiometer(19GHz):
(d) Microwave radiometer(85GHz):
Directly measures the emission from precipitation particularly in low frequencies



Excellent!!

Global Precipitation Product



TRMM
TMI



Aqua
AMSR-E



ADEOS-II
AMSR



DMSP
SSM/I

Microwave radiometer algorithm

Product from each sensor

Mix

Composite
product

30 min.

6 hour

1 day

0.5degree

1 month



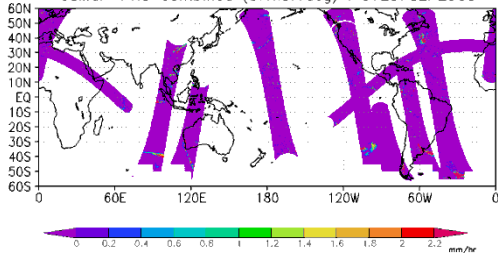
Geo. Satellite

Infrared radiometer
Cloud motion vector

Composite algorithm of
IR and MWR

0.1degree · 30min

GSMaP V4.5 Combined (0.1x0.1deg) : 01Z07SEP2003

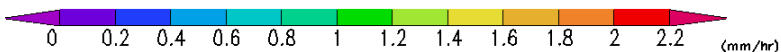
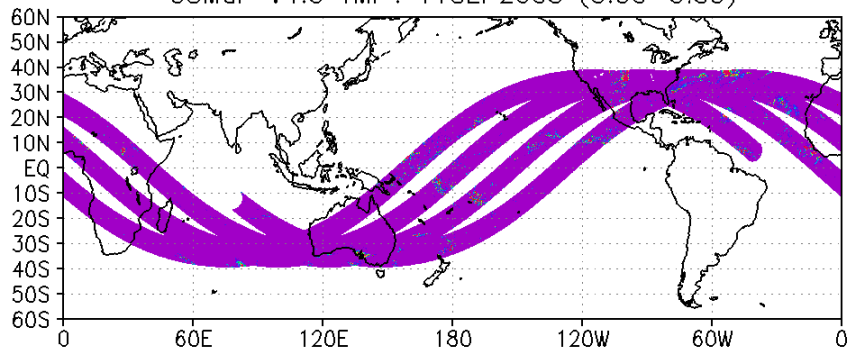


TRMM/TMI, Aqua/AMSR-E,
ADEOS-II/AMSR, DMSP/SSM/I
(F13, 14, 15)による1時間の
データ

6 hourly MWR combined map

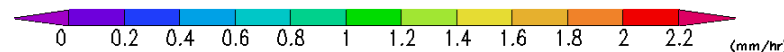
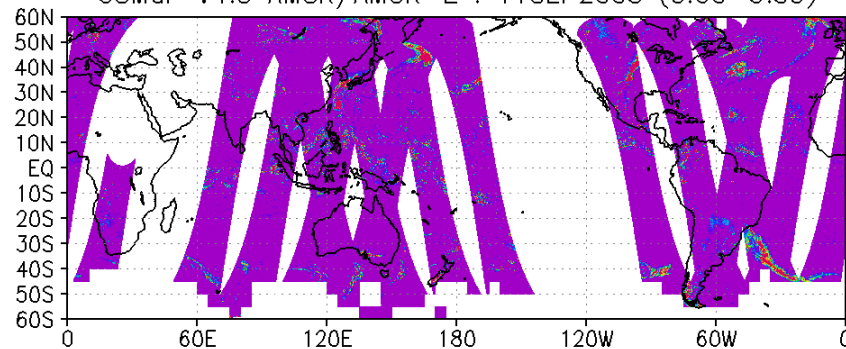
TMI

GSMaP V4.5 TMI : 11SEP2003 (0:00-5:59)



AMSR & AMSR-E

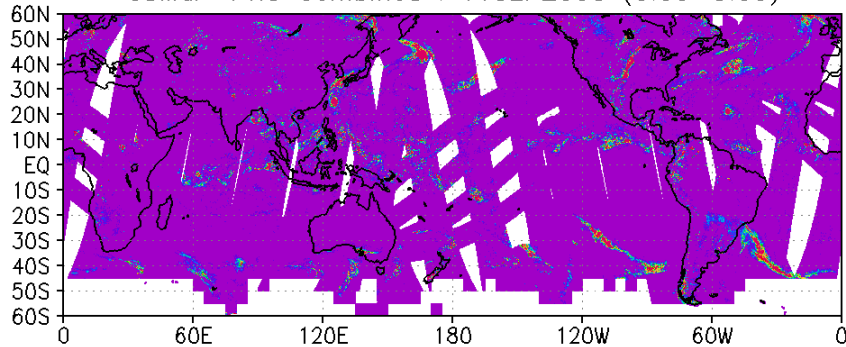
GSMaP V4.5 AMSR/AMSR-E : 11SEP2003 (0:00-5:59)



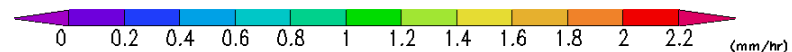
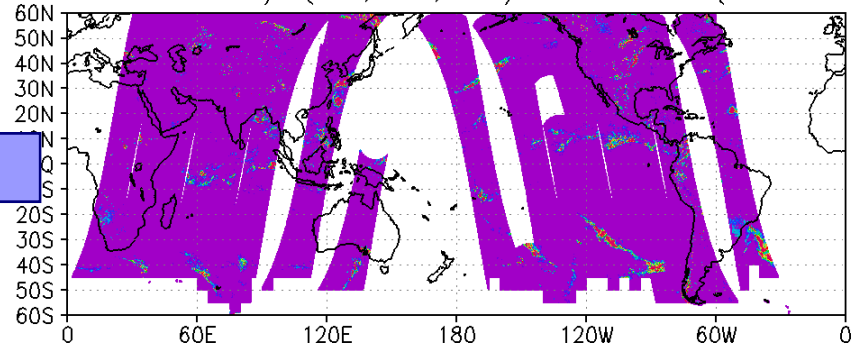
Combined
6 hourly

SSM/I (F13, F14, F15)

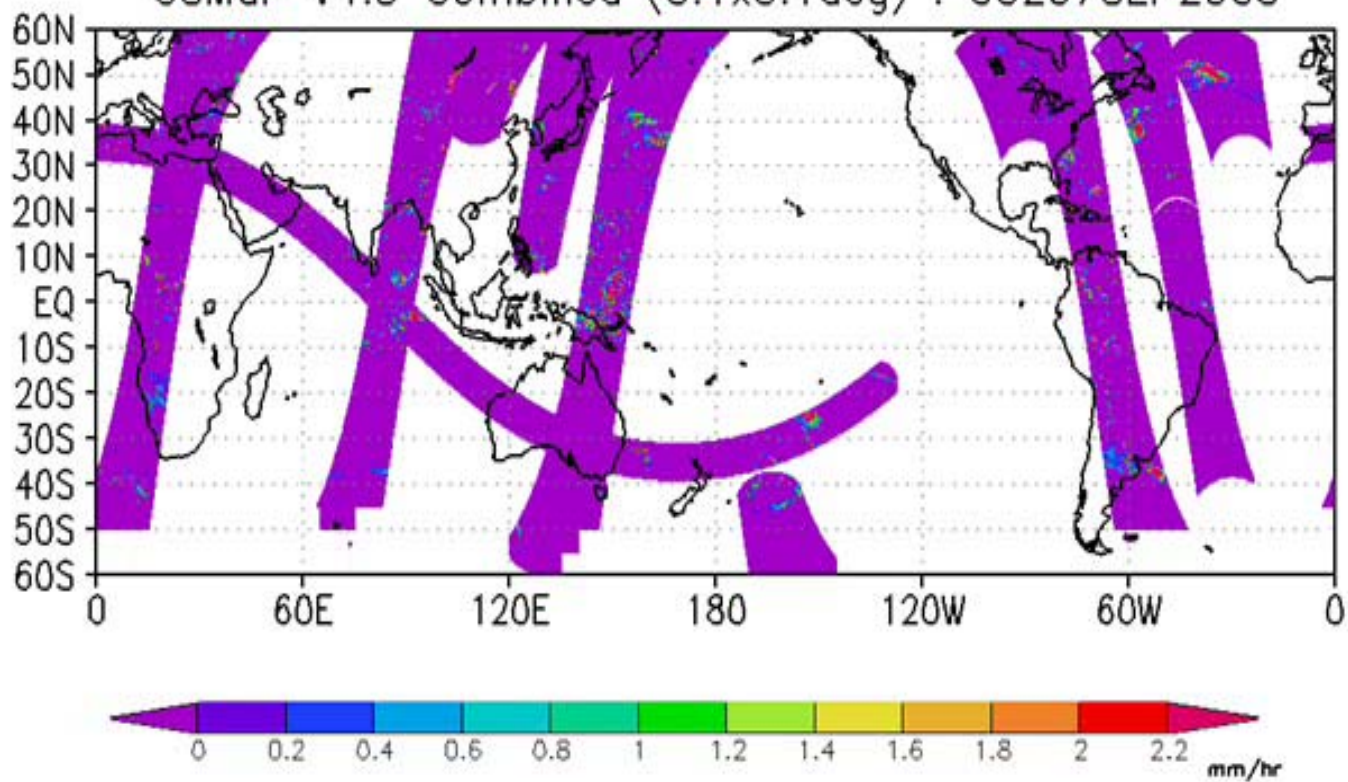
GSMaP V4.5 Combined : 11SEP2003 (0:00-5:59)



GSMaP V4.5 SSM/I (F13, F14, F15) : 11SEP2003 (0:00-5:59)



GSMaP V4.5 Combined (0.1x0.1deg) : 00Z07SEP2003



Global Precipitation product



TRMM
TMI



Aqua
AMSR-E



ADEOS-II
AMSR



DMSP
SSM/I

Microwave radiometer algorithm

Product from each sensor

Mix

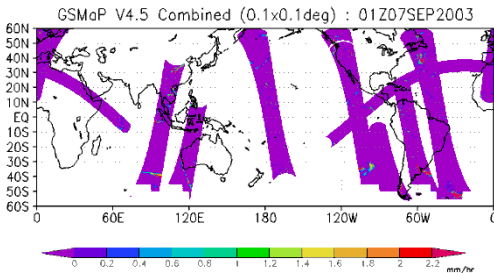
Composite product	1 hour
	6 hour
	1 day
0.1degree	1 month



Geo. Satellite

Infrared radiometer
Cloud motion vector

Composite algorithm of
IR and MWR
0.1degree · 30min



TRMM/TMI, Aqua/AMSR-E,
ADEOS-II/AMSR, DMSP/SSM/I
(F13, 14, 15)による1時間の
データ

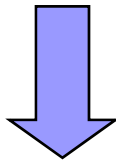
How can we get a global precipitation map with temporal resolution of 3 hours or less?

- Infrared radiometers (IR)

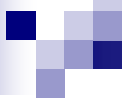
- can provide information on cloud top layers (not precipitation)
- Can ensure a global coverage with high temporal resolution (> 30 min) due to the geo-synchronous orbit (GEO)

- Microwave radiometers (MW)

- Can detect cloud structure and precipitation with high spatial resolution
- The major draw back is temporal sampling due low earth orbit satellite (LEO)



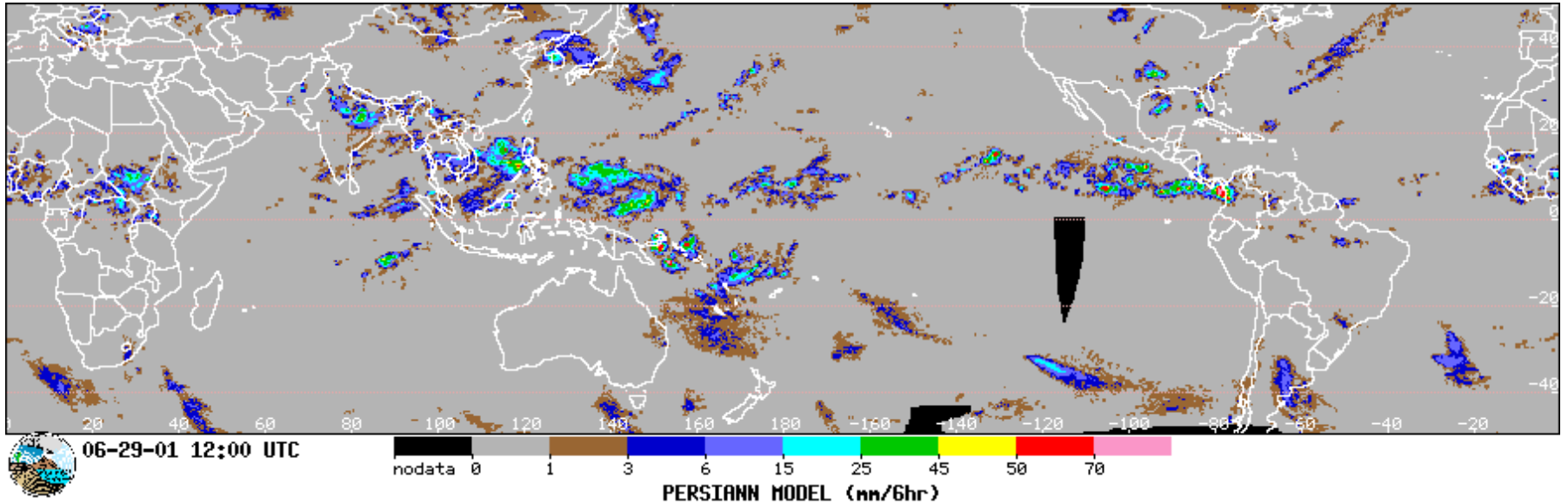
- The LEO-MW and GEO-IR radiometry are quite complementary for monitoring the highly variable parameters like precipitation.



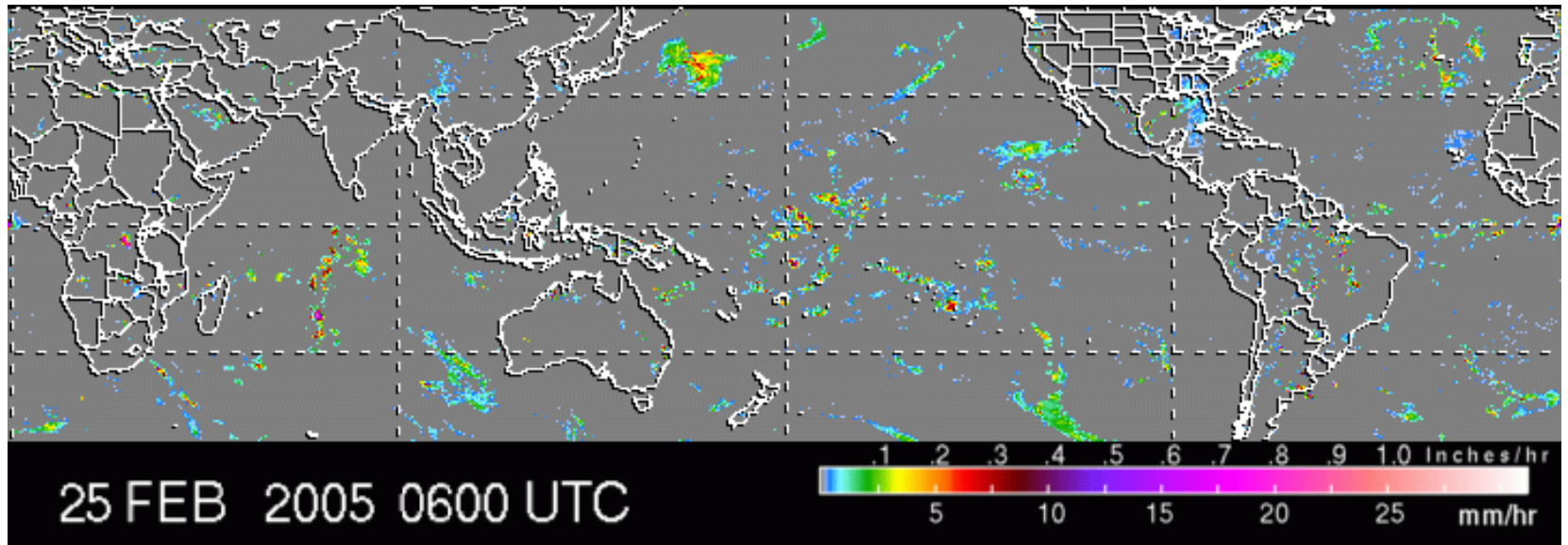
Global High Time/Space Resolution Precipitation Map

- CMORPH (CPC Morphing) – NOAA
- PERSIANN (Precipitation Estimation from Remotely Sensed Information using Artificial Neural Networks)
- University of California Irvine
- TRMM 3B42 – GSFC, NASA
- TRMM 3B42rt – GSFC, NASA
- NRL Blended - Naval Research Laboratory
- NESDIS Hydro Estimator (STAR) - NOAA
- Eumetsat Multi-Sensor Precipitation Estimates(MPE)

High Resolution Precipitation Products



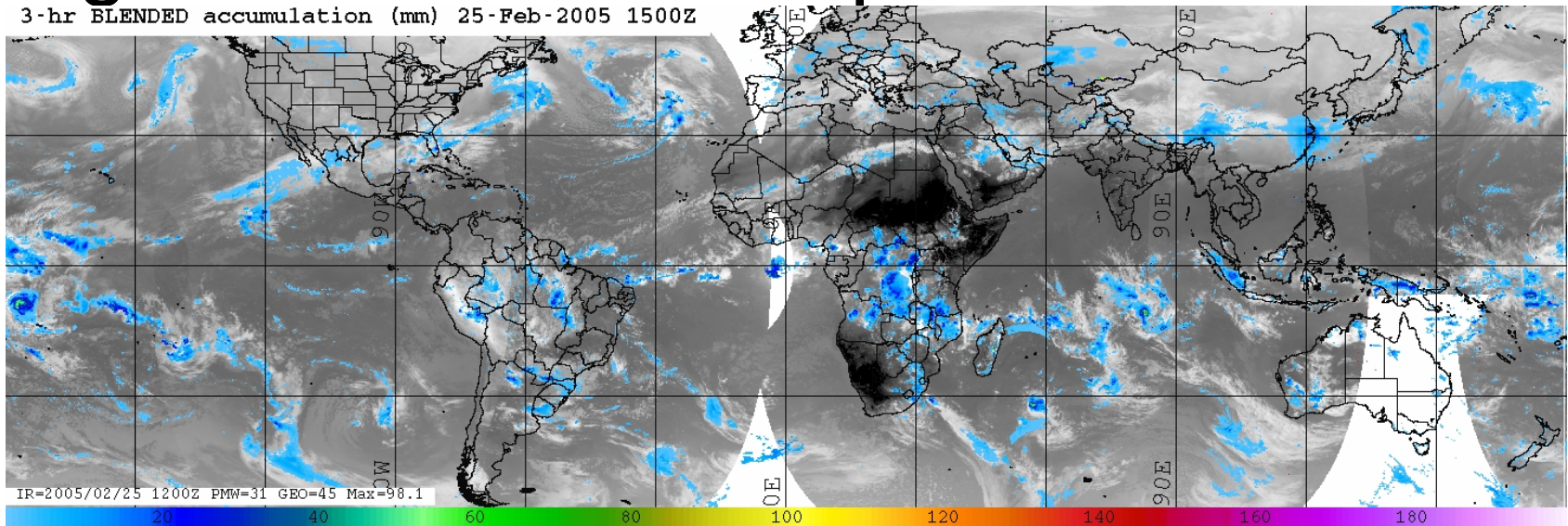
PERSIANN 6-hourly/0.25° real-time analyses



TRMM 3-hourly/0.25° real-time analyses

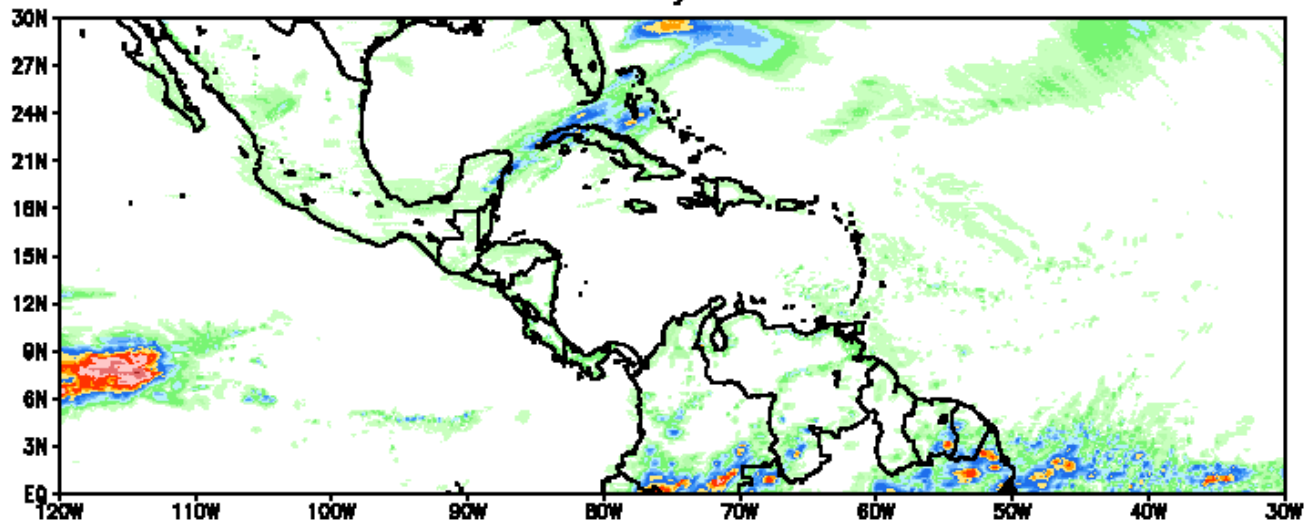
High Resolution Precipitation Products

3-hr BLENDED accumulation (mm) 25-Feb-2005 1500Z



NRL (Turk) 3-hourly/0.25° real-time analyses

CPC CMORPH February 28 2005 0000 UTC



CMORPH 30-minute/8 km real-time analyses



CMORPH -A High Time-Space Resolution Global Precipitation Analysis Using Passive Microwave and Infrared Data

<http://www.cpc.ncep.noaa.gov/products/janowiak/cmorph.html>
Joyce et al., 2004, J. Hydrometeorology

- Team: Bob Joyce, John Janowiak, Pingping Xie
(Climate Prediction Center, NOAA)
- Concept:
 - Take maximum advantage of accuracy of microwave estimates and coverage of IR
 - Don't use IR to estimate precipitation – all methods developed so far have significant and difficult-to-quantify errors, particularly on fine scales
 - Use IR to estimate storm motion instead – errors are smaller and easier to understand

Algorithm Output Information

- Spatial Resolution: ~ **8 km** (at equator)
- Domain: **60N-60S** (global longitude)
- Update Frequency: **30 minutes**
- Data Latency (~ **15 hours**; **2.5 hrs** for “QMORPH”)
- Source of Real-Time Data: **NESDIS/NCEP**
- Source of Archive Data: **NESDIS/NCEP**
- Capability of Producing Retrospective Data:
beg’g in 1-2 months – back to ~1998

Global Precipitation Climatology Project (GPCP)

(part of WCRP/GEWEX)

NASA, NOAA, DWD, Universities, EUMETSAT, JMA

GPCP Global Precipitation Products

- **Monthly, 2.5° merged analysis [1979-present]**
(Adler et al., 2003, submitted to *J. Hydromet.*;
Huffman et al., 1997, *BAMS*)
- **Pentad, 2.5 ° merged analysis [1979-present]** (Xie
et al., 2003--accepted *J. Clim.*)
- **Daily, 1° merged analysis [1997-present]**
(Huffman et al. 2001, *J. Hydromet.*)

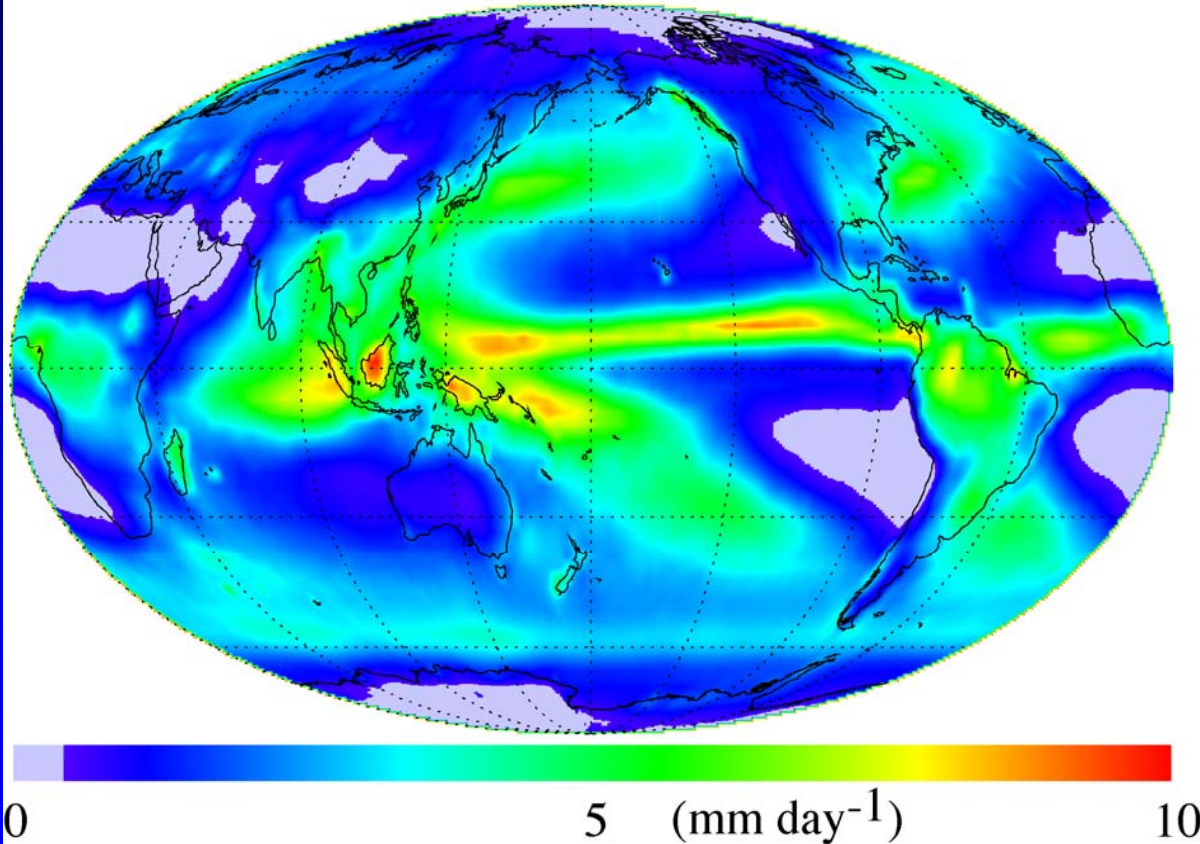
[products are integrated, i.e. they add up]

produced ~ 3 months after observation time

see www.precip.gsfc.nasa.gov

23-Year Climatology

The Global Precipitation Climatology Project (GPCP)



A 23-Year Precipitation Climatology (1979-2001)
Based on Observations from Multiple Satellites

GPCP Monthly Product

- SSM/I, geo-IR, TOVS, OLR, gauges
- Stepwise bias removal
- Blending using inverse error weights
- Final error fields
- WCRP/GEWEX
- Adler et al. (2003) J. Hydromet. (submitted)

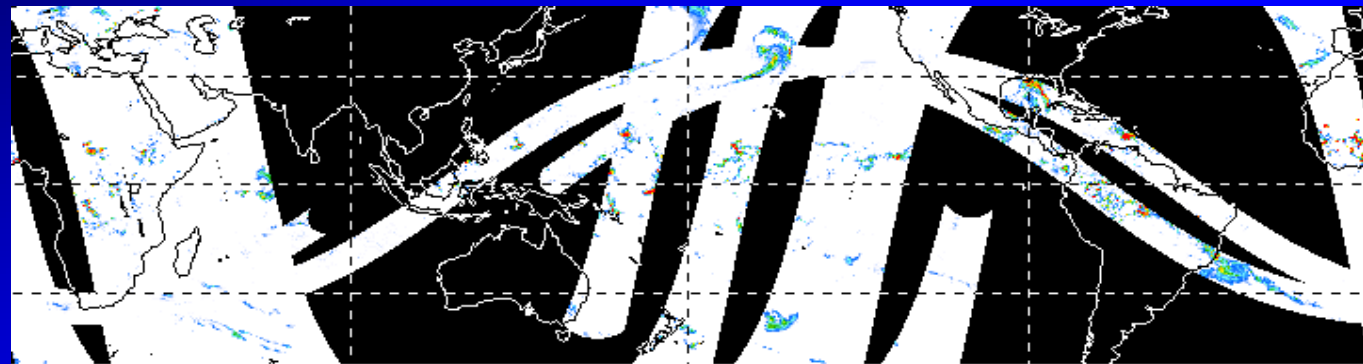
precip.gsfc.nasa.gov

Global total = 2.6 mm/d (Ocean [2.8 mm/d] Land[2.1 mm/d])

TRMM Multi-Satellite Real-Time Precipitation Estimates

3B40RT

Combined
microwave (TRMM
and TRMM-calibrated
SSM/I)



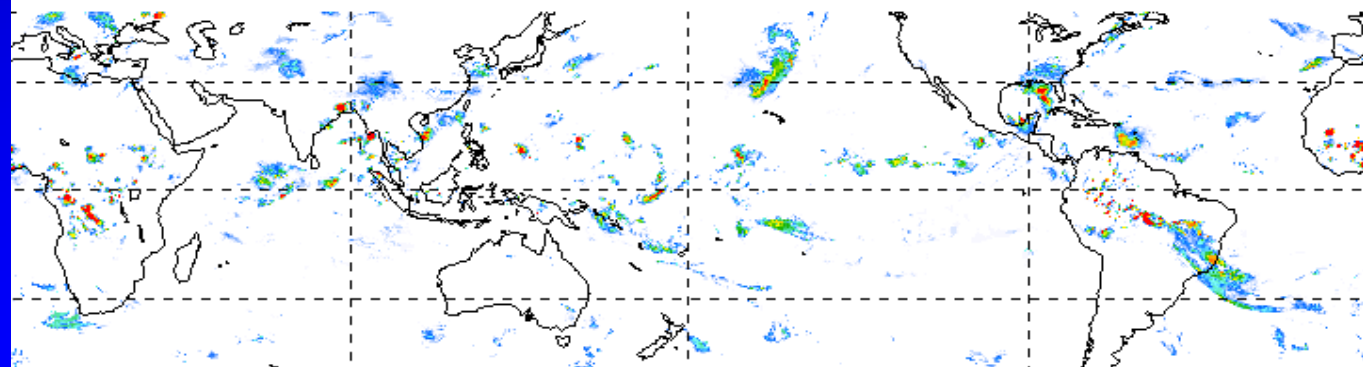
HQ Merge (mm/h)

18Z 24 Sep 2002



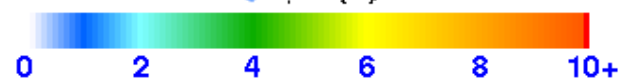
3B41RT

Microwave-
calibrated geo-IR
estimate
(Geo-IR from
NOAA/CPC)



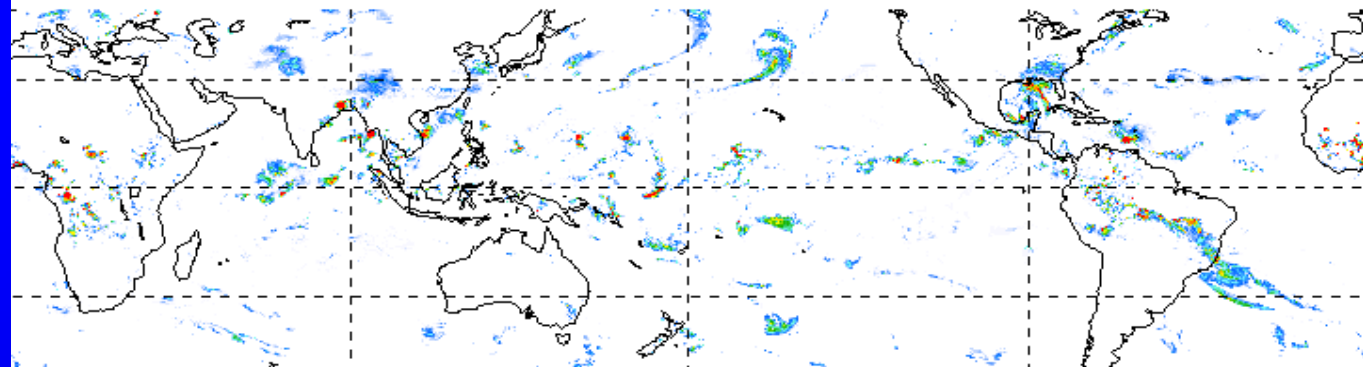
VAR (mm/h)

18Z 24 Sep 2002



3B42RT

Merged microwave
and geo-IR
estimates



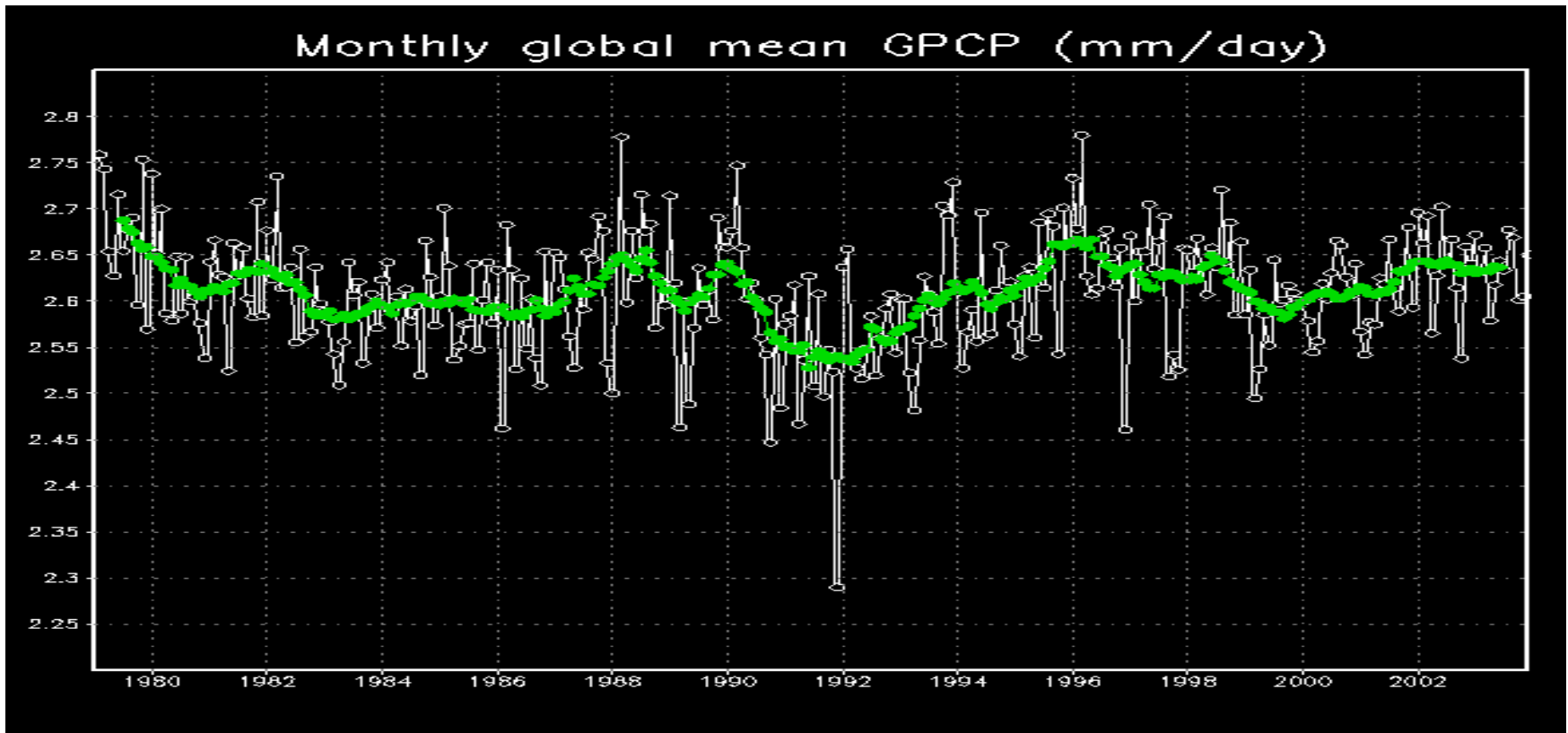
HQ+VAR Merge (mm/h)

18Z 24 Sep 2002



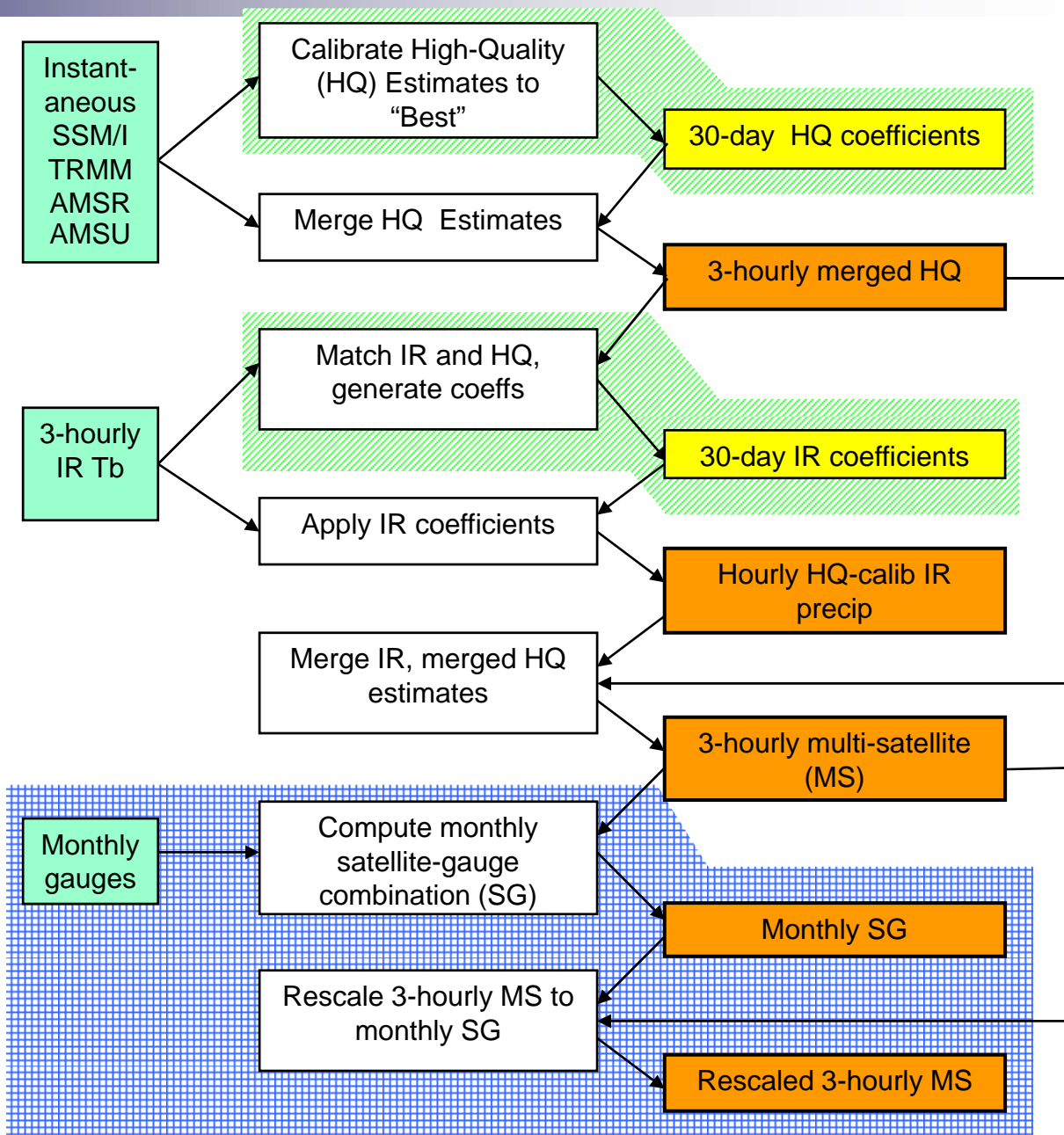
Multi-satellite Precipitation Analysis (MPA)

George Huffman, Bob Adler, Dave Bolvin, Eric Nelkin
NASA/GSFC



Algorithm Process

- The “real” MPA is the post-real-time Version 6 3B42
- The current real-time 3B42RT that runs 10 hr after real time is a first look
- We plan to replace the 10-hr run with a 4-hr “early” and 7-hr “final” to better support operations



Algorithm Output Information

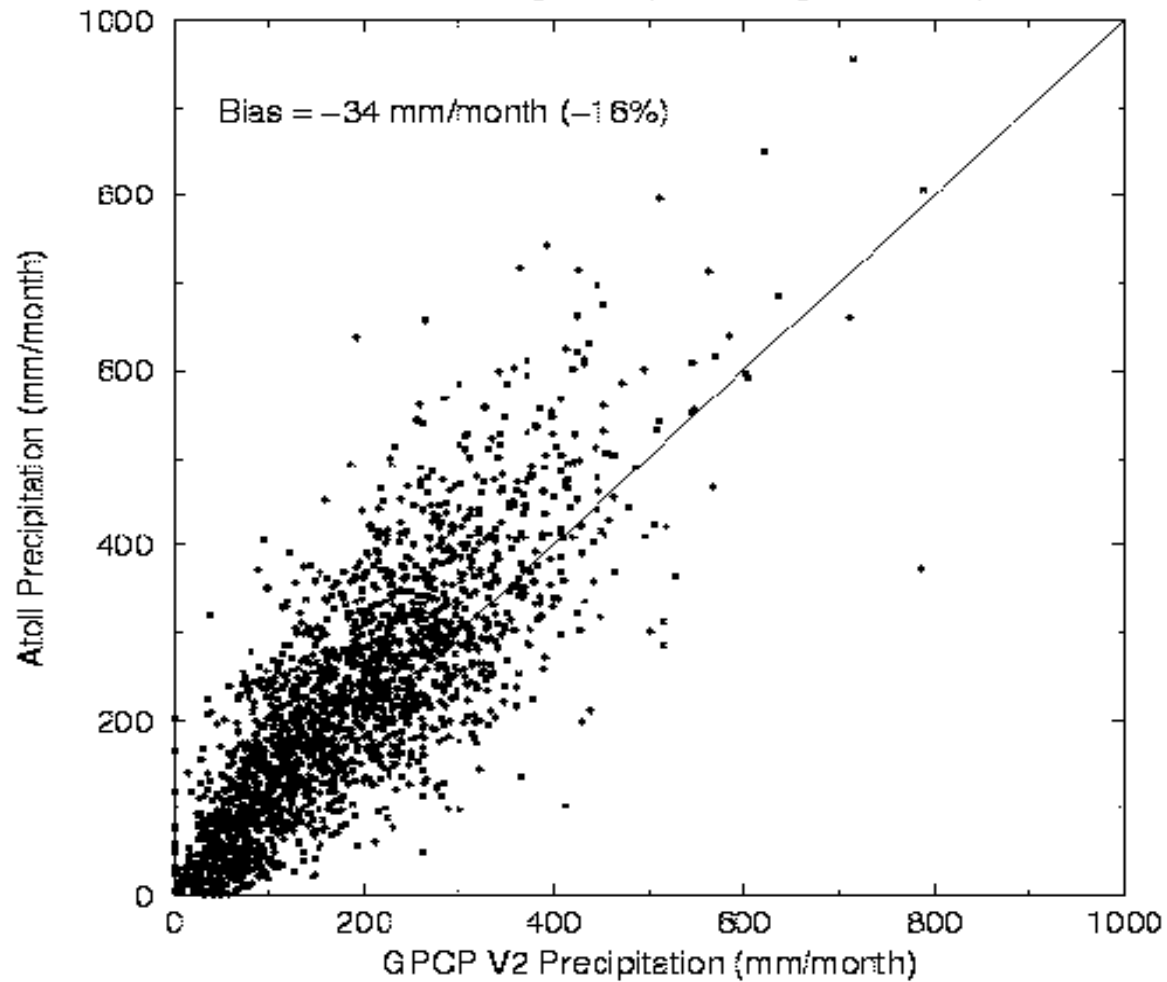
- **Spatial Resolution**
 - $0.25^{\circ} \times 0.25^{\circ}$
- **Spatial Coverage**
 - 50° N-S (60° possible)
- **Update Frequency**
 - 3-hr (RT), monthly (V.6)
- **Data Latency**
 - 10 hr (RT; plan move to 7 & 4),
2 weeks after month (V.6)

■ Strengths and Weaknesses of Underlying Assumptions

- “All” MW are used
- Aggregating MW to 3-hr maps introduces time errors at fine scale
- Intercalibration of MW and cal. of IR to MW traceable; good, except bad if the calibrator goes bad
- Different calibrators are used for RT (TMI) and V.6 (TCI and gauge)
- VAR scheme for IR assumes that instantaneously colder clouds rain more
- VAR scheme for IR takes calibration from a month of data; stable, but stiff
- HQ-VAR combination scheme is priority - HQ, else VAR; minimum assumptions, but introduces boundaries

GPCP V2 vs. Pacific Atolls

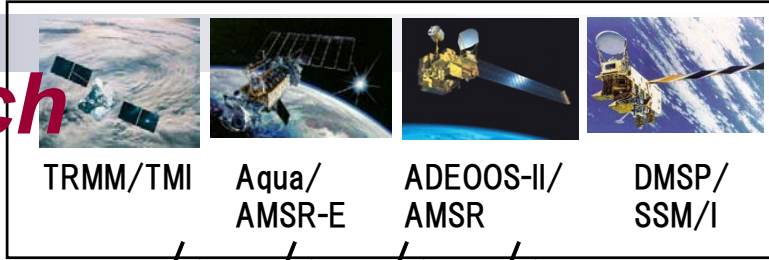
Jan 1979 - Aug 2001 (Two Gauge Minimum)





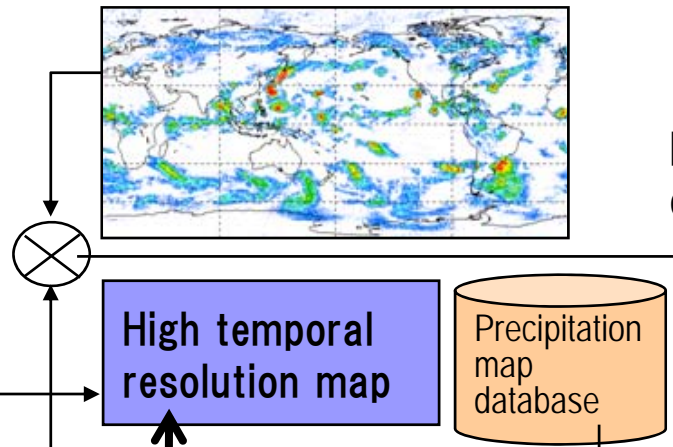
GLOBAL SATELLITE MAPPING OF PRECIPITATION (GSMAP)

Four pillars of the research



GEO meteorological satellite

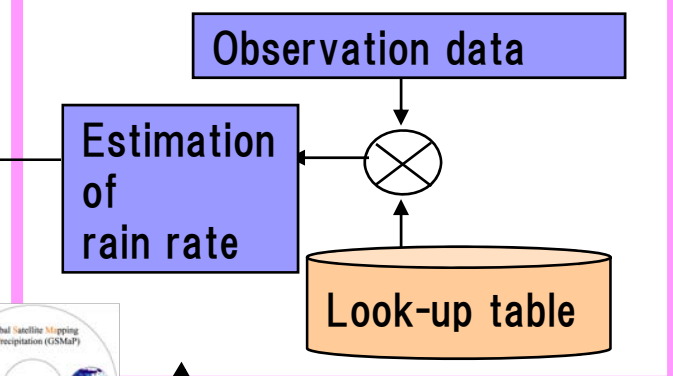
Production of global precipitation maps



Improvement of algorithm

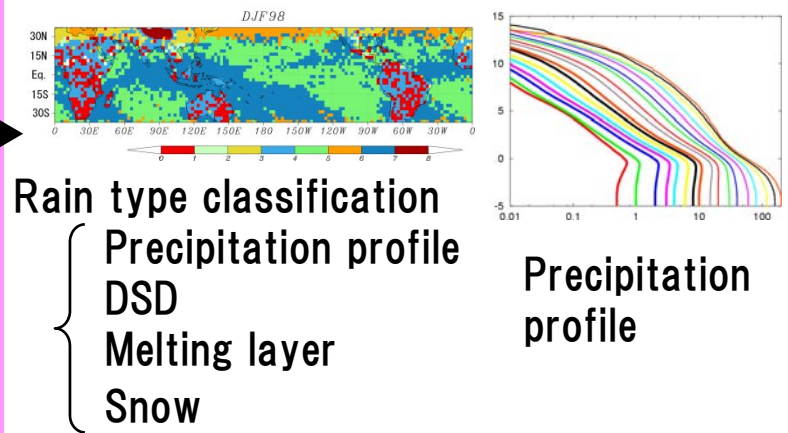


Algorithm development



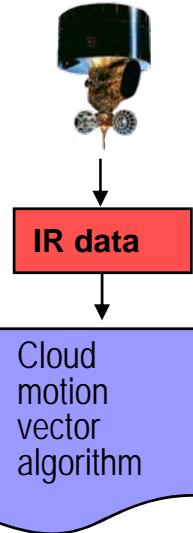
Radiative transfer equation

Precipitation physical model development



- Rain type classification
- Precipitation profile
 - DSD
 - Melting layer
 - Snow

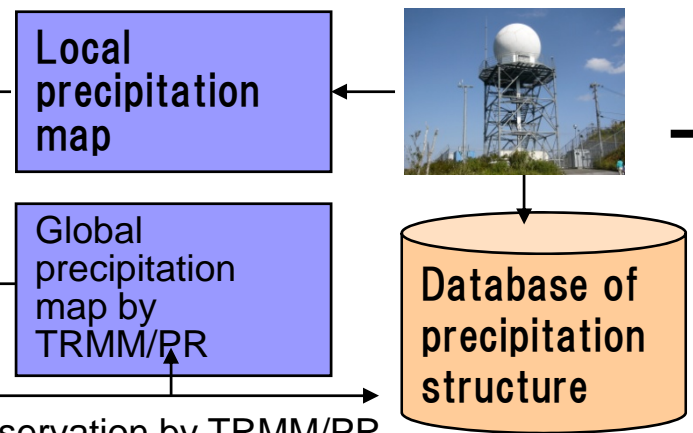
Precipitation profile



Data dissemination



Ground radar observation



Observation by TRMM/PR

Global Precipitation Product



TRMM
TMI



Aqua
AMSR-E



ADEOS-II
AMSR



DMSP
SSM/I

Microwave radiometer algorithm

Product from each sensor

Mix

Composite
product

30 min.

6 hour

1 day

0.5degree

1 month

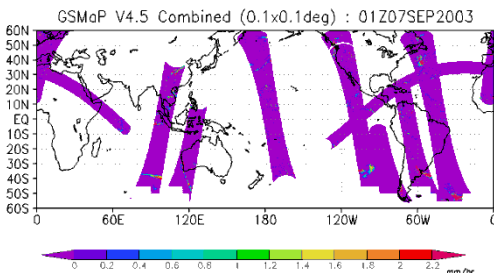


Geo. Satellite

Infrared radiometer
Cloud motion vector

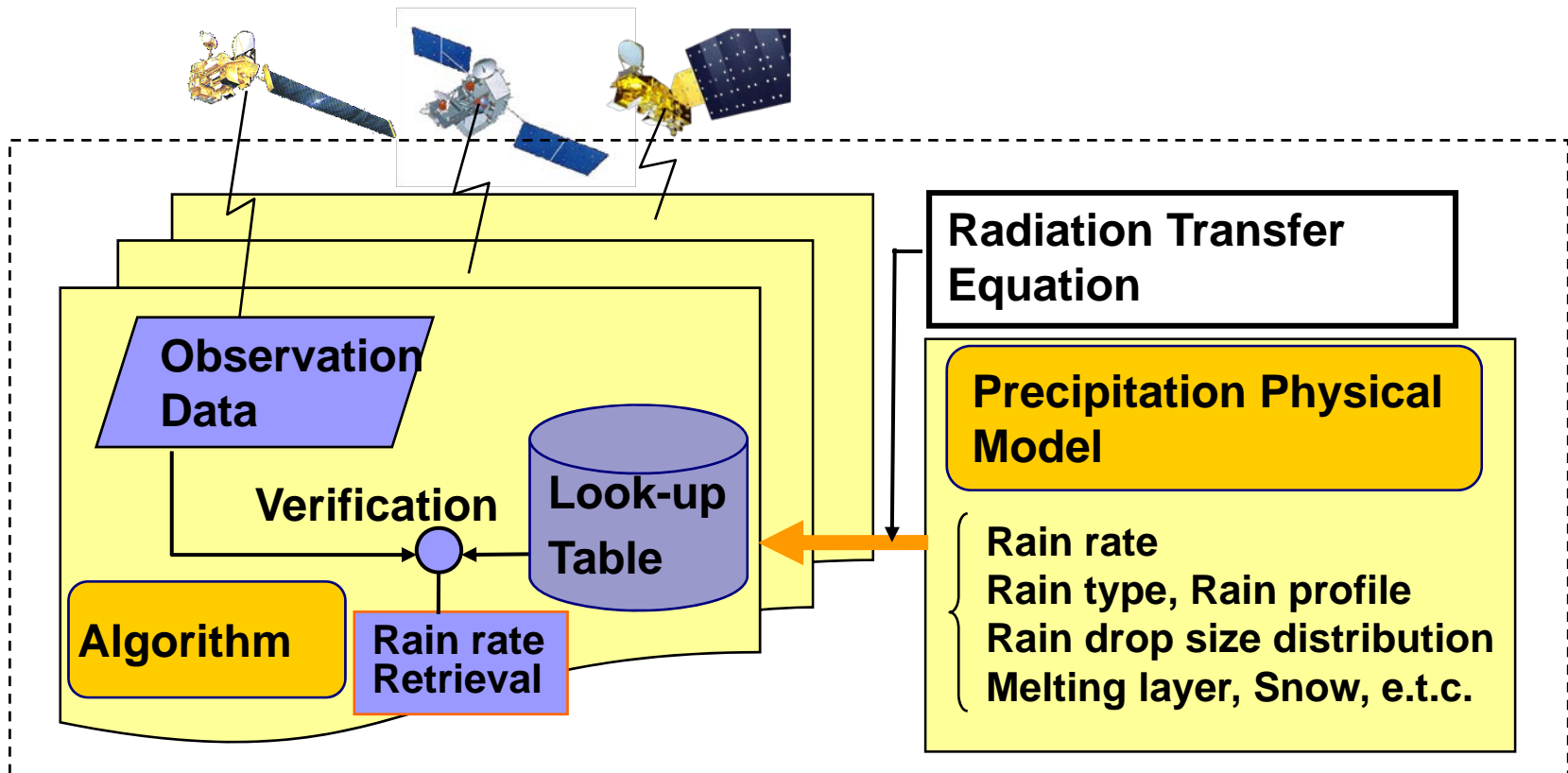
Composite algorithm of
IR and MWR

0.1degree · 30min



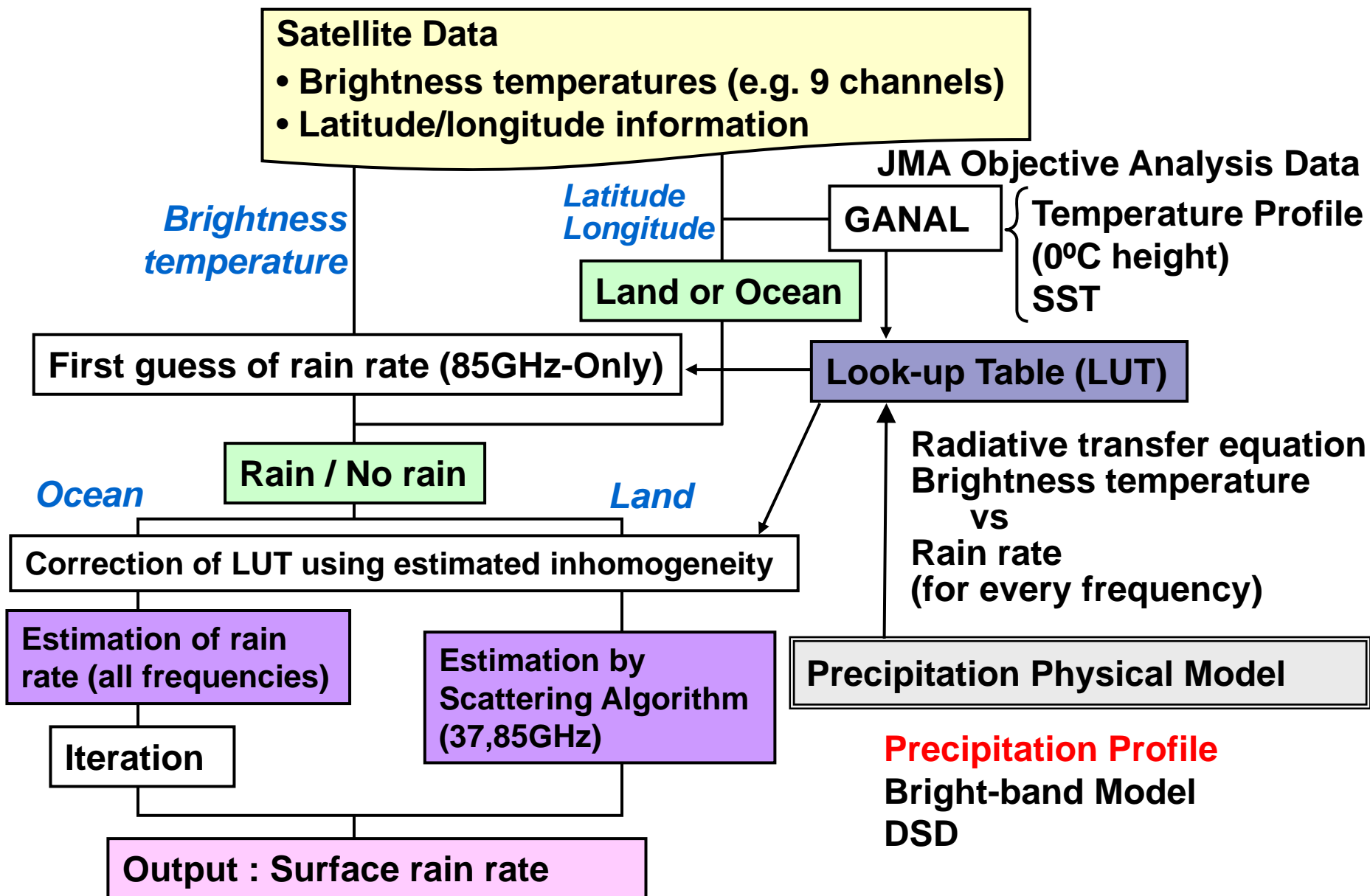
TRMM/TMI, Aqua/AMSR-E,
ADEOS-II/AMSR, DMSP/SSM/I
(F13, 14, 15)による1時間の
データ

Basis of Rain Rate Retrieval by Microwave Radiometers

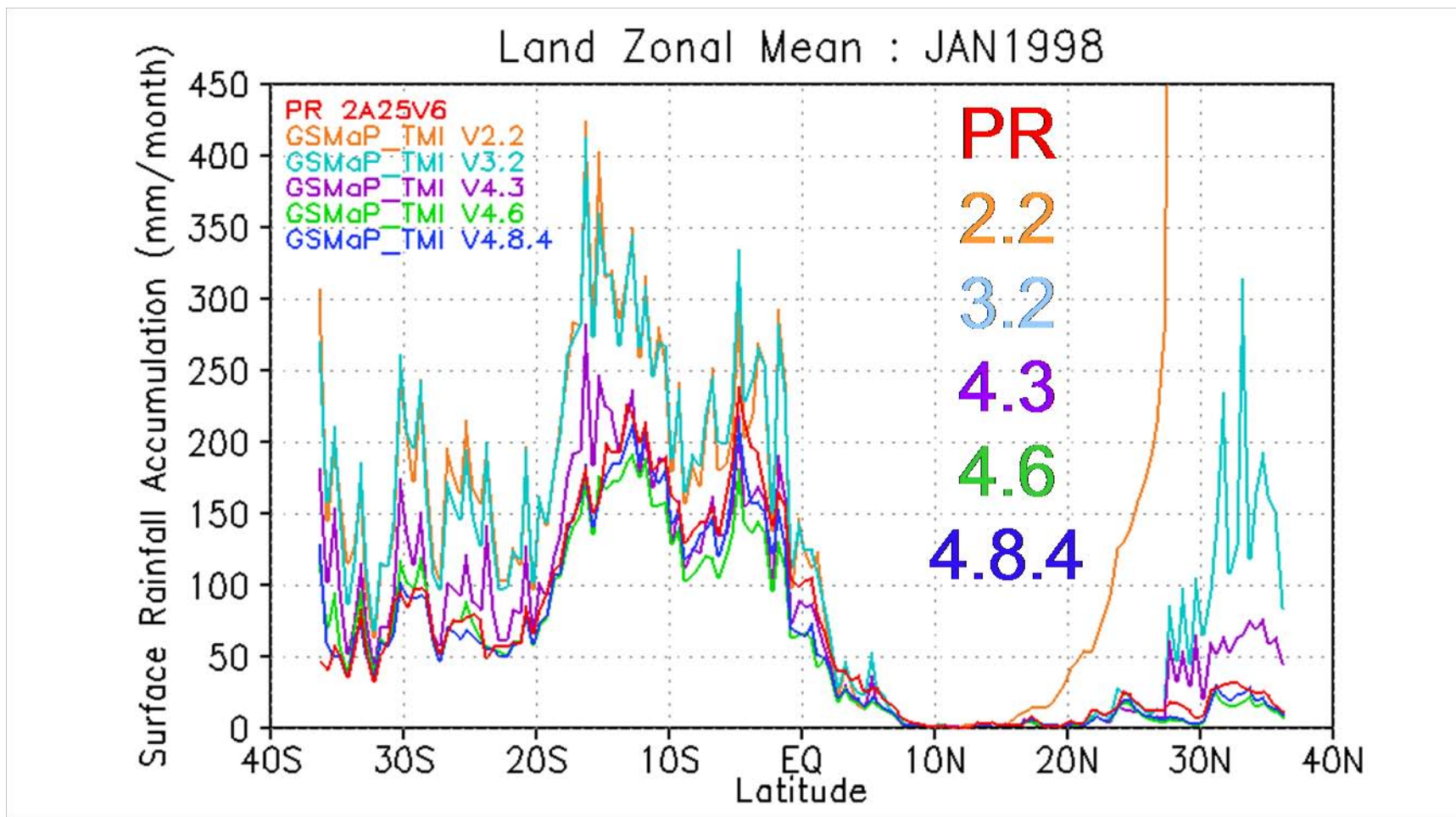


- Satellites observe the brightness temperature, integration of radiation and scattering power.
- The relation between rain rate and brightness temperature is tabulated by assuming precipitation physical model and calculating the radiative transfer equation. The rain rates giving the nearest brightness temperature values to the observed ones are considered to be the most appropriate estimation.

Flow Diagram of GSMaP MWR Algorithm

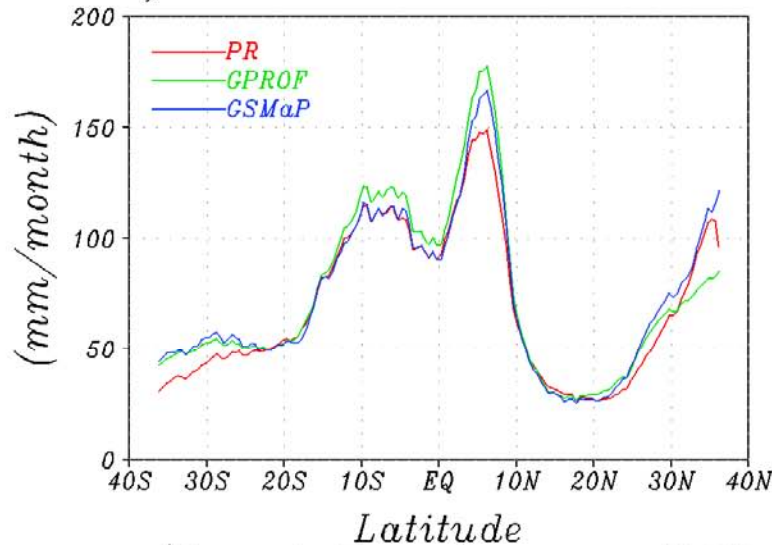


History of the algorithm modification

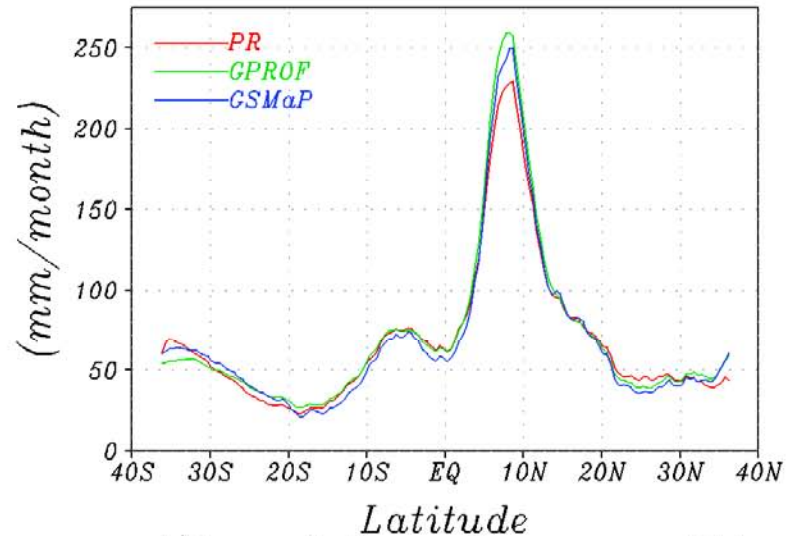


Comparison of TRMM rain rates by using TRMM/PR, TMI/GPROF, TMI/GSMaP algorithms (1998-2005)

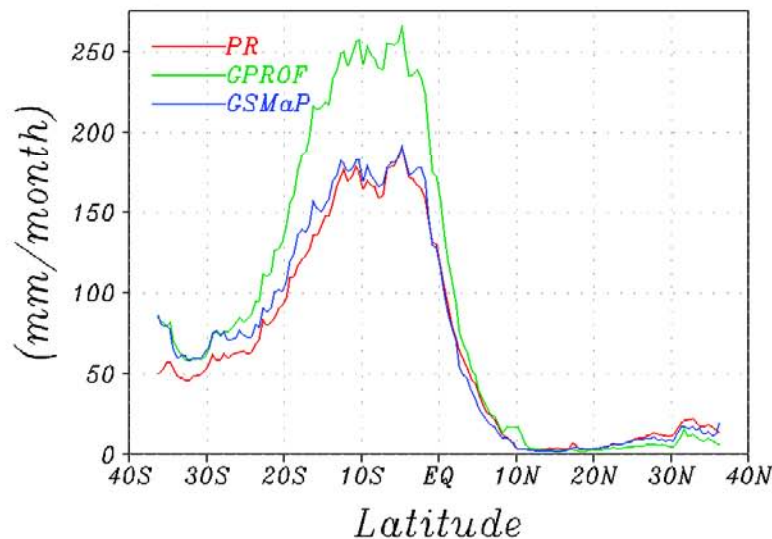
a) Ocean Zonal mean:DJF



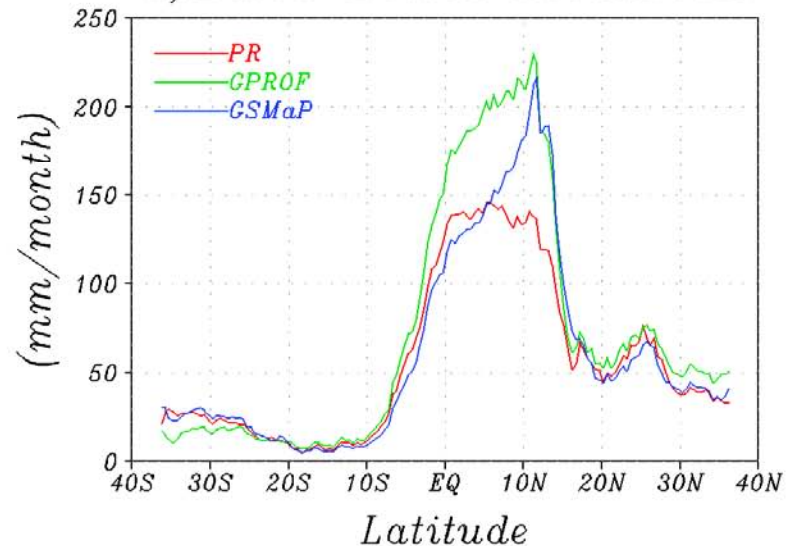
b) Ocean Zonal mean:JJA



c) Land Zonal mean:DJF



d) Land Zonal mean:JJA

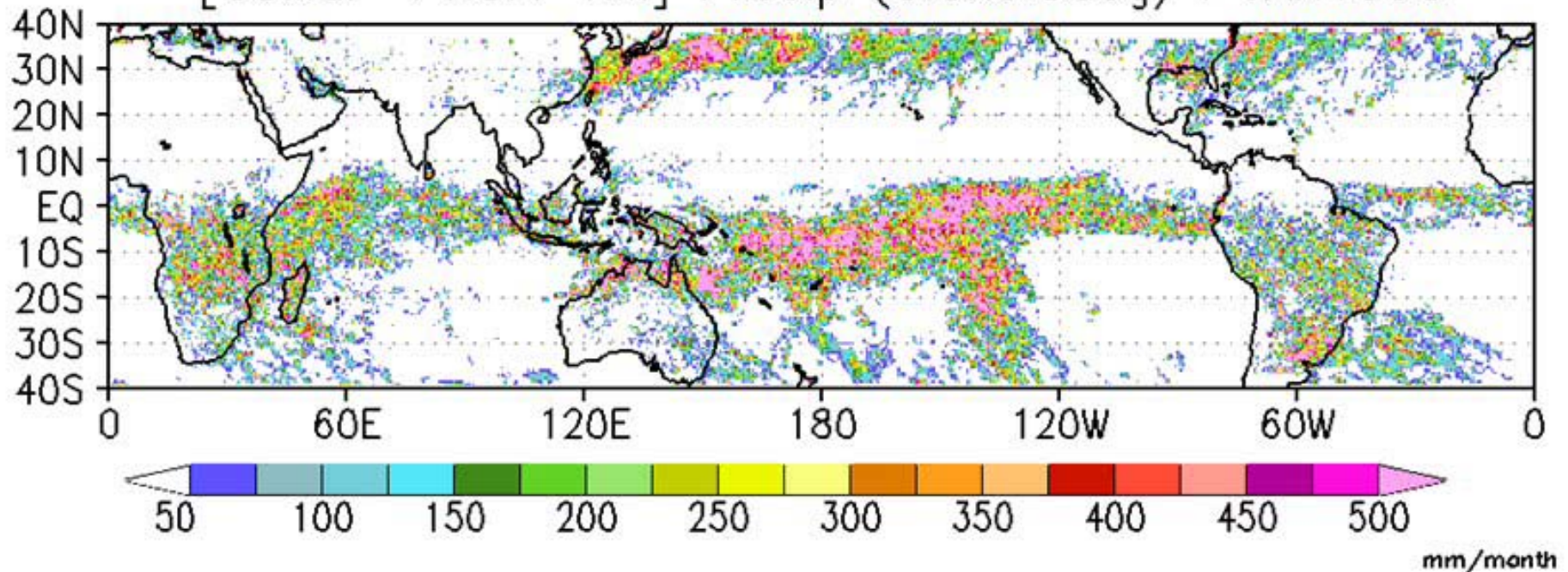


Approach of the GSMP project

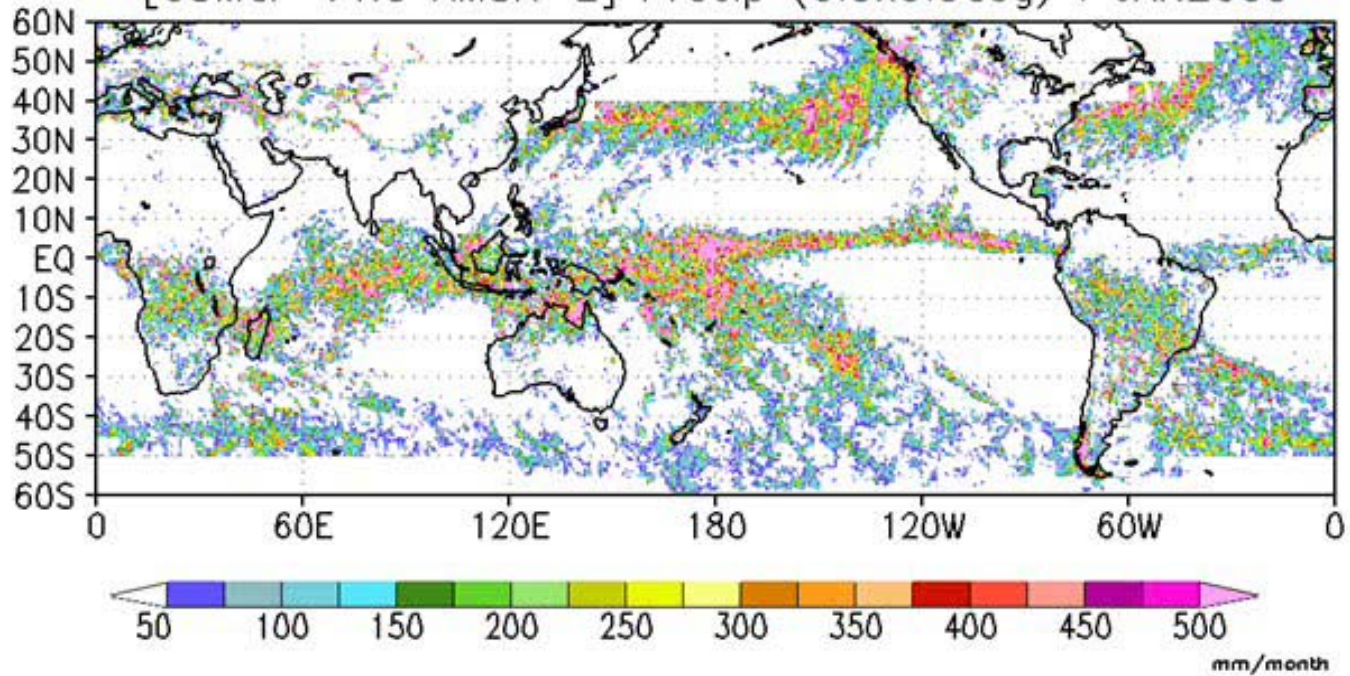
- We use the Aonashi Algorithm to retrieve rainfall rate.
- The sensors for the analysis are TMI, AMSR-E, AMSR, SSMI (F13, 14, 15).

Name	Data available
TRMM (TMI)	Jan. 1998 to Dec. 2005
Aqua (AMSR-E)	Jan. 2003 to Oct. 2005
ADEOS-II (AMSR)	Apr. 2003 to Oct. 2003
DMSP (SSMI:F13, F14, F15)	Sep. 2003, July. 2005 and several

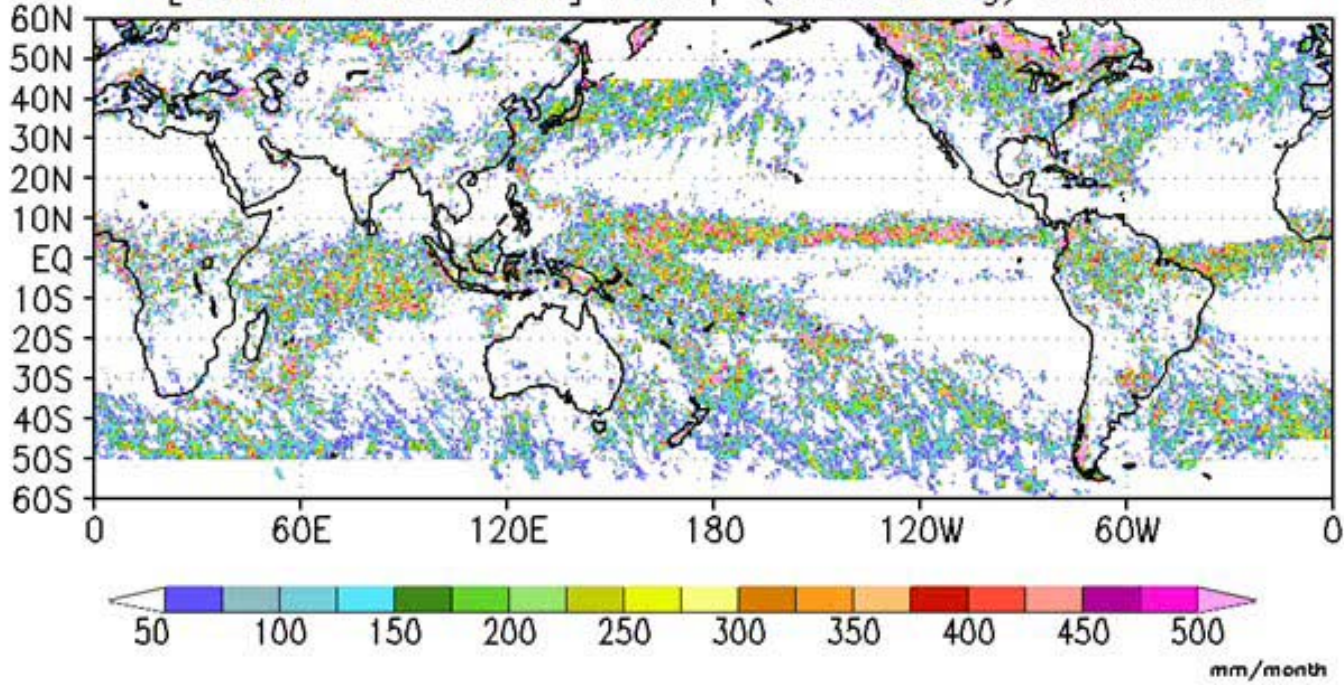
[GSMaP V4.5.1 TMI] Precip (0.5x0.5deg) : JAN1998



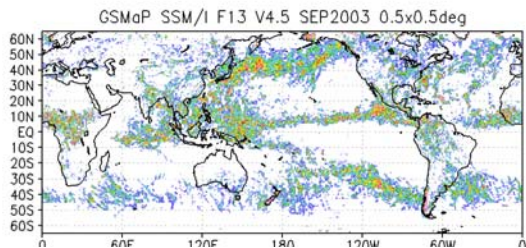
[GSMaP V4.5 AMSR-E] Precip (0.5x0.5deg) : JAN2003



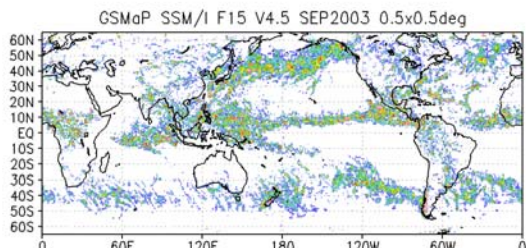
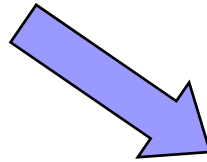
[GSMaP V4.5 AMSR] Precip (0.5x0.5deg) : APR2003



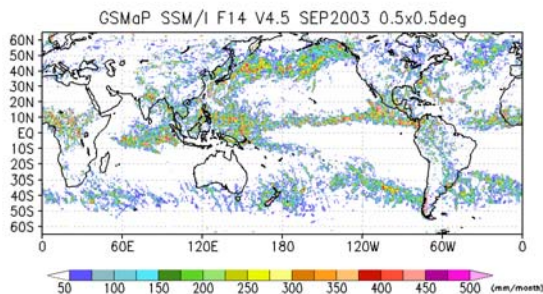
Monthly precipitation accumulation from DMSP/SSMI (F13, 14, 15) for Sep. 2003



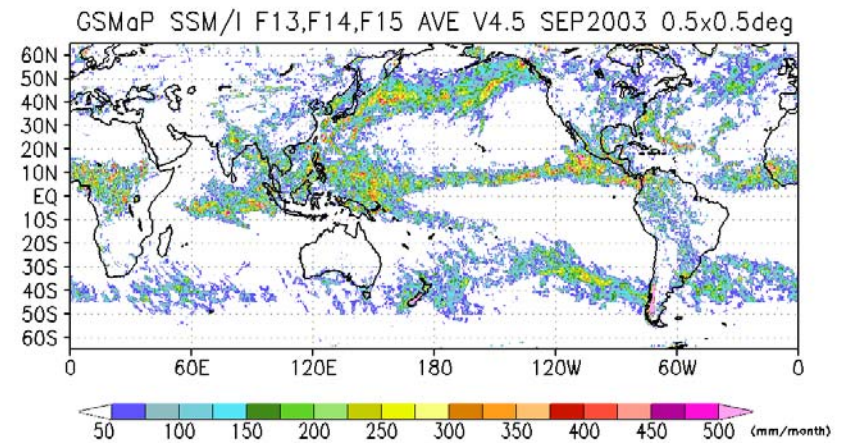
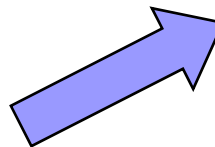
F13



F15



F14



GrADS: COLA/ICES

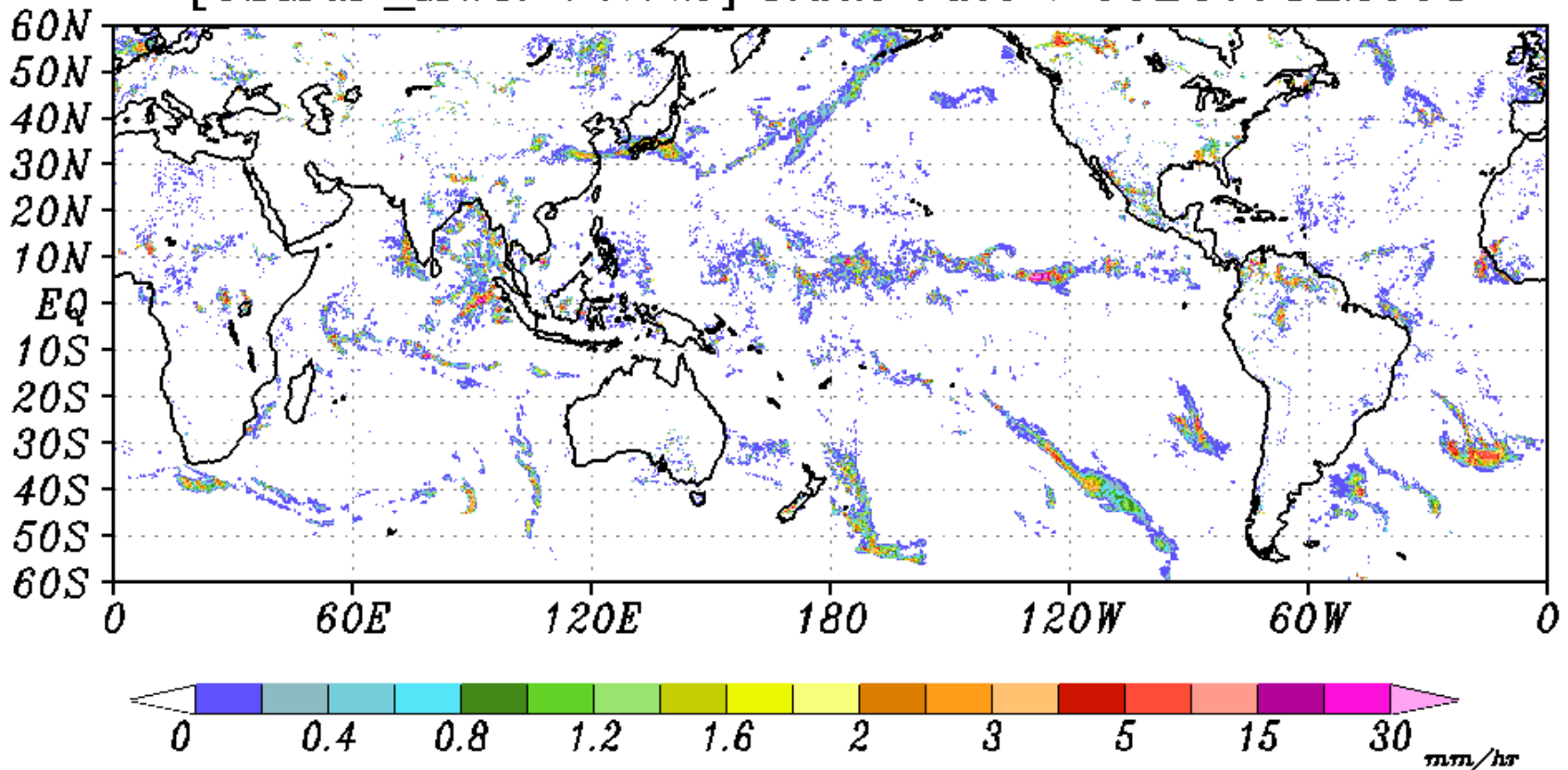
multi_print_rainmap_mth.gs

2005-10-13-17:16

Integrated 6-hour microwave radiometer precipitation map (GSMaP_MWR)

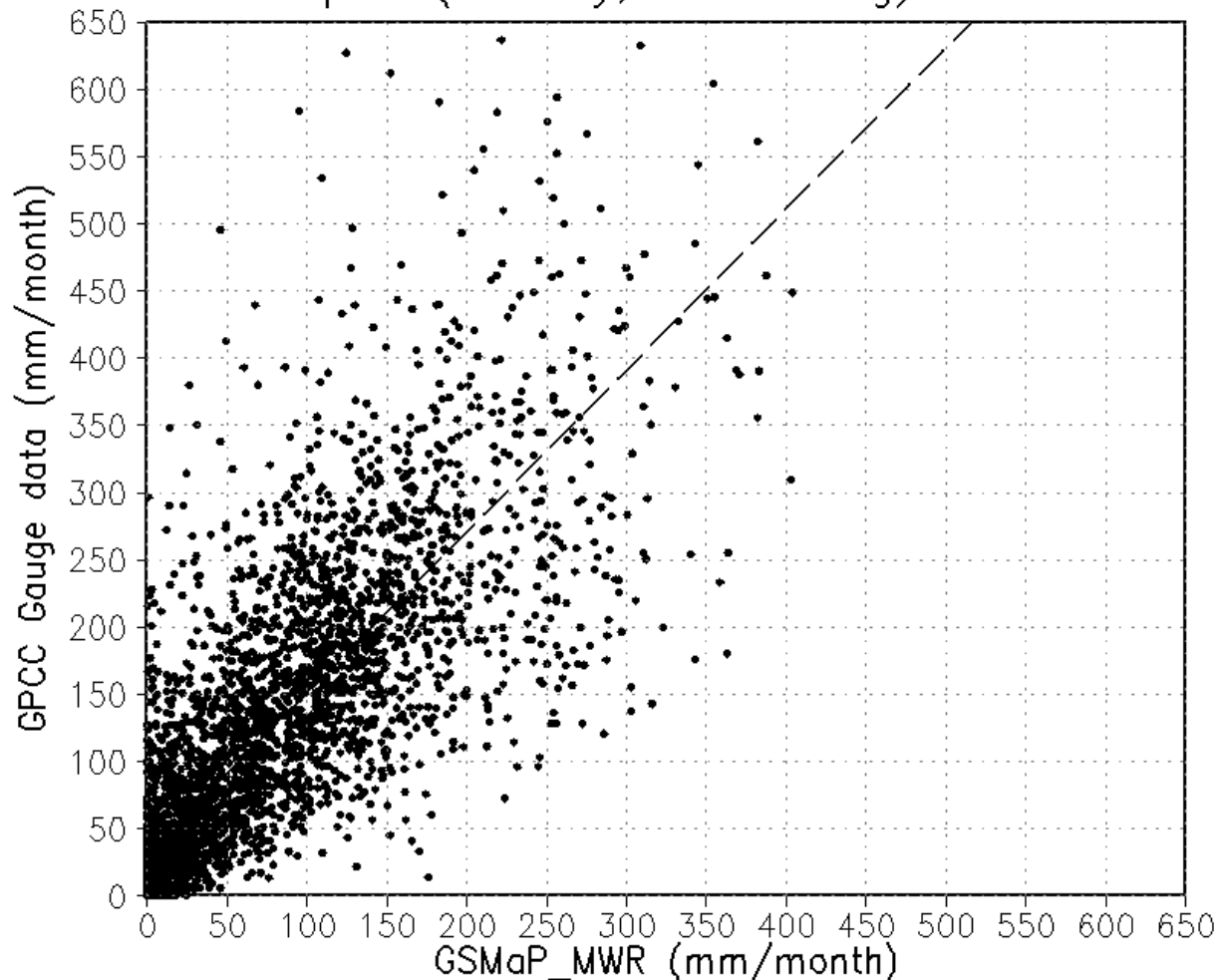
MWR(TMI+AMSR+AMSR-E+F13, 14, 15 SSM/I)

[GSMaP_MWR V4.7.2] Rain rate : 00Z01JUL2003



Comparison of monthly rain rates by ground-based rain gauge (GPCC) with GSMaP_MWR

LAND Tropics (Monthly, 1.0x1.0 deg): 2003–2005



● GPCC Monthly Precipitation (Monitoring) Product (Rudolf et al. 2005)

□ ground-based rain gauge
□ about 7000 rain gauges in the world

□ 1.0° × 1.0°

□ monthly average

● Analysis method

• Tropical Area (20S ~ 20N)

• There are at least 2 rain gauges in the 1.0° × 1.0°

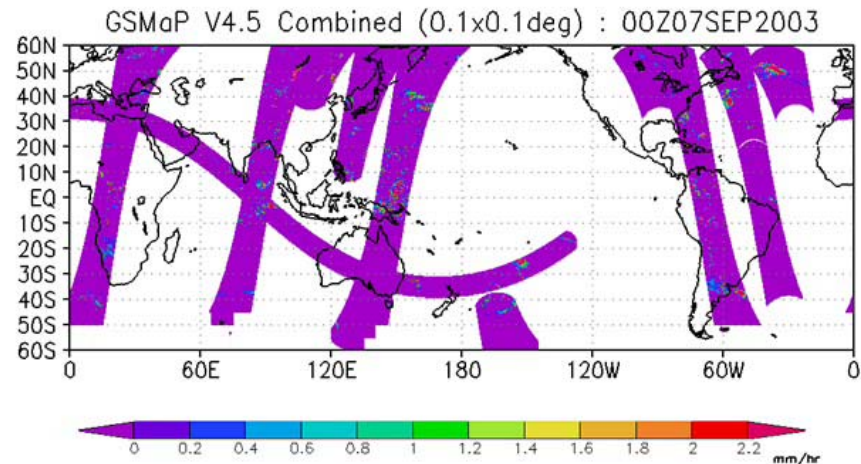
• 2003-2005

Regression line : $y=1.20x + 30.8$ (mm/month) Correlation coefficient : 0.79

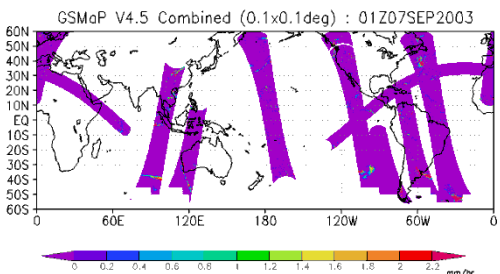
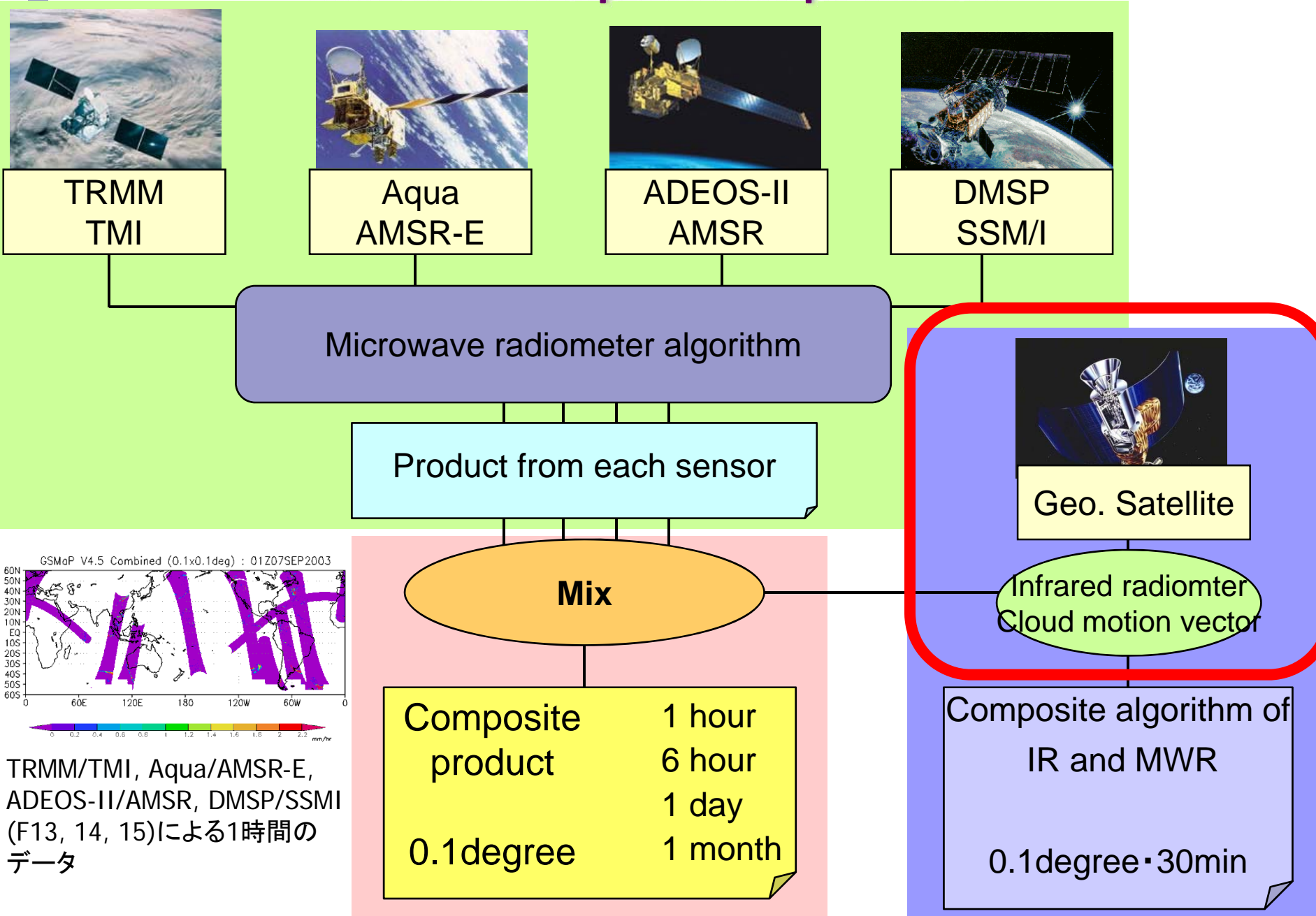
If we need a global precipitation map with higher resolution, how should we do?

- Solution

- ?????



Global Precipitation product



TRMM/TMI, Aqua/AMSR-E, ADEOS-II/AMSR, DMSP/SSM/I (F13, 14, 15)による1時間のデータ

Composite product	1 hour
	6 hour
	1 day
0.1degree	1 month

Composite algorithm of IR and MWR

0.1degree · 30min



Approaches

- There are so many products to realize the 3 hours or less resolution.
- What is the GSMP approach?

How do we combine the MWR and IR data?

- Combination of the moving vector and Kalman filtering method
- The moving vector method was introduced by Joyce et al. [2004].
 - Joyce R., J. Janowiak, P. Arkin, and P. Xie, CMORPH: A method that produces global precipitation estimates from passive microwave and infrared data at high spatial and temporal resolution, J. Hydrometeorology, 487-503, 2004
 - Advantage
 - MWR based approach (not Tb but cloud motion)
 - Fast processing time
 - Disadvantage
 - Not include the developing and decaying process of precipitation

New!!

- Kalman filter approach
 - Refine precipitation rate on Kalman gain after propagating the rain pixel
 - The Kalman gain is determined from the database on the relationship between the IR Tb and surface rain rate.

State and observation equation used in Kalman filter

$$x_{k+1} = x_k + \sigma_w \quad (\textit{State Equation})$$

$$y_k = Hx_k + G + \sigma_v \quad (\textit{Observation Equation})$$

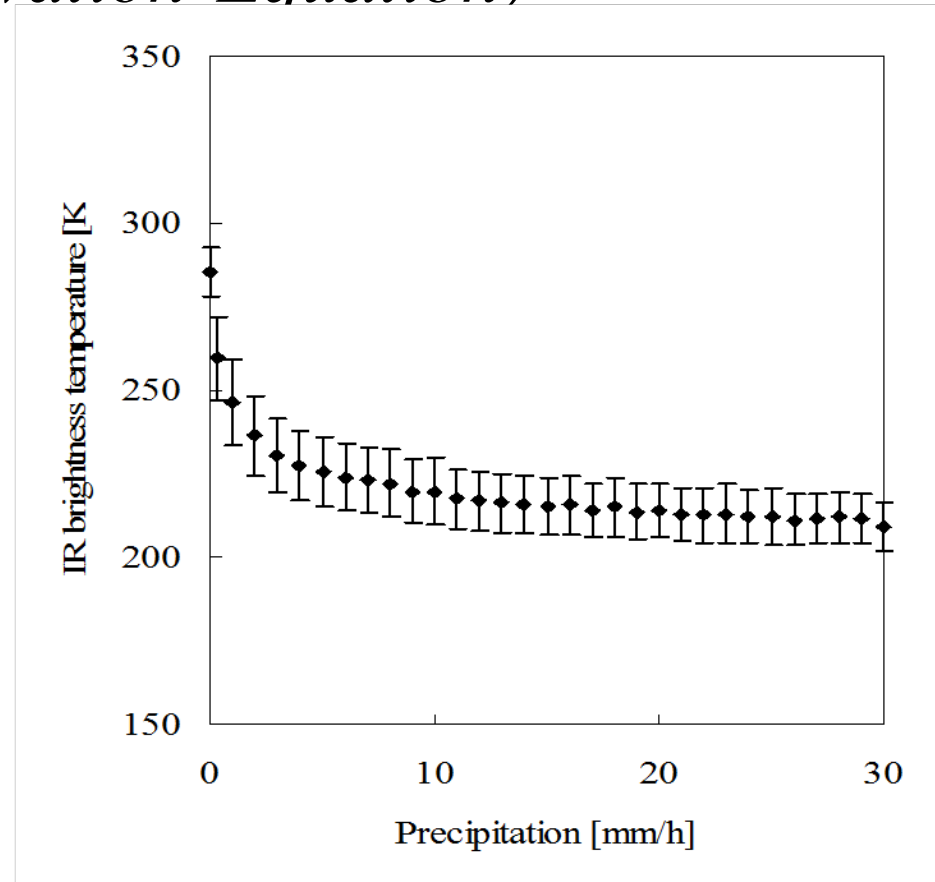
x_k : Rain rate at time k

y_k : Infrared Tb

x_{k+1} : Rain rate at time k+1

w : System noise

v : Observation noise



Kalman Filter

$$\alpha = \frac{\sigma_w^2}{\sigma_v^2}$$

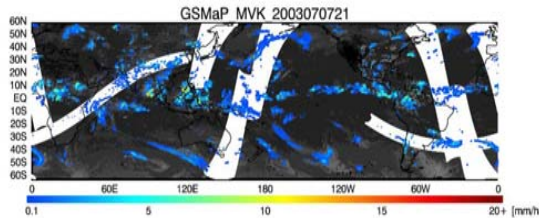
Predicted rain rate \bar{x}

IR Tb y

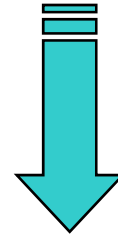
Obs. Noise σ_v

Refinement

$$\hat{x} = \bar{x} + K(y - \bar{x}) \quad K = \frac{\sqrt{\alpha^2 + 4\alpha} - \alpha}{2}$$



GSMaP \hat{x}

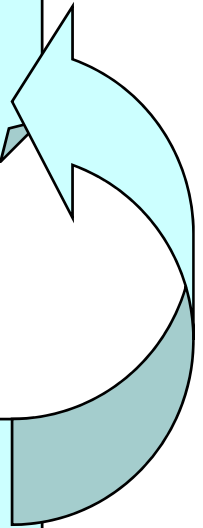


System Noise σ_w

Prediction

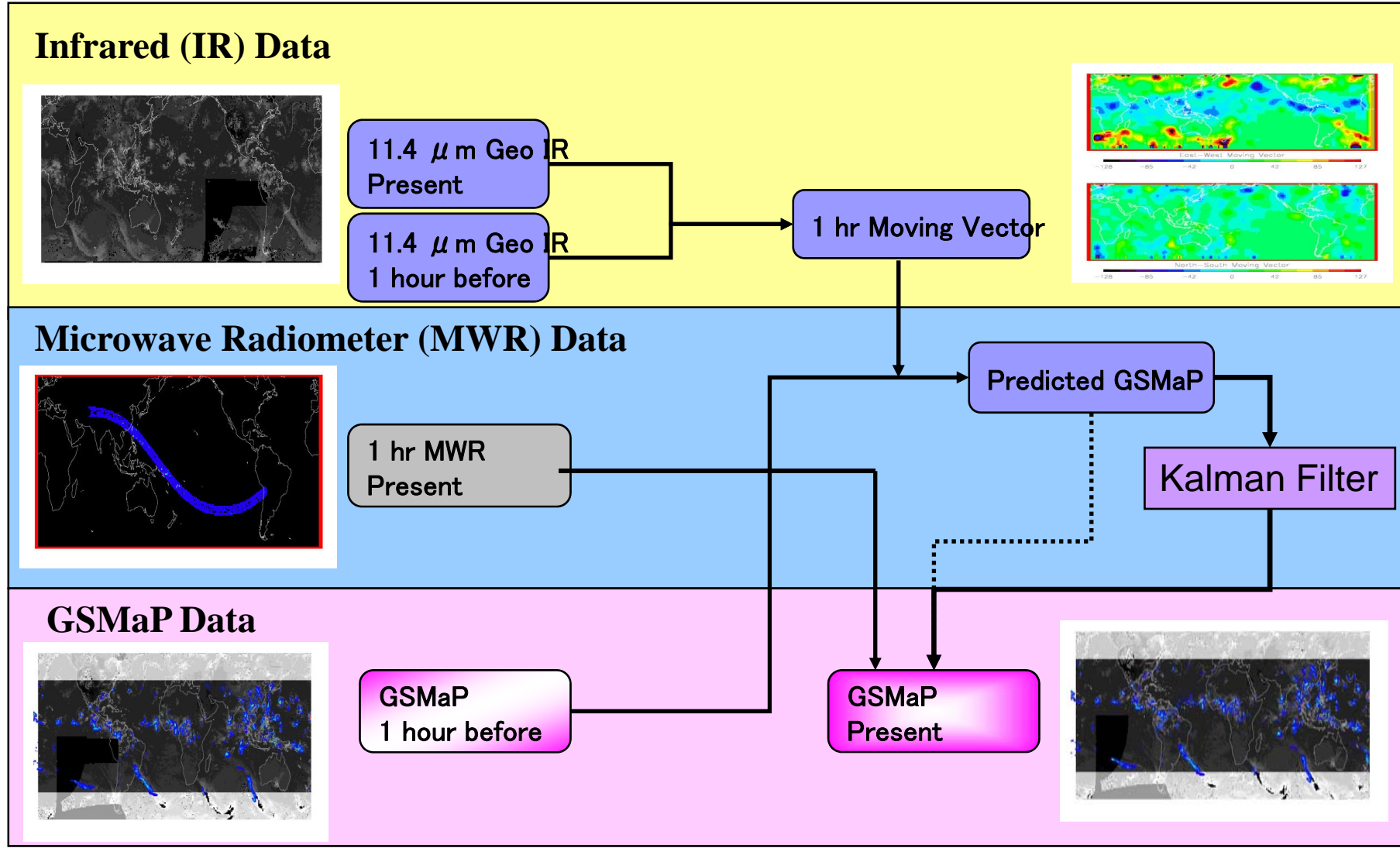
$$\bar{x}' = \hat{x}$$

Predicted rain rate \bar{x}'



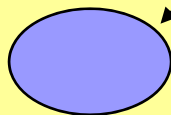
Production of high temporal (1 hr)/high spatial ($0.1^\circ \times 0.1^\circ$) resolution precipitation map (GSMaP)

Algorithm flow to predict the movement of raining areas by applying the cloud motion vector of the past 1 hour estimated from the IR cloud image



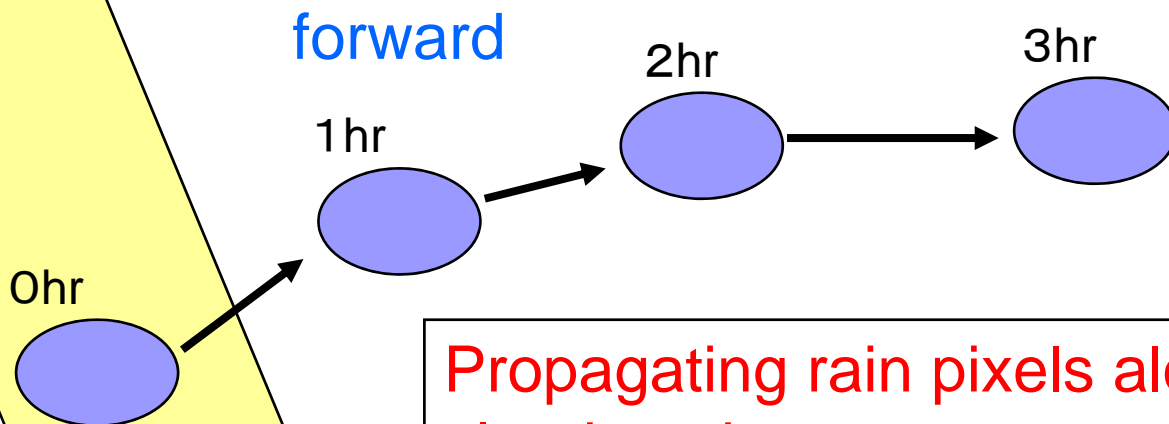
Backward process

Rain area obtained from the radiometer



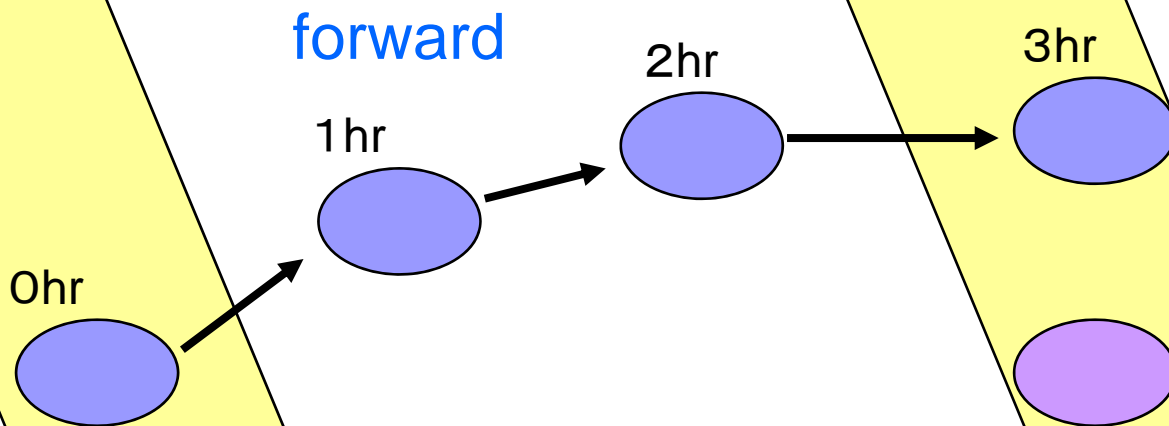
Swath of the sensor

Backward process



Propagating rain pixels along with cloud motion vector every hour

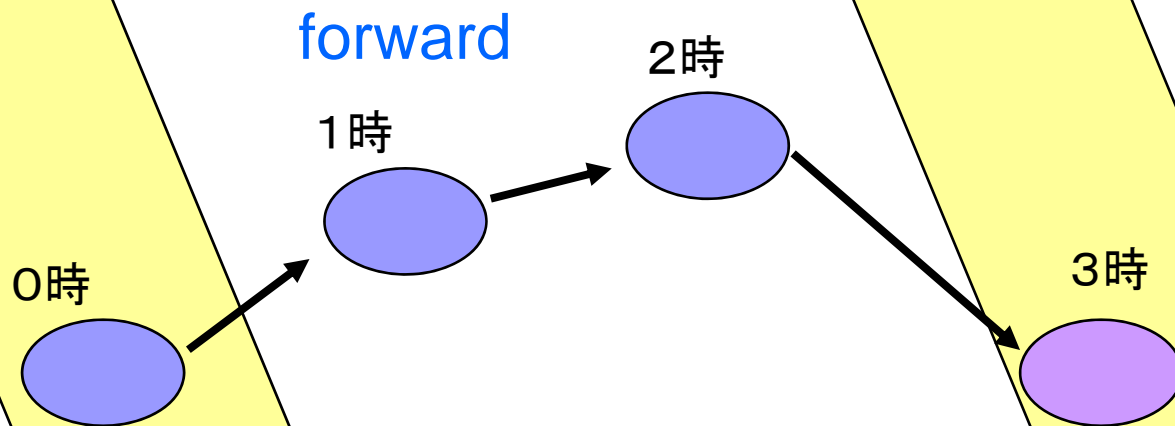
Backward process



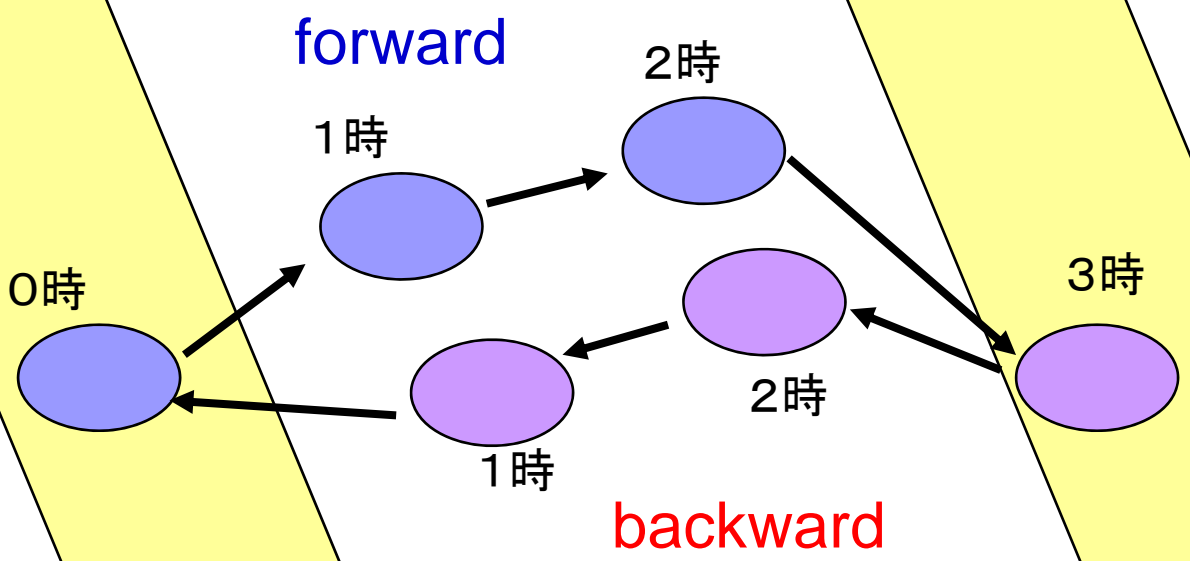
Newly identified rain area

Revisited Path of the microwave sensor

Backward process



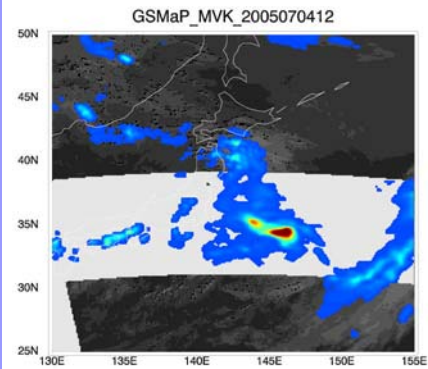
Backward process



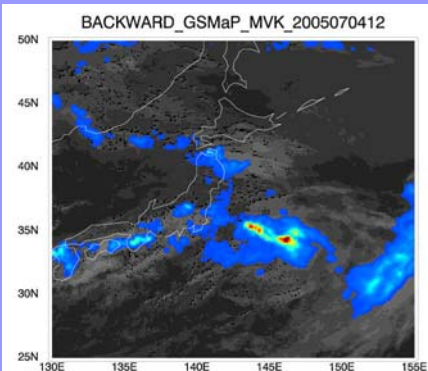
t

t+1

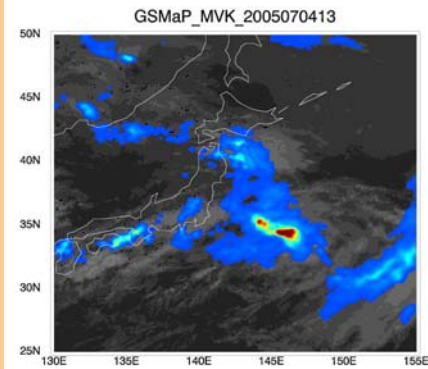
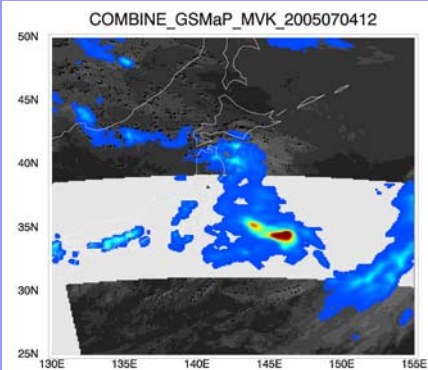
t+2



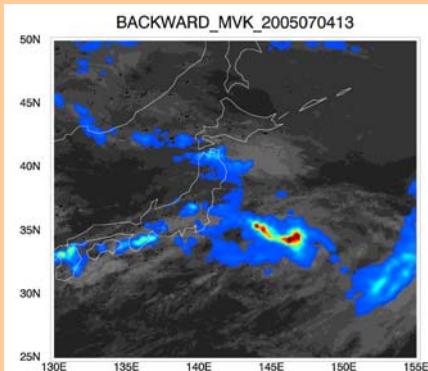
+



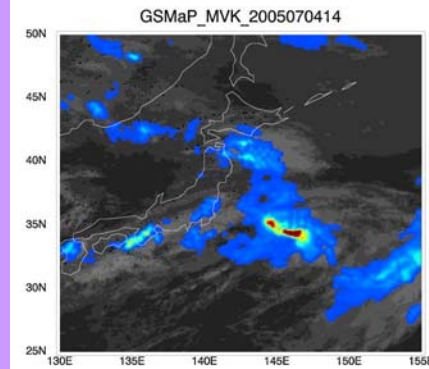
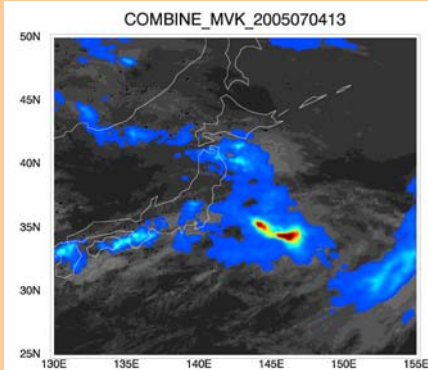
||



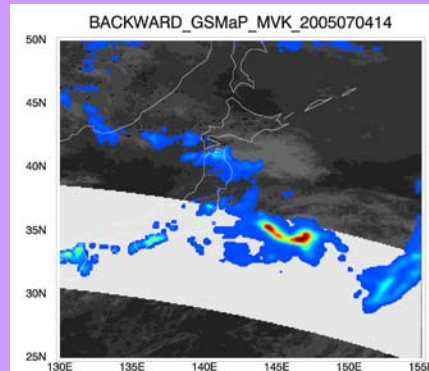
+



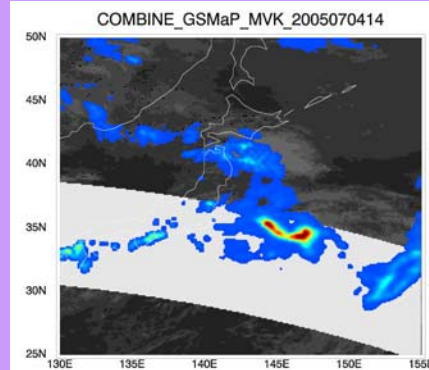
||



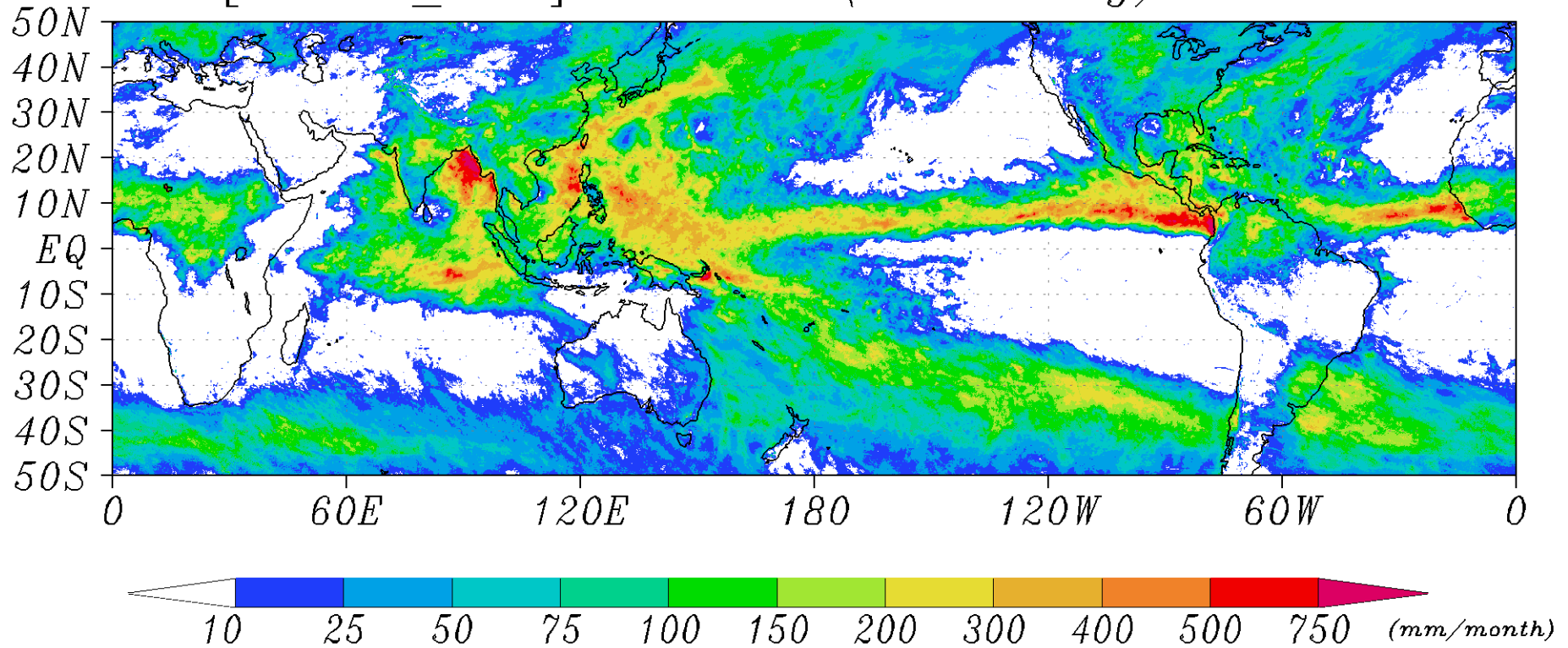
+



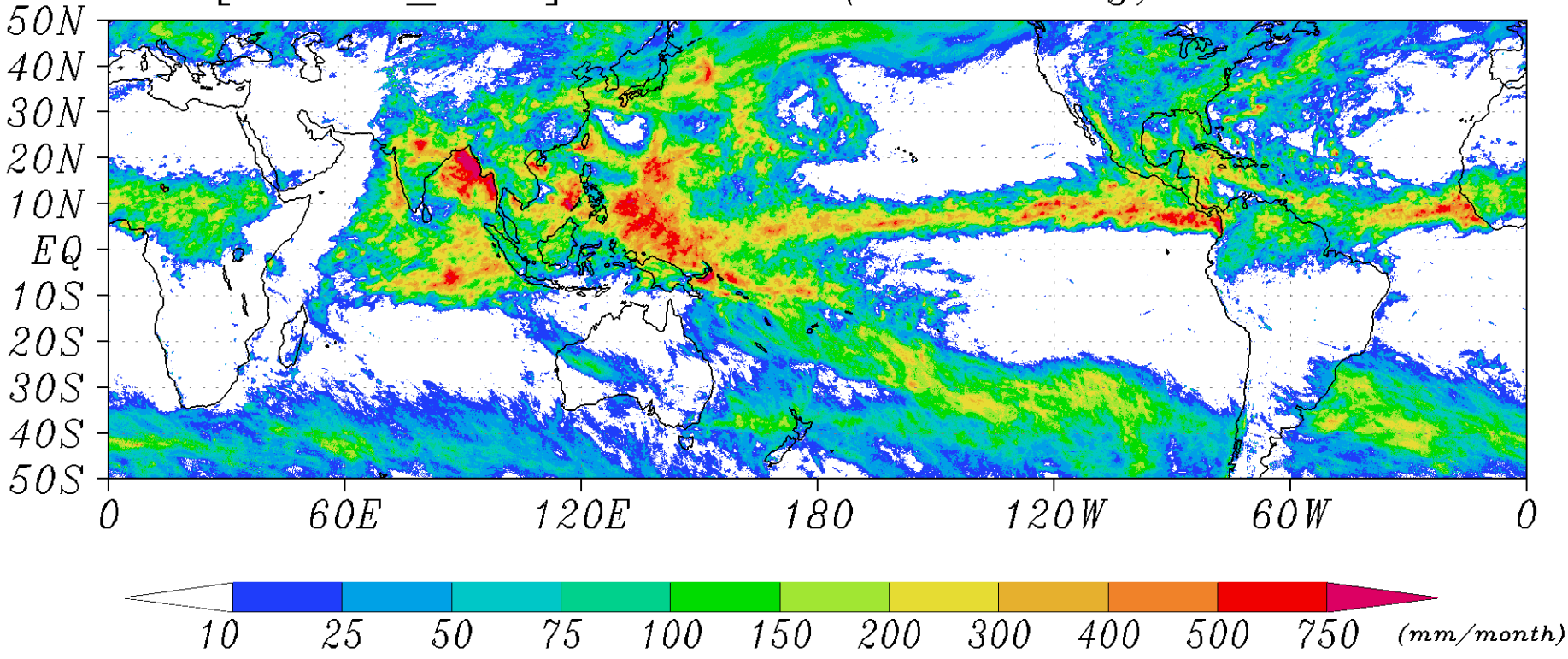
||



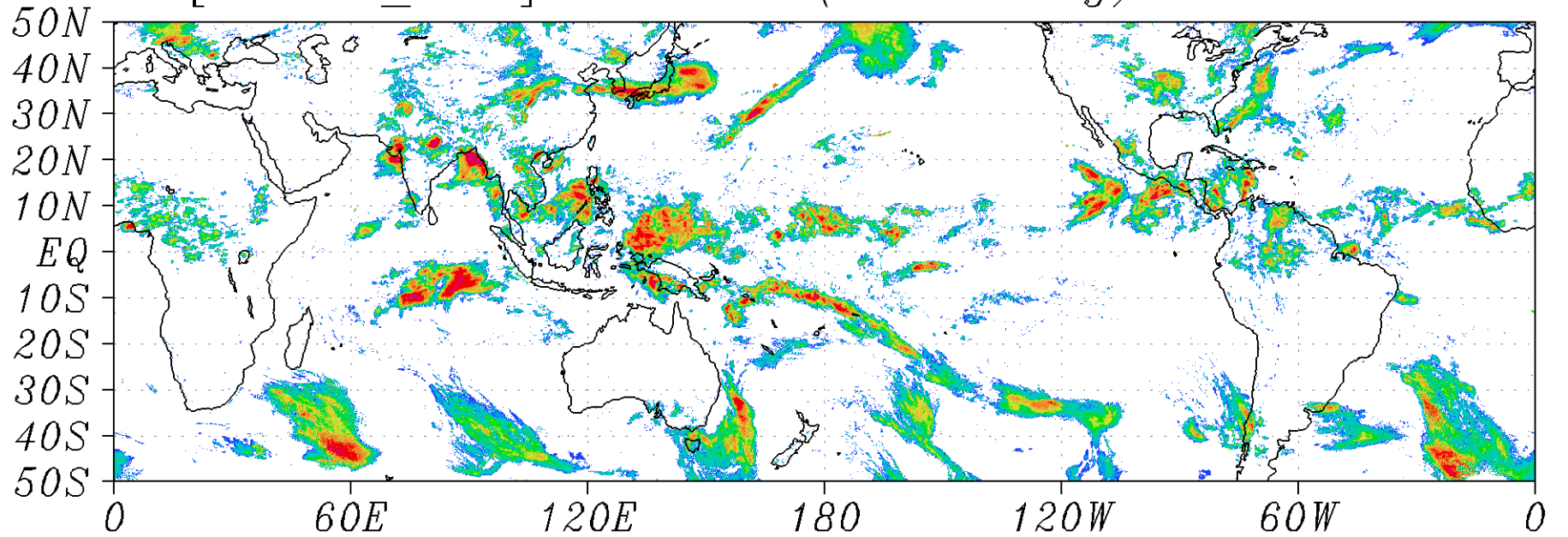
[GSMaP_MVK] Rain rate(0.1x0.1deg): JJA2005



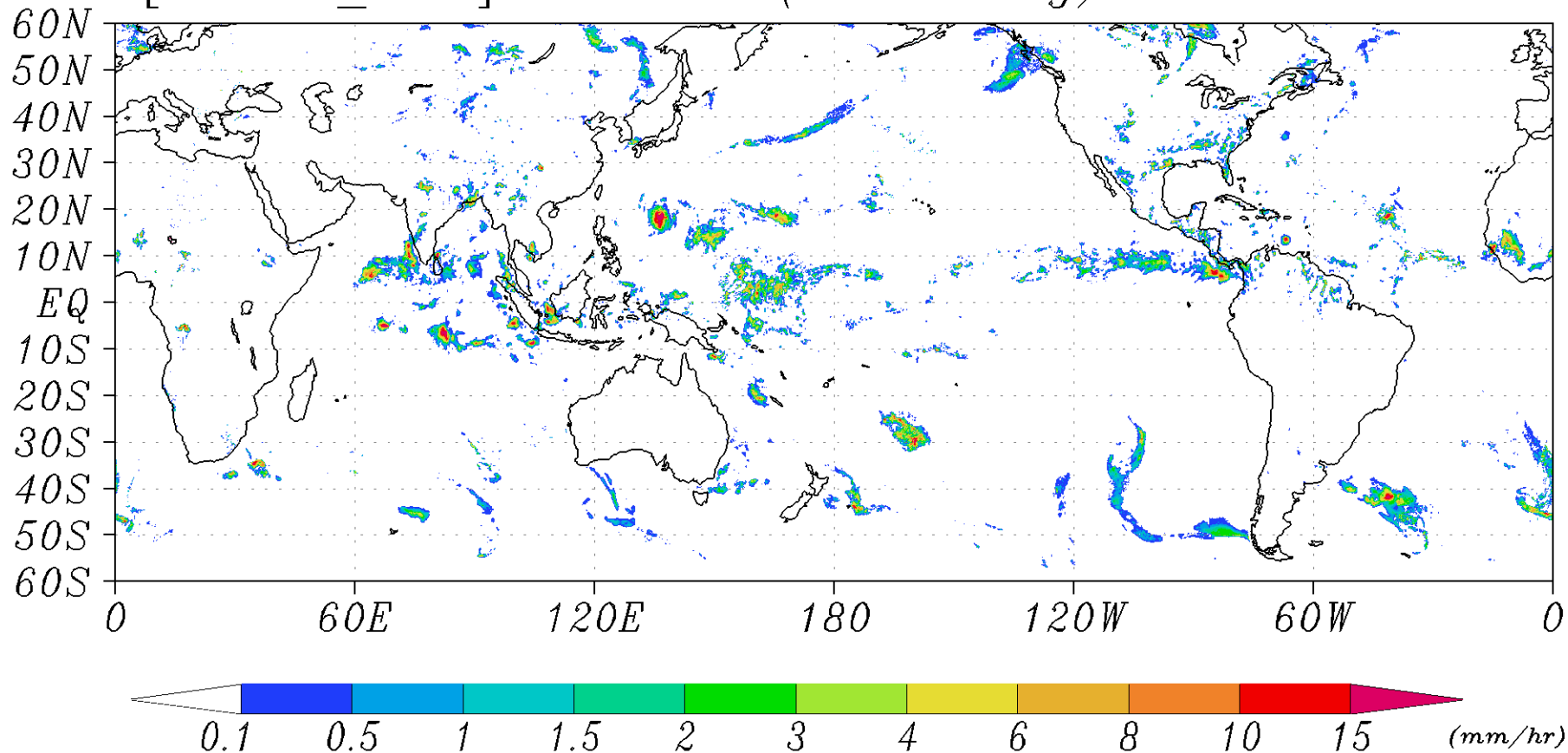
[GSMaP_MVK] Rain rate(0.1x0.1deg): JUL2005



[GSMaP_MVK] Rain rate(0.1x0.1deg): 01JUL2005



[GSMaP_MVK] Rain rate(0.1x0.1deg): 00Z15JUL2005

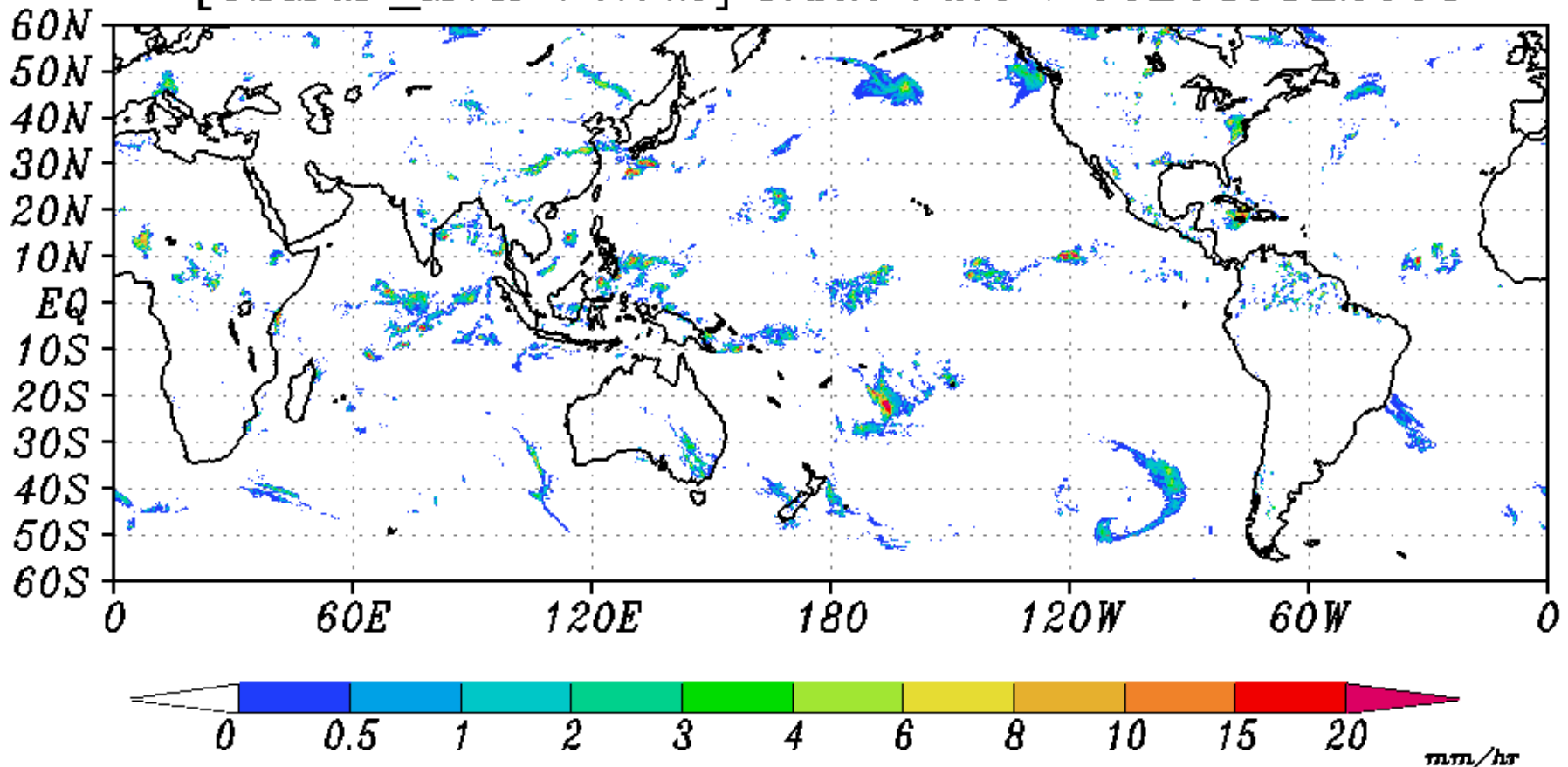


Combined global precipitation map

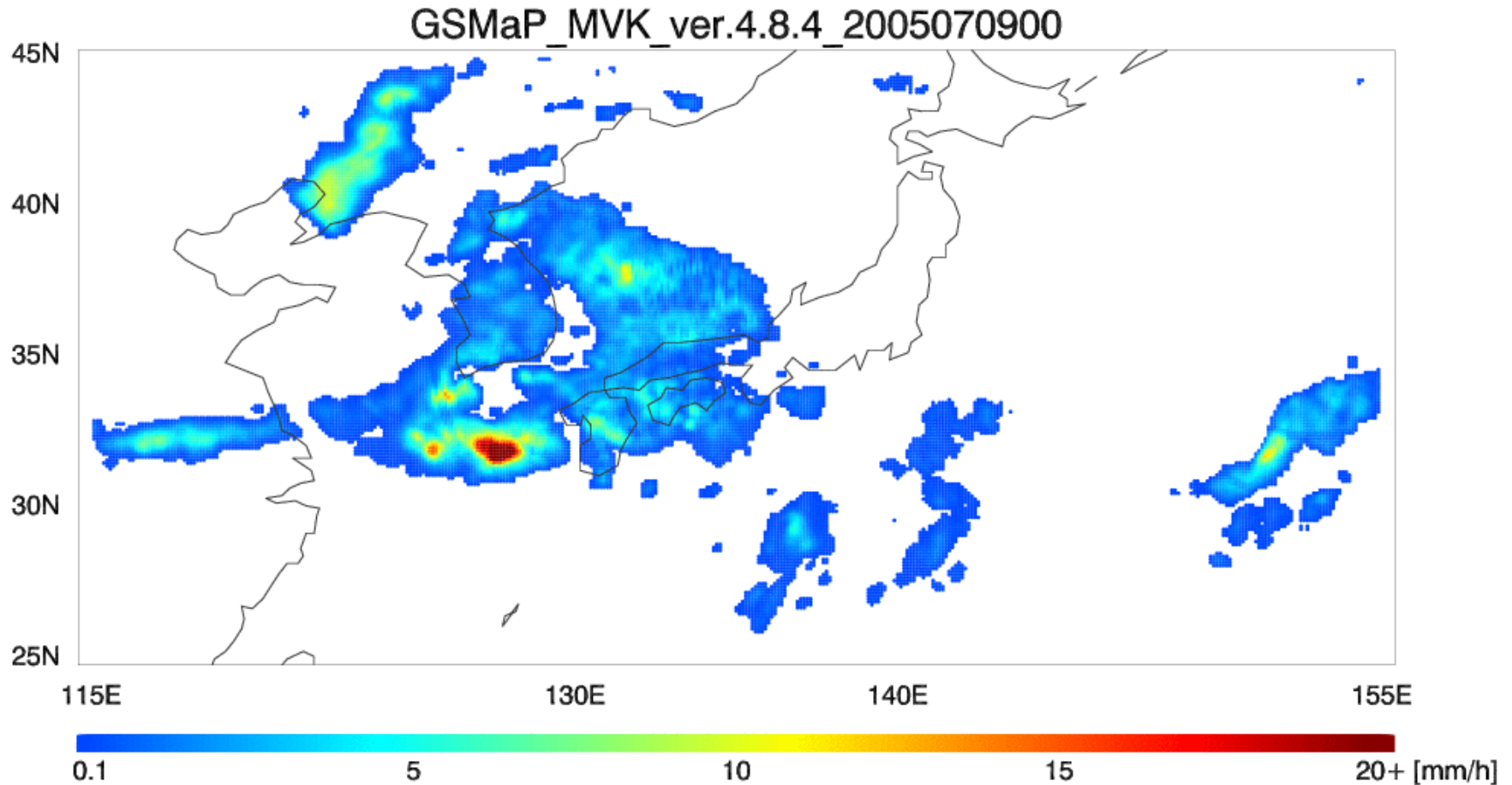
-MW radiometer + cloud motion vector with Kalman filter-
(0.1°, 1 hour, 8-10 July 2005)

MVK: MWR(TMI+AMSR+AMSR-E+F13, 14, 15 SSM/I)
+IR Cloud Motion Vector +Kalman Filter

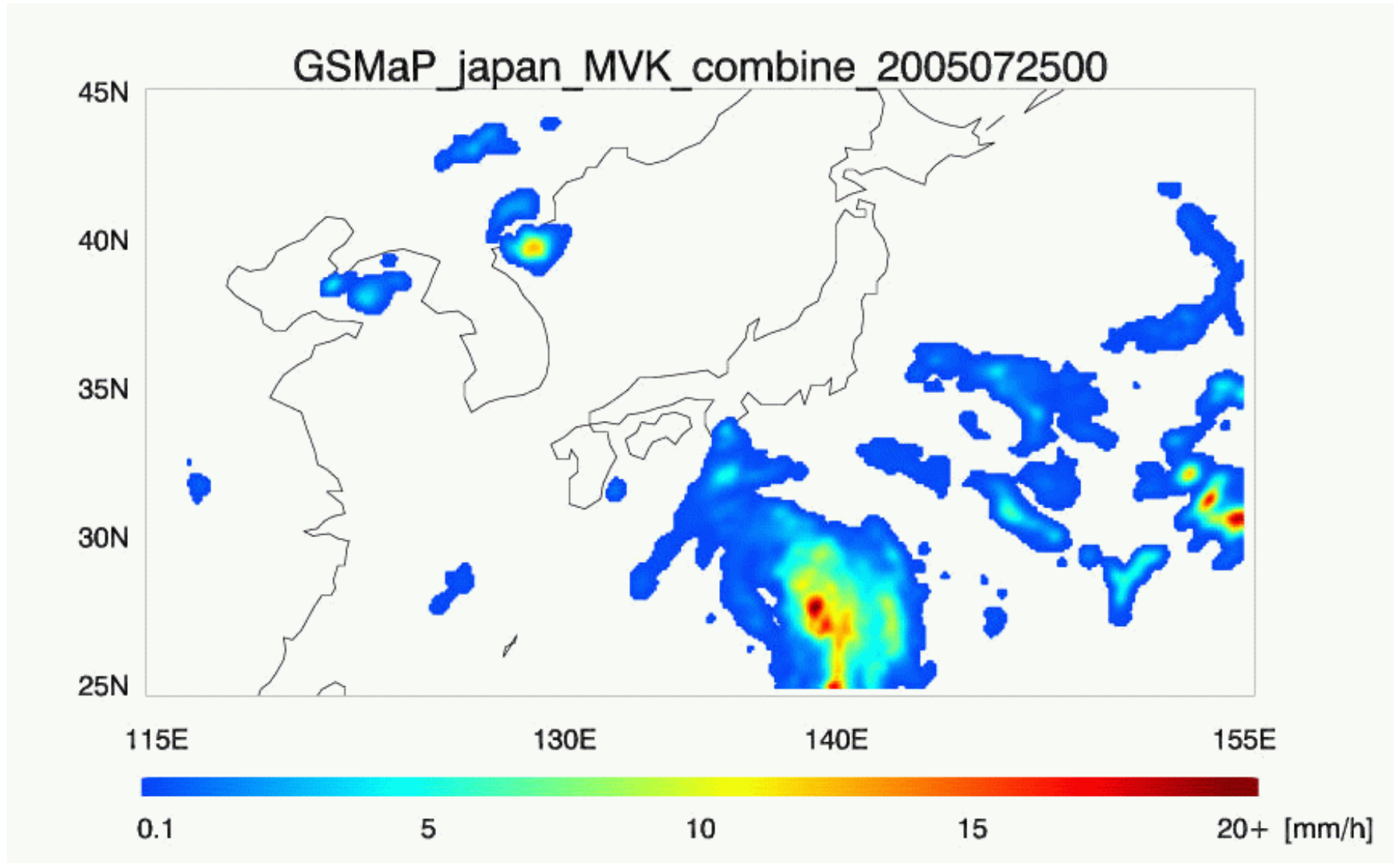
[GSMaP_MVK V4.7.2] Rain rate : 00Z08JUL2005



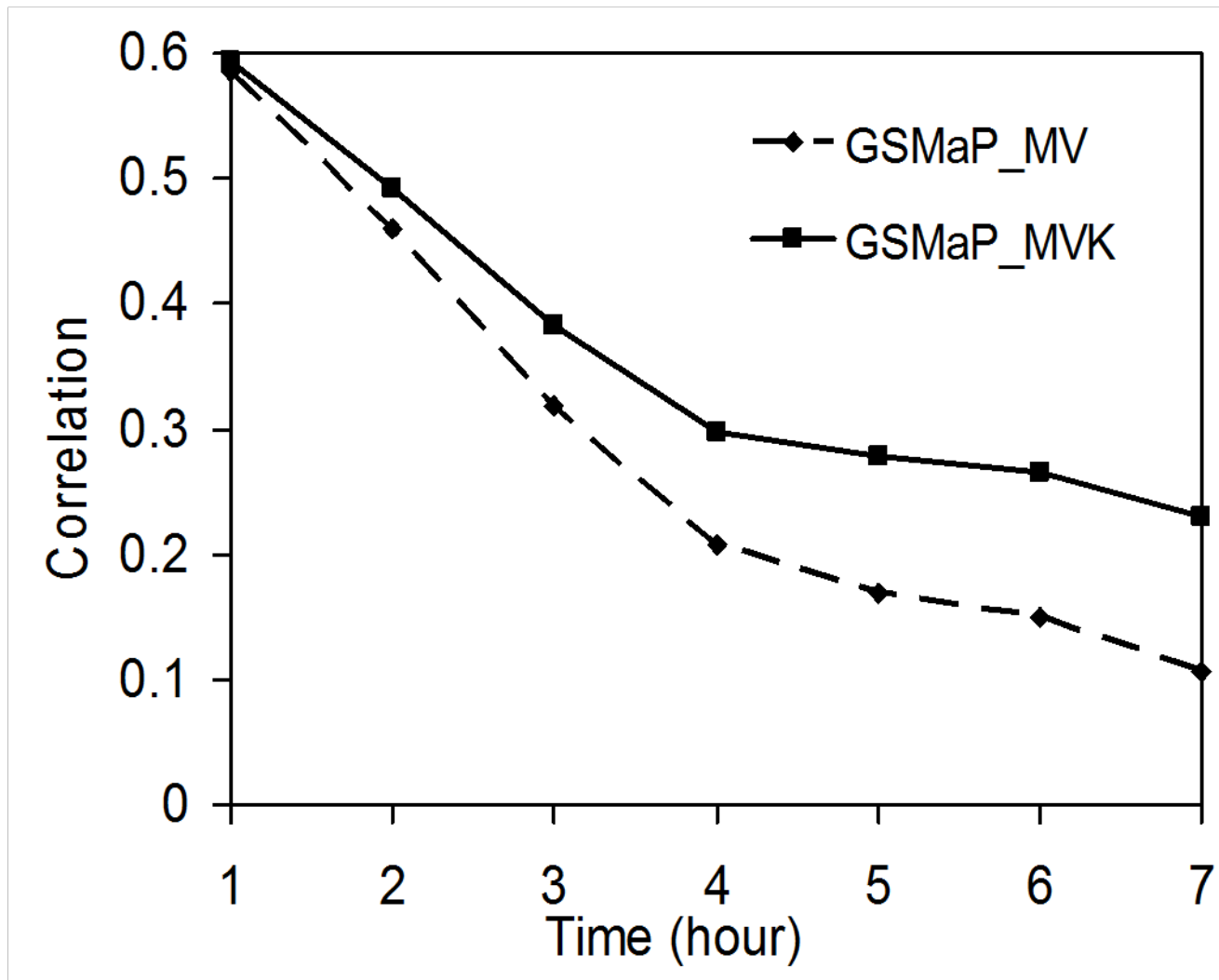
赤外・マイクロ波放射計 複合アルゴリズムによる 降水量(2005年7月9~10日)



赤外・マイクロ波放射計 複合アルゴリズムによる 降水量(台風200507号/BANYAN)



Correlation between radar and the GSMP product as a function of the past microwave satellite overpass

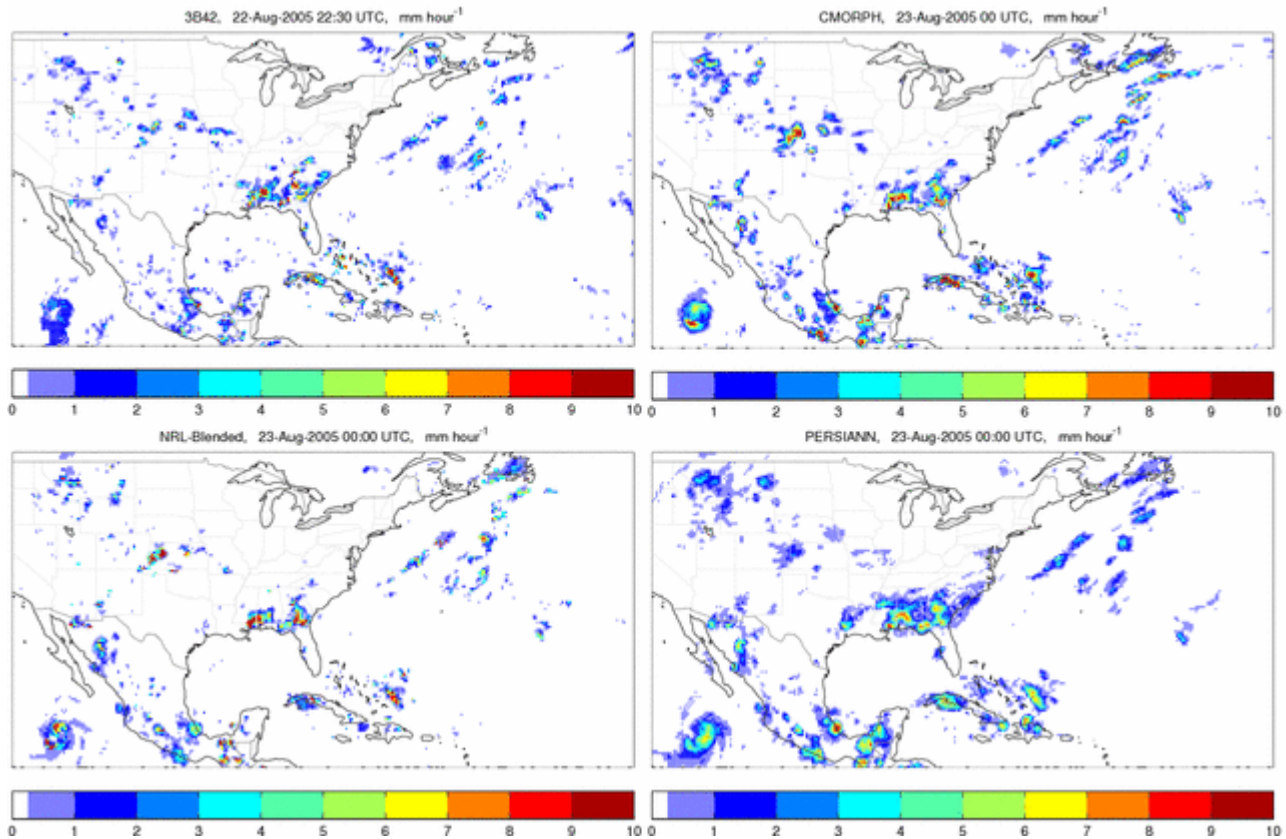


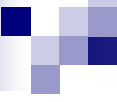


VALIDATION OF THE PRECIPITATION PRODUCTS

Hurricane Katrina – August 2005

TRMM 3B42, CMORPH, NRL, PERSIANN





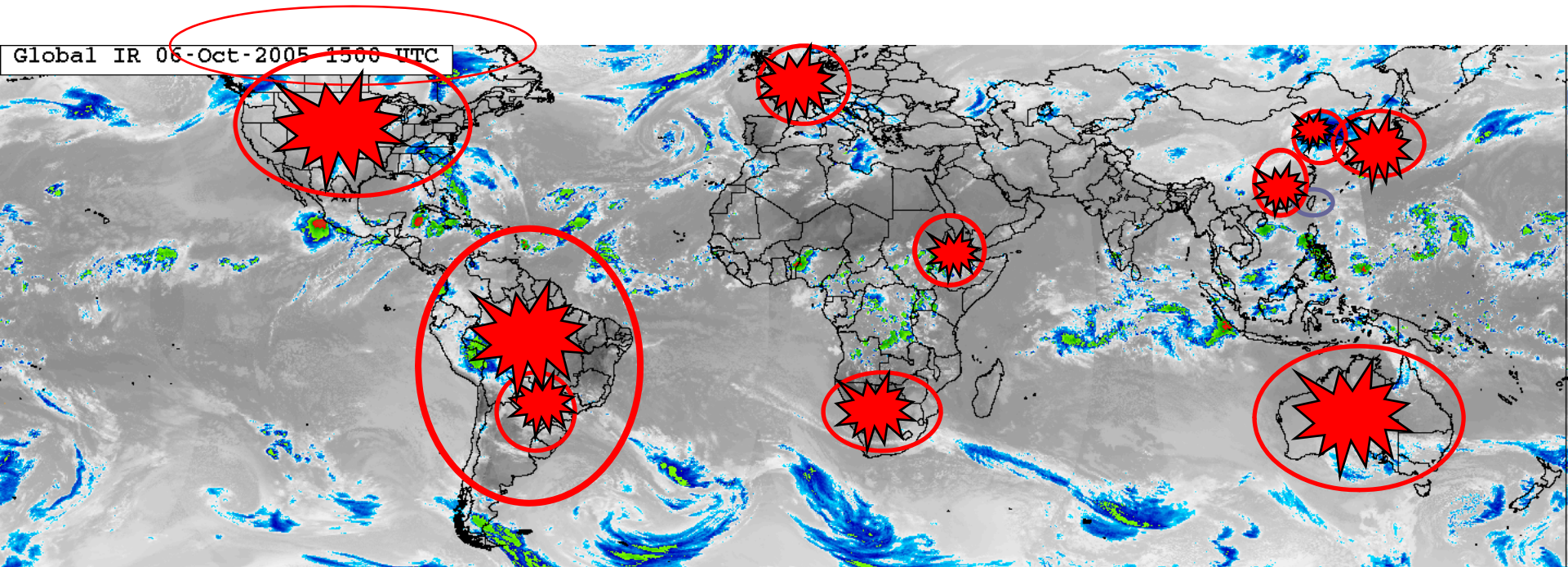
These products are very impressive, but how good are they really?

It is important to evaluate these new high resolution precipitation products to understand their errors and to identify a path to a consensus product that can be combined with gauge observations and other appropriate information and used for scientific and social applications

Program for the Evaluation of High Resolution Precipitation Products (PEHRPP)

- A comprehensive hypothesis-based collaborative effort to understand the capabilities and characteristics of these new HRPP (High Resolution Precipitation Products)
- Hypotheses:
 - HRPP errors can be characterized by comparing them to independent observations from rain gauges and radars.
 - Errors of and differences between HRPP are meaningful, in that they can be systematically related to precipitation characteristics and/or algorithm methodology.
 - Improved HRPP can be derived by combining products or methods based on the observed errors and differences.
 - HRPP spatial and temporal variability is realistic on scales appropriate for scientific studies (e.g., hydrology).
 - Numerical weather prediction forecasts of precipitation can be used to improve HRPP in some locations and times (e.g., high latitudes).
- Sponsored by the International Precipitation Working Group (Working Group of CGMS) with broad voluntary participation

Current/Proposed PEHRPP Suite 1 Validation Sites



Original:

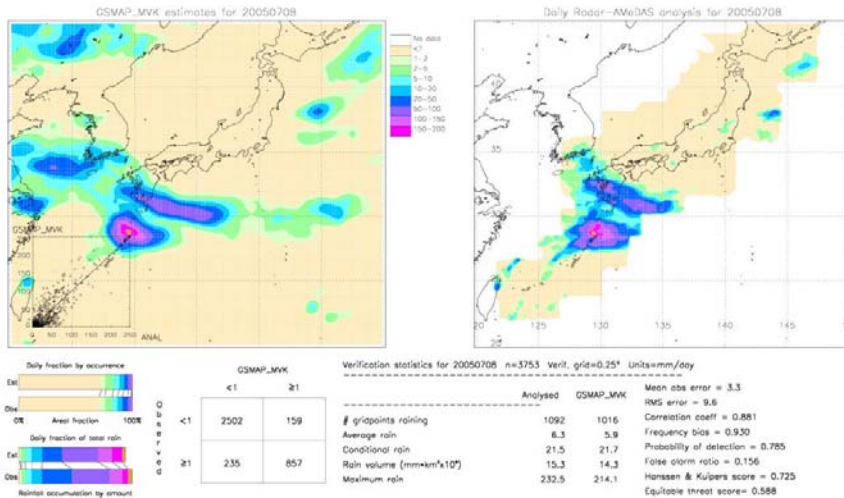
Australian continent (Ebert), CONUS (Janowiak), UK/Europe (Kidd)

New:

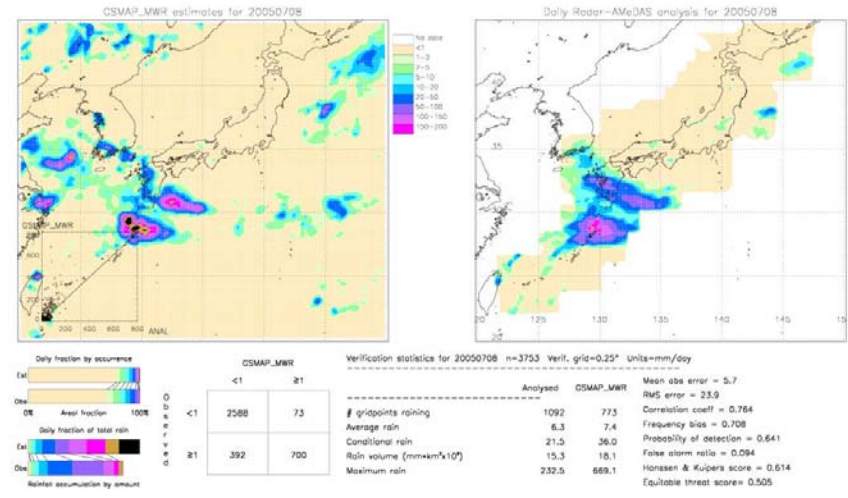
South America (Vila), S Africa (Pegram), Korea (Sohn), Taiwan (Jou), Japan (Ushio), Ethiopia/Sub-Saharan Africa (Dinko), Guangdong (Liang)...

Validation

GSMaP_MVK

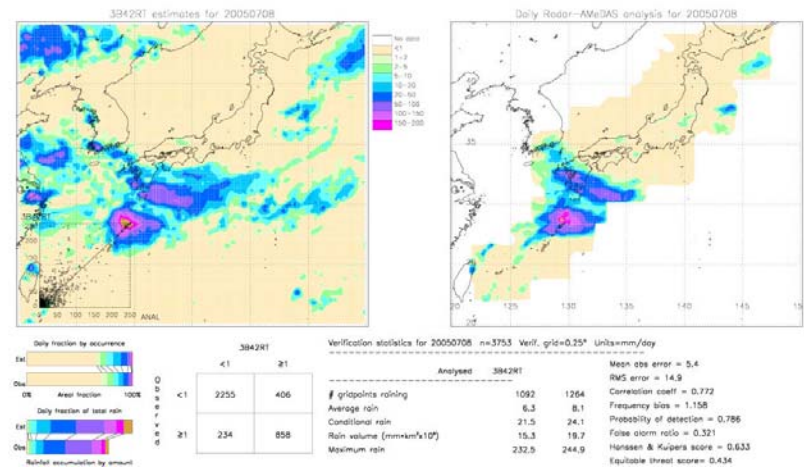
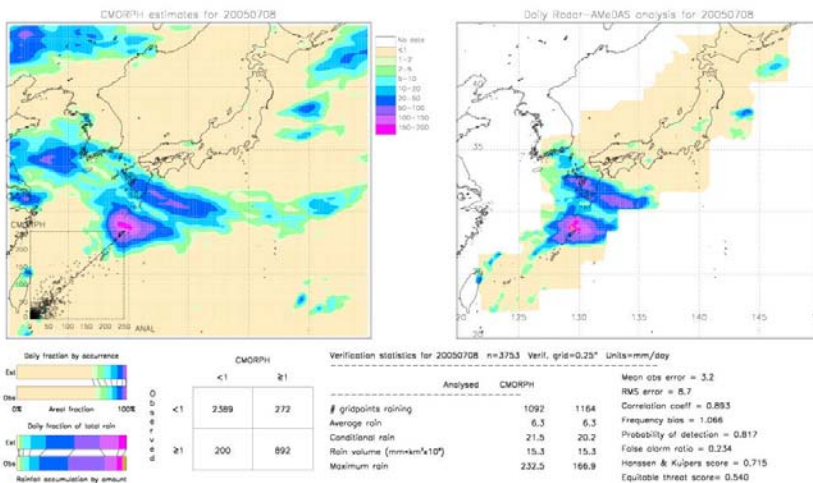


GSMaP_MWR



CMORPH(NOAA/CPC)

3B42RT(NASA)

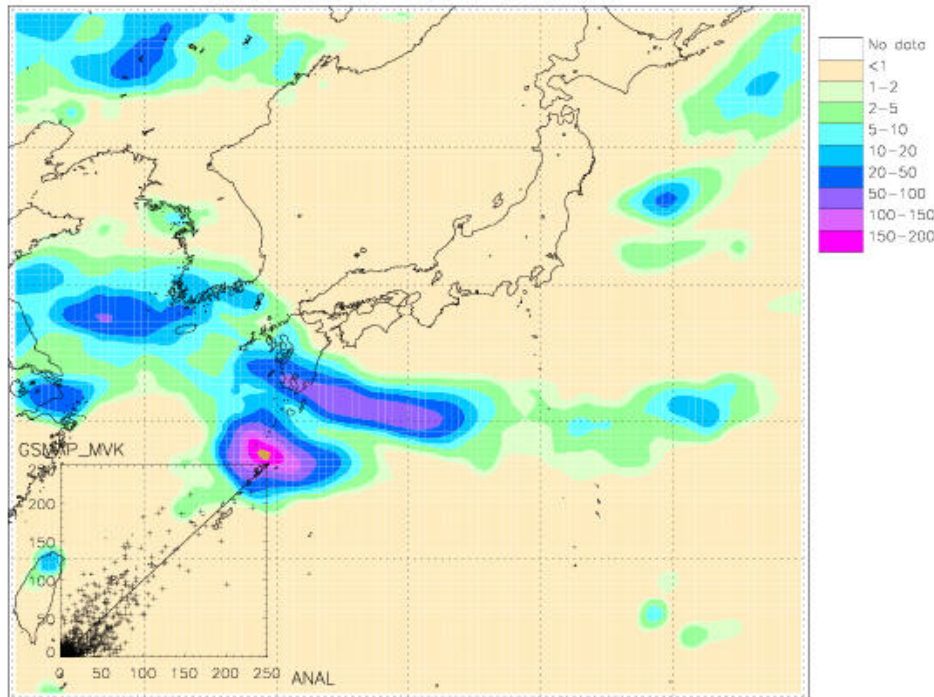


Example of validation of GSMaP_MVK using Radar-AMeDAS (8 July 2005)

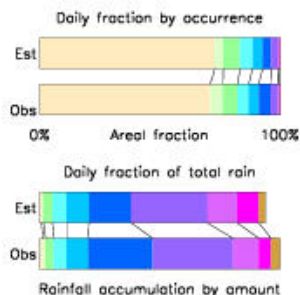
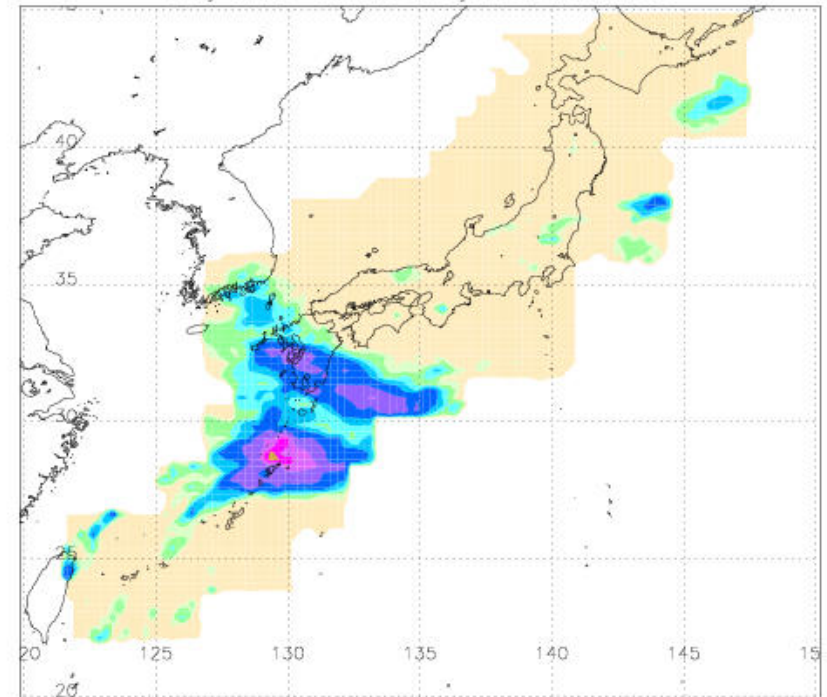
GSMaP_MVK

Radar-AMeDAS

GSMaP_MVK estimates for 20050708



Daily Radar-AMeDAS analysis for 20050708



Observed

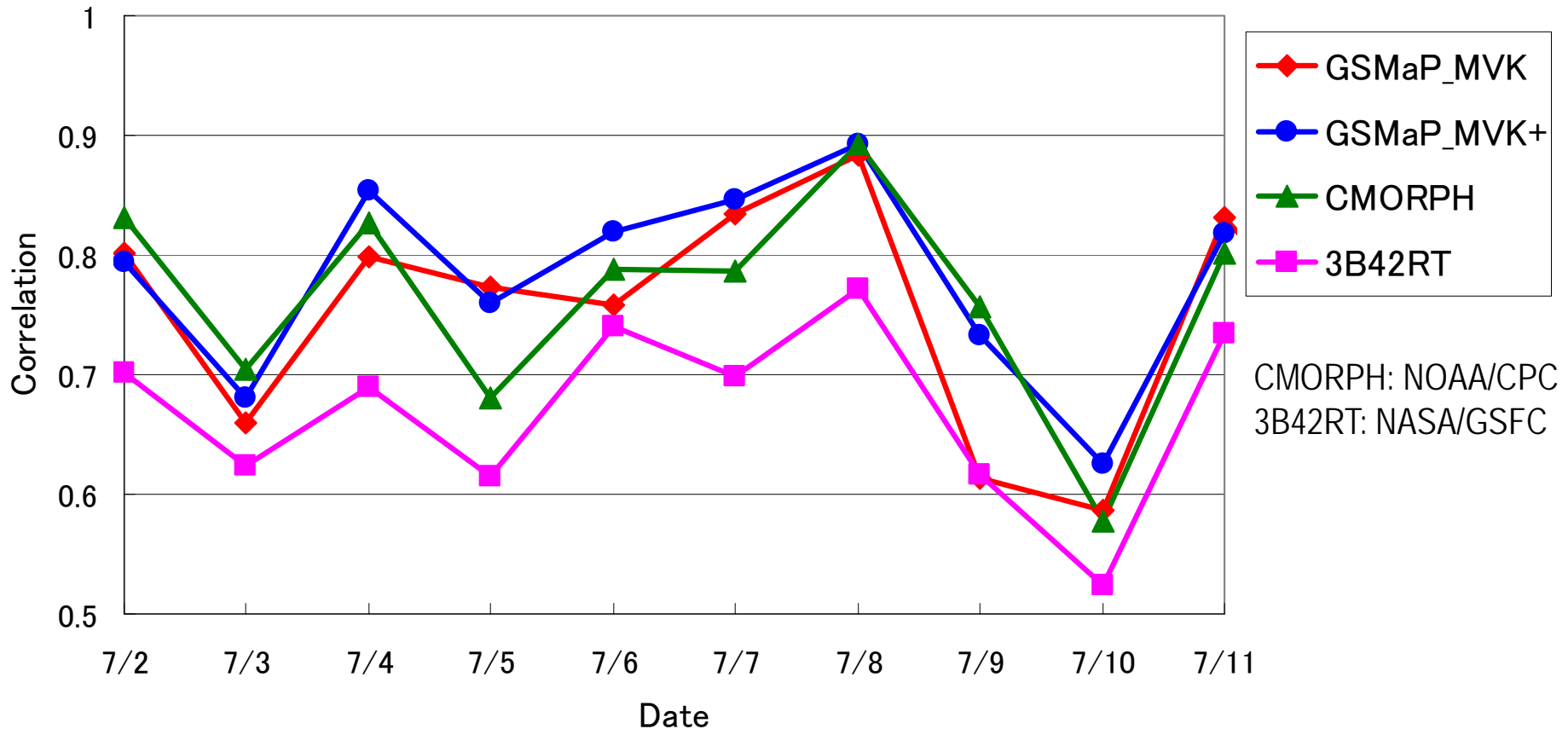
		GSMaP_MVK	
		<1	≥1
<1	<1	2502	159
	≥1	235	857

Verification statistics for 20050708 n=3753 Verif. grid=0.25° Units=mm/day

	Analysed	GSMaP_MVK	
# gridpoints raining	1092	1016	Mean abs error = 3.3
Average rain	6.3	5.9	RMS error = 9.6
Conditional rain	21.5	21.7	Correlation coeff = 0.881
Rain volume (mm*km ² *10 ⁶)	15.3	14.3	Frequency bias = 0.930
Maximum rain	232.5	214.1	Probability of detection = 0.785
			False alarm ratio = 0.156
			Hansen & Kuipers score = 0.725
			Equitable threat score = 0.588

Evaluation of various high resolution precipitation map using Radar-AMeDAS rain map

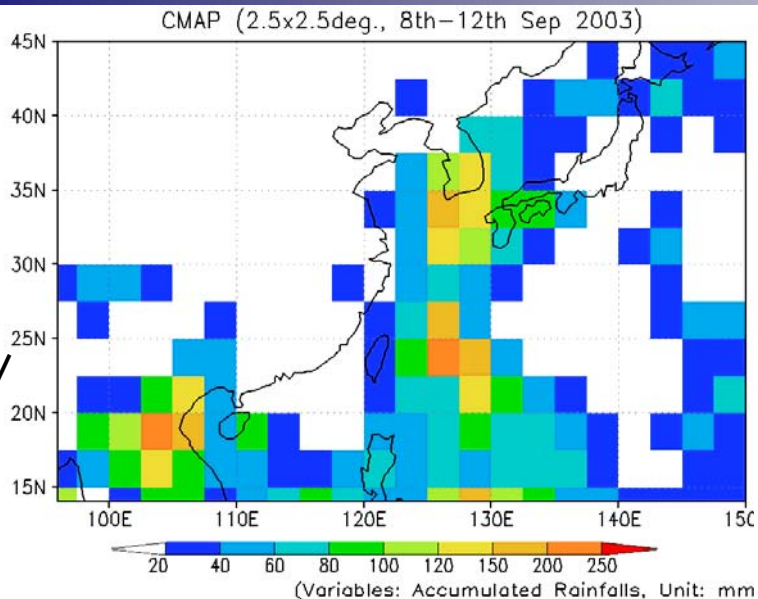
Daily variation of correlation coefficient ($0.25^\circ \times 0.25^\circ$) July, 2005



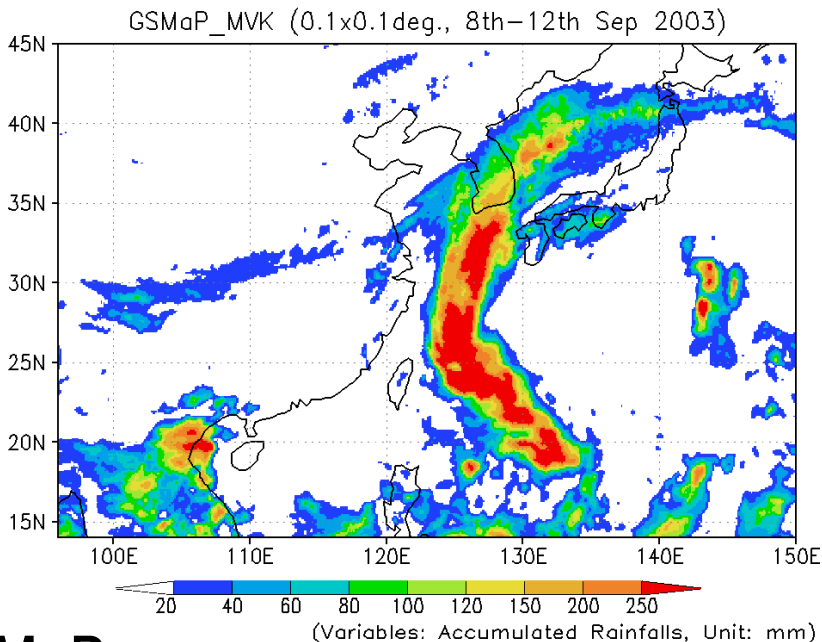
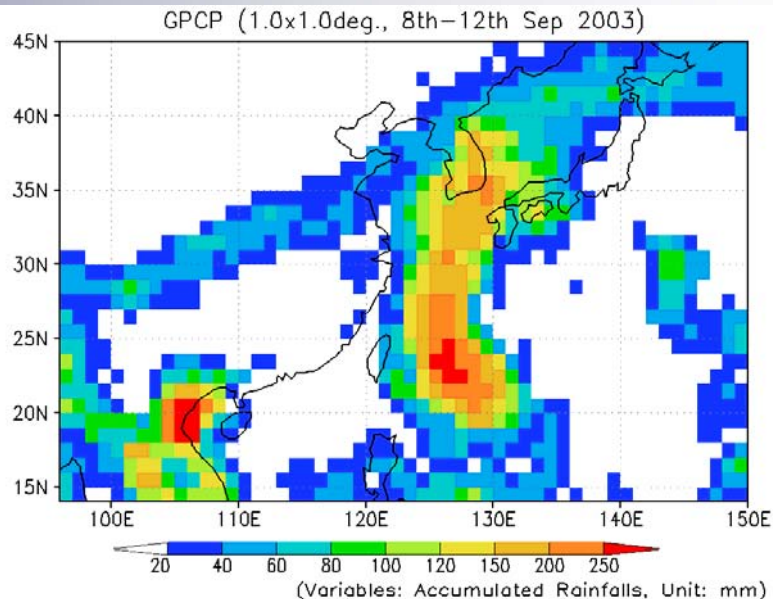
GSMaP_MVK shows high correlation with Radar-AMeDAS throughout the period.

GSMaP_MVK+, produced by adding NOAA AMSU rain rates to GSMaP_MVK, shows particularly high correlation.

CMAP
(NOAA/
CPC)



GPCP
Daily
(NASA/
GSFC)



GSMaP

降水マップの比較

(8-12 Sept. 2003)

(左上): CMAP, 2.5° 格子

(右上): GPCP Daily, 1.0° 格子

雨量計と衛星推定雨量

(IR, SSM/I, TOVS) 複合

(左下): GSMaP, 0.1° 格子

衛星推定雨量(TMI, AMSR-E, SSM/I)

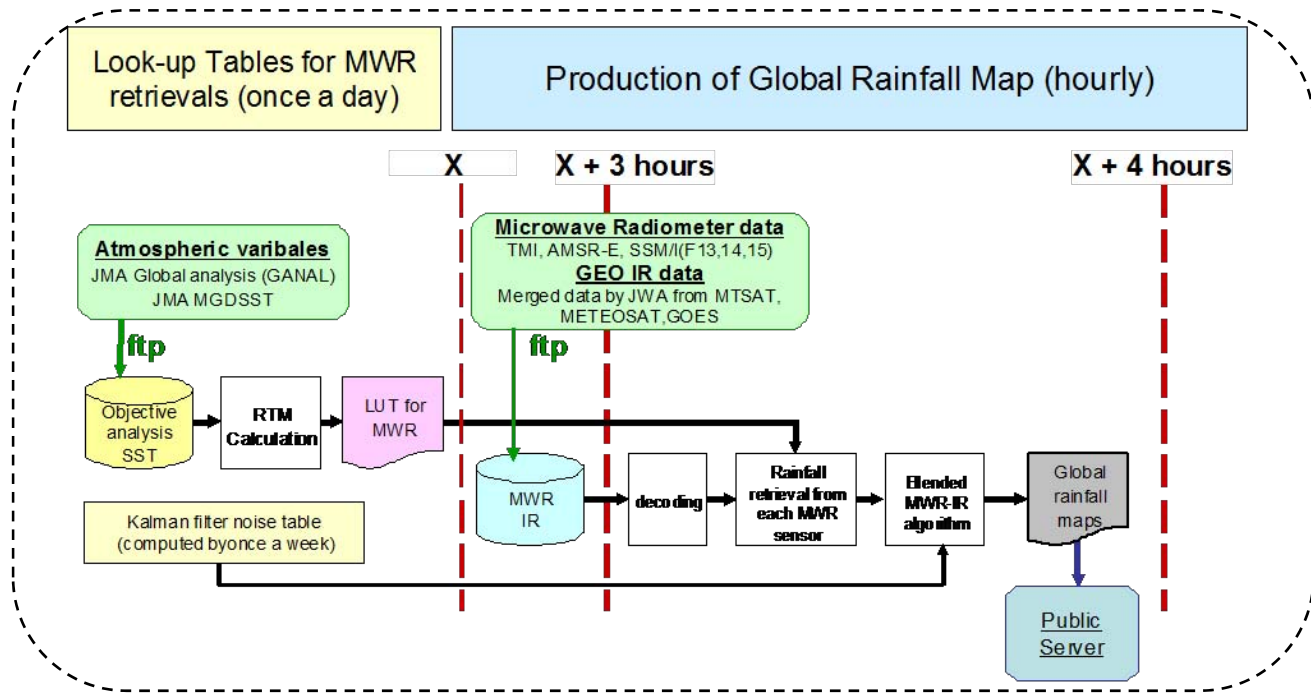
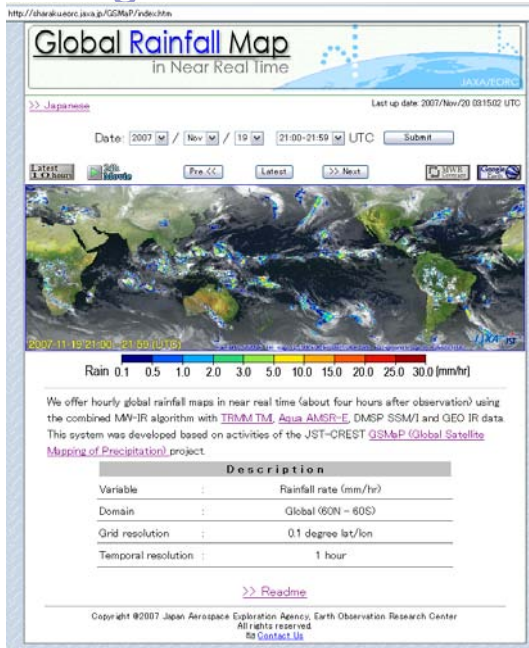
のIR補間



REAL TIME SYSTEM FOR APPLICATION

Construction of System for Near-Real-Time Global Rainfall Maps by GSMaP algorithms

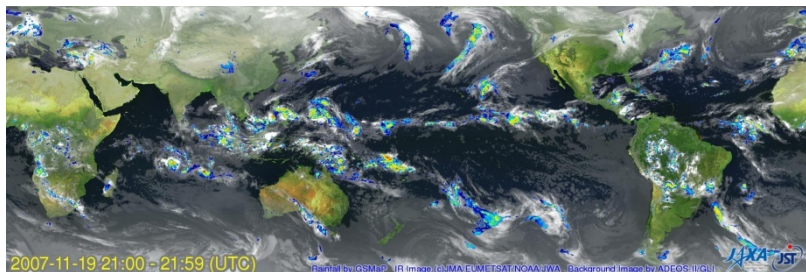
JAXA/EORC has started to release global rainfall data in near real time (about four hours after observations) on the Internet using GSMaP algorithms.

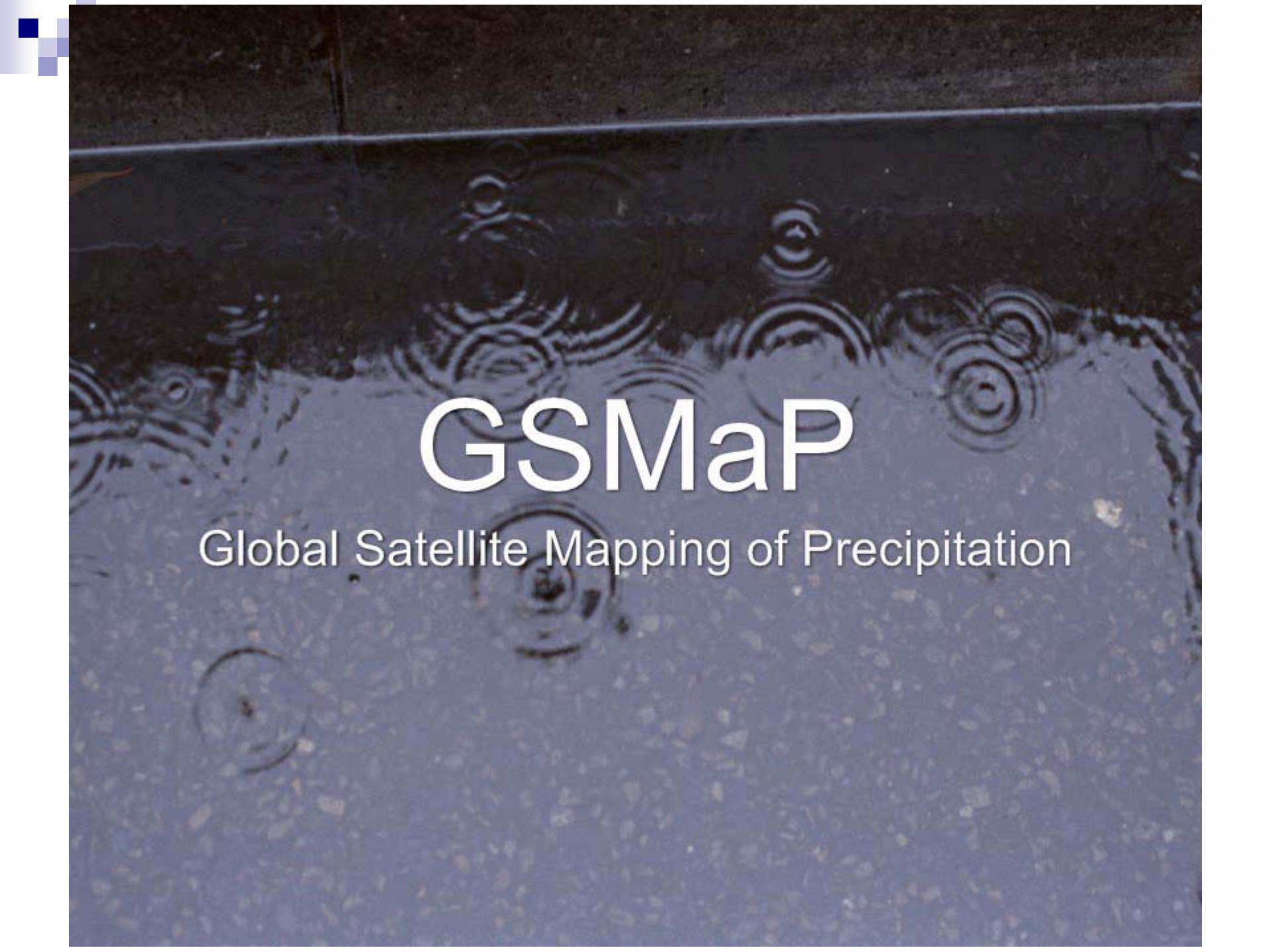


GSMaP NRT System in JAXA/EORC

Global Rainfall Map in Near Real Time by JAXA/EORC

<http://sharaku.eorc.jaxa.jp/GSMaP/>

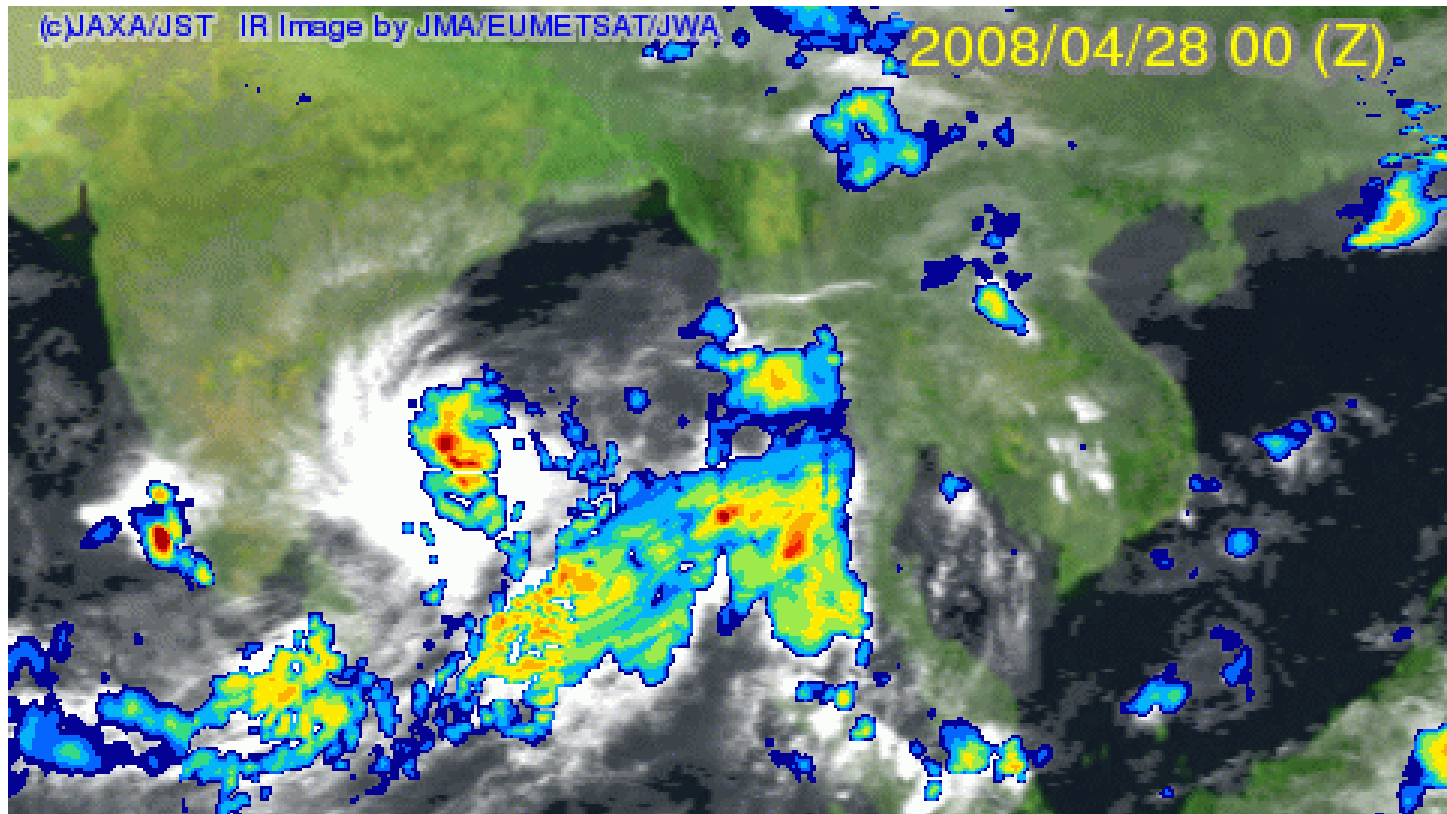




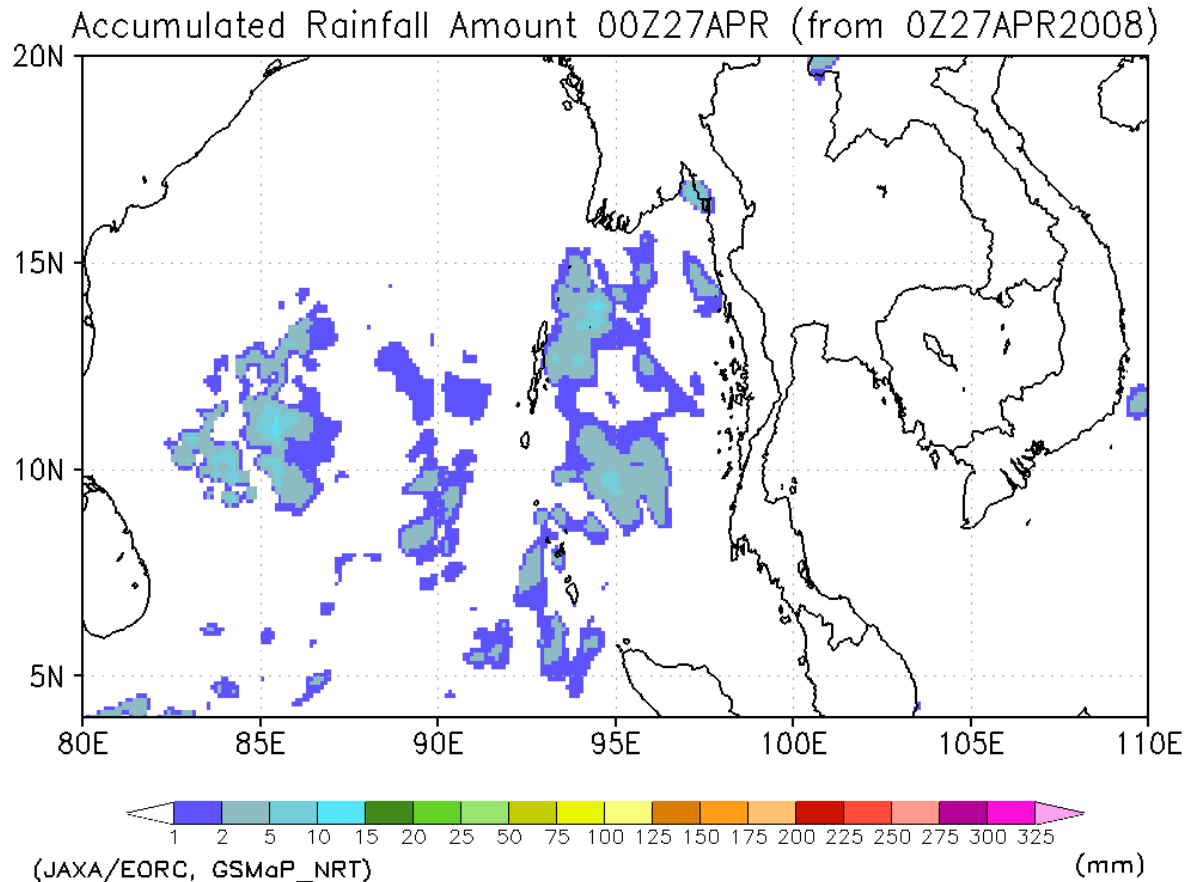
GSMaP

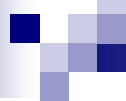
Global Satellite Mapping of Precipitation

Six hourly animation



Accumulated rainfall amount from Apr. 27 to May 5





Summary

- Needs for IR and MWR integration method are described.
- Some of the high resolution products are introduced.
- GSMaP_MVK product was introduced.

1 An Introduction to GrADS Software

The Grid Analysis and Display System (GrADS) is an interactive desktop tool to display earth science data. The followings are the features of GrADS.

Advantages

- **Free software.** Without any costs to introduce GrADS.
- **Easy installing.** GrADS is distributed for several operation systems; UNIX, Linux, Mac OSX, Sun, and Windows. In addition, pre-compiled versions are available.
- **Interactive handling.** It is suitable to quick-view data and is enable to calculate some kinds of functions easily.
- **Multiple file time series.** It is easy to display a time series such as latitude-time section.
- **Easy access to variable data formats.** GrADS deals with regardless of many types (i.e. 1-, 2-, and 4-byte integer (signed and unsigned) and float).

Disadvantages

- **Difficult page control.** It is difficult to settle map size and scale. There are a relatively few color variations although you can set some R-G-B colors.
- **Large file size of output figure.** An output file supports .eps format but in almost raster data.

1.1 Install

GrADS is distributed freely via the Internet. The latest version is 2.0 (The older versions are also available for old X-windows servers). Unless you want to optimize, customize etc., it is easy to use pre-compiled version.

At first, download the following files to operate GrADS from <http://www.iges.org/grads/downloads.html>.

- GrADS software (Choose one for your using OS)
- Supplementary Files (data.tar.Z)
- Supplementary Scripts (<http://www.iges.org/grads/gadoc/library.html>)

For the supplementary scripts, you can download all files by `wget` command.

```
[hoge@hoge src]$ wget -nc -np -r ftp://grads.iges.org/grads/scripts/
```

Next, uncompress and extract the downloaded files, and install GrADS. For the GrADS software,

```
[hoge@hoge src]$ tar xvfz grads-2.0.a3-bin-i686-pc-linux-gnu.tar.gz
grads-2.0a3/
grads-2.0a3/bin/
grads-2.0a3/bin/bufrscan
grads-2.0a3/bin/gribmap
```

```

...
grads-2.0a3/bin/grads
...
grads-2.0a3/COPYRIGHT
grads-2.0a3/INSTALL
[hoge@hoge src]$ cd grads-2.0a3/bin
[hoge@hoge bin]$ su
Password:
[hoge@hoge bin]# cp * /usr/local/bin
[hoge@hoge bin]# exit

```

For the supplementary (coast lines and fonts) files,

```

[hoge@hoge src]$ mkdir grads
[hoge@hoge src]$ cd grads
[hoge@hoge grads]$ tar xvfz ../data.tar.Z
[hoge@hoge grads]$ cd ../
[hoge@hoge src]$ su
Password:
[hoge@hoge src]# cp -r grads/ /usr/local/lib/
[hoge@hoge src]# exit

```

For the supplementary scripts,

```

[hoge@hoge src]$ cd grads.iges/org/grads/scripts/
[hoge@hoge scripts]$ su
Password:
[hoge@hoge scripts]# cp * /usr/local/lib/grads/
[hoge@hoge scripts]# exit

```

Add the environmental variable for GrADS.

```

[hoge@hoge hoge]$ vi .bashrc
## For GrADS (for >=2.0)
export GADDIR=/usr/local/lib/grads
## for GrDAS (for <2.0)
export GASCRP=/usr/local/lib/grads

```

```

[hoge@hoge hoge]$ vi .cshrc
## For GrADS (for >=2.0)
setenv GADDIR /usr/local/lib/grads
## For GrADS (for < 2.0)
setenv GASCRP /usr/local/lib/grads

```

1.2 Using GrADS gridded data file

The data description file for GrADS is called as “.ctl”. You may understand how the binary data is stored when you see the .ctl file. Get example.tar.Z (you may get the under part of <http://www.iges.org/grads/gadoc/downloads.html>) and confirm the data descriptions.

```

[hoge@hoge GrADS]$ tar xvfz example.tar.Z
model.ctl
model.dat
sample
[hoge@hoge GrADS]$ cat model.ctl
DSET    ^model.dat
OPTIONS little_endian
UNDEF   -2.56E33
TITLE   5 Days of Sample Model Output
XDEF    72 LINEAR 0.0 5.0
YDEF    46 LINEAR -90.0 4.0
ZDEF    7 LEVELS 1000 850 700 500 300 200 100
TDEF    5 LINEAR 02JAN1987 1DY
VARS    8
PS      0   99   Surface Pressure
U       7   99   U Winds
V       7   99   V Winds
Z       7   99   Geopotential Heights
T       7   99   Temperature
Q       5   99   Specific Humidity
TS      0   99   Surface Temperature
P       0   99   Precipitation
ENDVARS

```

In this example, the binary data set is named **model.dat**, the undefined, or missing, data value is **-2.56E33**, there are **72** grid points in the X direction, **46** in the Y direction, **7** levels, **5** times, and **8** variables. The variables **U**, **V**, **Z**, and **T** have **7** levels, the variable **Q** has **5** levels, and the variables **PS**, **TS**, and **P** has **one** level. The first dimension of these arrays vary from west to east, the second from south to north.

In this example the horizontal grids are Band Sequential (BSQ) and written in the following order: (02Jan1987, surface, PS), (02Jan1987, 1000 hPa, U), (02Jan1987, 850 hPa, U), ... (02Jan1987, 100 hPa, U), (02Jan1987, 1000 hPa, V), ... (02Jan1987, surface, TS), 02Jan1987, no demension, P), (03Jan1987, surface, PS), ... etc.

The further explanation of model.ctl is described as follows. See more information at Using GrADS Data Files (Section 4.0 in The Users Guide) or at About GrADS Gridded Data Sets in the online version of the users guide (<http://www.iges.org/grads/gadoc/descriptorfile.html>).

DSET data-set-name The name of the binary data set is “model.dat”. “^” is the proxy of a full path if the binary data set is in the same directory as .ctl file.

OPTIONS Byte order is little endian. If the format of a binary data is big endian, write “big_endian”.

UNDEF value The undefined, or missing, data value is -2.56E33. GrADS operations and graphics routines will ignore data with this value from this data set. *This is a required parameter even if there are no undefined data.*

TITLE string This data is 5 days of sample model output. You can write a brief description of the contents of the data set.

XDEF number LINEAR start increment The number of pixels (grid values in the X direction) is 72. The starting longitude is 0.0° with 5.0° increment from west to east. If the X dimension values go from east to west, write “xrev” at OPTIONS section.

YDEF number LINEAR start increment The number of lines (grid values in the Y direction) is 46. The starting longitude is -90.0° with 4.0° increment from south to north. If the Y dimension values go from north to south, write “yrev” at OPTIONS section.

ZDEF LEVELS value-list The number of arbitrary pressure levels are 7; 1000, 850, 700, 500, 300, 200, and 100 hPa.

TDEF number LINEAR start-time increment The number of times in the data set is 5. The start date is 2nd January, 2002 with 1 day increment (i.e. 2, 3, 4, 5, and 6 January, 2002).

VARs number This part indicates the start of the records describing the variables in the data set. There are eight variable records in this data, the first line with the following format:

abrev levs units description PS is abbreviation for this variable that is “Surface Pressure” (written at description part). A lev value of 0 indicates this variable has one “level” that does not correspond to a vertical level. If there are some vertical levels, the number of levels are described. The unit 99 means that the type of this variable is 4-byte float.

ENDVARS This ends the GrADS data description file.

[**Exercise 1**] Go through the sample (`[hoge@hoge GrADS]$ cat sample`) or the Tutorial (<http://www.iges.org/grads/gadoc/tutorial.html>) to get a feeling for how to use the basic capabilities of GrADS.

2 MTSAT

2.1 Outlines

The Multi-functional Transport Satellite - 1 (Replacement) (MTSAT-1R) is a geosynchronous satellite at 140°E launched on 26 February 2006 to fulfill a meteorological function and an aeronautical function, and has operated since 28 June 2006. MTSAT-1R was added a new observation channel in infrared to detect fog during nighttime and to improve observation accuracy of sea surface temperature. The observation channels and their band show following table. The field of view at nadir in visible (VIS) and infrared (IR) channels are about 1 km and 4 km with 10-bit (0–1023) gradation regardless of the channels.

Channel	Band [μm]
VIS	0.55–0.90
IR1	10.3–11.3
IR2	11.5–12.5
IR3	6.5–7.0
IR4	3.5–4.0

2.2 Extraction of gridded MTSAT-1R data

The Center for Environmental Remote Sensing (CEReS), Chiba University provides gridded dataset of VIS and IR channels on MTSAT-1R. Gridded dataset (format) that we defined are latitude & longitude oriented (to say another word, after geometric correction based on satellite position's information) format. However, we take into account re-calibration of radiometer (Tbb and Albedo%).

For the purpose of climatological long-term analysis, it is highly recommended that dataset consist of simple as binary (digital number stored), and text-based calibration table (look up table to convert digital number into physical variables such as Tbb or Albedo%). If new results provide “new calibration table”, they can easily apply to corrected variables by the replacement as of new calibration table, without any new calculations.

This part gives an explanation to read gridded MTSAT-1R data provided by CEReS. Each data file after the decompression for each channel contains a binary file of count number, and ten ASCII files of header information. The data files are stored in bz2 compression form for VIS and IRs.

Firstly, download one gridded data from the data server of MTSAT-1R (<ftp://mitsat-1r.cr.chiba-u.ac.jp/>), then confirm the archived data files.

```
[hoge@hoge MTSAT]$ wget ftp://mitsat-1r.cr.chiba-u.ac.jp/grid-MTSAT-1.01/200805/200805020530.ir.tar.bz2
[hoge@hoge MTSAT]$ tar xvfj 200805020530.ir.tar.bz2
IMG_DK01IR1_200805020530.geoss
IMG_DK01IR2_200805020530.geoss
...
hdr_ir4_200805020530_009.txt
hdr_ir4_200805020530_010.txt
```

Binary data (.geoss) are encoded in unsigned 2-byte values in big endian byte order. Since PC in this training course is in little endian byte order, re-encode the binary data using (dd) command.

```
[hoge@hoge MTSAT]$ cp IMG_DK01IR1_200805020530.geoss big_endian.geoss
[hoge@hoge MTSAT]$ dd if=big_endian.geoss of=little_endian.geoss conv=swab
```

Printing on the standard output the gridded file both endian, you may find the value from 0 to 1024 in the little endian file.

```
[hoge@hoge MTSAT]$ od -t u2 big_endian.geoss
0000000 44802 47618 47618 47618 47618 46082 46082
0000020 46082 46082 54274 51714 51714 51714 55810
...
[hoge@hoge MTSAT]$ od -t u2 little_endian.geoss
0000000 687 698 698 698 698 698 692 692
0000020 692 692 724 714 714 714 714 730
...
```

The data files are arrays of size 12000×12000 (longitude and latitude in 0.01°) for VIS and 3000×3000 (0.04°) for IRs. The range of the data is from 80°E to 160°W , and from 60°N to 60°S . The center of the first cell is 80.005°E (80.02°E) and 59.995°N (59.98°N) for VIS (IRs). That of the second cell is 80.015°E (80.06°E) and 59.995°N (59.98°N).

The .ctl file for IR of the gridded MTSAT-1R data are described as follows:

```
[hoge@hoge MTSAT]$ cat IR-count.ctl
DSET      ^IMG_DK01IR1_200805020530.geoss
OPTIONS   yrev little_endian
UNDEF     1023
TITLE     MTSAT-1R count number
XDEF      3000 LINEAR 80.02 0.04
YDEF      3000 LINEAR -59.98 0.04
ZDEF      1 LEVELS 1
TDEF      1 LINEAR 05:30Z02MAY2008 1HR
VARS      1
CN        0 -1,40,2   Count number
ENDVARS
```

That for VIS:

```
[hoge@hoge MTSAT]$ cat VIS-count.ctl
DSET      ^IMG_DK01VIS_200805020530.geoss
OPTIONS   yrev big_endian
UNDEF     1023
TITLE     MTSAT-1R count number
XDEF      12000 LINEAR 80.005 0.01
YDEF      12000 LINEAR -59.995 0.01
ZDEF      1 LEVELS 1
TDEF      1 LINEAR 05:30Z02MAY2008 1HR
VARS      1
CN        0 -1,40,2   Count number
ENDVARS
```

Draw the IR count number data using GrADS.

```
[hoge@hoge MTSAT]$ grads
...
Landscape mode? ('n' for portrait):
GX package Initialization: Size = 11 8.5
ga-> open IR-count.ct1
Scanning description file: IR-count.ct1
Data file IMG_DK01IR1_200805020530.geoss is open as file 1
LON set to 80.02 199.98
LAT set to -59.98 59.98
LEV set to 1 1
Time values set: 2008:5:2:5 2008:5:2:5
E set to 1 1
ga-> set grads off
ga-> set gxout grfill
ga-> set lon 80 200
ga-> set lat -60 60
ga-> set xlint 20
ga-> set ylint 15
ga-> set xlopts 1 4 0.15
ga-> set ylopts 1 4 0.15
ga-> d CN
Contouring: 200 to 900 interval 100
ga-> run cbarn
ga-> draw title MTSAT-1R IR1(CN) 20080502 0530UTC
ga-> enable print tmp.gx
ga-> print
ga-> disable print
Hardcopy output file is closed
ga-> !gxeps -c -i tmp.gx -o IMG_DK01IR1_200805020530.eps
ga-> quit
No hardcopy metafile open
GX package terminated
[hoge@hoge MTSAT]$ convert -rotate 90 IMG_DK01IR1_200805020530.eps ir1-count.eps
[hoge@hoge MTSAT]$ ggv ir1-count.eps
```

This CN value has no physical meanings. Thus, the CN value should be converted to brightness temperature using above convert table. The header file (.txt) are described in ASCII. There is a convert table between count number and brightness temperature (Tb) in the header file.

```
[hoge@hoge MTSAT]$ cat hdr_ir1_200805020530_001.txt
                Header Type #0 - Primary Header
                Header_Record_Length : 16
...
_UNIT:=KELVIN
```

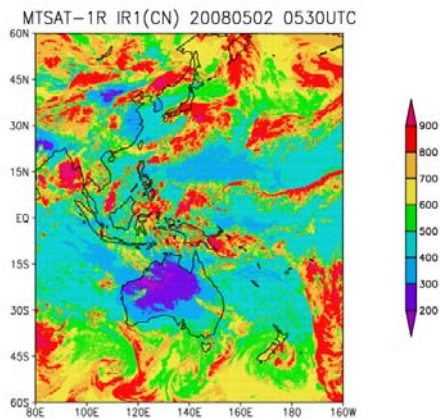


Figure 1: ir1-count.eps

```
0:=330.06
30:=327.69
60:=325.29
...
65535:=129.99
...
0 bytes left in header
```

Extract the convert table from the header file using (`awk`) command.

```
[hoge@hoge MTSAT]$ awk '/[0-9]:=/{print}' hdr_ir1_200805020530_001.txt | c
ut -d: -f1 > tmpa.txt
[hoge@hoge MTSAT]$ awk '/[0-9]:=/{print}' hdr_ir1_200805020530_001.txt | c
ut -d= -f2 > tmpb.txt
[hoge@hoge MTSAT]$ paste tmpa.txt tmpb.txt > tbbtable.txt
[hoge@hoge MTSAT]$ cat tbbtable.txt
0      330.06
30     327.69
60     325.29
...
65535  129.99
```

CEReS distributes a sample program to convert CN to Tb of gridded MTSAT-1R data. Get it from the data server and compile it.

```
[hoge@hoge programs]$ wget ftp://mtsatsat-1r.cr.chiba-u.ac.jp/support/c/readMT
SAT-1.01.tar.gz
[hoge@hoge programs]$ tar xvfz readMTSAT-1.01.tar.gz
readMTSAT-1.01/
readMTSAT-1.01/MTSAT-tbbctl
readMTSAT-1.01/count2tbb.c
readMTSAT-1.01/count2tbb.sh
```

```
readMTSAT-1.01/readme.txt
```

```
[hoge@hoge programs]$ cd readMTSAT-1.01
```

```
[hoge@hoge readMTSAT-1.01]$ gcc count2tbb.c -o count2tbb
```

Move to the directory at the sample data and execute the sample program.

```
[hoge@hoge MTSAT]$ /home/hoge/programs/readMTSAT-1.01/count2tbb little_endian.geoss
```

[Exercise 2] Draw the converted Tbb data using GrADS. The .ctl file as follows;

```
[hoge@hoge MTSAT]$ cat IR-tbb.ctl
```

```
DSET    ^tbb_little_endian.geoss
```

```
OPTIONS yrev
```

```
UNDEF  -999.0
```

```
TITLE  MTSAT-1R Tbb
```

```
XDEF 3000 LINEAR 80.02 0.04
```

```
YDEF 3000 LINEAR -59.98 0.04
```

```
ZDEF 1 LEVELS 1
```

```
TDEF 1 LINEAR 05:30Z02MAY2008 1HR
```

```
VARS 1
```

```
TBB    0 99 Tbb [K]
```

```
ENDVARS
```

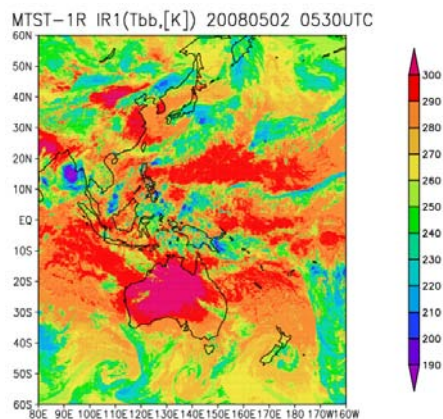


Figure 2: ir1-tbb.eps

CEReS does not only provides gridded geostationary satellites data of MTSAT-1R, but also those of the Fengyun (FY) -2C and -2D launched by China Meteorological Administration (located at 105°E and 86°E, respectively) and the Geostationary Operational Environmental Satellite (GOES) launched by the National Oceanic and Atmospheric Administration (NOAA) (located at 135°W and 75°W). Although there are some differences how to convert CN to Tbb depending on the satellites, you may read them easily. See each README file and sample program on the data server or refer to “CEReS 4VL Wiki” (<http://www.cr.chiba-u.jp/~4v1/> but in Japanese text only).

[**Exercise 2**] Make longitude-time section in IR1 Tbb at 0° in latitude from 90° to 180° in May 2008.

Procedure

1. Download the gridded IR data in May 2005.
2. Convert CN files to Tbb ones.
3. Draw it by GrADS utilizing **OPTIONS temprate** in .ctl file.

```
[hoge@hoge exercise2]$ cat exercise2.ctl
DSET `~%y4%m2%d2%h230.ir1tbb.geoss
OPTIONS yrev temprate
UNDEF -999.0
TITLE MTSAT-1R Tbb
XDEF 3000 LINEAR 80.02 0.04
YDEF 3000 LINEAR -59.98 0.04
ZDEF 1 LEVELS 1
TDEF 744 LINEAR 00Z01MAY2008 1hr
VARS 1
TBB 0 99 Tbb [K]
ENDVARS
```

```
[hoge@hoge exercise2]$ grads
...
ga-> open exercise2.ctl
ga-> set lat 0 0
ga-> set lon 90 180
ga-> set t 1 745
ga-> set xlint 15
ga-> set xlopts 1 4 0.15
ga-> set ylopts 1 4 0.15
ga-> set gxout grfill
ga-> set grads off
ga-> d tbb
ga-> run cbarn
ga-> draw title MTSAT-1R IR1 Tbb Lon.-Time Section at 0 deg
ga-> run cbarn
```

3 NOAA AVHRR

3.1 Outlines

The Television InfraRed Operational Satellite - Next-generation(TIROS-N/NOAA) series of polar orbiting meteorological satellites. The multiple NOAA satellites always operate (presently NOAA 17

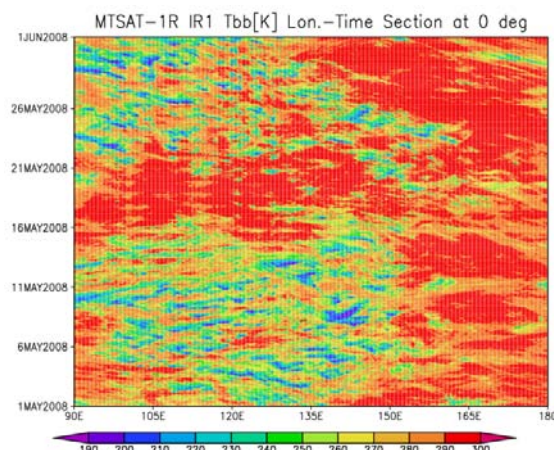


Figure 3: crosssection.eps

and 18). Each satellite observes at least two times in a day at a certain point with near-constant solar time. The orbit altitude is 830 and 870 km and that frequency is about 100 minutes. The NOAAs carry the Advanced Very High Resolution Radiometer (AVHRR) to observe cloud and land covers which data use in this program, in addition, the TIROS Operational Vertical Sounder (TOVS), the Advanced Microwave Sounding Unit (AMSU), and the Solar Backscatter Ultra-Violet Experiment (SBUV). The observation range and resolution of the AVHRR are 2700 km and 1 km, respectively.

Channels	Band [μm]
Red	0.58–0.68
Near-infrared	0.725–1.1
Thermal-infrared 1	3.55–3.93
Thermal-infrared 2	10.30–11.30
Thermal-infrared 3	11.50–12.50

3.2 Extraction of gridded NOAA AVHRR data

The NOAA AVHRR products provided by CERES are available from the Internet. The gridded data are archived in .bz2 format for each observation time.

At first, download an archived NOAA AVHRR data from <ftp://avhrr.cr.chiba-u.ac.jp/>, extract it, and confirm the contents.

```
[hoge@hoge AVHRR]$ wget ftp://avhrr.cr.chiba-u.ac.jp/disk2/products/200710/
n1807100204.tar.bz2
[hoge@hoge AVHRR]$ tar xvfj n1807100204.tar.bz2
n1807100204.mb1.gi : Red
n1807100204.mb2.gi : Near-infrared
n1807100204.mb3.gi : Thermal-infrared1
n1807100204.mb4.gi : Thermal-infrared1
n1807100204.mb5.gi : Thermal-infrared1
n1807100204.sza.gi : Solar zenith angle
```

```

n1807100204.saa.gi : Solar azimuth angle
n1807100204.sca.gi : Scan angle
n1807100204.nvi.gi : NDVI
n1807100204.sst.gi : SST

```

NOAA AVHRR products data (.gi) consist of header part (80 bytes), data part (70,948,872 byte), and footer part. In the data part, each variables are written as 2-byte integer in big endian. Each data are corresponds to the physical values as follows:

- Red and Near-infrared: Albedo (0.0, 100.0%) == (0, 1000)
- Thermal-infrared 1–3: Brightness Temperature (0.0, 320.0 K) == (0,3200)
- Solar zenith angle: (-360° , $+360^\circ$) == (-3600 , $+3600$)
- Solar azimuth angle: (-360° , $+360^\circ$) == (-3600 , $+3600$)
- Scan angle, SST: (0.0, 320.0 K) == (0, 3200)
- NDVI: (-1.0 , $+1.0$) == (-100 , $+100$)

Confirm the header part using sample program.

```

[hoge@hoge AVHRR]$ /home/hoge/programs/AVHRR/readheader n1807100204.mb4.gi
File name n1807100204.mb4.gi
(1) Number of lines per band          : 5562
(2) Number of bands in the image      : 1
(3) Number of bytes per line          : 12756
(4) Number of label records           : 0
(5) Number of bytes in one label record : 0
(6) Data_organization                 : 2
(7) Data type                          : 2
(8) Starting_byte_number              : 80
(9) p file identifier                 : imag

```

Note: Data type 1:byte,2:integer*2,3:integer*4,4:real*4,5:real*8,6:complex*8,7:complex*16

The data files are arrays of size 6378×5562 (longitude and latitude in 1 km) from west to east, and north to south. The range of the data is from 100°E to 170.022095°E , and from 60°N to 9.97971°N . The .ctl in this format:

```

[hoge@hoge exercise2]$ cat avhrr.ctl
DSET ^n1807100204.mb1.gi
OPTIONS yrev little_endian
UNDEF 0
TITLE AVHRR Red
XDEF 6378 LINEAR 100 0.01097869
YDEF 5562 LINEAR 19.97971 0.00899322
ZDEF 1 LEVELS 1

```

```
TDEF 1 LINEAR 04Z02OCT2007 1hr
VARS 1
RED 0 -1,40,2 Tbb [K]
ENDVARS
```

[Exercise 3] Draw the other band and products referring to above .ctl file.

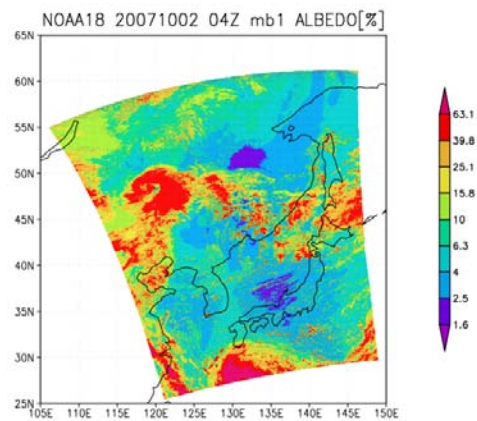


Figure 4: n1807100204.mb1-albedo.eps

This product does not take any atmospheric correction and sensor degradation correction since these corrections do not incorporate a product making routine developed by Global Imaging Corp. Thus, you should pay attention the characteristics of the data.



TRMM Tropical
Rainfall
Measuring
Mission



TRMM Data Handling

Takuji Kubota

Earth Observation Research Center (EORC)

Japan Aerospace Exploration Agency (JAXA)



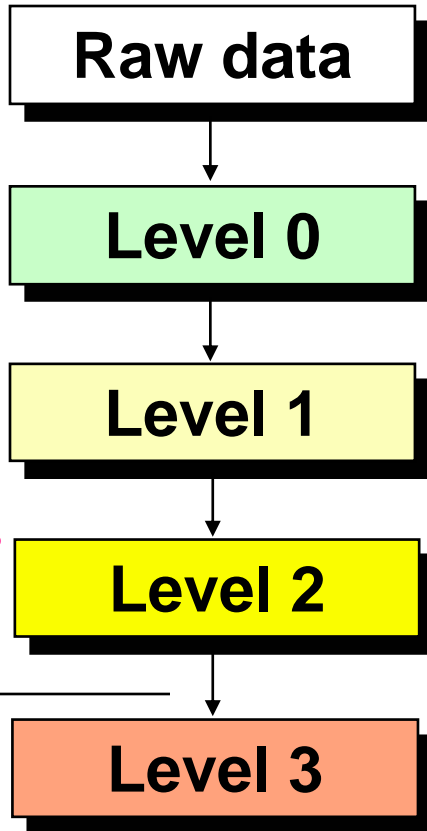
Contents

- **TRMM Data Overview**
- **Analyzing Tools**
- **Tutorial for PPS Orbit Viewer**



TRMM Data Overview

Data Processing for Standard Products



Transferred from TRMM

Quality checked raw data

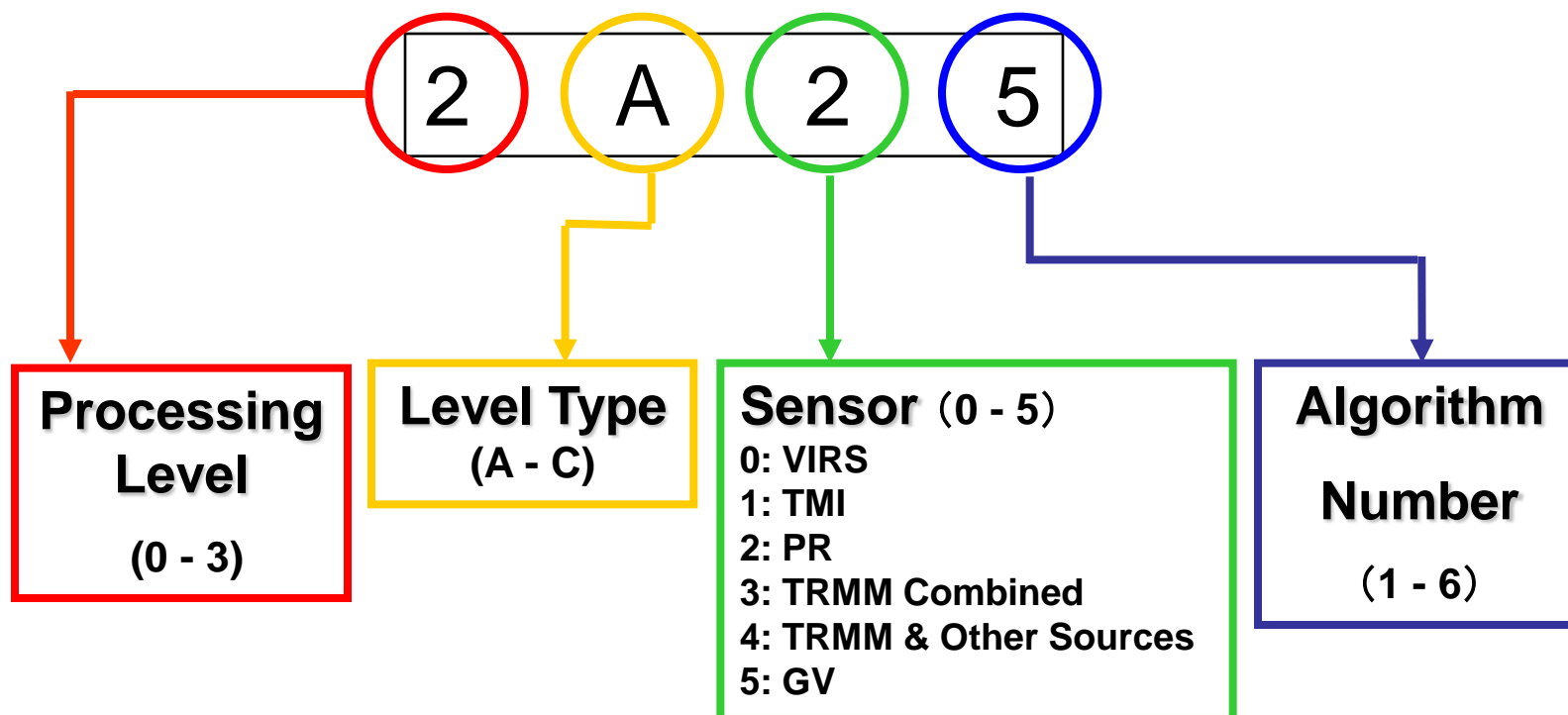
Calibrated data (PR received power etc.)

Geophysical parameters (rain rate, etc.)

Temporary and spatially averaged (monthly mean rainfall)



Standard Product Naming Rules



Point CERES and LIS products have different naming rules because they are processed and distributed by other NASA Centers.

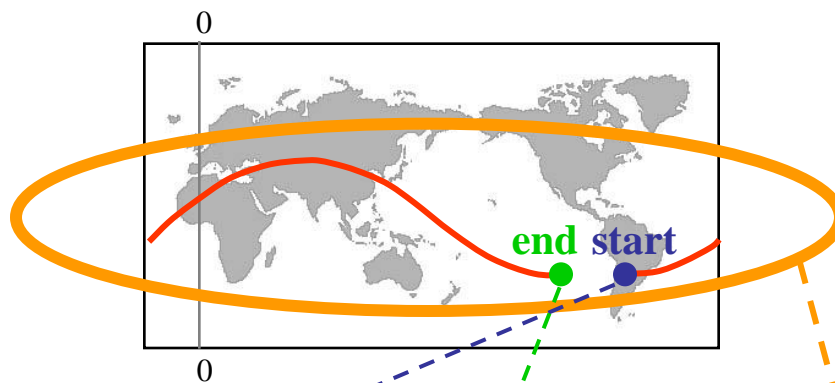


Examples of Level 1-2 Products

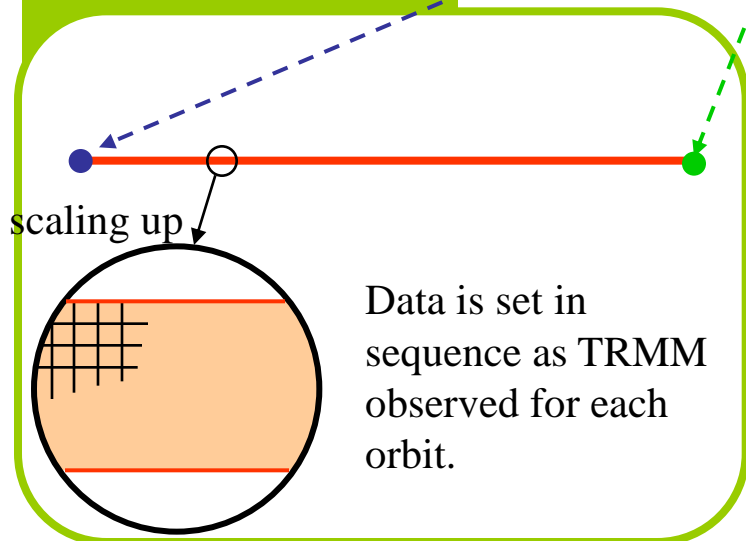
Data Product	Description
1B01: Visible and Infrared Radiance (VIRS)	Calibrated VIRS (0.63, 1.6, 3.75, 10.8, and 12 um) radiances at 2.2 km resolution over a 720 km swath
1B11: Microwave Brightness Temperature (TMI)	Calibrated TMI (10.65, 19.35, 21, 37, and 85.5 GHz) brightness temperatures at 5 to 45 km resolution over a 760 km swath
2A12: Hydrometeor Profile (TMI)	TMI Hydrometeor (cloud liquid water, prec. water, cloud ice, prec. ice) profiles in 14 layers at 5 km horizontal resolution, along with latent heat and surface rain, over a 760 km swath
2A25: Radar Rainfall Rate and Profile (PR)	PR (13.8 GHz) rain rate, reflectivity, and attenuation profiles, at 4 km horizontal, and 250 m vertical, resolutions, over a 220 km swath



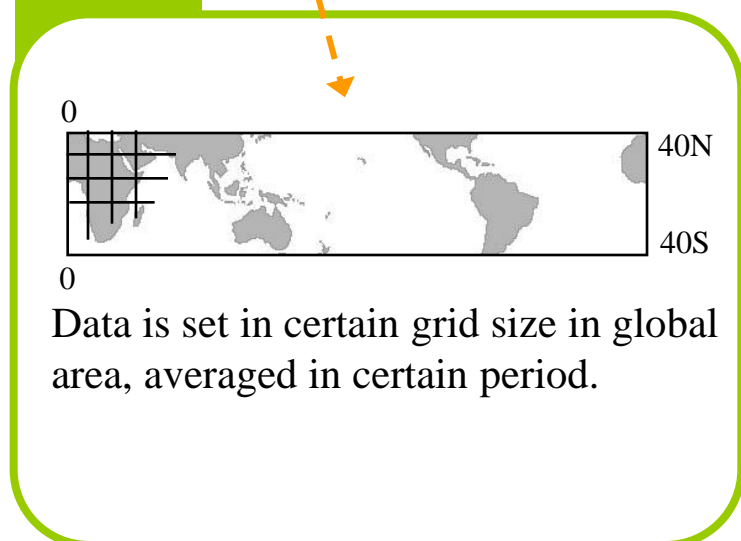
Level and Data Array



Level 1 and Level 2



Level 3



GSMaP dataset in the afternoon session is Level 3 product.



Data Format

■ HDF-EOS Format

HDF (Hierarchical Data Format), Specifying Satellite observation.

■ Structure of HDF Format

Metadata + Scientific Data Sets (SDS) + V data

Category	Characteristics	Example
Metadata	Detailed description of file in text format	algorithm version, pixel count number, etc.
SDS (Scientific Data Sets)	multi-dimension matrix data consisting from data elements in same type	radar reflectivity, rain
Vdata	table data which can combine data in different type	data by each scan



Note for data handling (1)

maneuver

■ Orbit maintenance maneuver (Delta-V maneuver)

To keep satellite altitude at appropriate range.
Currently, operated once in 7-10 days.

■ 180 degree yaw maneuver

To avoid VIRS radiation cooling unit to go sun side.
Operated once in 2-4 weeks

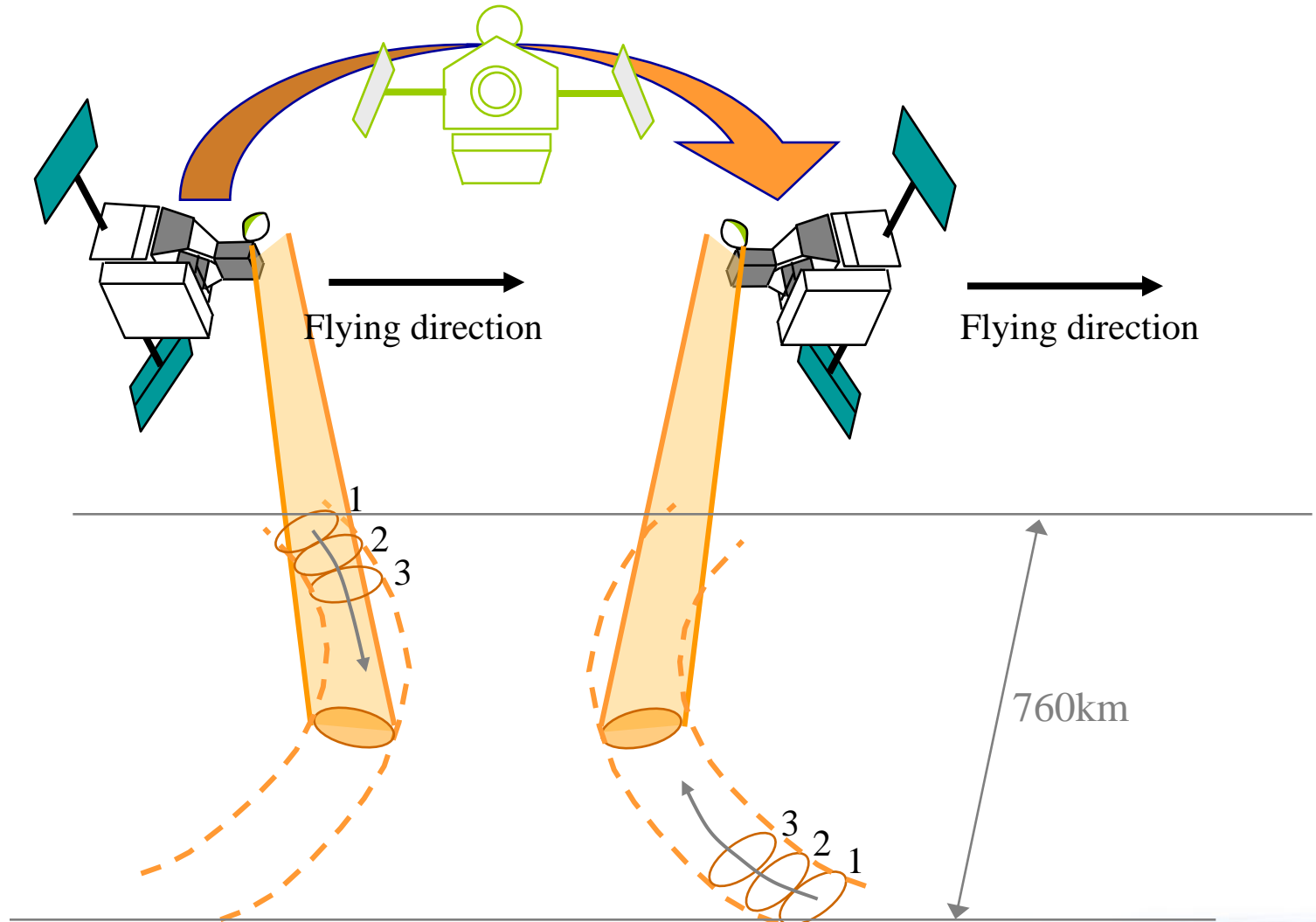
Point

Since satellite flying direction is reversed at this maneuver, scan direction is also reversed. Need to check geolocation of each scan data in the same time.

■ 90 degree yaw maneuver

To assess PR cross-track antenna pattern.
Operated once in half year.

180-degree Yaw Maneuver





Note for Data Handling (2)

Other factor for erroneous observation

■ Radio interference

example in Australia, etc.

■ Natural phenomena

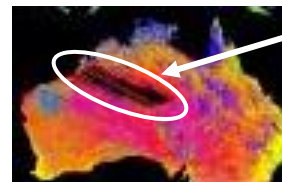
Leonid meteor shower, etc.

■ Sensor maintenance

operated in non-observation mode

■ Trouble in solar array panel

VIRS stopped operation from 6 Sep. to 17 Oct. 2002



Point

PR is not observe these area because the same frequency to PR is used in the ground.



Note for Data Handling (3)

Handling of missing data

Each missing scan filled by “Missing Value” to indicate they are mission data

Data type	1-byte integer	2-byte integer	4-byte integer	4-byte real	8-byte real
Max. of missing value*	-99	-9999	-9999	-9999.9	-9999.9

※ Numeric value lower than upper indicates mission data or invalid

When all data in a orbit is missing, scan data is omitted and “Orbit Size” in Metadata element will be “0”.



Note for Data Handling (4)

TRMM altitude change

At Launch : about 350km
 After Aug. 2001 : about 403 km

Characteristics of TRMM Instruments

	Swath Width (km)		Ground Resolution (km)	
	Pre-boost	Post-boost	Pre-boost	Post-boost
VIRS	720	833	2.2	2.4
TMI	760	878	4.4*	5.1*
PR	215	247	4.3	5.0

* Ground resolutions of TMI are those at 85.5 GHz (highest resolution).



Note for Data Handling (4)

TRMM altitude change

Observation in August 2001 is;

Altitude of orbit	Start date & orbit number	End date & orbit number	Data distribution
350km	2001/8/1 21164	2001/8/7 21267	YES
Altitude rising period	2001/8/7 21268	2001/8/24 21540	Empty granule
402.5 km	2001/8/25 21541	2001/8/31 21649	YES

PR Level 3 product for August 2001 was made from about 13 days (1-7 Aug. and 25-31 Aug.) eliminated data during altitude rising period

Point

Note that using data in different version number. Version number is confirmed from file name.



Analyzing Tools



How to Get the TRMM Online Data (1)

- PR/TMI/VIRS Data
 - DAAC (Goddard Distributed Active Archive Center - NASA/GSFC)
 - <http://disc.sci.gsfc.nasa.gov/data/datapool/TRMM/>
 - Level 1, 2, 3 standard products available
 - Precipitation Processing System (PPS) - NASA/GSFC
 - <http://pps.gsfc.nasa.gov/>
 - PPS Toolkit, HDF information
 - Gridded text data (3G68) available
(ftp://trmmopen.gsfc.nasa.gov/pub/)
- LIS (Home Page/download data)
 - <http://thunder.msfc.nasa.gov/>
- TRMM Realtime System
 - <http://pps.gsfc.nasa.gov/trmmrt/index.htm>
- TRMM 3 Hourly Global Rainfall - NASA/GSFC
 - <http://trmm.gsfc.nasa.gov/>
 - Near real-time 3-hourly rainfall data (3B40RT, 3B41RT, 3B42RT)



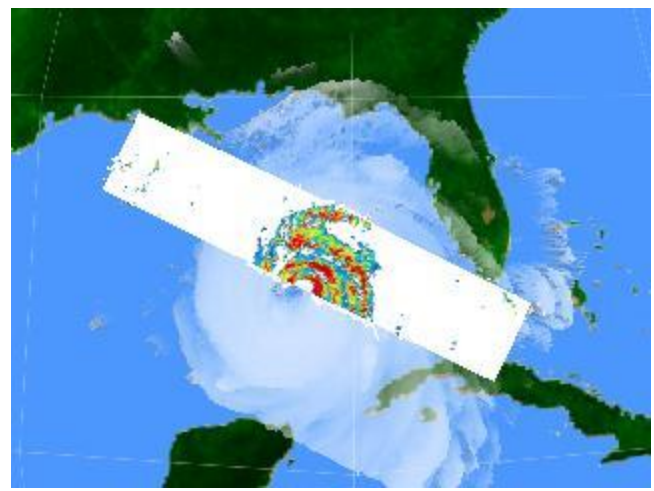
How to Get the TRMM Online Data (2)

- EOC home page - JAXA/EOC
 - <http://www.eorc.jaxa.jp/en/about/distribution/index.html>
 - Satellite information and images, data order
- EORC TRMM home page - JAXA/EORC
 - http://www.eorc.jaxa.jp/TRMM/index_e.htm
 - TRMM data in Asia monsoon and Japan area
 - Tropical cyclone database
 - http://sharaku.eorc.jaxa.jp/TYP_DB/index_e.shtml
 - TRMM Realtime Tropical Cyclone Monitoring (images only)
 - http://sharaku.eorc.jaxa.jp/trmm/RT/index_e.html
- GSMaP_NRT home page - JAXA/EORC
 - <http://sharaku.eorc.jaxa.jp/GSMaP/index.htm>
 - GSMaP Data Handling will be introduced in the afternoon session

JAXA/EORC Tropical Cyclone Database (for TRMM, AMSR-E and AMSR)

http://sharaku.eorc.jaxa.jp/TYP_DB/index_e.shtml

Browse **images**, **3D movies** and **data** of tropical cyclones observed by TRMM, Aqua/AMSR-E, Midori-II/AMSR are available.



Super Typhoon SONGDA(22W)
T0418

[Track Chart\(JPEG, 500x500\)](#)
 Period : Aug 27,2004 - Sep 07,2004
 Region : North Western Pacific
 Maximum Sustained Winds : 130kt (Category 4)
 Number of TRMM/PR,TMI,VIRS Observation : 19
 Number of Aqua/AMSR-E Observation : 17
 Number of Midori-II/AMSR Observation : 0

Observation Area	PR 3D	PR/VIRS Image	TMI Image/Precipitation	Water Vapor	
	No Data	No Data			Date/Time: Aug 28,2004 02:26(UTC) Satellite/Sensor: Aqua/AMSR-E Path Number: 193MA Lat/Lon: 2.0S-17.6N 156.2E-173.3E Download L1B(V02) L2AP0(V02) L2WV0(V02)
	No Data	No Data			Date/Time: Aug 28,2004 14:41(UTC) Satellite/Sensor: Aqua/AMSR-E Path Number: 088MD Lat/Lon: 6.1N-25.5N 156.2E-173.8E Download L1B(V02) L2AP0(V02) L2WV0(V02)
					Date/Time: Aug 28,2004 19:47(UTC) Satellite/Sensor: TRMM/PR,VIRS,TMI Orbit Number: 38683 Lat/Lon: 7.40N-20.42N 154.75E-159.26E Download 1B01(V6) 1B11(V6) 2A12(V6) 2A23(V6) 2A25(V6)



TRMM Analysis Tool

● PPS/TSDIS Orbit Viewer

- For quick look. Easy to make browse image.
- For UNIX, Linux and Windows.
- **<http://pps.gsfc.nasa.gov/tsdis/TSDISorbitViewer/release.html>**
- Demonstration later.

● HDF Group (Univ. of Illinois)

- C and FORTRAN library for reading and writing HDF format data.
- For UNIX and Linux.
- http://www.hdfgroup.org/products/hdf4_tools/

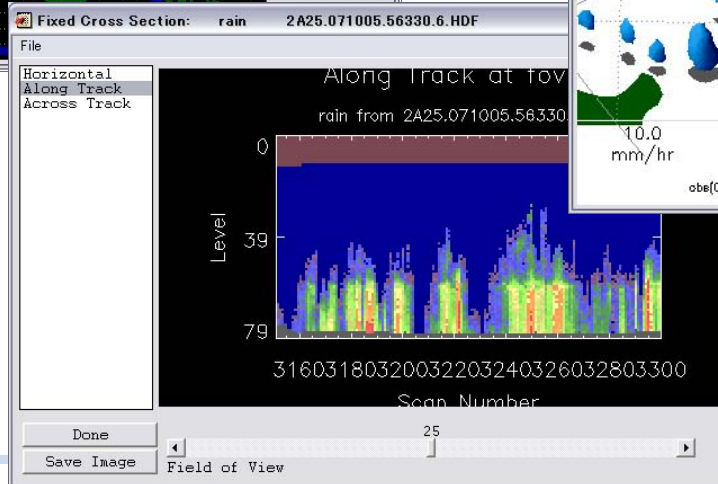
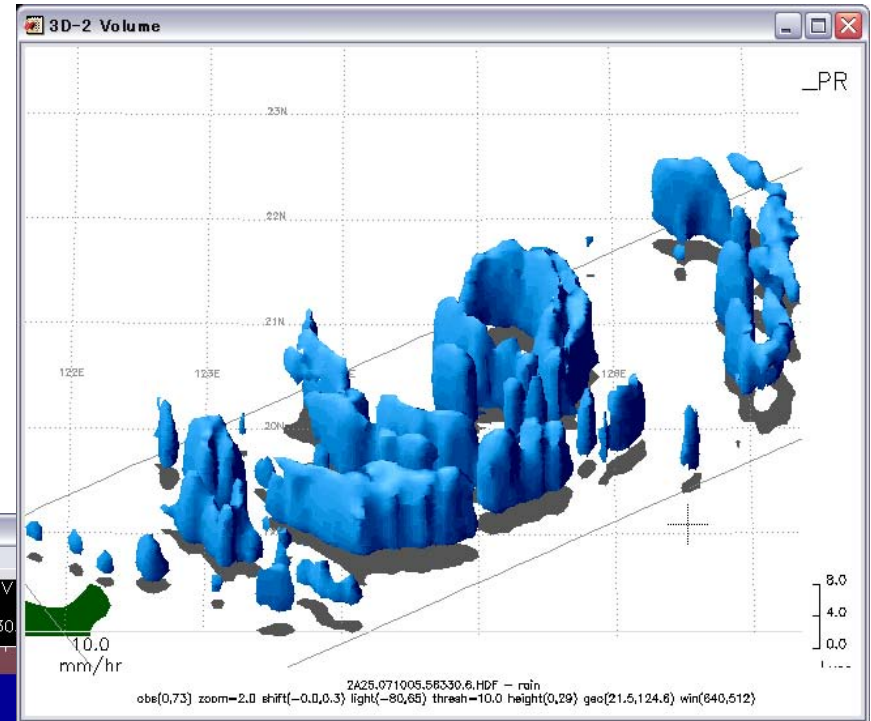
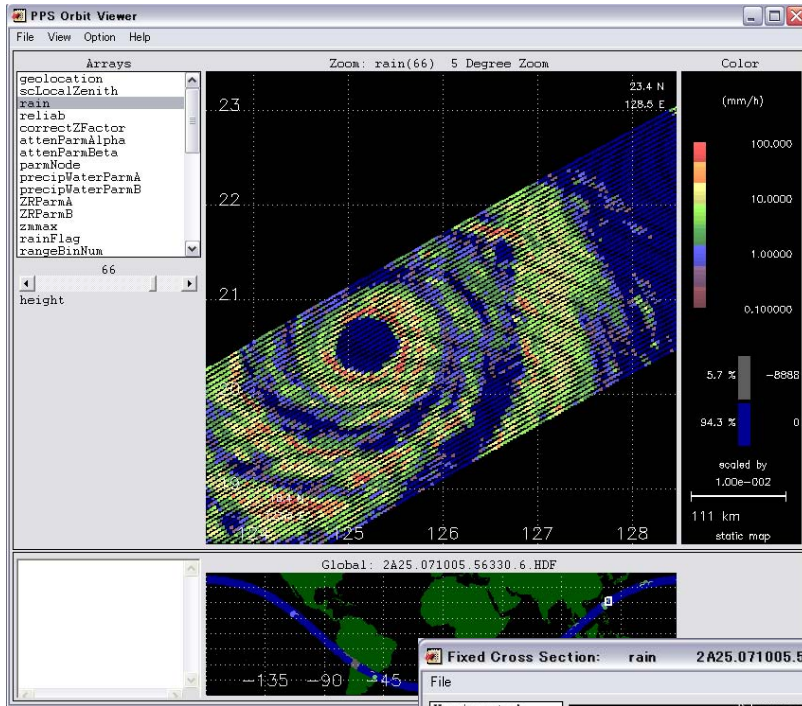
● PPS/TSDIS Toolkit

- C and FORTRAN library based HDF Library.
- For TRMM data (PR, TMI, VIRS, COMB, GV) only.
- For UNIX and Linux.
- <http://pps.gsfc.nasa.gov/tsdis/tsdistk.html>



Tutorial for *PPS Orbit Viewer*

Sample Image of Orbit Viewer





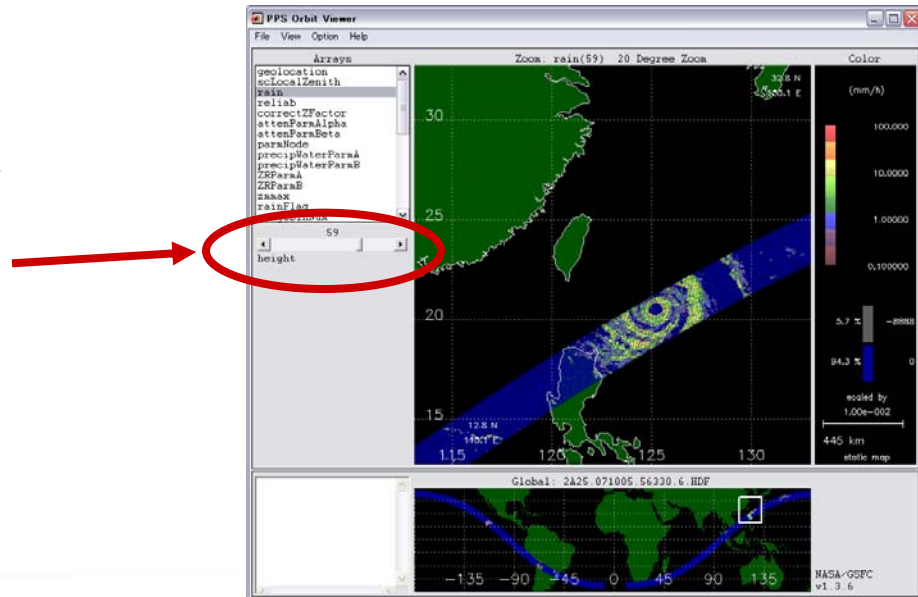
Let's practice ! (1)

- 1. Start orbit viewer.**
- 2. Open
TRMM_orbit/2A25.071005.56330.6.HDF.**
- 3. Select 'e_SurfRain' in Arrays.**
- 4. Click east of Philippines in the bottom panel.**
- 5. Click anywhere in the PR path.**
- 6. You can select 'Option'- 'Zoom resolution', or 'Interpolate Data'.**

Let's practice ! (2)

1. Select 'rain' in Arrays.
2. Click east of Philippines in the bottom panel.
3. Control 'vertical layer slider'. ("1" is a space side layer, 80 is a ground side layer)

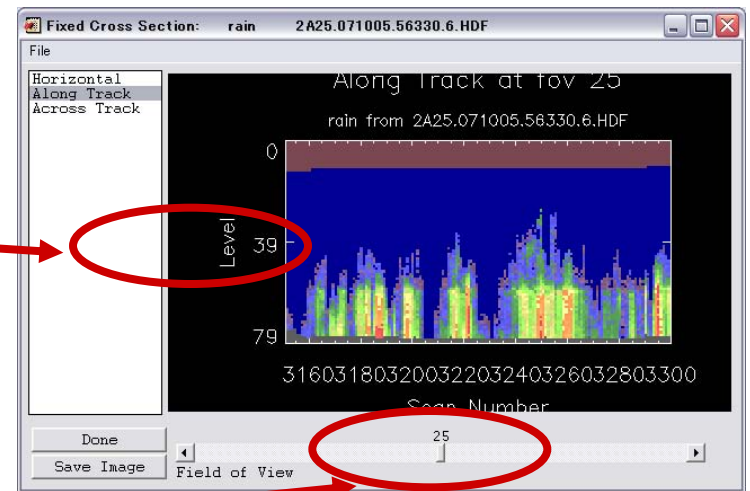
Vertical layer slider
(ex., '80'=ground,
'20'=5km altitude,
'40'=10km altitude)



Let's practice ! (3)

- Select the 'View'- 'Array'- 'Fixed_Cross_Section' menu item, and a new window will appear.
- Select 'Along Track'.
- To change the displayed element of the fixed dimension, move the slider at the bottom.

'Level 39' means about 10km altitude.

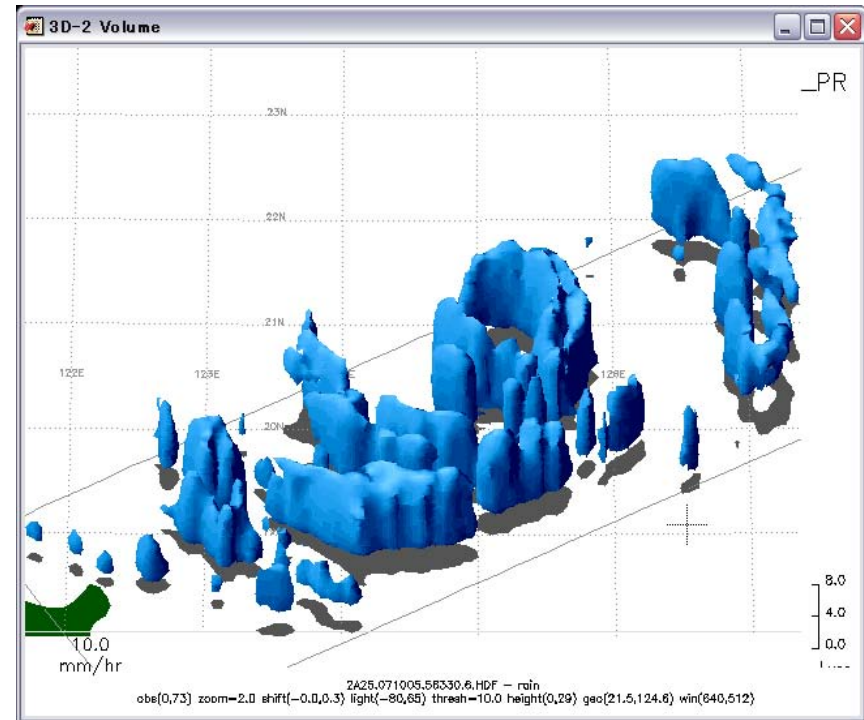
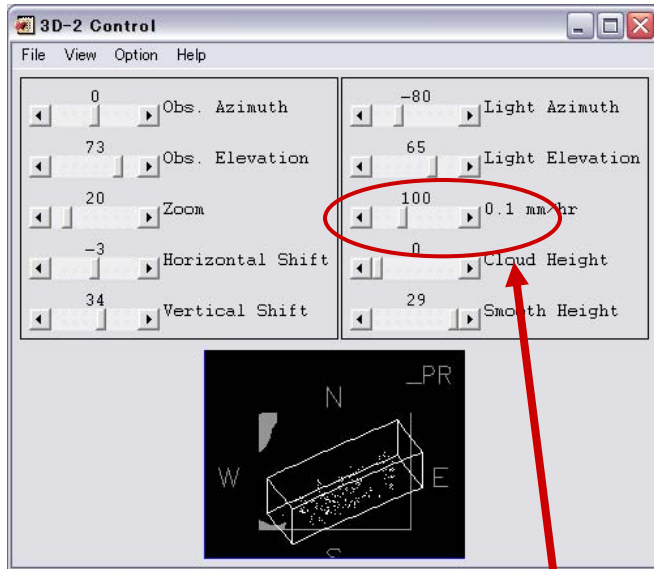


Slider

Let's practice ! (4)

- Select the 'View'- 'Array'- '3D_Viewer' menu item, and a new window will appear.
- Click 'Select data'.
- Try to menu sliders of the 3D Control Window.

3D Control Window





Let's practice ! (5)

- **Many sample data are set up. Try to open another data using the Orbit Viewer.**

Look at Data Sample (1)

In the directory 'TRMM_orbit',

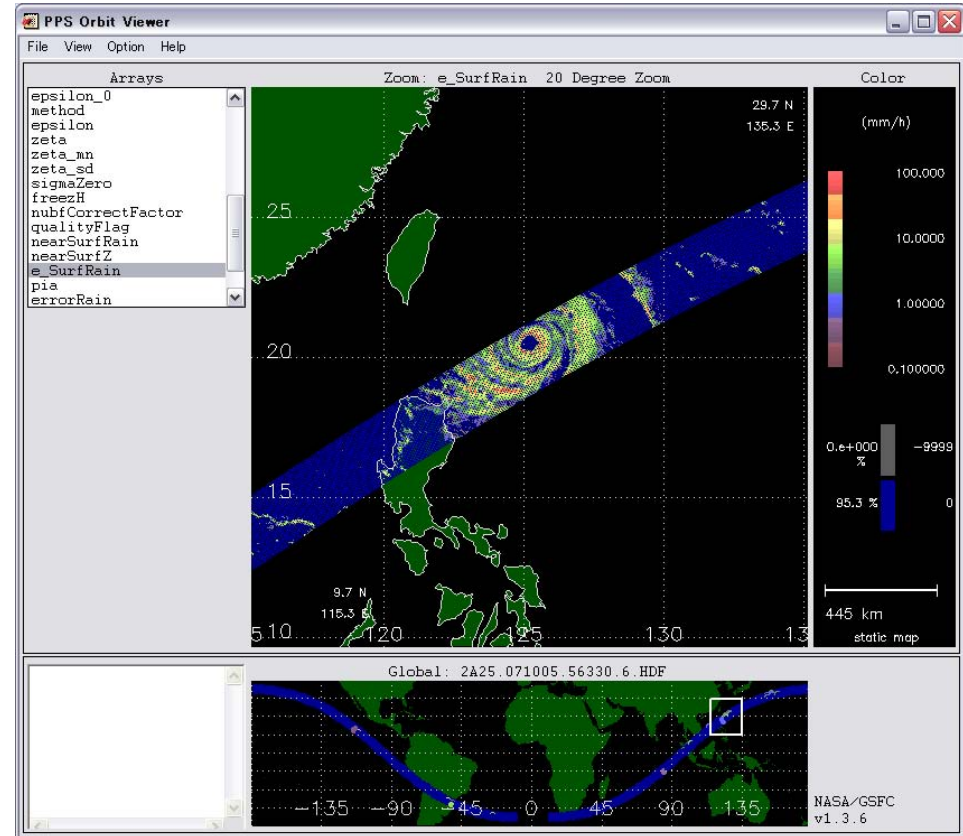
1B01.071005.56330.6.HDF
(VIRS)

1B11.071005.56330.6.HDF
(TMI Brightness Temperature)

2A12.071005.56330.6.HDF
(TMI rain rate)

2A25.071005.56330.6.HDF
(PR Rain rate)

3A25.071001.6A.HDF
(Monthly PR Rain rate)

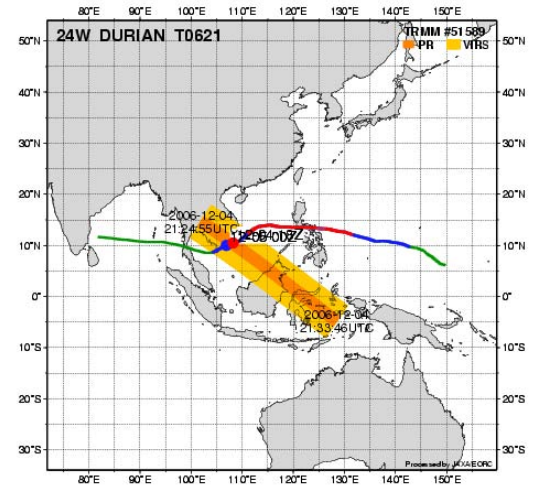
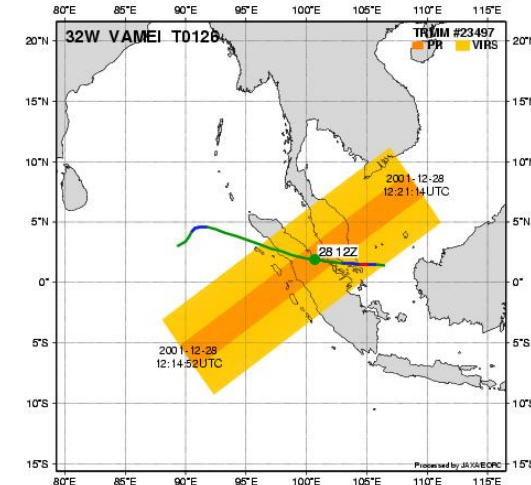
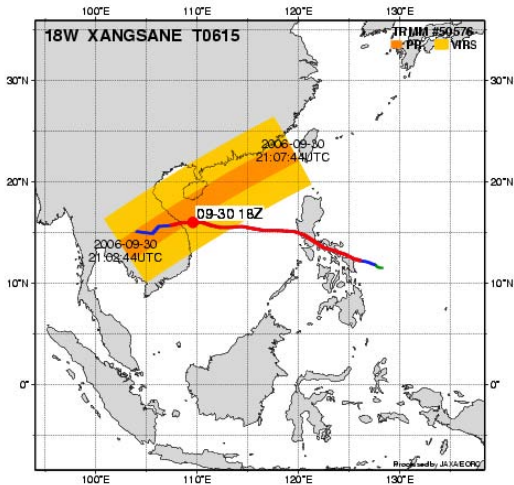
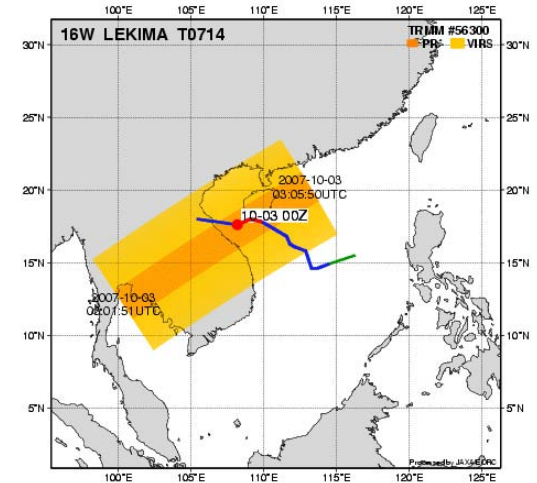
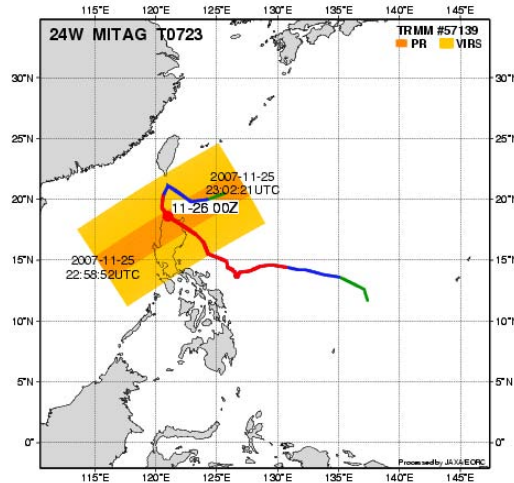
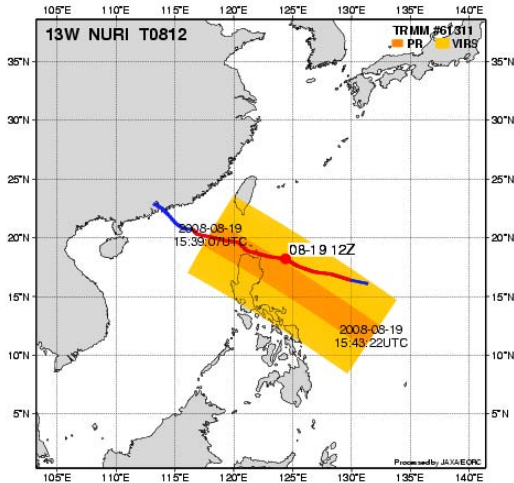




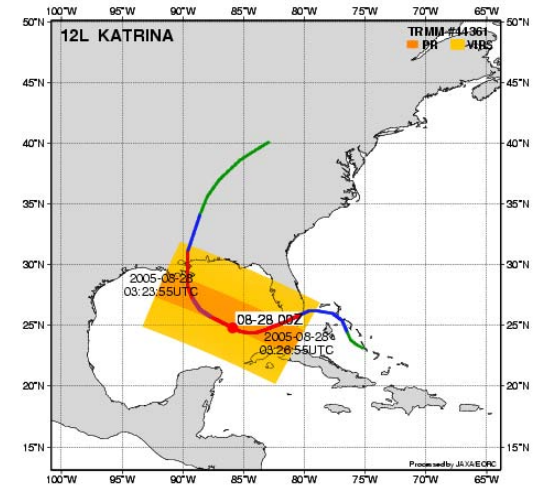
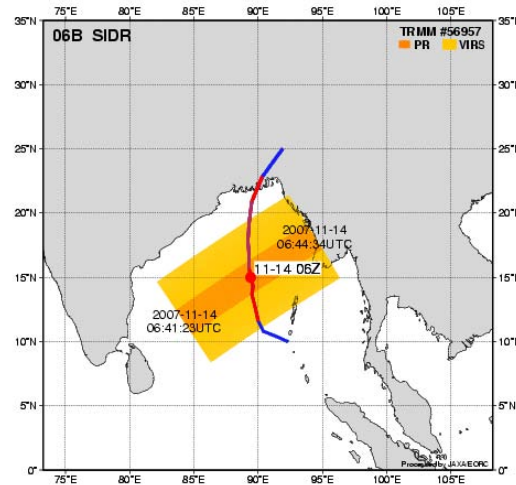
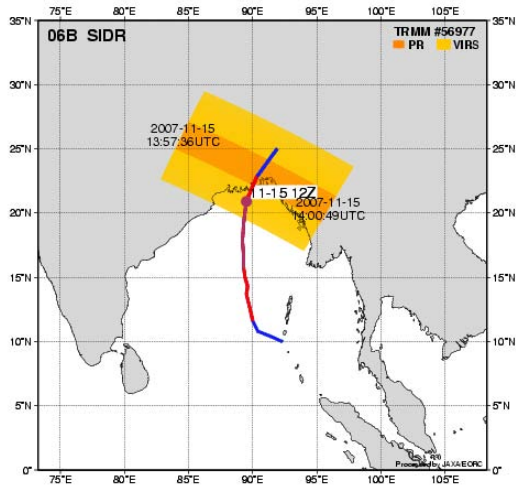
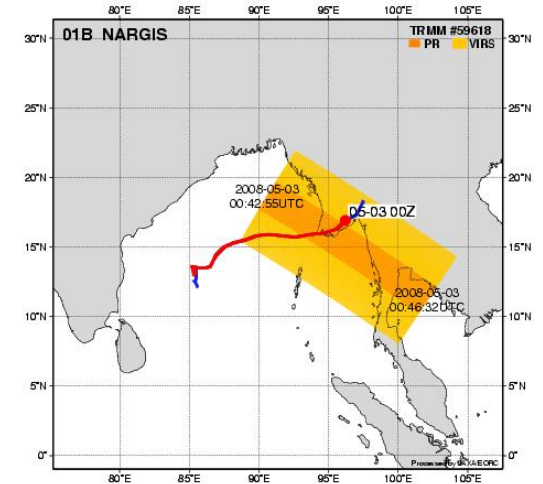
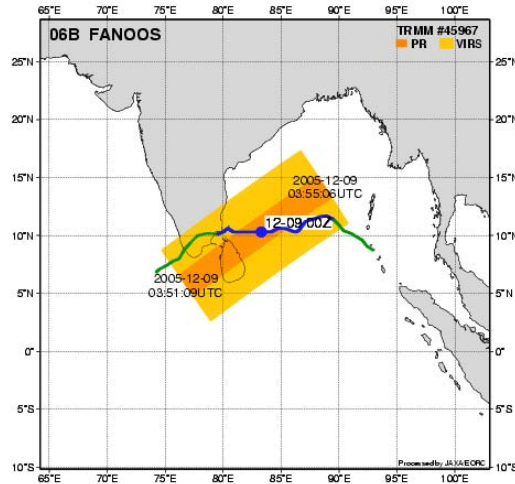
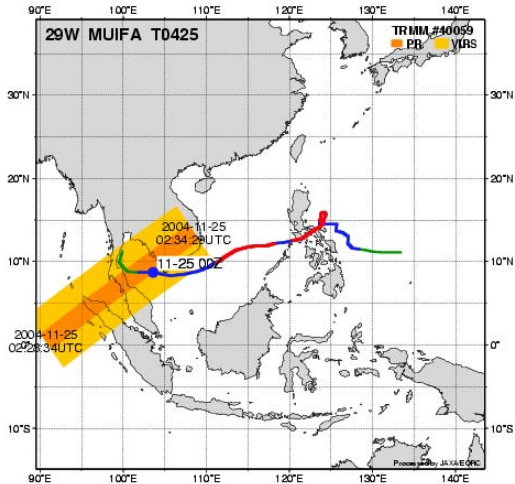
Look at Data Sample (2)

- **“TC_DB” folder includes 12 sample data of TRMM archived at JAXA/EORC Tropical Cyclone Database**
(http://sharaku.eorc.jaxa.jp/TYP_DB/index_e.shtml)
 - 1B01...HDF (VIRS)
 - 1B11...HDF (TMI Brightness Temperature)
 - 2A12...HDF (TMI rain rate)
 - 2A25...HDF (PR Rain rate)
- **See images in TC_DB/list for your reference.**

TC_DB List (1)



TC_DB List (2)





TRMM Tropical
Rainfall
Measuring
Mission



GSMaP Data Handling

Takuji Kubota

Earth Observation Research Center (EORC)

Japan Aerospace Exploration Agency (JAXA)



Contents

- **GSMaP Data Overview**
- **Handling of Precipitation data**



GSMaP Data Overview

Global rainfall map by multi-satellites

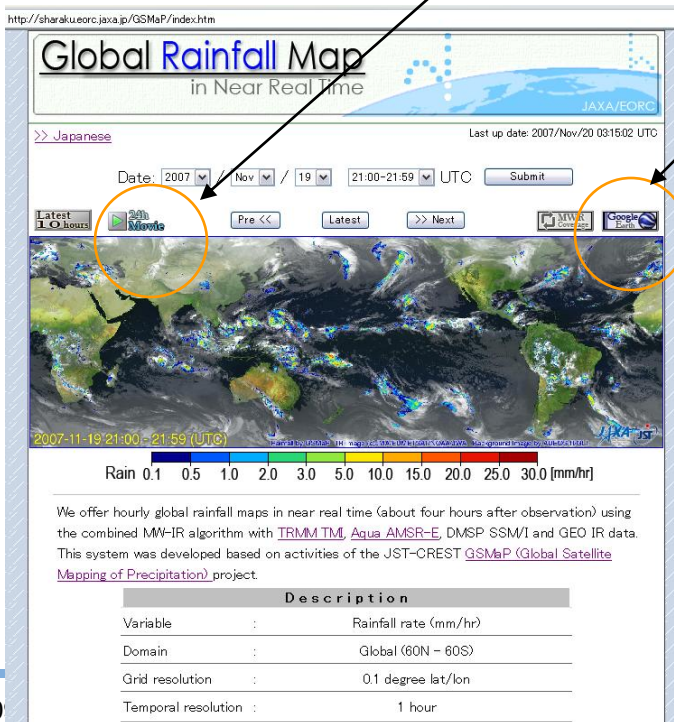
Global Rainfall Map in Near Real Time by JAXA/EORC

<http://sharaku.eorc.jaxa.jp/GSMaP/>

We have started to release hourly global rainfall data (0.1x0.1deg. lat/lon) in near real time (about **four hours** after observations) and visualize the latest data quickly.

Movie Button

Google Earth Button



Global Rainfall Map
in Near Real Time
JAXA/EORC

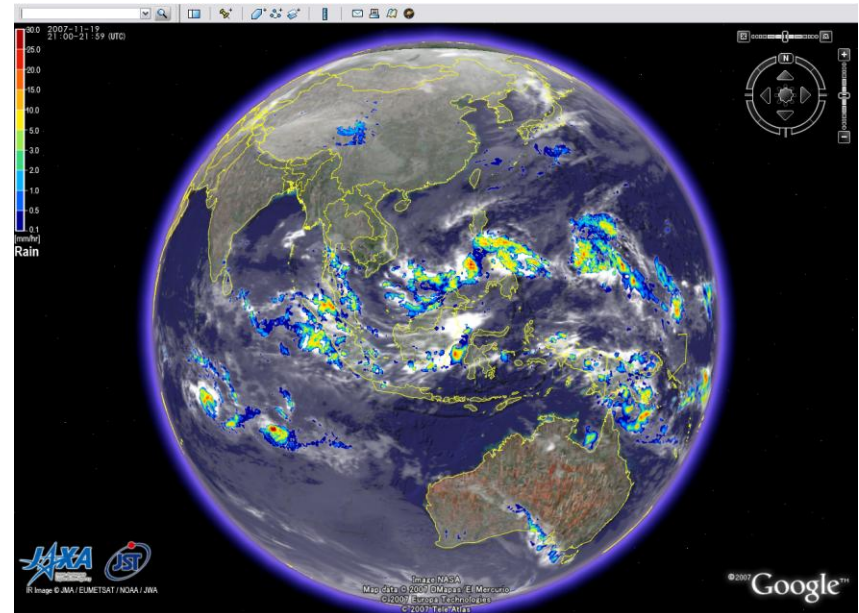
Date: 2007 / Nov / 19 / 21:00-21:59 UTC

20h Movies

Google Earth

Rain 0.1 0.5 1.0 2.0 3.0 5.0 10.0 15.0 20.0 25.0 30.0 (mm/hr)

Description	
Variable	Rainfall rate (mm/hr)
Domain	Global (60N - 60S)
Grid resolution	0.1 degree lat/lon
Temporal resolution	1 hour





How to Get the GSMP Online Data

● **GSMP_NRT (NRT:Near-real-time) by JAXA/EORC**

- <http://sharaku.eorc.jaxa.jp/GSMP/index.htm>
- Details will be presented later.

● **GSMP Data Archive Center**

- <http://www.gsmap.aero.osakafu-u.ac.jp/>
- GSMP Standard version (post-processing)
- Period: 1998-2006



GSMaP_NRT: Near-Real-time Data

● JAXA's site

- Data will be archived about 4 hours after observation.
 - Ex., Data of 00:00-0:59UTC will be put at about 5 UTC.

● FTP

- ftp hokusai.eorc.jaxa.jp

- **When you want to use GSMaP data after IHP Training Course**, please send your e-mail to **trmm_real@jaxa.jp**

- **Data are free ! We just need your registration.**



Basic Information

● Temporal resolution

- 1 hour (hourly data)

● Grid resolution

- 0.1 degrees latitude/longitude grid
- 10km at the equator

● Domain

- Global (60N-60S)

● Data latency

- 4 hours after observation

● Data Period

- 1 December 2007 – present in JAXA site
- *Data during 1998-2006 is archived in GSMP Data Archive Center.*



File Naming Rules

- **Data and flag files are named according to the following rules;**
 - **Hourly Rain Rate data:**
 - `gsmmap_nrt_YYYYMMDD.HHNN.dat`
 - **Satellite Information Flag:**
 - `gsmmap_nrt.YYYYMMDD.HHNN.sateinfo.dat`
 - **Observation Time Flag:**
 - `gsmmap_nrt.YYYYMMDD.HHNN.timeinfo.dat`
 - **where,**
 - **YYYY: 4-digit year**
 - **MM: 2-digit month**
 - **DD: 2-digit day**
 - **HH: 2-digit hour**
 - **NN: 2-digit minute (currently fixed as 00)**



FTP Information

● FTP Directory Information

● Hourly Rain Rate data;

● Latest 24 hour data:

- /realtime/latest/

● Archive:

- /realtime/archive/YYYY/MM/DD/

● Satellite Information Flag;

- /realtime/sateinfo/YYYY/MM/DD/

● Observation Time Flag;

- /realtime/timeinfo/YYYY/MM/DD/

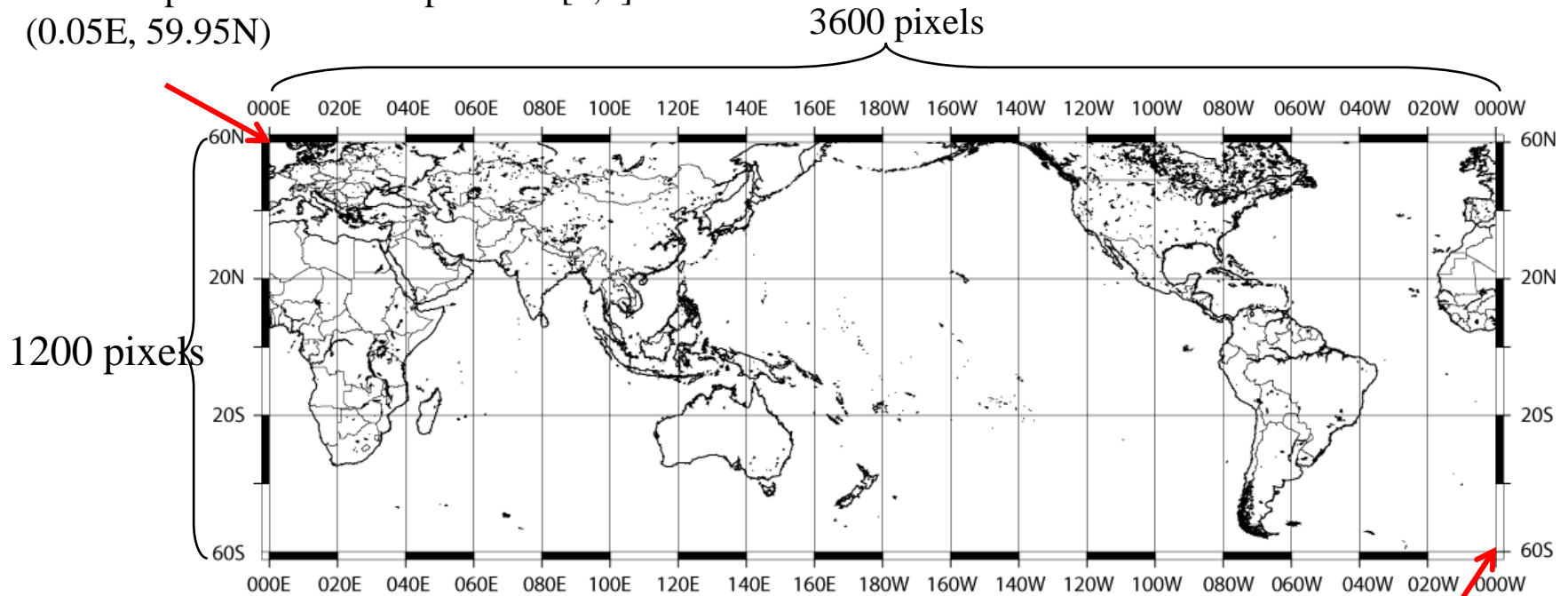


Data Format

- **All binary files**
 - little-endian byte order platform
 - archived with compressed using "gzip".
- **Grid of those files**
 - 3600 x 1200 pixels
 - longitude-latitude elements corresponding to a 0.1 x 0.1 degree grid that covers the global region from 60N to 60S.
 - The center longitude and latitude of the first pixel [1,1] (left top corner) is [0.05E, 59.95N] (*see next slide*).
- **File Size**
 - Approximately 800 Kbyte (with gzip), and 17 Mbyte (uncompress).

Data Coverage Map

The first pixel is on left-top corner [1,1]:
(0.05E, 59.95N)



The last pixel is on right-bottom corner [3600:1200]:
(0.05W, 59.95S)

Data Coverage Map (Rain and Flag data)



Definition of Missing Data

“Hourly Rain Rate” data are stored in 4-byte float plain binary format.
Unit is [mm/hr].

Negative value denotes missing in observation data or no retrieval was done in microwave retrieval algorithm

Value	Description
(positive)	Hourly rain rate [mm/hr].
-4	Missing due to low temperature in microwave retrieval algorithm.
-8	Missing due to sea ice in microwave retrieval algorithm.
-999	Missing due to no observation

Satellite Information Flag

- **Satellite Information Flag:**
 - **gsmmap_nrt.YYYYMMDD.HH NN.sateinfo.dat**
- **Each bit in flag responses to satellite/sensor respectively**
- **value of flag indicates accumulated value of all satellite and/or sensor name.**

Pixel Value		Description	
Value	Bit	Sensor Category	Satellite/Sensor
1	0	Microwave radiometer aboard low orbital satellite	TRMM/TMI
2	1		Aqua/AMSR-E
4	2		DMSP-F13/SSM/I
8	3		DMSP-F14/SSM/I
16	4		DMSP-F15/SSM/I
65536	16	Infrared Imager aboard Geo-stationary meteorological satellite	GOES-EAST
131072	17		GOES-WEST
262144	18		INDEX
524288	19		METEOSAT
1048576	20		MTSAT
-(negative)	31	No microwave radiometer observation	

Observation Time Flag

- **Observation Time Flag:**
 - **gsmmap_nrt.YYYYMMDD.HH NN.timeinfo.dat**
- **“Observation Time Information Flag” indicates relative time of latest microwave radiometer observation at each pixel.**
- **0 means start time of the file (HH in file name). Values are stored as indicated in right table.**

Value	Description
+X	If value is positive, microwave radiometer observation is available at the pixel during time period of the file. X ($0 \leq X < 1$) indicates relative observation time of latest microwave radiometer, and is stored as differences from the start time of the file. For example, if UTC of the file (HH) = “01” and X = 0.2, observation time of the pixel will be 01:12 UTC.
-Y	If value is negative, NO microwave radiometer observation is available at the pixel during time period of the file. Y indicates relative observation time of latest microwave radiometer, and stored as differences from the start time of the file. For example, if UTC of the file (HH) = “01” and Y = -2.5, latest observation time of microwave radiometer at the pixel will be 23:30 UTC of previous day.
-999	Missing data.



GrADS Control File

- **Sample control files of the Grid Analysis and Display System (GrADS) for each product are also available from ftp server.**
 - **Hourly Rain Rate data:**
 - **/realtime/archive/GSMaP_NRT.hourly.rain.ctl**
 - **Satellite Information Flag:**
 - **/realtime/satinfo/GSMaP_NRT.hourly.sat.ctl**
 - **Observation Time Flag:**
 - **/realtime/timeinfo/GSMaP_NRT.hourly.time.ctl**

Summary of GSMaP_NRT Products

No	Parameter [unit]	Data format	Coverage	Grid size	Horizontal resolution	Temporal resolution	FTP directory
1	Hourly Rain Rate [mm/h]	4-byte float plain binary, little-endian	Global (60° N-60° S)	3600 x 1200	0.1 degree grid box	Hourly	Latest 24-hr: /realtime/latest/ Archive: /realtime/archive/ YYYY/MM/DD/
2	Satellite Information Flag	4-byte signed integer plain binary, little-endian					/realtime/sateinfo/ YYYY/MM/DD/
3	Observation Time Flag	4-byte float plain binary, little-endian					/realtime/timeinfo/ YYYY/MM/DD/
4	Hourly Rain Rate in text format [mm/h]	ASCII, CSV format		200 rows x 400 lines			/realtime/txt/AAAB BBB/YYYY/MM/DD/
5	Daily Accumulated Rainfall [mm/day]	4-byte float plain binary, little-endian	Global (60N-60S)	1440 x 480	0.25 degree grid box	Daily (accumulation from 00Z to 23Z of the specified day)	/realtime/daily/00 Z-23Z/YYYYMM/
6						Daily (accumulation from 12Z of previous day to 11Z of the specified day)	/realtime/daily/p1 2Z-11Z/YYYYMM/



Handling of Precipitation data



Mission List

- Rainfall gridded Data is put in Directry 'GSMaP_DATA'
- Draw a figure of global distribution of rainfall by GrADS.
 - Open GrADS control file (GSMaP_NRT.hourly.rain.ctl) by GrADS and draw it by a command 'd precip'.
 - open GSMaP_NRT.hourly.rain.ctl
 - set gxout grfill
 - d precip
- Draw a figure of your favorite area, for example, 80E-90E, 17N-27N.
 - Examlle;
 - set lon 80 90
 - set lat 17 27
 - d precip
- Compute a daily mean by GrADS and draw a figure of a daily mean.
 - Example;
 - set lon 80
 - set lat 17
 - set t 1 24
 - d precip
- Draw a figure of time series at your favorite location.



TRMM Tropical
Rainfall
Measuring
Mission



Satellite data/images access through JAXA/EORC www/ftp site

Misako KACHI

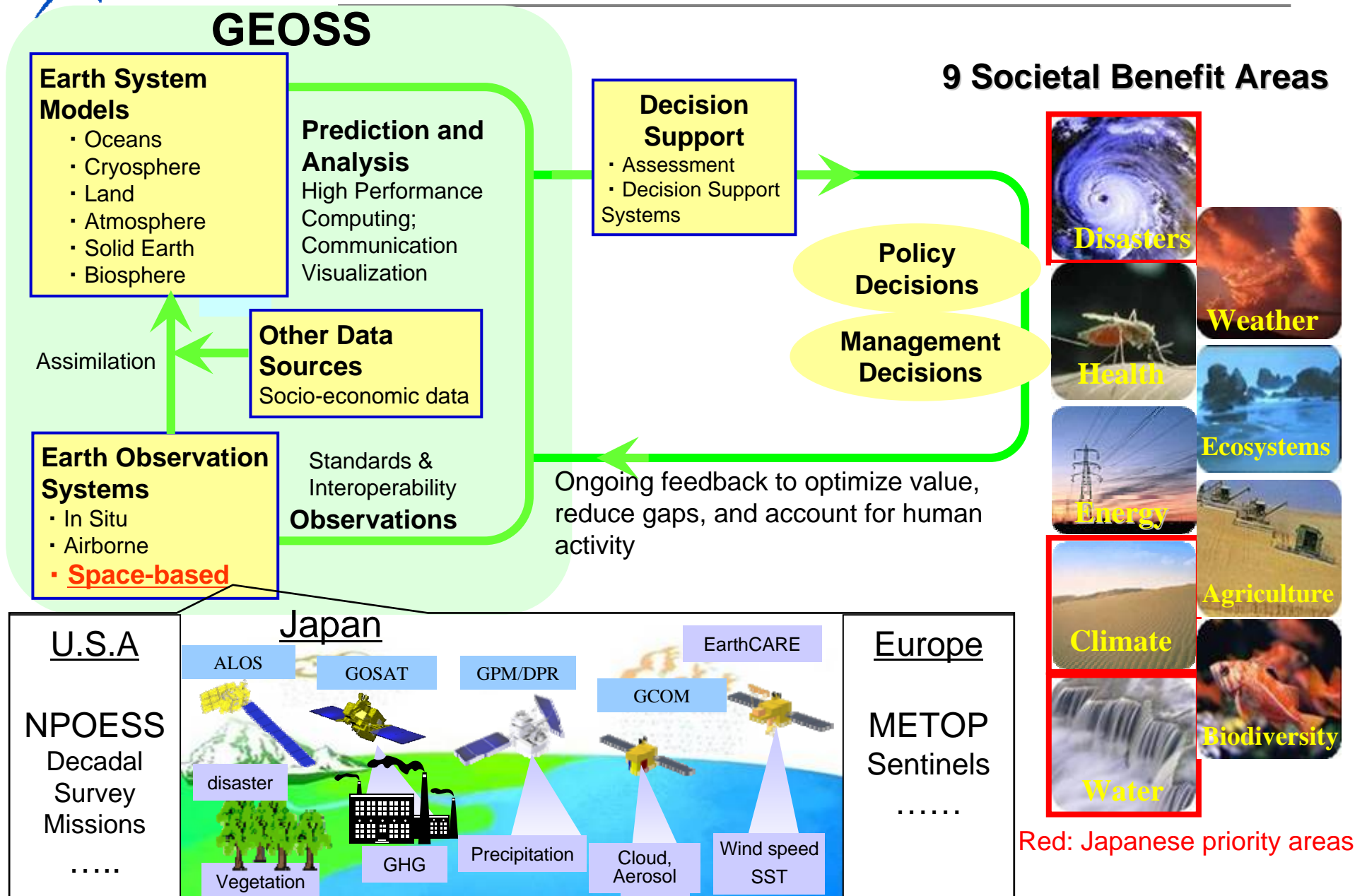
Earth Observation Research Center (EORC)
Japan Aerospace Exploration Agency (JAXA)

Contents

- JAXA Introduction (DVD video - 14min)
- JAXA's water related missions
 - Tropical Rainfall Measuring Mission (TRMM)
 - Advanced Microwave Scanning Radiometer for EOS-Aqua (AMSR-E)
 - Advanced Land Observing Satellite (ALOS)
 - Future missions: GCOM-W/-C, GPM
- Satellite data access to TRMM/AMSR-E data via www/ftp site
 - TRMM/AMSR-E standard products
 - JAXA/EORC Tropical Cyclone Database
 - TRMM Tropical Cyclone Monitoring
 - Global Precipitation Map in Near Real Time
 - Latent Heating Research Product
 - Others
- JAXA activities for hydrological applications
 - Collaboration with IFNet/ICHARM
 - Collaboration with University of Tokyo
 - Sentinel Asia/Sentinel Asia for Environment (DVD video, if there is enough time)
- Appendix: List of TRMM www/data sites



GEOSS 10yr Implementation Plan





JAXA's water related missions

- TRMM (1997 ~)
 - Precipitation Radar (PR)
 - TRMM Microwave Imager (TMI)
- ADEOS-II (2002 ~ 2003)
 - Global Imager (GLI)
 - Advanced Microwave Scanning Radiometer (AMSR)
 - SeaWinds
- Aqua (2002 ~)
 - Advanced Microwave Scanning Radiometer for EOS (AMSR-E)
- ALOS (2006 ~)

Tropical Rainfall Measuring Mission (TRMM)

- Major characteristics
 - **Focused on rainfall observation.**
First instantaneous rainfall observation by three different sensors (PR, TMI, VIRS). **PR, active sensor, can observe three-dimensional structure of rainfall.**
 - Targeting tropical and subtropical region, and chose non-sun-synchronous orbit (inc. angle 35 degree) to observe diurnal variation.
- Major achievement in Japan
 - Demonstration of high quality and high reliability of a satellite onboard precipitation radar
 - Improvement of MWR precipitation retrieval by PR 3D observation
 - Pioneering precipitation system climatology by PR observation
 - Operational use in NWP etc.
 - New products including all-weather SST, global soil moisture



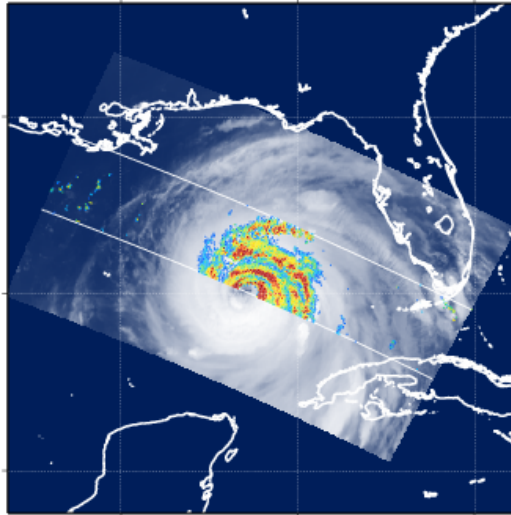
Launch	28 Nov. 1997 (JST)
Altitude	About 350km (since 2001, boosted to 402km to extend mission operation)
Inc. angle	About 35 degree, non-sun-synchronous orbit
Design life	3-year and 2month (still operating)
Instruments	<p>Precipitation Radar (PR)</p> <p>TRMM Microwave Imager (TMI)</p> <p>Visible Infrared Scanner (VIRS)</p> <p>Lightning Imaging Sensor (LIS)</p> <p>CERES (not in operation)</p>



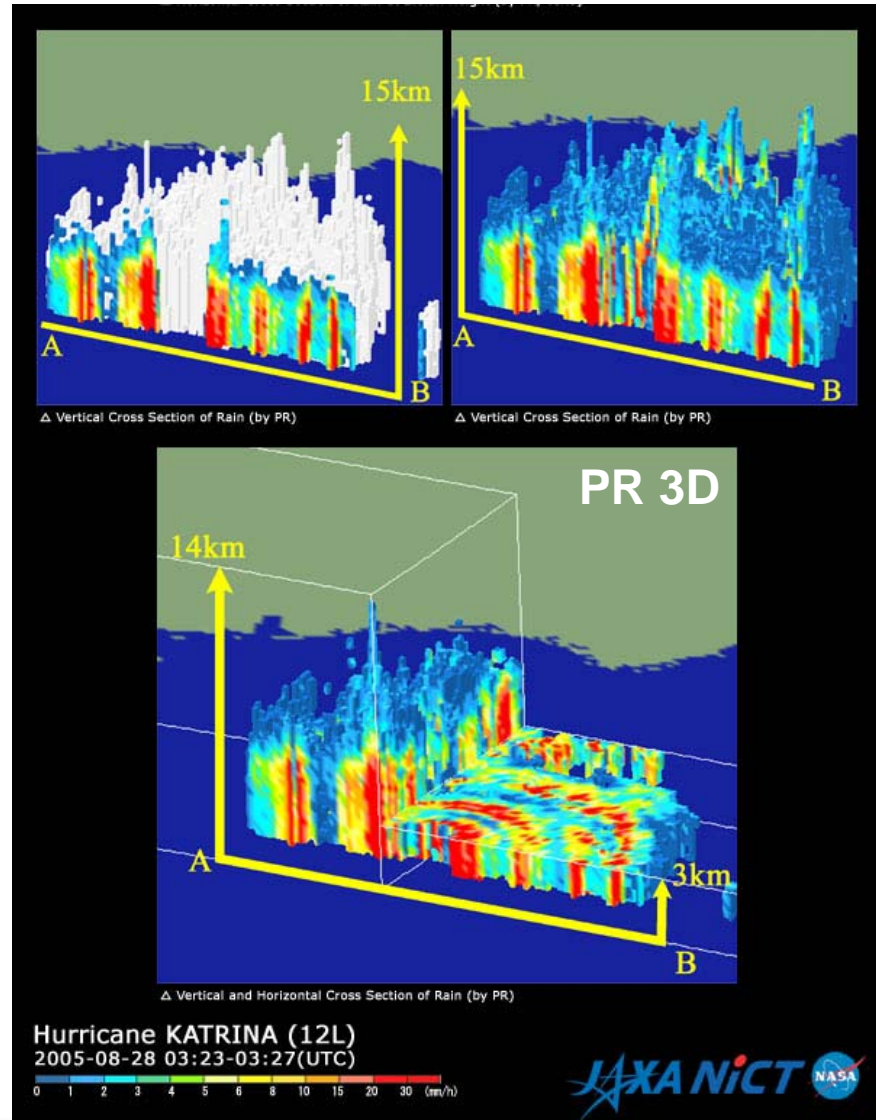
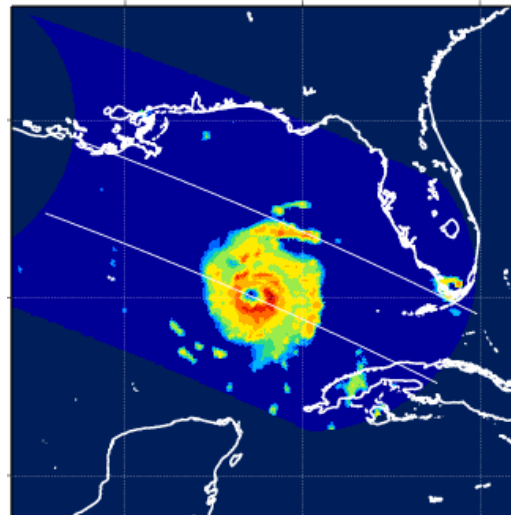
Observation of 3-dimensional Structure of Tropical Cyclones

Hurricane Katrina in 2005

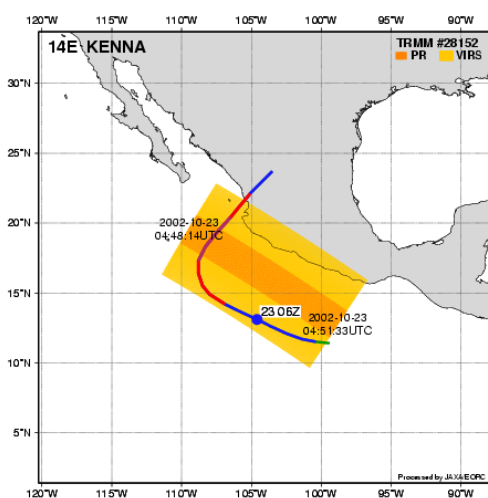
PR & IR image



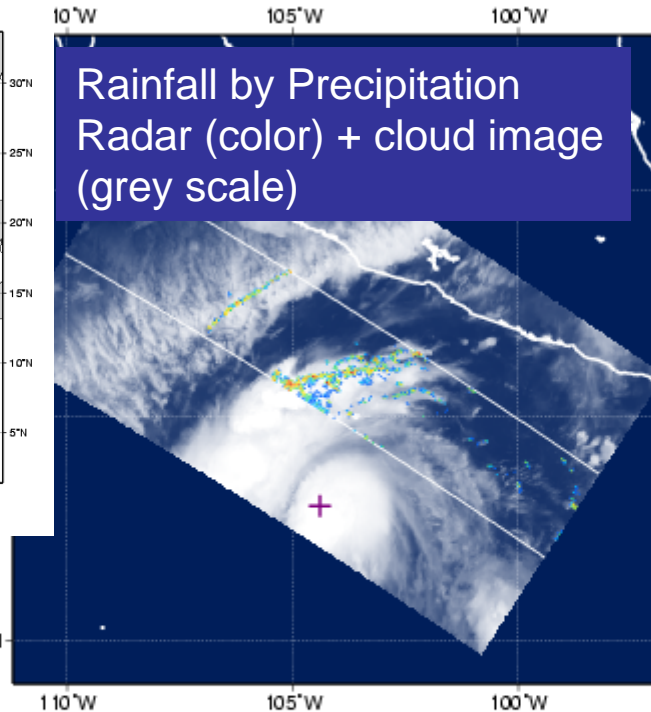
TMI image



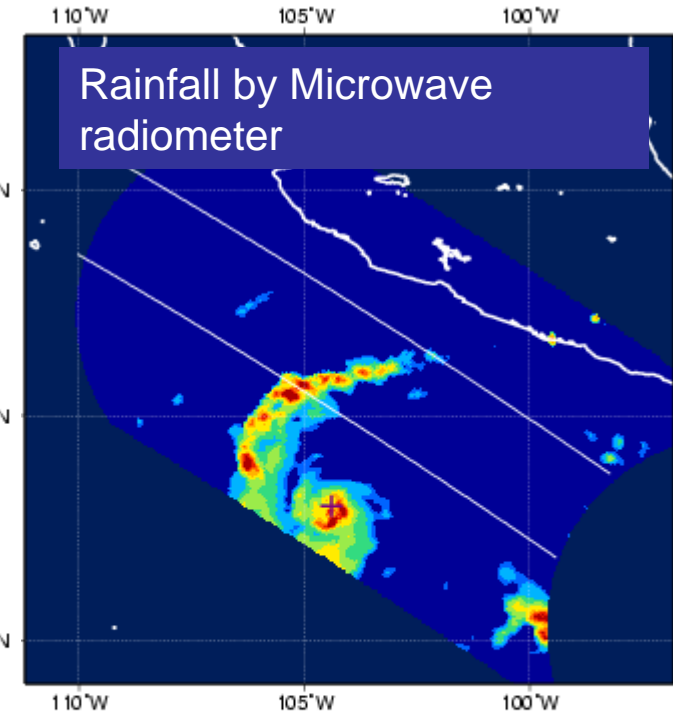
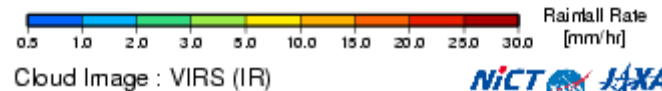
Tropical cyclone observation impact in forecasts



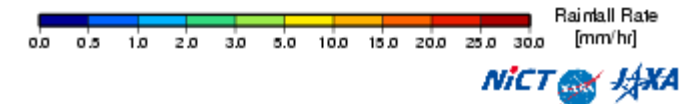
Hurricane KENNA
in 2002



KENNA (14E) Rainfall Rate by TRMM/PR
2002-10-23 04:49 (UTC) Orbit Number 28152
2A25.02 1023.28 152.5A.14E.KENNA.HDF (Ver.5A)



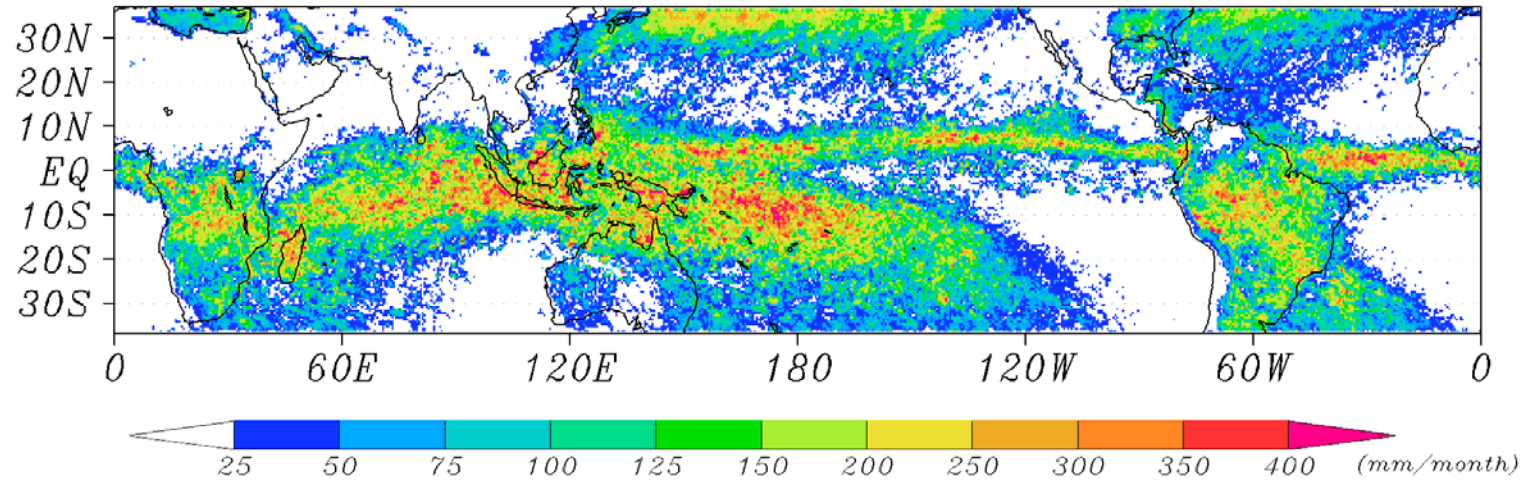
KENNA (14E) Rainfall Rate by TRMM/TMI
2002-10-23 04:51 (UTC) Orbit Number 28152
2A12.02 1023.28 152.5A.14E.KENNA.HDF (Ver.5A)



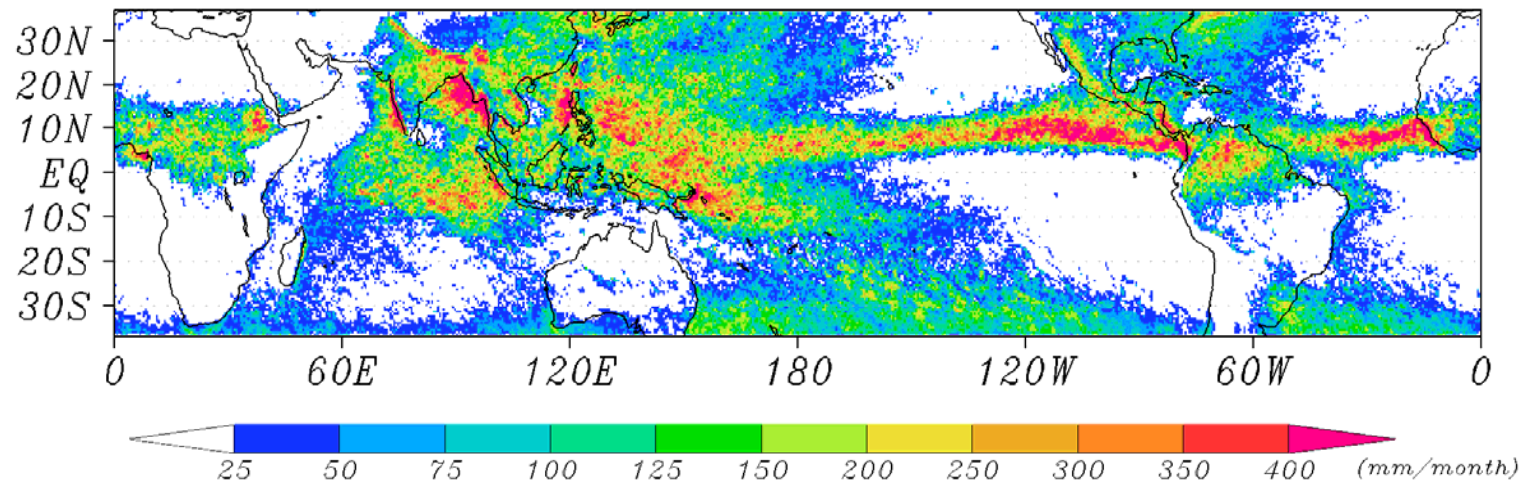
Structure of "eye" of hurricane (denote in +) is not recognized in cloud image (left), but clearly seen in microwave radiometer observation (right). In consequence, 24-hr forecast regarding intensity by NOAA Tropical Prediction Center was corrected.

TRMM PR climatology

TRMM PR 3A25 Rain rate (0.5x0.5deg) : JAN(1998-2007)



TRMM PR 3A25 Rain rate (0.5x0.5deg) : JUL(1998-2007)





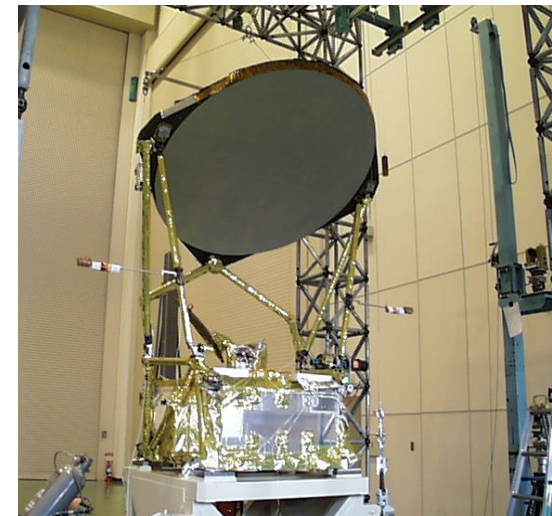
Advanced Microwave Scanning Radiometer for EOS

■ Mission status

- Continuous observation over 6-years after the launch on May 4, 2002 onboard NASA's EOS Aqua satellite.
- Stable brightness temperature records, except the loss of 89GHz-A data from November 2004.
- Operation of the Aqua satellite will be maintained at least until 2011, according to NASA senior review.

■ Instrument characteristics

- Multi-frequency microwave radiometer with dual polarization capability (developed by JAXA).
- High-spatial resolution compared to existing instruments by large size antenna.
- C-band (6.9GHz) channels for estimating SST and soil moisture.
- Afternoon (1:30 pm) equatorial crossing time that is currently unique for microwave radiometers.



Pre-launch AMSR-E in Tsukuba Space Center

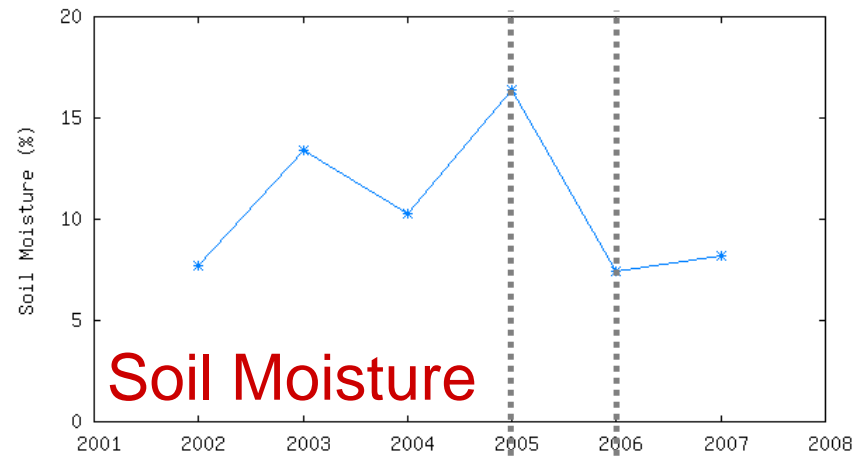
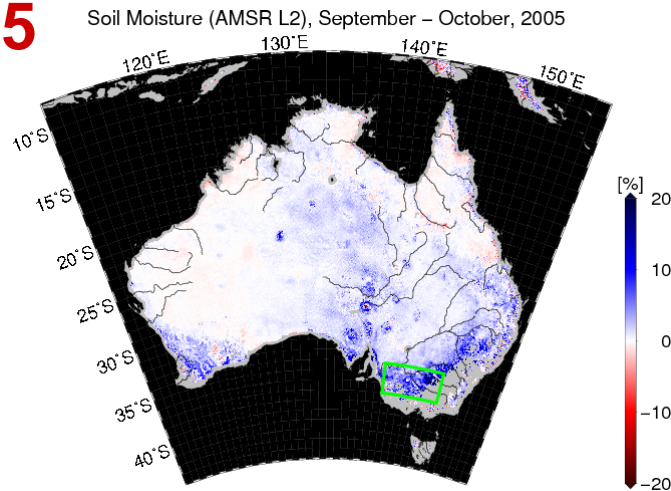




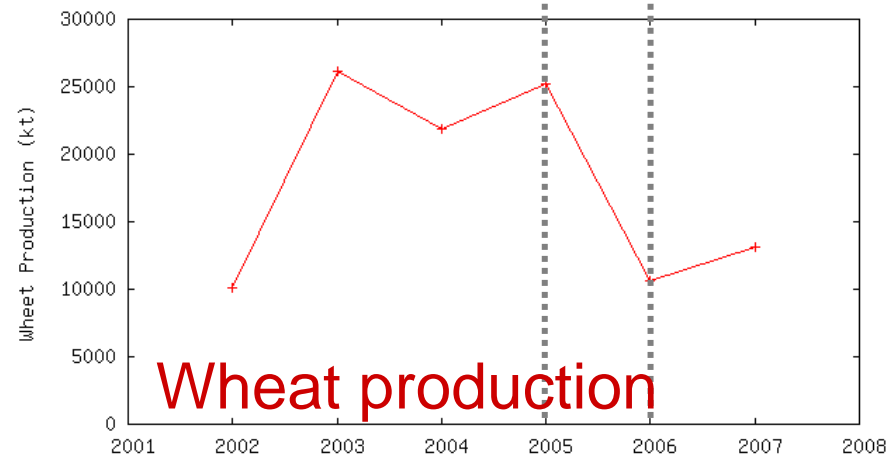
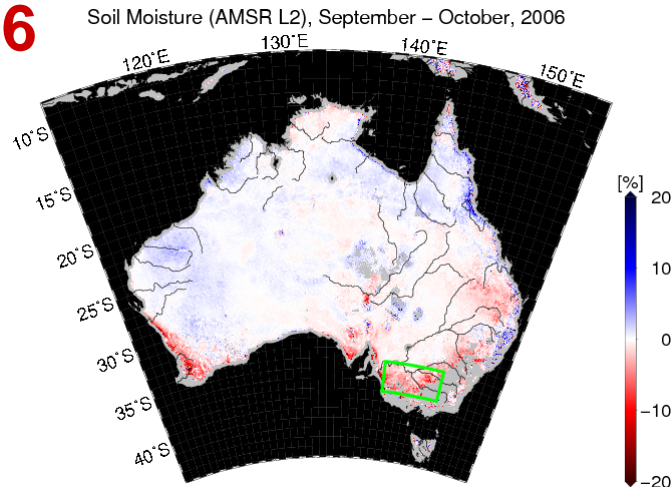
Soil Moisture observation

- AMSRE soil moisture anomalies over south-eastern Australia (green rectangle) averaged Sep.-Oct. 2005 and 2006 are compared to wheat production.

2005



2006



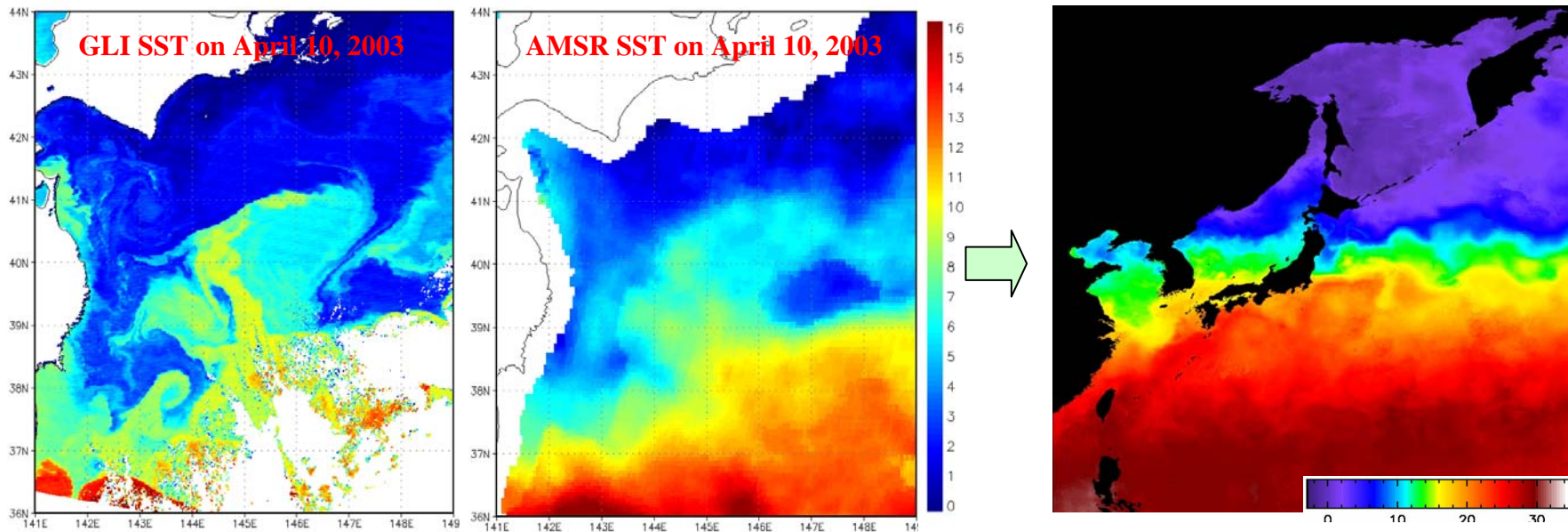
Source: Australian Bureau of Agricultural and Resource Economics





All weather SST

- C-band (7GHz) channels are indispensable for retrieving global sea surface temperature and soil moisture. All-weather, frequent measurements enables analyses of rapid changes of SST.
- Time-proven infrared measurement and microwave observations are in complementary situation in terms of spatial resolution and error sources.
- AMSR-E and various infrared sensor data are merged by objective analysis to obtain cloud-free high-resolution SST image.

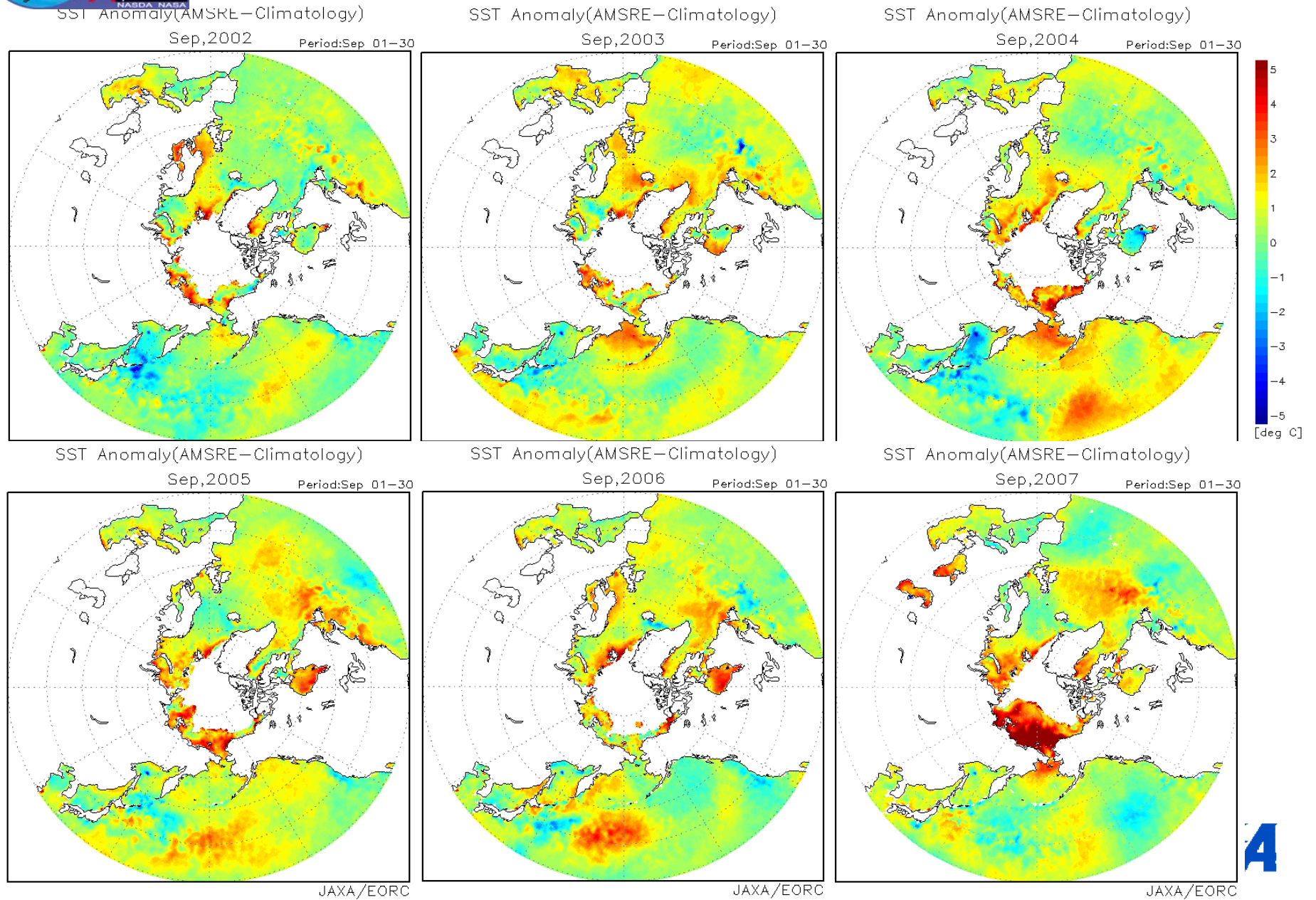


SST images around east coast of Japan on April 10, 2003 obtained by GLI (left) and AMSR (right). Differences of spatial resolution and influence of clouds (lower-left white areas in GLI image) are clearly seen.

New Generation Sea Surface Temperature (NGSST) by NGSST group (led by Professor Hiroshi Kawamura of Tohoku University).



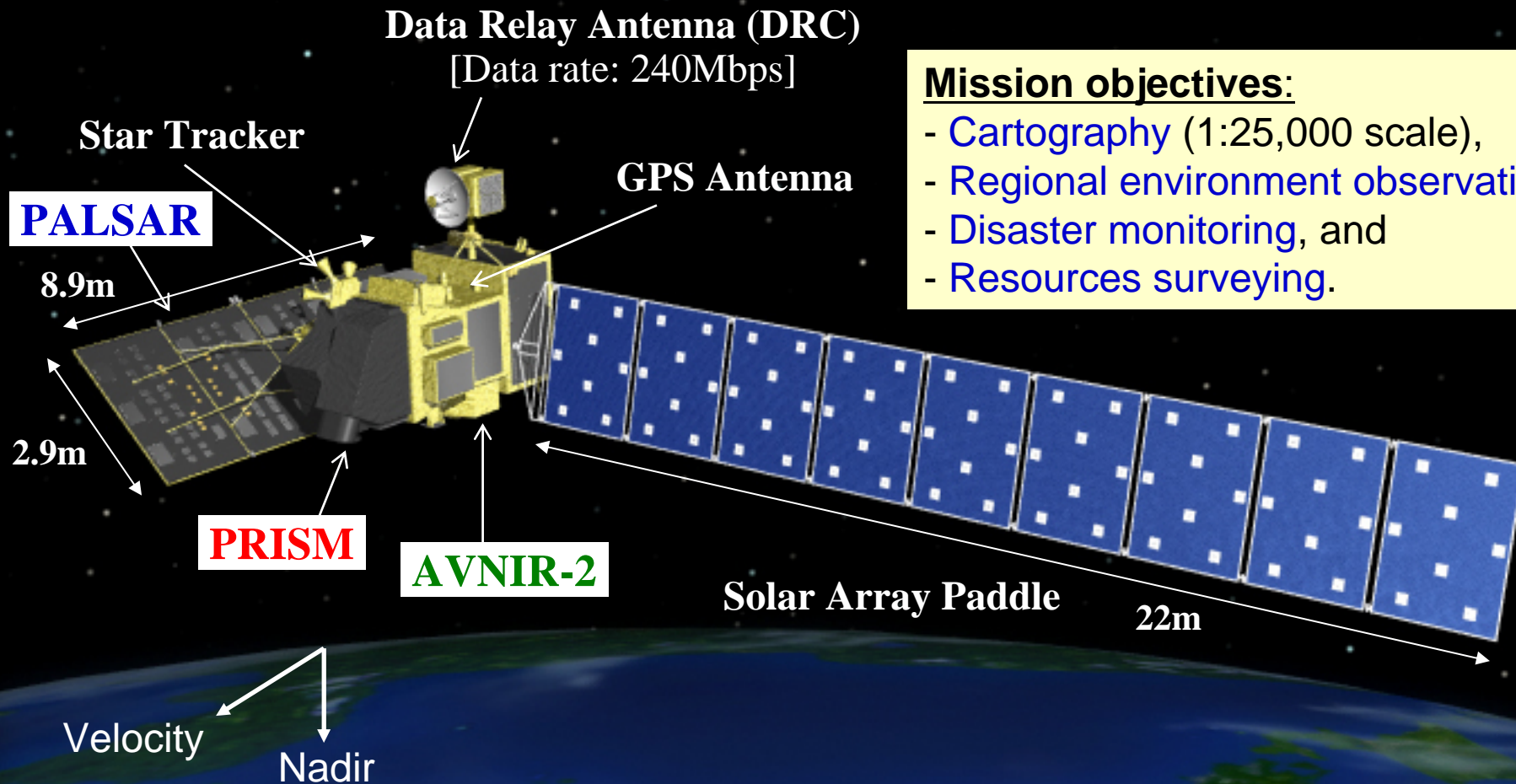
SST anomaly in northern high latitudes



ALOS "Daichi"

(Advanced Land Observing Satellite)

Jan. 24, 2006: Launch by H-IIA #8 from TNSC
Aug. 30, 2007: 1.6 year (583 days) after launch



- Mission objectives:**
- Cartography (1:25,000 scale),
 - Regional environment observation,
 - Disaster monitoring, and
 - Resources surveying.

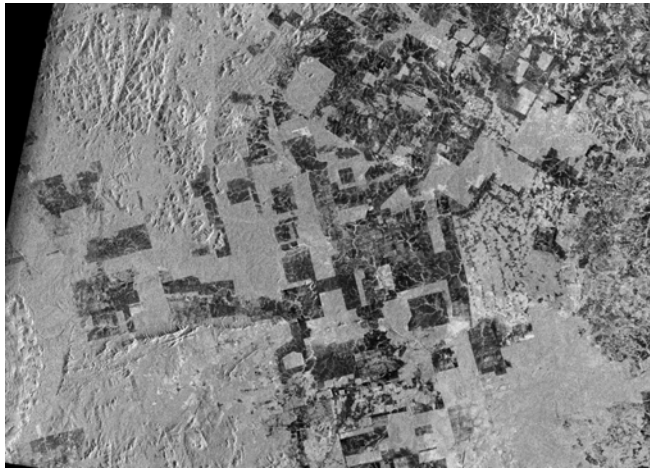
PRISM : Panchromatic Remote-sensing Instrument for Stereo Mapping
AVNIR-2: Advanced Visible and Near Infrared Radiometer type 2
PALSAR: Phased Array type L-band Synthetic Aperture Radar

ALOS Characteristics

Launch Date	10:33am, January 24 th , 2006 (JST)
Orbit	Sun-synchronous
Local Time at DN	10:30am +/- 15 min.
Altitude	691.65 km @Equator
Inclination	98.16 degrees
Recurrent Period	46 days (Sub-cycle: 2 days)
Revolution	14 + 27/46 (/day), 671 (/recurrent)
Period	98.7 minutes
Longitude Repeatability	+/-2.5 km @Equator
Data Collection	1 DRTS (Data Relay Test Satellite), 240 Mbps HSSR (High Speed Solid state Recorder) + DT (X-band direct downlink), 120 Mbps
Yaw Steering	Off / On
Attitude Error each axis	2.0e-4 degree (determination) 0.1 deg. (maintain)
Satellite Mass	4,000 Kg
Power	7 KW @EOL



Deforestation Monitoring in Amazon



JERS-1 SAR (Oct., 1996)

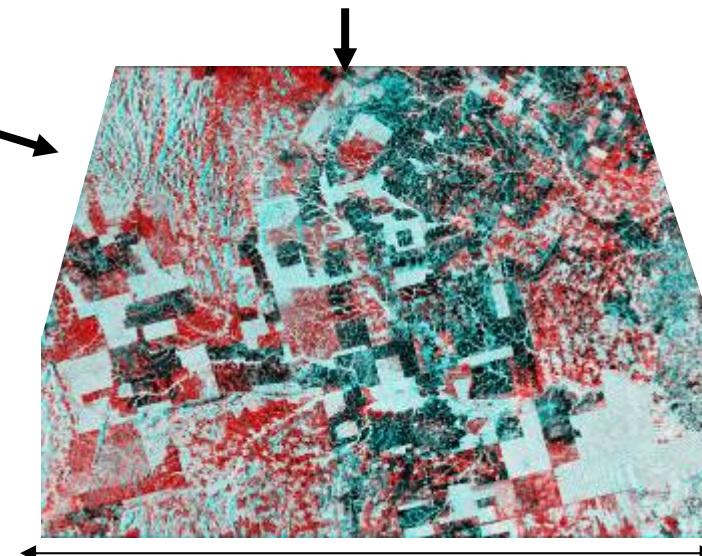


ALOS PALSAR (Jun., 2006)



Above image shows one of most popular deforestation site.

Red shows deforestation area during 10years



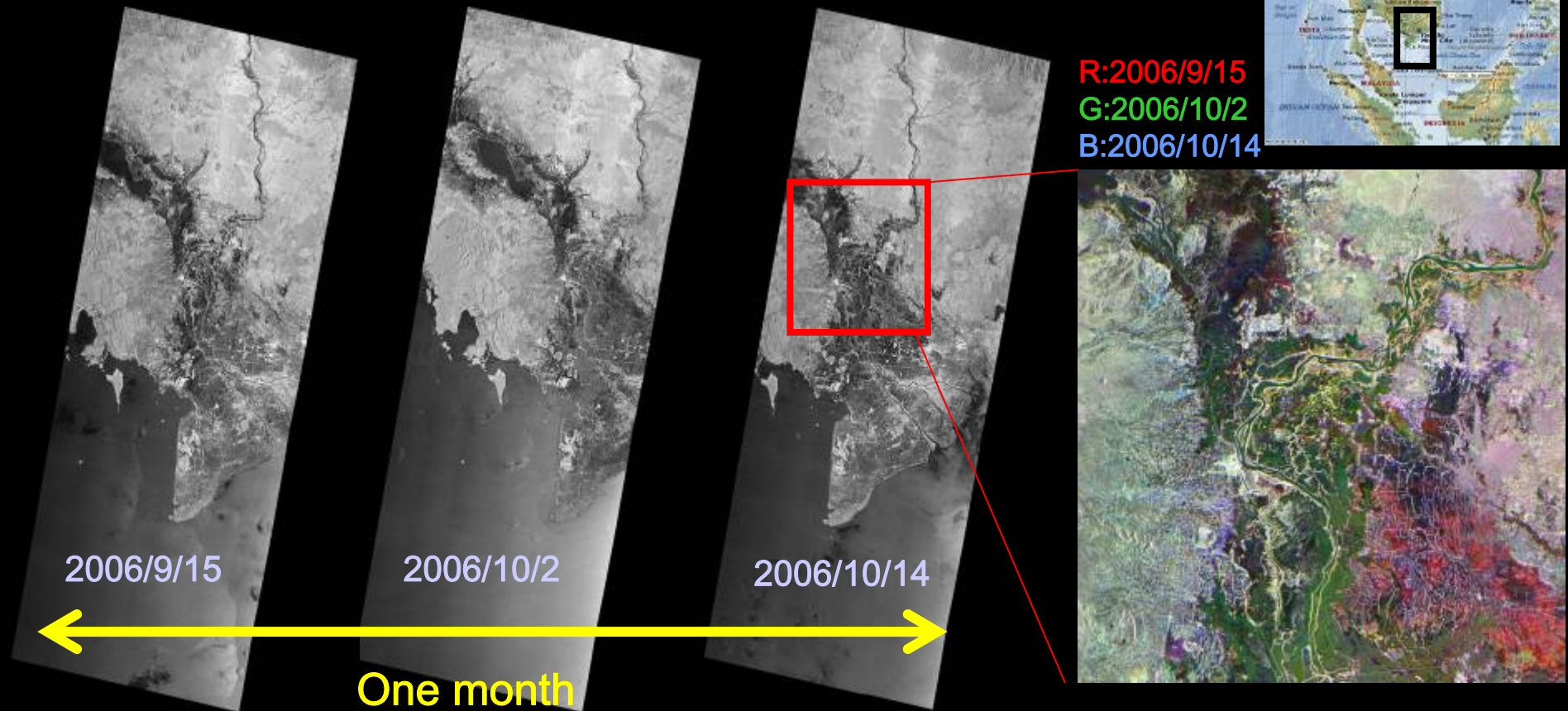
100km

10 year image comparison using JERS-1/SAR with ALOS/PALSAR.

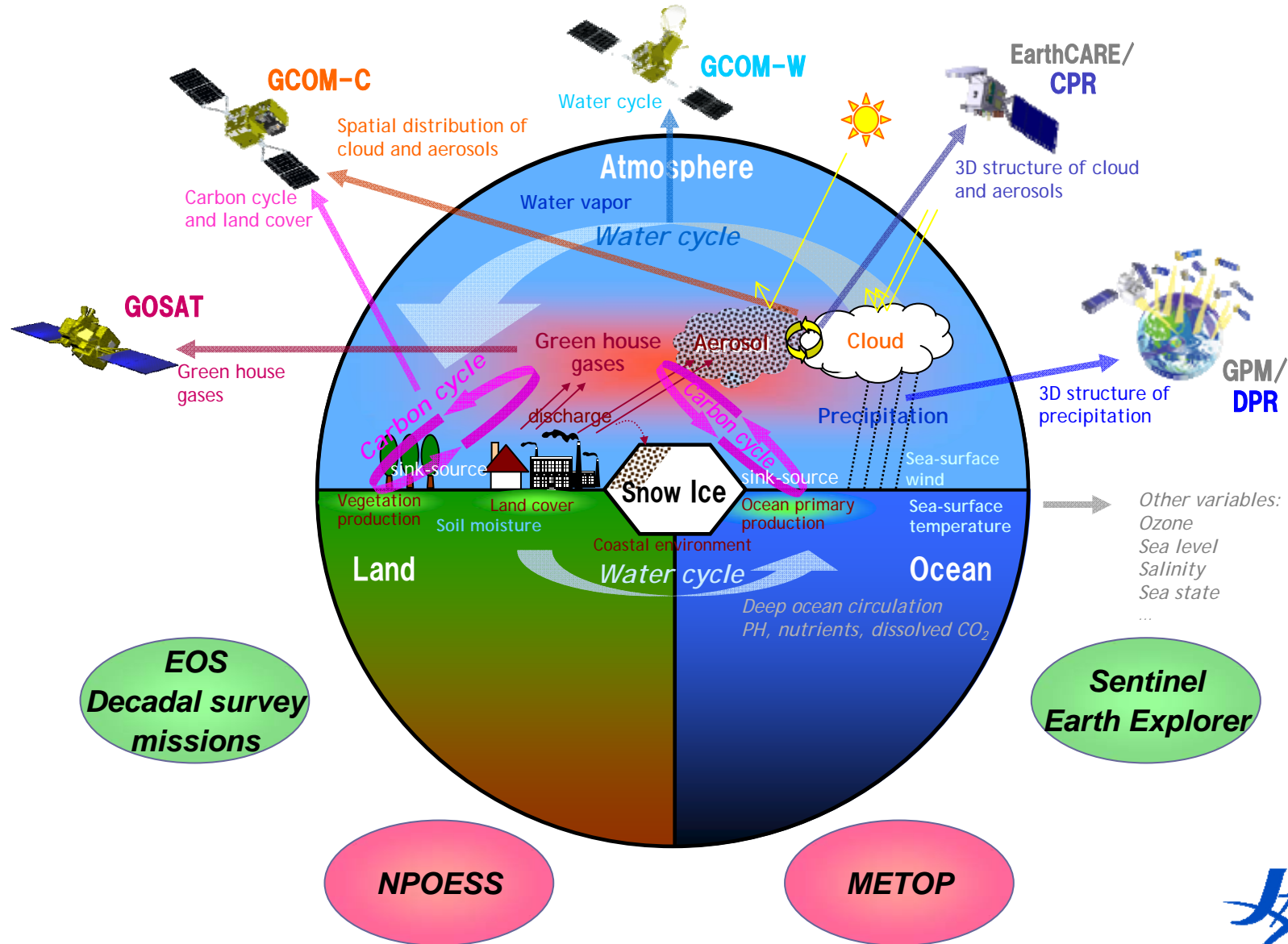
Grasp of flooding area at Mekong Delta



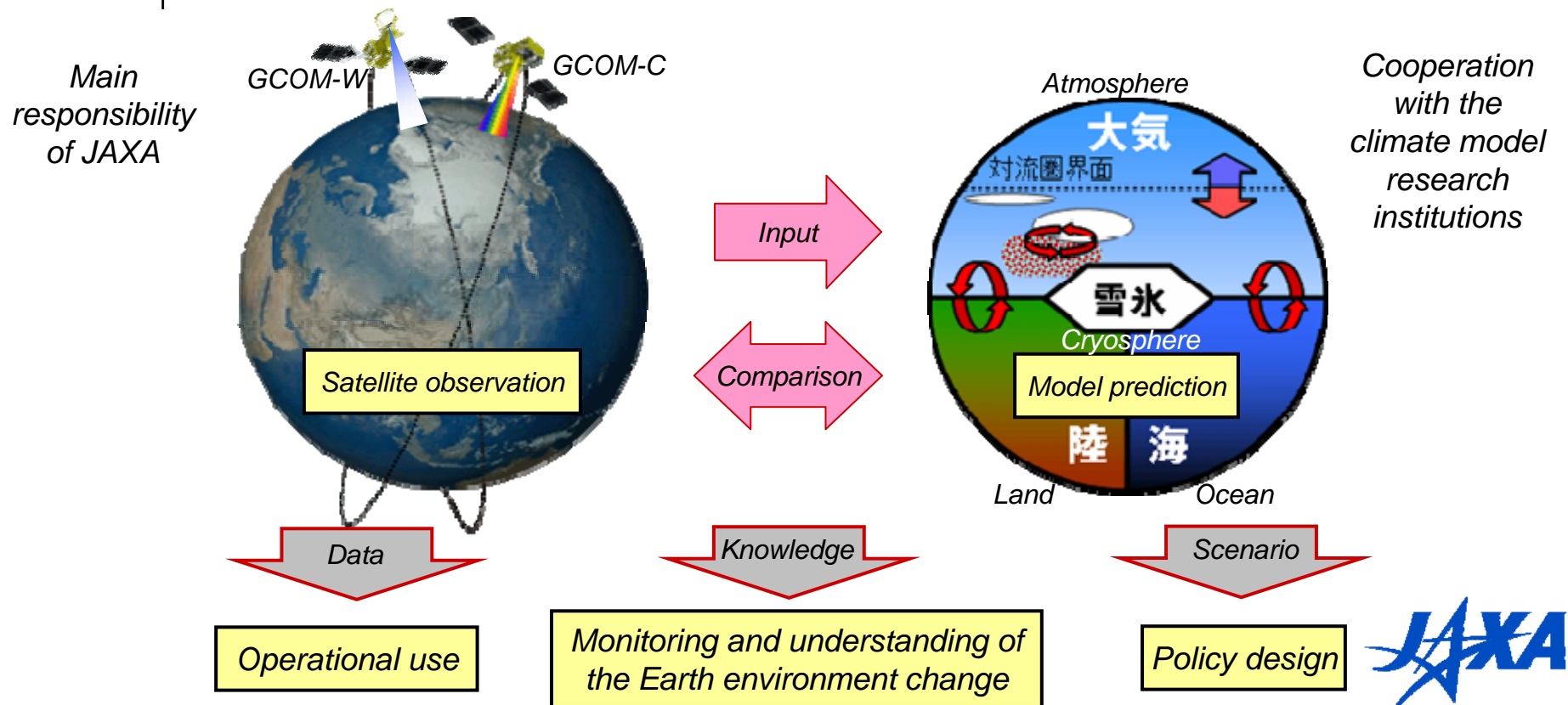
R:2006/9/15
G:2006/10/2
B:2006/10/14



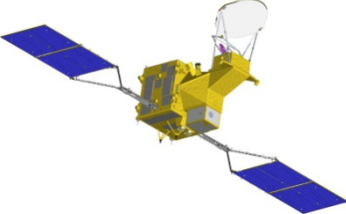
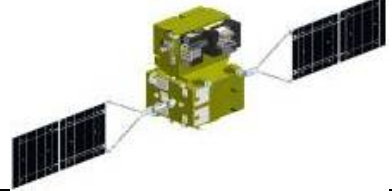
- From September 2006 to October 2006, we observed Mekong Delta continuously, using PALSAR/ScanSAR. Mekong Delta is affected by flooding every rainy season.
- We made color composite 3 season images about enclosed by red rectangle.
- On the composite image, color shows area having any change. Generally, flooding area appears darker than other area because of weak backscattering. Thus, we can assume that red area around plain was flooded after September 15 and Yellow area around Mekong river was flooded after October 2.
- Continuous observation by ScanSAR enables time series analysis of flooding area.



- Demonstrate long-term global observation of various geophysical parameters for understanding climate variability and water cycle.
- Two medium-sized satellites, three generations with one year overlap to ensure 10-15 years stable data records.
- Cooperation with climate models and direct contribution to operational users.



GCOM 1st Generation

	GCOM-W1	GCOM-C1
Orbit	Type : Sun-synchronous, sub-recurrent Altitude : 699.6 km Inclination : 98.19 degrees Local time of ascending node : 13:30	Type : Sun-synchronous, sub-recurrent Altitude : 798 km Inclination : 98.6 degrees Local time of ascending node : 10:30
Satellite overview		
Mission life	5 years	
Launch vehicle	H2A launch vehicle	
Mass	1940kg (AMSR2 404 kg)	2020 kg (SGLI 480 kg included)
Instrument	AMSR 2	Second Generation Global Imager (SGLI)
Launch (target)	January 2012	January 2014 (TBD)

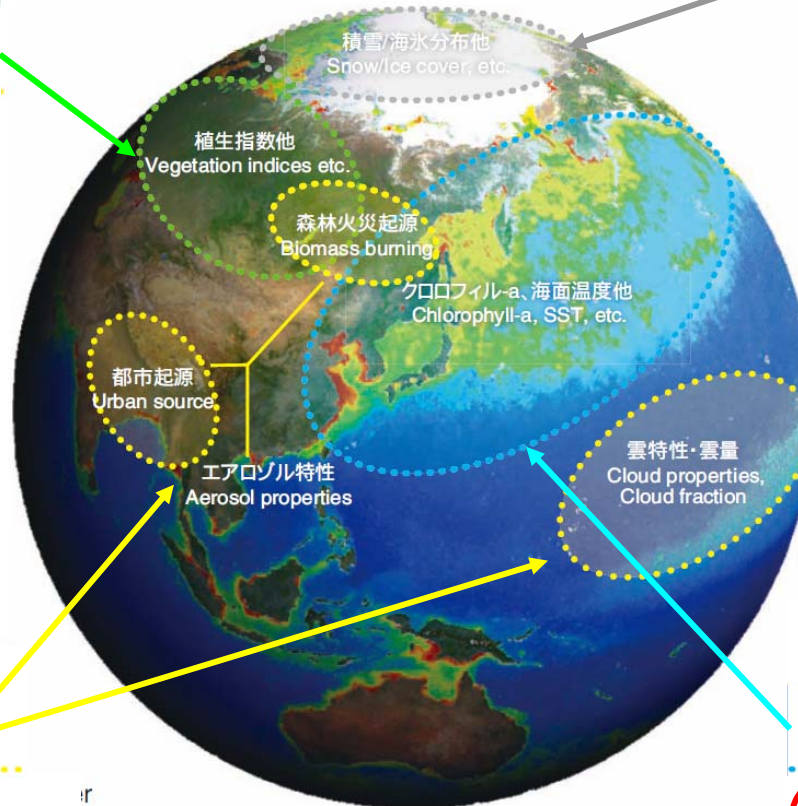
Most of the parameters are compatible with GCOS requirement

陸/Land

- Vegetation indices
- Soil moisture
- Biomass burning
- Land surface temp.

雪氷/Cryosphere

- Snow impurity
- Snow grain size
- Sea ice extent
- Snow depth/extent



大気/Atmosphere

- Aerosol properties
- Cloud properties
- Precipitable water
- Precipitation

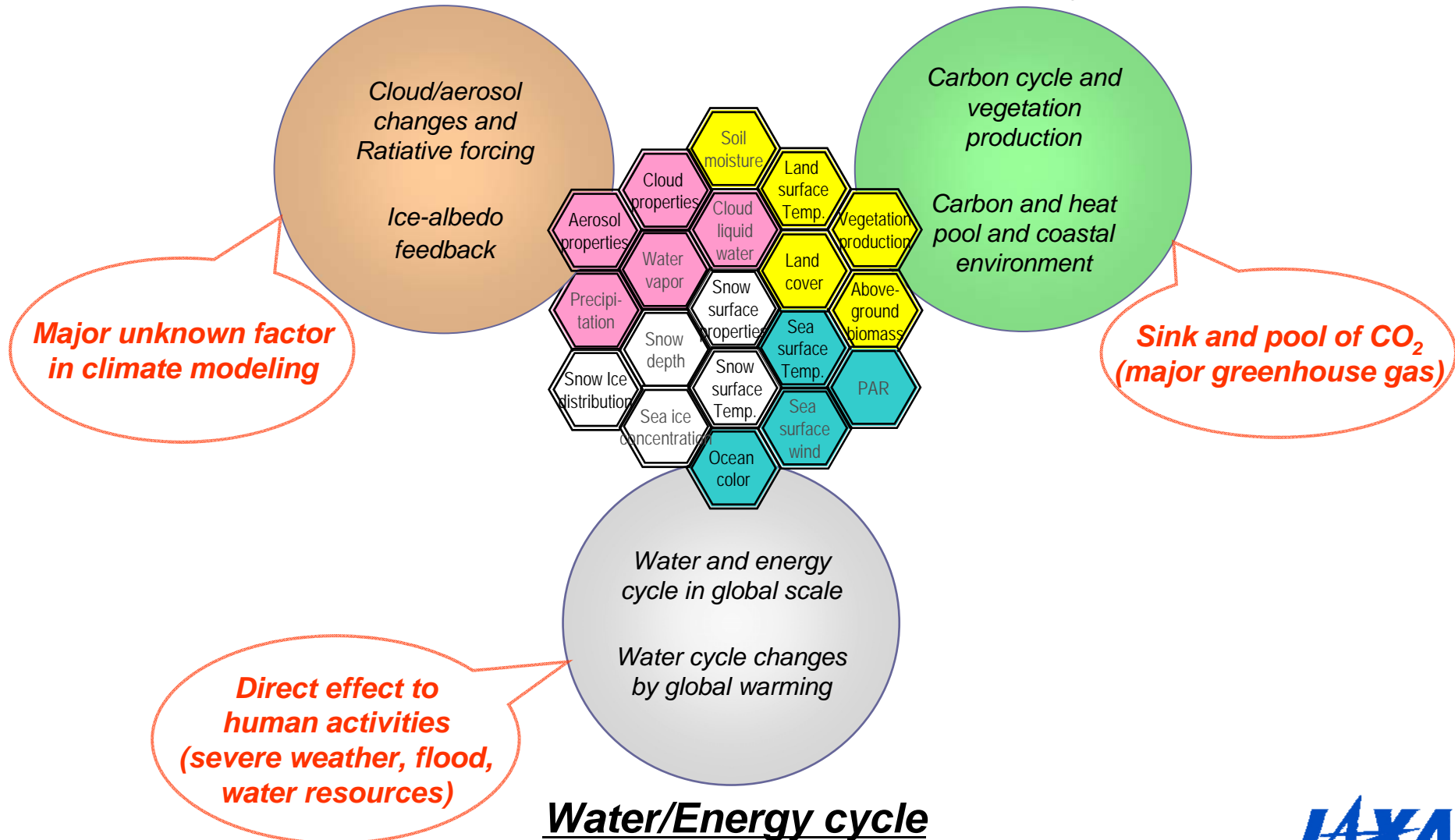
海洋/Ocean

- Sea surface temperature
- Sea surface wind speed
- Chlorophyll-a
- Suspended solid

GCOM observation targets

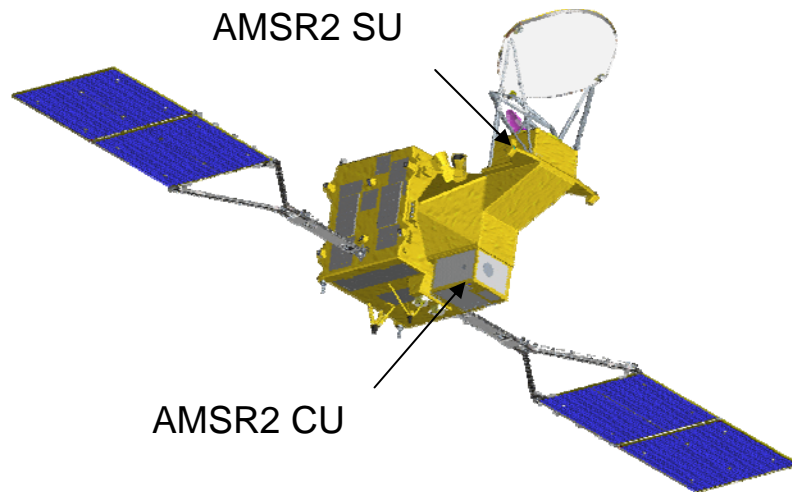
Radiation budget

Carbon cycle



GCOM-W1 Satellite

- Targets of GCOM-W are water-energy cycle, and will carry the Advanced Microwave Scanning Radiometer-2 (AMSR2).
- AMSR2 will continue AMSR-E observations (water vapor, cloud liquid water, precipitation, SST, sea surface wind speed, sea ice concentration, snow depth, and soil moisture).

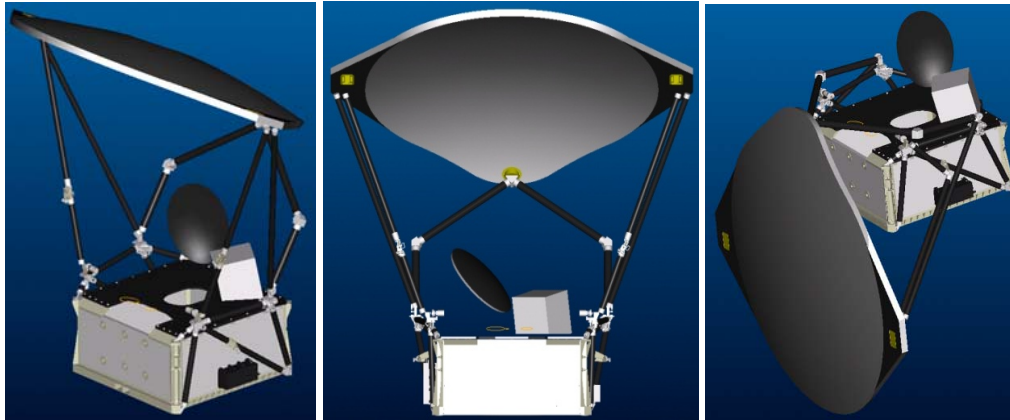


GCOM-W (Water)

Orbit	Sun synchronous orbit Altitude: 699.6km (on Equator) Inclination: 98.186° Local sun time: 13:30±15min
Life	5 years
Launch	January 2012 by H-IIA Rocket
Satellite scale	5.1m (X) X 17.6m (Y) X 5.0m (Z) (on-orbit)
Satellite mass	Total 1,940kg Mission mass: 404kg (AMSR2) Bus mass (dry): 1,391kg Propellant: 144kg
Power generation	More than 4050W (EOL)



Overview of AMSR2 instrument



Deployed

Stowed

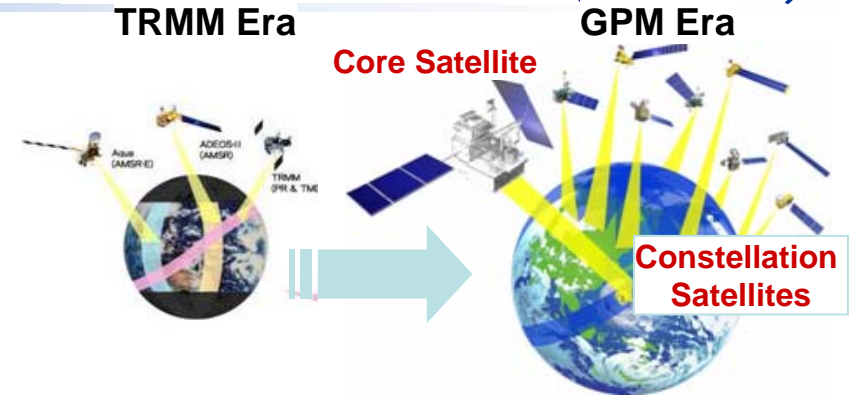
- Deployable main reflector system with 2.0m diameter.
- Frequency channel set is identical to that of AMSR-E except 7.3GHz channel for RFI mitigation.
- Two-point external calibration with the improved HTS (hot-load).
- Deep-space maneuver will be considered to check the consistency between main reflector and CSM.

AMSR2 characteristics	
Scan	Conical scan
Swath width	1450km
Antenna	2.0m offset parabola
Digitalization	12bit
Incidence angle	nominal 55 degree
Polarization	Vertical and Horizontal
Dynamic range	2.7-340K

AMSR2 Channel Set				
Center Freq. [GHz]	Band width [MHz]	Polarization	Beam width [deg] (Ground res. [km])	Sampling interval [km]
6.925/7.3	350	V and H	1.8 (35 x 62)	10
10.65	100		1.2 (24 x 42)	
18.7	200		0.65 (14 x 22)	
23.8	400		0.75 (15 x 26)	
36.5	1000		0.35 (7 x 12)	
89.0	3000		0.15 (3 x 5)	5

Global Precipitation Measurement (GPM)

- The Global Precipitation Measurement (GPM) is a follow-on and expanded mission of the Tropical Rainfall Measuring Mission (TRMM)



Core Satellite (JAXA, NASA)

Dual-frequency precipitation radar (DPR)

GPM Microwave Imager (GMI)

- Precipitation with high precision
- Discrimination between rain and snow
- Adjustment of data from constellation satellites

(launch in 2013)

Constellation Satellites (International Partners)

Microwave radiometers

Microwave sounders

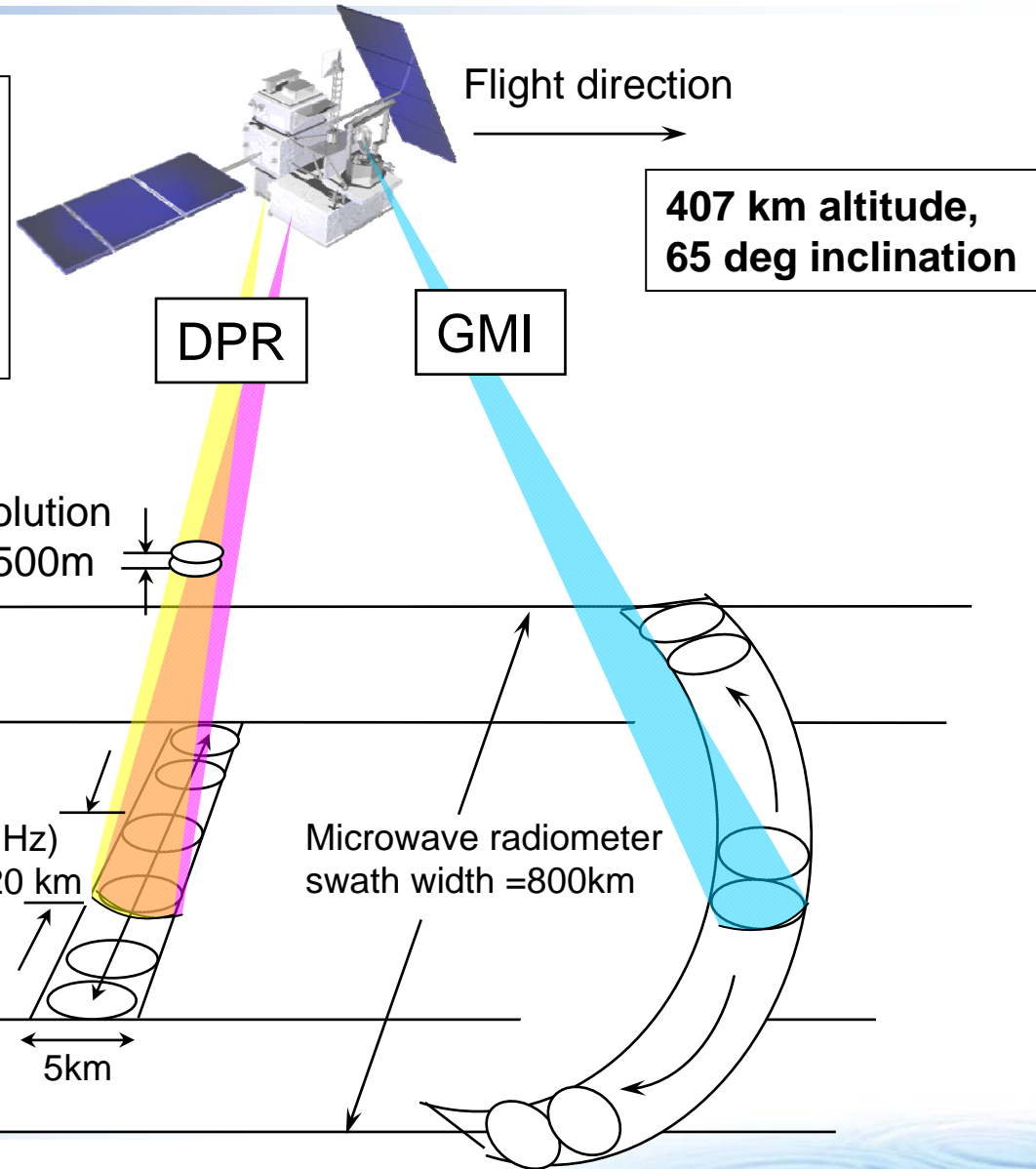
- Global precipitation every 3 hours

(launch around 2013)

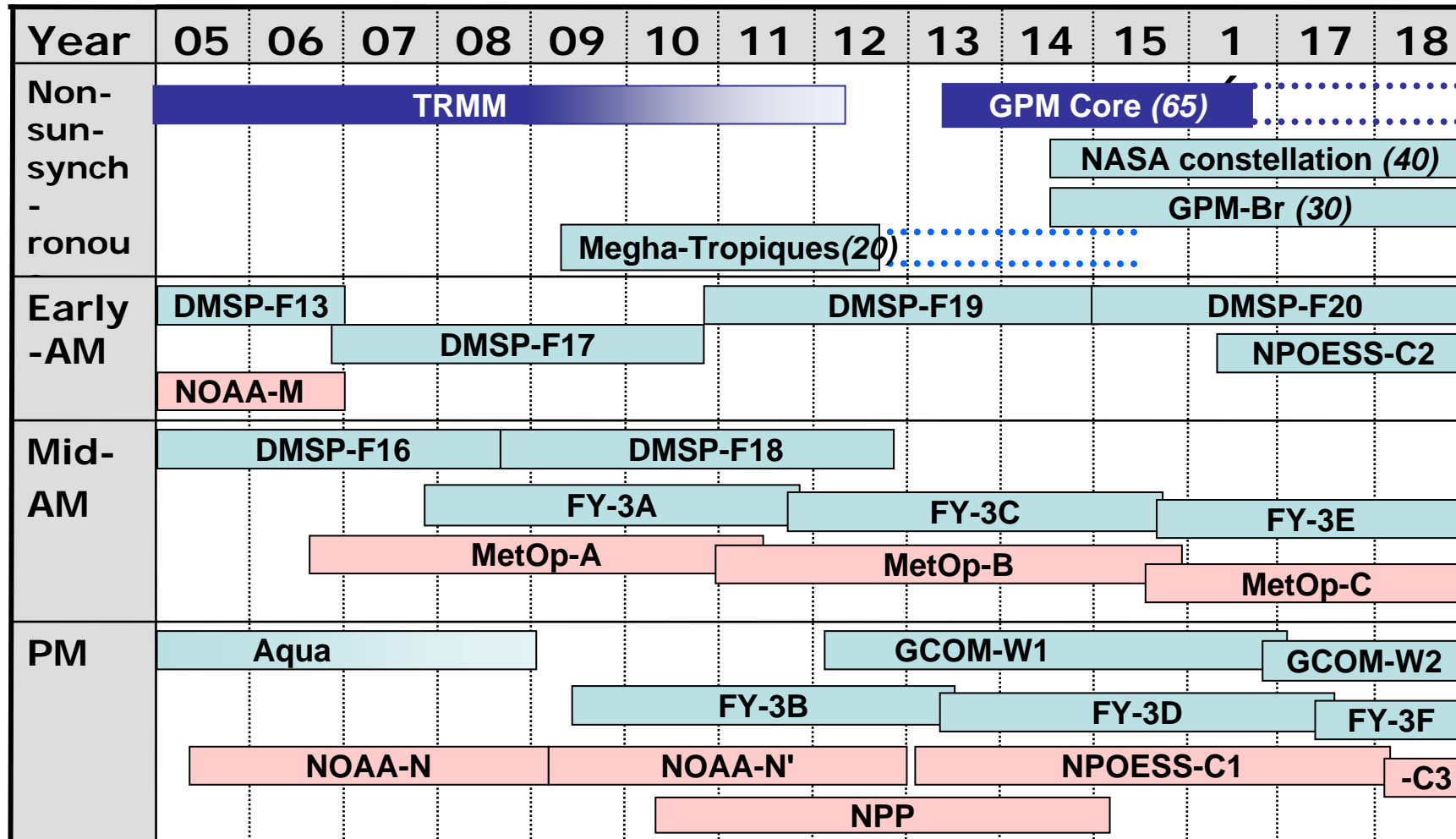
- Improve the accuracy of both long-term and short-term weather forecasts
- Improve water resource management in river control and irrigation systems for agriculture

Sensors aboard GPM core satellite

Dual-frequency precipitation radar (DPR) consists of Ku-band (13.6GHz) radar : **KuPR** and Ka-band (35.5GHz) radar : **KaPR**

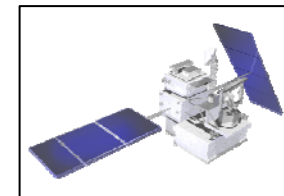
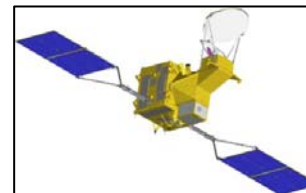


Precipitation Satellite Missions



Current and future conical scanning microwave radiometers

Sensor	SSM/I	TMI	AMSR-E	SSMIS	Windsat	AMSR2	GMI	MIS
Satellite	DMSP series (~F15)	TRMM	Aqua	DMSP series (F16~)	Coriolis	GCOM W1	GPM	NPOESS C2
Provider	DoD, U.S.	NASA	JAXA	DoD, U.S.	NASA	JAXA	NASA	NOAA/NRL
Freq. [GHz]	19.35 - 85.5	10.65 - 85.5	6.93 - 89.0	19.35 - 183.3	6.8 - 37.0	6.93 - 89.0	10.65 - 183.3	6 - TBD
Antenna size [m]	0.61	0.61	1.6	0.61	1.8	2.0	1.2	1.8





TRMM
Tropical Rainfall Measuring Mission

Satellite data access to TRMM/AMSR-E



data via www/ftp site

TRMM Web site:
http://www.eorc.jaxa.jp/TRMM/index_e.htm

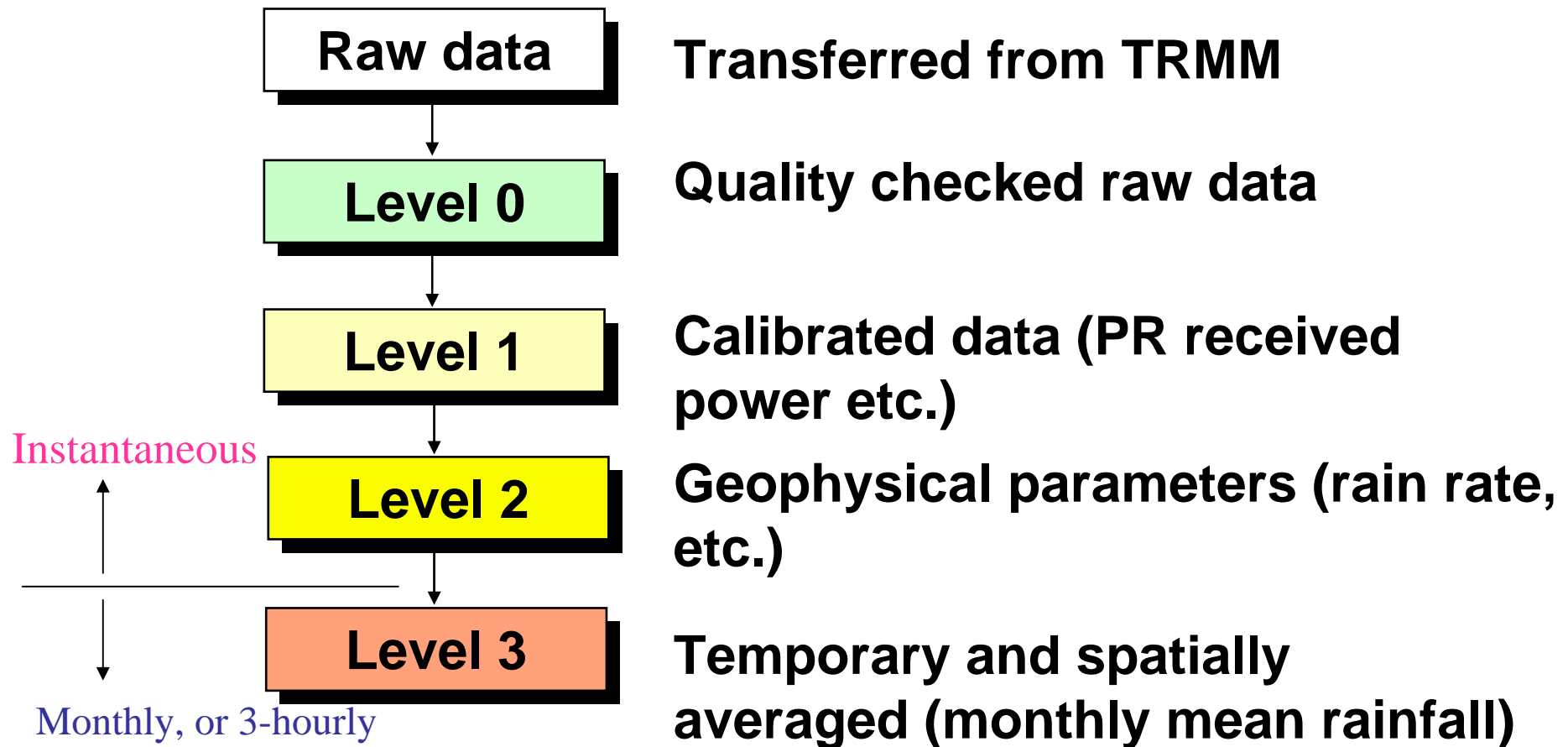
AMSR-E Web site:
http://sharaku.eorc.jaxa.jp/AMSR/index_e.htm

Satellite Product Categories

- Standard Product
 - Operational product that produced
- Subset Product
 - Sub-set of specific region or area, produced from standard product.
- Research Product
 - Product that uses research algorithm and is produced mainly for research objectives. Products are not produced operationally.
- Near Real-time Product
 - Product that is released in near real-time in order to meet requirement for operational uses, such as numerical weather prediction. Products are released within 3-to-4 hours after satellite observation to operational agencies, but geolocation accuracy could be worse than standard product in several kilometers.

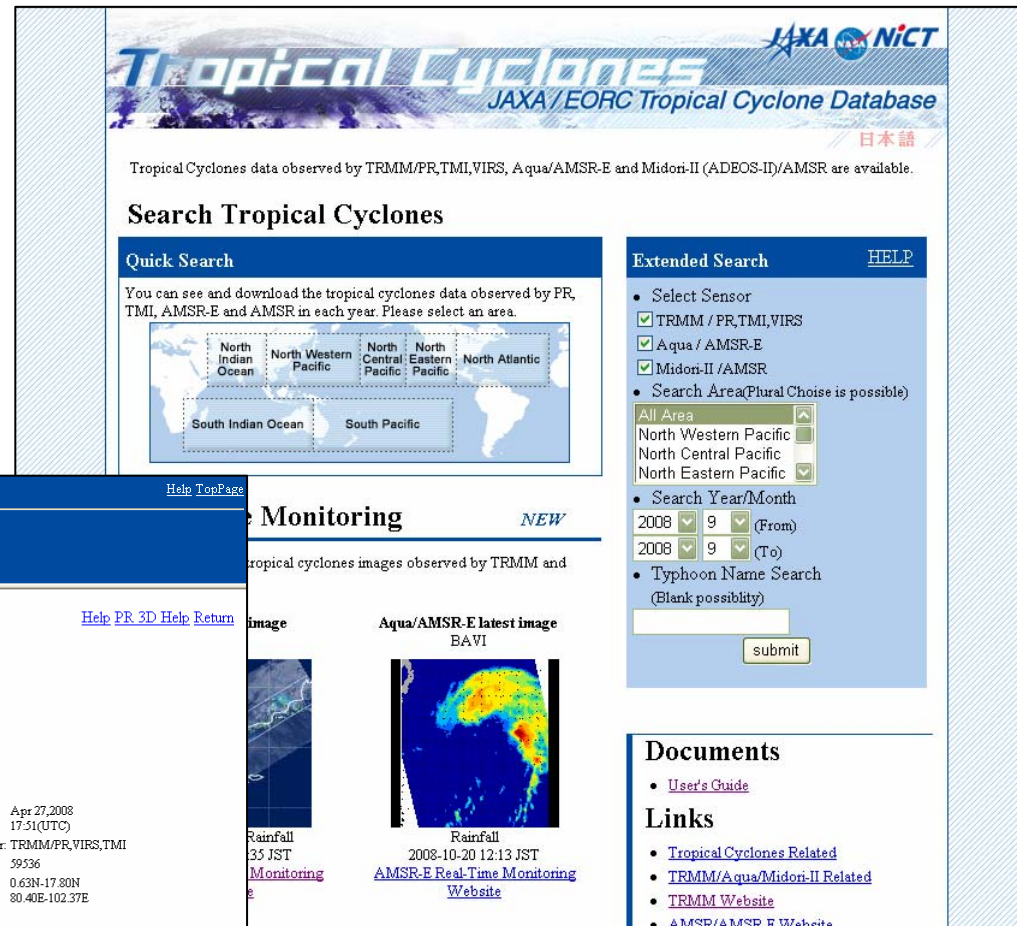


Data Processing for Standard Products (TRMM/PR as example)



JAXA/EORC Tropical Cyclone Database

- Browse images, **3D movies** and data of tropical cyclones observed by TRMM, AMSR-E, AMSR are available.
- Updated 1-1.5 months after observation.



Tropical Cyclones
 JAXA/EORC Tropical Cyclone Database
 日本語

Tropical Cyclones data observed by TRMM/PR,TMI,VIRS, Aqua/AMSR-E and Midori-II (ADEOS-II)/AMSR are available.

Search Tropical Cyclones

Quick Search

You can see and download the tropical cyclones data observed by PR, TMI, AMSR-E and AMSR in each year. Please select an area.

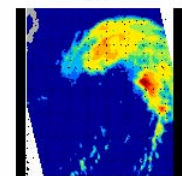
North Indian Ocean
 North Western Pacific
 North Central Pacific
 North Eastern Pacific
 North Atlantic
 South Indian Ocean
 South Pacific

Extended Search [HELP](#)

- Select Sensor
 - TRMM / PR,TMI,VIRS
 - Aqua / AMSR-E
 - Midori-II /AMSR
- Search Area(Plural Choise is possible)
 - All Area
 - North Western Pacific
 - North Central Pacific
 - North Eastern Pacific
- Search Year/Month
 - 2008 (From)
 - 2008 (To)
- Typhoon Name Search (Blank possibility)

Monitoring *NEW*

Tropical cyclones images observed by TRMM and Aqua/AMSR-E latest image

 Rainfall 05 JST Monitoring
 Aqua/AMSR-E latest image BAVI
 Rainfall 2008-10-20 12:13 JST
[AMSR-E Real-Time Monitoring Website](#)

Documents

- [User's Guide](#)

Links

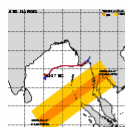
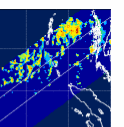
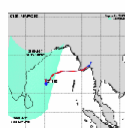
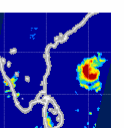
- [Tropical Cyclones Related](#)
- [TRMM/Aqua/Midori-II Related](#)
- [TRMM Website](#)
- [AMSR/AMSR-E Website](#)

Typhoon search [Help](#) [TopPage](#)

Area: Year:

Tropical Cyclone NARGIS(01B)

[Track Chart\(JPEG, 500x500\)](#)
 Period : Apr 27,2008 - May 03,2008
 Region :North Indian Ocean
 Maximum Sustained Winds : 115kt (Category 4)
 Number of TRMM/PR,TMI,VIRS Observation : 7
 Number of Aqua/AMSR-E Observation : 7
 Number of Midori-II/AMSR Observation : 0

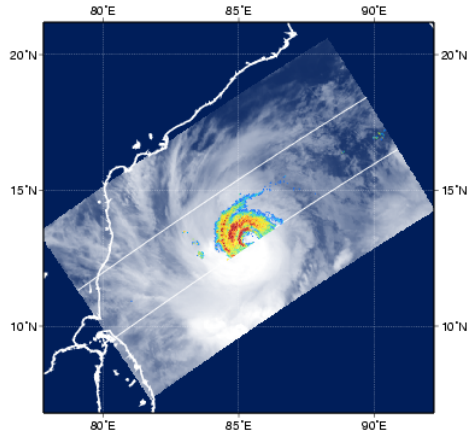
Observation Area	PR 3D	PR/VIRS Image	TMI/AMSR/AMSR-E Precipitation	Water Vapor
				No Data
	No Data	No Data		No Data

Date/Time: Apr 27,2008 17:51(UTC)
 Satellite/Sensor: TRMM/PR,VIRS,TMI
 Orbit Number: 39536
 Lat/Lon: 0.63N-17.80N 80.40E-102.37E
 Download: [1B01\(V6\)](#) [1B11\(V6\)](#) [2A12\(V6\)](#) [2A23\(V6\)](#) [2A25\(V6\)](#)

Date/Time: Apr 27,2008 20:17(UTC)
 Satellite/Sensor: Aqua/AMSR-E
 Path Number: 14244

http://sharaku.eorc.jaxa.jp/TYP_DB/index_e.shtml

Example of Tropical Cyclone Database

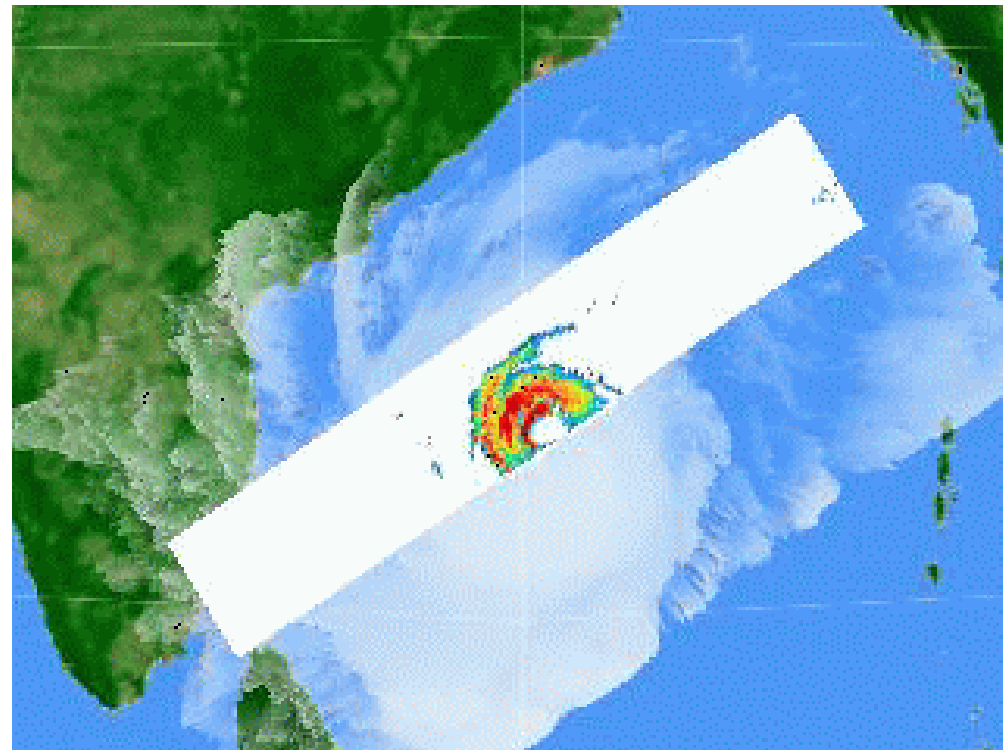
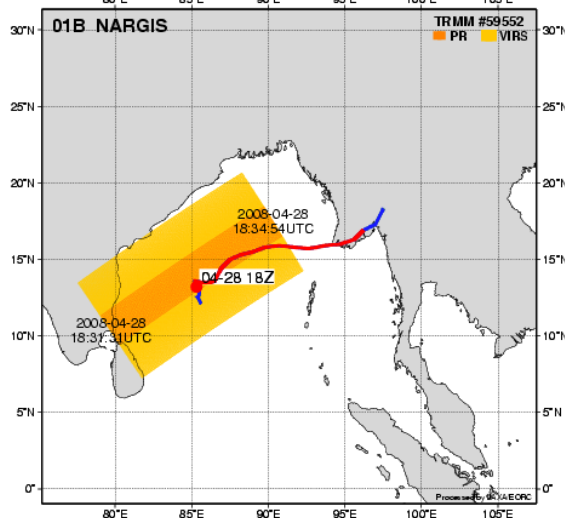


NARGIS (01B) Rainfall Rate by TRMM/PR
 2008-04-28 18:33 (UTC) Orbit Number 59552
 2A25.080428.59552.6.01B.NARGIS.HDF (Ver.6)
 Rainfall Rate [mm/hr]
 Cloud Image : VIRS (IR)

TRMM/PR 3D Observation of the cyclone attack in Myanmar

Date/Time: Apr 28, 2008 18:33(UTC)
 Satellite/Sensor: TRMM/PR, VIRS
 Lat/Lon: 8.20N-18.84N, 79.66E-90.30E

Track Chart and Observation Area





TRMM Tropical Cyclone Real-Time Monitoring

- Global regions (Asia, Americas, Oceania)
- Operating in near-real time (3-6 hours after observation)
- Browse images of PR, TMI and storm tracks are available

Tropical Cyclones TRMM Real-Time Monitoring

Top 日本語

Information Last up date : Oct. 22, '08 10:0Z

The TRMM real-time monitoring for tropical cyclones is now available. The coverage expands to the global area. (March 26, 2007)

Links

Tropical Cyclones Database

You can access to online archive of images, movies and data of tropical cyclones observed by TRMM/Aqua/Midori-II satellites.

AMSRE Typhoon Real-Time Monitoring

Japanese version only.

Last Two Months

Asia

Show All Typhoons

Show Active Typhoons

America

Show All Typhoons

Show Active Typhoons

Oceania

Show All Typhoons

Show Active Typhoons

Image

PR/VIRS Image

TMI Image

Observation Area

Asia

03B(THREE)

Satellite Obs.

- Date/Time : Oct. 22, '08, 0335Z
- Lat/Lon : 8.4N-21.5N, 44.7E-58.8E

Info. (Oct. 22, '08, 0000Z)

- Pressure : - hPa
- Winds : 30 kt

TRMM Real-Time Monitoring for Tropical Cyclones

Asia

Top > Asia 日本語

Last Two Months Last up date : Oct. 22, '08 10:0Z

» 03B(THREE)	Oct. 20 -	» 18W(HAGUPIT_T0814)	Sep. 18 -Sep. 24
» 14W(FOURTEEN)	Aug. 26 -Aug. 28	» 19W(JANGMI_T0815)	Sep. 23 -Sep. 30
» 15W(SINLAKU_T0813)	Sep. 8 -Sep. 20	» 20W(MEKKHALA_T0816)	Sep. 28 -Sep. 30
» 16W(SIXTEEN)	Sep. 10 -Sep. 11	» 21W(HIGOS_T0817)	Sep. 30 -Oct. 4
		» 22W(TWENTYTWO)	Oct. 14 -Oct. 15
		» 23W(BAVI_T0818)	Oct. 19 -Oct. 20

Recent Images

PR/VIRS Image

TMI Image

Observation Area

03B(THREE)

Satellite Obs.

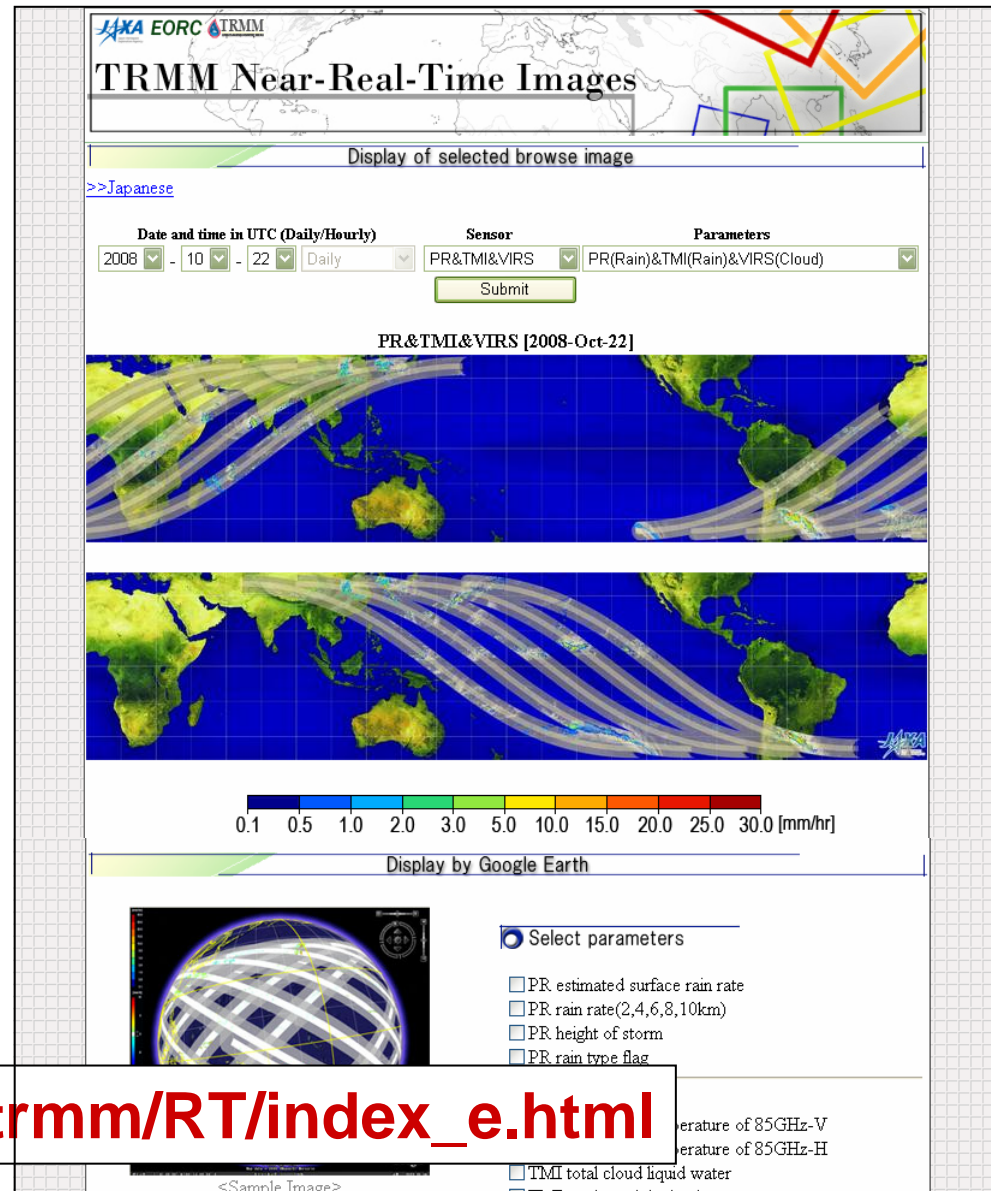
- Date/Time : Oct. 22, '08, 0335Z
- Lat/Lon : 8.4N-21.5N, 44.7E-58.8E

Info. (Oct. 22, '08, 0000Z)

- Pressure : - hPa
- Winds : 30 kt

TRMM Near Real Time Images

- Operational from Feb. 2008
- Visualize TRMM near-real time data 3-6 hours after observation
- Easy browsing, easy selection of dates and parameters. Displaying user selected regions with zoom-up and down
- Overlaying multi-parameters.
- Displaying by Google Earth.



TRMM Near-Real-Time Images
 Display of selected browse image
 >>Japanese

Date and time in UTC (Daily/Hourly): 2008 - 10 - 22 Daily
 Sensor: PR&TMI&VIRS
 Parameters: PR(Rain)&TMI(Rain)&VIRS(Cloud)
 Submit

PR&TMI&VIRS [2008-Oct-22]

0.1 0.5 1.0 2.0 3.0 5.0 10.0 15.0 20.0 25.0 30.0 [mm/hr]

Display by Google Earth

Select parameters

- PR estimated surface rain rate
- PR rain rate(2,4,6,8,10km)
- PR height of storm
- PR rain type flag
- TMI total cloud liquid water

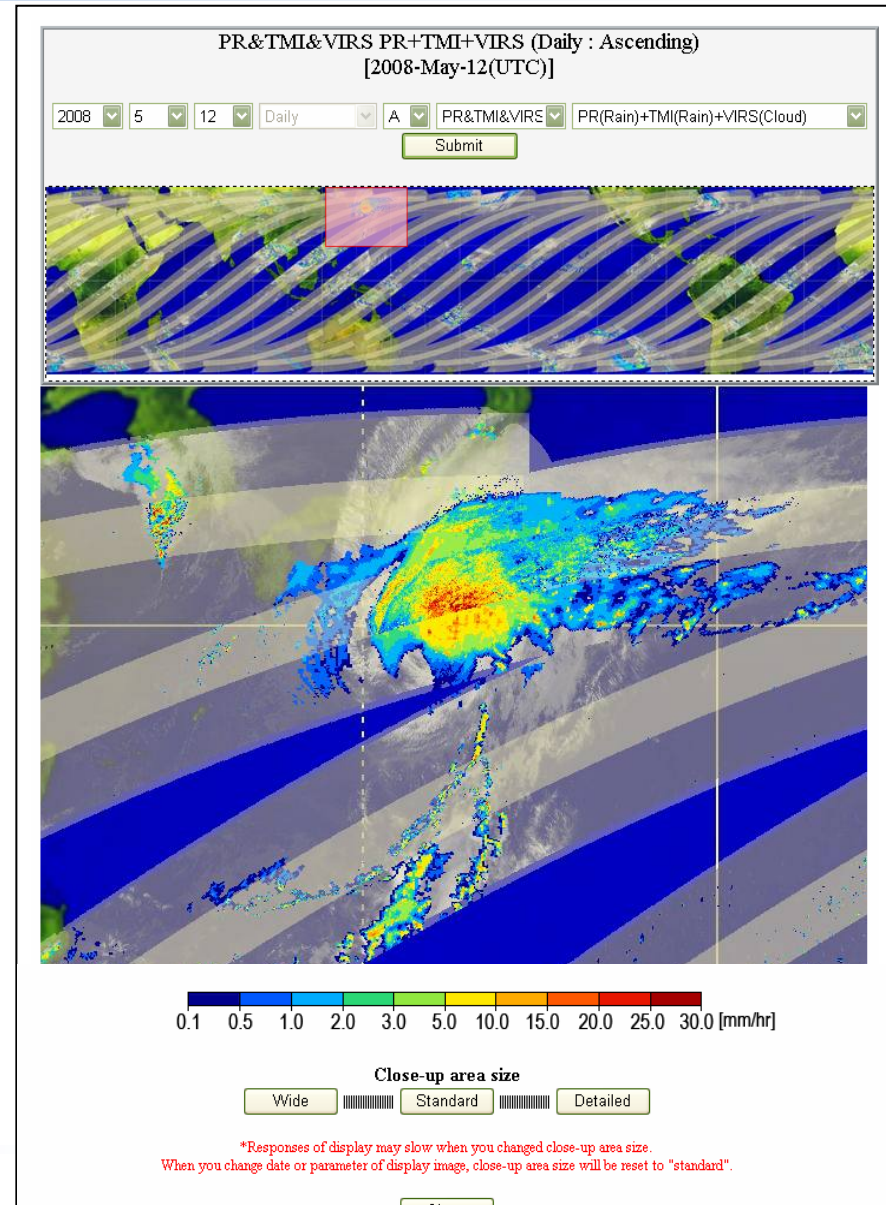
temperature of 85GHz-V
 temperature of 85GHz-H

<Sample Image>

http://sharaku.eorc.jaxa.jp/trmm/RT/index_e.html

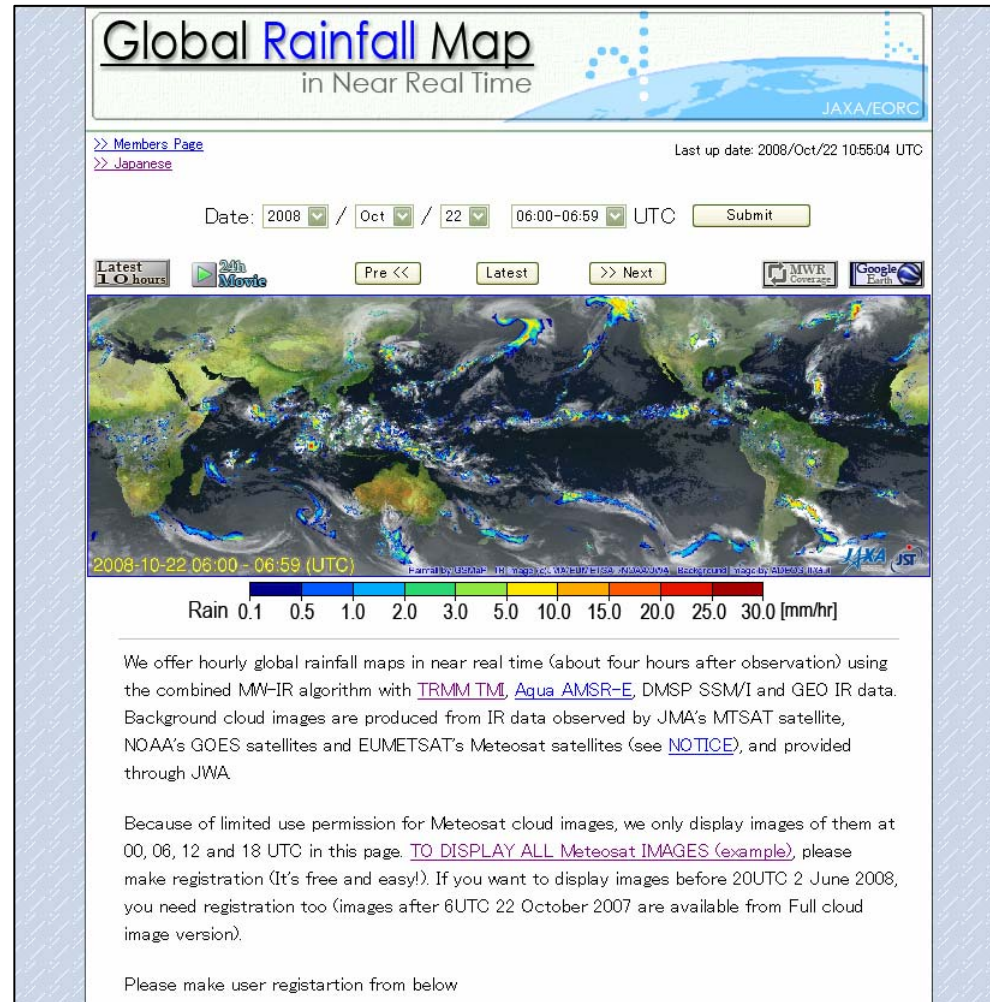
TRMM Near Real Time Images (cont.)

- Data are averaged in 0.05-degree lat/lon grid for each orbit
- Standard products
 - PR surface rainfall
 - PR 20-layer rain rate (2,4,6,8,10km)
 - PR storm height
 - PR rain type
 - TMI surface rainfall
 - TMI brightness temperature for 85GHz-V/H
 - TMI total cloud water content
 - TMI total cloud ice content
 - VIRS IR channel
- Reference images
 - TMI-PR differences
 - PR(rain) + TMI (rain) + VIRS(cloud)
 - PR(rain) + VIRS(cloud)
- Research products
 - will be added. (e.g., TMI SST, VIRS SST, etc.)



Global Rainfall Map in Near Real Time

- Displaying global rainfall map merging TRMM, AMSR-E and other satellite information
- Available 4-hr after observation
- Browse images, 24-hr animation, displaying by Google Earth
- 0.1-degree lat/lon grid, hourly products
- Data are also available via password protected ftp site
- Based on JST/CREST GSMaP algorithm



Global Rainfall Map
in Near Real Time
JAXA/EORC

>> [Members Page](#) Last up date: 2008/Oct/22 10:55:04 UTC
>> [Japanese](#)

Date: 2008 / Oct / 22 06:00-06:59 UTC

Latest 10 hours 24h Movie Pre << Latest >> Next

2008-10-22 06:00 - 06:59 (UTC)

Rain 0.1 0.5 1.0 2.0 3.0 5.0 10.0 15.0 20.0 25.0 30.0 [mm/hr]

We offer hourly global rainfall maps in near real time (about four hours after observation) using the combined MW-IR algorithm with [TRMM TMI](#), [Aqua AMSR-E](#), DMSP SSM/I and GEO IR data. Background cloud images are produced from IR data observed by JMA's MTSAT satellite, NOAA's GOES satellites and EUMETSAT's Meteosat satellites (see [NOTICE](#)), and provided through JWA.

Because of limited use permission for Meteosat cloud images, we only display images of them at 00, 06, 12 and 18 UTC in this page. [TO DISPLAY ALL Meteosat IMAGES \(example\)](#), please make registration (It's free and easy!). If you want to display images before 20UTC 2 June 2008, you need registration too (images after 6UTC 22 October 2007 are available from Full cloud image version).

Please make user registration from below

<http://sharaku.eorc.jaxa.jp/GSMaP/>

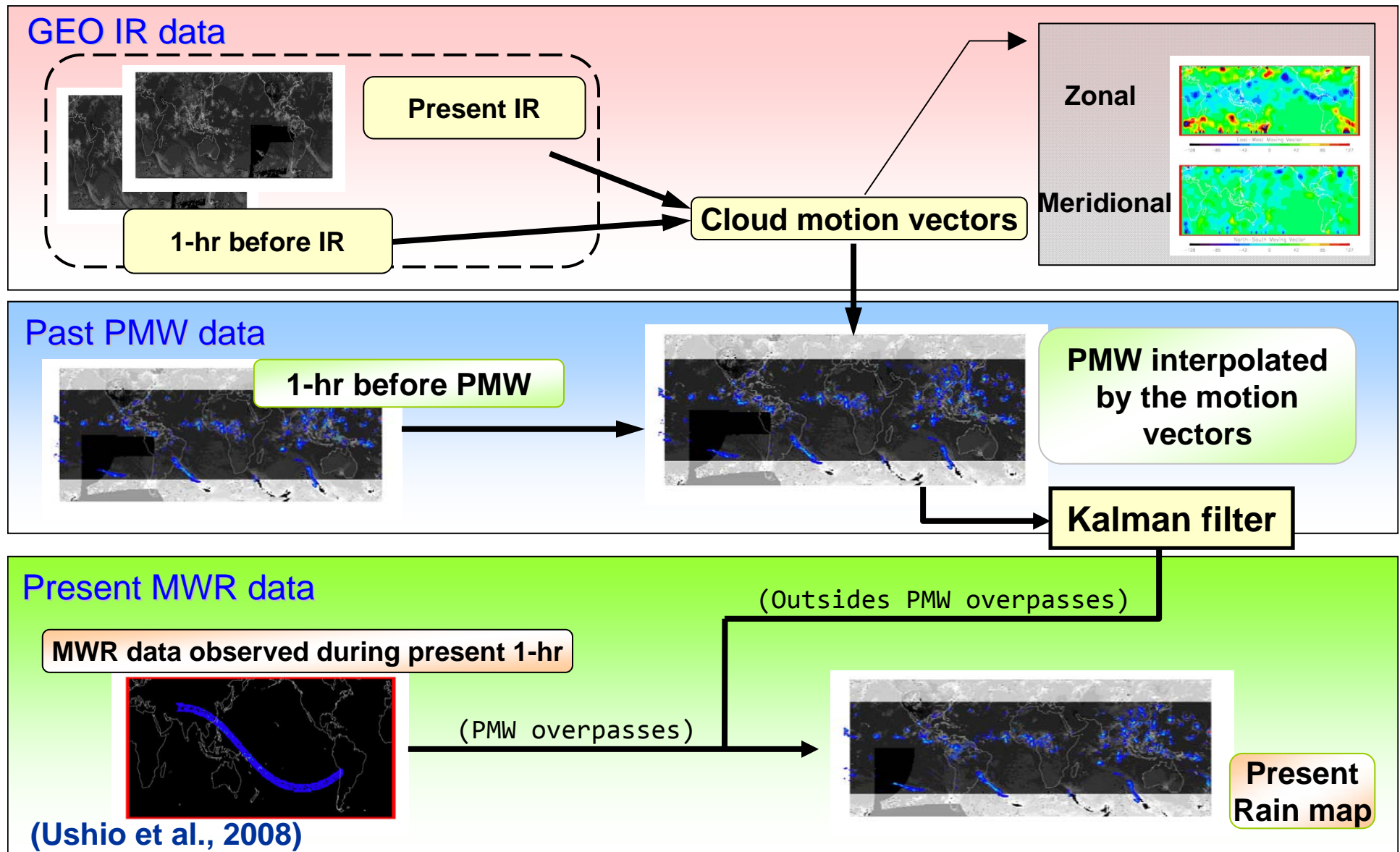


Global Satellite Mapping of Precipitation (GSMaP)

- GSMaP team (Osaka-prefecture Univ., Osaka Univ., MRI, JAXA, NICT, more) funded by JST/CREST. **Details will be presented by Dr. Ushio.**
- Production of high precision and high resolution global precipitation map by using satellite-borne microwave radiometers.
 - Retrievals from microwave radiometers (TMI, AMSR-E, AMSR, SSM/Ix3)
 - Utilization of precipitation radar, GEO's visible and IR radiometers
- Combination of the moving vector (Joyce et al., 2004) and Kalman filtering method
 - The moving vector method was used in CMORPH
 - Advantage: MWR based approach (not Tb but cloud motion), Fast processing time
 - Disadvantage: Not include the developing and decaying process of precipitation
 - New Kalman filter approach
 - Refine precipitation rate on Kalman gain after propagating the rain pixel
 - The Kalman gain is determined from the database on the relationship between the IR Tb and surface rain rate.
- Real time version is developed by JAXA.

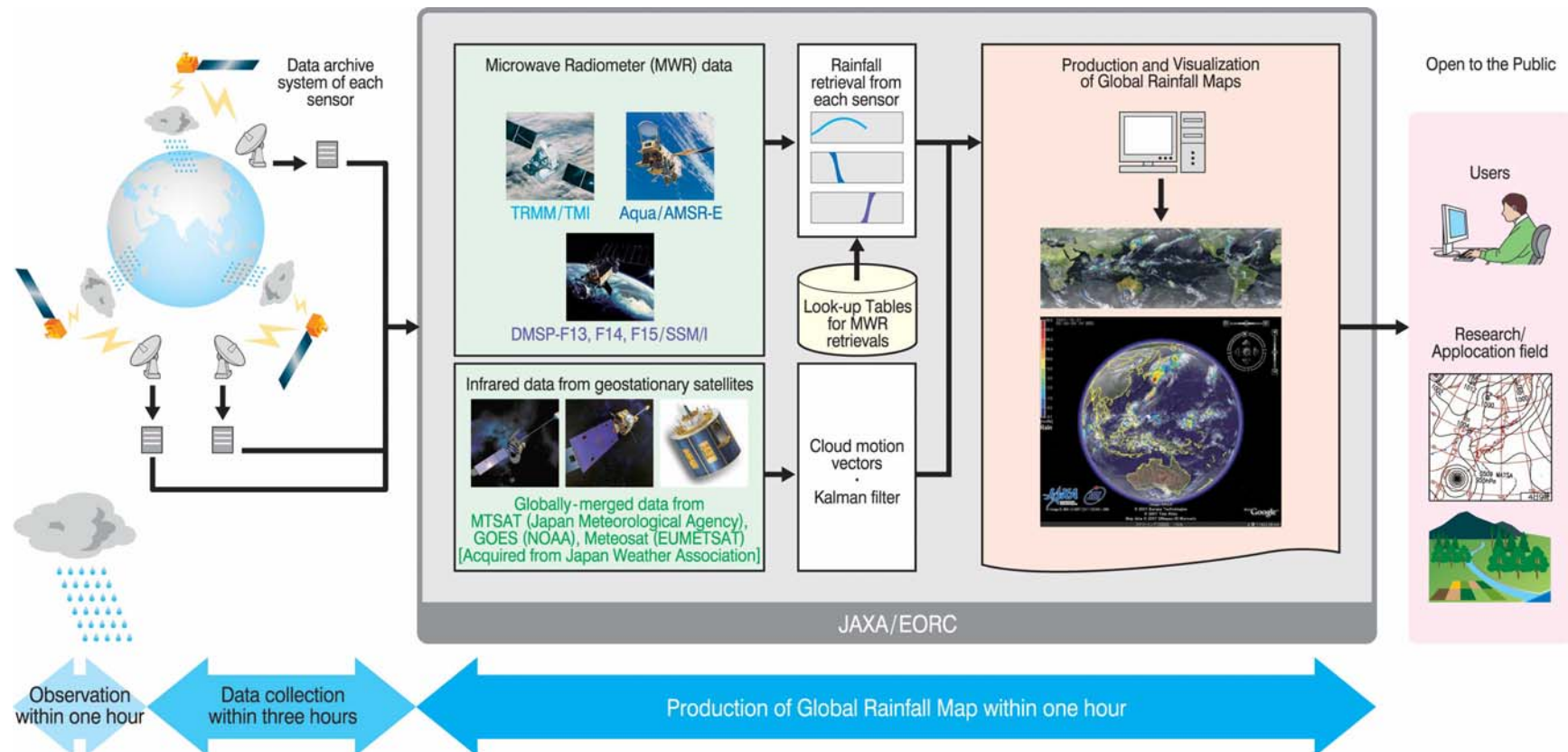


Flowchart of GSMaP algorithm



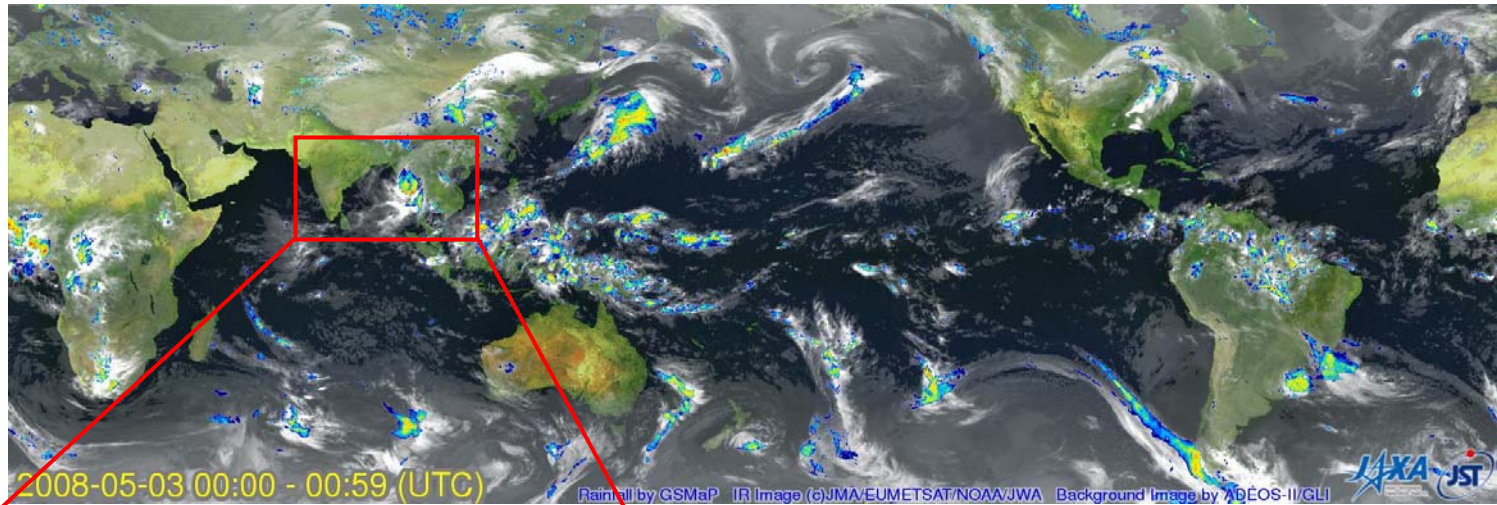
Processing Flow of GSMaP_NRT

- Observation data by microwave radiometer (MWR) and Geostationary satellite available within three hours from observation are utilized in the GSMaP_NRT system .
- These data are collected and processed at the system, and output products (rainfall) are delivered to users within four hours after observation.



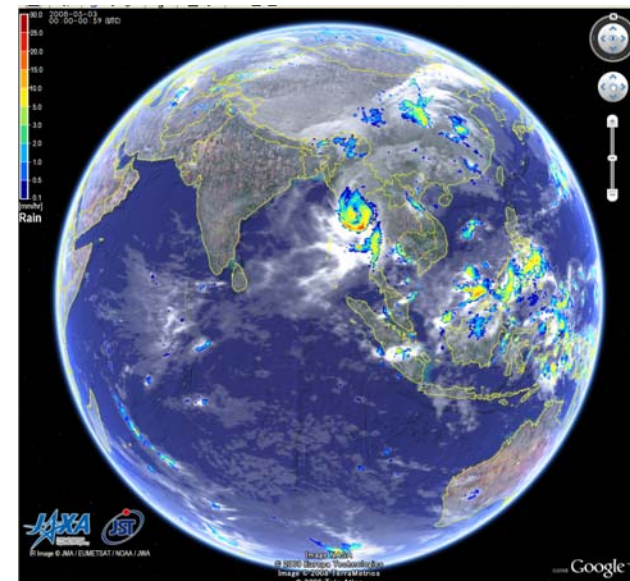
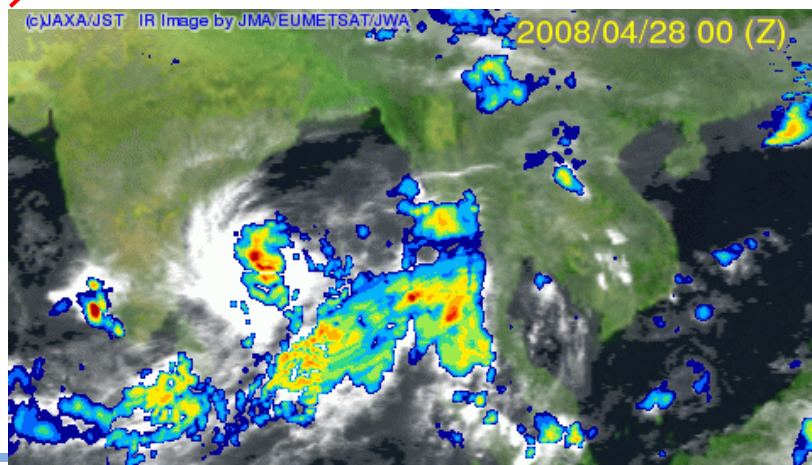


GSMaP_NRT observed cyclone attack in Myanmar (May 2008)

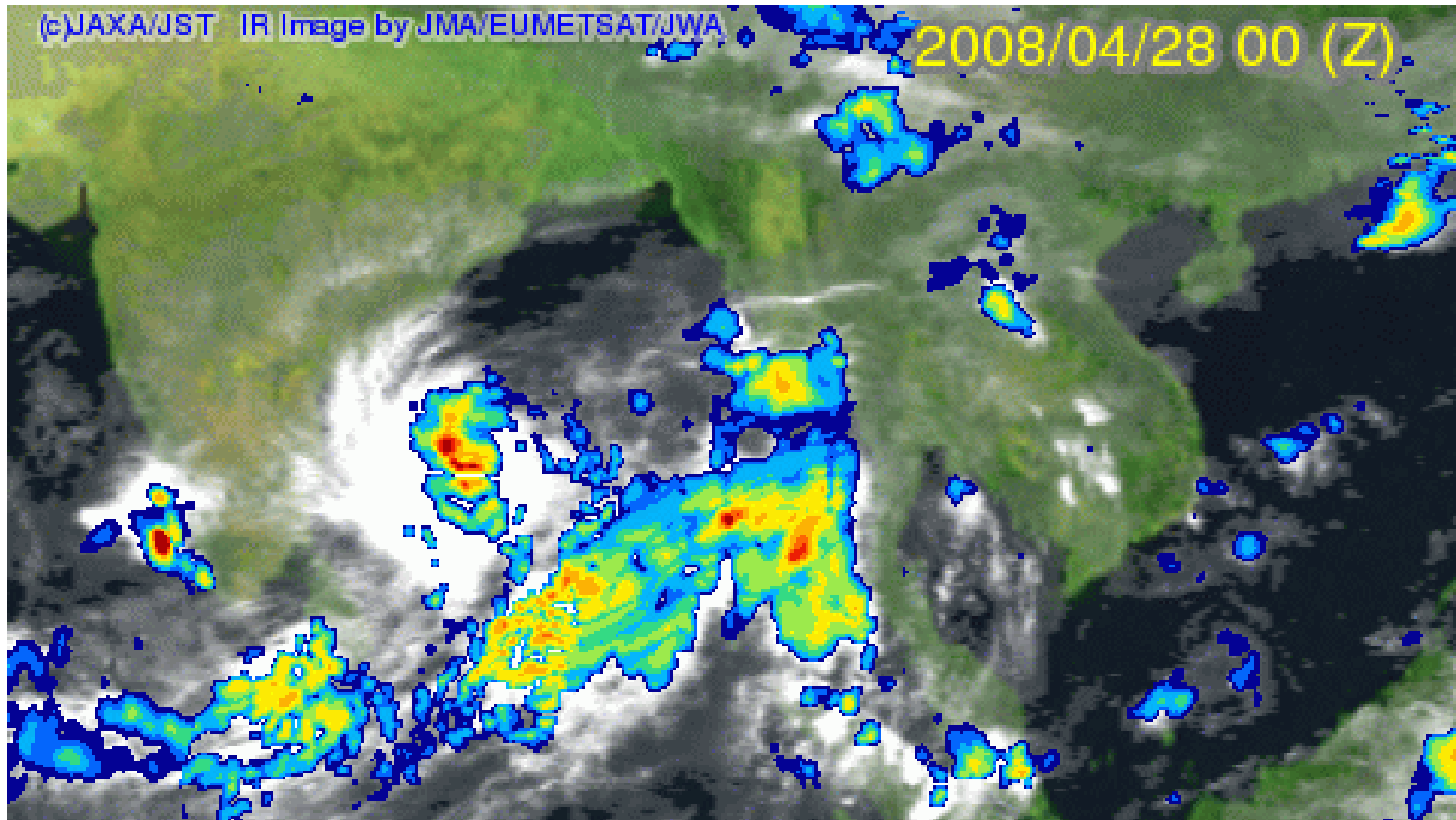


00Z
May 3,
2008

April 28~May 3



Animation of every 6 hours



April 28~May 4, 2008

Latent Heat Research Product

- Latent heating profile estimated by PR 3-D observation
- All data are available during PR observation period (updating every 1-month)
- Base on Spectral Latent Heating (SLH) algorithm (Shige et al., 2004, 2007, 2008)
- Orbital (non-grid, grid) and monthly data in 0.5-degree lat/lon grid are available

Latent Heat Research Product

Last Update : Oct. 08, 08

Data

- [L2 LH NonGrid \(Orbit, NoneGrid\)](#)
- [L2 LH Grid \(Orbit, Grid\)](#)
- [L3 LH \(Month, Grid\)](#)
- [Product Explanation](#)
- [Sample Program](#)
- [Papers](#)

User Registration

I inform it of a version change, the data update situation to the FTP site and maintenance information by an email when I have you do user's registration. User registration form is [here](#).

What's New

Oct. 08, 2008
Upload data of Sep. 2008

Sep. 10, 2008
Our Web and ftp systems will not be available from 10:00(JST), Sep. 25 to 14:00(JST), Sep. 25 due to our facility maintenance. We apologize for any inconvenience.

Sep. 10, 2008
We've carried out renewal of this website.

Sep. 09, 2008

About This Web Site

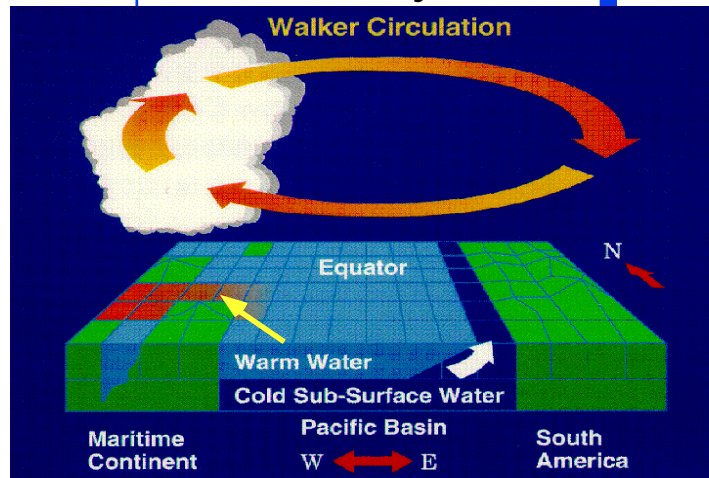
The latent heat research product is based on the Spectral Latent Heating (SLH) algorithm (Shige, Takayabu et al., 2004, 2007). The algorithm uses TRMM PR information (convective/stratiform classification, precipitation top height (PTH), precipitation rates at the surface, melting level, etc.) to retrieve heating profiles utilizing lookup tables. Heating profile lookup tables for the three rain types - convective, shallow stratiform, and anvil rain (deep stratiform with a melting level) - were derived from numerical simulations of tropical clouds utilizing a cloud-resolving model (CRM). For convective and shallow stratiform regions, the lookup table is based on the PTH. However, PR cannot observe PTH accurately enough for the anvil regions because of its insensitivity to the small ice-phase hydrometeors. Thus, for the anvil region, the lookup table refers to the precipitation rate at the melting level instead of PTH. (Please refer to [papers](#) in detail.)

<http://www.eorc.jaxa.jp/TRMM/lh/index.html>

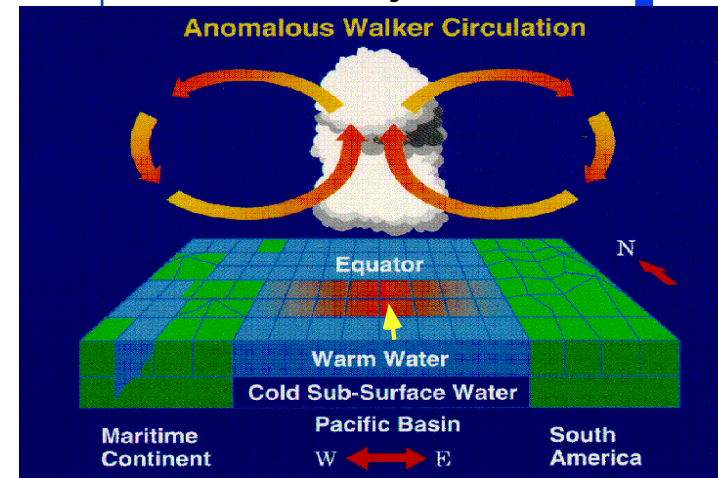
Atmospheric Circulation Dynamics

Tropical rainfall and atmospheric circulation

Atmospheric circulation
of normal years



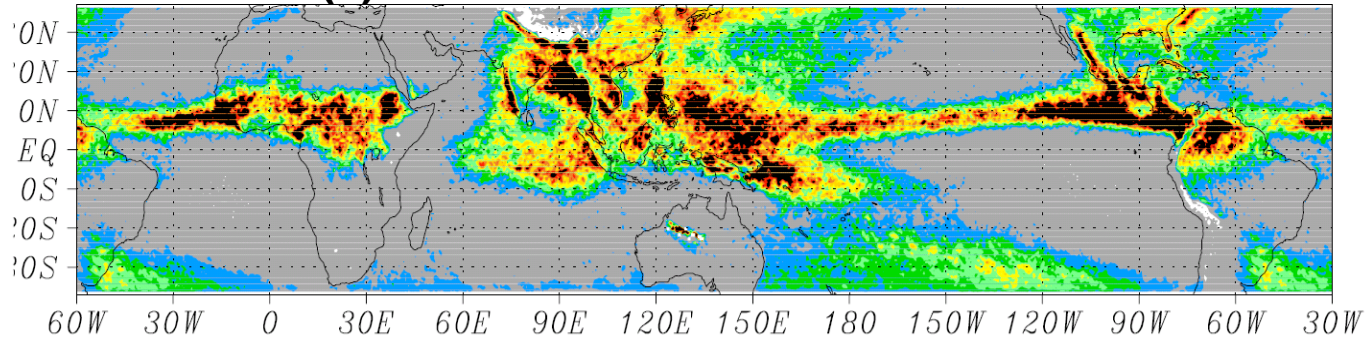
Atmospheric circulation of
El Niño years



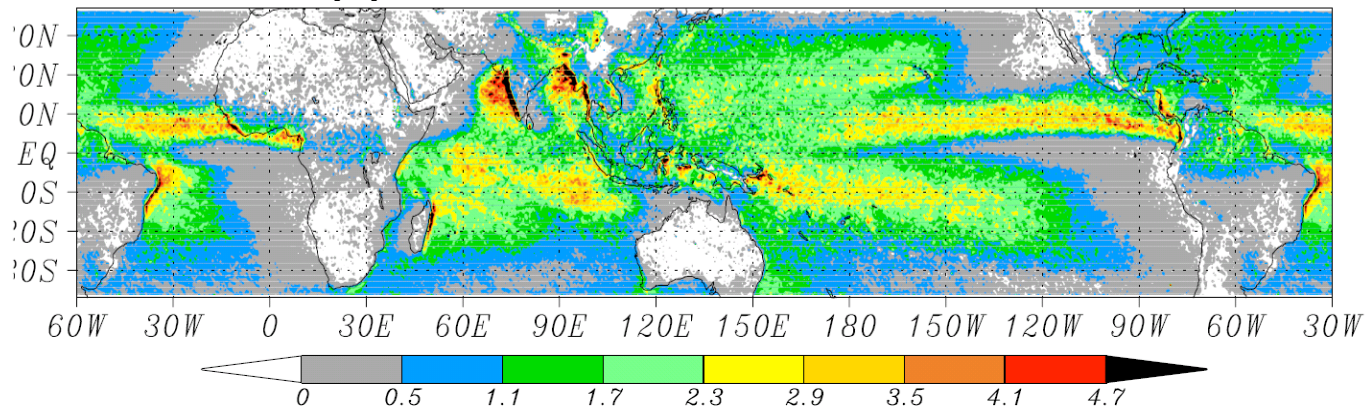
Tropical rainfall: Primary **“heat”** engine for the atmospheric circulation on the Earth. Its fixed quantitative observations are essential to the research on climate change and abnormal weather.

Latent heat observed by TRMM

(a) Latent heat at altitude of 7.5km



(b) Latent heat at altitude of 2km



(Shige, Takayabu, et al., 2004, 2007, 2008)

Latent heat distribution during December, January, and February using TRMM PR 3D data between 1998 and 2007. The data can be utilized for evaluation of global water & energy cycle and for improvement of climate models.



AMSR-E Level 3 Browse Images

- Displaying browse images of AMSR-E Level 3 (daily) products
 - brightness temperatures
 - water vapor
 - cloud liquid water
 - precipitation
 - sea surface wind
 - sea surface temperature
 - sea ice concentration
 - snow water equivalence
 - soil moisture

Level 3 ブラウズ画像 [Home]

Brightness Temperature 6GHz-V	AMSR	AMSR-E	Sea Surface Wind	AMSR	AMSR-E
Brightness Temperature 36GHz-V	AMSR	AMSR-E	Sea Surface Temperature	AMSR	AMSR-E
Brightness Temperature 89GHz-V	AMSR	AMSR-E	Sea Ice Concentration	AMSR	AMSR-E
Water Vapor	AMSR	AMSR-E	Snow Water Equivalence	AMSR	AMSR-E
Cloud Liquid Water	AMSR	AMSR-E	Soil Moisture	AMSR	AMSR-E
Precipitation	AMSR	AMSR-E			

Aqu AMSR-E 2008/10/20 Descending
Sea Surface Temperature (Shibata V5.1.1)

Aqu AMSR-E 2008/10/20 Descending
Water Vapor (Shibata V5.0.1)

Sea Surface Temperature AMSR-E

Another Browse Images

- Near Real Time Brightness Temperature/Radar AMeDAS (Around Japan)
- High Resolution Images
- Anomaly
- SSM / I (1987 - 1999)

Aqu AMSR-E 2008/10/20 Descending
Sea Ice Concentration (Shibata V5.1.1)

Sea Ice Concentration AMSR-E

Sorry, some products cannot be seen because of data deficit of 89GHz channel (receiver A).
Browse images processed at EORC are available on this page. EORC is doing test processing of geophysical products by using "research algorithms" in addition to the "standard algorithms" used in the Earth Observation Center (EOC). Therefore, you will find multiple images for some geophysical parameters. Through the algorithm inter-comparison, EORC is trying to improve the products in cooperation with the AMSR investigators.
Version numbers used in this page are defined for the EORC test processing, and are not identical to that of EOC official release version.

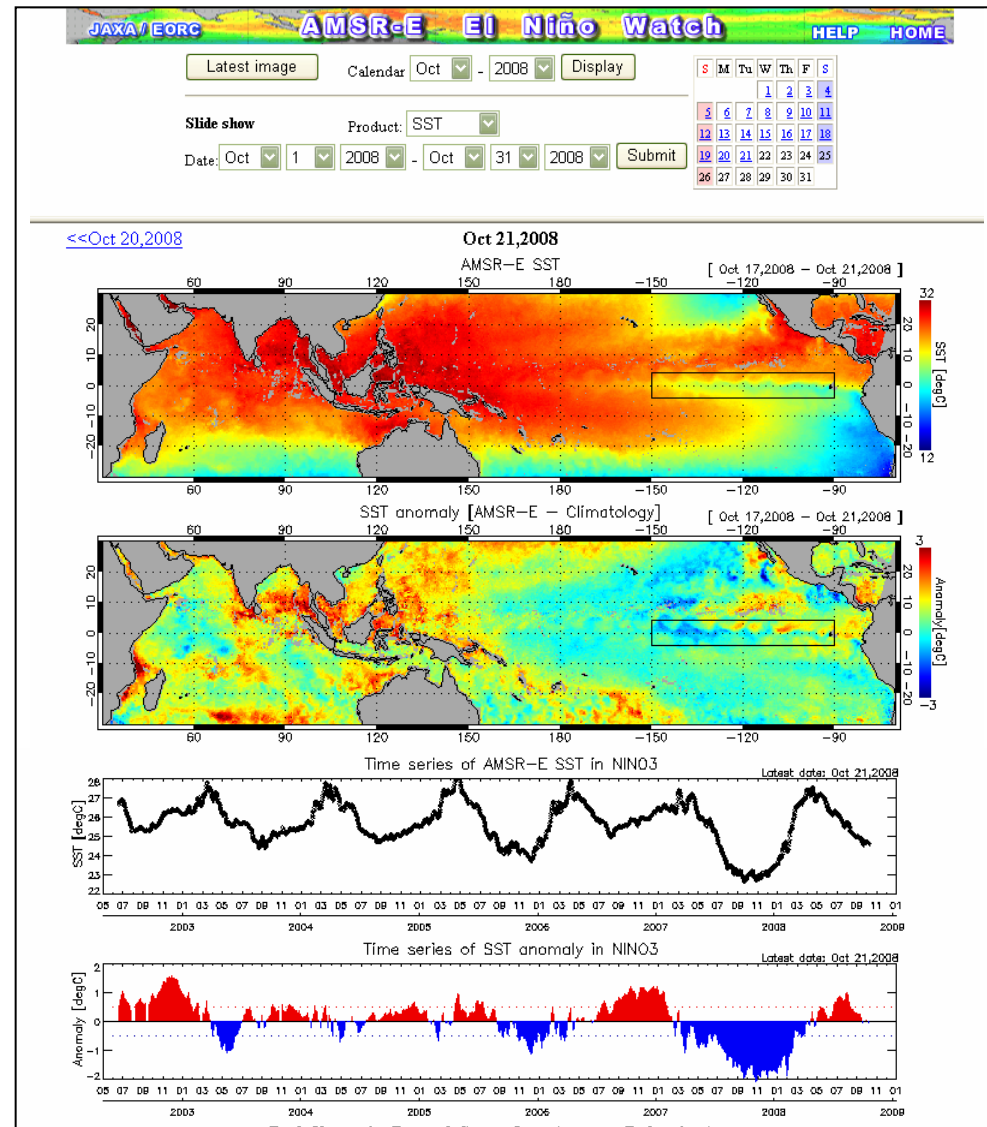
宇宙航空研究開発機構 地球観測研究センター
JAXA EORC Earth Observation Research Center
ALL RIGHTS RESERVED.

http://sharaku.eorc.jaxa.jp/cgi-bin/adeos2/amsl/l3brws/l3brws_top.cgi?lang=e



El Niño Watch

- Daily monitoring of sea surface temperature (SST) by AMSR-E and its anomaly from climatology (30-yr average) over the tropical Pacific region
- Images have archived since June 2002.



<http://sharaku.eorc.jaxa.jp/cgi-bin/amsr/elni2/elni2.cgi?lang=e>



Arctic Sea-Ice Monitor by AMSR-E

- Daily monitoring of Arctic sea-ice concentration by AMSR-E
- Images have archived since June 2002.
- Collaboration with International Arctic Research Center (IARC)

IARC-JAXA Information System

Home Welcome News Research Facilities Data For Users Links

Home > Arctic sea-ice monitor by AMSR-E

Arctic Sea-Ice Monitor by AMSR-E

Latest image | Calendar: | Slide show: [Oct 2008\(3.10MB\)>>](#)

Oct 21, 2008
AMSR-E Sea Ice Concentration 200810:1

Click the image to enlarge.

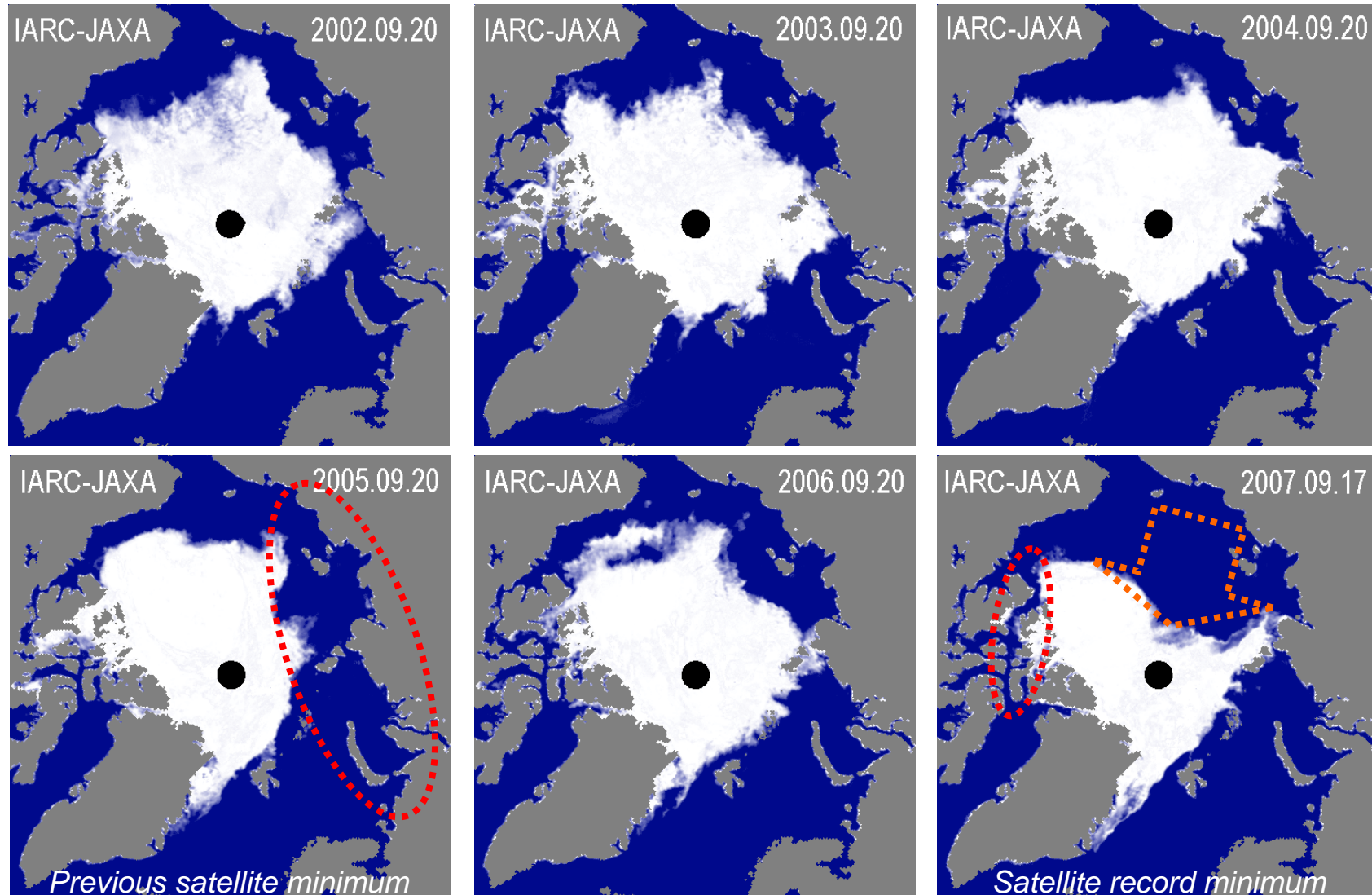
Powered by: Links: AMSR/AMSR-E Science Earth Observation Research Center (EORC/JAXA)

<http://www.ijis.iarc.uaf.edu/cgi-bin/seaice-monitor.cgi?lang=e>





Changes in AMSR-E sea ice extent

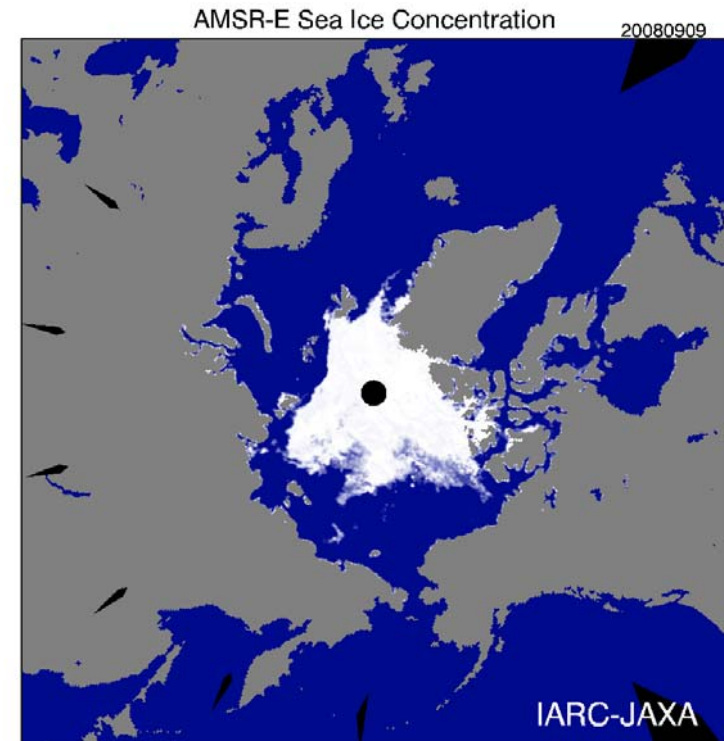
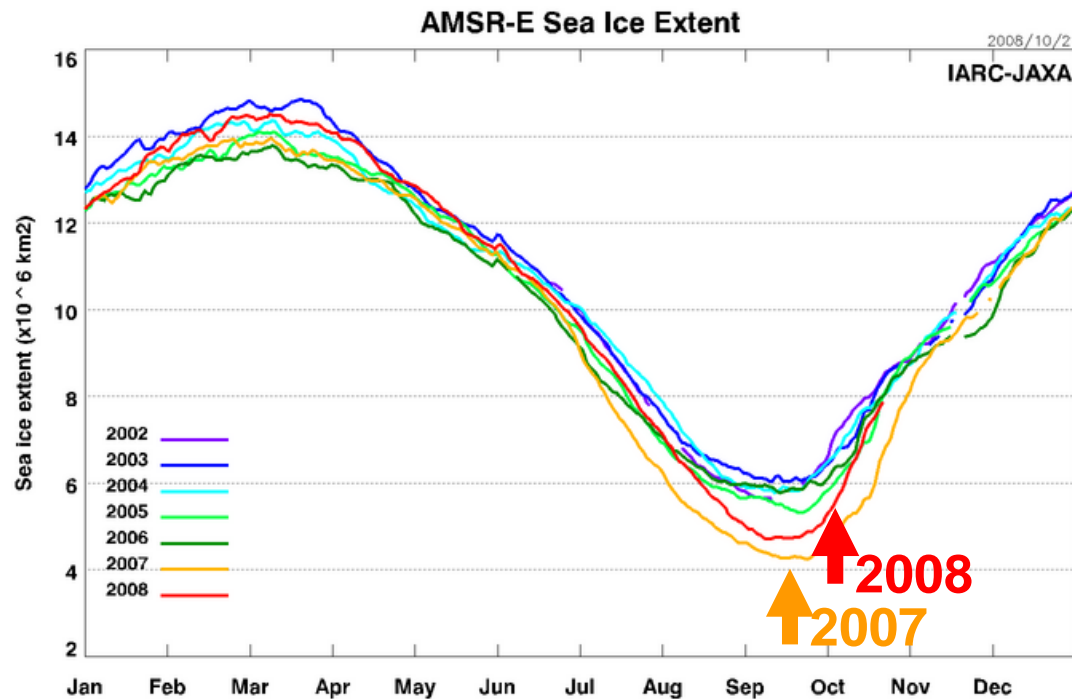


AMSR-E sea ice extent over northern polar region around September 20 of recent 6 years (2002-2007). Images are available at the Arctic Sea-Ice Monitor site maintained by the International Arctic Research Center (<http://www.ijis.iarc.uaf.edu/en/index.htm>).



Recent status of ice extent

Minimum ice extent of 2008: 470.8 km² (recorded at 9 Sep. 2008)

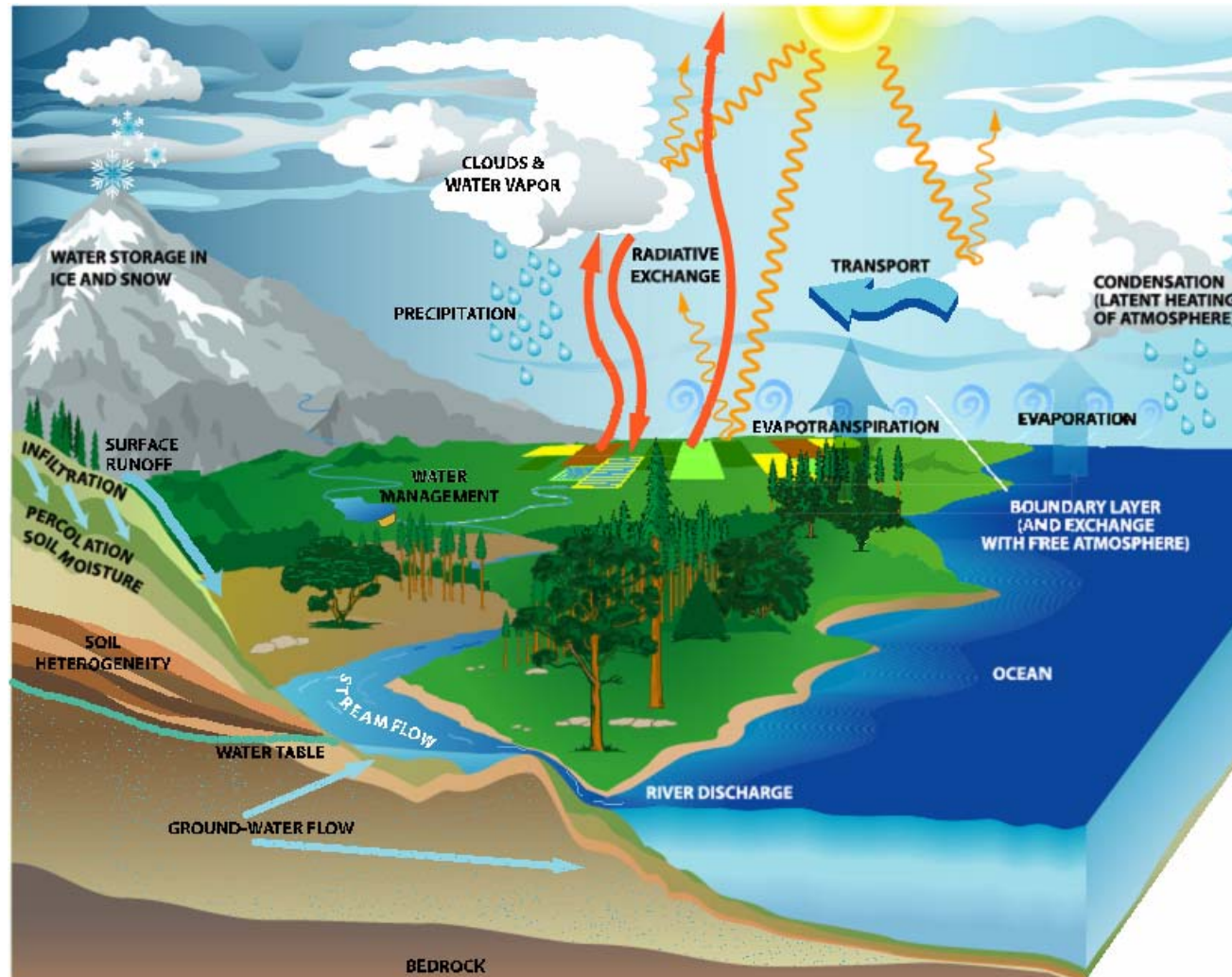


Time series of AMSR-E sea ice extent over Arctic Oceans. Daily updates are available at the Arctic Sea-Ice Monitor site maintained by the International Arctic Research Center (<http://www.ijis.iarc.uaf.edu/en/index.htm>).



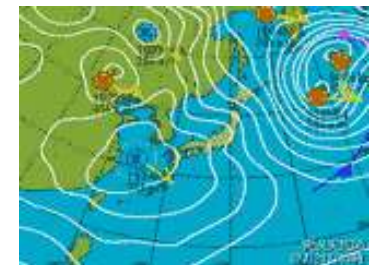


JAXA activities for hydrological applications



Rainfall Measurement and our life

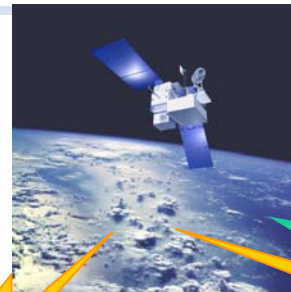
- Rain affects most everyone's life & work;
 - Food production; and
 - Flood and drought.
- Rain is a key variable in;
 - Weather prediction models;
 - Climate models; and
 - Air-sea interaction models, etc.
- Rain is one of hardest meteorological parameters to measure;
 - because of its spatial and temporal variability;
 - contribution by rainfall measuring satellites is highly expected; and
 - Appearance of TRMM satellite



Collaboration in Global Flood Alert System

(<http://www.internationalfloodnetwork.org>)

JAXA are collaborated with IFNet and UNESCO/ICHARM for improving satellite rainfall estimation for utilization in flood warning.



GPM
(Global Precipitation Measurement)

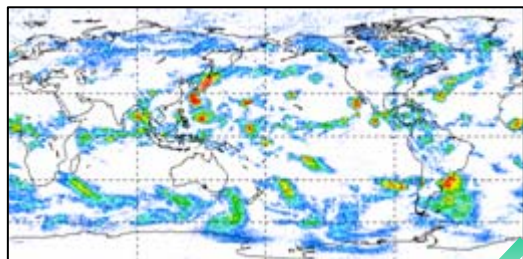
Raw Data

Precipitation Information around the Upstream



Ground Stations
(NASA, JAXA)

On-Line



Data Processing System (NASA, JAXA)
Real-time 3-hourly Precipitation Data

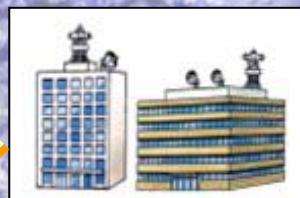
On-Line



Estimation of precipitation probability

Present Precipitation > Estimated Precipitation Probability

E-mail



Disaster Prevention Organizations of the concerned countries

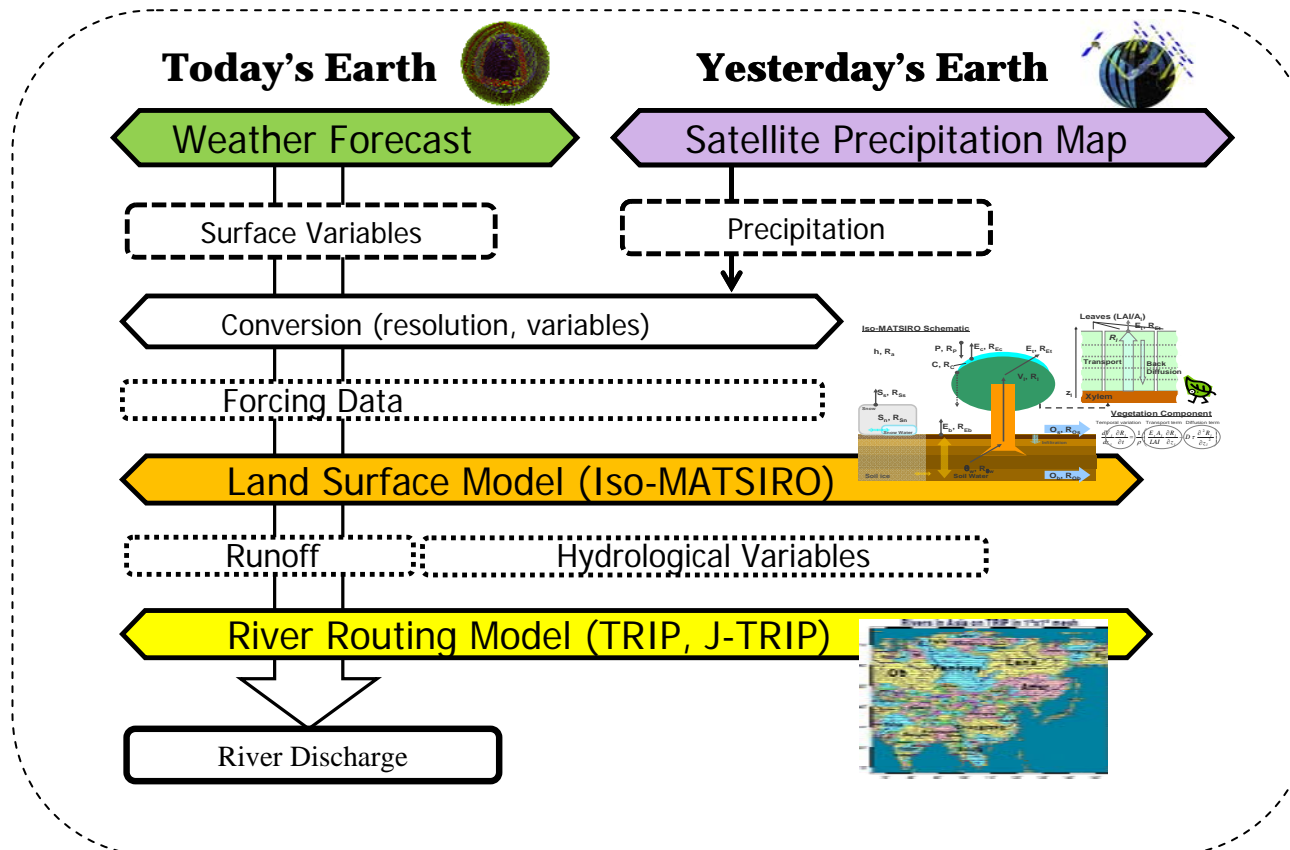
Flood Alert !



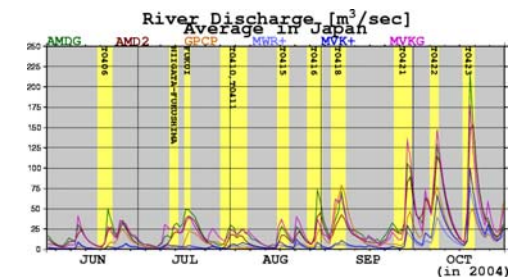
Collaboration with Univ. of Tokyo

Prof. Oki's group (Univ. of Tokyo) and JAXA are developing Global Land Data Assimilation System, which can provide information of river discharge

System flowchart of Prof. Oki's group

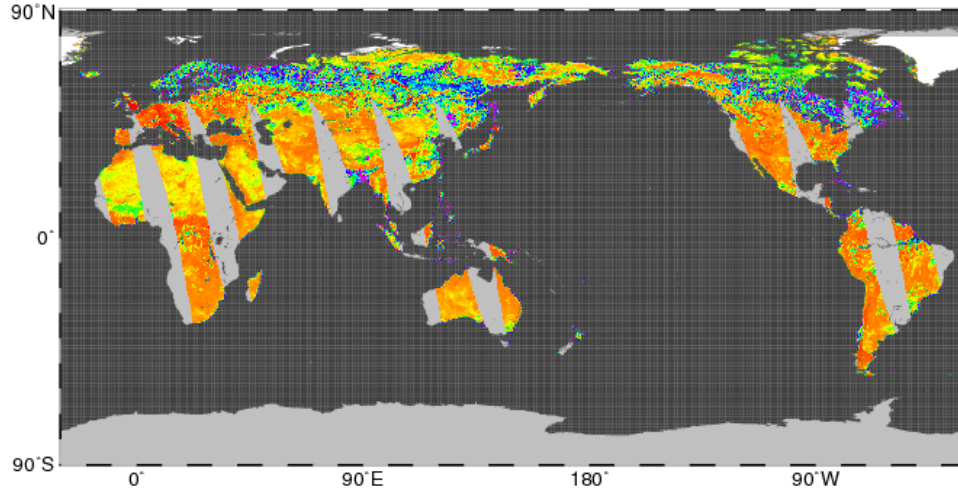


Initial results:
River Discharge
Daily time series, average
all over Japan

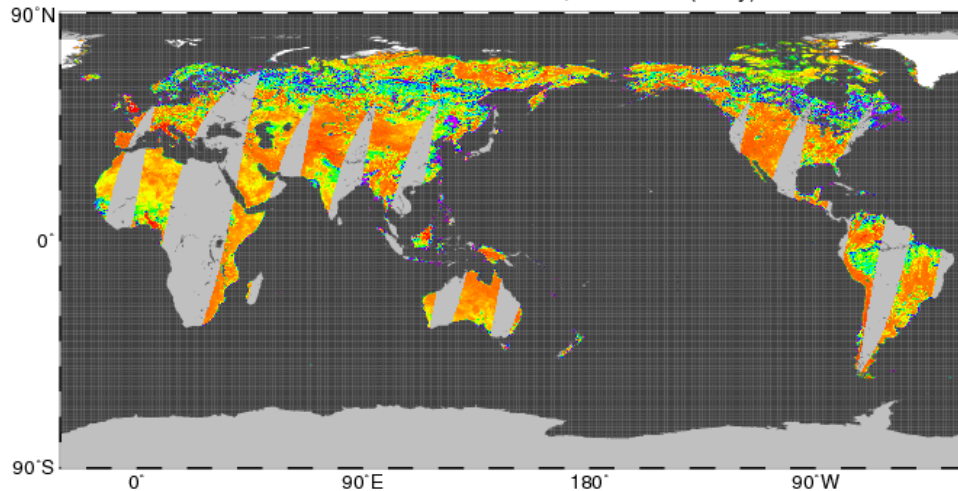


Results of Today's Earth

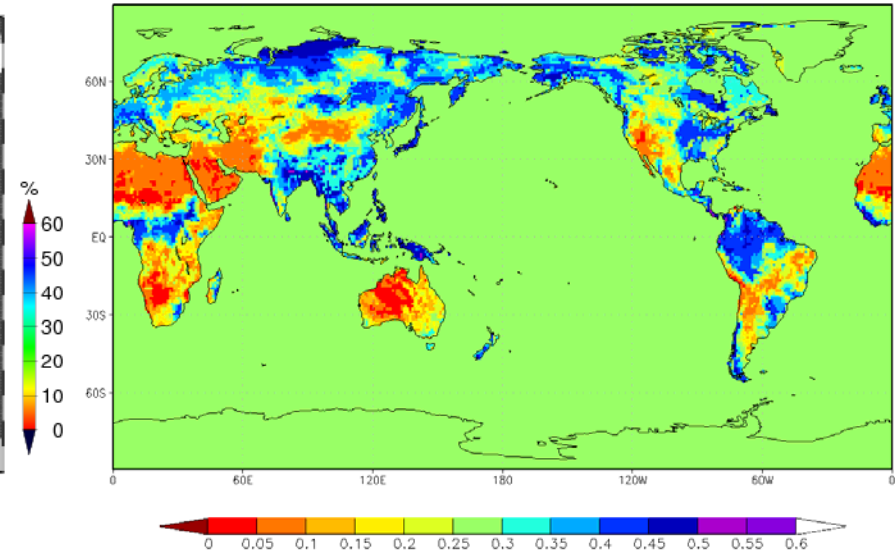
AQUA/AMSR-E SM Jul. 01, 2008 ASC (Daily)



AQUA/AMSR-E SM Jul. 01, 2008 DES (Daily)



5cm soil moisture [m**3/m**3]: 2008/07/01/00Z(INIT) 00-06Z



Left: AMSR-E soil moisture observation at 1 Jul. 2008 (by Dr. Fujii, JAXA)

Right: 5cm Soil moisture model results by Today's Earth

What is Sentinel Asia?

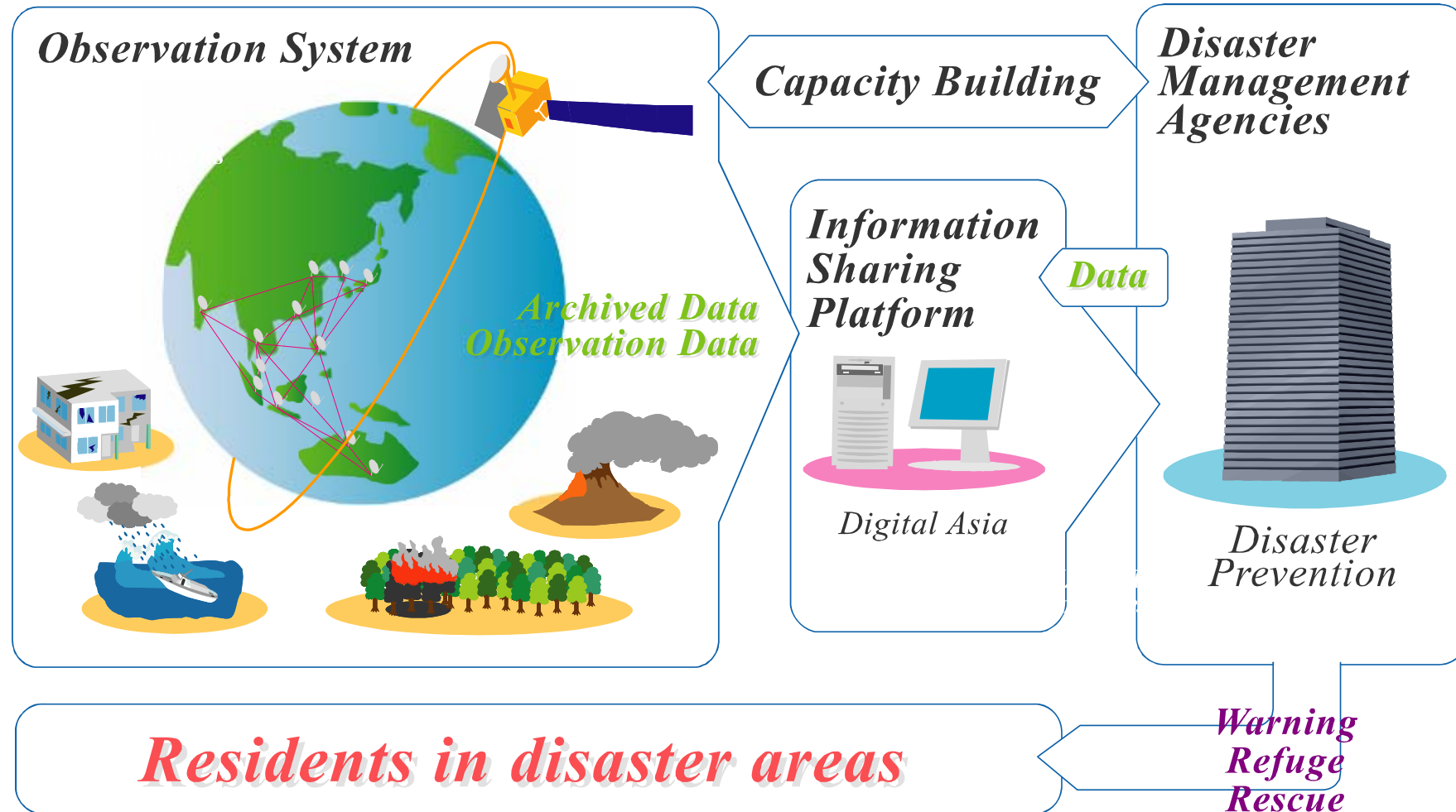
- Sentinel Asia is a "voluntary and best-efforts-basis initiatives" led by the APRSAF (Asia-Pacific Regional Space Agency Forum) to share disaster information in the Asia-Pacific region on the Digital Asia (Web-GIS) platform and to make the best use of earth observation satellites data for disaster management in the Asia-Pacific region.
- Sentinel Asia is to initially be an internet-based, node-distributed, information distribution backbone, eventually distributing relevant satellite and in-situ spatial information on multiple hazards in the Asia-Pacific region.



The screenshot shows the Sentinel Asia website interface. At the top, there is a green header with the text "Sentinel Asia" and "Disaster Management Support System in the Asia-Pacific Region". Below the header is a navigation menu with links for Home, About Sentinel Asia, JPT Members, Library, FAQ, and Contact Us. The main content area is titled "Welcome to Sentinel Asia Web Site" and contains several sections: "Emergency Observation", "Wildfire Monitoring", "Flood Monitoring", "MTSAT Imagery", "Capacity Building", "Web Forum", and "Emergency Observation Request". A "Current Topics" section lists several earthquake events in China from May 2008, with links to JAXA/EORC and SAR data. A footer note indicates the page was last updated on 06/03/2008 at 22:53:20.

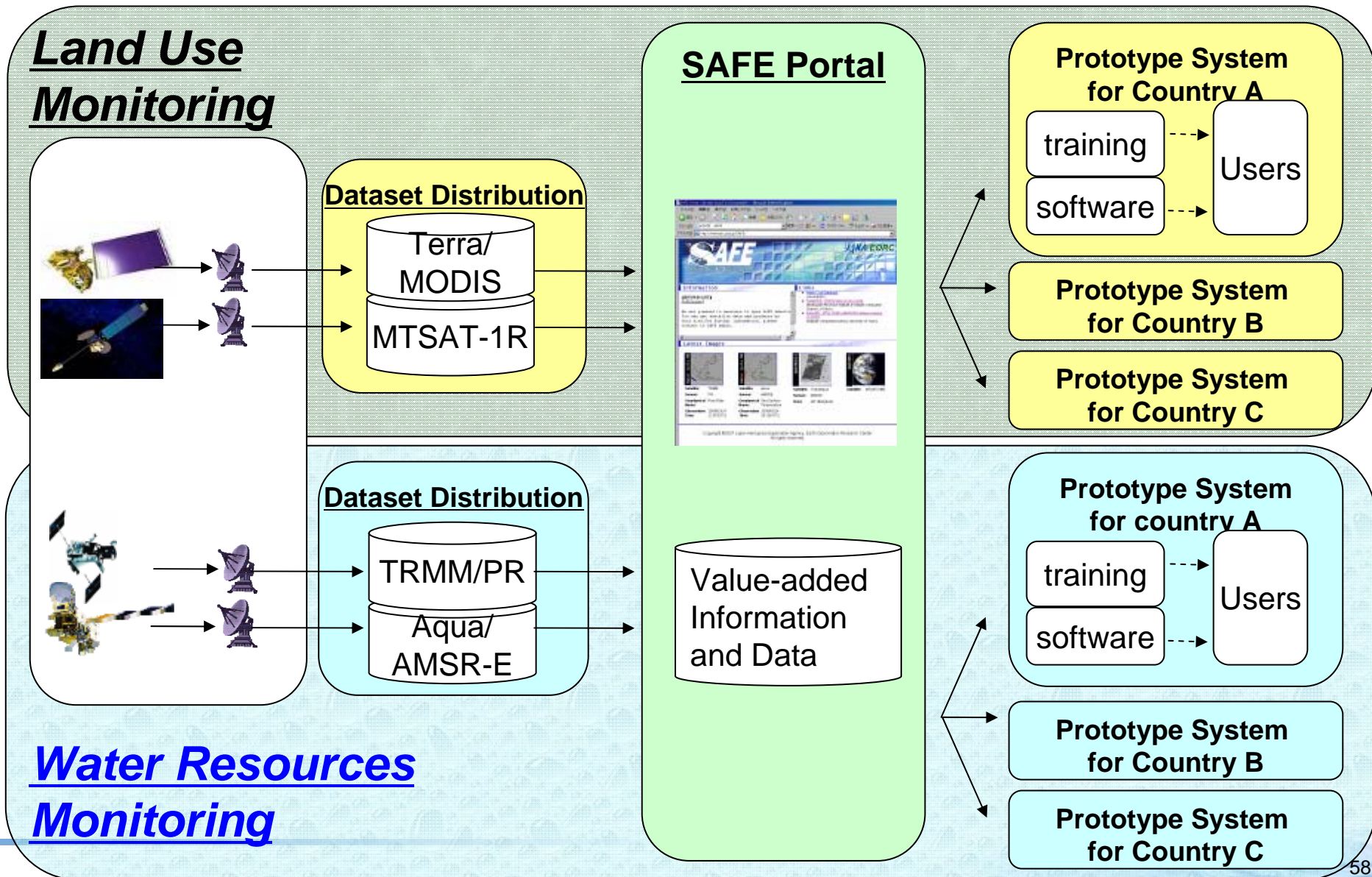
<http://dmss.tksc.jaxa.jp/sentinel/>

Overview of Sentinel Asia



Sentinel Asia For Environment (SAFE)

(expansion of Sentinel Asia)





Appendix

TRMM Online data (1)

- Standard Product
 - PR/TMI/VIRS Data
 - Earth Observation Data and Information System - JAXA/EORC
 - <https://www.eorc.jaxa.jp/iss/jsp/indexEn.html>
 - Need registration
 - DAAC (Goddard Distributed Active Archive Center) - NASA/GSFC
 - <http://lake.nascom.nasa.gov/data/dataset/TRMM/index.html>
 - LIS (Home Page/download data) - NASA/MSFC
 - <http://thunder.msfc.nasa.gov/>
- Subset Product
 - Level 3 Selected Monthly Rainfall Data Set - JAXA/EORC
 - http://www.eorc.nasda.go.jp/TRMM/imgdt/L3_data/index.htm
 - TRMM Specific Area Data Set - JAXA/EORC
 - http://www.eorc.jaxa.jp/TRMM/data/monitoring/TSD/gisp_e.htm
 - PR subset for Japan and GAME Area (1997.12-2000.9, 2004.4-2005.2)
- TRMM Gridded Rainfall Products (text) - NASA/GSFC/TSDIS
 - <ftp://trmmopen.gsfc.nasa.gov/pub/>

TRMM Online data (2)

- Near Real-time Product (Level 1 & 2)
 - TRMM Realtime System - NASA/GSFC
 - <http://tsdis.gsfc.nasa.gov/trmmrt/index.htm>
 - Need registration
- Near Real-time rain map (research)
 - 3B40RT (HQ MW only), 3B41RT (Geo-stationary IR data), 3B42RT (MWR+IR) - NASA/GSFC
 - Online data available within 10 hours
 - <http://trmm.gsfc.nasa.gov/>
 - GSMaP - JAXA/JST
 - <http://sharaku.eorc.jaxa.jp/GSMaP/>
 - Online data available within 4 hours
 - Need registration for NRT use
 - Past data are available from JST/CREST GSMaP web site:
http://www.radar.aero.osakafu-u.ac.jp/~gsmmap/index_english.html
- Research Product
 - VIRS Sea Surface Temperature - JAXA/EORC
 - http://www.eorc.jaxa.jp/TRMM/data/monitoring/day_vrs/index_e.htm
 - TMI Sea Surface Temperature - JAXA/EORC
 - Under construction (coming soon)